Harnessing the potential of *Pseudomonas putida* as a robust platform for the synthesis of bioactive natural products

Inaugural-Dissertation

zur Erlangung des Doktorgrades
der Mathematisch-Naturwissenschaftlichen Fakultät
der Heinrich-Heine-Universität Düsseldorf

vorgelegt von

Nora Lisa Bitzenhofer
aus Tettnang

Laupheim, November 2023

Aus dem Institut für Molekulare Enzymtechnologie
der Heinrich-Heine-Universität Düsseldorf

Gedruckt mit der Genehmigung der
Mathematisch-Naturwissenschaftlichen Fakultät
der Heinrich-Heine-Universität Düsseldorf

Referent: Prof. Dr. Karl-Erich Jaeger
Korreferent: Prof. Dr. Martina Pohl

Tag der mündlichen Prüfung: 23. Mai 2024

Für meine Eltern und meinen Bruder

A. TABLE OF CONTENT

B. ABBREVIATIONS

3-MB	3-methylbenzoate
AA	amino acid
AAAH	aromatic AA hydroxylases
ABC	ATP-binding cassette
Ab^R	antibiotic resistance marker
ACP	acyl-carrier protein
ATP	adenosine triphosphate
BCE	before the Christian Era
BGC	biosynthetic gene cluster
c.	circa
Cas9	CRISPR-associated protein 9
CoA	coenzyme A
CRAGE	*chassis*-independent recombinase-assisted genome engineering
CRISPR	clustered regularly interspaced short palindromic repeats
CRISPRa	CRISPR activation
CRISPRi	CRISPR interference
Cti	*cis-trans* isomerase
dCas9	dead Cas9
DCPK	dicyclopropyl ketone
DNA	deoxyribonucleic acid
DNP	*Dictionary of Natural Products*®
ED	Entner-Doudoroff
EMP	Embden-Meyerhof-Parnas
FA	fatty acid
FAD	flavin adenine dinucleotide
FDA	*Food and Drug Administration*
FMN	flavin mononucleotide
FPP	farnesyl pyrophosphate
GC	guanine-cytosine
GRAS	generally recognized as safe
GUS	β-glucuronidase
HAA	3-(hydroxyalkanoyloxy)alkanoic acid
HPLC	high-performance liquid chromatography
HV	host–vector
IM	inner membrane
IPA	indole-3-pyruvic acid
IPTG	isopropyl-β-D-1-thiogalactopyranoside
kb	kilobase
LacZ	β-galactosidase
LPS	lipopolysaccharide
MAP	2-methyl-3-n-amylpyrrole
MATE	multidrug and toxic compound extrusion
MBC	4-methoxy-2,2′-bipyrrole-5-carbaldehyde
MBS	mutational biosynthesis
MFS	major facilitator superfamily
mRNA	messenger RNA
MS	mass spectrometry
MVA	mevalonate
n.d.	not determined
NAD(P)	nicotinamide adenine dinucleotide (phosphate)
NDP	nucleoside diphosphate
NMR	nuclear magnetic resonance
NP	natural product
NRP	non-ribosomal peptide
NRPS	non-ribosomal peptide synthase
NT	non-template
OE	outside end
OM	outer membrane
OMP	outer membrane protein
OMV	outer membrane vesicle
oriR	origin of replication
PAM	protospacer adjacent motif
PCA	phenazine-1-carboxylic acid
PCP	peptidyl-carrier protein
PDA	photodiode array
PDB	precursor-directed biosynthesis
PE-H	polyester hydrolase
Pel	pellicle
PG	peptidoglycan
PK	polyketide
PKS	polyketide synthase
PLP	pyridoxal phosphate
PP	pentose phosphate
PPTase	phosphopantetheinyl transferase
PQS	*Pseudomonas* quinolone signal

Psl	polysaccharide synthesis locus
RBS	ribosome binding site
RL	rhamnolipid
RNA	ribonucleic acid
RNAP	RNA polymerase
RND	resistance-nodulation-division
rRNA	ribosomal RNA
SAM	S-adenosyl methionine
SEVA	Standard European Vector Architecture
sgRNA	single guiding RNA
SMR	small multidrug resistance
sRNA	small RNA
T	template
T7RP	T7 RNA polymerase
TCA	tricarboxylic acid cycle
TREX	transfer and expression
TTP	thiamine pyrophosphate
UV	ultraviolet
yTREX	TREX system applicable for yeast cloning

C. SUMMARY

Natural products (NPs) are a valuable source of potentially useful pharmaceutical compounds and have been a focus of scientific research for a long time. Obtaining these compounds from the native producer is often limited or even impossible, which highlights the significance of recombinant production in appropriate microbial hosts. As *Pseudomonas putida* has already demonstrated to be a promising heterologous host, this thesis aimed to establish strategies for harnessing the potential of *P. putida* as a robust production platform for several NPs.

First, the criteria identified by prior research for generating a robust *Pseudomonas chassis* were reviewed and applied in subsequent studies. For stable and straightforward strain generation, a fully modular genetic toolbox was established, which enables the random as well as site-specific chromosomal integration in different genomic loci. This toolbox could be used for the integration of genes encoding biosynthetic pathways and other bioprocess-relevant features in subsequent studies. Pathway engineering was then carried out using the established vector series to genomically introduce genes involved in precursor supply or entire additional precursor biosynthetic pathways.

Further, the release and extracellular storage of the produced NP was pursued with different strategies. For the first time, engineering the formation of outer membrane vesicles, a native stress response in Gram-negative bacteria, was explored to support NP biosynthesis in *P. putida*. Using a two-phase cultivation with polyurethane foam cubes as an adsorbent resulted in the extracellular accumulation of the major part of produced prodiginines and arcyriaflavin A, with over 95% of each compound recovered from the cubes. Finally, access to diverse NPs and their derivatives was enabled by combining biology with classical chemistry to build tailored biosynthetic pathways. Namely, production of new-to-nature hydroxylated and cyclic prodiginines was achieved through a hybrid synthesis route that involves adding chemically prepared building blocks as well as artificial biosynthetic pathway expansion or late-stage chemical conversion of the bioproduct, respectively. This showcase underlined the value of combining different biosynthetic concepts like (combinatorial) biosynthesis, muta-, and semisynthesis. By applying all mentioned strategies, the recombinant production of several NP classes was realized in *P. putida* KT2440, which include rhamnolipids, terpenes, and especially alkaloids such as prodiginines, violacein, and arcyriaflavin A.

In conclusion, genetic as well as biosynthetic tools were established, and engineering strategies were investigated to help to ensure strain stability, to access diverse NPs, and to enhance bioprocess productivity of the chosen host organism. These findings contribute to research aimed at harnessing the potential of *P. putida* as a recombinant production host and may significantly minimize the effort required to generate an optimal *chassis* organism hosting novel biosynthetic pathways in the future.

D. ZUSAMMENFASSUNG

Naturstoffe stellen eine bedeutende Ressource für die Entwicklung wichtiger Pharmazeutika dar und befinden sich schon seit längerer Zeit im Fokus der wissenschaftlichen Forschung. Der natürliche Produzent dieser Naturstoffe kann jedoch häufig nicht als Quelle dieser Stoffe dienen, weshalb sich die rekombinante Produktion in einem geeigneten mikrobiellen Wirt als vielversprechende Alternative erwiesen hat. Das Ziel dieser Arbeit bestand darin, verschiedene Strategien zu entwickeln, um *Pseudomonas putida*, der bereits zuvor als vielversprechender heterologer Wirt beschrieben wurde, als eine robuste Produktionsplattform für diverse Naturstoffe zu etablieren.

Hierfür wurden wesentliche Kriterien, die aus der bisherigen Forschung zur Erzeugung robuster *Chassis* bekannt sind, zusammengetragen und in unterschiedlichen Studien angewandt. Eine modulare Toolbox wurde entwickelt, die sowohl eine zufällige als auch gezielte genomische Integration von Genen, die Biosynthesewege oder andere Bioprozess-relevante Funktionen kodieren, in verschiedene Genom-Loci ermöglicht. Dies wurde in weiteren Studien erfolgreich zur Stammerzeugung eingesetzt. So konnten auch Gene, die an der Synthese von Vorstufenmolekülen beteiligt sind oder sogar ganze alternative Synthesewege kodieren, in das Genom integriert werden, um die Biosynthese der jeweiligen Naturstoffe zu optimieren.

Im weiteren Verlauf wurde die Produktivität durch Freisetzung und extrazelluläre Anreicherung des Naturstoffs optimiert, wofür verschiedene Strategien untersucht wurden. Erstmals wurde in *P. putida* die Bildung von sogenannten *outer membrane vesicles*, eine natürliche Stressantwort von Gram-negativen Bakterien, gezielt genetisch beeinflusst und ein Einfluss auf die Naturstoffproduktion beobachtet. Außerdem führte eine Zweiphasenkultivierung mit Polyurethanschaumwürfeln als Adsorbens dazu, dass die extrazelluläre Akkumulation von Prodigininen und Arcyriaflavin A erhöht wurde und über 95% der produzierten Menge aller untersuchten Naturstoffe in den Schwämmen zu finden war. Abschließend konnten mithilfe der Kombination aus Biologie und klassischer Chemie maßgeschneiderte Biosynthesewege entwickelt und damit ein Zugang zu verschiedenen Naturstoffen und deren Derivaten ermöglicht werden. Es konnte durch eine hybride Syntheseroute, welche sowohl die Zugabe chemisch hergestellter Vorstufen als auch eine artifizielle Erweiterung des Biosyntheseweges beziehungsweise eine späte chemische Umsetzung des Bioprodukts beinhaltet, die Bildung neuartiger hydroxylierter und zyklischer Prodiginine erreicht werden. Anhand dieses Beispiels konnte verdeutlicht werden, wie vielversprechend die Kombination unterschiedlicher Biosynthesekonzepte wie die (kombinatorische) Biosynthese, Muta- und Semisynthese ist. Durch Anwendung all dieser Strategien konnte die rekombinante Produktion mehrerer Naturstoffklassen in *P. putida* KT2440 realisiert werden. Diese Klassen umfassen

Rhamnolipide, Terpene sowie insbesondere Alkaloide, wie Prodiginine, Violacein und Arcyriaflavin A.

Zusammenfassend wurden in dieser Arbeit genetische und biosynthetische Werkzeuge entwickelt sowie *engineering*-Strategien untersucht, die für die Gewährleistung der genetischen Stabilität der erzeugten Stämme, den Zugang zu verschiedenen Naturstoffen und die Verbesserung der Produktivität des Bioprozesses von zentraler Bedeutung sind. Diese Ergebnisse tragen zur Weiterentwicklung des Potenzials von *P. putida* als rekombinantem Wirt für die Naturstoffproduktion bei. Die so entwickelten Werkzeuge können helfen, den Aufwand, der für die Entwicklung eines optimalen *Chassis*-Organismus für neue Biosynthesewege erforderlich ist, erheblich zu reduzieren.

I. INTRODUCTION

Since ancient times, nature has been a source of remedies for a wide variety of diseases and ailments. The documentation reaches back to c. 1600 BCE when the knowledge of ancient Egyptian medicine was summarized in the Ebers Papyrus. This 20-meter-long papyrus documents an understanding of versatile topics spanning wound treatment to contraception, with early mentions of narcotics such as opium and cannabis[1]. Since then, natural products (NPs) have served as powerful therapeutics and inspiration for drug design, culminating in the `golden era` of antibiotics (1940s to 1960s)[2,3], which gave mankind one of the biggest medical breakthroughs of the 20th century[4,5]. While NPs find application in the treatment of diverse diseases, the field of antibiotics perhaps most prominently demonstrates their utmost relevance. Most classes of antibiotics currently in use were developed during these years, and to date, more than three-quarters of the approved antibiotics are based on NPs or their derivatives, again underlining the value of these compounds as antibiotic scaffolds[6,7]. However, the research pipeline for new antibiotics is depleted, while the urgency to discover new antimicrobial agents has grown due to increased antibiotic resistances[8]. In fact, deaths associated with infections by multidrug-resistant bacteria are expected to further increase in the coming years and could overtake cancer as the leading cause of death by 2050[9]. Therefore, research in this field must be intensified in order to combat this threat[10,11]. Biotechnology can make valuable contributions to the discovery and production of relevant compounds. To do so, it requires an in-depth understanding of the molecular framework and biosynthesis of NPs[12,13].

I.1. Natural products

In the broadest sense, NPs are defined as any chemical compounds that occur naturally in biological organisms. These compounds can be derived from primary metabolism, from building blocks such as sugars, amino acids (AAs), lipids, and nucleic acids. However, the term ‘natural product’ typically refers to secondary metabolites which are basically derivatives of primary metabolites, but often synthesized through more complex pathways. Unlike primary metabolites, these molecules are not essential for the organism’s basic metabolism and reproduction[14]. They often exhibit various biological effects, including antibacterial, antifungal, anticancer, and immunosuppressive properties[6,15,16], as well as promoting cell survival or adaptability to changing environmental conditions[17–20].

NPs are produced from a limited number of primary metabolites (e.g., D-glucose, isopentyl diphosphates, L-tryptophan, L-phenylalanine, acetyl-CoA, malonyl-CoA) as building blocks. Their structural architectures are generated by a limited number of enzyme classes (e.g., oxidoreductases, decarboxylases, transferases, isoprenoid synthases) in conjunction with certain chemical reactions (e.g., Aldol- and *Claisen* condensation, C-N condensation, *Mannich* reaction)[21]. The combination of precursors, reactions and enzymes results in the formation of a

diverse range of NPs, which comprise approximately 200 000 to 350 000 compounds, with the estimations based on the compounds listed in various NP databases, such as the *Dictionary of Natural Products*® (DNP)[22–24]. According to the DNP, the majority of the representatives are produced by plants (67%), animals (13%), fungi (10%), and bacteria (9%) (**Figure I-1**)[25]. Although plants have been reported to have the highest number of NPs with terpenoids as their largest group[18,25–27], bacteria exhibit the highest percentage of bioactive products in a medically relevant context. The relative amount is three- to seven-fold higher compared to plants or animals[25,26]. More than 50% of antibacterial agents which were approved by the FDA (*Food and Drug Administration*) are of bacterial origin[28]. Furthermore, bacterial NPs exhibit additional activities besides their use as antibacterial agents[25,29]. In particular, they are utilized as antineoplastic[30,31], antifungal[32,33], antiviral[34], and anti-inflammatory agents[35].

The bacterial divisions with the highest number of (bioactive) NPs are actinobacteria (or actinomycetota), including *Streptomyces* or *Mycobacterium*, proteobacteria, such as *Pseudomonas*[29,36–38], and cyanobacteria (**Figure I-1**)[25]. The discovery of streptothricin[39] and streptomycin[40] in the 1940s brought special attention to the *Streptomyces* species and today it is estimated that 30 to 45% of the compounds described as originating from microorganisms actually derive from these species[25,29]. These include antibiotic classes such as β-lactams, aminoglycosides, peptides, and tetracyclines[4]. Additionally, rare actinomycetes biosynthesize other frequently utilized antibiotics, such as gentamicin produced by *Micromonospora purpurea*, erythromycin by *Saccharopolyspora erythraea*, and vancomycin by *Amycolatopsis orientalis*[41]. Besides the already mentioned divisions and species, *Bacillus* species also serve as a source of NPs, predominantly producing peptide antibiotics like lantibiotics[42–45].

The genes responsible for the biosynthesis, regulation, protection from, or export of NPs are typically arranged in close proximity to each other and are encoded in so-called biosynthetic gene clusters (BGC). These BGCs can vary in size from a few kilobases (kb) to over 100 kb[46,47].

Regarding the structural architecture, NPs are often described as chemically intricate[48]. In the early 2000s, structural studies demonstrated that these compounds contain more sp^3-hybridized bridgehead atoms and multiple chiral centers compared to small molecules of synthetic origin[49–51]. The classification and categorization of molecular structures of these products provides valuable data and enables the development of sophisticated tools for NP research. Besides the DNP, other NP-specific databases have been created to simplify the study of NPs[52–56].

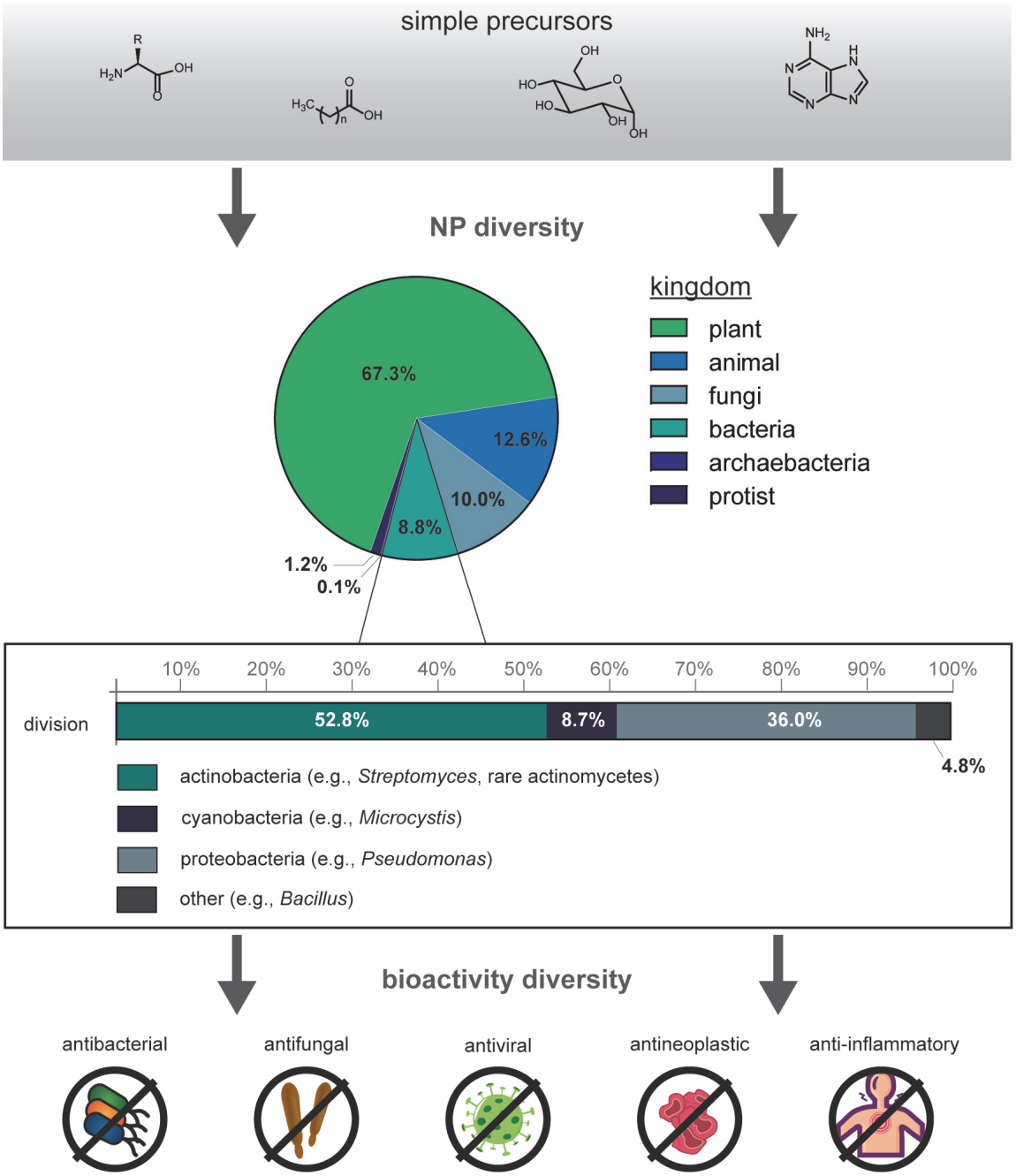

Figure I-1: Distribution of NPs in six different kingdoms of life.
Overview of the distribution of NPs derived from different primary metabolites (f.l.t.r., AAs, fatty acids, sugars, and nucleobases) into six kingdoms based on the categorization of the *Dictionary of Natural Products* (DNP) (http://dnp.chemnetbase.com) (top). For bacterial NPs, the most prominent producers are shown (middle). More than half are produced by *Streptomyces* and rare actinomycetes. However, cyanobacteria, *Bacillus* and *Pseudomonas* species are also known producers of bioactive NPs[25]. The most promising bioactivities of the bacterial NPs, for which they are frequently applied, are for example antibacterial, antifungal, or anti-inflammatory effects (bottom).

A widely accepted NP classification, determined by their structural scaffold, their enzymatic biochemistry, and by the starting precursors, was introduced by Walsh and Tang, leading to six general groups of NPs[21]: polyketides, peptides, phenylpropanoids, isoprenoids and terpenoids, purines and pyrimidines, as well as alkaloids. Polyketides, peptides, and alkaloids constitute the largest groups in bacteria and account for over half of the bacterial NPs[25]. Alkaloids, in

particular, are highly intriguing due to the large number of bioactive compounds found within this class.

I.2. Alkaloids

Alkaloids are a large group of bioactive natural products with about 40 000 compounds listed in the *Dictionary of Alkaloids*[57]. They are found in many organisms like plants, animals, and different microorganisms[58–62]. Most of the overall isolated alkaloids thus far are in fact from plants but as already mentioned above, they also occur in bacteria.

Alkaloids are essentially natural nitrogen-containing organic compounds that often have complex heterocyclic structures. Due to their structural scaffold containing one or more nitrogen as heteroatoms, alkaloids readily form hydrogen bonds with proteins, enzymes, and receptors[63]. In the presence of other functional groups, this explains the extraordinary bioactivity of alkaloids. The broad activity spectrum comprises antimicrobial, anticancer, antimalaria, and anti-inflammatory properties[16,64–66]. Due to their high bioactivities, they play an important role in both traditional and modern medicine and are being studied intensively to better understand their usage and effects[16,64,67–69]. Based on the scaffold, alkaloids can be divided into several classes, including pyridines, pyrimidines, pyrrolidines, pyrroles, indoles, (iso-)quinolines, and quinolones (**Figure I-2**)[16].

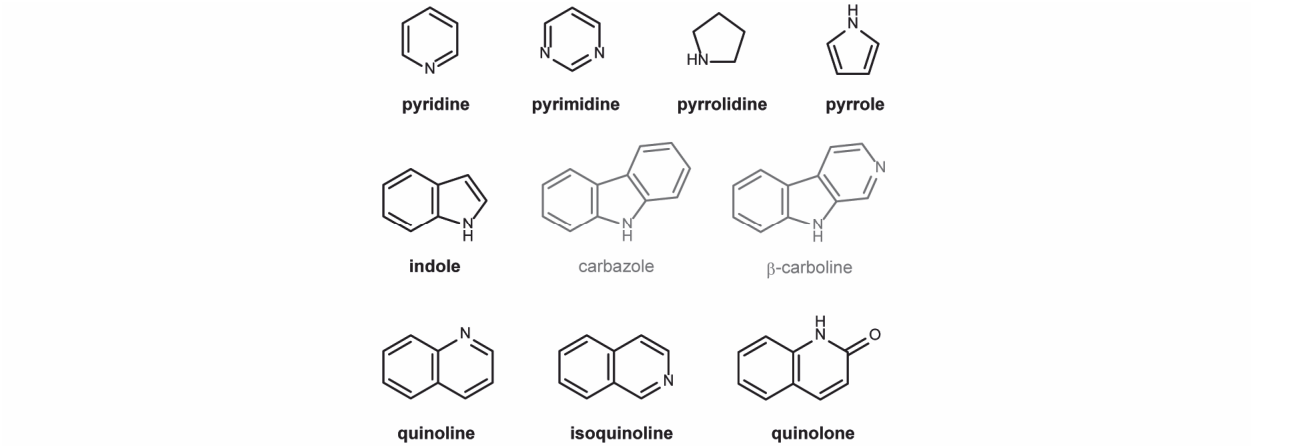

Figure I-2: Scaffolds of different classes of alkaloids (adapted from Cushnie et al. 2014[16]).
Eight scaffolds of heterocyclic alkaloids are exemplarily shown in black. The gray structures represent important subclasses of the indole alkaloids such as the indolocarbazoles. Other classes of bioactive alkaloids whose scaffolds are not shown here are aaptamines, acridines, imidazoles, indolizidines, 1,3,4-oxadiazoles, piperazines, piperidines, 2-pyridones, and thiazoles.

I.2.1. Three representatives of the bacterial alkaloids

Based on the structural classification outlined in the previous chapter, this section will delve into three classes of bacterial alkaloids in more detail which were the focus of this thesis: the pyrrole alkaloids, the indole alkaloids, and the quinoline alkaloids.

Pyrrole alkaloids: An intriguing class, which is widespread in both terrestrial and marine environments, are the pyrrole alkaloids. One of the very notable members is the prodiginine family, which consists of tripyrrolic and bright red NPs produced by various marine and terrestrial bacteria[70]. The three rings of the basic structure are typically referred to as ring A, B, and C (**Figure I-3**, A). Prodiginines can be divided into two categories: one group includes prodiginines with alkyl chain substituents, such as prodigiosin and undecylprodigiosin[71]. The other category encompasses cyclized derivatives like butyl-meta-cycloheptylprodigiosin and cycloprodigiosin[72,73]. The latter, in contrast to the straight-chain variants, contains a hexane ring between the third and fourth positions of the pyrrole ring C, with a methyl group attached to this ring[74]. Marine species from different genera, such as *Pseudoalteromonas*[75–77], *Vibrio*[78–80], or *Zooshikella* species[81,82], produce the cyclic prodiginines usually in a mixture with the straight-chain variant[72,80,82].

However, the most widely recognized compound among the prodiginine family is the straight-chain prodigiosin (**14**), which possesses a pentyl chain on the pyrrole ring C. It occurs in *Serratia* species such as *Serratia marcescens*[83–86], in *Hahella chejuensis*[87,88], *Streptomyces coelicolor*, and *S. griseoviridis*[89–91]. The well-described *S. marcescens* prodigiosin BGC, known as the '*pig* cluster', is comprised of 14 unidirectionally arranged genes (*pigA* to *pigN*) stretched over 21 kb (**Figure I-3**, B)[92]. The associated enzymes participate in the biosynthesis of the tripyrrole structure of prodigiosin (**14**). Specifically, the enzymes PigB, PigD, and PigE are responsible for the synthesis of the monopyrrole MAP (2-methyl-3-*n*-amylpyrrole, **4**). The enzymes PigA, PigF to PigJ, as well as PigM and PigN are responsible for the synthesis of MBC, also known as 4-methoxy-2,2′-bipyrrole-5-carbaldehyde (**13**). The final condensation reaction between MAP and MBC is catalyzed by the ligase PigC (**Figure I-3**, C)[93,94]. The current understanding of the functions of PigK and PigL remains vague. PigK may serve as a chaperon assisting in the folding of other Pig enzymes[95]. The gene *pigL* encodes for a 4′-phosphopantetheinyl transferase, thus an involvement in the phosphopantetheinylation reaction in the MBC pathway has been suggested[94]. Based on the localization at the inner membrane, it has been postulated that the last biosynthetic enzymes of the precursor pathways, PigB and PigN/F, as well as the enzyme PigC form a membrane-associated protein complex for the condensation reaction[94,96,97].

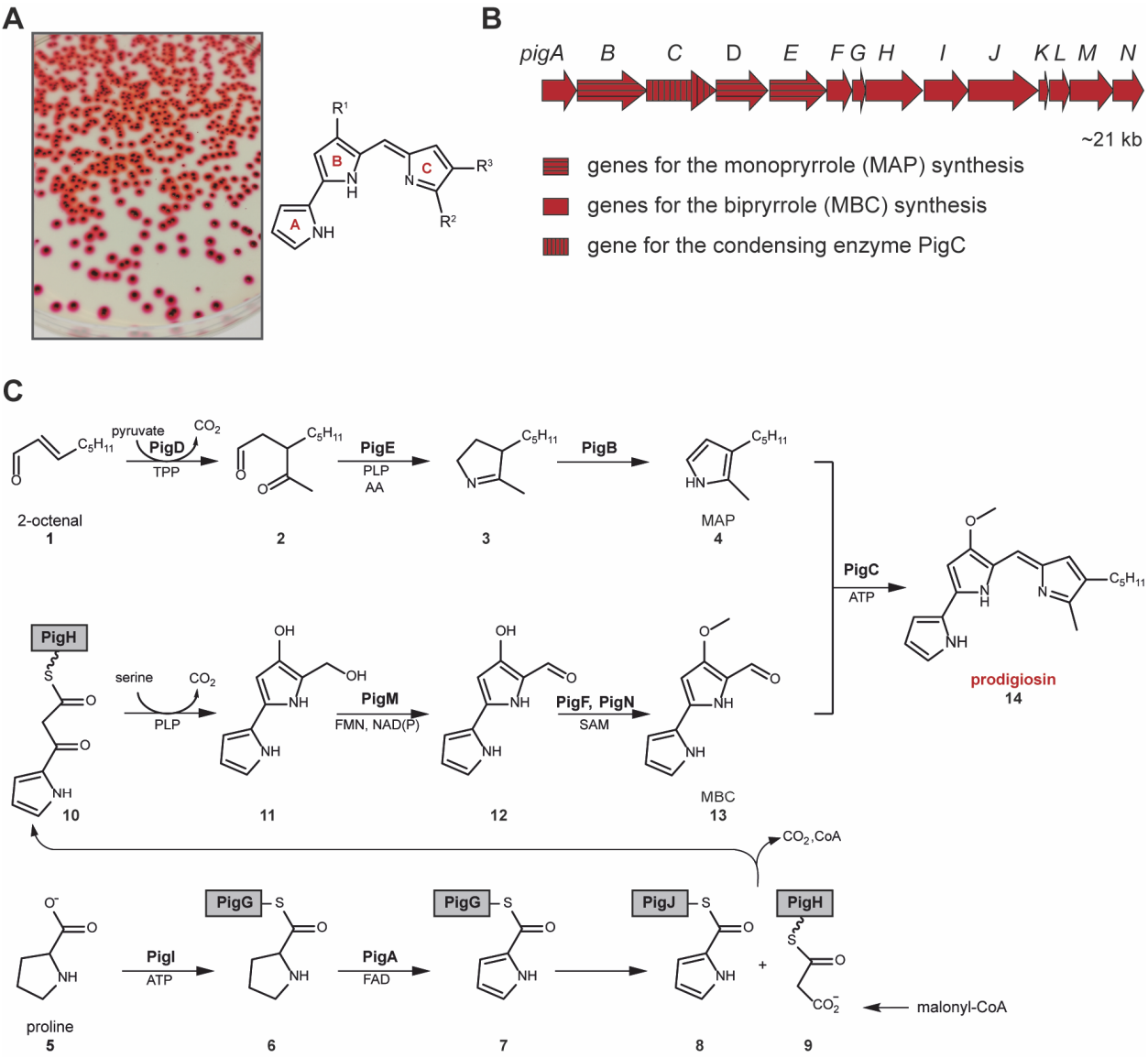

Figure I-3: The biosynthetic pathway of the tripyrrole prodigiosin (adapted from Williamson et al. 2005, 2006[93,94] and N. Bitzenhofer 2018[98]).
A: The typical red color of prodiginines is shown by a prodigiosin-producing bacterium (*Pseudomonas putida* pig21[99]). The basic structure of prodiginines is given, consisting of three pyrrole rings, labeled A, B, and C. The structural diversity of the prodiginine family is due to the varying substituents at the 2-(R^2) and 3-(R^3) positions of the C-ring. **B**: The BGC responsible for the biosynthesis of prodigiosin (**14**) in *Serratia marcescens* is displayed. This so-called '*pig* gene cluster' contains 14 unidirectional genes (about 21 kb). Enzymes for the MAP (**4**) synthesis are encoded by *pigB*, *pigD* and *pigE*, which are represented by horizontally striped arrows. The associated enzymes of the genes *pigA*, *pigF* to *pigJ*, *pigM* and *pigN* are responsible for the production of MBC (**13**) (genes are indicated by blank arrows). The vertical striped arrow indicates the *pigC* gene, which encodes for the ligase PigC responsible for the terminal reaction. **C**: The biosynthesis of prodigiosin is based on a bifurcated pathway utilizing 2-octenal (**1**) and proline (**5**) as precursors. The final condensation reaction between MAP (**4**) and MBC (**13**) ultimately results in the tripyrrole prodigiosin (**14**), which is intensively red colored. TTP: thiamin pyrophosphate; PLP: pyridoxal phosphate; AA: amino acids; ATP: adenosine triphosphate; FAD: flavin adenine dinucleotide; FMN: flavin mononucleotide; NAD(P): nicotinamide adenine dinucleotide (phosphate); SAM: *S*-adenosyl methionine.

Numerous scientific studies have revealed the bioactive properties of prodigiosin and its derivatives, which makes them prospective drug candidates[95,100]. On the one hand, prodigiosin is considered to exert an anticancer effect by inducing apoptosis in specific cancer cells[101–105]. Prodigiosin-triggered destruction of cancer cells can be attributed to its function as an anion transporter that binds to biologically significant anions, causing a shift in the pH gradient and

leading to the acidification of the cancer cells[106,107]. On the other hand, these tripyrroles have been reported to be antibacterial agents. Four mechanisms of action have been proposed: as mitogen-activated protein kinase regulators, pH modulators, bacterial DNA cleavage agents and cell cycle inhibitors[108]. Several bacterial species are sensitive to the antagonistic effects of prodigiosin[109–112]. Notably, the cyclic derivatives appear to exhibit greater antimicrobial activity against certain Gram-positive and -negative bacteria compared to the straight-chain variants[82]. Furthermore, prodiginines demonstrated antimalaria[90,113], antiviral[114], and immunosuppressive activities[115]. A comparison of straight-chain and cyclic variants revealed higher antifungal activity for the latter[82,116].

Since prodigiosin and its derivatives exhibit a range of properties, which are relevant for the potential use as therapeutic drugs, there is great interest in gaining access to these compounds via high-level production as well as novel structural variants. Thus, this class is still widely studied in NP research.

Indole alkaloids: Among the alkaloids, the indole-containing alkaloids are highly abundant in nature and show a range of structural and therapeutic properties, which include antimicrobial, anticancer and anti-inflammatory activities[117]. Two examples of this wide field are the bisindoles violacein and rebeccamycin. Both are biosynthesized by oxidative dimerization of two L-tryptophan units, and both demonstrated great potential as therapeutic agents.

Violacein (**19**) and its byproduct deoxyviolacein (**20**), which both exhibit striking purple hues (**Figure I-4**, A), are produced by the Gram-negative bacterium *Chromobacterium violaceum*[118]. In addition, other species have been described to produce these types of compounds[119–124]. The biosynthesis of these bisindole alkaloids in *C. violaceum* involves five enzymes, VioA to VioE. The corresponding genes are all located within the unidirectional *vioABCDE* operon (about 7 kb) (**Figure I-4**, B)[125,126].

The indolocarbazole bisindole rebeccamycin (**23**) or its derivatives rebeccamycin aglycon (**21**) and arcyriaflavin A (deschloro-rebeccamycin aglycon) share all an indolo[2,3-a]carbazole scaffold[127]. Rebeccamycin shows a yellow coloration and is naturally produced by the actinomycete *Lentzea aerocolonigenes* (formerly referred to as *Lechevalieria aerocolonigenes*)[128–130]. For the biosynthesis of the indolocarbazole several catalytic steps are required. The associated bidirectional gene cluster contains 11 genes (about 26 kb), whereby eight genes encode enzymes directly involved in the biosynthesis (RebG,O,D,C,P,M,F,H). Two genes (*rebU* and *rebT*) seem to be involved in resistance and secretion of the compound as they encode for putative antibiotic transporters[131,132]. In addition, the *reb* cluster contains a regulator-encoding gene (*rebR*) which belongs to the LuxR family and might be functioning as a transcription activator similar to the regulatory mechanism of the *vio* genes[131,133,134].

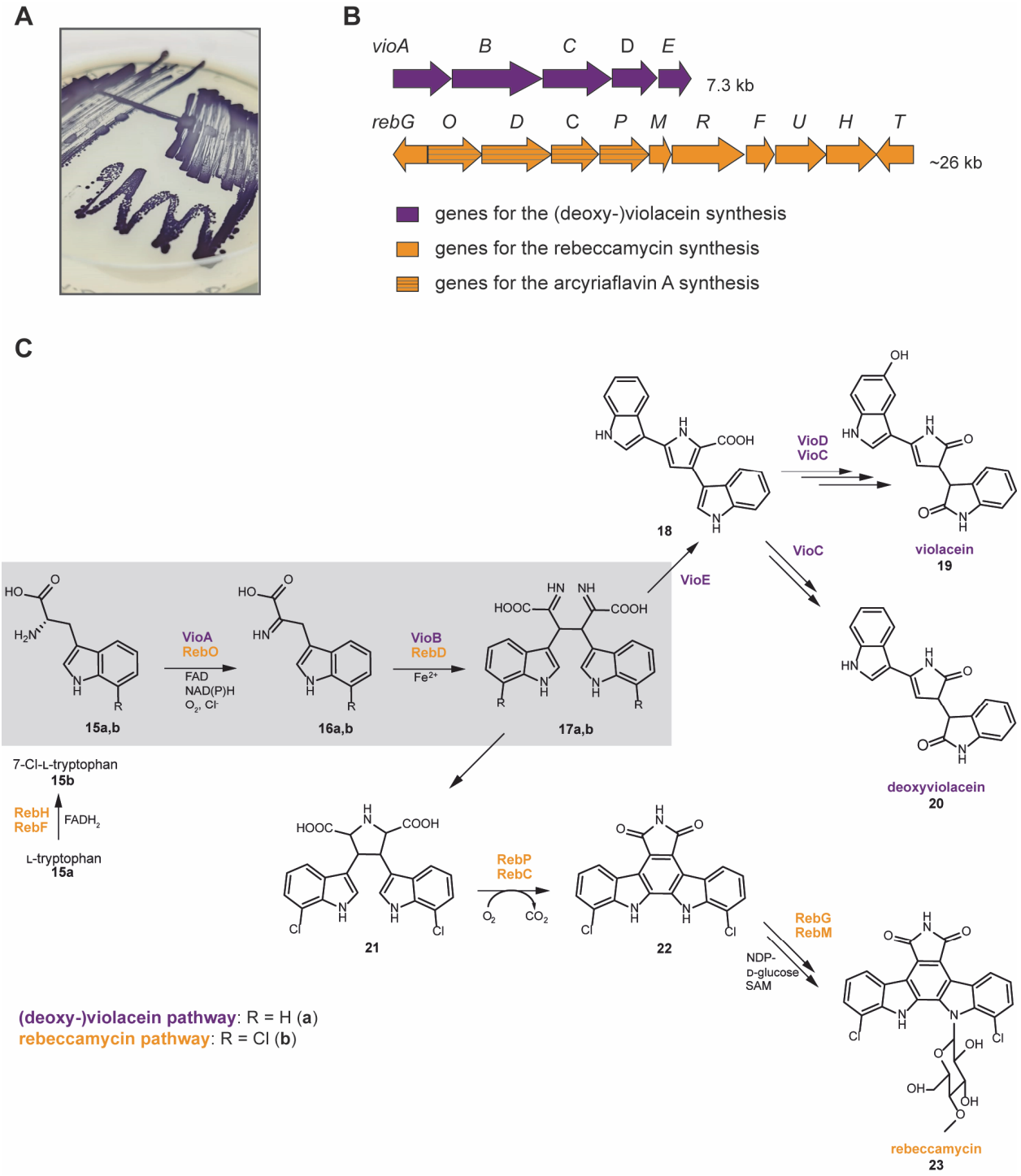

Figure I-4: The biosynthetic pathways of the bisindoles violacein and rebeccamycin (adapted from Füller et al. 2016[135]).
A: Violacein-producing bacterium (*P. putida* vio12[136]) with the typical purple color. **B**: Representation of the *vio* (purple) and *reb* (orange) BGCs from *C. violaceum* and *L. aerocolonigenes*, respectively. Regarding the *reb* cluster, genes essential for the synthesis of both rebeccamycin (*rebGODCPMRFUHT*) and its derivative arcyriaflavin A (*rebODCP*), which are indicated by horizontally striped arrows, are shown. **C**: The initial formation of the indole-3-pyruvic acid (IPA) imine dimer (**17a,b**) is comparable for violacein and rebeccamycin catalyzed by the homologous enzymes VioA,B and RebO,D, respectively (gray box). Further synthesis of violacein (**19**) is performed by VioE, VioC, and VioD. In addition, the byproduct deoxyviolacein (**20**) can be produced without the involvement of VioD. For rebeccamycin (**23**) biosynthesis, an initial chlorination of L-tryptophan is necessary (**15a** → **15b**). The terminal steps are catalyzed by RebP, RebC, RebG, and RebM. FAD: flavin adenine dinucleotide; NAD(P): nicotinamide adenine dinucleotide (phosphate); SAM: *S*-adenosyl methionine; NDP: nucleoside diphosphate.

The syntheses of violacein and rebeccamycin are based on closely related initial enzymatic steps catalyzing the oxidation of an L-tryptophan unit to the indole-3-pyruvic acid (IPA) imine (**16a,b**) (**Figure I-4**, C)[135]. In the case of rebeccamycin biosynthesis (**23**), this step is preceded by chlorination of L-tryptophan (**15a** → **15b**). In both cases, the imine formation is followed by oxidative coupling of two imines to the IPA imine dimer (**17a,b**). At this stage, the synthesis pathways diverge to form the respective end products. The (deoxy-)violacein synthesis involves an intramolecular rearrangement by VioE, which results in the formation of protodeoxyviolaceic acid (**18**). VioD and VioC can then convert **18** to violacein (**19**) and deoxyviolacein (**20**), respectively[126,137]. Typically, these two compounds exist in a mixture. In contrast, for the biosynthesis of rebeccamycin, **17b** is spontaneously converted into chlorinated chromopyrrolic acid (**21**), followed by the formation of the rebeccamycin aglycon (**22**), which is enzymatically catalyzed by RebC and RebO. RebG and RebM perform the final steps to yield rebeccamycin (**23**) which include the introduction of a D-glucose moiety by a β-glycosidic linkage and a methylation step[131,138].

Both groups of compounds exhibit several promising biological activities for therapeutical use. For violacein, these activities include antibacterial, antiviral, and antitumoral effects[139–141]. Several studies have demonstrated its impact on both pathogenic and non-pathogenic bacteria[142–144]. In addition, extensive research has been dedicated to examining the underlying mechanism regarding anti-cancer properties. These efforts have shown that violacein modulates important processes in cancer, such as inhibiting proliferative signaling, inducing cell death, and preventing metastasis and invasion[145–150]. Like violacein, rebeccamycin and its derivatives have also demonstrated antibacterial effects against Gram-positive bacteria[128,151]. However, their potential in cancer treatment is of greater interest since rebeccamycin is a DNA intercalating agent and functions as a topoisomerase I inhibitor[128,152]. Becatecarin, a water-soluble variant of rebeccamycin, has even undergone phase I and II in clinical trials, e.g., for the treatment of lung and breast cancer[153–156]. Derivatives of the indolocarbazole, such as arcyriaflavin A, have further been investigated in the context of treating human cytomegalovirus infections and, more recently, endometriosis[157–159].

The diverse and highly relevant bioactivities of the violacein and rebeccamycin-type compounds illustrate the potential and importance of indole alkaloids. Thus, targeted biotechnological production of these compounds holds significant value.

Quinoline alkaloids: In recent years, the class of quinoline and quinolone alkaloids has attracted significant attention in the pharmaceutical research due to their diverse bioactivities ranging from antimalaria to anticancer aspects[160–164]. Although quinoline alkaloids are mostly abundant in plants, bacteria also represent promising sources for the discovery of such compounds. The *Pseudomonas* quinolone signal (PQS), a quorum sensing modulator in the *Pseudomonas* genus, and the aurachins, a group of farnesylated quinoline alkaloids are well-known examples of this class[165].

Aurachins have been first described in the myxobacterium *Stigmatella aurantiaca*[166], before other producer species have been found including *S. erecta*[167] as well as actinomycetes like *Rhodococcus* and *Streptomyces* species[168–170]. The compounds in this class can be categorized into two structural types based on the position of the farnesyl chain: the C-type aurachins possess the farnesyl chain at the C3 position and the A-type aurachins at the C4 position of the quinolone motif. Major aurachins which belong to these categories are aurachin C and D (C-type), and aurachin A and B (A-type). The BGCs for the biosynthesis of these four compounds is divided into three different loci in *S. aurantica*, referred to as gene locus I-III. Locus I contains the genes responsible for the formation of aurachin D and then C (**Figure I-5**, A). The genes in gene loci II and III are responsible for the formation of aurachins B and A, respectively[171]. For a more detailed description of the biosynthesis, a focus will be given to the C-type group (aurachin D and aurachin C). In *S. aurantiaca*, the biosynthesis of aurachin C (**28**) involves a type II polyketide synthase (PKS) in the conversion of anthranilic acid (**24**) to 4-hydroxy-2-methylquinoline (**26a**)[172,173]. This intermediate is then farnesylated by the membrane-bound prenyltransferase AuaA to form aurachin D (**27**). In a final enzymatic step, *N*-hydroxylation occurs catalyzed by the Rieske monooxygenase [2Fe-2S] AuaF (**Figure I-5**, B)[171,174].

Aurachins were initially found to possess antimicrobial activity against Gram-positive bacteria and certain fungi[176]. The structural similarity between aurachins and the known electron transport inhibitor, 2-heptyl-4-hydroxyquinoline-*N*-oxide (HQNO), suggested the same cellular targets. This was confirmed in various studies[166,177,178]. Moreover, further investigations revealed cytotoxic effects on different mammalian cell lines, especially for aurachin D[176,179]. Antiparasitic activity has been demonstrated in the malarian pathogen *Plasmodium falciparum* FcB1 and *Trypanosoma brucei gambiense*, causing African sleeping sickness. A direct comparison indicated significantly higher antiparasitic activity of aurachins B, C and E over aurachin D[167,176,180].

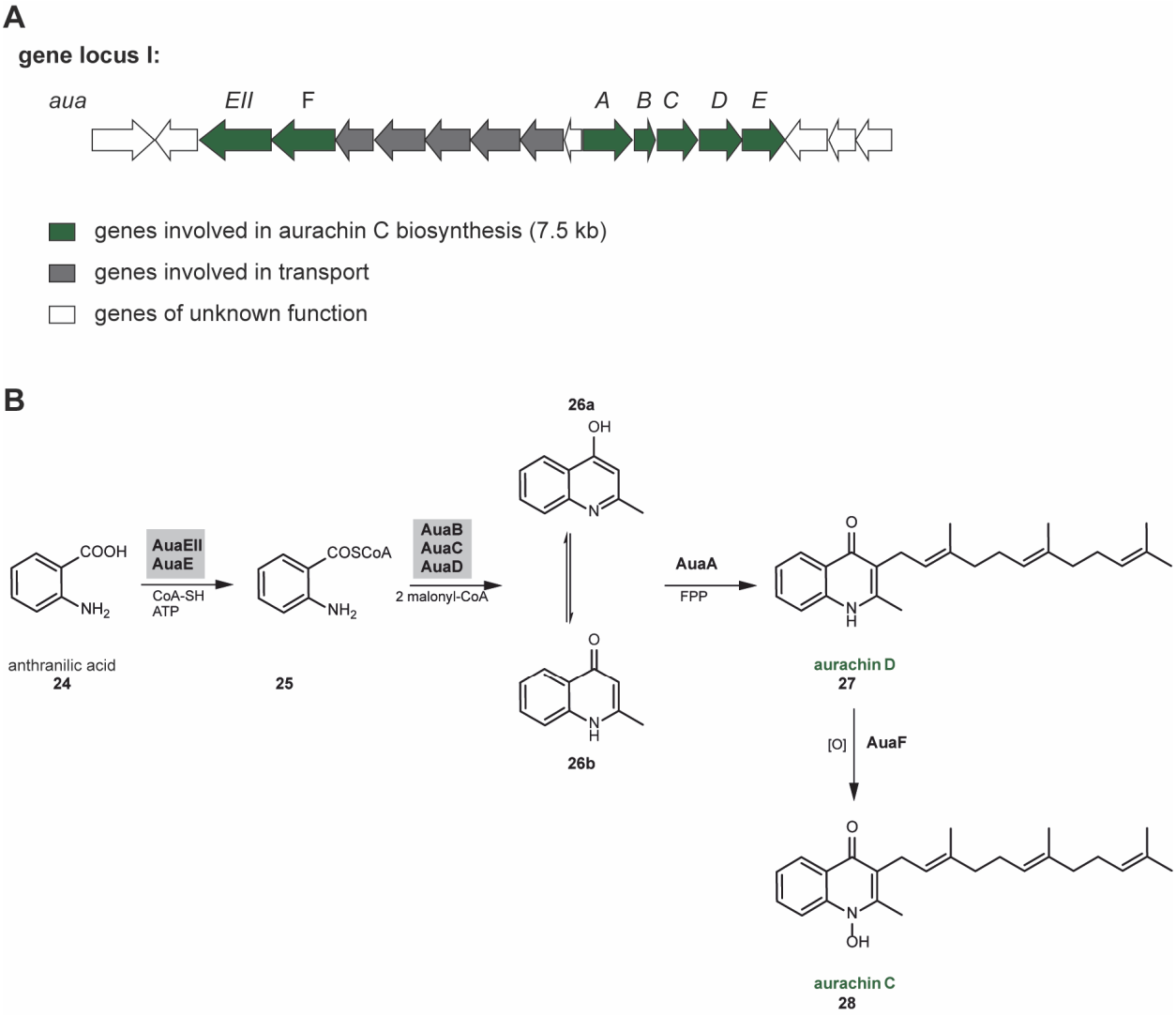

Figure I-5: The biosynthetic pathway of the farnesylated quinoline aurachin C (adapted from Pistorius et al. 2011[171]; Sester et al. 2020[175]).
A: Architecture of the *aua* gene cluster for aurachin C biosynthesis. In *S. aurantiaca*, genes encoding for enzymes responsible for the synthesis of aurachins are divided into three gene loci (I to III). Gene locus I contains the seven genes *auaA-EII* (green arrows) necessary for aurachin C production. This locus also contains genes responsible for aurachin transport (gray arrows) and genes with yet unknown function (white arrows). **B**: Aurachin C (**28**) is synthesized from anthranilic acid (**24**). The initial steps involve a type-II PKS (enzymes are highlighted by gray boxes). It results in the production of 4-hydroxy-2-methylquinoline (**26a**) which undergoes tautomerization into 2-methyl-1H-quinolin-4-one (**26b**). AuaA is responsible for transferring the farnesyl side chain from FPP to **26b**, thereby leading to the formation of aurachin D (**27**). The final catalytic step in the biosynthesis of aurachin C (**28**) involves the *N*-hydroxylation by AuaF. CoA: coenzyme A; ATP: adenosine triphosphate; FPP: farnesyl pyrophosphate.

The overview of NPs, particularly the detailed review of some bacterial alkaloids, underlines the great potential of these compounds. However, a major challenge is obtaining the natural products in sufficient amounts for further characterization studies and applications. One approach to address this issue is to use the native producers for large-scale biosynthesis. However, under standard cultivation conditions, the expression of biosynthetic genes and product yields are often low. Therefore, one strategy can be to activate BGCs within the producer, for example, utilizing a library of diverse activator genes[181]. Since other aspects such as pathogenicity or difficult handling in the laboratory may render the native producers unattractive for a biotechnological application, another commonly employed strategy is therefore

to facilitate NP formation by the heterologous expression of the BGCs in alternative microbial hosts[182,183].

I.3. Recombinant NP biosynthesis

Over the past 40 years, the significance of NPs has increased, with 50 to 70% of approved drugs being NPs, derivatives, or NP biosimilars[6,184,185]. Because of their intricacy and complex stereochemistry, these compounds are challenging to synthesize chemically. Extracting them from their natural hosts, such as plants or fungi, is often environmentally impractical and time-consuming. Moreover, a fungal or bacterial producer may be pathogenic, not cultivable under laboratory conditions, or may show insufficient growth or product titers[26,186].

Therefore, expressing a BGC heterologously in a genetically accessible, non-harmful and highly productive host presents a promising alternative for NP production (**Figure I-6**)[182,183,187–189]. Notably, this approach also presents opportunities to incorporate novel engineering techniques in NP biosynthesis, leading to increased production titers or to structurally modified compounds. The initial step in recombinant NP production is always the identification and selection of known or novel BGCs. In particular, the search for novel gene clusters has been facilitated and expedited by bioinformatics developments in recent years, as genome mining can be used to screen genome sequences for the presence of new BGCs[56,190–195]. After (*in silico*) identification of suitable biosynthetic genes, recombinant host selection and its manipulation including stable integration of often large BGCs and, if necessary, engineering of metabolic fluxes need to be realized. A further challenge that should not be underestimated is the analytical detection, isolation, and structural elucidation of the produced compound, especially for novel NPs using, for instance, high-performance liquid chromatography (HPLC), mass spectrometry (MS), and nuclear magnetic resonance (NMR) spectroscopy. Once all necessary procedures are completed, NPs can be employed to investigate the biological effects and determine their mechanism of action[196].

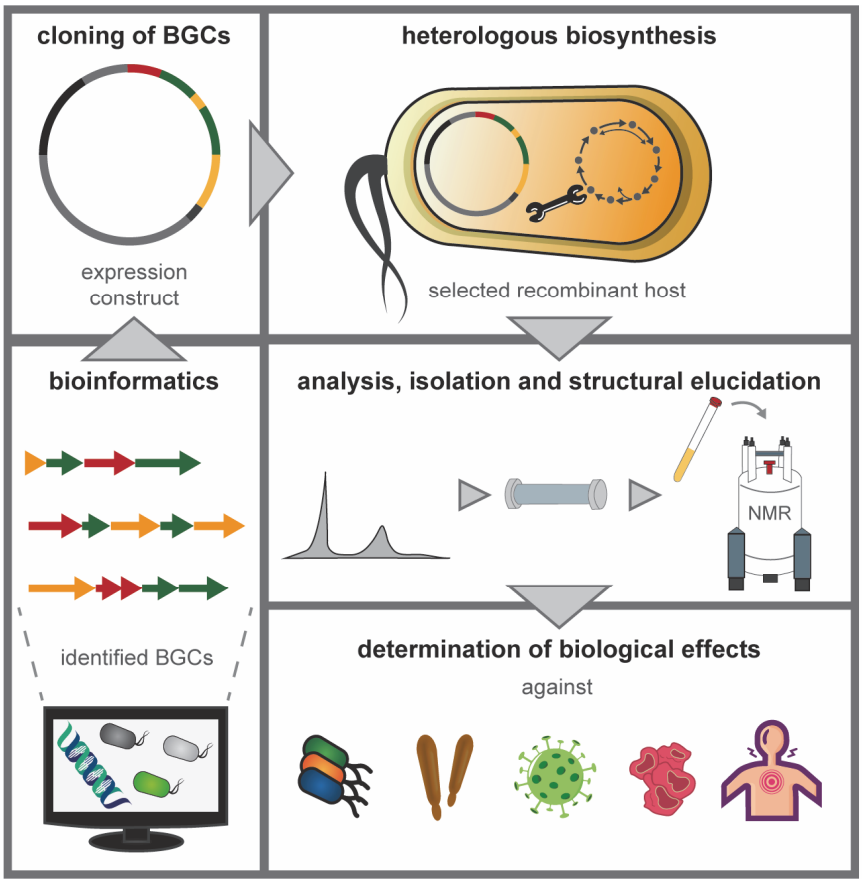

Figure I-6: Procedure of bioactive NP production in heterologous hosts (adapted from Brötz-Oesterhelt et al. 2023[196]).
Several steps are necessary for the biosynthetic NP production in recombinant hosts. These include identifying and cloning BGCs e.g., using bioinformatic approaches such as genome mining. Selecting a suitable organism is critical for enabling stable expression of biosynthetic genes and achieving high-yield production. The next step involves conducting bioanalytical methods (e.g., HPLC-MS measurements), isolating the compound via column chromatography-based techniques, and ultimately determining their structure (e.g., by NMR). Then, the effect of the produced NP against microbes, viruses, cancer cells, or inflammation can be investigated.

The selection of an optimal production host certainly requires special consideration, as the recombinant biotransformation of bioactive NPs bears several critical points[197]. These include (i) ensuring effective transfer of biosynthetic genes and stable integration[182,198], (ii) coordinated and regulated gene expression as well as enzyme activity[182], (iii) overcoming non-optimal metabolic fluxes or low precursor or cofactor supply[188], and (iv) dealing with the NP bioactivities that can cause stress for the producer resulting in impaired strain stability and reduced growth. Thus, researchers have turned to various heterologous hosts over time. For terpene production, these include especially yeasts, such as *Saccharomyces cerevisiae*, as well as aerobic and anaerobic phototrophic bacteria[199–201]. Another common choice is the widely used host *E. coli*, and well-studied *Streptomyces* strains, like *S. coelicolor*, *S. lividans*, and *S. albus*, which are specifically used for expression of large BGCs[202,203]. In addition, the metabolically versatile bacterial strain *Pseudomonas putida* is useful for the production of various types of NPs[204]. This organism possesses several advantageous inherent properties for recombinant biosynthesis, which will be elaborated in the following chapter.

I.3.1. *Pseudomonas putida* as cell factory

The Gram-negative rod-shaped soil bacterium *P. putida* has demonstrated biotechnological potential in the last decades as an appropriate cell factory[205–207]. Especially, *P. putida* KT2440 is an intriguing representative for biotechnological use, due to its HV-1 (host–vector system safety level 1) certification[208,209]. Overall, the *Pseudomonas* genus is a highly heterogeneous bacterial group, found in various environments and niches[207,210]. *P. putida* can grow in a range of diverse and often extreme habitats. Its remarkable capacity to metabolize diverse carbon sources positions *P. putida* as a promising candidate for various biotechnological applications. Additionally, it exhibits the ability to grow in low-nutrient environments, which accounts for its widespread distribution[211].

The central carbon metabolism of *P. putida* features a distinctive circular structure known as the EDEMP cycle. It is composed of enzymes from the Entner-Doudoroff (ED), the Embden-Meyerhof-Parnas (EMP), and the pentose phosphate (PP) pathways. Glucose degradation primarily occurs through the ED pathway. The resulting triose phosphate is then partially recycled into hexose phosphate through a cycle involving the EMP and PP pathways[212,213]. Implementing cyclic glycolysis and recycling parts of the triose phosphate enable adjustment of NADPH synthesis to meet anabolic requirements and increase robustness to oxidative stress[214,215]. However, most of the triose phosphates generated by the ED pathway are metabolized through the tricarboxylic acid (TCA) cycle to produce reducing equivalents and biomass precursors[216]. Although *P. putida* has such a versatile metabolism, it has a rather low background profile of secondary metabolites, which facilitates the detection of recombinantly produced ones[204,217,218]. In addition, *P. putida* has demonstrated its ability to withstand xenobiotics through different adaptation strategies[219], which renders the suitability to produce bioactive NPs. Furthermore, its relatively high GC-content of approximately 62% suggests it for the recombinant biosynthesis of NPs from GC-rich species, like actinobacteria or myxobacteria[220–223].

Due to these reasons, *P. putida* has already successfully been applied as a recombinant host for producing numerous NPs such as AA-derived compounds, biosurfactants (e.g., rhamnolipids (RL)), terpenoids, as well as polyketides (PKs) and non-ribosomal peptides (NRPs)[204,211,224] (**Figure I-7**).

The shikimate pathway in bacteria supplies precursor compounds for aromatic AAs which can all serve as the building blocks for NPs. *P. putida* strains have thus been developed to produce various compounds from these precursors, such as chorismate-derived anthranilic acid (**24**) at approximately 1.5 g L^{-1}[225], and different carbocyclic aromatic secondary metabolites such as phenazines, in particular phenazine-1-carboxylic acid (PCA) (over 400 mg L^{-1})[226–228] and the resulting pyocyanin product[229]. Besides, those AA-derived compounds include the bisindole alkaloids deoxyviolacein (**20**) (up to 1.5 g L^{-1})[230], and violacein (**19**)[99,136].

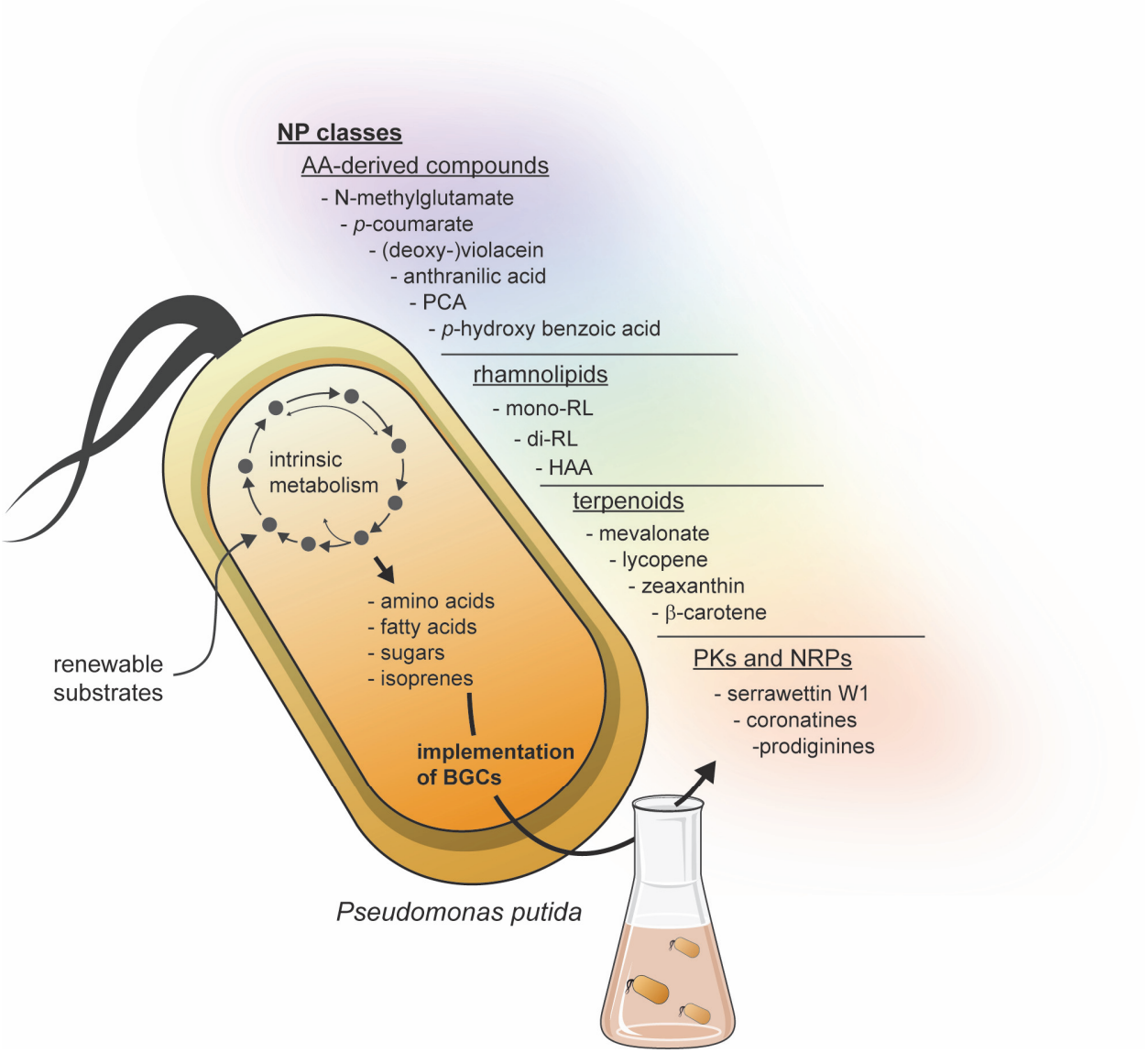

Figure I-7: *P. putida* as a cell factory for biotechnological applications (adapted from Loeschcke and Thies 2015, 2020[204,224]).
In the field of recombinant biosynthesis of NPs, *P. putida* has emerged as a widely used heterologous host. The synthesis of the products is achieved by implementing corresponding BGCs and utilizing intrinsically metabolized building blocks from the primary metabolism. A diverse range of NP classes has been examined, including amino acid (AA)-derived compounds, rhamnolipids (RLs), terpenoids, as well as polyketides (PKs) and non-ribosomal peptides (NRPs). PCA: phenazine-1-carboxylic-acid; HAA: 3-(hydroxyalkanoyloxy)alkanoic acid. BGC: biosynthetic gene cluster.

In addition to human pathogenic *Pseudomonas aeruginosa*, a well-studied native RLs producer[231], *P. putida* constitutes a promising alternative for industrial biosurfactant production[232]. Generally, RLs entail a hydrophobic unit consisting of two molecules of hydroxy fatty acids (FA) which form 3-(hydroxyalkanoyloxy)alkanoic acid (HAA), and one (mono-RL) or two rhamnose units (di-RL) that make up the hydrophilic part[233]. Upon expressing the *rhlAB*(*C*) operon from *P. aeruginosa*, *P. putida* can produce mono- and di-RLs, as well as the precursor HAA[136,234–237]. In a fed-batch bioreactor, nearly 15 g L^{-1} of mono-RLs were achieved during recombinant production[238].

For heterologous terpene biosynthesis, yeasts, like *S. cerevisiae*, as well as aerobic and anaerobic bacteria such as *Rhodobacter capsulatus* have been described as viable hosts[199,201]. However, the ability to produce terpenoids from isoprenoid precursors has also been demonstrated in *P. putida*. Its tolerance towards isoprenoids makes it a promising candidate for production[223]. To date, *P. putida* has been successfully employed to synthesize different terpenoids encompassing carotenoids like lycopene, zeaxanthin, and β-carotene[239–242].

PKs and NRPs comprise the last group of recombinantly produced NPs in *P. putida*. These highly diverse compounds are formed by condensation of basic AAs or carboxylic building blocks[243]. The functional modification of the acyl-carrier protein (ACP) or peptidyl-carrier protein (PCP) domains by a phosphopantetheinyl transferase (PPTase) is critical for their performance. As the genes encoding a PPTase are often not located within the PKS/NRPS gene cluster, an effective producer of PKs and NRPs has to be additionally equipped with this gene. *P. putida* intrinsically possesses a PPTase with a broad substrate spectrum that activates both ACP and PCP domains[244,245] and has been successfully used to recombinantly produce PKs and NRPs such as flaviolin, coronatin, and serrawetin W1[246–248]. An interesting PK/NRP hybrid NP is the tripyrrole prodigiosin (**14**). *P. putida* is capable to produce prodigiosin in high titers compared to other hosts like *E. coli*[249]. Multiple studies have dealt with the production of prodigiosin or prodiginine derivatives in *P. putida*[99,239,250–253]. These efforts led to an optimized producer strain reaching over 1 g L^{-1} prodigiosin[254].

The above examples of different classes of NPs produced in *P. putida* species underline the potential this organism has for the recombinant biosynthesis of bioactive products. However, specific genetic and metabolic engineering strategies must be considered that enable and optimize production. These strategies will be discussed in the following chapters.

I.3.1.1. Genetic tools for *Pseudomonas putida*

Since its complete sequencing in 2002[255], the repertoire of genetic tools for engineering *P. putida* KT2440 has been continuously expanded, making the bacterium a highly amenable host for genetic engineering. This toolbox includes elements for genome editing and genetic regulatory elements such as origins of replication (oriR), promoters, ribosome binding sites (RBS), and transcriptional terminators[256].

The integration of single biosynthetic genes or smaller BGCs is often accomplished by utilizing plasmids including standardized series such as the Standard European Vector Architecture (SEVA)[257–260]. Introduction of respective genes onto plasmids enables efficient generation of a producer strain and versatile utilization in different strains[259,261]. Exchangeable components like oriR, antibiotic resistance markers (Ab^R), as well as constitutive and inducible promoter elements have resulted in a range of recombinant plasmids, making customization easier. The oriR plays a crucial role in plasmid construction as it determines the copy number, thereby, affecting the protein yield[262]. Further, there are also temperature-sensitive plasmids that become unstable at higher temperatures, and integrative plasmids, also known as suicide vectors, containing an oriR unable to replicate in *P. putida*[246,257,263,264]. These plasmids are commonly used for plasmid-curing and genomic recombinant integration strategies, respectively. The Ab^R consisting of the antibiotic gene and its native promoter is important for maintaining plasmids. *P. putida* has a natural resistance to chloramphenicol and triclosan (irgasan)[265,266], which is frequently utilized in selective medium for the isolation of *Pseudomonas* species. Nevertheless, the toolbox for *P. putida* has several resistance markers available (e.g., kanamycin, tetracycline, gentamicin, or streptomycin/spectinomycin)[257,259].

Promoters are essential for functional gene expression and directly impact expression levels through their regulation, which can be constitutive, positively, or negatively regulated. Several constitutive promoters, both native and synthetic, have been utilized in *P. putida*[260,267]. In contrast to constitutive promoters, inducible promoters that respond to external signals, so-called inducers, provide a better fine-tuning of gene expression (**Table I-1**)[212,256,268,269]. When working with inducible expression systems, it is essential to consider the promoter's leakiness, known as basal expression, the inducer working concentration as well as the level of induced expression compared to the basal expression level, which is referred to as the dynamic range.

Other elements influencing the protein yield by affecting the secondary structure and stability of the messenger RNA (mRNA) include the RBS spacer, i.e., the distance between the RBS and the start codon, and the transcriptional terminators[270,271]. The RBS determines translation rates of the mRNA. Hence, the exact transcription sequence, including all elements such as the RBS sequence and spacer, can serve as regulatory elements to impact protein production levels[272].

Table I-1: Widely used inducible expression systems for *Pseudomonas* species.
DCPK: dicyclopropyl ketone, IPTG: isopropyl-β-D-1-thiogalactopyranoside, 3-MB: 3-menthylbenzoate, n.d.: not determined; [1]names of the promoters are given, preceded by the regulator proteins.

regulator/promoter system[1]	inducer	regulation	inducer concentration	leakiness	references
AlkS/P_{alkB}	short chain alkanes (e.g. DCPK)	positive	0.001 to 0.05% (*w*/*v*)	low	[268,273]
AntR/P_{antA}	anthranilate	negative	0.01 to 10 mM	low	[274]
AraC/P_{BAD}	L-arabinose	positive	1 to 100 mM	very low	[268,275]
LacIq/P_{trc},P_{lacUV5}	IPTG	negative	up to 3 mM	n.d.	[276,277]
MtlR/P_{mtlE}	D-mannitol	positive	0.1 to 1% (*w*/*v*)	low	[278,279]
NagR/P_{nagAa}	salicylic acid	positive	1 mM	n.d.	[279]
NahR/P_{sal}	salicylic acid	positive	0.001 to 5 mM	low	[268,280]
RhaRS/P_{rhaB}	L-rhamnose	positive	1 to 10 mM	low	[268,274]
TetR/P_{tetA}	anhydrotetracycline	negative	approx. 1 µM	low	[278]
XylS/P_m	3-MB	positive	0.05 to 0.5 mM	low	[268]

Besides the introduction on a replicative plasmid, the genomic integration proves to be a promising approach as it leads to higher genetic stability and less burden, particularly, for the expression of large BGCs[256]. Here, a distinction is made between random chromosomal integration and site-specific integration, for example, achieved through recombineering strategies.

Random integration entails incorporating genetic elements into a random location within the genome using transposons, such as the Tn5 transposon, to generate a strain library[239,281–283]. The suitable strains can be selected by identifying the particular product using visible outputs (e.g., for prodiginines or violacein, these products themselves can act as color-indicators) or by utilizing a transcriptional reporter, such as fluorescent proteins[99,247,251,284]. For larger BGCs, both the transfer and expression (TREX) system and the enhanced yTREX system, which allows for yeast recombinational cloning, serve as appropriate tools[99,239,251]. Using the (y)TREX system, the gene cluster, flanked by outside ends (OE), is randomly integrated into the genome, facilitated by the Tn5 transposase. The integrated genes can then be selectively expressed using either two T7 RNA polymerase (T7RP)-dependent promoters or, in the case of a gene cluster with unidirectional genes, using a chromosomal promoter[239]. In the first case, it is necessary to integrate a T7RP-encoding plasmid into *P. putida*. Instead relying on chromosomal promoters, recombinant production of prodigiosin has uncovered favored integration loci, particularly in the rRNA-coding operons of *P. putida*. This has resulted not only in high expression and product levels, but also in high genetic stability[251]. One benefit of utilizing Tn5 transposition is the ability to perform multiple sequential Tn5 integrations, assuming different selection markers are accessible or implemented.

However, random integration may not be advantageous for all applications and could require significant effort in screening the resulting strain library, depending on the detectability of the

biological product. Site-specific integration abolishes the necessity to examine an enormous library by minimizing variability and instead defining the genomic locus. For example, BGCs can be embedded into specific locations within the chromosome by addressing *attB* sequence motifs within the tRNA-encoding genes via IntB13 site-specific recombinase[285–287]. Furthermore, CRAGE (*chassis*-independent recombinase-assisted genome engineering) permits genomic integration at a previously transposon-based inserted 'landing pad'[288]. In addition, Tn7 transposition can be considered[240,267,289,290]. Here, the Tn7 transposase inserts a gene sequence at the *att*Tn7 site, a specific location in the genome of most bacteria that appears only once or twice[291,292]. In *P. putida* and other prokaryotes, the recognition site of the Tn7 proteins is in the *glmS* gene, which is essential, making it unlikely for this site to be lost in bacterial chromosomes[291]. Since insertion occurs downstream of the essential gene, transposition events are not lethal but lead to stable strains. Moreover, the *att*Tn7 site is often located near the chromosome's replication origin. This implies that the biosynthetic genes are present in at least two copies throughout bacterial growth due to continuous cell division and DNA replication enabling efficient transcription[293,294]. As Tn7 transposition can only occur once in the one available *att*Tn7 site in *P. putida*, genetic engineering is limited with this system.

Transposon systems are well suited for introducing BGCs into the genome, but are less ideal for knockouts, as they can only disrupt genes and not delete them. To address this issue, the genetic toolbox provides methods that use homologous recombination, which are facilitated by recombinases like RecET[246,295]. An advantage of these methods is that undesired genes can be deleted and BGCs can be inserted simultaneously. However, the requirement for antibiotic selection marker could limit some applications. For this purpose, methods for scar- and marker-less engineering have been expanded by incorporating counter-selection tools, including the homing endonuclease I-SceI[209,286,296], the levansucrase SacB[297–299], or CRISPR/Cas9[269,300]. Over the last decades, the presented tools have not only been utilized for the integration and expression of BGCs but also for engineering strategies to optimize NP production – for example via gene deletion or introduction, the implementation of sophisticated regulation, or enzyme engineering.

I.3.1.2. Systems metabolic engineering for recombinant NP biosynthesis

The recombinant NP production depends not only on integrating respective biosynthetic genes but also on several other factors that influence yield in biosynthesis. To overcome limitations in productivity, systems metabolic engineering using tools for regulatory and pathway engineering have been applied to NP production in *P. putida*, which will be outlined in the following section (**Figure I-8**)[187,301,302].

Regulatory elements have already been described as an important tool in the genetic toolbox of *P. putida* in chapter I.3.1.1. The engineering of regulatory elements, particularly promoters, has been proven to be an effective approach to enhance production. This has been

demonstrated for several NPs, such as prodigiosin, glidobactin A, coronatines, and RLs[247,254,303]. Furthermore, the utilization of alternative RBS and start codons has been shown to impact the titers of prodigiosin and glidobactin A[254]. In addition to these adaptations, protein assembly regulation and pathway control can also be attained through transcriptional, post-transcriptional and post-translational regulation[256]. The CRISPR system has applications in genome-editing methods but can also be employed to regulate gene expression using a catalytically inactive Cas9 enzyme (dead Cas9, dCas9). This edited system can be used to decrease transcription by obstructing the DNA for the RNA polymerase (RNAP), known as CRISPR interference (CRISPRi), or to activate transcription (CRISPRa)[304,305]. The CRISPRa complex, in contrast, recruits and stabilizes the RNAP. While CRISPRi is already well-established for use in metabolic engineering in *P. putida*[306–308], for CRISPRa only pioneering work has been done in *P. putida* so far[309]. Further widely applied and popular methods for metabolic engineering are small RNA (sRNA)-based strategies due to their independence from additional heterologous proteins[310,311]. sRNAs can up- or down-regulate target genes through interaction with their mRNA. In addition to the strategies that control transcription or translation rates, another direct approach for controlling protein assembly and enzyme activity is via post-translational regulation. It enables a more precise control over protein levels, but it is energetically unfavorable as resources are invested in the production of dispensable proteins[312]. The addition of a hybrid Nla/SsrA proteolytic tag at the desired gene enables protein activation or degradation based on conditional proteolysis. This way, the use of a post-translational system helped to reduce basal expression and to improve inducibility in *P. putida*[313].

In addition to engineering transcriptional and translational machineries, effective activation of biosynthetic pathways, especially for PK- and NRP-type compounds, is crucial. Despite possessing an intrinsic PPTase with the ability to activate a wide range of carrier proteins, studies have indicated that co-expression of an additional PPTase can result in improved production titers in *P. putida*, as recently observed for glidobactin A and docosahexaenoic acid[254,285,314].

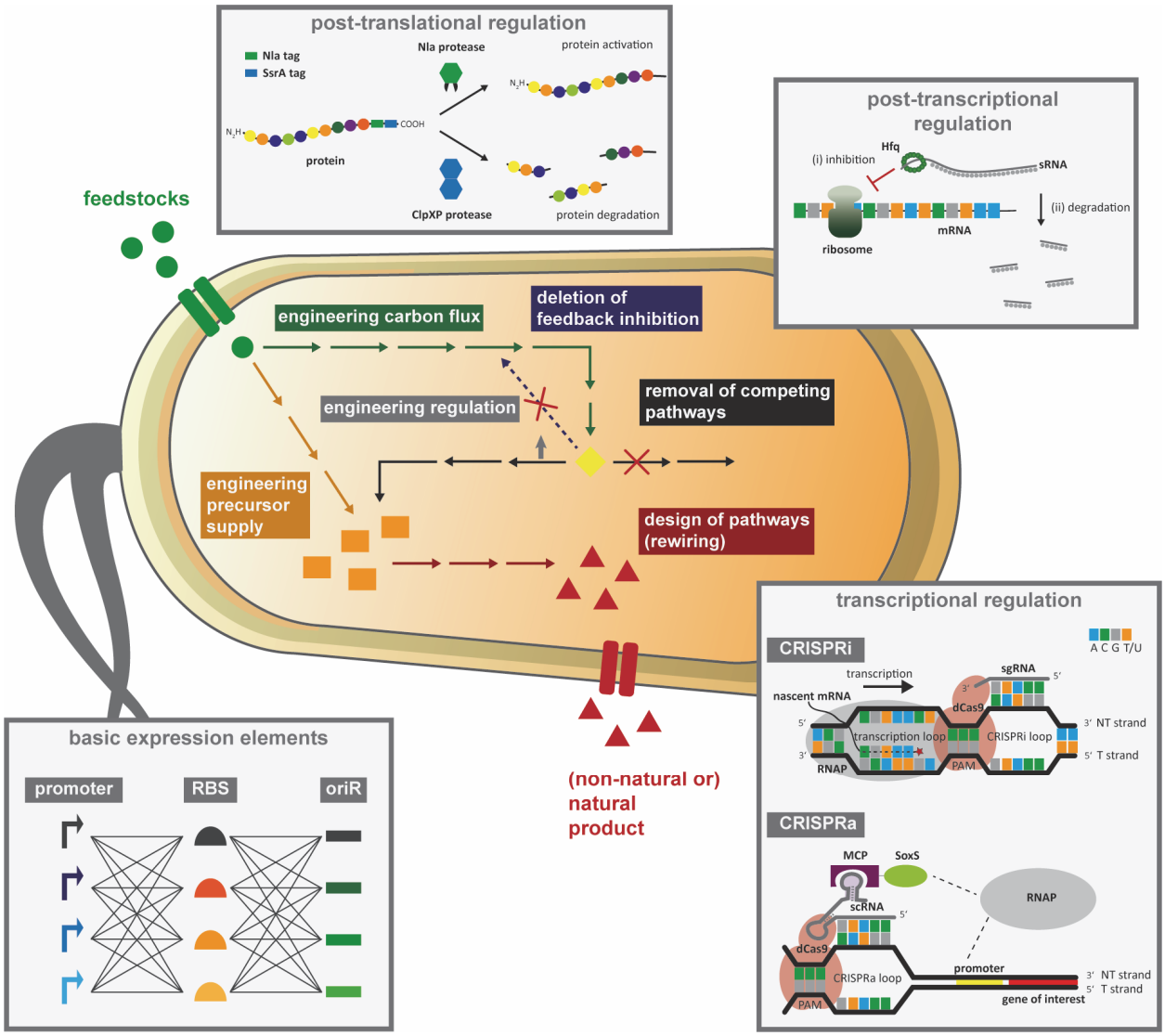

Figure I-8:Strategies and procedures of systems metabolic engineering for recombinant NP production (adapted from Ko et al. 2020[301], Fernández-Cabezón and Nikel 2020[302]).
Engineering the carbon flux and precursor supply, removal of competing pathways as well as feedback inhibition, design of (non-natural) biosynthetic pathways for NP production, and engineering of pathway regulation which includes the change of basic expression elements, transcriptional, post-transcriptional, and post-translation regulation, are key strategies in metabolic engineering. RBS: ribosome binding site; sgRNA: single guiding RNA, RNAP: RNA polymerase, NT: non-template; T: template; MCP-SoxS: transcriptional activator; mRNA: messenger RNA; sRNA: small RNA.

Systems metabolic engineering involves not only regulating biosynthetic enzyme production but also ensuring that sufficient metabolites are available. Optimizing precursor supply is a major determinant for achieving high yields. This is typically achieved by overexpressing enzymes which catalyze rate-limiting steps[315] or integrating new precursor pathways. For instance, the genes of the mevalonate (MVA) pathway from *Myxococcus xanthus* have been integrated in *P. putida* to enhance flux from acetyl-CoA to the isoprenoid precursor required for geranic acid production[223]. Besides over- and co-expression, intrinsic metabolic networks can be interrupted to reduce or abolish competing pathways or product degradation enzymes[225,254,316]. Feedback-inhibition loops, which naturally protect cells from wasteful biosynthesis of compounds which are not needed at high levels, often interfere with productivity. Enzyme engineering strategies,

such as rational design, can generate feedback-inhibition-resistant mutants to further support NP production. The combined use of the last two strategies has led to improved titers of anthranilic acid and *p*-hydroxy benzoic acid in *P. putida*[225,316]. Rerouting metabolic pathways, for example, for the generation of alternative sugar catabolic routes or improvement of the carbon flux towards a desired product and rewiring pathways for the production of non-native products are strategies that result in optimized production or even in the generation of new-to-nature compounds[303,317,318].

I.3.2. Biosynthetic concepts for NPs and derivatives

Regarding the recombinant production of NPs, the last chapters emphasized the selection of an appropriate organism, genetic tools as well as engineering strategies to obtain desirable titers of the target compound. In the following, a summary will be given on the biosynthetic concepts available to reach the final product. This will shed light on how to access derivatives and non-native products, which are of great interest in NP research. The following chapter will present different concepts involved in converting a precursor into a highly valuable product (**Figure I-9**) and give examples for recombinant production of bacterial alkaloids mentioned in chapter I.2.1.

In vitro biocatalysis using isolated enzymes has gained popularity as a sustainable and greener manufacturing process compared to traditional chemical approaches (**Figure I-9**,i)[319–321]. It also offers advantages over *in vivo* biotransformation, such as direct substrate availability for the enzymes, which may be hampered *in vivo* by transport limitations due to poor cellular uptake. Further, an easier and less expensive product recovery and downstream processing is expected since no cells need to be disrupted and no separation is required from a multitude of cellular components. *In vitro* conversion of chemically synthesized MAP and MBC analogs with the enzyme PigC and other ligating enzymes, such as TamQ and ThreaP from *Pseudoalteromonadaceae* strains, showcased the promiscuous properties of these enzymes and led to a variety of prodiginine derivatives including cyclic variants[252,322–324].

On the other hand, whole-cell biotransformation is a promising approach, especially for the production of complex products derived from multi-step biosynthetic cascades. So far, classic biosynthesis is the most frequently applied method (**Figure I-9**, ii) and has been used for the recombinant production of a multitude of NPs[204,224]. Combinatorial biosynthesis is an expanded form of classical biosynthesis (**Figure I-9**, iii). This method involves combining biosynthetic pathways or catalytical parts, to end up with a more efficient biosynthesis or with new and modified NP structures[325]. Combination of the violacein pathway with the tryptophan halogenase RebH and the flavin reductase RebF has resulted in chlorinated derivatives of violacein and deoxyviolacein[326,327]. Combinatorial biosynthesis has also been applied for the production of cycloprodigiosin in preliminary studies. For this, the *pig* gene cluster was

integrated in *P. putida* and the gene encoding for the enzyme Prub680, a cyclase from *P. rubra*, was co-expressed[327].

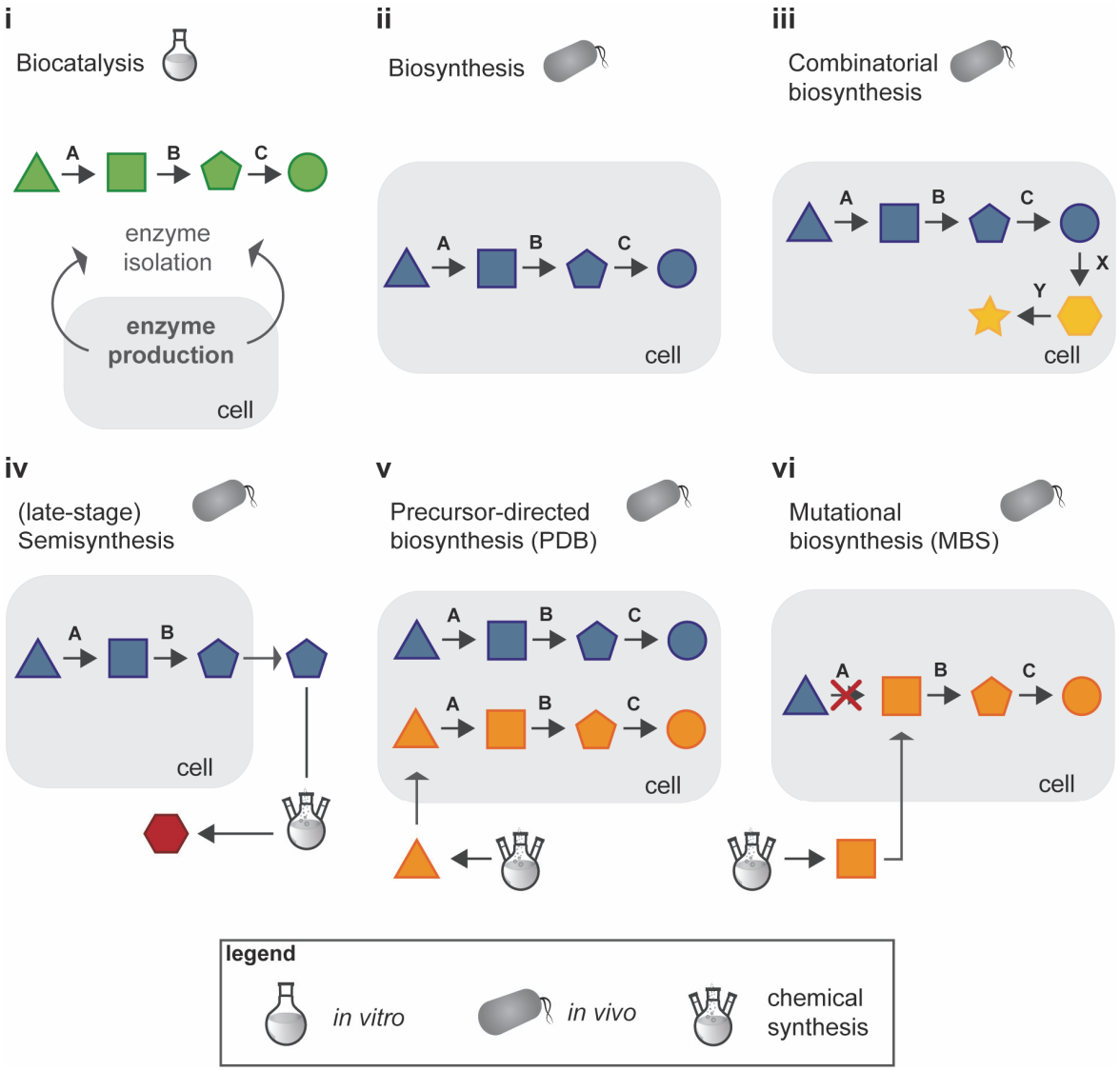

Figure I-9: Biosynthetic concepts to produce a diversity of NPs in heterologous hosts.
Different biosynthetic concepts for the synthesis of NPs or their derivatives are shown. These include *in vitro* biocatalysis (**i**), biosynthesis (**ii**), combinatorial biosynthesis (**iii**), semisynthesis with late-stage chemical derivatization (**iv**), as well as mutational synthesis (precursor-directed biosynthesis (PDB, **v**) and mutasynthesis (MBS, **vi**)). The geometric shapes represent precursors, biosynthetic intermediates, and final products. Shapes of the same color belong to the same synthesis pathways. The capital letters denote the enzymes involved.

Biosynthesis and combinatorial biosynthesis rely on naturally occurring pathways or catalytic reactions which restricts the diversity of accessible compounds. Approaches combining biology with classical synthetic chemistry allow access to a more diverse portfolio of xenobiotic compounds. Minor variations (e.g., halogenations or esterifications) are often introduced by chemical derivatization of a biologically produced NP. This method is referred to as semisynthesis (**Figure I-9**, iv)[328–331]. Prominent examples include the synthesis of artemisinin from biosynthesized artemisic acid, or the synthesis of englerin A from biosynthesized guaia-6,10(14)diene[330]. As the semisynthetic approaches are often hampered by poor

stereoselectivity[332], another focus is laid on the conversion of a chemically synthesized artificial precursor leading to structurally modified products. The precursor-directed biosynthesis (PDB) and mutational biosynthesis (MBS), also known as mutasynthesis, are two methods applicable for this purpose.

PDB is achieved by adding biosynthetic precursor analogs to a non-modified NP producer (**Figure I-9**, v). Thus, the biosynthetic machinery of the producer can be accessed without time-consuming genetic manipulations. This has been successfully demonstrated for the production of novel aurachins by feeding halogenated anthranilic acids to *S. erecta*[175]. However, the yields of the derivatives produced via PDB are affected by the competition between natural and non-natural precursors. Low concentrations of the desired compounds often result in difficulties separating them from the natural variants[333].

Mutasynthesis is a promising approach merging chemical synthesis with biosynthesis via genetically modified producer strains. By generating mutants with blocked key biosynthetic steps and feeding them with precursor analogs, called mutasynthons, biosynthesis of non-natural products is possible without formation of the original product (**Figure I-9**, vi)[334]. A prerequisite for MBS is the availability of genetic and functional information on the biosynthesis of the targeted NP. An additional issue could arise if the biosynthetic step to be deleted provides an essential intermediate for the producer's growth. Nonetheless, MBS can be used to overcome PDB limitations, specifically those involving reactions which result in complex mixtures of challenging-to-separate products or limit non-natural product formation due to a competition with natural precursors[335]. Thus, mutasynthesis proves to be a practical and effective alternative to produce non-natural NPs. Besides *in vitro* conversion, prodigiosin derivatization has also been pursued using MBS. For this purpose, the gene *pigD* was deleted to block the synthesis of the monopyrrole MAP in the first catalytic step. As the precursor MBC is still biosynthesized, pathway manipulation allowed for the establishment of a mutasynthesis platform in *P. putida* to produce cyclic and non-cyclic prodiginines by introduction of chemically synthesized MAP analogs[252,322]. The production of novel compounds by PDB and MBS requires some knowledge concerning the NP's biosynthetic pathway with several crucial factors to be considered: the cellular uptake of the artificial precursor by the producer, potential toxic side-effects of non-native biosynthetic intermediates, and the acceptance of artificial precursors as well as intermediates by the biosynthetic machinery[333].

The application and potential of different biosynthetic concepts have been shown in this chapter. However, these concepts do not have to be considered separately, as combinations of them enable an extended and rapid access to derivatives and NP libraries. The recently coined term CHEM-BIO-CHEM refers to strategies using a combination of muta- and semisynthesis, while implementation of MBS and combinatorial biosynthesis can be referred to as CHEM-BIO-BIO strategies[328,329,332].

I.4. Stress responses in *Pseudomonas*

In biotechnological NP production, the associated substrates and biosynthetic products often cause severe stress to the bacterial hosts, which is why the study of stress response mechanisms has become relevant in this context.

Bacteria have various strategies to alleviate stress caused by prevailing environmental conditions in their natural habitat. These stress response mechanisms are advantageous for survival and can be leveraged for efficient recombinant production by whole-cell biotransformation, which requires an organism that can cope with the associated stress. *Pseudomonas* species are found in different habitats all over the world, exposed to drought, extreme temperatures, and other factors causing environmental stress[336,337]. To survive such harsh conditions and to cope with the impact they have on cellular functions, Pseudomonads have evolved different intrinsic mechanisms against osmotic, desiccation, heat and cold, oxidative, as well as chemical stress (**Figure I-10**)[338–341].

The different stressors can occur as single factors, or in combination; in addition, one stressor can also give rise to additional stress factors. For example, while oxidative stress is mainly caused by exposure to UV light or hydrogen peroxide[342–344], it can also arise in conjunction with solvent, antibiotic, or osmotic stress[345–348]. While the *Pseudomonas* clade is perhaps most famous for a high solvent tolerance, the stress tolerance traits are in fact diverse and are coming into focus of biotechnological research. These diverse evolved response strategies can be triggered individually and more specifically in reaction to a certain stress, but also simultaneously, so resulting stress responses to various stressors often exhibit certain similarities.

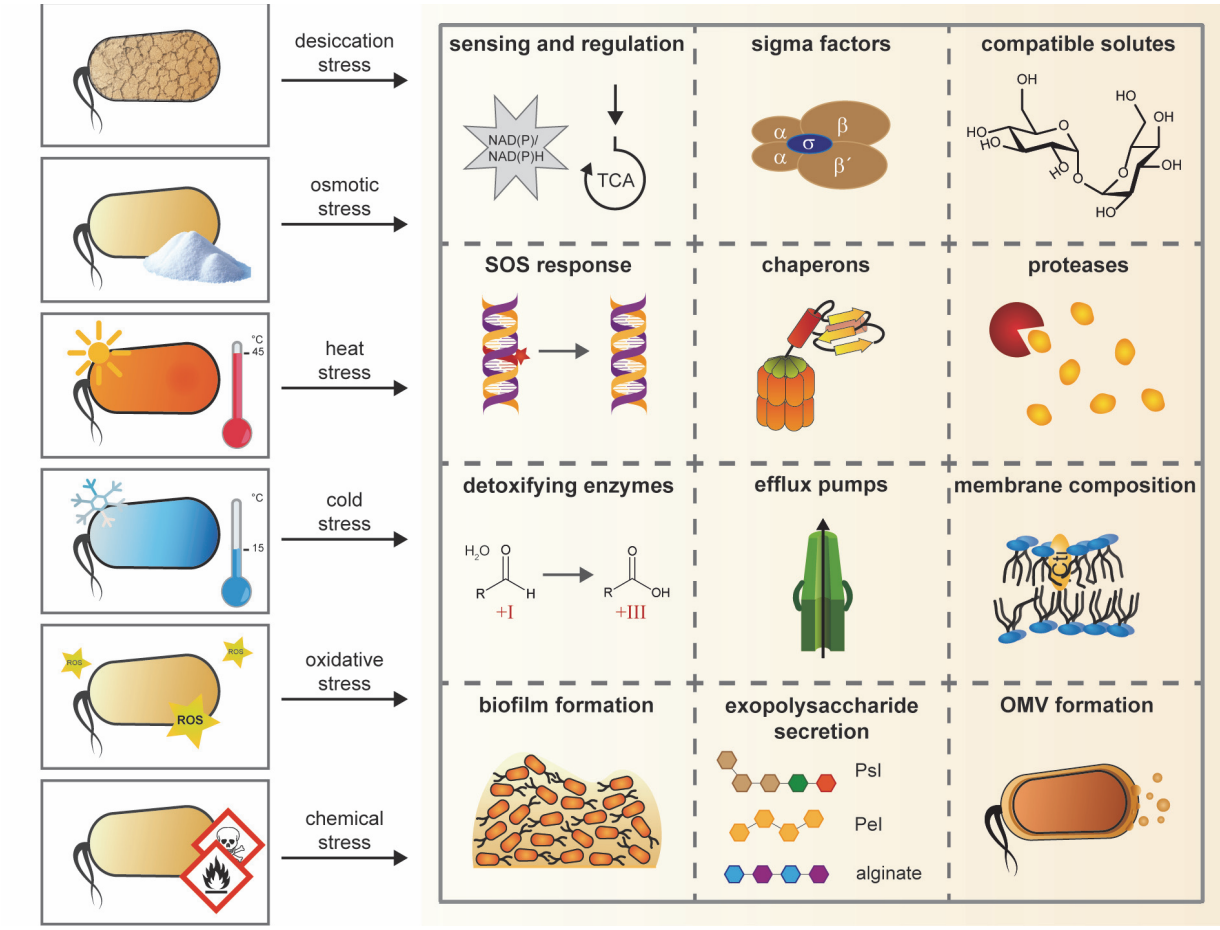

Figure I-10: Environmental stresses and evolved response mechanisms in *Pseudomonas* species.
Schematic overview of stresses caused by different harsh environments. To overcome the harmful effects of the environmental stresses, *Pseudomonas* species have evolved diverse response strategies including protection, repair, detoxification, as well as the prevention of intrusion or the extrusion of the stressor. NAD(P): nicotinamide adenine dinucleotide (phosphate); Psl: polysaccharide synthesis locus; Pel: pellicle; OMV: outer membrane vesicle.

The mechanisms of this stress response network encompass strategies for protection and repair, for conversion or extrusion of the stressor, as well as strategies to keep the stressor out of the cell. From an energetic point of view, these strategies are highly demanding, which is why proteins involved in energy metabolism are typically upregulated in stress-induced cells[349–351].

In addition, alternative sigma factors are used for transcription initiation of genes linked to stress mechanisms, in order to help the cell to respond to physiological changes[338,352]. Compatible solutes, such as the disaccharide trehalose or glutamate and its derivatives, are small organic molecules protecting the cell from desiccation, due to osmotic stress, temperature, or oxidative stress[353,354]. They accumulate intracellularly to regulate osmotic pressure and maintain cellular homeostasis[355–357].

As the stressors can cause damages to DNA, proteins, or other cellular components, repair mechanisms have been developed including the SOS system, chaperons, and proteases. The SOS system responds to DNA damage and promotes its integrity. It is tightly regulated and involves induction of multiple proteins, with the proteins LexA and RecA playing key roles[358]. Chaperons and proteases are crucial for any kind of proteotoxic stress, preventing aggregation

or misfolding, as well as enabling degradation of denatured proteins and proteins that are no longer required[359–363].

Dealing with the stressor includes the elimination of harmful compounds, especially solvents or antimicrobials, by redox enzymes or the extrusion of the stressor by efflux transporters. Both mechanisms play crucial roles in the bacterial stress response helping to decrease the intracellular stressor concentration[364–366]. *Pseudomonas* species have a large repertoire of such detoxifying enzymes[367–369] and are equipped with many efflux transporters which belong to the RND (resistance-nodulation-division)-, the SMR (small multidrug resistance)-, and the MATE (multidrug and toxic compound extrusion)-family, as well as ABC-binding cassette (ABC)- and major facilitator superfamily (MFS) transporters[351,370–374].

Extreme temperatures, solvents, or hydrophobic antibiotics can also affect the bacterial membrane and its fluidity. Thus, altering the membrane composition is a further strategy to cope with the stress-induced effects on the cell envelope[338,375,376]. The integrity of the inner membrane (IM) can be maintained by converting *cis* unsaturated FAs into their *trans* configuration by the periplasmic enzyme *cis*-*trans*-isomerase (Cti)[377,378]. This response decreases the membrane fluidity counteracting the effect of destabilizing substances like solvents. In addition, it is a very fast process independent of transcriptional activation or *de novo* synthesis of FAs.

Bacteria growing in biofilms are more resistant to different stressors[379]. The secretion of polysaccharides, which are major components of the biofilm matrix, facilitates its formation[380]. Examples include capsulate polysaccharides such as alginate and levan, as well as the aggregative polysaccharides Psl (polysaccharide synthesis locus) and pellicle (Pel)[381]. Besides the polysaccharides, the formation of so-called outer membrane vesicles (OMVs) also supports biofilm formation by increasing the cell surface hydrophobicity[382]. However, vesiculation is not exclusively involved in biofilm formation, but is a response to different stressors[383–385]. Their biogenesis, biological functions and the potential biotechnological exploitation of their formation are discussed in the next chapter.

I.4.1. Outer membrane vesicle formation

OMVs are formed from the outer membrane (OM) by Gram-negative bacteria, typically ranging in sizes from 20 to 300 nm in diameter[386,387]. They carry membrane components, lipopolysaccharides (LPS), peptidoglycan (PG), proteins (membrane-bound, periplasmic, cytoplasmic), and nucleic acids[388]. Vesiculation occurs under different conditions including the exposure to antibiotics or other toxicants, as well as a lack of nutrients[389]. Thus, they play a crucial role in the bacterial stress response network supporting survival. In addition, vesiculation has also been described in context with release of hydrophobic molecules such as prodigiosin, violacein, or PQS in the native producers, where OMVs potentially function as a delivery vehicle and extracellular reservoir[390–392]. Besides these compounds, enzymes enabling the catabolism of otherwise unavailable polymeric substrates were described to be exported in OMVs[393].

The underlying mechanism of vesiculation is not completely understood. It has been described as a very fast process which does not involve transcriptional regulation[382,394]. However, over the last years, different models have been proposed and proteins affecting OMV formation have been described for some Gram-negative bacteria including *E. coli*, *P. aeruginosa*, *Salmonella* and *Vibrio* species (**Figure I-11**)[386,387,389,395]. The models explain the OMV biogenesis due to decreased linkages between the OM and the PG layer leading to bulging of the OM. This can be caused by a lack or decreased presence of specific outer membrane proteins (OMPs), such as Lpp or OmpA, or by the activity of PG degrading enzymes[387,396,397]. Modification of the OM structure is an additional trigger for OMV formation. Changes in the OM structure result, for example, from LPS modifications or accumulation of phospholipids in the outer leaflet of the OM due to a non-functional Mla ABC transporter system, which would usually maintain the asymmetry of the lipid bilayer[395,398–400]. Accumulation of misfolded proteins or other molecules in the periplasm leads to an increase of periplasmic pressure which can also induce vesicle formation in Gram-negative bacteria[401–403].

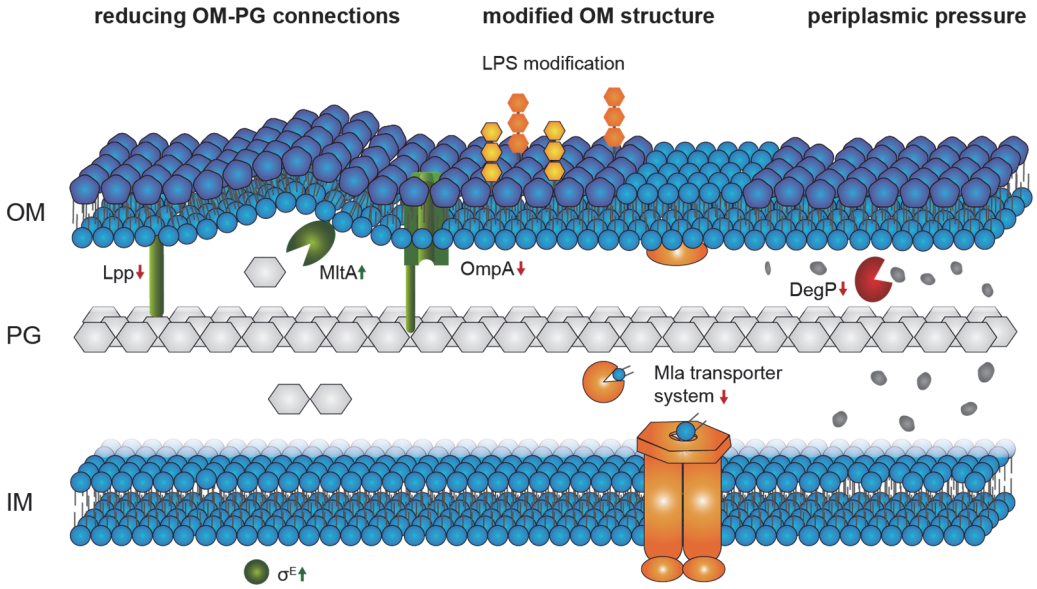

Figure I-11: Proposed models for OMV biogenesis in Gram-negative bacteria (adapted from Juodeikis & Carding 2022[395]).
Mechanisms activating OMV formation in Gram-negative bacteria include the reduction of local connections between the outer membrane (OM) and the peptidoglycan (PG), the modification of the OM structure, as well as increasing periplasmic pressure. Examples of targets which are involved in these mechanisms are shown in the figure. The underlying regulation of these processes/proteins are presented by arrows. Green arrows indicate upregulation, red arrows indicate downregulation. IM: inner membrane; LPS: lipopolysaccharide.

The OMV biogenesis thus relies on many different mechanisms which can be naturally affected by the organism, the growth phase, or the kind of exposed stress[395]. Recently, OMVs have gained attention as a target in strain engineering to support the production of NPs[404,405]. This observation is considerably promising for further research, particularly with regards to the suitability of different genetic targets for OMV biogenesis and the various classes of NPs.

I.5. Outline of this thesis

NPs are widely distributed in nature and have a multitude of biological activities that make them valuable for pharmaceutical applications. Biosynthesis using heterologous microbial host strains is a promising approach to access large amounts of NPs in high yields. Many recombinant hosts suffer from low tolerance against high product concentrations, organic solvents, or temperature, limiting their overall titers. A suitable host organism may be engineered to facilitate an effective recombinant NP biosynthesis. Pseudomonads are endowed with remarkable stress-coping mechanisms, so the HV-1 certified strain *Pseudomonas putida* KT2440 represents an attractive starting point. This thesis focused on the generation and characterization of a robust *P. putida chassis* for recombinant NP biosynthesis.

For this purpose, a general overview about the potential of *Pseudomonas* species in the context of intrinsic stress response mechanisms and available engineering tools was given first (**II.1**). To evaluate the host capacities of *P. putida*, the biosynthetic pathways of different bacterial alkaloids like prodiginines, arcyriaflavin A and violacein were implemented as models and different tools were applied to harness the host's potential:

(i) A fully modular genetic toolbox was established allowing the stable random as well as site-specific integration of biosynthetic genes into the *P. putida* genome (**II.2**).

(ii) OMV formation was identified as a responsible factor for tolerance towards production, supporting product yields. The targeted exploitation of this stress response strategy was investigated for the production of different NP classes (**II.3** and **II.4**).

(iii) Access to desired NPs and to non-natural derivatives was explored via different biosynthetic concepts as shown for prodiginine production in *P. putida* (**II.5**).

This way, this thesis investigated different bioprocess and genetic approaches to support the production of a value compound of interest in *P. putida* and to further establish this host as a NP cell factory.

II. RESULTS

The following chapter consists of six manuscripts that built the framework of this thesis: Five have already been published in peer-reviewed journals and one is about to be published in a peer-reviewed journal. The present work and publications are based on collaborative projects within the BMBF project ´NO-STRESS`, as part of the innovation lab 'AutoBioTech' within the project "Modellregion, BioRevierPLUS: BioökonomieREVIER Innovationscluster Biotechnologie & Kunststofftechnik", and the interdisciplinary PhD project ´ARcyria` (Bioeconomy Science Center). I would like to mention my colleagues Dr. Luzie Kruse, Dr. Robin Weihmann, and Dr. Sonja Kubicki (Institute of Molecular Enzyme Technology, HHU Düsseldorf), my collaborators from the Department of Environmental Biotechnology, Helmholtz Center for Environmental Research (UFZ) (Dr. Hermann Heipieper and Dr. Christian Eberlein), and from the Institute of Bioorganic Chemistry (HHU Düsseldorf) of Prof. Dr. Jörg Pietruszka for the great and fruitful cooperation. The work of my bachelor and master students, especially of Carolin Höfel, Anka Sieberichs and Maximilian Spindler, is also worth mentioning. Each publication or manuscript includes a statement of my own contributions.

II.1. Strategies for the generation of robust *Pseudomonas chassis*

PUBLICATION I

Towards robust *Pseudomonas* cell factories to harbour novel biosynthetic pathways

Nora Lisa Bitzenhofer*, Luzie Kruse*, Stephan Thies, Benedikt Wynands, Thorsten Lechtenberg, Jakob Rönitz, Ekaterina Kozaeva, Nicolas Thilo Wirth, Christian Eberlein, Karl-Erich Jaeger, Pablo Iván Nikel, Hermann J. Heipieper, Nick Wierckx, Anita Loeschcke

Essays in Biochemistry (**2021**) 65(2):319-336.

The online version is available at: 10.1042/EBC20200173

Status: published

Own contribution:

Writing parts of the manuscript, designing and preparing the figures.

Check for updates

Essays in Biochemistry (2021) EBC20200173
https://doi.org/10.1042/EBC20200173

PORTLAND PRESS

Review Article

Towards robust *Pseudomonas* cell factories to harbour novel biosynthetic pathways

Nora Lisa Bitzenhofer[1,*], Luzie Kruse[1,*], Stephan Thies[1], Benedikt Wynands[2], Thorsten Lechtenberg[2], Jakob Rönitz[2], Ekaterina Kozaeva[3], Nicolas Thilo Wirth[3], Christian Eberlein[4], Karl-Erich Jaeger[1], Pablo Iván Nikel[3], Hermann J. Heipieper[4], Nick Wierckx[2] and Anita Loeschcke[1]

[1]Institute of Molecular Enzyme Technology, Heinrich-Heine-University, Düsseldorf, Germany; [2]Institute of Bio- and Geosciences IBG-1: Biotechnology, Forschungszentrum Jülich, Germany; [3]The Novo Nordisk Foundation Center for Biosustainability, Technical University of Denmark, Lyngby, Denmark; [4]Department of Environmental Biotechnology, Helmholtz Centre for Environmental Research (UFZ), Leipzig, Germany

Correspondence: Anita Loeschcke (a.loeschcke@fz-juelich.de) or Nick Wierckx (n.wierckx@fz-juelich.de)

Biotechnological production in bacteria enables access to numerous valuable chemical compounds. Nowadays, advanced molecular genetic toolsets, enzyme engineering as well as the combinatorial use of biocatalysts, pathways, and circuits even bring new-to-nature compounds within reach. However, the associated substrates and biosynthetic products often cause severe chemical stress to the bacterial hosts. Species of the *Pseudomonas* clade thus represent especially valuable *chassis* as they are endowed with multiple stress response mechanisms, which allow them to cope with a variety of harmful chemicals. A built-in cell envelope stress response enables fast adaptations that sustain membrane integrity under adverse conditions. Further, effective export machineries can prevent intracellular accumulation of diverse harmful compounds. Finally, toxic chemicals such as reactive aldehydes can be eliminated by oxidation and stress-induced damage can be recovered. Exploiting and engineering these features will be essential to support an effective production of natural compounds and new chemicals. In this article, we therefore discuss major resistance strategies of Pseudomonads along with approaches pursued for their targeted exploitation and engineering in a biotechnological context. We further highlight strategies for the identification of yet unknown tolerance-associated genes and their utilisation for engineering next-generation *chassis* and finally discuss effective measures for pathway fine-tuning to establish stable cell factories for the effective production of natural compounds and novel biochemicals.

Introduction

Microbial biotechnology can provide chemical compounds that are essential for modern societies in multiple sectors, e.g. as pharmaceuticals and chemical building blocks. However, efficient microbial production using whole (living) cells requires a host that can cope with the associated stress. Aside from temperature or osmotic stress, this includes severe chemical stress caused by high concentrations of substrates and products needed to establish economically viable processes.

Bacteria have evolved numerous strategies to alleviate chemical stress and members of the *Pseudomonas* clade are especially well-equipped with such traits [1]. This has likely contributed to the development of the soil bacterium *Pseudomonas putida* and its relatives into versatile microbial cell factories during the past few decades, enabling the biosynthesis of various compounds including secondary metabolites like rhamnolipids, terpenes, polyketides, and non-ribosomal peptides, organic acids, alcohols, and aromatics [2–4]. Most of these products are not natively synthesised by the host strain, thus confronting cells with novel and – in parts – harmful chemistry, as many hydrophobic and antibiotic products

*These authors contributed equally to this work.

Received: 06 February 2021
Revised: 01 May 2021
Accepted: 24 May 2021

Version of Record published: 05 July 2021

PORTLAND PRESS

Essays in Biochemistry (2021) EBC20200173
https://doi.org/10.1042/EBC20200173

tend to corrupt enzyme or membrane integrity. The *Pseudomonas* clade thus appears to provide an intriguing starting point to shed light on xenobiotic tolerance in the context of biotechnological applications such as plastics upcycling [5], aromatics production [4], and *trans*-metabolism [6].

Nowadays, even the production of new-to-nature compounds with potentially advantageous properties is coming into reach via engineering and combinatorial use of enzymes, pathways, and hosts, or hybrid bio- and chemical synthesis [7,8]. For example, the strain *P. putida* KT2440 was artificially equipped with parts of the polyketide synthase-/non-ribosomal peptide synthetase-type pathways for coronatine and prodigiosin biosynthesis to provide platforms that could incorporate supplemented unnatural amino acids or pyrrole precursors into new small molecules [9–11]. Another recent example challenged *P. putida* with xenobiotic organofluorine metabolites by use of a *Streptomyces* fluorinase and purine nucleotide phosphorylase for the synthesis of fluoronucleotides and fluorosugars [12].

The host's robustness is evidently becoming a central aspect in strain development in the face of increasingly demanding production processes and targeted chemistry. Pseudomonads may benefit from their built-in characteristics when utilised as hosts [13–16]. For example, the solvent-tolerant *P. putida* S12 outperformed *E. coli* in the production of *p*-hydroxystyrene in biphasic cultures [17]. However, targeted engineering will likewise be necessary, especially for processes involving new-to-*Pseudomonas* compounds. The known robustness-associated features of different *Pseudomonas* strains can be assigned to three major strategies: (i) keeping stressors out of the cell by reducing permeability, (ii) eliminating stressors in the cell by export or conversion, and (iii) recovery of damaged structures. The molecular bases of these strategies have been comprehensively reviewed before with emphasis on organic solvent tolerance [18,19]. In this article, we discuss these leading tolerance and resistance strategies against a broader range of chemical stressors and their targeted exploitation in *Pseudomonas* platform strains along with future application perspectives (see Box 1 for key terms and concepts).

Box 1 Key terms and concepts

***Chassis*, host:** A microorganism with specific metabolic and robustness abilities (native or engineered), which allow functioning and purposeful utilisation.
Cell factory: An engineered *chassis*, which is utilised for biosynthesis of a product.
Engineering: Targeted or untargeted genetic modification aiming to adapt *chassis* abilities or cell factory performance.
Bioproduction: Biosynthesis of a product in an organism.
***Pseudomonas* bioproduction strains:** We focus on *P. putida* KT2440, *P. putida* S12, *P. putida* DOT-T1E, and *P. taiwanensis* VLB120 (because these are the hosts most widely described in the literature centred on chemical stress tolerance as reviewed in this article). Notably, the taxonomic status of *P. putida* strains is debated – with implications on their safety status. While strain KT2440 is generally accepted to be non-pathogenic and has HV1 status certified by the U.S. Food and Drug Administration (FDA) [20], regulatory matters for all other strains of the species are inconsistent, hampering biotechnological exploitation. A taxonomic revision of the *P. putida* clade has been suggested that proposed a new species *P. alloputida* [21], which encompasses the above-mentioned strains and distinguishes them from other species within the *P. putida* group including clinical isolates. Here, we refer to this proposed species as *P. putida* for the sake of consistency with prior literature.
HV1 status: A strain (together with a plasmid), which is certified as host–vector (HV) system safety level 1 (i.e. HV1), can be handled in a P1 (or biosafety level 1) facility.
Resistance, tolerance, robustness: Ability of an organism to withstand adverse conditions (this article's focus lies on chemical compounds). The mechanistic differences that can be assigned to the terms [22] are usually not resolved in biotechnological research; here, we use these terms interchangeably.
Stressor: An environmental condition (pH, temperature, ionic strength etc.) or a chemical compound (organic solvent, toxic substance etc.), that causes cellular and/or metabolic stress resulting, e.g., in impaired growth or cell death.
Toxicant: A toxic chemical compound, which can act as a causative agent of chemical stress (i.e. as stressor) in an organism via diverse mechanisms.
Chemical stress: Summary of adverse effects exerted by chemicals including corruption of membrane integrity, damage of macromolecules (DNA and proteins), and interference with metabolism (e.g. inhibition of protein biosynthesis).
Xenobiotic: A chemical compound foreign to an organism or an ecological system.

Essays in Biochemistry (2021) EBC20200173
https://doi.org/10.1042/EBC20200173

New-to-*Pseudomonas* compound: A xenobiotic to a *Pseudomonas* host.
New-to-nature compound: A chemical compound, which does not occur naturally.

How Pseudomonads deal with toxic chemicals

In this chapter, we highlight the prominent natural stress responses of Pseudomonads, which allow them to sustain cell envelope integrity in the presence of toxicants, and to effectively export or eliminate them. We discuss the usefulness of these features for biotechnological applications and point out approaches for their targeted exploitation and engineering.

Built-in cell envelope stress response as support of bioproduction

A key feature of *Pseudomonas* strains making them so interesting for biotechnological applications is their inherent stress response and resistance to a variety of stress parameters, including antibiotics and solvents. In particular, solvent resistance has been extensively investigated. Solvents and other (hydrophobic) chemicals mainly affect the cell envelope by accumulation in the outer membrane or crossing it via porins, thus reaching the cytoplasmic membrane [23,24]. This can lead to the loss of essential membrane functions (cell integrity, enzymatic matrix, barrier for diffusion and electrochemical gradients) due to impaired membrane stability [25]. To maintain a specific degree of membrane fluidity, bacteria can adapt their lipid composition by biosynthesis of saturated lipids [26]. Besides, *Pseudomonas* species bear two powerful short-term adaption mechanisms [27] (Figure 1A,B).

A characteristic and almost unique adaptive response to environmental stress is the conversion of *cis* unsaturated membrane fatty acids into their corresponding *trans* configuration [28,29]. This very fast process neither consumes ATP nor involves cofactors [30] and is also independent of *de novo* protein and fatty acid biosynthesis. The periplasmic enzyme *cis-trans*-isomerase (Cti) converts the fatty acid residues palmitoleic acid (C16:1Δ9*cis*) and *cis*-vaccenic acid (C18:1Δ11*cis*) of phospholipids in the cytoplasmic membrane [28,29], leaving the position of the double bond unaltered. The shift from *cis*- to *trans*-fatty acids reduces membrane fluidity [23]. The gene for Cti (PP_2376 for *P. putida* KT2440) is present in all so far listed 34 *Pseudomonas* genomes in the Pfam database and could even be applied as a helpful molecular marker for the upcoming reorganisation of the genus (http://pfam.xfam.org/family/PF06934). This feature contributes to their inherent robustness [31]. Further engineering of this feature to improve bioproduction has not been described, although it might be thinkable: In *Escherichia coli*, expression of *cti* improved tolerance and carboxylic acid production [32], and *Pseudomonas* strains with additional copies of *cti* showed an increase in the level of *trans*-fatty acids [33].

In addition to rapid alteration in the phospholipids, Pseudomonads, like all Gram-negative bacteria, use vesiculation as a defence mechanism against various chemical (and non-chemical) stresses [34]. They release outer membrane vesicles (OMVs) with a diameter between 20 and 500 nm into the extracellular space, thereby altering the composition of the lipopolysaccharide (LPS) layer, the most distal part of their bacterial cell envelope. OMV formation and its numerous functions have been reviewed in detail [27,34–37]. The fast release of OMVs plays a major role in stress response, leading to a more hydrophobic bacterial surface and thus enhancing biofilm formation [38]. Bacteria living in biofilms or microcolonies are significantly more tolerant to antibiotics, solvents, and other forms of environmental stress [38,39], and this enhanced tolerance can be exploited in biofilm biocatalysis [40]. Furthermore, OMVs were shown to be crucial for unlocking otherwise unavailable polymeric substrates by exporting ligninolytic enzymes [41]. Vesiculation was also described to be naturally associated with the bacterial export of secondary metabolites like prodigiosin [42], the *Pseudomonas* quinolone signal (PQS) [43], and violacein [44], where OMVs may function as delivery vehicles. The mechanism could similarly support biotechnological production processes and even facilitate downstream processing. Vesiculation may even shield cells from a full toxicant dose, as OMVs were suggested to serve not only as an extracellular reservoir for a bacterial product but also as a non-cellular target [37,45]. The genetic basis of OMV formation is not yet entirely understood but could be connected to a range of genes [37]. Such knowledge has already been successfully applied for the engineering of hypervesiculation to support cell viability under stress conditions [46] or protein secretion in *E. coli* [47], but has not yet been utilised in the context of optimising *Pseudomonas* biotechnology and will certainly require fine-tuning to avoid extensive loss of lipids and membrane integrity [48,49]. The above-mentioned urgent response mechanisms enable *Pseudomonas* species to react quickly to emerging adverse conditions, making them robust candidates for whole-cell biotransformation processes and accessing new-to-nature chemistry.

PORTLAND PRESS

Essays in Biochemistry (2021) EBC20200173
https://doi.org/10.1042/EBC20200173

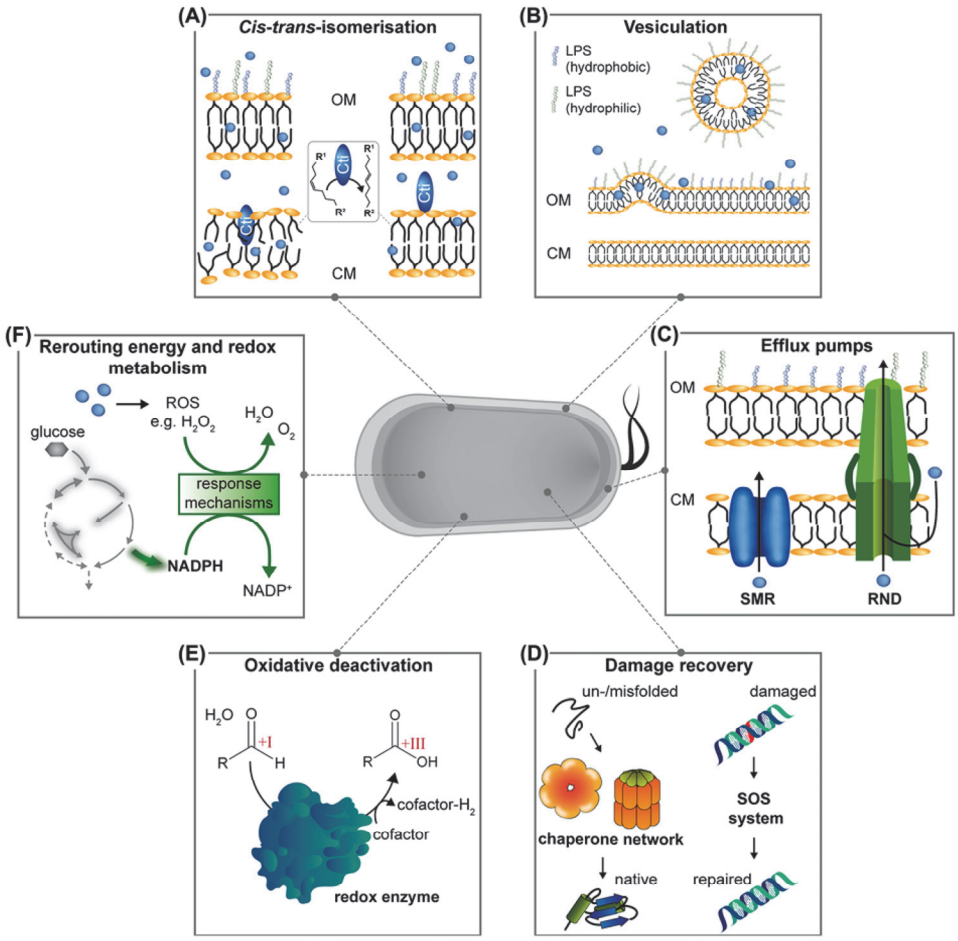

Figure 1. *Pseudomonas* natural stress response mechanisms against harmful chemicals

Bacteria counter chemical stress (blue spheres) with different mechanisms: (**A**) stabilising membrane adaptation by *cis-trans*-isomerase (Cti); (**B**) release of outer membrane vesicles and concomitant cell surface alteration by removal of hydrophilic lipopolysaccharides (LPSs); (**C**) export of chemicals via efflux transporters (RND, resistance-nodulation-division transporter family; SMR, small multidrug resistance transporter family); (**D**) damage recovery, e.g. by chaperones (like ClpB and GroEL/ES) that support correct protein folding and assembly, or DNA repair via the SOS response; (**E**) aldehyde elimination via oxidation (oxidation states of carbonyl carbon indicated in red); (**F**) rerouting of energy and redox metabolism to provide reducing equivalents for response mechanisms inactivating reactive oxygen species (ROS) and energy-demanding tolerance mechanisms. While vesiculation and chaperone-aided protein folding are ubiquitous stress responses in Gram-negative bacteria, *cis-trans*-isomerisation is a rather specific feature of Pseudomonads. Here, redox and efflux transporter equipment differs in individual strains. CM, cytoplasmic membrane; OM, outer membrane.

Essays in Biochemistry (2021) EBC20200173
https://doi.org/10.1042/EBC20200173

Table 1 Resistance-mediating extrusion transporters in *Pseudomonas*

Name	Superfamily	Substrate(s)*	Representative host(s)	References
TtgABC, ArpABC, MexAB-OprM	RND	Antibiotics, heavy metals, mono- and polycyclic aromatics, short- and long-chain alcohols, polyphenols (e.g. naringenin, quercetin, phloretin), monoterpenoids, bipyridyls	*P. putida* KT2440, DOT-T1E, S12, GS1 *P. taiwanensis* VLB120 *P. aeruginosa* PAO1 *P. syringae* B728a	[52–58,60,61,70,71]
TtgDEF	RND	Aromatic solvents (i.e. toluene and styrene), monoterpenoids (i.e. geraniol), long-chain alcohols	*P. putida* DOT-T1E, GS1	[55,61,71]
TtgGHI, SrpABC	RND	Mono- and polycyclic aromatics (e.g. toluene and styrene, biphenyls), long-chain alcohols	*P. putida* DOT-T1E, S12 *P. taiwanensis* VLB120	[55,56,59,70,71]
MexCD-OprJ	RND	Antibiotics, polyphenols (i.e. phloretin), triclosan, acriflavine, alkaloids (i.e. berberine)	*P. aeruginosa* PAO1 *P. syringae* B728a	[54,72]
MexEF-OprN	RND	Antibiotics, polyphenols (i.e. phloretin), triclosan, alkaloids (i.e. berberine), formaldehyde†, glycolaldehyde†, vanillin†, 2,2-bipyridyl	*P. putida* KT2440 *P. aeruginosa* PAO1 *P. syringae* B728a	[54,62,72–75]
MexHI-OpmD	RND	Phenazines (i.e. 5-methylphenazine-1-carboxylate), antibiotics	*P. aeruginosa* PAO1, PA14	[65,67]
ParXY-TtgC MexXY-OprM	RND	Antibiotics	*P. putida* KT2440 *P. aeruginosa* PAO1	[53,76]
TtgK	MFS	Toluene	*P. putida* DOT-T1E	[77]
PP_1271-73‡	MFS	4-Hydroxybenzoate, vanillin†, 3-chlorobenzoate†, propionate, toluene†	*P. putida* KT2440, S12	[66,68,69,75,78]
PP_3349‡	MFS	Formaldehyde†	*P. putida* KT2440	[73]
PP_3658‡	MFS	Formaldehyde†	*P. putida* KT2440	[73]
Psyr_0228§	MFS	Antibiotics	*P. syringae* B728a	[72]
Ttg2ABC	ABC	Antibiotics, toluene, *p*-coumarate, heavy metals, *tert*-butyl hydroperoxide	*P. putida* KT2440, DOT-T1E	[15,77]
Psyr_0541§	SMR	Antibiotics, alkaloids (i.e. berberine)	*P. syringae* B728a	[72]
EmrE	SMR	Antibiotics	*P. aeruginosa* PAO1	[79]
NorM_PS	MATE	Antibiotics, 4′,6-diamidino-2-phenylindole	*P. stutzeri* ATCC 14405	[80]

This table provides an overview of the most important efflux transporters, their superfamily, substrates, and hosts. It does not provide a complete list of efflux transporters. Abbreviations: MFS, major facilitator superfamily; RND, resistance-nodulation-division transporter family; SMR, small multidrug resistance; ABC, ATP-binding cassette; MATE, multidrug and toxic compound extrusion.
*Substrates are representative as many transporters have a broad substrate range. Substrate spectrum can differ between representative hosts.
†Suggested substrate due to a responsive up-regulation of the transporter; an actual contribution to resistance was not investigated.
‡Transporter name not available; locus tag of *P. putida* KT2440 used as reference.
§Transporter name not available; locus tag of *P. syringae* B728a used as reference.

Chemical export machinery avoids intracellular accumulation of toxicants

The active extrusion of molecules plays a major role in the resistance of bacteria towards various toxic compounds because the invasion of toxic chemicals cannot be prevented completely by cell envelope stress response mechanisms (Figure 1C). Implicated efflux transporters are structurally and mechanistically diverse [50] and are categorised into different families [51] (Table 1).

In Pseudomonads, efflux transporters of the resistance-nodulation-division (RND) family belong to the critical repertoire conveying resistance towards a broad spectrum of toxicants including antibiotics [52,53], biocides [54], heavy metals [51], mono- and polycyclic aromatics [55–59], short- and long-chain alcohols [59,60], (cyclo-)alkanes [59], monoterpenoids [61], and aldehydes [62]. Several different RND efflux pumps are present in *Pseudomonas* [63], however, strains commonly used in biotechnological applications differ in their equipment, which may have direct implications on their suitability as workhorses for specific product categories (Table 1).

The efflux pumps TtgABC, TtgDEF, and TtgGHI were thoroughly studied in the past and they all contribute to toluene resistance in *P. putida* DOT-T1E [55]. Unlike TtgDEF and TtgGHI, TtgABC belongs to the core genome of *P. putida* [64] and is especially relevant for the extrusion of antibiotics. TtgDEF is genetically co-localised with a toluene degradation cluster, extrudes toluene and styrene, and is present in *P. putida* DOT-T1E and *P. putida* GS1 [18,61]. TtgGHI is a key determinant regarding resistance towards aromatic solvents such as toluene and styrene, enabling growth in the presence of a second phase of these solvents [18,59]. Consequently, strains harbouring this efflux pump are considered to be solvent-tolerant, while the absence of TtgDEF and TtgGHI in *P. putida* KT2440 renders this strain sensitive to solvents.

PORTLAND PRESS

Essays in Biochemistry (2021) EBC20200173
https://doi.org/10.1042/EBC20200173

In addition to RND efflux transporters, ATP-binding cassette (ABC), major facilitator superfamily (MFS), multidrug and toxic compound extrusion (MATE), and small multidrug resistance (SMR) transporters were also suggested or shown to be involved in resistance to a wide variety of biotechnologically interesting stressors in *Pseudomonas* (Table 1). However, only a few representatives have been identified and sufficiently characterised. Thus, for many, the substrate spectrum has not been (fully) revealed, yet.

The extrusion of toxicants is likely an ancient mechanism relevant for *Pseudomonas* (and other bacteria) in their ecologic niche, e.g. to resist plant antimicrobials and natural antibiotics [51] or to enable growth on natural petroleum seeps. The large diversity and broad substrate spectrum of efflux transporters enabled an adaptation to many different anthropogenic substances including synthetic antibiotics [65], solvent contaminants [55], and halogenated aromatics [54,66]. Furthermore, efflux transporters are not only important for the export of exogenous toxicants but can also extrude natively produced molecules such as phenazines [67] or heterologous products such as *p*-hydroxybenzoate [68] and propionate [69]. Besides, the extrusion of solvents also increases the degree of freedom regarding the extractant selection in biphasic fermentation for *in situ* removal of toxic substrates or products and can thus alleviate the toxic effect of compounds that are not subject to efficient extrusion themselves [19]. Therefore, the microbial production of bulk chemicals (e.g. butanol or phenol), high-value compounds such as flavonoids (e.g. naringenin) and alkaloids (e.g. berberine), or even new-to-nature compounds could benefit from the broad substrate spectrum of efflux transporters in the future.

Dealing with the toxicant: detoxification and damage recovery

In addition to keeping or bringing toxicants out of the cells, bacteria also prevent or repair damage caused by a stressor (Figure 1D). For instance, DNA damage activates the bacterial SOS system, which maintains DNA integrity and replication via high- and low-fidelity repair mechanisms [81]. Mutants deficient in DNA repair genes, thus, show higher sensitivity to reactive compounds [82]. The up-regulation of chaperones from the heat shock protein families, like GroEL/ES or ClpB, is a ubiquitous response in bacteria to any kind of proteotoxic stress of physical or chemical nature [83,84], including the presence of solvents or aldehydes [62,85]. Accordingly, chaperone overexpression in *P. putida* improved tolerance to reactive wastewater components and enabled the valorisation of those compounds [62,84].

Furthermore, Pseudomonads are especially well-equipped to eliminate reactive and thus harmful compounds via conversion by a large set of redox enzymes (Figure 1E). Aldehydes, including the 'sleeping giant of sustainable chemistry' 5-hydroxymethylfurfural (HMF) [86] or the flavour compound vanillin, bear especially high potential to do harm as they are very reactive molecular species towards a plethora of nucleophiles, such as amino- or thiol- functionalities in, e.g., proteins or DNA [62]. Pseudomonads can rapidly convert toxic aldehydes into less noxious alcohol or acid derivatives. In contrast to *E. coli*, which primarily reduces aldehydes [87], Pseudomonads almost exclusively rely on oxidative deactivation [88]. This is of particular interest in the context of biotechnological processes where alcohols and aldehydes are to be oxidised into corresponding acids, such as the production of the plastic monomer 2,5-furandicarboxylic acid (FDCA) from HMF [89–91] or conversion of the monoterpenoid geraniol into geranic acid [61].

In *P. putida* KT2440, the periplasmic pyrroloquinoline quinone (PQQ)-dependent alcohol dehydrogenases PedE and PedH can oxidise a wide range of alcohols and aldehydes [92]. Both enzymes are highly expressed in *P. putida* KT2440 even in the absence of aldehydes or alcohols [93]. This high metabolic preparedness suggests that *P. putida* regularly encounters such toxicants in its natural habitat. The use of periplasmic enzymes seems logical from a tolerance perspective, as it may prevent high concentrations of aldehydes in the cytoplasm. It should be noted that the *ped* cluster encoding the above-mentioned dehydrogenases is not well conserved among Pseudomonads, and strains like *P. taiwanensis* VLB120 completely lack the cluster (pseudomonas.com [94]). However, Pseudomonads have a large repertoire of other dehydrogenases, and recent studies point to the involvement of, e.g., molybdenum-dependent enzymes [95–97].

The *Pseudomonas* redox equipment is also of particular interest for metabolisation of alternative substrates: Oxidases catalyse the first steps in the utilisation of alcohols as carbon source, including plastic monomers like ethylene glycol and 1,4-butanediol [93,98,99]. The targeted overexpression of glycolate oxidase was employed to avoid accumulation of the toxic intermediates glycolaldehyde and glyoxal during ethylene glycol metabolisation [99]. Similarly, *Pseudomonas* oxidation capacity was enhanced to increase FDCA production by co-expression of recombinant oxidases [91]. Such biotechnological oxidations require very high specific activities, with correspondingly high demand on the electron transport chain to regenerate redox cofactors. This, and also the use of true oxidases that produce H_2O_2, impose significant oxidative stress, which Pseudomonads are also well-equipped to handle [100] (Figure 1F).

Essays in Biochemistry (2021) EBC20200173
https://doi.org/10.1042/EBC20200173

Table 2 Approaches to exploring tolerance features

Aim	Approach	Examples	Application note	References
Identification of natural genetic tolerance determinants	Identify single key factors via untargeted loss/gain-of-function studies	Tn*5* transposon mutagenesis; expression of (meta)genomic library	Potential false positives in loss-of-function approach with production strain (biosynthesis potentially compromised)	[106,107]
Identification of natural genetic tolerance determinants	Identify single key factors via targeted function validation	Gene expression after screening of geno- and phenotypes	Can ultimately lead to an understanding of networks	[70,143]
Identification of natural genetic tolerance determinants	Reveal multifactorial networks by addressing each gene	Transcript-/proteomics; sequence screening; enrichment within TRMR library	Applicable for studies with production strains, except TRMR (biosynthesis potentially compromised)	[62,68,103,116]
Creation of new features	Adapt strain via untargeted tolerance-induction with stress	Enrichment of mutants during TALE	Relevant for new-to-*Pseudomonas* and new-to-nature products; rather only for exposure (in production strain, biosynthesis potentially compromised)	[98,113,114]

This feature is connected with a metabolic architecture geared towards formation of NADPH, the metabolic currency to counteract oxidative stress, upon exposure to oxidative agents [101]. Notably, oxidation of alcohols or aldehydes may also be detrimental when they are the desired end product of synthetic pathways or occur as biosynthetic intermediates, which may require gene inactivation [96,102]. Thus, complete understanding of *Pseudomonas*' extensive oxidative enzymatic repertoire is indispensable to gain insights into 'tolerance-by-conversion' mechanisms and to enable microbial catalysis of new substrates and products.

Perspectives in tolerance and cell factory engineering

In this chapter, we discuss the present toolbox of methods for the identification of tolerance-associated genes and their utilisation for engineering next-generation *chassis* with enhanced tolerance. Beyond that, we highlight key emergent strategies for pathway fine-tuning to establish stable cell factories for the effective production of natural compounds and novel biochemicals.

Identification and implementation of tolerance-related genes

Identifying the genetic background of tolerant phenotypes is of major interest for developing robust production strains for industrial applications. So far, various methods have been explored (Table 2).

The most conventional method for linking bacterial phenotypes to genes appears to be random gene inactivation via transposon mutagenesis. Screening for loss of tolerance and the identification of the transposon integration site in such clones was foundational in identifying, e.g. solvent pumps [59,103–105]. In contrast, gain of tolerance can be utilised to identify respective factors in (meta)genomic libraries of tolerant bacteria using susceptible strains for expression [106,107]. Both strategies are powerful to identify single key factors for tolerance but miss complex interacting networks.

With the emergence of respective technologies, it became possible to study whole transcriptomes (via microarrays or RNA-Seq) or proteomes to reveal multifactorial responses to exposure or biosynthesis of the stressor [62,68,103]. Moreover, advanced sequencing technologies facilitated the comparative analysis of complete genomes from related strains with different phenotypes to deduce tolerance-associated genes by sequence homology analysis or matching conspicuous phenotypes with outstanding genes [70,108–110]. Furthermore, the massive progress in sequencing technology evoked a reinvigoration of adaptive laboratory evolution (ALE) [111]. The strategy involves exposing a bacterial strain to a sublethal concentration of the stressor, which is usually increased over subsequential cultivations. This enables the development of robust strains and the elucidation of the genetic background conveying the tolerance [111,112]. This approach, designated as tolerance ALE (TALE) [113], is straightforward but rather time-consuming in dependence on the basic growth rate and the speed of adaption [93,113,114].

To achieve high throughput, recent studies combined the selection methodology of ALE with the 'targeting each gene' concept of transposon libraries and tracked the population dynamics in mixed cultures exposed to stress to quantify which mutant strains were enriched [15,61,115]. Conceptually similar, trackable multiplex recombineering (TRMR) of a barcoded cassette with a strong promoter and ribosome-binding site (RBS) upstream of virtually every gene allowed quantification of each mutant in mixed culture under stress conditions [116]. This strategy has not yet

PORTLAND PRESS

Essays in Biochemistry (2021) EBC20200173
https://doi.org/10.1042/EBC20200173

been applied in Pseudomonads but was suitable, e.g., to identify several genes contributing to furfural tolerance in *E. coli* [116].

Most of the described approaches are suitable for the elucidation of tolerance-associated genes and at the same time for the implementation of tolerance in a host (Figure 2). However, the typical methodology relies on exposure to externally applied stressors, although the actual motivation often was the efficient biotechnological production of the compound. Even though this might be sufficient for many membrane-permeable compounds [69], further studies directly focusing on production and the associated response [68] will be useful to identify tolerance-related genes with applicability in bioproduction. Notably, ALE-type strategies are of limited use for this approach, since stress-induced selection processes are likely to yield suppressor mutations that abolish biosynthesis of the xenobiotic stressor. Here, the use of 'omics' technologies appears favourable to uncover sensory and regulatory networks evoking multilevel responses to a production.

While major components of the *Pseudomonas* response to chemical stress could be identified (Figure 1), it is important to note that many of the mentioned studies suggest tolerance to rely on complex and highly diverse networks [81,117–119], meaning this feature is generally not trivial to transfer from one organism to another. Moreover, the formation of resistance determinants such as multicomponent efflux pumps, which have to be operated constantly to effectively lower the intracellular concentration of a toxicant, is associated with a high energy demand which can lead to reduced biomass yield, productivity, and even in some cases reduced tolerance [19,25,120–123]. It is therefore not practical to aim at creating one fully robust strain that can cope with any kind of stressor. For biotechnological use, it appears more attractive to isolate uniquely adapted [124–126] or to create new strains with distinct properties enabling the *à la carte* selection of the most appropriate *chassis* for a specific product or process [120].

Since so far, descriptions of the targeted engineering of *Pseudomonas chassis* with optimised resistance for effective biotechnological applications are scarce [62,69,99,120,127], conclusions about generally successful strategies for strain development cannot yet be drawn. Based on studies with other chassis [85,128–130], we propose that due to the high metabolic costs, removal of dispensable energy-intensive cellular features [120], along with fine-tuning the expression of the tolerance-conveying gene(s), is essential for the construction of an optimal biotechnological cell factory. The latter is important for efflux pumps, where too strong expression can destabilise the membrane [60]. This fine-tuning can be achieved through controllable and stable gene expression. For *Pseudomonas*, a range of well-characterised, adjustable expression systems is available including inducible promoters with low leakiness (e.g. XylS/*Pm*, RhaRS/P_{rhaBAD}, AntR/P_{antA}, AraC/P_{araB}) [131–133], or synthetic libraries of constitutive promoters with defined activities [132,134]. The use of plasmids for gene introduction enables rapid construction of different strains [135]. Nevertheless, genomic integration is usually preferable for avoiding problems such as plasmid instability or plasmid-related growth impairment [136–138]. For chromosomal integration, different genetic tools are available and already summarised in previous reviews [3]. A distinction can be made between randomised (e.g. via transposon Tn*5*) [139,140] and site-specific integration. Especially prominent here are transposon Tn*7* [132,134] and homologous recombination facilitated by recombinases (e.g. RecET) [141]. Counterselection strategies for genomic modifications including gene deletions have also been successfully adapted to *Pseudomonas* (e.g. by use of *sacB*, CRISPR-Cas9, or I-*Sce*I) [142]. This array of tools, together with an increasing understanding of tolerance traits, will facilitate the generation of *chassis* with specifically adapted tolerance features in the near future.

Engineering of optimal flux in cell factories with novel pathways

The biosynthetic repertoire of *Pseudomonas* together with implementation of heterologous pathways allows the utilisation of various substrates and synthesis of highly diverse products such as aromatics, glycolipids, and terpenoids [2–4]. *De novo* biosynthesis of fluorometabolites from mineral fluoride has recently paved a new way to fluorinated building blocks [12]. An ideal cell factory for respective biotechnological applications is composed of a *chassis* that exhibits inherent or engineered tolerance to the involved substrate and product, and a metabolic pathway with optimal flux between the two. As discussed above, imbalances in a catabolic pathway can lead to accumulation of toxic compounds such as aldehydes that require elimination [99]. Also for anabolic recombinant pathways like multistep terpenoid biosynthesis, toxicity of biosynthetic intermediates is discussed as one major challenge for effective production [144]. Optimal balancing of intrinsic or recombinant pathways may thus become necessary, especially when the involved biocatalysts are confronted with non-natural substrates, affecting reaction rates and the overall catalytic efficiency (Figure 3).

Prominent catabolic routes in *Pseudomonas* exploited in both the context of bioremediation and the production of, e.g., muconic acid and derivatives thereof [145], are cleavage pathways involved in the degradation of various

Essays in Biochemistry (2021) EBC20200173
https://doi.org/10.1042/EBC20200173

PORTLAND PRESS

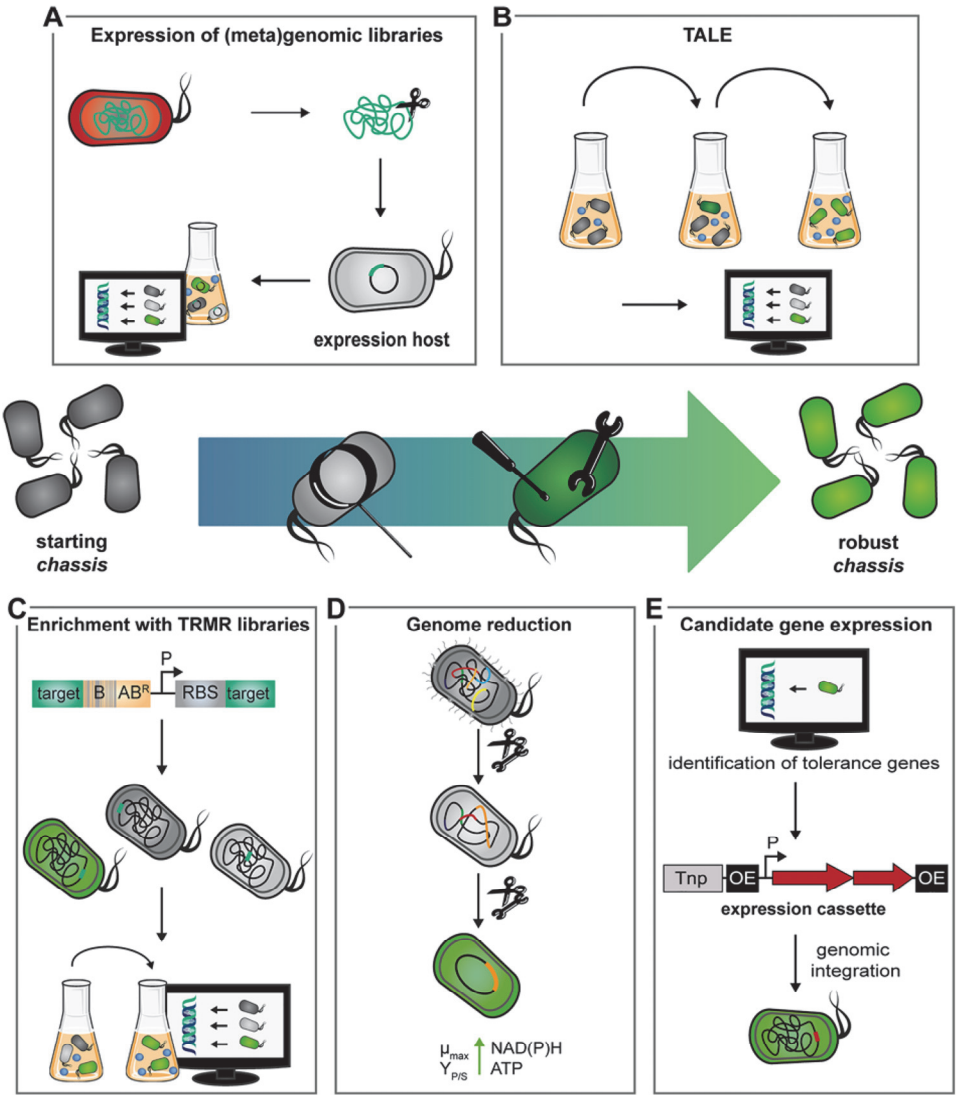

Figure 2. Engineering *Pseudomonas* strains with optimised tolerance

Depicted are five approaches to building robust *chassis* (green cells) with tolerance to chemical stress (blue spheres). (**A**) (Meta)genomic libraries, e.g. of strains living in habitats with harsh environmental conditions, are promising to screen for tolerance-conveying genes by expression and exposure to a stressor. (**B**) In TALE, adaptive changes accumulate during long-term selection under stress-inducing conditions and can be identified by whole-genome sequencing. (**C**) TRMR facilitates the genomic integration of a DNA cassette with a sequence barcode for tracking (B), an antibiotic resistance gene (AB^R), a strong promoter (P), and an RBS upstream of virtually every gene. Under stress conditions, the strains overexpressing genes that confer enhanced tolerance are specifically enriched within the barcoded library. (**D**) The removal of energy-intensive features during genome reduction can free capacities (in form of NAD(P)H and ATP) required to sustain tolerance, maximal growth rates and production yields. (**E**) Previously identified resistance-associated candidate genes are integrated into the genome of a 'starting *chassis*' by different genetic tools, e.g. a transposon (Tnp, transposase encoding region; OE, outside end of transposon).

PORTLAND PRESS

Essays in Biochemistry (2021) EBC20200173
https://doi.org/10.1042/EBC20200173

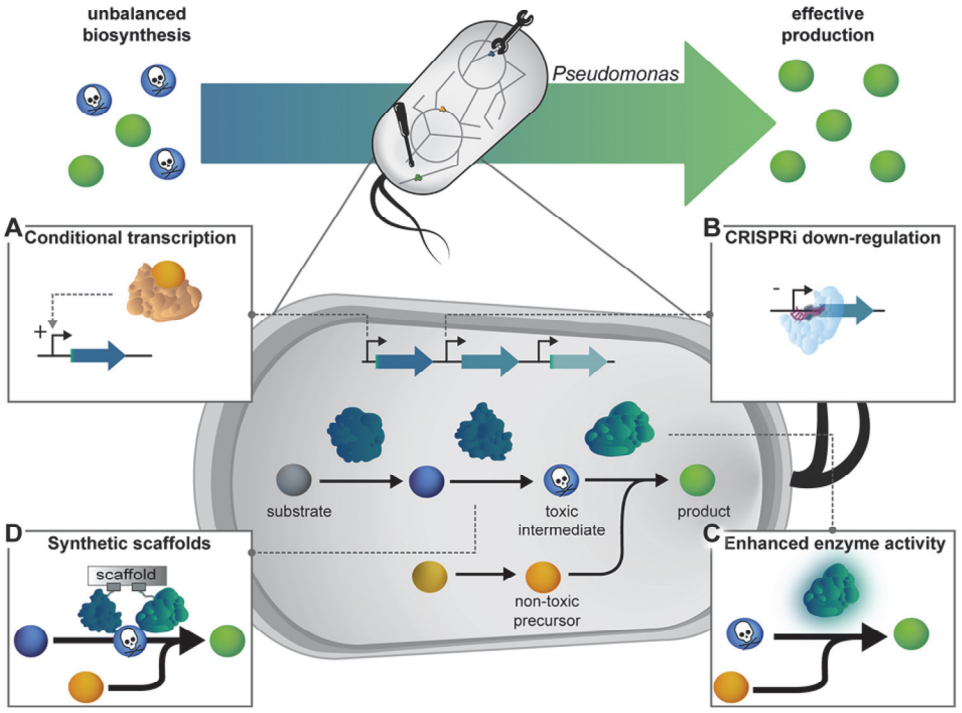

Figure 3. Key emergent strategies for pathway balancing

At the metabolite level (spheres), an unbalanced biosynthesis can lead to accumulation of toxic intermediates in native or synthetic biochemical networks. Sophisticated regulation and balancing of metabolic fluxes towards and from the toxic intermediate can support effective production of targeted end-products. (**A**) Dynamic control via a transcription regulator activates the reactions leading to the toxic intermediate strictly under the condition that its reaction partner (orange sphere) is available at sufficient concentrations for effective conversion into the desired product. (**B**) Tight transcription control can be achieved by CRISPR-interference. (**C**) Enzymes with enhanced activity facilitate effective conversion and synthesis of the desired end-product. (**D**) Synthetic scaffolds increase local concentrations of pathway enzymes for effective substrate-channelling with decreased diffusion of intermediates.

aromatic chemicals. Extensive studies on the *ortho*-cleavage pathway's kinetics revealed that the overall flux is controlled by substrate uptake as well as by the enzymatic reactions forming and consuming the toxic intermediate catechol [146]. Bioproduction of novel building blocks derived from muconic acid requires an in-depth understanding of pathway regulation. For instance, when exposed to halogenated analogues of the pathway substrates, the cells accumulate halogenated catechols [147–149]. This phenomenon can be attributed to both a significantly reduced activity of the catechol-1,2-dioxygenases on substituted catechols [150] and a different (or lacking) response of the pathway regulators, preventing an efficient metabolic flux.

Protein engineering combined with a suitable screening assay can be a viable strategy to adapt a key enzyme towards accepting alternative substrates. Engineering of the prodigiosin ligase is a successful example of this [151,152]. As previously discussed, enhancing the expression level of a detoxifying oxidase was key for the utilisation of ethylene glycol [99]. In another case, accumulation of toxic glycolaldehyde as intermediate of installed xylose catabolism was avoided by deletion of a regulator leading to derepression of its conversion [127]. In both cases, adjusting the metabolic flow was thus key for the effective utilisation of both new-to-*Pseudomonas* substrates.

Balancing the expression of two biosynthetic genes was key to the production of bisdemethoxycurcumin in *P. putida* KT2440 to avoid the accumulation of undesirable intermediates and toxic effects [153]. Generally, the use

Essays in Biochemistry (2021) EBC20200173
https://doi.org/10.1042/EBC20200173

PORTLAND PRESS

of promoters with stringently adjustable expression strength and genome integration of expression cassettes appears favourable to achieve stable and controlled expression of biosynthetic genes, as discussed above in the context of tolerance-associated genes. Modular cloning methods allow efficient assembly and testing of various constructs [154–156]. However, adapting the expression of one gene to release enzymatic bottlenecks is not always a feasible option to avoid the effect of toxic intermediates. The kinetic parameters of certain enzyme–substrate combinations can be significantly inferior compared with other reactions within the same pathway, even at high concentrations of the catalyst. In these cases, the upstream enzyme levels need to be adjusted to avoid a metabolic imbalance at the bottleneck. Using multiple promoter systems, which can control expression of different genes independently, may be necessary [153,157]. Expression strengths can be further tuned through the use of translation initiation sequences of defined strengths, designed either with bioinformatic tools like the RBS Calculator for a given gene (https://salislab.net/software/predict_rbs_calculator) or standardised by balancing elements controlling transcription and translation initiation (bicistronic designs) [158].

Furthermore, a dynamic regulation approach can be employed to balance the biochemical activities based on metabolite concentrations: CRISPR-interference [159–161] as well as conditional proteolysis systems [162] have been implemented in *Pseudomonas* and can be used to down-regulate biochemical functions leading up to the toxic intermediate (e.g. by coupling the output to a suitable expression system, biosensor or riboswitch). For enhancing *E. coli*-based biodiesel production, where the desired product consists of precursors originating from two independent pathways that include a toxic intermediate, metabolite-inducible expression systems could be developed to allow a conditional activation of the toxicity-generating reactions only when the availability of the second precursor reached a threshold [163]. Aside from avoiding stress, such mechanisms are also ideal for avoiding unwanted intrinsic down-regulation of biosynthetic networks by key intermediates, which often occurs in biosynthetic pathways and impairs product yield. Another emerging strategy to achieve a higher and more balanced flux is to spatially organise enzymes within synthetic scaffolds [164,165] to create high local concentrations of metabolites and enzymes, with well-defined stoichiometry to support immediate conversion without diffusion of intermediates. All these strategies (Figure 3) together with an increasing understanding of tolerance traits will be instrumental for effective production applications and expanding the catalytic landscape of *Pseudomonas* towards novel chemistries [12,166].

Conclusion

Proof-of-principle studies on the microbial production of many different compounds of interest are abundant in current literature. However, efficient high-level production of such compounds is relatively rare, because often the producer microbes typically applied to this end encounter challenging chemistries at multiple levels. Construction of robust cell factories will therefore be critical to take the next steps on the path towards sustainable bioproduction. Based on the current state of research, bacteria from the *Pseudomonas* clade represent especially promising *chassis* organisms in that respect. Here, unlocking new strains with unique tolerance features and knowledge-guided improvement of established *chassis* based on the biochemical characterisation of such traits will play an important role. This approach can enable the rapid construction of new synthetic hosts to finally establish a '*chassis à la carte*' selection with specifically adapted tolerance features for any biotechnological application.

Summary

- Efficient bioproduction of chemical compounds using whole cells as biocatalysts is often hampered by the limited ability of microbial hosts to cope with the stress linked to production.
- Pseudomonads are endowed with effective stress responses to many chemicals of biotechnological relevance.
- Understanding of the underlying tolerance mechanisms is increasing but their targeted exploitation and engineering is only just starting.
- A powerful molecular genetic toolbox will aid the construction of *chassis* with specific tolerance features to obtain optimised hosts for biotechnology.
- Pathway balancing strategies can further improve effective bioproduction of natural and new-to-nature compounds.

PORTLAND PRESS

Essays in Biochemistry (2021) EBC20200173
https://doi.org/10.1042/EBC20200173

Competing Interests

N.T.W. and P.I.N. have filed patent applications on the use of engineered *Pseudomonas putida* strains to produce novel halogenated molecules.

Funding

This work was supported by the German Federal Ministry of Education and Research via the project NO-STRESS [grant numbers 031B0852A (to J.R., T.L., B.W. and N.W.), 031B0852B (to N.L.B., L.K., S.T., A.L. and K.-E.J.), 031B085C (to C.E. and H.J.H.)]; the Federal Ministry of Education and Research [grant numbers LipoBiocat/031B0837A (to S.T. and K.-E.J.), GlycoX/161B0866A (to S.T., A.L. and K.-E.J.)]; The Novo Nordisk Foundation [grant numbers NNF20CC0035580, *LiFe*, NNF18OC0034818 (to P.I.N.)]; the Danish Council for Independent Research (*SWEET*) [grant number 8021-00039B]; the European Union's Horizon 2020 Research and Innovation Programme [grant number 814418 (*SinFonia*)]; the Novo Nordisk Foundation as part of the Copenhagen Bioscience Ph.D. Programme [grant number NNF17CC0026768 (to E.K.)]; and the European Union's Horizon 2020 Research and Innovation Programme for the project MIX-UP [grant number 870294 (to N.W.)].

Author Contribution

A.L., S.T. and N.W. conceived the concept. A.L. directed the writing. N.L.B., L.K., S.T., A.L., B.W., T.L., J.R., E.K., C.E. and N.T.W. wrote the manuscript. N.L.B., L.K., E.K. and N.T.W. conceived and prepared the figures. A.L., K.-E.J., H.J.H., N.W. and P.I.N. edited the manuscript. All authors discussed and approved the manuscript.

Acknowledgements

The authors would like to acknowledge the work by many researchers in the field of *Pseudomonas* microbiology and biotechnology who have made authoritative contributions to our current understanding of this bacterium, the work of whom could not always be cited because of space reasons.

Abbreviations

ABC, ATP-binding cassette (transporter family); ALE, adaptive laboratory evolution; Cti, *cis*–*trans* isomerase; FDCA, 2,5-furandicarboxylic acid; HMF, 5-hydroxymethylfurfural; HV1, host–vector (HV) system safety level 1; LPS, Lipopolysaccharide; MATE, multidrug and toxic compound extrusion (transporter family); MFS, major facilitator superfamily (transporter family); OMV, outer membrane vesicle; PQQ, pyrroloquinoline quinone; PQS, *Pseudomonas* quinolone signal; RBS, ribosome binding site; RND, resistance-nodulation-division (transporter family); SMR, small multidrug resistance (transporter family); TALE, tolerance ALE; TRMR, trackable multiplex recombineering.

References

1 Thorwall, S., Schwartz, C., Chartron, J.W. and Wheeldon, I. (2020) Stress-tolerant non-conventional microbes enable next-generation chemical biosynthesis. *Nat. Chem. Biol.* **16**, 113–121, https://doi.org/10.1038/s41589-019-0452-x

2 Weimer, A., Kohlstedt, M., Volke, D.C., Nikel, P.I. and Wittmann, C. (2020) Industrial biotechnology of *Pseudomonas putida:* advances and prospects. *Appl. Microbiol. Biotechnol.* **104**, 7745–7766, https://doi.org/10.1007/s00253-020-10811-9

3 Loeschcke, A. and Thies, S. (2020) Engineering of natural product biosynthesis in *Pseudomonas putida*. *Curr. Opin. Biotechnol.* **65**, 213–224, https://doi.org/10.1016/j.copbio.2020.03.007

4 Schwanemann, T., Otto, M., Wierckx, N. and Wynands, B. (2020) *Pseudomonas* as versatile aromatics cell factory. *Biotechnol. J.* **15**, 1900569, https://doi.org/10.1002/biot.201900569

5 Wilkes, R.A. and Aristilde, L. (2017) Degradation and metabolism of synthetic plastics and associated products by *Pseudomonas* sp.: capabilities and challenges. *J. Appl. Microbiol.* **123**, 582–593, https://doi.org/10.1111/jam.13472

6 Nikel, P.I. and de Lorenzo, V. (2018) *Pseudomonas putida* as a functional chassis for industrial biocatalysis: From native biochemistry to *trans*-metabolism. *Metab. Eng.* **50**, 142–155, https://doi.org/10.1016/j.ymben.2018.05.005

7 Yan, F., Burgard, C., Popoff, A., Zaburannyi, N., Zipf, G., Maier, J. et al. (2018) Synthetic biology approaches and combinatorial biosynthesis towards heterologous lipopeptide production. *Chem. Sci.* **9**, 7510–7519, https://doi.org/10.1039/C8SC02046A

8 Khan, M.S.A. and Atlaf, M.M. (2019) Hybrid bioactive products and combinatorion biosynthesis. *New and Future Developments in Microbial Biotechnology and Bioengineering*, pp. 131–139, Elsevier, https://doi.org/10.1016/B978-0-444-63504-4.00010-4

9 Gemperlein, K., Hoffmann, M., Huo, L., Pilak, P., Petzke, L., Müller, R. et al. (2017) Synthetic biology approaches to establish a heterologous production system for coronatines. *Metab. Eng.* **44**, 213–222, https://doi.org/10.1016/j.ymben.2017.09.009

10 Klein, A.S., Domröse, A., Bongen, P., Brass, H.U.C., Classen, T., Loeschcke, A. et al. (2017) New prodigiosin derivatives obtained by mutasynthesis in *Pseudomonas putida*. *ACS Synth. Biol.* **6**, 1757–1765, https://doi.org/10.1021/acssynbio.7b00099

11 Habash, S.S., Brass, H.U.C., Klein, A.S., Klebl, D.P., Weber, T.M., Classen, T. et al. (2020) Novel prodiginine derivatives demonstrate bioactivities on plants, nematodes, and fungi. *Front. Plant Sci.* **11**, 579807, https://doi.org/10.3389/fpls.2020.579807

Essays in Biochemistry (2021) EBC20200173
https://doi.org/10.1042/EBC20200173

12 Calero, P., Volke, D.C., Lowe, P.T., Gotfredsen, C.H., O'Hagan, D. and Nikel, P.I. (2020) A fluoride-responsive genetic circuit enables *in vivo* biofluorination in engineered *Pseudomonas putida*. *Nat. Commun.* **11**, 5045, https://doi.org/10.1038/s41467-020-18813-x
13 Ochsner, U.A., Reiser, J., Fiechter, A. and Witholt, B. (1995) Production of *Pseudomonas aeruginosa* rhamnolipid biosurfactants in heterologous hosts. *Appl. Environ. Microbiol.* **61**, 3503–3506, https://doi.org/10.1128/aem.61.9.3503-3506.1995
14 Ankenbauer, A., Schäfer, R.A., Viegas, S.C., Pobre, V., Voß, B., Arraiano, C.M. et al. (2020) *Pseudomonas putida* KT2440 is naturally endowed to withstand industrial-scale stress conditions. *Microb. Biotechnol.* **13**, 1145–1161, https://doi.org/10.1111/1751-7915.13571
15 Calero, P., Jensen, S.I., Bojanovič, K., Lennen, R.M., Koza, A. and Nielsen, A.T. (2018) Genome-wide identification of tolerance mechanisms toward *p*-coumaric acid in *Pseudomonas putida*. *Biotechnol. Bioeng.* **115**, 762–774, https://doi.org/10.1002/bit.26495
16 Klein, A.S., Brass, H.U.C., Klebl, D.P., Classen, T., Loeschcke, A., Drepper, T. et al. (2018) Preparation of cyclic prodiginines by mutasynthesis in *Pseudomonas putida* KT2440. *ChemBioChem* **19**, 1545–1552, https://doi.org/10.1002/cbic.201800154
17 Verhoef, S., Wierckx, N., Westerhof, R.G.M., de Winde, J.H. and Ruijssenaars, H.J. (2009) Bioproduction of *p*-hydroxystyrene from glucose by the solvent-tolerant bacterium *Pseudomonas putida* S12 in a two-phase water-decanol fermentation. *Appl. Environ. Microbiol.* **75**, 931–936, https://doi.org/10.1128/AEM.02186-08
18 Ramos, J.-L., Sol Cuenca, M., Molina-Santiago, C., Segura, A., Duque, E., Gómez-García, M.R. et al. (2015) Mechanisms of solvent resistance mediated by interplay of cellular factors in *Pseudomonas putida*. *FEMS Microbiol. Rev.* **39**, 555–566, https://doi.org/10.1093/femsre/fuv006
19 Kusumawardhani, H., Hosseini, R. and de Winde, J.H. (2018) Solvent tolerance in bacteria: fulfilling the promise of the biotech era? *Trends Biotechnol.* **36**, 1025–1039, https://doi.org/10.1016/j.tibtech.2018.04.007
20 Kampers, L.F.C., Volkers, R.J.M. and Martins dos Santos, V.A.P. (2019) *Pseudomonas putida* KT2440 is HV1 certified, not GRAS. *Microb. Biotechnol.* **12**, 845–848, https://doi.org/10.1111/1751-7915.13443
21 Keshavarz-Tohid, V., Vacheron, J., Dubost, A., Prigent-Combaret, C., Taheri, P., Tarighi, S. et al. (2019) Genomic, phylogenetic and catabolic re-assessment of the *Pseudomonas putida* clade supports the delineation of *Pseudomonas alloputida* sp. nov. *Pseudomonas inefficax* sp. nov. *Pseudomonas persica* sp. nov., and *Pseudomonas shirazica* sp. nov. *Syst. Appl. Microbiol.* **42**, 468–480, https://doi.org/10.1016/j.syapm.2019.04.004
22 Balaban, N.Q., Helaine, S., Lewis, K., Ackermann, M., Aldridge, B., Andersson, D.I. et al. (2019) Definitions and guidelines for research on antibiotic persistence. *Nat. Rev. Microbiol.* **17**, 441–448, https://doi.org/10.1038/s41579-019-0196-3
23 de Bont, J. (1998) Solvent-tolerant bacteria in biocatalysis. *Trends Biotechnol.* **16**, 493–499, https://doi.org/10.1016/S0167-7799(98)01234-7
24 Sandoval, N.R. and Papoutsakis, E.T. (2016) Engineering membrane and cell-wall programs for tolerance to toxic chemicals: beyond solo genes. *Curr. Opin. Microbiol.* **33**, 56–66, https://doi.org/10.1016/j.mib.2016.06.005
25 Heipieper, H.J., Neumann, G., Cornelissen, S. and Meinhardt, F. (2007) Solvent-tolerant bacteria for biotransformations in two-phase fermentation systems. *Appl. Microbiol. Biotechnol.* **74**, 961–973, https://doi.org/10.1007/s00253-006-0833-4
26 Zhang, Y.-M. and Rock, C.O. (2008) Membrane lipid homeostasis in bacteria. *Nat. Rev. Microbiol.* **6**, 222–233, https://doi.org/10.1038/nrmicro1839
27 Eberlein, C., Baumgarten, T., Starke, S. and Heipieper, H.J. (2018) Immediate response mechanisms of Gram-negative solvent-tolerant bacteria to cope with environmental stress: *cis-trans* isomerization of unsaturated fatty acids and outer membrane vesicle secretion. *Appl. Microbiol. Biotechnol.* **102**, 2583–2593, https://doi.org/10.1007/s00253-018-8832-9
28 Heipieper, H.J., Meinhardt, F. and Segura, A. (2003) The *cis-trans* isomerase of unsaturated fatty acids in *Pseudomonas* and *Vibrio:* biochemistry, molecular biology and physiological function of a unique stress adaptive mechanism. *FEMS Microbiol. Lett.* **229**, 1–7, https://doi.org/10.1016/S0378-1097(03)00792-4
29 Heipieper, H.J., Diefenbach, R. and Keweloh, H. (1992) Conversion of *cis* unsaturated fatty acids to *trans,* a possible mechanism for the protection of phenol-degrading *Pseudomonas putida* P8 from substrate toxicity. *Appl. Environ. Microbiol.* **58**, 1847–1852, https://doi.org/10.1128/AEM.58.6.1847-1852.1992
30 Von Wallbrunn, A., Richnow, H.H., Neumann, G., Meinhardt, F. and Heipieper, H.J. (2003) Mechanism of *cis-trans* isomerization of unsaturated fatty acids in *Pseudomonas putida*. *J. Bacteriol.* **185**, 1730–1733, https://doi.org/10.1128/JB.185.5.1730-1733.2003
31 Junker, F. and Ramos, J.L. (1999) Involvement of the *cis/trans* isomerase Cti in solvent resistance of *Pseudomonas putida* DOT-T1E. *J. Bacteriol.* **181**, 5693–5700, https://doi.org/10.1128/JB.181.18.5693-5700.1999
32 Tan, Z., Yoon, J.M., Nielsen, D.R., Shanks, J.V. and Jarboe, L.R. (2016) Membrane engineering *via trans* unsaturated fatty acids production improves *Escherichia coli* robustness and production of biorenewables. *Metab. Eng.* **35**, 105–113, https://doi.org/10.1016/j.ymben.2016.02.004
33 Holtwick, R., Meinhardt, F. and Keweloh, H. (1997) *cis-trans* isomerization of unsaturated fatty acids: cloning and sequencing of the *cti* gene from *Pseudomonas putida* P8. *Appl. Environ. Microbiol.* **63**, 4292–4297, https://doi.org/10.1128/AEM.63.11.4292-4297.1997
34 Mozaheb, N. and Mingeot-Leclercq, M.-P. (2020) Membrane vesicle production as a bacterial defense against stress. *Front. Microbiol.* **11**, 60221, https://doi.org/10.3389/fmicb.2020.600221
35 Kulp, A. and Kuehn, M.J. (2010) Biological functions and biogenesis of secreted bacterial outer membrane vesicles. *Annu. Rev. Microbiol.* **64**, 163–184, https://doi.org/10.1146/annurev.micro.091208.073413
36 Schertzer, J.W. and Whiteley, M. (2013) Bacterial outer membrane vesicles in trafficking, communication and the host-pathogen interaction. *J. Mol. Microbiol. Biotechnol.* **23**, 118–130, https://doi.org/10.1159/000346770
37 Schwechheimer, C. and Kuehn, M.J. (2015) Outer-membrane vesicles from Gram-negative bacteria: biogenesis and functions. *Nat. Rev. Microbiol.* **13**, 605–619, https://doi.org/10.1038/nrmicro3525
38 Baumgarten, T., Sperling, S., Seifert, J., von Bergen, M., Steiniger, F., Wick, L.Y. et al. (2012) Membrane vesicle formation as a multiple-stress response mechanism enhances *Pseudomonas putida* DOT-T1E cell surface hydrophobicity and biofilm formation. *Appl. Environ. Microbiol.* **78**, 6217–6224, https://doi.org/10.1128/AEM.01525-12

PORTLAND PRESS

Essays in Biochemistry (2021) EBC20200173
https://doi.org/10.1042/EBC20200173

39 Atashgahi, S., Sánchez-Andrea, I., Heipieper, H.J., van der Meer, J.R., Stams, A.J.M. and Smidt, H. (2018) Prospects for harnessing biocide resistance for bioremediation and detoxification. *Science* **360**, 743–746, https://doi.org/10.1126/science.aar3778
40 Halan, B., Karande, R., Buehler, K. and Schmid, A. (2016) Catalytic *Pseudomonas taiwanensis* VLB120△C biofilms thrive in a continuous pure styrene generated by multiphasic segmented flow in a capillary microreactor. *J. Flow Chem.* **6**, 39–42, https://doi.org/10.1556/1846.2015.00037
41 Salvachúa, D., Werner, A.Z., Pardo, I., Michalska, M., Black, B.A., Donohoe, B.S. et al. (2020) Outer membrane vesicles catabolize lignin-derived aromatic compounds in *Pseudomonas putida* KT2440. *Proc. Natl. Acad. Sci. U.S.A.* **117**, 9302–9310, https://doi.org/10.1073/pnas.1921073117
42 Tan, D., Fu, L., Sun, X., Xu, L. and Zhang, J. (2020) Genetic analysis and immunoelectron microscopy of wild and mutant strains of the rubber tree endophytic bacterium *Serratia marcescens* strain ITBB B5-1 reveal key roles of a macrovesicle in storage and secretion of prodigiosin. *J. Agric. Food Chem.* **68**, 5606–5615, https://doi.org/10.1021/acs.jafc.0c00078
43 Mashburn, L.M. and Whiteley, M. (2005) Membrane vesicles traffic signals and facilitate group activities in a prokaryote. *Nature* **437**, 422–425, https://doi.org/10.1038/nature03925
44 Choi, S.Y., Lim, S., Cho, G., Kwon, J., Mun, W., Im, H. et al. (2020) *Chromobacterium violaceum* delivers violacein, a hydrophobic antibiotic, to other microbes in membrane vesicles. *Environ. Microbiol.* **22**, 705–713, https://doi.org/10.1111/1462-2920.14888
45 Domröse, A., Klein, A.S., Hage-Hülsmann, J., Thies, S., Svensson, V., Classen, T. et al. (2015) Efficient recombinant production of prodigiosin in *Pseudomonas putida*. *Front. Microbiol.* **6**, 972, https://doi.org/10.3389/fmicb.2015.00972
46 McBroom, A.J. and Kuehn, M.J. (2007) Release of outer membrane vesicles by Gram-negative bacteria is a novel envelope stress response. *Mol. Microbiol.* **63**, 545–558, https://doi.org/10.1111/j.1365-2958.2006.05522.x
47 Ojima, Y., Sawabe, T., Konami, K. and Azuma, M. (2020) Construction of hypervesiculation *Escherichia coli* strains and application for secretory protein production. *Biotechnol. Bioeng.* **117**, 701–709, https://doi.org/10.1002/bit.27239
48 Llamas, M.A., Ramos, J.L. and Rodriguez-Herva, J.J. (2000) Mutations in each of the *tol* genes of *Pseudomonas putida* reveal that they are critical for maintenance of outer membrane stability. *J. Bacteriol.* **182**, 4764–4772, https://doi.org/10.1128/JB.182.17.4764-4772.2000
49 Schwechheimer, C., Sullivan, C.J. and Kuehn, M.J. (2013) Envelope control of outer membrane vesicle production in Gram-negative bacteria. *Biochemistry* **52**, 3031–3040, https://doi.org/10.1021/bi400164t
50 Henderson, P.J.F., Maher, C., Elbourne, L.D.H., Eijkelkamp, B.A., Paulsen, I.T. and Hassan, K.A. (2021) Physiological functions of bacterial "multidrug" efflux pumps. *Chem. Rev.* **121**, 5417–5478, https://doi.org/10.1021/acs.chemrev.0c01226
51 Blanco, P., Hernando-Amado, S., Reales-Calderon, J., Corona, F., Lira, F., Alcalde-Rico, M. et al. (2016) Bacterial multidrug efflux pumps: much more than antibiotic resistance determinants. *Microorganisms* **4**, 14, https://doi.org/10.3390/microorganisms4010014
52 de Bont, J.A.M. and Kieboom, J. (2001) Identification and molecular characterization of an efflux system involved in *Pseudomonas putida* S12 multidrug resistance. *Microbiology* **147**, 43–51, https://doi.org/10.1099/00221287-147-1-43
53 Puja, H., Comment, G., Chassagne, S., Plésiat, P. and Jeannot, K. (2020) Coordinate overexpression of two RND efflux systems, ParXY and TtgABC, is responsible for multidrug resistance in *Pseudomonas putida*. *Environ. Microbiol.* **22**, 5222–5231, https://doi.org/10.1111/1462-2920.15200
54 Chuanchuen, R., Karkhoff-Schweizer, R.R. and Schweizer, H.P. (2003) High-level triclosan resistance in *Pseudomonas aeruginosa* is solely a result of efflux. *Am. J. Infect. Control* **31**, 124–127, https://doi.org/10.1067/mic.2003.11
55 Rojas, A., Duque, E., Mosqueda, G., Golden, G., Hurtado, A., Ramos, J.L. et al. (2001) Three efflux pumps are required to provide efficient tolerance to toluene in *Pseudomonas putida* DOT-T1E. *J. Bacteriol.* **183**, 3967–3973, https://doi.org/10.1128/JB.183.13.3967-3973.2001
56 Yao, X., Tao, F., Tang, H., Hu, H., Wang, W. and Xu, P. (2020) Unique regulator SrpR mediates crosstalk between efflux pumps TtgABC and SrpABC in *Pseudomonas putida* B6-2 (DSM 28064). *Mol. Microbiol.* **115**, 131–141
57 Henríquez, T., Stein, N.V. and Jung, H. (2020) Resistance to bipyridyls mediated by the TtgABC efflux system in *Pseudomonas putida* KT2440. *Front. Microbiol.* **11**, 1974, https://doi.org/10.3389/fmicb.2020.01974
58 Terán, W., Krell, T., Ramos, J.L. and Gallegos, M.-T. (2006) Effector-repressor interactions, binding of a single effector molecule to the operator-bound TtgR homodimer mediates derepression. *J. Biol. Chem.* **281**, 7102–7109, https://doi.org/10.1074/jbc.M511095200
59 Kieboom, J., Dennis, J.J., de Bont, J.A.M. and Zylstra, G.J. (1998) Identification and molecular characterization of an efflux pump involved in *Pseudomonas putida* S12 solvent tolerance. *J. Biol. Chem.* **273**, 85–91, https://doi.org/10.1074/jbc.273.1.85
60 Basler, G., Thompson, M., Tullman-Ercek, D. and Keasling, J. (2018) A *Pseudomonas putida* efflux pump acts on short-chain alcohols. *Biotechnol. Biofuels* **11**, 136, https://doi.org/10.1186/s13068-018-1133-9
61 Schempp, F.M., Hofmann, K.E., Mi, J., Kirchner, F., Meffert, A., Schewe, H. et al. (2020) Investigation of monoterpenoid resistance mechanisms in *Pseudomonas putida* and their consequences for biotransformations. *Appl. Microbiol. Biotechnol.* **104**, 5519–5533, https://doi.org/10.1007/s00253-020-10566-3
62 Jayakody, L.N., Johnson, C.W., Whitham, J.M., Giannone, R.J., Black, B.A., Cleveland, N.S. et al. (2018) Thermochemical wastewater valorization via enhanced microbial toxicity tolerance. *Energy Environ. Sci.* **11**, 1625–1638, https://doi.org/10.1039/C8EE00460A
63 Godoy, P., Molina-Henares, A.J., De La Torre, J., Duque, E. and Ramos, J.L. (2010) Characterization of the RND family of multidrug efflux pumps: *in silico* to *in vivo* confirmation of four functionally distinct subgroups. *Microb. Biotechnol.* **3**, 691–700, https://doi.org/10.1111/j.1751-7915.2010.00189.x
64 Passarelli-Araujo, H., Jacobs, S.H., Franco, G.R. and Venancio, T.M. (2021) Phylogenetic and population structure analyses uncover pervasive misclassification and help assessing the biosafety of *Pseudomonas alloputida* for biotechnological applications. *bioRxiv*, https://doi.org/10.1101/2020.12.22.423983
65 Sekiya, H., Mima, T., Morita, Y., Kuroda, T., Mizushima, T. and Tsuchiya, T. (2003) Functional cloning and characterization of a multidrug efflux pump, MexHI-OpmD, from a *Pseudomonas aeruginosa* mutant. *Antimicrob. Agents Chemother.* **47**, 2990–2992, https://doi.org/10.1128/AAC.47.9.2990-2992.2003

Essays in Biochemistry (2021) EBC20200173
https://doi.org/10.1042/EBC20200173

66 Wang, Y., Morimoto, S., Ogawa, N. and Fujii, T. (2011) A survey of the cellular responses in *Pseudomonas putida* KT2440 growing in sterilized soil by microarray analysis. *FEMS Microbiol. Ecol.* **78**, 220–232, https://doi.org/10.1111/j.1574-6941.2011.01146.x
67 Sakhtah, H., Koyama, L., Zhang, Y., Morales, D.K., Fields, B.L., Price-Whelan, A. et al. (2016) The *Pseudomonas aeruginosa* efflux pump MexGHI-OpmD transports a natural phenazine that controls gene expression and biofilm development. *Proc. Natl. Acad. Sci. U.S.A.* **113**, E3538–E3547, https://doi.org/10.1073/pnas.1600424113
68 Verhoef, S., Ballerstedt, H., Volkers, R.J.M., de Winde, J.H. and Ruijssenaars, H.J. (2010) Comparative transcriptomics and proteomics of *p*-hydroxybenzoate producing *Pseudomonas putida* S12: novel responses and implications for strain improvement. *Appl. Microbiol. Biotechnol.* **87**, 679–690, https://doi.org/10.1007/s00253-010-2626-z
69 Ma, C., Mu, Q., Xue, Y., Xue, Y., Yu, B. and Ma, Y. (2020) One major facilitator superfamily transporter is responsible for propionic acid tolerance in *Pseudomonas putida* KT2440. *Microb. Biotechnol.* **14**, 386–391
70 Volmer, J., Neumann, C., Bühler, B. and Schmid, A. (2014) Engineering of *Pseudomonas taiwanensis* VLB120 for constitutive solvent tolerance and increased specific styrene epoxidation activity. *Appl. Environ. Microbiol.* **80**, 6539–6548, https://doi.org/10.1128/AEM.01940-14
71 Rojas, A., Duque, E., Schmid, A., Hurtado, A., Ramos, J.-L. and Segura, A. (2004) Biotransformation in double-phase systems: physiological responses of *Pseudomonas putida* DOT-T1E to a double phase made of aliphatic alcohols and biosynthesis of substituted catechols. *Appl. Environ. Microbiol.* **70**, 3637–3643, https://doi.org/10.1128/AEM.70.6.3637-3643.2004
72 Helmann, T.C., Ongsarte, C.L., Lam, J., Deutschbauer, A.M. and Lindow, S.E. (2019) Genome-wide transposon screen of a *Pseudomonas syringae mexB* mutant reveals the substrates of efflux transporters. *mBio* **10**, e02614–19, https://doi.org/10.1128/mBio.02614-19
73 Roca, A., Rodríguez-Herva, J.-J., Duque, E. and Ramos, J.L. (2008) Physiological responses of *Pseudomonas putida* to formaldehyde during detoxification. *Microb. Biotechnol.* **1**, 158–169, https://doi.org/10.1111/j.1751-7915.2007.00014.x
74 Henriquez, T., Baldow, T., Lo, Y.K., Weydert, D., Brachmann, A. and Jung, H. (2020) Involvement of MexS and MexEF-OprN in resistance to toxic ion chelators in *Pseudomonas putida* KT2440. *Microorganisms* **8**, 1782, https://doi.org/10.3390/microorganisms8111782
75 Simon, O., Klaiber, I., Huber, A. and Pfannstiel, J. (2014) Comprehensive proteome analysis of the response of *Pseudomonas putida* KT2440 to the flavor compound vanillin. *J. Proteomics* **109**, 212–227, https://doi.org/10.1016/j.jprot.2014.07.006
76 Masuda, N., Sakagawa, E., Ohya, S., Gotoh, N., Tsujimoto, H. and Nishino, T. (2000) Contribution of the MexX-MexY-OprM efflux system to intrinsic resistance in *Pseudomonas aeruginosa*. *Antimicrob. Agents Chemother.* **44**, 2242–2246, https://doi.org/10.1128/AAC.44.9.2242-2246.2000
77 García, V., Godoy, P., Daniels, C., Hurtado, A., Ramos, J.-L. and Segura, A. (2009) Functional analysis of new transporters involved in stress tolerance in *Pseudomonas putida* DOT-T1E. *Environ. Microbiol. Rep.* **2**, 389–395, https://doi.org/10.1111/j.1758-2229.2009.00093.x
78 Volkers, R.J.M., Ballerstedt, H., Ruijssenaars, H., de Bont, J.A.M., de Winde, J.H. and Wery, J. (2009) *trgI,* toluene repressed gene I, a novel gene involved in toluene-tolerance in *Pseudomonas putida* S12. *Extremophiles* **13**, 283–297, https://doi.org/10.1007/s00792-008-0216-0
79 Li, X., Poole, K. and Nikaido, H. (2003) Contributions of MexAB-OprM and an EmrE homolog to intrinsic resistance of *Pseudomonas aeruginosa* to aminoglycosides and dyes. *Antimicrob. Agents Chemother.* **47**, 27–33, https://doi.org/10.1128/AAC.47.1.27-33.2003
80 Nie, L., Grell, E., Malviya, V.N., Xie, H., Wang, J. and Michel, H. (2016) Identification of the high-affinity substrate-binding site of the multidrug and toxic compound extrusion (MATE) family transporter from *Pseudomonas stutzeri*. *J. Biol. Chem.* **291**, 15503–15514, https://doi.org/10.1074/jbc.M116.728618
81 Maslowska, K.H., Makiela-Dzbenska, K. and Fijalkowska, I.J. (2019) The SOS system: A complex and tightly regulated response to DNA damage. *Environ. Mol. Mutagen.* **60**, 368–384, https://doi.org/10.1002/em.22267
82 Roca, A., Rodríguez-Herva, J.-J., Duque, E. and Ramos, J.L. (2008) Physiological responses of *Pseudomonas putida* to formaldehyde during detoxification. *Microb. Biotechnol.* **1**, 158–169, https://doi.org/10.1111/j.1751-7915.2007.00014.x
83 Hartl, F.U., Bracher, A. and Hayer-Hartl, M. (2011) Molecular chaperones in protein folding and proteostasis. *Nature* **475**, 324–332, https://doi.org/10.1038/nature10317
84 Bösl, B., Grimminger, V. and Walter, S. (2006) The molecular chaperone Hsp104—a molecular machine for protein disaggregation. *J. Struct. Biol.* **156**, 139–148, https://doi.org/10.1016/j.jsb.2006.02.004
85 Mukhopadhyay, A. (2015) Tolerance engineering in bacteria for the production of advanced biofuels and chemicals. *Trends Microbiol.* **23**, 498–508, https://doi.org/10.1016/j.tim.2015.04.008
86 Galkin, K.I. and Ananikov, V.P. (2019) When will 5-hydroxymethylfurfural, the "sleeping giant" of sustainable chemistry, awaken? *ChemSusChem* **12**, 2976–2982, https://doi.org/10.1002/cssc.201900592
87 Kunjapur, A.M., Tarasova, Y. and Prather, K.L.J. (2014) Synthesis and accumulation of aromatic aldehydes in an engineered strain of *Escherichia coli*. *J. Am. Chem. Soc.* **136**, 11644–11654, https://doi.org/10.1021/ja506664a
88 Xu, Q., Zheng, Z., Zou, L., Zhang, C., Yang, F., Zhou, K. et al. (2020) A versatile *Pseudomonas putida* KT2440 with new ability: selective oxidation of 5-hydroxymethylfurfural to 5-hydroxymethyl-2-furancarboxylic acid. *Bioprocess. Biosyst. Eng.* **43**, 67–73, https://doi.org/10.1007/s00449-019-02205-7
89 Koopman, F., Wierckx, N., de Winde, J.H. and Ruijssenaars, H.J. (2010) Efficient whole-cell biotransformation of 5-(hydroxymethyl)furfural into FDCA, 2,5-furandicarboxylic acid. *Bioresour. Technol.* **101**, 6291–6296, https://doi.org/10.1016/j.biortech.2010.03.050
90 Hsu, C.-T., Kuo, Y.-C., Liu, Y.-C. and Tsai, S.-L. (2020) Green conversion of 5-hydroxymethylfurfural to furan-2,5-dicarboxylic acid by heterogeneous expression of 5-hydroxymethylfurfural oxidase in *Pseudomonas putida* S12. *Microb. Biotechnol.* **13**, 1094–1102, https://doi.org/10.1111/1751-7915.13564
91 Pham, N.N., Chen, C.-Y., Li, H., Nguyen, M.T.T., Nguyen, P.K.P., Tsai, S.-L. et al. (2020) Engineering stable *Pseudomonas putida* S12 by CRISPR for 2,5-furandicarboxylic acid (FDCA) production. *ACS Synth. Biol.* **9**, 1138–1149, https://doi.org/10.1021/acssynbio.0c00006

PORTLAND PRESS

Essays in Biochemistry (2021) EBC20200173
https://doi.org/10.1042/EBC20200173

92 Wehrmann, M., Billard, P., Martin-Meriadec, A., Zegeye, A. and Klebensberger, J. (2017) Functional role of lanthanides in enzymatic activity and transcriptional regulation of pyrroloquinoline quinone-dependent alcohol dehydrogenases in *Pseudomonas putida* KT2440. *mBio* **8**, e00570–17, https://doi.org/10.1128/mBio.00570-17

93 Li, W.-J., Narancic, T., Kenny, S.T., Niehoff, P.-J., O'Connor, K., Blank, L.M. et al. (2020) Unraveling 1,4-butanediol metabolism in *Pseudomonas putida* KT2440. *Front. Microbiol.* **11**, 382, https://doi.org/10.3389/fmicb.2020.00382

94 Winsor, G.L., Griffiths, E.J., Lo, R., Dhillon, B.K., Shay, J.A. and Brinkman, F.S.L. (2016) Enhanced annotations and features for comparing thousands of *Pseudomonas* genomes in the Pseudomonas genome database. *Nucleic Acids Res.* **44**, D646–D653, https://doi.org/10.1093/nar/gkv1227

95 Zheng, Z., Xu, Q., Tan, H., Zhou, F. and Ouyang, J. (2020) Selective biosynthesis of furoic acid from furfural by *Pseudomonas putida* and identification of molybdate transporter involvement in furfural oxidation. *Front. Chem.* **8**, 587456, https://doi.org/10.3389/fchem.2020.587456

96 Graf, N. and Altenbuchner, J. (2014) Genetic engineering of *Pseudomonas putida* KT2440 for rapid and high-yield production of vanillin from ferulic acid. *Appl. Microbiol. Biotechnol.* **98**, 137–149, https://doi.org/10.1007/s00253-013-5303-1

97 Adewunmi, Y., Namjilsuren, S., Walker, W.D., Amato, D.N., Amato, D.V., Mavrodi, O.V. et al. (2019) Antimicrobial activity of, and cellular pathways targeted by, *p*-anisaldehyde and epigallocatechin gallate in the opportunistic human pathogen *Pseudomonas aeruginosa*. *Appl. Environ. Microbiol.* **86**, e02482–19, https://doi.org/10.1128/AEM.02482-19

98 Li, W.-J., Jayakody, L.N., Franden, M.A., Wehrmann, M., Daun, T., Hauer, B. et al. (2019) Laboratory evolution reveals the metabolic and regulatory basis of ethylene glycol metabolism by *Pseudomonas putida* KT2440. *Environ. Microbiol.* **21**, 3669–3682, https://doi.org/10.1111/1462-2920.14703

99 Franden, M.A., Jayakody, L.N., Li, W.-J., Wagner, N.J., Cleveland, N.S., Michener, W.E. et al. (2018) Engineering *Pseudomonas putida* KT2440 for efficient ethylene glycol utilization. *Metab. Eng.* **48**, 197–207, https://doi.org/10.1016/j.ymben.2018.06.003

100 Akkaya, Ö., Pérez-Pantoja, D.R., Calles, B., Nikel, P.I. and de Lorenzo, V. (2018) The metabolic redox regime of *Pseudomonas putida* tunes its evolvability toward novel xenobiotic substrates. *mBio* **9**, e01512–18, https://doi.org/10.1128/mBio.01512-18

101 Nikel, P.I., Fuhrer, T., Chavarría, M., Sánchez-Pascuala, A., Sauer, U. and de Lorenzo, V. (2021) Reconfiguration of metabolic fluxes in *Pseudomonas putida* as a response to sub-lethal oxidative stress. *ISME J.*, https://doi.org/10.1038/s41396-020-00884-9

102 Di Gioia, D., Luziatelli, F., Negroni, A., Ficca, A.G., Fava, F. and Ruzzi, M. (2011) Metabolic engineering of *Pseudomonas fluorescens* for the production of vanillin from ferulic acid. *J. Biotechnol.* **156**, 309–316, https://doi.org/10.1016/j.jbiotec.2011.08.014

103 Reva, O.N., Weinel, C., Weinel, M., Boöhm, K., Stjepandic, D., Hoheisel, J.D. et al. (2006) Functional genomics of stress response in *Pseudomonas putida* KT2440. *J. Bacteriol.* **188**, 4079–4092, https://doi.org/10.1128/JB.00101-06

104 Ramos, J.L., Duque, E., Godoy, P. and Segura, A. (1998) Efflux pumps involved in toluene tolerance in *Pseudomonas putida* DOT-T1E. *J. Bacteriol.* **180**, 3323–3329, https://doi.org/10.1128/JB.180.13.3323-3329.1998

105 Li, X.-Z., Zhang, L. and Poole, K. (1998) Role of the multidrug efflux systems of *Pseudomonas aeruginosa* in organic solvent tolerance. *J. Bacteriol.* **180**, 2987–2991, https://doi.org/10.1128/JB.180.11.2987-2991.1998

106 Kapardar, R.K., Ranjan, R., Grover, A., Puri, M. and Sharma, R. (2010) Identification and characterization of genes conferring salt tolerance to *Escherichia coli* from pond water metagenome. *Bioresour. Technol.* **101**, 3917–3924, https://doi.org/10.1016/j.biortech.2010.01.017

107 Louis, P. and Galinski, E.A. (1997) Characterization of genes for the biosynthesis of the compatible solute ectoine from *Marinococcus halophilus* and osmoregulated expression in *Escherichia coli*. *Microbiology* **143**, 1141–1149, https://doi.org/10.1099/00221287-143-4-1141

108 Abraham, W.P., Raghunandanan, S., Gopinath, V., Suryaletha, K. and Thomas, S. (2020) Deciphering the cold adaptive mechanisms in *Pseudomonas psychrophila* MTCC12324 isolated from the arctic at 79° N. *Curr. Microbiol.* **77**, 2345–2355, https://doi.org/10.1007/s00284-020-02006-2

109 Hosseini, R., Kuepper, J., Koebbing, S., Blank, L.M., Wierckx, N. and Winde, J.H. (2017) Regulation of solvent tolerance in *Pseudomonas putida* S12 mediated by mobile elements. *Microb. Biotechnol.* **10**, 1558–1568, https://doi.org/10.1111/1751-7915.12495

110 Dunlop, M.J., Dossani, Z.Y., Szmidt, H.L., Chu, H.C., Lee, T.S., Keasling, J.D. et al. (2011) Engineering microbial biofuel tolerance and export using efflux pumps. *Mol. Syst. Biol.* **7**, 487, https://doi.org/10.1038/msb.2011.21

111 Sandberg, T.E., Salazar, M.J., Weng, L.L., Palsson, B.O. and Feist, A.M. (2019) The emergence of adaptive laboratory evolution as an efficient tool for biological discovery and industrial biotechnology. *Metab. Eng.* **56**, 1–16, https://doi.org/10.1016/j.ymben.2019.08.004

112 Kusumawardhani, H., Furtwängler, B., Blommestijn, M., Kaltenytė, A., van der Poel, J., Kolk, J. et al. (2021) Adaptive laboratory evolution restores solvent tolerance in plasmid-cured *Pseudomonas putida* S12: a molecular analysis. *Appl. Environ. Microbiol.* **87**, e00041–21, https://doi.org/10.1128/AEM.00041-21

113 Mohamed, E.T., Werner, A.Z., Salvachúa, D., Singer, C.A., Szostkiewicz, K., Rafael Jiménez-Díaz, M. et al. (2020) Adaptive laboratory evolution of *Pseudomonas putida* KT2440 improves *p*-coumaric and ferulic acid catabolism and tolerance. *Metab. Eng. Commun.* **11**, e00143, https://doi.org/10.1016/j.mec.2020.e00143

114 Kuepper, J., Otto, M., Dickler, J., Behnken, S., Magnus, J., Jäger, G. et al. (2020) Adaptive laboratory evolution of *Pseudomonas putida* and *Corynebacterium glutamicum* to enhance anthranilate tolerance. *Microbiology* **166**, 1025–1037, https://doi.org/10.1099/mic.0.000982

115 Thompson, M.G., Incha, M.R., Pearson, A.N., Schmidt, M., Sharpless, W.A., Eiben, C.B. et al. (2020) Fatty acid and alcohol metabolism in *Pseudomonas putida:* functional analysis using random barcode transposon sequencing. *Appl. Environ. Microbiol.* **86**, e01665–20, https://doi.org/10.1128/AEM.01665-20

116 Glebes, T.Y., Sandoval, N.R., Gillis, J.H. and Gill, R.T. (2015) Comparison of genome-wide selection strategies to identify furfural tolerance genes in *Escherichia coli*. *Biotechnol. Bioeng.* **112**, 129–140, https://doi.org/10.1002/bit.25325

117 Roncarati, D. and Scarlato, V. (2017) Regulation of heat-shock genes in bacteria: from signal sensing to gene expression output. *FEMS Microbiol. Rev.* **41**, 549–574, https://doi.org/10.1093/femsre/fux015

118 Shingler, V. (2003) Integrated regulation in response to aromatic compounds: from signal sensing to attractive behaviour. *Environ. Microbiol.* **5**, 1226–1241, https://doi.org/10.1111/j.1462-2920.2003.00472.x

Essays in Biochemistry (2021) EBC20200173
https://doi.org/10.1042/EBC20200173

119 Vogt, S.L. and Raivio, T.L. (2012) Just scratching the surface: an expanding view of the Cpx envelope stress response. *FEMS Microbiol. Lett.* **326**, 2–11, https://doi.org/10.1111/j.1574-6968.2011.02406.x
120 Wynands, B., Otto, M., Runge, N., Preckel, S., Polen, T., Blank, L.M. et al. (2019) Streamlined *Pseudomonas taiwanensis* VLB120 chassis strains with improved bioprocess features. *ACS Synth. Biol.* **8**, 2036–2050, https://doi.org/10.1021/acssynbio.9b00108
121 Putriņš, M., Ilves, H., Lilje, L., Kivisaar, M. and Hõrak, R. (2010) The impact of ColRS two-component system and TtgABC efflux pump on phenol tolerance of *Pseudomonas putida* becomes evident only in growing bacteria. *BMC Microbiol.* **10**, 110, https://doi.org/10.1186/1471-2180-10-110
122 Blank, L.M., Ionidis, G., Ebert, B.E., Bühler, B. and Schmid, A. (2008) Metabolic response of *Pseudomonas putida* during redox biocatalysis in the presence of a second octanol phase. *FEBS J.* **275**, 5173–5190, https://doi.org/10.1111/j.1742-4658.2008.06648.x
123 Isken, S., Derks, A., Wolffs, P.F.G. and de Bont, J.A.M. (1999) Effect of organic solvents on the yield of solvent-tolerant *Pseudomonas putida* S12. *Appl. Environ. Microbiol.* **65**, 2631–2635, https://doi.org/10.1128/AEM.65.6.2631-2635.1999
124 Bollinger, A., Thies, S., Katzke, N. and Jaeger, K. (2020) The biotechnological potential of marine bacteria in the novel lineage of *Pseudomonas pertucinogena*. *Microb. Biotechnol.* **13**, 19–31, https://doi.org/10.1111/1751-7915.13288
125 Cruden, D.L., Wolfram, J.H., Rogers, R.D. and Gibson, D.T. (1992) Physiological properties of a *Pseudomonas* strain which grows with *p*-xylene in a two-phase (organic-aqueous) medium. *Appl. Environ. Microbiol.* **58**, 2723–2729, https://doi.org/10.1128/AEM.58.9.2723-2729.1992
126 Ramos, J.L., Duque, E., Huertas, M.J. and Haïdour, A. (1995) Isolation and expansion of the catabolic potential of a *Pseudomonas putida* strain able to grow in the presence of high concentrations of aromatic hydrocarbons. *J. Bacteriol.* **177**, 3911–3916, https://doi.org/10.1128/JB.177.14.3911-3916.1995
127 Bator, I., Wittgens, A., Rosenau, F., Tiso, T. and Blank, L.M. (2020) Comparison of three xylose pathways in *Pseudomonas putida* KT2440 for the synthesis of valuable products. *Front. Bioeng. Biotechnol.* **7**, 480, https://doi.org/10.3389/fbioe.2019.00480
128 Gong, Z., Nielsen, J. and Zhou, Y.J. (2017) Engineering robustness of microbial cell factories. *Biotechnol. J.* **12**, 1700014, https://doi.org/10.1002/biot.201700014
129 Qi, Y., Liu, H., Chen, X. and Liu, L. (2019) Engineering microbial membranes to increase stress tolerance of industrial strains. *Metab. Eng.* **53**, 24–34, https://doi.org/10.1016/j.ymben.2018.12.010
130 Schalck, T., Van den Bergh, B. and Michiels, J. (2021) Increasing solvent tolerance to improve microbial production of alcohols, terpenoids and aromatics. *Microorganisms* **9**, 249, https://doi.org/10.3390/microorganisms9020249
131 Martínez-García, E. and de Lorenzo, V. (2017) Molecular tools and emerging strategies for deep genetic/genomic refactoring of *Pseudomonas*. *Curr. Opin. Biotechnol.* **47**, 120–132, https://doi.org/10.1016/j.copbio.2017.06.013
132 Zobel, S., Benedetti, I., Eisenbach, L., de Lorenzo, V., Wierckx, N. and Blank, L.M. (2015) Tn7-based device for calibrated heterologous gene expression in *Pseudomonas putida*. *ACS Synth. Biol.* **4**, 1341–1351, https://doi.org/10.1021/acssynbio.5b00058
133 Calero, P., Jensen, S.I. and Nielsen, A.T. (2016) Broad-host-range ProUSER vectors enable fast characterization of inducible promoters and optimization of *p*-coumaric acid production in *Pseudomonas putida* KT2440. *ACS Synth. Biol.* **5**, 741–753, https://doi.org/10.1021/acssynbio.6b00081
134 Elmore, J.R., Furches, A., Wolff, G.N., Gorday, K. and Guss, A.M. (2017) Development of a high efficiency integration system and promoter library for rapid modification of *Pseudomonas putida* KT2440. *Metab. Eng. Commun.* **5**, 1–8, https://doi.org/10.1016/j.meteno.2017.04.001
135 Martínez-García, E., Goñi-Moreno, A., Bartley, B., McLaughlin, J., Sánchez-Sampedro, L., Pascual del Pozo, H. et al. (2020) SEVA 3.0: an update of the Standard European Vector Architecture for enabling portability of genetic constructs among diverse bacterial hosts. *Nucleic Acids Res.* **48**, D1164–D1170, https://doi.org/10.1093/nar/gkz1024
136 Jahn, M., Vorpahl, C., Türkowsky, D., Lindmeyer, M., Bühler, B., Harms, H. et al. (2014) Accurate determination of plasmid copy number of flow-sorted cells using droplet digital PCR. *Anal. Chem.* **86**, 5969–5976, https://doi.org/10.1021/ac501118v
137 Lindmeyer, M., Jahn, M., Vorpahl, C., Müller, S., Schmid, A. and Bühler, B. (2015) Variability in subpopulation formation propagates into biocatalytic variability of engineered *Pseudomonas putida* strains. *Front. Microbiol.* **6**, 1042, https://doi.org/10.3389/fmicb.2015.01042
138 Mi, J., Sydow, A., Schempp, F., Becher, D., Schewe, H., Schrader, J. et al. (2016) Investigation of plasmid-induced growth defect in *Pseudomonas putida*. *J. Biotechnol.* **231**, 167–173, https://doi.org/10.1016/j.jbiotec.2016.06.001
139 Nikel, P.I. and de Lorenzo, V. (2013) Implantation of unmarked regulatory and metabolic modules in Gram-negative bacteria with specialised mini-transposon delivery vectors. *J. Biotechnol.* **163**, 143–154, https://doi.org/10.1016/j.jbiotec.2012.05.002
140 Domröse, A., Hage-Hülsmann, J., Thies, S., Weihmann, R., Kruse, L., Otto, M. et al. (2019) *Pseudomonas putida* rDNA is a favored site for the expression of biosynthetic genes. *Sci. Rep.* **9**, 7028, https://doi.org/10.1038/s41598-019-43405-1
141 Choi, K.R., Cho, J.S., Cho, I.J., Park, D. and Lee, S.Y. (2018) Markerless gene knockout and integration to express heterologous biosynthetic gene clusters in *Pseudomonas putida*. *Metab. Eng.* **47**, 463–474, https://doi.org/10.1016/j.ymben.2018.05.003
142 Martin-Pascual, M., Batianis, C., Bruinsma, L., Asin-Garcia, E., Garcia-Morales, L., Weusthuis, R.A. et al. (2021) A navigation guide of synthetic biology tools for *Pseudomonas putida*. *Biotechnol. Adv.* **49**, 107732, https://doi.org/10.1016/j.biotechadv.2021.107732
143 Thummeepak, R., Pooalai, R., Harrison, C., Gannon, L., Thanwisai, A., Chantratita, N. et al. (2020) Essential gene clusters involved in copper tolerance identified in *Acinetobacter baumannii* clinical and environmental isolates. *Pathogens* **9**, 60, https://doi.org/10.3390/pathogens9010060
144 Zhang, C. and Hong, K. (2020) Production of terpenoids by synthetic biology approaches. *Front. Bioeng. Biotechnol.* **8**, 347, https://doi.org/10.3389/fbioe.2020.00347
145 Kohlstedt, M., Starck, S., Barton, N., Stolzenberger, J., Selzer, M., Mehlmann, K. et al. (2018) From lignin to nylon: cascaded chemical and biochemical conversion using metabolically engineered *Pseudomonas putida*. *Metab. Eng.* **47**, 279–293, https://doi.org/10.1016/j.ymben.2018.03.003
146 Sudarsan, S., Blank, L.M., Dietrich, A., Vielhauer, O., Takors, R., Schmid, A. et al. (2016) Dynamics of benzoate metabolism in *Pseudomonas putida* KT2440. *Metab. Eng. Commun.* **3**, 97–110, https://doi.org/10.1016/j.meteno.2016.03.005

PORTLAND PRESS

Essays in Biochemistry (2021) EBC20200173
https://doi.org/10.1042/EBC20200173

147 Brooks, S.J., Doyle, E.M., Hewage, C., Malthouse, J.P.G., Duetz, W. and O'Connor, K.E. (2004) Biotransformation of halophenols using crude cell extracts of *Pseudomonas putida* F6. *Appl. Microbiol. Biotechnol.* **64**, 486–492, https://doi.org/10.1007/s00253-003-1488-z
148 Lynch, R.M., Woodley, J.M. and Lilly, M.D. (1997) Process design for the oxidation of fluorobenzene to fluorocatechol by *Pseudomonas putida*. *J. Biotechnol.* **58**, 167–175, https://doi.org/10.1016/S0168-1656(97)00146-6
149 Arensdorf, J.J. and Focht, D.D. (1994) Formation of chlorocatechol meta cleavage products by a Pseudomonad during metabolism of monochlorobiphenyls. *Appl. Environ. Microbiol.* **60**, 2884–2889, https://doi.org/10.1128/AEM.60.8.2884-2889.1994
150 Jiménez, J.I., Pérez-Pantoja, D., Chavarría, M., Díaz, E. and de Lorenzo, V. (2014) A second chromosomal copy of the *catA* gene endows *Pseudomonas putida* mt-2 with an enzymatic safety valve for excess of catechol. *Environ. Microbiol.* **16**, 1767–1778, https://doi.org/10.1111/1462-2920.12361
151 Brands, S., Brass, H.U.C., Klein, A.S., Pietruszka, J., Ruff, A.J. and Schwaneberg, U. (2020) A colourimetric high-throughput screening system for directed evolution of prodigiosin ligase PigC. *Chem. Commun.* **56**, 8631–8634, https://doi.org/10.1039/D0CC02181D
152 Brands, S., Sikkens, J.G., Davari, M.D., Brass, H.U.C., Klein, A.S., Pietruszka, J. et al. (2021) Understanding substrate binding and the role of gatekeeping residues in PigC access tunnels. *Chem. Commun.* **57**, 2681–2684, https://doi.org/10.1039/D0CC08226K
153 Incha, M.R., Thompson, M.G., Blake-Hedges, J.M., Liu, Y., Pearson, A.N., Schmidt, M. et al. (2020) Leveraging host metabolism for bisdemethoxycurcumin production in *Pseudomonas putida*. *Metab. Eng. Commun.* **10**, e00119, https://doi.org/10.1016/j.mec.2019.e00119
154 Young, R., Haines, M., Storch, M. and Freemont, P.S. (2021) Combinatorial metabolic pathway assembly approaches and toolkits for modular assembly. *Metab. Eng.* **63**, 81–101, https://doi.org/10.1016/j.ymben.2020.12.001
155 Casini, A., Storch, M., Baldwin, G.S. and Ellis, T. (2015) Bricks and blueprints: methods and standards for DNA assembly. *Nat. Rev. Mol. Cell Biol.* **16**, 568–576, https://doi.org/10.1038/nrm4014
156 Valenzuela-Ortega, M. and French, C. (2021) Joint universal modular plasmids (JUMP): A flexible vector platform for synthetic biology. *Synth. Biol.* **6**, 1–11, https://doi.org/10.1093/synbio/ysab003
157 Li, J. and Ye, B.-C. (2021) Metabolic engineering of *Pseudomonas putida* KT2440 for high-yield production of protocatechuic acid. *Bioresour. Technol.* **319**, 124239, https://doi.org/10.1016/j.biortech.2020.124239
158 Mutalik, V.K., Guimaraes, J.C., Cambray, G., Lam, C., Christoffersen, M.J., Mai, Q.-A. et al. (2013) Precise and reliable gene expression via standard transcription and translation initiation elements. *Nat. Methods* **10**, 354–360, https://doi.org/10.1038/nmeth.2404
159 Tan, S.Z., Reisch, C.R. and Prather, K.L.J. (2018) A robust CRISPR interference gene repression system in *Pseudomonas*. *J. Bacteriol.* **200**, e00575–e00617, https://doi.org/10.1128/JB.00575-17
160 Kim, S.K., Yoon, P.K., Kim, S., Woo, S., Rha, E., Lee, H. et al. (2020) CRISPR interference-mediated gene regulation in *Pseudomonas putida* KT2440. *Microb. Biotechnol.* **13**, 210–221, https://doi.org/10.1111/1751-7915.13382
161 Batianis, C., Kozaeva, E., Damalas, S.G., Martín-Pascual, M., Volke, D.C., Nikel, P.I. et al. (2020) An expanded CRISPRi toolbox for tunable control of gene expression in *Pseudomonas putida*. *Microb. Biotechnol.* **13**, 368–385, https://doi.org/10.1111/1751-7915.13533
162 Volke, D.C., Turlin, J., Mol, V. and Nikel, P.I. (2020) Physical decoupling of XylS/ Pm regulatory elements and conditional proteolysis enable precise control of gene expression in *Pseudomonas putida*. *Microb. Biotechnol.* **13**, 222–232, https://doi.org/10.1111/1751-7915.13383
163 Zhang, F., Carothers, J.M. and Keasling, J.D. (2012) Design of a dynamic sensor-regulator system for production of chemicals and fuels derived from fatty acids. *Nat. Biotechnol.* **30**, 354–359, https://doi.org/10.1038/nbt.2149
164 Lemmens, L.J.M., Ottmann, C. and Brunsveld, L. (2020) Conjugated protein domains as engineered scaffold proteins. *Bioconjug. Chem.* **31**, 1596–1603, https://doi.org/10.1021/acs.bioconjchem.0c00183
165 Conrado, R.J., Wu, G.C., Boock, J.T., Xu, H., Chen, S.Y., Lebar, T. et al. (2012) DNA-guided assembly of biosynthetic pathways promotes improved catalytic efficiency. *Nucleic Acids Res.* **40**, 1879–1889, https://doi.org/10.1093/nar/gkr888
166 Nieto-Domínguez, M. and Nikel, P.I. (2020) Intersecting xenobiology and neometabolism to bring novel chemistries to life. *ChemBioChem* **21**, 2551–2571, https://doi.org/10.1002/cbic.202000091

II.2. A genetic toolbox for engineering *P. putida*

PUBLICATION II

The modular pYT vector series employed for chromosomal gene integration and expression to produce carbazoles and glycolipids in *P. putida*

Robin Weihmann*, Sonja Kubicki*, **Nora Lisa Bitzenhofer**, Andreas Domröse, Isabel Bator, Lisa-Marie Kirschen, Franziska Kofler, Aileen Funk, Till Tiso, Lars M. Blank, Karl-Erich Jaeger, Thomas Drepper, Stephan Thies, Anita Loeschcke

FEMS Microbes (**2023**) 4:xtac030.

The online version is available at: 10.1093/femsmc/xtac030

Status: published

Supporting Information can be found in the Appendix (**Chapter V.1**)

Own contribution:

Planning and performing arcyriaflavin A experiments and analyzing the data, writing parts of the manuscript.

FEMS Microbes, 2023, 4, 1–17
DOI: 10.1093/femsmc/xtac030
Advance access publication date: 19 December 2022
Research Article – Microbes & Metabolism

The modular pYT vector series employed for chromosomal gene integration and expression to produce carbazoles and glycolipids in *P. putida*

Robin Weihmann[1,2], Sonja Kubicki[1,2], Nora Lisa Bitzenhofer[1], Andreas Domröse[1], Isabel Bator[2,3], Lisa-Marie Kirschen[1], Franziska Kofler[1], Aileen Funk[1], Till Tiso[2,3], Lars M. Blank[2,3], Karl-Erich Jaeger[1,2,4], Thomas Drepper[1,2], Stephan Thies[1,2,*], Anita Loeschcke[1,2,*]

[1]Institute of Molecular Enzyme Technology, Heinrich Heine University Düsseldorf at Forschungszentrum Jülich GmbH, 52428 Jülich, Germany
[2]Bioeconomy Science Center (BioSC), Forschungszentrum Jülich GmbH, 52425 Jülich, Germany
[3]iAMB - Institute of Applied Microbiology, ABBt - Aachen Biology and Biotechnology, RWTH Aachen University, 52074 Aachen, Germany
[4]Institute of Bio-and Geosciences IBG 1: Biotechnology, Forschungszentrum Jülich GmbH, 52428 Jülich, Germany
*Corresponding author: Institute of Molecular Enzyme Technology, Heinrich Heine University Düsseldorf at Forschungszentrum Jülich GmbH, Wilhelm-Johnen-Straße 52428 Jülich, Germany. E-mail: a.loeschcke@fz-juelich.de; s.thies@fz-juelich.de
#equally contributed
Editor: Swaine Chen

Abstract

The expression of biosynthetic genes in bacterial hosts can enable access to high-value compounds, for which appropriate molecular genetic tools are essential. Therefore, we developed a toolbox of modular vectors, which facilitate chromosomal gene integration and expression in *Pseudomonas putida* KT2440. To this end, we designed an integrative sequence, allowing customisation regarding the modes of integration (random, at *att*Tn7, or into the 16S rRNA gene), promoters, antibiotic resistance markers as well as fluorescent proteins and enzymes as transcription reporters. We thus established a toolbox of vectors carrying integrative sequences, designated as pYT series, of which we present 27 ready-to-use variants along with a set of strains equipped with unique 'landing pads' for directing a pYT interposon into one specific copy of the 16S rRNA gene. We used genes of the well-described violacein biosynthesis as reporter to showcase random Tn5-based chromosomal integration leading to constitutive expression and production of violacein and deoxyviolacein. Deoxyviolacein was likewise produced after gene integration into the 16S rRNA gene of *rrn* operons. Integration in the *att*Tn7 site was used to characterise the suitability of different inducible promoters and successive strain development for the metabolically challenging production of mono-rhamnolipids. Finally, to establish arcyriaflavin A production in *P. putida* for the first time, we compared different integration and expression modes, revealing integration at *att*Tn7 and expression with NagR/P_{nagAa} to be most suitable. In summary, the new toolbox can be utilised for the rapid generation of various types of *P. putida* expression and production strains.

Keywords: toolbox, chromosomal gene integration, synthetic biology, *Pseudomonas putida*, carbazoles, glycolipids

Introduction

Natural products represent a rich source for valuable chemical compounds. Heterologous expression of the respective biosynthetic genes is one key technology for studying the intriguing biochemical synthesis pathways or bioactivities of these natural products.

Aside from many other microbes (Ke and Yoshikuni 2020), the Gram-negative soil bacterium *Pseudomonas putida* has been established as a remarkable host for natural product biosynthesis (Loeschcke and Thies 2020, Weimer et al. 2020). While a truly wide range of applications has been reported, production of rhamnolipids and aromatic building blocks are counted to the most prominent ones (Loeschcke and Thies 2020, Schwanemann et al. 2020, Weimer et al. 2020). The bacterium's potential in this regard is linked to specific advantageous features, including simple cultivation, a versatile metabolism but low background of intrinsic natural products and a remarkable xenobiotic tolerance (Thorwall et al. 2020, Bitzenhofer et al. 2021). The strain KT2440 is, in addition, HV1 certified (Kampers, Volkers and Martins dos Santos 2019).

The rising number of studies in the field has shown that the cloning and expression strategy is decisive for the effectivity in the construction of expression strains. The previously common gene expression from plasmids typically requires the use of antibiotics and can come with growth defects and issues in the reproducibility of results (Mi et al. 2016, Cook et al. 2018). Therefore, integrative vectors, which are applicable in *P. putida*, have been built and multiple distinct tools targeting different integration sites have been established (Loeschcke and Thies 2020, Martín-Pascual et al. 2021). Here, the chosen site of integration might be a crucial factor to yield effective production strains. In previous studies, transposon integration at random chromosomal positions (Fu et al. 2008, Nikel and de Lorenzo 2013, Martínez-García et al. 2014, Domröse et al. 2017, Gemperlein et al. 2017, Thompson et al. 2020) or at the *att*Tn7 site (Choi and Schweizer 2006, Zobel et al. 2015, Hernandez-Arranz et al. 2019, Bator et al. 2020), as well as gene

Received: August 5, 2022. Revised: November 3, 2022. Accepted: December 16, 2022

integration at specific integration sites, which is realised by recombineering and rendered especially effective, e.g. by recombinases like RecET and aided by SacB, I-SceI or Cas9 (Elmore et al. 2017, Choi and Lee 2020, 2020, Cook et al. 2021), have emerged as particularly relevant. Among others, the ribosomal RNA encoding regions, have been identified as especially suitable for the integration and expression of biosynthetic gene clusters (Domröse et al. 2019, Otto et al. 2019, Nazareno, Acharya and Dumenyo 2021).

Modular concepts can facilitate effectivity in cloning procedures and minimise the effort for testing different strain construction strategies. Hence, the development of modular systems, which allow a standardised combination of DNA elements, represents a central aspect of the methodology in the field of Synthetic Biology and Biotechnology (Nora et al. 2019). The modularity of such systems can bring about full flexibility for the compilation of functional DNA 'parts', allowing re-usage of constructs and their effective usability upon exchange among researchers. The key concept implies that a variation of one component creates a new construct, but leaves the structure unimpaired in its changeability with regard to the same component or other components, thus retaining the construct's amenability to further changes.

In this sense, the design principles of the BioBrick standards were developed (Knight 2003), which have since accelerated research advances. Among others, the SEVA (Standard European Vector Architecture) plasmid series in particular is widely applied by the *Pseudomonas* research community (Martínez-García et al. 2020, Schuster and Reisch 2021, Valenzuela-Ortega and French 2021). In this context, target sequence independent cloning methods emerged that facilitated the effective cloning of parts in the desired sequence. The use of type IIS restriction enzymes represents one option to introduce standard coupling sequences of DNA parts for effective gene cluster cloning from multiple parts (Engler, Kandzia and Marillonnet 2008, van Dolleweerd et al. 2018, Valenzuela-Ortega and French 2021). These endonucleases catalyse DNA hydrolysis adjacent to their recognition site and can thus generate freely defined overhangs at the ends of DNA fragments, which can be employed as couplers (Yan et al. 2018). Moreover, ligation-independent methods, like commercially available In-Fusion® cloning, which are based on the annealing of complementary ends of DNA fragments, likewise enables the assembly of individual parts with standard coupling sequences (Bird et al. 2014). In addition, yeast-mediated recombineering, which is also independent of endonuclease recognition sequences, has proven to be useful for the assembly of plasmid constructs carrying larger gene clusters (Montiel et al. 2015, Weihmann et al. 2020, Alam et al. 2021).

For *P. putida* in particular, a series of plasmids with standardised architecture have been established (Calero, Jensen and Nielsen 2016, Martínez-García et al. 2020). In addition, we report here a toolkit for the effective standardised and ligase-independent assembly as well as chromosomal integration of larger gene clusters *via* a mode of choice and their expression, which can be useful for production strain construction.

We aimed to construct a designated set of vectors as a versatile toolbox for the effective construction of *P. putida* expression strains, which facilitates standardised cloning procedures and offers different chromosomal integration methods (transposons Tn5 or Tn7, and *rrn* interposon). Applications are demonstrated by establishing different biosyntheses: we employed the well-described violacein biosynthesis, which has been commonly used as reporter pathway before, for the validation of constitutive expression *via* Tn5-mediated integration aiming to exploit strong host promoters, and expression *via* specifically targeted *rrn* interposon integration. For metabolically challenging rhamnolipid biosynthesis, tight control of expression has been described as crucial for strain stability, hence it appeared most suitable to validate inducible expression modules introduced by Tn7 integrative elements. Finally, we used arcyriaflavin A biosynthesis, which has not been introduced in *P. putida* before, to compare all three integration and expression modes to identify the most suitable procedure for this case. We thus present the construction of strains constitutively producing violaceins, optimisation of a rhamnolipid expression module and first-time construction of an arcyriaflavin A producing strain.

Material and methods

Bacterial strains and standard cultivation media

Escherichia coli strains DH5α (Grant et al. 1990) and S17-1 (Simon, Priefer and Pühler 1983) as well as *P. putida* KT2440 (Bagdasarian et al. 1981, Nelson et al. 2002) and derived strains (all *P. putida* strains used for expression studies are listed in Table S6) were cultivated in LB (lysogeny broth) medium (10 g L^{-1} tryptone, 5 g L^{-1} yeast extract, 10 g L^{-1} NaCl, Carl Roth, Karlsruhe, Germany) or in TB medium (Terrific broth, modified, Carl-Roth Karlsruhe, Germany: 12 g L^{-1} Casein, enzymatically digested, 24 g L^{-1} yeast extract, 9.4 g L^{-1} dipotassium phosphate, 2.2 g L^{-1} monopotassium phosphate, 4 mL L^{-1} glycerol). LB agar plates were prepared with 15 g L^{-1} Agar-Agar, Kobe I, Carl Roth®, Karlsruhe, Germany. If appropriate, antibiotics were added at the following concentrations [μg mL^{-1}]: ampicillin (Ap), 100 (*E. coli*); kanamycin (Km), 50 (*E. coli*) or 25 (*P. putida*); streptomycin (Sm), 25 (*E. coli*); chloramphenicol (Cm), 25 (*E. coli*); gentamicin, 4 (*E. coli*) or 25 (*P. putida*); tetracycline, 10 (*E. coli*) or 50 (*P. putida*). Irgasan (25 μg mL^{-1}) was exclusively supplemented to agar plates after conjugation. *E. coli* was cultivated at 37°C, *P. putida* at 30°C. If not specified otherwise, cell densities given as OD (optical density) refer to measurements of liquid cultures in a Spectrophotometer (Genesys 20, ThermoFisher Scientific, Waltham, MA, USA) using 1 mL samples in cuvettes with 1 cm path length.

General molecular genetic methods

Standard molecular genetic methods were basically conducted as described previously (Green and Sambrook 2012). After amplification in *E. coli* DH5α, plasmid DNA was isolated with the innuPREP Plasmid Mini Kit (Analytik Jena AG, Jena, Germany). The DNeasy Blood & Tissue Kit (Quiagen® GmbH, Hilden, Germany) was used to isolate genomic DNA of bacterial strains. We utilised restriction endonuclease enzymes and phosphatase FastAP (ThermoFisher Scientific GmbH, Walkham, USA), as well as I-SceI (New England Biolabs, Ipswich, MA, US) according to the instructions given by manufacturers. The innuPREP DOUBLEpure Kit (Analytik Jena AG, Jena, Germany) was used to purify DNA fragments. Commercial services were employed for the synthesis of oligonucleotide primers as well as the sequences 'pYT_core' and '16S landing site', and moreover for sequencing of cloned vectors (Eurofins Genomics GmbH, Ebersberg, Germany). All used plasmids and oligonucleotides are listed in Tables S4 and S5.

Design of random DNA sequences

The YT_core sequence was generated *in silico* and obtained by gene synthesis. To create random DNA sequences as coupling regions for assembly cloning in pYT vectors, we used the Random DNA Sequence generator of the Sequence Manipulation Suite (Stothard 2000). In addition, we excluded canonical RBS sequences

Table 1. Ready-to-use pYT vector and strain sets.

pYT vector toolbox					
Vector	**Backbone resistance**	**Integrating resistance marker**	**Transcription reporter**	**Integration elements**	**Reference/GenBank ID**
pYTRW10K_0 × 5	Km^R	-	-	Tn*5*	This study/ON366562
pYTRW07K_0G5	Km^R	Gm^R	-	Tn*5*	This study/ON366565
pYTRW08K_0C5	Km^R	Cm^R	-	Tn*5*	This study/ON366564
pYTRW09K_0T5	Km^R	Tc^R	-	Tn*5*	This study/ON366563
pYTRW11K_0S5	Km^R	Sm^R	-	Tn*5*	This study/ON366561
pYTRW13K_3G5	Km^R	Gm^R	mCherry	Tn*5*	This study/ON366560
pYTRW14K_7G5	Km^R	Gm^R	LacZ	Tn*5*	This study/ON366559
pYTRW15K_2G5	Km^R	Gm^R	mTagBFP2	Tn*5*	This study/ON366558
pYTRW16K_1G5	Km^R	Gm^R	eYFP	Tn*5*	This study/ON366557
pYTRW17K_6G5	Km^R	Gm^R	PE-H	Tn*5*	This study/ON366556
pYTRW18K_3T5	Km^R	Tc^R	mCherry	Tn*5*	This study/ON366555
pYTRW20K_0Ti1	Km^R	Tc^R	-	LP-L/R	This study/ON366554
pYTRW28K_0Ti1	Km^R	Tc^R	-	LP-L/R_SacB	This study/ON366549
pYTRW21K_1Ti1	Km^R	Tc^R	eYFP	LP-L/R	This study/ON366553
pYTRW26K_1Ti1	Km^R	Tc^R	eYFP	LP-L/R_SacB	This study/ON366551
pYTRW22K_7Ti1	Km^R	Tc^R	LacZ	LP-L/R	This study/ON366552
pYTRW27K_7Ti1	Km^R	Tc^R	LacZ	LP-L/R_SacB	This study/ON366550
pYTSK00K_0 × 7	Km^R	-	-	Tn*7*	This study/ON366548
pYTSK01K_0G7	Km^R	Gm^R	-	Tn*7*	Tiso et al. 2020/MT522186
pYTSK02A_0G7	Ap^R	Gm^R	-	Tn*7*	This study/ON366547
pYTSK31K_1G7	Km^R	Gm^R	eYFP	Tn*7*	This study/ON366546
pYTSK54K_7G7	Km^R	Gm^R	LacZ	Tn*7*	This study/ON366545
pYTSK55K_2G7	Km^R	Gm^R	mTagBFP2	Tn*7*	This study/ON366544
pYTSK56K_3G7	Km^R	Gm^R	mCherry	Tn*7*	This study/ON366543
pYTSK58K_6G7	Km^R	Gm^R	PE-H	Tn*7*	This study/ON366542
pYTSK65K_8G7	Km^R	Gm^R	GUS	Tn*7*	This study/ON366541
pYTNB01K_1G7	Km^R	Gm^R	NagR/P_{nagAa}-eYFP	Tn*7*	This study/ON366566
pSEVA512S-16S-pad	Vector carries the landing pad with Gm^R and homology arms to 16S genes				This study/ON366567
Strains for pYT application					
Strain	**Resistance**	**Characteristics**			**Reference**
P. putida RW16SA	Gm^R	carries landing pad for pYT interposon in 16S gene of *rrnA*			This study
P. putida RW16SB	Gm^R	carries landing pad for pYT interposon in 16S gene of *rrnB*			This study
P. putida RW16SC	Gm^R	carries landing pad for pYT interposon in 16S gene of *rrnC*			This study
P. putida RW16SD	Gm^R	carries landing pad for pYT interposon in 16S gene of *rrnD*			This study
P. putida RW16SE	Gm^R	carries landing pad for pYT interposon in 16S gene of *rrnE*			This study
P. putida RW16SF	Gm^R	carries landing pad for pYT interposon in 16S gene of *rrnF*			This study
P. putida RW16SG	Gm^R	carries landing pad for pYT interposon in 16S gene of *rrnG*			This study

and used prediction tools to exclude promoters [BPROM, (Solovyev and Salamov 2011)], and terminators [ARNold (Naville et al. 2011)], that could interfere with gene expression. Sequences with start or stop codons were excluded or they were removed manually. The recognition sites of restriction endonucleases (I-*Ppo*I, PI-*Sce*I, *Asi*SI, *Eco*RI, I-*Sce*I, *Mau*BI, I-*Ceu*I, *Sal*I, PI-*Psp*I, *Mlu*I, *Nco*I, *Xho*I, *Sac*I, *Kpn*I) were likewise excluded. Finally, the generated sequences were compared *via* BLASTN with the entire NCBI database and to each other to exclude similarity to known sequences to prevent unwanted recombination events.

Yeast recombinational cloning and *in vitro* cloning procedures

Specific cloning procedures for the construction of the ready-to-use pYT vector and strain sets (Table 1) are detailed in the supplementary material. In brief, yeast recombinational cloning was used for multiple cloning steps including the construction of the three basic vectors pYTRW010K_0 × 5, pYTRW020K_0Ti1, pYTSK00K_0 × 7 (as detailed in Fig. S2), and subsequently for the integration of biosynthesis, marker or reporter modules into these. To this end, pYT vectors were linearised by restriction endonuclease digestion with I-*Sce*I (biosynthesis modules), *Mau*BI (reporters) or *Sal*I (markers), depending on the modules to be cloned, followed by dephosphorylation with FastAP. Respective DNA inserts were obtained by PCR, during which ca. 30 bp suitable homology arms were added (see Table S5). Promoter elements and rhamnolipid biosynthetic genes *rhlAB* were introduced in one reaction at the I-*Sce*I site of the vector and therefore designed to overlap with each other. Preparation of competent cells of uracil auxotrophic *Saccharomyces cerevisiae* VL6-48 (ATCC® MYA-3666, LGC Standards GmbH, Wesel, Germany) (Kouprina et al. 1998, Noskov et al. 2002) and vector assembly by recombinational cloning was performed in the yeast cells as described before (Gietz and Schiestl 2007, Domröse et al. 2017, Weihmann et al. 2020). Yeast cultures were grown in 1 mL of SD^{-Ura} medium to isolate assembled plasmids with the innuPREP Plasmid Mini-Kit according to the corresponding manual—with exception of cell lysis, which was performed by incubation of the cells with 200 U mL^{-1} *Arthrobacter luteus* Lyticase (Sigma-Aldrich Chemie GmbH, Hamburg, Germany) in the kit's resuspension buffer at 37°C for

2–5 h). For various cloning steps, including the integration of *vio* or *reb* biosynthetic genes, a promoter, reporters or markers in pYT vectors, the *in vitro* In-Fusion® HD cloning kit (Takara Bio. Inc., Kusatsu, Japan) was used, which facilitates the ligase-free assembly based on the annealing of complementary single-stranded 5' overhangs, which are generated by a 3' exonuclease. To this end, pYT vectors were linearised by digestion with the endonuclease I-SceI (or other nucleases as appropriate) and the DNA inserts were amplified by PCR using primers with 20 bp overhangs to other fragments or the linear pYT vector. The parts were combined for the assembly reaction as defined by the manufacturer. All PCR templates are summarised in Table S4.

Plasmid transfer and genomic integration in *P. putida*

Bacterial conjugation was used to transfer vectors to the *P. putida* KT2440 wild type or derivatives thereof. For standard mating, *E. coli* S17-1 was first transformed with the respective vector. The donor was then incubated together with the *P. putida* recipient for 5–16 h at 30°C in 200 μL of LB medium on a cellulose acetate membrane on LB-agar. The mixture was finally plated on LB-agar (supplemented with Irg and an appropriate antibiotic depending on the used construct) and incubated at 30°C overnight. After transfer of constructs for Tn5-based genomic integration in *P. putida* KT2440, clones carrying the transposon were selected with different antibiotics depending on the pYT marker. Clones expressing biosynthetic genes or reporter genes were selected on LB-agar based on specific phenotypes. For clones, which were further characterised in terms of metabolite production, loss of the Km^R backbone resistance was verified by plating on accordingly supplemented agar to exclude spontaneous plasmid co-integration. For *rrn* integration, seven *P. putida* strains were constructed, each possessing an appropriate landing pad in one of the seven 16S genes. The landing pad cassette was obtained from commercial gene synthesis services, cloned into pSEVA512S and the resulting plasmid pSEVA512S-16S-pad was transferred to *P. putida* KT2440. Clones were selected on LB-agar with Gm/Irg, followed by replica-plating on Gm (landing pad marker) and Tc (vector backbone marker) to identify double crossover variants. PCR analyses with forward primers binding in the upstream region of individual *rrn* operons and a reverse primer binding in the Gm^R-conveying *aacC1* gene, followed by sequencing of PCR products, identified seven strains (RW16-A to RW16S-G) with correct integration in the seven different 16S genes (see details in Fig. S3). For gene integration at the landing pads, appropriate pYT vectors were transferred to these strains *via* conjugation. Either, the conjugation mix was transferred in liquid LB medium containing Tc and 250 g L^{-1} sucrose for 2 days before a sample was plated on LB selection medium (Tc/Irg) containing 250 g L^{-1} sucrose to directly obtain single colonies resulting from a double crossover event. Alternatively, cells were plated and incubated on selection medium (Tc/Irg), before several single colonies were re-streaked on antibiotic-containing LB-agar and incubated overnight. For SacB-based counter-selection, single colonies from these plates were then streaked on YT agar plates (10 g L^{-1} yeast extract, 20 g L^{-1} tryptone, 250 g L^{-1} sucrose, and 36 g L^{-1} agar) containing 25% (*w/V*) sucrose and incubated for 2 days. Resulting colonies (about 10–100) were screened for Km (vector backbone marker) and Gm (landing pad marker) sensitivity (Elmore et al. 2017). Successful integration of the gene cluster was corroborated by PCR using forward primers, which bind in the upstream regions of *rrn* operons and reverse primers in the introduced biosynthetic *vio* genes. Successful integration of the Tn7 transposon into the *attTn7* site was confirmed by colony PCR using previously established primers, which are designed to bind to the *glmS* region and Tn7 ends (Choi et al. 2005).

Detection of hydrolytic enzyme reporter activity

For qualitative detection of β-galactosidase (LacZ) or β-glucuronidase (GUS) activity in *P. putida* clones, strains were incubated on LB-agar supplemented with 40 mg L^{-1} X-Gal (5-Bromo-4-chloro-3-indolyl-3-D-galactopyranoside; Sigma-Aldrich) or with 75 mg L^{-1} X-Gluc (5-Bromo-4-chloro-3-indolyl-3-D-glucuronide; Sigma-Aldrich) (Horwitz et al. 1964, Frampton, Restaino and Blaszko 1988). Polyester hydrolase activity (PE-H) was detected on LB-agar containing 8.8 mL L^{-1} Impranil® DLN-SD (COVESTRO, Leverkusen, Germany) (Molitor et al. 2020). If appropriate, sodium salicylate in a final concentration of 5 mM and antibiotics were supplemented. For the quantitative determination of LacZ, GUS and PE-H activity in *P. putida*, assays with chromogenic substrates ONPG (*o*-nitrophenyl-β-D-galactopyranosid) (Miller 1972, Weihmann et al. 2020), pNPG (*p*-nitrophenyl-β-D-glucuronosid) (Cui et al. 2016) and pNP ester (here *p*-nitrophenyl-β-D-octanoat) (Bollinger et al. 2020) were used. For the ONPG assay, cell extracts were prepared following previously established protocols (Miller 1972, Weihmann et al. 2020) by mixing 10 μL samples of *P. putida* cultures with 390 μL of diluted Z-buffer; 25 μL chloroform and 25 μL Z-buffer were added, and the mix was incubated for 3 min at 30°C. For the ONPG assay, 400 μL ONPG substrate solution (0.8 mg L^{-1} in diluted Z-buffer) were added to the cell extract. The mixture was incubated for 2 min at 30°C. Afterwards, 400 μL stop solution (1 M Na_2CO_3) was added and cell debris was removed by centrifugation (22°C, 15 min, 3000 g). The *o*-nitrophenol absorption of the samples was finally measured at 420 nm in the microplate reader TECAN Infinite M1000 PRO (Tecan Deutschland GmbH, Crailsheim, Germany). To calculate β-galactosidase activities as Miller units, cell densities of the bacterial cultures (measured at 580 nm in the same device), were taken into account. To prepare the pNPG and pNPO assays, the cells were diluted 1:10 and pellets (1 min, 18 000 g) were suspended in 100 mM PBS (pH 6.8) or 100 mM KP_i (pH 7.2) buffer containing 0.1 mg mL^{-1} polymixin B (incubation: 1 h, 37°C). For the pNPG assay, 50 μL substrate solution (PBS buffer containing 0.5 g L^{-1} pNPG (0.793 mM)) was added to 50 μL of the whole cell extract in a microtiter plate (incubation: 2 min, 37°C). The reaction was stopped by adding 100 μL of stop solution (1 M Na_2CO_3). For the pNPO assay, 180 μL substrate solution (100 mM KP_i-buffer containing 20 mM pNPO) was added to 20 μL of the whole cell extract in a microtiter plate. The *p*-nitrophenol absorption of samples at 410 nm was measured in the microplate reader, allowing calculation of β-glucuronidase and esterase activities in U mL^{-1}. These were divided by the corresponding cell densities, also measured with the TECAN Infinite M1000 PRO at 580 nm.

Detection of fluorescence reporters

For qualitative detection of fluorescence reporters in *P. putida*, corresponding strains were streaked on LB-agar supplemented with salicylate (5 mM final concentration), if necessary, and incubated at 30°C overnight. Subsequently, fluorescence of eYFP and mCherry was documented on a Blue/Green LED transilluminator (Nippon Genetics Europe GmbH; 430–530 nm) and of mTagBFP2 on the CAMAG TLC® Visualizer 2 (CAMAG AG & Co. GmbH 366 nm).

For the determination of *in vivo* fluorescence intensity in the context of reporter validation, samples of *P. putida* expression

cultures were pelleted (1 mL, 1 min, 18 000 g) and washed three times in 1 mL Tris-HCl buffer (100 mM; pH 8; 1 min; 18 000 g). For fluorescence measurements in a TECAN Infinite M1000 PRO, 200 μL of this suspension were transferred to microtiter plates (Greiner Bio-One International GmbH; MTP 96-well). The excitation and emission wavelengths were matched to the fluorescence reporters mTagBFP2 (λ_{maxEx} = 399 nm, λ_{maxEm} = 454 nm) (Subach et al. 2011), eYFP (λ_{maxEx} = 513 nm; λ_{maxEm} = 527 nm) (Spiess et al. 2005) and mCherry (λ_{maxEx} = 587 nm; λ_{maxEm} = 610 nm) (Shaner et al. 2004). In addition, the measured fluorescence intensities were divided by the corresponding cell densities, also measured with the TECAN Infinite M1000 PRO at 580 nm. In the context of rhamnolipid production, fluorescence of *P. putida* was measured in cultures grown in Flowerplates® (m2p-labs GmbH; Flowerplate® MTP-B) in a BioLector® I (m2p-labs GmbH) equipped with an eYFP filter module (λ_{Ex} = 508 nm; λ_{Em} = 532 nm) and BioLection 2 software. For cell density normalisation of fluorescence, the biomass (measured as scattered light at 620 nm by the same instrument) was used.

Expression of violacein biosynthetic genes and product analysis

Precultures of *P. putida* strains carrying *vio* biosynthetic genes were inoculated in 0.8 mL TB medium and incubated overnight in FlowerPlates® at 30°C under constant shaking at 1400 rpm in a ThermoMixer® C (Eppendorf AG, Hamburg, Germany). These cultures were used to inoculate main cultures in 0.8 mL TB to $OD_{750\,nm}$ = 0.05 as starting cell density in FlowerPlates®. After shaking incubation (1400 rpm) of cultures at 30°C in a ThermoMixer® C or in a Biolector System (m2p-labs GmbH), cells from 500 μL culture were harvested for analysis of violacein production. Cell samples were extracted with 0.5 mL ethanol (p.a.) and crude extracts were cleared by centrifugation. For a qualitative determination of the composition of violaceins, 10 μL samples were subjected to HPLC-PDA analysis using an Accucore™ C18 Column (50 × 4.6 mm, 2.6 μm particle size, 80 Å pores) equipped with a guard column filled with the same material (Thermo Fisher Scientific GmbH, Walkham, USA) and previously developed methods (Sánchez et al. 2006, Lee et al. 2013, Domröse et al. 2017). The column oven temperature was set to 30°C, and the flow rate to 1 mL min^{-1}. The mobile phase was composed of dH_2O with 0.1% (V/V) formic acid (A) and acetonitrile with 0.1% (V/V) formic acid (B) and applied for gradient elution as previously described (Domröse et al. 2017). Peaks obtained in chromatograms (recorded at 600 nm) were evaluated regarding the retention times and PDA spectra, using previously published data for reference (Sánchez et al. 2006, Lee et al. 2013, Domröse et al. 2017) (violacein, 5.9 min, λ_{max} = 374, 571 nm; deoxyviolacein, 6.3 min, λ_{max} = 372, 562 nm; prodeoxyviolacein, 5.6 min, λ_{max} = 418, 610 nm). To estimate violacein concentrations in crude extracts, the absorption at 575 nm was measured with a Spectrophotometer (Genesys 20, ThermoFisher Scientific, Waltham, MA, USA) using 1 mL 1:10 diluted samples. Accumulation of the typical violacein/deoxyviolacein mixture or (almost) exclusively deoxyviolacein was evaluated using the molar extinction coefficients of violacein (ε_{575} [M^{-1} cm^{-1}] = 25 400) and deoxyviolacein (ε_{575} [M^{-1} cm^{-1}] = 15 700), respectively (Rodrigues et al. 2012).

Expression of rhamnolipid biosynthetic genes and product analysis

Precultures of *P. putida* strains carrying rhamnolipid biosynthetic genes were prepared in 1 mL LB medium in FlowerPlates® at 30°C shaking at 1200 rpm in a ThermoMixer® C (Eppendorf AG, Hamburg, Germany). Main cultures in sterile 48-well FlowerPlates® were inoculated to an $OD_{580\,nm}$ = 0.05 in 1.2 mL LB medium supplemented with 10 g L^{-1} glucose and appropriate antibiotics. They were incubated in a BioLector I system at 30°C shaking at 1200 rpm. If appropriate, inducers were added after 3.5 h to a final concentration of 10 mM (L-arabinose or L-rhamnose), 2 mM (sodium salicylate or D-mannitol), or 0.5 μM (anhydrotetracycline). After 24 h, 500 μL samples of the culture broth (cell-free) were taken, and 500 μL acetonitrile were added. After incubation at 4°C overnight and subsequent centrifugation (2 min, 11 000 g), the samples were filtrated (Phenex RC syringe filters, 0.2 μm, Ø 4 mm (Phenomenex, Torrance, USA). To determine rhamnolipid and HAA concentrations, 5 μL samples were subjected to HPLC-CAD analyses using previously developed methods (Behrens et al. 2016, Tiso et al. 2016). We employed a NUCLEODUR C18 Gravity column (150 × 4.6 mm, 3 μm particle size, 110 Å pores; Macherey-Nagel GmbH & Co. KG, Düren, Germany), a column oven temperature of 40°C, a flow rate of 1 mL min^{-1}, and a mobile phase of acetonitrile (A) and ultra-pure water with 0.2% (V/V) formic acid (B), which were applied for gradient elution as previously described. The stated amounts of rhamnolipids represent the sum of all detectable congeners, which were quantified in samples using chromatographically purified compounds as references as previously described (Behrens et al. 2016) The main congeners showed signals at retention times of 9.4 min (C10-C10) and 7.1 min (Rha-C10-C10).

Expression of arcyriaflavin A biosynthetic genes and product analysis

Precultures were prepared for *P. putida* strains with *rebODCP* genes in 100 mL Erlenmeyer flasks containing 10 mL LB medium and incubated at 30°C and 130 rpm for 16 h. Main cultures were inoculated from precultures in 10 mL LB medium to an optical density of $OD_{580\,nm}$ = 0.05 using 100 mL flasks. Cells were cultivated at 30°C and 130 rpm for 4 h and were then supplemented with 1 mM L-trytophan (stock prepared in dH_2O). Additionally, expression of arcyriaflavin A genes was induced with 2 mM sodium salicylate (stock prepared in 70% (V/V) EtOH) in the strain carrying the respective expression cassette in the *att*Tn7 site. Cells were harvested after a total incubation time of 48 h by centrifugation for 15 min at 5000 rpm and 4°C. Arcyriaflavin A was extracted from the cell pellet with 1 mL ethanol (p.a.) and crude extracts were analysed by HPLC-PDA as described above for the other indolocarbazole (deoxy)violacein (Domröse et al. 2017). The arcyriaflavin A signal was assigned by comparative evaluation of retention times and PDA spectra (6.7 min, λ_{max} = 282, 316 nm) with a reference (purity ≥98% (HPLC); Tocris Bioscience, Bristol, United Kingdom) (Fig. S6). Based on a calibration curve (0 to 0.33 mg mL^{-1}), arcyriaflavin A titres were thus calculated from peaks areas obtained in the chromatograms recorded at 316 nm.

Analysis of *rhl* transcript levels

Pseudomonas putida cell material equivalent to $OD_{580\,nm}$ = 2 in 1 mL was harvested after 6 h of cultivation by centrifugation. Total RNA isolation, DNase treatment, RT-qPCR as well as the data quality control (Bustin et al. 2009) and evaluation were performed as previously described (Tiso et al. 2020) using the primers PA-*rhlB*_fw RT and PA-*rhlB*_rv RT (Kõressaar et al. 2018). Copy numbers of *rhlB* transcript per OD were approximated based on the initially extracted total RNA from cells equivalent to $OD_{580\,nm}$ = 2 in 1 mL. Quality control and calibration are shown in Fig. S7.

Results

Conceptualisation of the modular yTREX toolbox

The production of valuable compounds can be implemented in microbial hosts by heterologous gene expression, for which the use of effective cloning technologies and chromosomal integration of expression cassettes represent key success factors. We therefore set out to construct a fully modular toolbox for the chromosomal integration of target genes or gene clusters in *P. putida* KT2440. We designed a DNA cassette that would chromosomally integrate in three different modes and allow addition or exchange of individual elements like target genes, promoters, transcription reporters or resistance markers *via* designated standard procedures (Fig. 1). To facilitate yeast recombineering and conjugational transfer from *Escherichia coli* to the host bacterium, we chose the integrative sequence to be carried in the yTREX vector backbone, which is equipped with respective genetic elements (Domröse et al. 2017). We denoted the toolbox as pYT vector series (YT for yTREX toolbox).

Three chromosomal integration modes: The integrative sequence was defined by flanking elements that would convey chromosomal integration with the help of transposons or an interposon for both, untargeted or site-specific integration in genomic *loci via* transposition or homologous recombination (Fig. 1). The first option is the random transposon Tn5, which uses a 'cut and paste' mechanism and has evolved to low frequency genomic integration (Reznikoff 2008). This transposon requires only one *tnp* gene as well as the OE-L and OE-R ('left' and 'right' outer ends) for effective functioning. It therefore typically facilitates very robust gene delivery and can yield strains, in which target genes integrate downstream of a chromosomal promoter and biosynthesis is thus readily implemented (Martínez-García et al. 2014, Domröse et al. 2017, Nazareno, Acharya and Dumenyo 2021). The identification of such clones among all clones obtained after random transposition is dependent on effective screening methods like the use of transcription reporters that provide an easily detectable readout.

Previously, the use of transposon Tn5 led us to the identification of the *P. putida* ribosomal RNA (rRNA)-encoding genes (also: *rrn* operons or rDNA) as exceptionally suitable chromosomal *loci* for gene cluster integration and expression (Domröse et al. 2019). We therefore further aimed to facilitate direct *rrn* targeting *via* homologous recombination as a second option. The rRNA is encoded in seven *rrn* operons in *P. putida* KT2440, denoted with A, B, C, D, E, F, and G (Nelson et al. 2002, Belda et al. 2016). We chose to facilitate specific integration in one of these seven 16S rRNA genes, which are the first genes downstream of the respective *rrn* promoters, followed by 23S and 5S rRNA genes. Since the seven 16S gene sequences are 99.93–100% identical, targeting of a specific copy is ensured by pre-installation of unique sequences as 'landing pads' in each 16S gene.

The third option is the site-specific chromosomal integration of genes with the help of the Tn7 transposase (Peters and Craig 2001). The transposon Tn7, encoded by the genes *tnsABCD* and defined by the transposon outer ends integrates with high efficiency into the bacterial chromosome. Here, partner proteins direct integration into the *att*Tn7 site. In *P. putida* KT2440 and many other bacteria, this site is located near the chromosomal origin of replication, so the genetic information is present at least in duplicate at most times of bacterial growth due to ongoing DNA replication (Slager and Veening 2016). The transposon Tn7 has been used in many studies for the fast generation of stable expression strains, for example, to allow comparison of promoter strengths or biosensor modules independent of chromosomal positioning effects (Choi et al. 2005, Choi and Schweizer 2006, Damron et al. 2013, Zobel et al. 2015).

The transposon-based options are in principle applicable in a variety of host bacteria since Tn5 integrates randomly and the *att*Tn7 site occurs (mostly only once) in the genome of most bacteria because it is defined by being located adjacent to the essential *glmS* (glutamine-fructose-6-phosphate aminotransferase) gene (Peters and Craig 2001). These three integration modes define three different basic vectors of the pYT series.

Modular adaptability of the integrative sequence: The pYT vector series shall facilitate delivery of chosen genetic modules into the bacterial chromosome and is hence designed for straightforward adaptability. Within the borders of the integrating sequence, all elements of the cassette, which we denoted as YT_core, can be freely chosen or exchanged. This modularity is granted by restriction endonuclease and homing endonuclease recognition sequences that define 'slots', which are framed by randomised sequences (Fig. 1). Elements like target genes, transcription reporters or resistance markers can thus be inserted at these designated positions *via* restriction and ligation or *via* assembly of complementary strands in yeast recombinational cloning or methods like In-Fusion® cloning, for which the framing sequences next to the 'slots' are utilised as standardised recombination sites. This shall allow straightforward primer design for appropriate insert amplification and thus easy adaptation to the specific experimental requirements of various research questions: The central recognition site of homing endonuclease I-*Sce*I facilitates vector linearisation for the integration of a gene cluster of interest at the cluster integration site (CIS, see Fig. S1 for details). By linearisation with *Asi*SI or PI-*Sce*I, additional elements like promoters can be added upstream of the target genes. Hydrolysis at the sites for *Mau*BI or I-*Ceu*I enables the addition of a transcription reporter, linearisation at the sites for *Sal*I or PI-*Psp*I the inclusion of a resistance marker gene. We additionally included a set of common restriction sites as multiple cutter region (*Mlu*I, *Nco*I, *Xho*I, *Sac*I, *Kpn*I, and *Eco*RI). These endonuclease recognition sites do not occur within the majority of here used transcription reporter or resistance marker genes (encoding eYFP, mCherry, mTagBFP2, LacZ, GUS, PE-H, Gm^R, Tc^R, Sm^R, Cm^R, see Table S1). This allows cloning or an exchange of a resistance marker in a construct, in which a reporter has already been introduced, and *vice versa* in most cases. The homing endonuclease sites were additionally included to allow cloning or an exchange of elements in constructs already carrying larger target gene clusters, which may contain restriction sites within their sequences, or if new reporter or marker genes will be used, which contain such sites. Finally, the site for homing endonuclease I-*Ppo*I allows transfer of fully 'loaded' YT_core cassettes between the three different vector types for integration *via* Tn5, Tn7 or into *rrn* genes.

Construction and validation of the pYT toolbox modules

Based on the vector designs conveying the three integration modes, three basic vectors were constructed. To this end, the YT_core sequence (Fig. S1), which was obtained as a gene synthesis fragment, was assembled with respective flanking sequences into the backbone of the yTREX vector, which replicates in *E. coli* with pMB1 ori to a mid copy number (Domröse et al. 2017). Cloning procedures are summarised in Fig. S2. In brief, pYT vectors conveying Tn5 transposition were equipped with the *tnp* gene and OE sequences of transposon Tn5. To facilitate integration in a 16S gene, we first introduced synthetic landing pad sequences in the *P.*

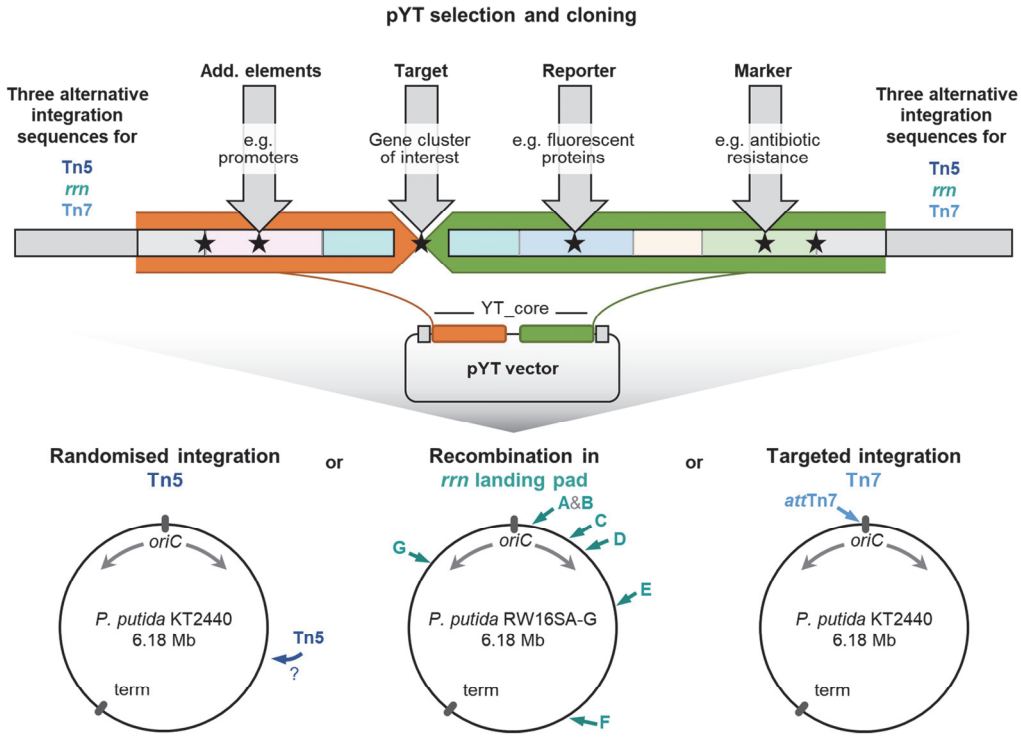

Figure 1. Concept of the modular pYT vector series. First, a suitable vector from an existing library can be selected. Relevant elements defining the integrative YT_core sequence are depicted schematically. Details are given in Fig. S1. Orange and green regions denote sequences framing the gene cluster of interest, which is to be expressed. Vectors with different resistance markers, reporter genes and chromosomal integration modes are available. If necessary, adaptations for other required vector features can be made *via* standardised procedures. The integration of target genes of interest can be realised *via* conventional, ligase-independent or yeast recombinational cloning; positions of homing endonuclease recognition sites are indicated by black asterisks. Cloned vectors facilitate generation of expression strains *via* integration at different genomic positions (marked in the schematic representations of *P. putida* KT2440 chromosomes): Three vector series are available enabling random Tn5 transposition, recombination-based integration at pre-installed landing pads in one of the 16S rRNA-encoding genes of *P. putida* KT2440 *rrn* operons (denoted with A to G), and targeted transposon Tn7 integration at the *att*Tn7 site.

putida KT2440 genome 630 bp downstream of the 16S promoter P1 (Domröse et al. 2019) by recombination, thus generating *P. putida* strains RW16SA, -B, -C, -D, -E, -F, and -G (carrying the landing pad in the 16S rRNA gene of the *rrn* operons A, B, C, D, E, F, or G, respectively) (**Figure S3**). In respective pYT vectors for gene integration at this position, 500 bp sequences homologous to landing pad sequences were added on each end of the YT_core. Vectors for gene delivery to *att*Tn7 were equipped with the *tnsABCD* genes and OE sequences of transposon Tn7.

Making use of the standardised YT_core cloning slots for ligase-free module insertion (Fig. S1), different marker and reporter genes were cloned in the vectors (Table S2).

We verified the functionality of the chosen resistance marker genes, which were cloned together with the respective promoters to convey Gm^R, Cm^R, Tc^R, and Sm^R (Sutcliffe 1979, Prentki and Krisch 1984, Antoine and Locht 1992, Schweizer 1993) (Fig. 2A). The selection marker Km^R was additionally included in the plasmid backbone to be used for the selection of *E. coli* clones which are grown for plasmid amplification to ensure they really maintain the replicative plasmid and not only carry the transposon or interposon in the chromosome. Further, we tested the applicability of selected reporter genes (*eYFP* and *lacZ*) to facilitate identification of expressing clones after Tn5 transposition (Fig. 2B). Further evaluation was performed using the fluorescent proteins eYFP, mCherry, and mTagBFP2, as well as the enzymes β-galactosidase (LacZ), β-glucuronidase (GUS), and polyester hydrolase (PE-H) (Miller 1972; Jefferson, Burgess and Hirsh 1986, Shaner et al. 2004, Spiess et al. 2005, Subach et al. 2011, Bollinger et al. 2020), after Tn7 transposition. In addition to qualitative evaluation of reporter expression after integration at *att*Tn7 (Fig. S4), we validated the suitability of the established reporters for providing a quantitative read-out. To this end, the previously established *nagR*-P_{nagAa}-PA_*rhlAB* cassette (consisting of mono-rhamnolipid biosynthetic genes under control of a salicylate-inducible promoter (Tiso et al. 2020)), was cloned in the I-SceI site of vectors, which were additionally equipped with different reporter genes. After integration into the *P. putida* KT2440 chromosome, a differential read-out over a wide range of inducer concentrations could be verified (Fig. 2C).

Therefore, a collection of 27 pYT vectors along with landing pad carrying strains for *rrn* integration was established as ready-to-use and easily expandable toolbox (Table 1). The cloning procedures are detailed in the supplementary information. All vectors

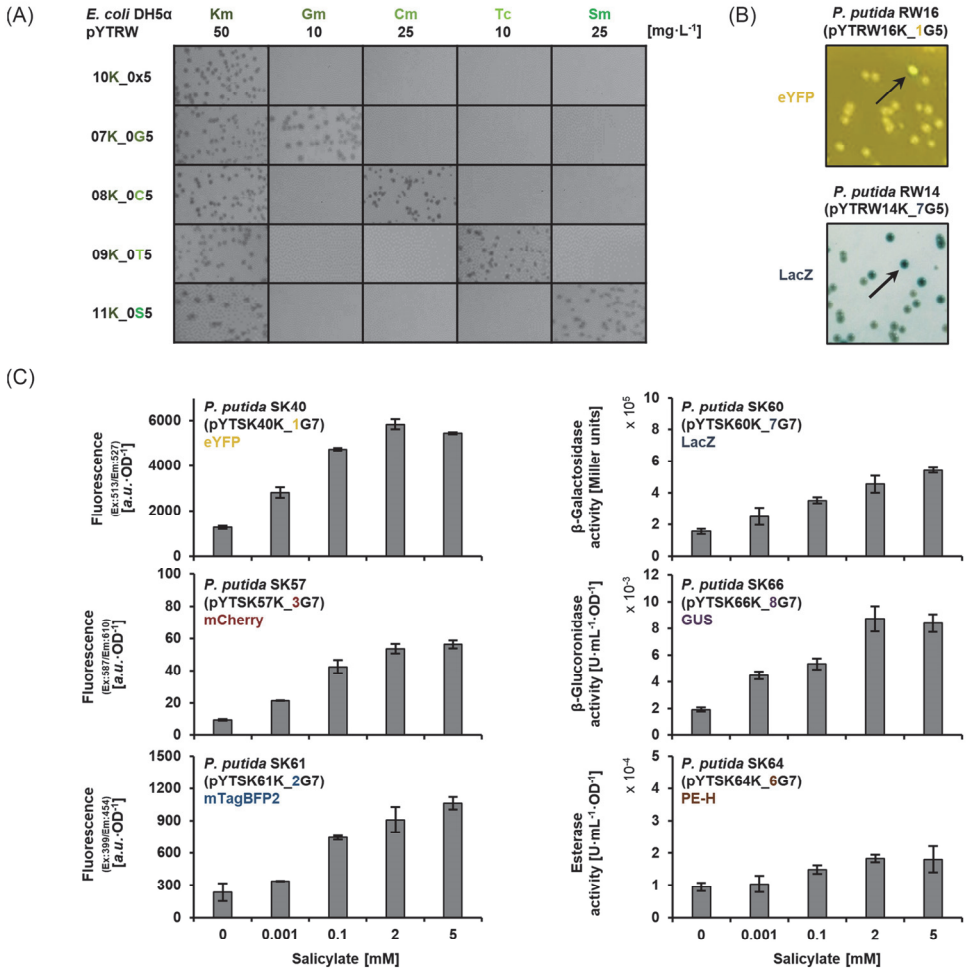

Figure 2. Functional validation of pYT marker and reporter modules. **(A)** Selective growth of *E. coli* DH5α cells after transformation with pYT vectors carrying different resistance markers. Marker gene indicating characters in vector names are highlighted. **(B)** Phenotypes of *P. putida* cells after random transposon Tn5 integration of pYT cassettes with different transcription reporters. Arrows indicate exemplary expressing clones. **(C)** Reporter signal quantified after differential salicylate induction of *P. putida* strains after integration of pYT cassettes at the *att*Tn7 site. Reporter gene indicating characters in vector names are highlighted. Data represent the mean of three independent experiments with error bars indicating the corresponding standard deviations.

and strains can be obtained from the authors upon request. The sequences were deposited at NCBI GenBank. The applied vector nomenclature, which includes the initials of the creator as well as a unique number and further indicates the plasmid backbone resistance (e.g. K for Km^R), the reporter (e.g. 1 for eYFP), the marker (e.g. G for Gm^R) and the integration mode (e.g. 5 for Tn5) is explained in Table S3.

Constitutive expression of *vio* genes by Tn5 transposition and *rrn*-integration

The transposon Tn5 has been successfully used for integration and expression of multiple genes in various hosts including *P. putida* (de Lorenzo et al. 1998, Nikel and de Lorenzo 2013, Martínez-García et al. 2014, Domröse et al. 2017). To verify functionality of transposon Tn5 elements in the new vector setup of our present study, we used the well-described *vio* genes encoding the biosynthesis of violacein and deoxyviolacein. Accumulation of these violet pigments served as easy-to-detect reporter for expression tool development for *P. putida* before (Domröse et al. 2017, Choi et al. 2018). In our own previous work, random Tn5 transposition facilitated the integration of *vio* genes downstream of chromosomal promoters leading to metabolite production in a fraction of clones (Domröse et al. 2017). We therefore sought to benchmark the new setup against those previous findings on strain construction and violacein production.

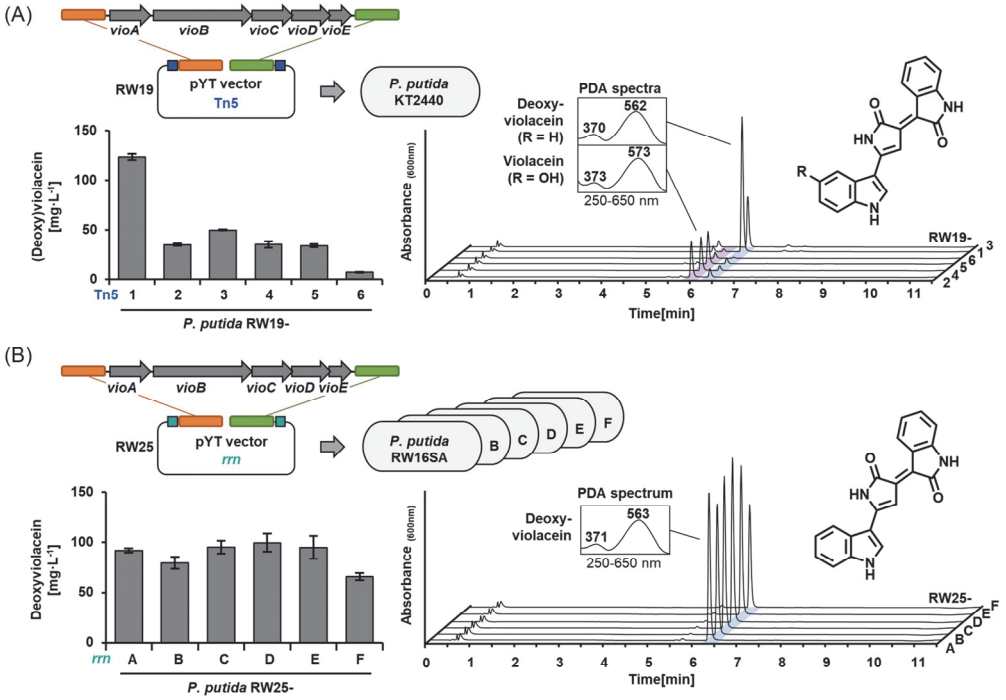

Figure 3. Violacein and deoxyviolacein production of *P. putida* after pYT-mediated *vio* gene integration *via* Tn5 transposition or into *rrn* operons. **(A)** Cloning scheme of pYT construct as well as product titres and corresponding HPLC-PDA analyses obtained after random transposon Tn5 integration of the *vioABCDE* gene cluster. **(B)** Cloning scheme of pYT construct as well as product titres and corresponding HPLC-PDA analyses obtained after interposon integration of *vioABCDE* into the landing pads within *rrn* operons of *P. putida* RW16SA-F. Biosynthesis of (deoxy)violacein was verified by HPLC-PDA analyses of extracts. PDA spectra of product peaks in chromatograms (recorded at 600 nm) are shown. Titres were estimated by spectrophotometrical measurements. Data represent the mean of three independent experiments with error bars indicating the corresponding standard deviations.

We selected the vector pYTRW09K_0T5, which carries Tc^R as integrating resistance marker. The genes *vioA*, *vioB*, *vioC*, *vioD*, *vioE* (7.3 kb) from *Chromobacterium violaceum* ATCC 12472 were PCR-amplified adding homologous cloning overhangs and assembled into the vector, which was linearised with I-SceI, by In-Fusion® cloning generating vector pYTRW19K_0T5_vioABCDE.

The vector was transferred into *P. putida* KT2440 by conjugation to insert *vio* genes in the chromosome *via* Tn5 transposition. Plating on Tc-containing agar plates yielded hundreds of clones, as we expected from previous work with the Tn5 transposon in the host (Domröse et al. 2017, 2019). Among these, about 15% exhibited a violet-blueish colour. Six selected clones designated as RW19-1, -2, -3, -4, -5, and -6 produced violacein and deoxyviolacein at titres between 10 and 123 mg L^{-1}, as determined by established spectrophotometry and HPLC-PDA analysis (Domröse et al. 2017) (Fig. 3A). The (almost) exclusive production of deoxyviolacein in two clones was traced back to nucleotide deletions in the *vioD*-encoded oxygenase (Fig. S5). The titres are in the same range as previously obtained with the yTREX tool (Domröse et al. 2017). Therefore, the transposon Tn5 version of the pYT vector series is functional and suitable for rapid generation of recombinant expression strains.

Targeted gene integration at defined positions was addressed as next step. The integration of biosynthetic genes in the *P. putida* rDNA was previously shown to promote high-level constitutive gene expression, especially in *rrnA*, *rrnC*, and *rrnD* (Domröse et al. 2019). To verify functionality of the pYT interposon elements for gene integration into *P. putida rrn* genes with pre-installed landing pads (see Fig. 2; Fig. S3), we again used the *vio* genes of *C. violaceum*. To assess the benefit of levansucrase-encoding *sacB* as counter selection marker (Gay et al. 1985), we cloned the genes *vioABCDE* in the I-SceI site of vector pYTRW21K_1Ti1 (without the *sacB* gene), yielding pYTRW24K_1Ti1, and also generated the analogous pYTRW25K_1Ti1 (with the *sacB* gene). Both vectors were equipped with the Tc^R integrating resistance marker.

The vectors were transferred into the landing pad-carrying *P. putida* RW16SA, -B, -C, -D, -E, -F, and -G by conjugation. After transfer of pYTRW024K_1Ti1 (without the *sacB* gene), plating on Tc-containing agar plates yielded several clones, among which, however, almost all tested clones showed resistance against Tc and Gm, which indicated single crossover integration. After transfer of pYTRW25K_1Ti1 (with the *sacB* gene), only 5–15 clones were obtained on Tc- and sucrose-containing agar plates. These showed a typical colour-phenotype of *vio*-expressing colonies. Further, they

exhibited only resistance to Tc, but sensitivity to Gm, indicating a double crossover event that led to the intended deletion of the resistance cassette Gm^R at the landing pad. Finally, PCR analyses and sequencing confirmed that six strains carrying the *vio* genes in the 16S gene of *rrnA*, *rrnB*, *rrnC*, *rrnD*, *rrnE*, or *rrnF* could be obtained as expected. These were denoted as *P. putida* RW25-A, -B, -C, -D, -E, and -F. Despite several attempts, we were not able to integrate the *vio* genes in the *rrn* operon G. Notably, this *rrn* operon is in contrast to all others located on the (-) strand (Domröse et al. 2019). However, we have no hypothesis as to why gene cluster integration into this landing pad was unsuccessful, after the installation of the landing pad posed no difficulties.

The six strains produced deoxyviolacein at titres between 66 and 100 mg L^{-1}, as determined spectrophotometrically and by HPLC-PDA analysis Fig. 3B. The production of deoxyviolacein was again caused by nucleotide deletions in the *vioD*-encoded oxygenase (Fig. S5). Since the *vioD* sequence on plasmids was intact, the deletions must have taken place during or after chromosomal integration. The specific occurrence of mutations in *vioD*—presumably upon expressions—suggests a distinct toxicity of violacein, which is not exerted by deoxyviolacein. Higher antibacterial activity of violacein compared to deoxyviolacein has been observed before (Wang et al. 2012). Since the MIC (minimal inhibitory concentration) of violacein has been described to be in the range of 18.5 mg L^{-1} (*Pseudomonas aeruginosa*) (Subramaniam, Ravi and Sivasubramanian 2014) and 28.7 mg L^{-1} (*E. coli*) (Priya, Srinivasa and Mariappan 2018), growth of *P. putida* may be impaired at higher production titres. While the compound has previously been successfully produced in several heterologous hosts including *P. putida* (Fang et al. 2015, Domröse et al. 2017, Zhang et al. 2017, Choi et al. 2021), genetic instability of some *E. coli* and *P. putida* production strains was noted in this context (Sarovich and Pemberton 2007, Philip, Sarovich and Pemberton 2009, Domröse et al. 2017).

Taken together, our results suggest that violacein production is problematic, but the host *P. putida* is suitable for the constitutive and stable production of deoxyviolacein. Interestingly, the previously described clean deletion of *vioD* led to much lower titres of deoxyviolacein (10 and 21 mg L^{-1}) (Domröse et al. 2017) compared to the here presented results, which might suggest a beneficial effect of partial gene deletion. The deoxyviolacein titres, which were obtained after use of the rDNA interposon, being in the range of the best producers after transposon Tn5 integration, corroborates the suitability of the *rrn loci* for gene integration and expression. Moreover, the tendencies of production-to-*rrn* operon correlation were similar to previous observations: While previously reported tendencies of lower production after integration in *rrnB*, *rrnE*, and *rrnF* (Domröse et al. 2019) are partly matched by violacein titres (*rrnE* does not match), the integration into *rrnA*, *rrnC* and *rrnD*, which previously led to highest *pig* gene expression and prodigiosin production (Domröse et al. 2019), was also especially suitable for violacein production. Therefore, the rDNA interposon version of the pYT vector series is functional and suitable for the generation of recombinant expression strains.

Optimisation of *rhl* expression modules at the *att*Tn7 site

In previous studies, the transposon Tn7 has been applied to introduce genes reliably into the genome of different organisms. The introduction of genes in one defined chromosomal position is particularly suitable for comparative studies of expression modules (*e.g.* varying the promoter, the RBS, the biosynthetic or accessory genes). For rhamnolipids, the specific expression mode has already been shown to be important in the optimisation of production strains and can contribute to increasing production stability without loss of titres (Tiso et al. 2020, Sathesh-Prabu et al. 2021). We hence chose to apply our toolbox for the integration and expression of *rhl* genes encoding biosynthesis of rhamnolipids at the *att*Tn7 site.

To compare different regulatory elements to drive the expression of the rhamnolipid biosynthetic genes *rhlA* and *rhlB* of *Pseudomonas aeruginosa* PAO1, they were assembled into pYT vectors along with a constitutive or one of five inducible promoters: P_{lac}, *araC*-P_{BAD}, *rhaRS*-*rhaP*$_{BAD}$, *nagR*-P_{nagAa}, *mtlR*-P_{mtlE}, *tetR*-P_{tetA}. The *E. coli* P_{lac} of the lactose-inducible operon without its repressor gene *lacI* was chosen as constitutive expression system (de Lorenzo et al. 1993). The *araC*-P_{BAD} module from *E. coli* was used to facilitate L-arabinose-inducible expression (Calero, Jensen and Nielsen 2016). The *E. coli rhaRS-P rhaP*$_{BAD}$ module was chosen for L-rhamnose-inducible expression (Calero, Jensen and Nielsen 2016). For these systems, the transporter genes *araE* and *rhaT* were additionally included under the control of the P_{tac} promoter to improve the transport of the inducers L-arabinose and L-rhamnose, respectively, into the cells (Calero, Jensen and Nielsen 2016). The P_{tetA} from *E. coli* was used for anhydrotetracycline-inducible expression (Chai et al. 2012). The *mtlR*-P_{mtlE} module from *Pseudomonas protegens* Pf-5 was chosen as D-mannitol-inducible system (Hoffmann and Altenbuchner 2015) and the *nagR*-P_{nagAa} from *Comamonas testosteroni* for salicylate-inducible expression (Verhoef et al. 2010). All templates used for PCR amplification of the named elements are summarised in Table S4. The expression system modules and the genes *rhlA* and *rhlB* were assembled in the I-SceI-linearised vector pYTSK01K_0G7, which provides Gm^R as integrating marker, *via in vivo* recombination in *Saccharomyces cerevisiae* VL6-48. The BCD2 (BiCistronic Design) element, which consists of two Shine-Dalgarno sequences and a small leader peptide (Mutalik et al. 2013), was employed for translation initiation of *rhlA* and utilised as standardised cloning linkage between biosynthetic genes and expression system modules; accordingly, the respective sequence was integrated into corresponding oligonucleotide primers (Table S5). The resulting vectors (pYTSK03,08,09,10,12,13K_0G7) were subsequently equipped with the *eYFP* reporter gene (Aymoz et al. 2016), generating vectors pYTSK33,38,39,40,42,43K_1G7 which carry the promoters P_{lac}, *araC*-P_{BAD}, *rhaRS*-*rhaP*$_{BAD}$, *nagR*-P_{nagAa}, *mtlR*-P_{mtlE}, and *tetR*-P_{TetA}, respectively (Fig. 4A).

The vectors were transferred into *P. putida* by conjugation resulting in high numbers of Gm-resistant clones. Integration of the recombinant transposon at the *att*Tn7 site was verified by colony PCR using previously established primers (Choi et al. 2005) in all respective strains *P. putida* SK33, SK38, SK39, SK40 (Tiso et al. 2020), SK42, and SK43.

We comparatively assessed the performance of the strains with different expression system modules on the levels of transcription and expression as well as production. First, the transcription and expression levels of the biosynthetic operon *rhlAB* and downstream encoded *eYFP* reporter were determined by RT-qPCR as transcript copies of *rhlB* as well as *via* eYFP fluorescence (Fig. 4A). Stronger expression of *rhlAB* genes seemed to be accompanied by likewise higher eYFP fluorescence after 24 h, most prominently in case of the D-mannitol-inducible *mtlR*-P_{mtlE} system (SK42), followed by the group of *araC*-P_{BAD}, *nagR*-P_{nagAa} and *tetR*-P_{tetA} (SK38, SK40, and SK43). Finally, P_{lac} showed weakest expression. Our findings of an overall correlation of the eYFP reporter fluorescence with *rhlB* transcript levels indicate the usefulness of the reporter. However, it should be noted, that both

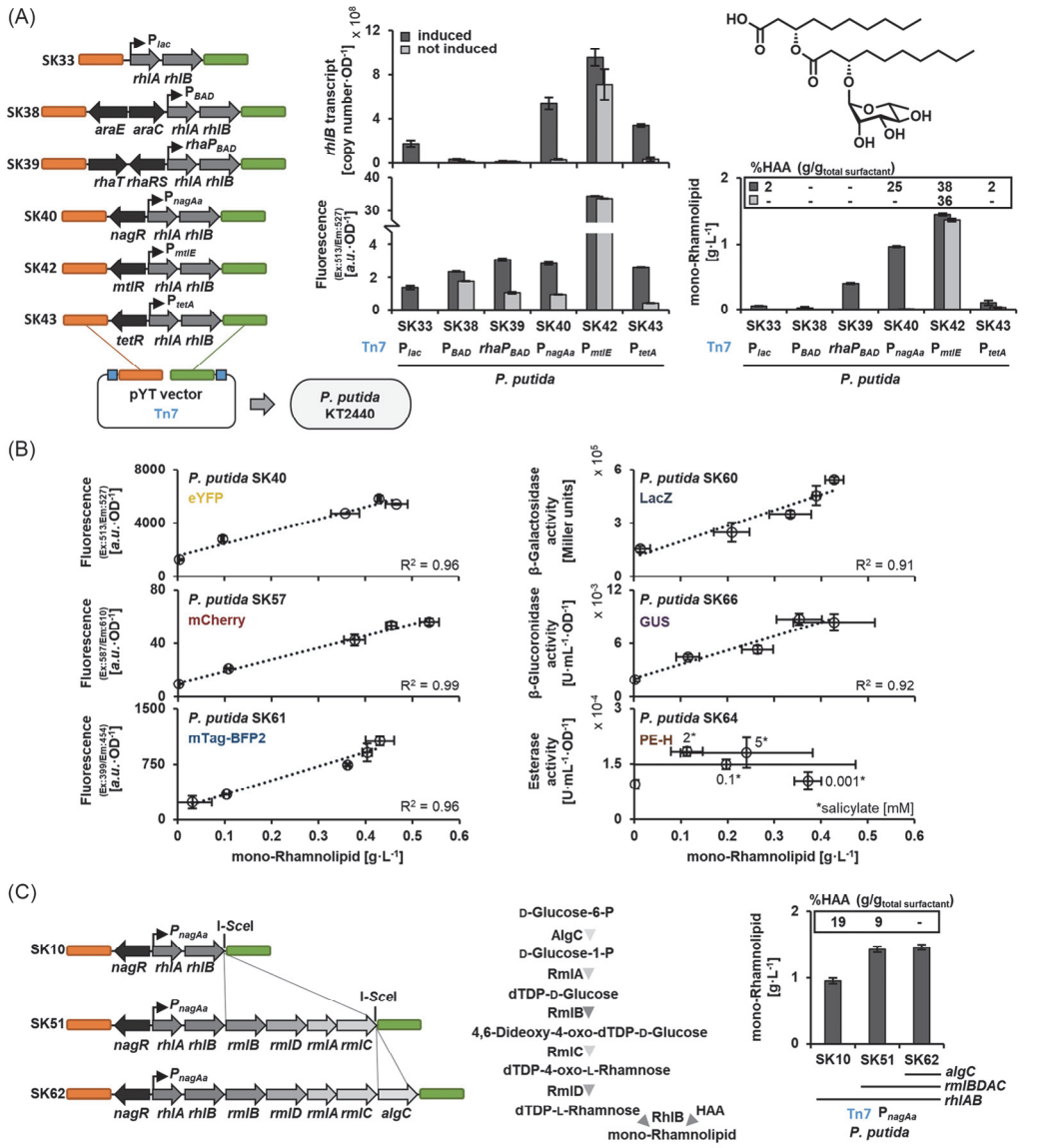

Figure 4. Evaluation of different *att*Tn7-integrated expression modules for rhamnolipid production in *P. putida*. **(A)** Cloning schemes of pYT constructs as well as *rhlB* transcript levels, eYFP reporter fluorescence, and titres of mono-rhamnolipids obtained after Tn7 integration and expression of *rhlAB* with different promoters. The fraction (g/g) of HAA per total surfactant, *i.e.* the sum of mono-rhamnolipids and HAA, is shown as inset. The commonly dominant C10-C10 mono-rhamnolipid congener is depicted. **(B)** Correlation of reporter signals (*i.e.* fluorescence or enzyme activity) and mono-rhamnolipid titres depending on different salicylate inducer concentrations in strains carrying *rhlAB* and reporter genes under control of *nagR*-P_{nagAa}. Increasing salicylate concentrations (0, 0.001, 0.1, 2, and 5 mM) correspond to increasing mono-rhamnolipid titres with the exception of the PE-H-expressing strain (where salicylate concentrations are indicated for each data point). **(C)** Titre of mono-rhamnolipids and HAA fraction upon biosynthetic module expansion with *rmlBDAC* and *algC* genes for improved supply of the precursor dTDP-L-rhamnose to reduce HAA accumulation. Biosynthetic products were quantified by HPLC-CAD analyses. Data represent the mean of three independent experiments with error bars indicating the corresponding standard deviations.

were determined as end point measurements: thus, putative dynamic underlying processes remain undiscovered. For example, the *araC*-P_{BAD} and *rhaRS*-*rhaP*$_{BAD}$-driven systems (SK38 and 39) yielded a fluorescence comparable to *nagR*-P_{nagAa}, and *tetR*-P_{TetA} (SK40 and SK43) despite a lower initial expression. Both parameters are generally influenced by different factors including post-translational oxygen-dependent maturation of eYFP required for fluorescence, which can take significant time during fast bacterial growth (Drepper et al. 2007, 2010). Furthermore, RT-qPCR depicts an equilibrium of transcript levels at a given time and values are thus not only indicative of transcription strength but also result from previously discussed RNA degradation mechanisms (Pearson, Pesci and Iglewski 1997) that have not been fully elucidated for the natively adopted *rhlAB* operon from *P. aeruginosa* until now. Therefore, a correlation of reporter fluorescence and transcript levels should be interpreted cautiously.

Constitutive strong expression can be problematic for the stability of rhamnolipid production (Tiso et al. 2020). For a promoter system similar to the very strong *mtlR*-P_{mtlE} (from the related *Pseudomonas fluorescens* DSM50106), a high basal expression in *P. putida* KT2440 has already been reported (Hoffmann and Altenbuchner 2015). We therefore also analysed expression under non-inducing conditions revealing a very high basal expression without addition of the inducer D-mannitol for strain SK42. Hence, the respective promoter system may not be attractive for production purposes.

To assess the promoters' suitability for production, the supernatants of all cultures were analysed with regard to the achieved titres of mono-rhamnolipids and their aglycon precursor 3-(3-hydroxyalkanoyloxy) alkanoic acid (HAA), which typically accumulates as unwanted side product due to incomplete conversion, by established HPLC-CAD analysis (Tiso et al. 2020). Strains with P_{lac}, *araC*-P_{BAD}, and *tetR*-P_{TetA} (SK33, SK38, and SK43) showed only low mono-rhamnolipid titres (ca. 0.02-0.1 g L^{-1}), presumably because the expression of *rhlAB* is too weak. On the other hand, in the stronger *nagR*-P_{nagAa}-based (SK40) and *mtlR*-P_{mtlE}-based (SK42) expression strains, high mono-rhamnolipid titres of ca. 1 and 1.4 g L^{-1}, respectively, were found. However, a large amount of the aglycon HAA (25%–38% ($g/g_{total\ surfactant}$)) accumulated, especially in strain SK42 with *mtlR*-P_{mtlE}. This may be due to a limited availability of the precursor dTDP-L-rhamnose, which is generated from the central carbon metabolism in *P. putida*, at times of strong expression. In summary, the salicylate-inducible promoter *nagR*-P_{nagAa} facilitated strong gene expression with relatively low background without induction as well as relatively high mono-rhamnolipid production with lower levels of the aglycon intermediate, so we chose this promoter system for further studies.

To further elucidate the usefulness of the transcription reporters in our toolbox collection, we next analysed how the salicylate-induced production of rhamnolipids correlates with the output of different transcriptional reporters (eYFP, mCherry, mTagBFP2, LacZ, GUS, PE-H; see Fig. 2) at different induction strength. To this end, the respective pYT vectors were cloned by yeast-mediated recombineering of reporter genes into pYTSK10_0G7 (Tiso et al. 2020) and the *P. putida* strains SK57, SK61, SK60, SK66, and SK64 were constructed. Expression was induced during cultivation with different salicylate concentrations (0.001-5 mM), reporter fluorescence and enzyme activities were determined after 24 h and correlated with the mono-rhamnolipid titres for each inducer concentration (Fig. 4B). Interestingly, despite potential influences of chromophore maturation dynamics in GFP variants (Drepper et al. 2007, 2010) or the amplifying effect in enzyme-based assays (Iyer et al. 2001), the reporter signals (with the exception of PE-H) correlated remarkably well with the mono-rhamnolipid titres (R^2 = 0.92–0.99). Only the PE-H activity does not correlate with product levels, which might be related to the enzyme's influence on the *P. putida* metabolism or even rhamnolipid stability. Our results indicate that tracking the expression of the *rhlAB* operon *via* transcriptional reporters could in principle provide an indication of mono-rhamnolipids production. However, the determination of the rhamnolipid titres should not solely be based on reporter readout; nevertheless, the use of transcriptional reporters is certainly a powerful tool to indicate expression levels and, in the presented case as well as in previous studies (Weihmann et al. 2020), it may serve to estimate product titres.

To finally showcase the utilisation and recycling of homing endonuclease site I-*Sce*I for successive addition of expression modules, we chose to expand the *rhl* expression cassette by dTDP-L-rhamnose biosynthetic genes to reduce accumulation of the aglycon HAA and thus optimise *nagR*-P_{nagAa}-based mono-rhamnolipid production (Fig. 4C). To this end, the *P. aeruginosa* genes encoding for the enzymes RmlA, B, C, and D and the phosphoglucomutase AlgC, which are required for the conversion of glucose-6-phosphate to dTDP-L-rhamnose, were cloned downstream of the *rhlAB* genes in vector pYTSK10_0G7. In line with the toolbox concept of modularity, we could make use of the I-*Sce*I site, which was not destroyed but recycled in the previous cloning step of *rhl* genes, multiple times. The resulting vectors pYTSK51_0G7 and pYTSK62_0G7 were used to generate strains *P. putida* SK51 (additionally equipped with *rml* genes) and SK62 (additionally equipped with *rml* genes and *algC*), respectively. These strains showed a reduced HAA level upon coexpression of *rml* genes and even complete conversion of HAA to mono-rhamnolipid upon additional *algC* coexpression, respectively, with a mono-rhamnolipid titre of 1.45 g L^{-1}. Thus, a qualitative improvement in the production of mono-rhamnolipids by expression of associated genes could be achieved.

The here presented maximal titres of mono-rhamnolipids match previously reported levels, which were obtained under similar cultivation conditions with especially strong constitutive promoters (Tiso et al. 2020). However, the amount of unconverted HAA was massively decreased with the approach presented here. Since the delivery of reactants through the additional expression of heterologous genes has proven useful for an optimisation of biosynthetic flux and product titres in particular for *P. putida* and rhamnolipid biosynthesis but also beyond that (Cabrera-Valladares et al. 2006, Zhang et al. 2012, Sánchez-Pascuala et al. 2019, Troost et al. 2019), the demonstrated method of homing endonuclease I-*Sce*I utilisation and recycling of the site can be helpful for various applications. Occurrence of this nuclease recognition site in biosynthetic genes is highly unlikely, so it can be used, recycled, and re-used for modular extensions multiple times. In summary, our toolbox facilitated the construction of different mono-rhamnolipid production strains, the identification of a most suitable promoter, evaluation of diverse transcription reporters, and the quantitative and qualitative optimisation of production.

Comparison of integration and expression modes for *reb* gene expression

Since the pYT series was proven applicable for all three integration modes (Tn*5*, *rrn*, Tn*7*), we aimed to challenge our toolbox with the expression of biosynthetic genes of a compound which has not been produced in *P. putida* before, and to investigate how different modes of expression affect production. For this purpose, the biosynthetic genes of the indolocarbazole arcyriaflavin A, which

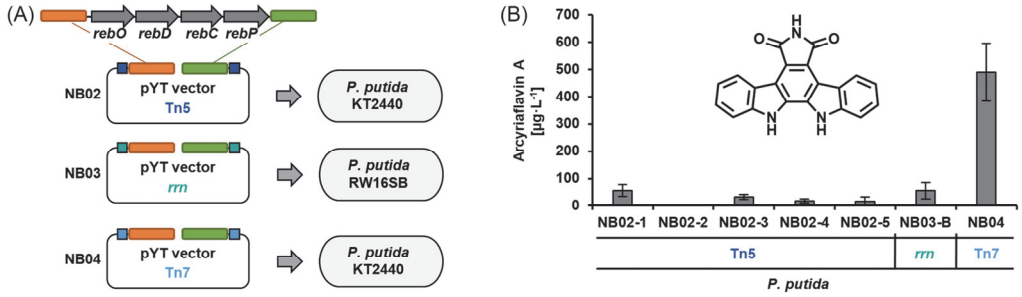

Figure 5. Comparison of different gene integration and expression modes for the production of acryriaflavin A in *P. putida*. **(A)** Cloning schemes of pYT constructs facilitating different integration and expression modes of the acryriaflavin A biosynthetic genes *rebODCP* in *P. putida*. **(B)** Acryriaflavin A titres quantified by HPLC-PDA analyses of crude cell extracts using commercial acryriaflavin A as reference. Data represent the mean of three independent experiments with error bars indicating the corresponding standard deviations.

occurs in the rebeccamycin pathway (Sánchez et al. 2002, 2005), were chosen.

The genes *rebO*, *rebD*, *rebC*, and *rebP* (7.4 kb) derived from the actinomycete *Lentzea aerocolonigenes* (ATCC 39243) (Bush et al. 1987, Sánchez et al. 2006) were integrated *via* In-Fusion® cloning into the I-*Sce*I-linearised pYT vectors pYTRW18K_3T5 and pYTRW26K_1Ti1 for Tn5 transposition and integration into the 16S rRNA genes, respectively. As *nagR*-P_{nagAa} was favourable for rhamnolipid production, we equipped vector pYTSK31K_1G7, which carries Tn7 elements, with this expression system module using the AsiSI site of the YT_core sequence (Fig. S1). In the resulting vector pYTNB01K_1G7, the promoter is placed upstream of the I-*Sce*I site, therefore allowing integration of a gene cluster here with suitable homology arms to the upstream and downstream sequences (CIS_up/dn). Hence, the same PCR product used for *reb* gene integration in the other two pYT vectors, could now be used for this third version (Fig. 5A). The resulting vectors pYTNB02K_3T5, pYTNB03K_1Ti1, and pYTNB04K_1G7 were transferred into the *P. putida* KT2440 wild type or strains RW-16SA-G carrying the landing pad in 16S rRNA genes by conjugation.

Interestingly, the implementation of a constitutive *rebODCP* gene expression by Tn5 transposition was more difficult than for violacein production. Here, conjugational transfer of pYTNB02K_3T5 had to be performed several times to obtain 100 to 200 clones. In contrast to the identification of strains readily expressing violacein biosynthetic genes after random transposition downstream of a chromosomal promoter, the expression of *reb* genes could not be visually detected by the formation of a colored biosynthetic product. Therefore, the clones obtained after conjugation were first analysed for mCherry reporter fluorescence under a Blue/Green transilluminator (λ = 450-530 nm). The mCherry fluorescence results from expression of the respective gene, which is located downstream of the *reb* genes as reporter for complete transcription of the *rebODCP* cluster. Based on the fluorescence signal, five clones (designated as *P. putida* KT2440 NB02-1,-2,-3,-4,-5) were finally selected for production studies. Moreover, with the *rrn* interposon, no double crossover integration could be identified in multiple attempts although counter selection using SacB was implemented, so that a clone with single crossover (in the 16S gene of *rrnB*; *P. putida* NB03-B) was selected for production studies. In contrast, a high number of clones with gene integration at *att*Tn7 was obtained without difficulties, providing strain NB04.

Production of acryriaflavin A was verified in all expression strains after cultivation in liquid medium (and induction with salicylate after an initial growth period in case of the NB04 strain carrying *rebODCP* under *nagR*-P_{nagAa} control at the *att*Tn7 site) by HPLC-PDA analysis using a commercial reference for comparison (Fig. S6). Compared with the other indolocarbazole, deoxyviolacein, which could be produced with high titres in Tn5- and *rrn*-based strains (more than 100 mg L^{-1}), a constitutive expression in analogously constructed strains was apparently less appropriate for acryriaflavin A production (titres of about 60 μg L^{-1}) (Fig. 5B). The difficulties encountered in the construction of these two strains as well as their low production titres suggest that the constitutive production of acryriaflavin A in *P. putida* is unfavourable. It is already known that acryriaflavin A derivatives can act as antimicrobial compounds (Sánchez, Méndez and Salas 2006, Schmidt, Reddy and Knölker 2012). This is also supported by the fact that the production titre with the inducible system is eightfold higher. The calculated titre of about 500 μg L^{-1} (approximately 0.25 mg L^{-1} day^{-1}) is comparable to concentrations of acryriaflavin derivatives already achieved in *E. coli* (Hyun et al. 2003, Casini et al. 2018).

Thus, integration into the *attTn7* site under control of the salicylate inducible promoter *nagR* P_{nagAa} was found to be most suitable for the production of acryriaflavin A. At present, the titres of the two L-tryptophan-derived indolocarbazoles deoxyviolacein and acryriaflavin A cannot be expected to be in a comparable range since the oxidase RebO has a clear preference for 7-chloro-L-tryptophan, which is the native substrate of the rebeccamycin pathway (Nishizawa, Aldrich and Sherman 2005). However, results obtained for deoxyviolacein production indicate that *P. putida* should be metabolically equipped for future optimisation towards higher acryriaflavin A titres. In summary, the construction of the different acryriaflavin A production strains again demonstrated the usefulness of the toolbox presented in this work, in that standardised procedures facilitated comparative evaluation of different integration and expression modes without requiring a new cloning strategy for each case.

In conclusion, the presented ready-to-use series of pYT vectors enabled the efficient construction of secondary metabolite producing *P. putida* strains by transfer and activation of heterologous gene clusters. Its modular architecture allowed standardisation of experimental workflows and the straightforward construction of different strains in parallel, facilitating the selection of the most promising ones.

The toolbox described here complements the available set of tools for the transfer and genomic integration of genes for the construction of *P. putida* expression strains (Loeschcke and Thies 2020, Martin-Pascual et al. 2021). These comprise highly effective tools applying random transposition (Fu et al. 2008, Martínez-García et al. 2014, Domröse et al. 2017), or site-specific integration realised *via* transposase-, integrase- or recombination-based strategies to construct stable and controllable expression strains (Hernandez-Arranz et al. 2019, Bator et al. 2020, Choi and Lee 2020, Zhang et al. 2020, Cook et al. 2021). In contrast to the named specific toolsets, the yTREX toolbox, combines the utilisation of three different favorable modes of genomic integration for biosynthesis gene clusters (Loeschcke and Thies 2020) with a fully modular design, which allows effective ligase-independent vector assembly (Domröse et al. 2017). The latter facilitates rapid construction of different strains and the exchange of modules between the toolbox vectors, thereby matching the current developments in synthetic *Pseudomonas* strain engineering towards standardised and modular genetic tools (de Lorenzo and Schmidt 2018, Martin-Pascual et al. 2021). Straightforward parallel cloning of different transposon or interposon constructs can be especially useful in recombinant production strain development. As illustrated here and in previous studies, the most promising locus for gene integration and mode of expression for a metabolic pathway cannot always be predicted beforehand (Domröse et al. 2015, Gießelmann et al. 2019, Tiso et al. 2020), so that only a comparative evaluation may help. In principle, the presented toolbox should be applicable with Gram-negative hosts other than *P. putida* for which protocols for conjugational transfer, Tn7 and Tn5 transposition are well established. The latter has been elegantly employed for the integration of landing pads to enable subsequent specific recombinational integration of biosynthetic gene clusters in diverse γ-Proteobacteria in an effective manner (Wang et al. 2019). The *rrn* integrative variant requires, of course, also the equipment of the target strain with landing pads. Notably, considering the high degree of conservation of 16S rRNA-encoding genes, the constructs used here to deliver landing pads to *P. putida* KT2440 should also be applicable in other *Pseudomonas* (Otto et al. 2019) and most probably in other Proteobacteria as well.

Acknowledgements

The authors gratefully acknowledge Sabrina Linden and Esther Knieps-Grünhagen for technical support.

Supplementary Data

Supplementary data is available at FEMSMC online.

Conflicts of interest statement. None declared

Funding

RW, SK, IB and TT obtained grants from the Bioeconomy Science Center which is financially supported by the Ministry of Culture and Science within the framework of the NRW Strategieprojekt BioSC (No. 313/323-400-002 13). The Ministry for Culture and Science funded a scholarship for AD within the CLIB Graduate Cluster Biotechnology. This work was further supported by the German Federal Ministry of Education and Research *via* the projects NO-STRESS (031B0852B, to NLB, ST, AL and KEJ), LipoBiocat (031B0837A, to ST and KEJ), and GlycoX (161B0866A, to ST, AL and KEJ). TT and LMB have been partially funded by the Deutsche Forschungsgemeinschaft (DFG, German Research Foundation) under Germany´s Excellence Strategy—Exzellenzcluster 2186 „The Fuel Science Center' ID: 390919832.

References

Alam K, Hao J, Zhang Y *et al.* Synthetic biology-inspired strategies and tools for engineering of microbial natural product biosynthetic pathways. *Biotechnol Adv* 2021;**49**:107759.

Antoine R, Locht C. Isolation and molecular characterization of a novel broad-host-range plasmid from *Bordetella bronchiseptica* with sequence similarities to plasmids from Gram-positive organisms. *Mol Microbiol* 1992;**6**:1785–99.

Aymoz D, Wosika V, Durandau E *et al.* Real-time quantification of protein expression at the single-cell level via dynamic protein synthesis translocation reporters. *Nat Commun* 2016;**7**:11304.

Bagdasarian M, Lurz R, Rückert B *et al.* Specific-purpose plasmid cloning vectors II. Broad host range, high copy number, RSF1010-derived vectors, and a host-vector system for gene cloning in *Pseudomonas*. *Gene* 1981;**16**:237–47.

Bator I, Wittgens A, Rosenau F *et al.* Comparison of three xylose pathways in *Pseudomonas putida* KT2440 for the synthesis of valuable products. *Front Bioeng Biotechnol* 2020;**7**:480.

Behrens B, Baune M, Jungkeit J *et al.* High performance liquid chromatography-charged aerosol detection applying an inverse gradient for quantification of rhamnolipid biosurfactants. *J Chromatogr A* 2016;**1455**:125–32.

Belda E, Van Heck RGA, Lopez-sanchez MJ *et al.* The revisited genome of *Pseudomonas putida* KT2440 enlightens its value as a robust metabolic chassis. *Environ Microbiol* 2016;**18**:3403–24.

Bird LE, Rada H, Flanagan J *et al.* DNA cloning and assembly methods. In: Valla S, Lale R (eds.), *Methods in Molecular Biology*. Vol **1116**. New York: Humana Press, 2014,119–31.

Bitzenhofer NL, Kruse L, Thies S *et al.* Towards robust *Pseudomonas* cell factories to harbour novel biosynthetic pathways. *Essays Biochem* 2021;**65**:319–36.

Bollinger A, Thies S, Knieps-Grünhagen E *et al.* A Novel Polyester Hydrolase From the Marine Bacterium *Pseudomonas aestusnigri* – Structural and Functional Insights. *Front Microbiol* 2020;**11**:114.

Bush JA, Long BH, Catino JJ *et al.* Production and biological activity of rebeccamycin, a novel antitumor agent. *J Antibiot (Tokyo)* 1987;**40**:668–78.

Bustin SA, Benes V, Garson JA *et al.* The MIQE guidelines: minimum information for publication of quantitative real-time PCR experiments. *Clin Chem* 2009;**55**:611–22.

Cabrera-Valladares N, Richardson A-P, Olvera C *et al.* Monorhamnolipids and 3-(3-hydroxyalkanoyloxy) alkanoic acids (HAAs) production using *Escherichia coli* as a heterologous host. *Appl Microbiol Biotechnol* 2006;**73**:187–94.

Calero P, Jensen SI, Nielsen AT. Broad-host-range ProUSER vectors enable fast characterization of inducible promoters and optimization of *p*-coumaric acid production in *Pseudomonas putida* KT2440. *ACS Synth Biol* 2016;**5**:741–53.

Casini A, Chang FY, Eluere R *et al.* A Pressure Test to Make 10 Molecules in 90 Days: external Evaluation of Methods to Engineer Biology. *J Am Chem Soc* 2018;**140**:4302–16.

Chai Y, Shan S, Weissman KJ *et al.* Heterologous expression and genetic engineering of the tubulysin biosynthetic gene cluster using Red/ET recombineering and inactivation mutagenesis. *Chem Biol* 2012;**19**:361–71.

Choi K-H, Gaynor JB, White KG *et al.* A Tn7-based broad-range bacterial cloning and expression system. *Nat Methods* 2005;**2**:443–8.

Choi KH, Schweizer HP. mini-Tn7 insertion in bacteria with single *att*Tn7 sites: example *Pseudomonas aeruginosa*. *Nat Protoc* 2006;**1**:153–61.

Choi KR, Cho JS, Cho IJ *et al.* Markerless gene knockout and integration to express heterologous biosynthetic gene clusters in *Pseudomonas putida*. *Metab Eng* 2018;**47**:463–74.

Choi KR, Lee SY. Protocols for RecET-based markerless gene knockout and integration to express heterologous biosynthetic gene clusters in *Pseudomonas putida*. *Microb Biotechnol* 2020;**13**:199–209.

Choi SY, Lim S, Yoon K *et al.* Biotechnological activities and applications of bacterial pigments violacein and prodigiosin. *J Biol Eng* 2021;**15**:10.

Cook TB, Jacobson TB, Venkataraman M V. *et al.* Stepwise genetic engineering of *Pseudomonas putida* enables robust heterologous production of prodigiosin and glidobactin A. *Metab Eng* 2021;**67**:112–24.

Cook TB, Rand JM, Nurani W *et al.* Genetic tools for reliable gene expression and recombineering in *Pseudomonas putida*. *J Ind Microbiol Biotechnol* 2018;**45**:517–27.

Cui W, Han L, Cheng J *et al.* Engineering an inducible gene expression system for *Bacillus subtilis* from a strong constitutive promoter and a theophylline-activated synthetic riboswitch. *Microb Cell Fact* 2016;**15**:199.

Damron FH, McKenney ES, Barbier M *et al.* Construction of mobilizable mini-Tn7 vectors for bioluminescent detection of gram-negative bacteria and single-copy promoter *lux* reporter analysis. *Appl Environ Microbiol* 2013;**79**:4149–53.

de Lorenzo V, Eltis L, Kessler B *et al.* Analysis of *Pseudomonas* gene products using *lacIq/Ptrp-lac* plasmids and transposons that confer conditional phenotypes. *Gene* 1993;**123**:17–24.

de Lorenzo V, Herrero M, Sánchez JM *et al.* Mini-transposons in microbial ecology and environmental biotechnology. *FEMS Microbiol Ecol* 1998;**27**:211–24.

de Lorenzo V, Schmidt M. Biological standards for the Knowledge-Based BioEconomy: what is at stake. *N Biotechnol* 2018;**40**:170–80.

Domröse A, Hage-Hülsmann J, Thies S *et al. Pseudomonas putida* rDNA is a favored site for the expression of biosynthetic genes. *Sci Rep* 2019;**9**:7028.

Domröse A, Klein AS, Hage-Hülsmann J *et al.* Efficient recombinant production of prodigiosin in *Pseudomonas putida*. *Front Microbiol* 2015;**6**:972.

Domröse A, Weihmann R, Thies S *et al.* Rapid generation of recombinant *Pseudomonas putida* secondary metabolite producers using yTREX. *Synth Syst Biotechnol* 2017;**2**:310–9.

Drepper T, Eggert T, Circolone F *et al.* Reporter proteins for *in vivo* fluorescence without oxygen. *Nat Biotechnol* 2007;**25**:443–5.

Drepper T, Huber R, Heck A *et al.* Flavin mononucleotide-based fluorescent reporter proteins outperform green fluorescent protein-like proteins as quantitative *in vivo* real-time reporters. *Appl Environ Microbiol* 2010;**76**:5990–4.

Elmore JR, Dexter GN, Salvachúa D *et al.* Engineered *Pseudomonas putida* simultaneously catabolizes five major components of corn stover lignocellulose: glucose, xylose, arabinose, p-coumaric acid, and acetic acid. *Metab Eng* 2020;**62**:62–71.

Elmore JR, Furches A, Wolff GN *et al.* Development of a high efficiency integration system and promoter library for rapid modification of *Pseudomonas putida* KT2440. *Metab Eng Commun* 2017;**5**:1–8.

Engler C, Kandzia R, Marillonnet S. A one pot, one step, precision cloning method with high throughput capability. *PLoS One* 2008;**3**:e3647.

Fang M-Y, Zhang C, Yang S *et al.* High crude violacein production from glucose by *Escherichia coli* engineered with interactive control of tryptophan pathway and violacein biosynthetic pathway. *Microb Cell Fact* 2015;**14**:8.

Frampton EW, Restaino L, Blaszko N. Evaluation of the β-glucuronidase substrate 5-bromo-4-chloro-3-indolyl-β-D-glucuronide (X-GLUC) in a 24-hour direct plating method for *Escherichia coli*. *J Food Prot* 1988;**51**:402–4.

Fu J, Wenzel SC, Perlova O *et al.* Efficient transfer of two large secondary metabolite pathway gene clusters into heterologous hosts by transposition. *Nucleic Acids Res* 2008;**36**:e113.

Gay P, le Coq D, Steinmetz M *et al.* Positive selection procedure for entrapment of insertion sequence elements in Gram-negative bacteria. *J Bacteriol* 1985;**164**:918–21.

Gemperlein K, Hoffmann M, Huo L *et al.* Synthetic biology approaches to establish a heterologous production system for coronatines. *Metab Eng* 2017;**44**:213–22.

Gießelmann G, Dietrich D, Jungmann L *et al.* Metabolic engineering of *Corynebacterium glutamicum* for high-level ectoine production: design, combinatorial assembly, and implementation of a transcriptionally balanced heterologous ectoine pathway. *Biotechnol J* 2019;**14**:1800417.

Gietz RD, Schiestl RH. High-efficiency yeast transformation using the LiAc/SS carrier DNA/PEG method. *Nat Protoc* 2007;**2**:31–5.

Grant SGN, Jessee J, Bloom FR *et al.* Differential plasmid rescue from transgenic mouse DNAs into *Escherichia coli* methylation-restriction mutants. *Proc Natl Acad Sci* 1990;**87**:4645–9.

Green M, Sambrook J. *Molecular Cloning: A Laboratory Manual*. 4th ed. Cold Spring Harbor, New York: Cold Spring Harbor Laboratory Press, 2012.

Hernandez-Arranz S, Perez-Gil J, Marshall-Sabey D *et al.* Engineering *Pseudomonas putida* for isoprenoid production by manipulating endogenous and shunt pathways supplying precursors. *Microb Cell Fact* 2019;**18**:152.

Hoffmann J, Altenbuchner J. Functional characterization of the mannitol promoter of *Pseudomonas fluorescens* DSM 50106 and its application for a mannitol-inducible expression system for *Pseudomonas putida* KT2440. *PLoS One* 2015;**10**:e0133248.

Horwitz JP, Chua J, Curby RJ *et al.* Substrates for cytochemical demonstration of enzyme activity. I. Some substituted 3-Indolyl-β-D-glycopyranosides. *J Med Chem* 1964;**7**:574–5.

Hyun CG, Bililign T, Liao J *et al.* The biosynthesis of indolocarbazoles in a heterologous *E. coli* host. *ChemBioChem* 2003;**4**:114–7.

Iyer M, Wu L, Carey M *et al.* Two-step transcriptional amplification as a method for imaging reporter gene expression using weak promoters. *Proc Natl Acad Sci* 2001;**98**:14595–600.

Jefferson RA, Burgess SM., Hirsh D. β-Glucuronidase from *Escherichia coli* as a gene-fusion marker. *Proc Natl Acad Sci* 1986;**83**:8447–51.

Kampers LFC, Volkers RJM, Martins dos Santos VAP. *Pseudomonas putida* KT2440 is HV1 certified, not GRAS. *Microb Biotechnol* 2019;**12**:845–8.

Ke J, Yoshikuni Y. Multi-chassis engineering for heterologous production of microbial natural products. *Curr Opin Biotechnol* 2020;**62**:88–97.

Knight T. Idempotent vector design for standard assembly of biobricks. *MIT Libr* 2003:1–11.

Kõressaar T, Lepamets M, Kaplinski L *et al.* Primer3_masker: integrating masking of template sequence with primer design software. *Bioinformatics* 2018;**34**:1937–8.

Kouprina N, Annab L, Graves J *et al.* Functional copies of a human gene can be directly isolated by transformation-associated recombination cloning with a small 3′ end target sequence. *Proc Natl Acad Sci USA* 1998;**95**:4469–74.

Lee ME,Anil A Han AS Tomlin CJ Dueber JE Expression-level optimization of a multi-enzyme pathway in the absence of a high-throughput assay. *Nucleic Acids Res* 2013;**41**:10668–78.

Loeschcke A, Thies S. Engineering of natural product biosynthesis in *Pseudomonas putida*. *Curr Opin Biotechnol* 2020;**65**:213–24.

Martin-Pascual M, Batianis C, Bruinsma L *et al.* A navigation guide of synthetic biology tools for *Pseudomonas putida*. *Biotechnol Adv* 2021;**49**:107732.

Martínez-García E, Aparicio T, de Lorenzo V *et al.* New transposon tools tailored for metabolic engineering of Gram-negative microbial cell factories. *Front Bioeng Biotechnol* 2014;**2**:46.

Martínez-García E, Goñi-Moreno A, Bartley B *et al.* SEVA 3.0: an update of the Standard European Vector Architecture for enabling portability of genetic constructs among diverse bacterial hosts. *Nucleic Acids Res* 2020;**48**:D1164–70.

Mi J, Sydow A, Schempp F *et al.* Investigation of plasmid-induced growth defect in *Pseudomonas putida*. *J Biotechnol* 2016;**231**:167–73.

Miller JH. Assay of β-Galactosidase. In: experiments in Molecular Genetics. *Cold Spring Harb Lab Cold Spring Harb New York* 1972:352–5.

Molitor R, Bollinger A, Kubicki S *et al.* Agar plate-based screening methods for the identification of polyester hydrolysis by *Pseudomonas* species. *Microb Biotechnol* 2020;**13**:274–84.

Montiel D, Kang H-S, Chang F-Y *et al.* Yeast homologous recombination-based promoter engineering for the activation of silent natural product biosynthetic gene clusters. *Proc Natl Acad Sci* 2015;**112**:8953–8.

Mutalik VK, Guimaraes JC, Cambray G *et al.* Precise and reliable gene expression via standard transcription and translation initiation elements. *Nat Methods* 2013;**10**:354–60.

Naville M, Ghuillot-Gaudeffroy A, Marchais A *et al.* ARNold: a web tool for the prediction of Rho-independent transcription terminators. *RNA Biol* 2011;**8**:11–3.

Nazareno ES, Acharya B, Dumenyo CK. A mini-Tn5-derived transposon with reportable and selectable markers enables rapid generation and screening of insertional mutants in Gram-negative bacteria. *Lett Appl Microbiol* 2021;**72**:283–91.

Nelson KE, Weinel C, Paulsen IT *et al.* Complete genome sequence and comparative analysis of the metabolically versatile *Pseudomonas putida* KT2440. *Environ Microbiol* 2002;**4**:799–808.

Nikel PI, de Lorenzo V. Implantation of unmarked regulatory and metabolic modules in Gram-negative bacteria with specialised mini-transposon delivery vectors. *J Biotechnol* 2013;**163**:143–54.

Nishizawa T, Aldrich CC, Sherman DH. Molecular analysis of the rebeccamycin L-amino acid oxidase from *Lechevalieria aerocolonigenes* ATCC 39243. *J Bacteriol* 2005;**187**:2084–92.

Nora LC, Westmann CA, Martins-Santana L *et al.* The art of vector engineering: towards the construction of next-generation genetic tools. *Microb Biotechnol* 2019;**12**:125–47.

Noskov V, Kouprina N, Leem SH *et al.* A genetic system for direct selection of gene-positive clones during recombinational cloning in yeast. *Nucleic Acids Res* 2002;**30**:e8.

Otto M, Wynands B, Drepper T *et al.* Targeting 16S rDNA for Stable Recombinant Gene Expression in *Pseudomonas*. *ACS Synth Biol* 2019;**8**:1901–12.

Pearson JP, Pesci EC, Iglewski BH. Roles of *Pseudomonas aeruginosa las* and *rhl* quorum-sensing systems in control of twitching motility. *J Bacteriol* 1997;**179**:5756–67.

Peters JE, Craig NL. Tn7: smarter than we thought. *Nat Rev Mol Cell Biol* 2001;**2**:806–14.

Philip DS, Sarovich DS, Pemberton JM. Complete sequence and analysis of the stability functions of pPSX, a vector that allows stable cloning and expression of Streptomycete genes in *Escherichia coli* K12. *Plasmid* 2009;**62**:39–43.

Prentki P, Krisch HM. *In vitro* insertional mutagenesis with a selectable DNA fragment. *Gene* 1984;**29**:303–13.

Priya D, Srinivasa KSR, Mariappan TK. Production of violacein pigment from *Chromobacterium violaceum* and its antibacterial activity and synergism on *E. coli* isolated from UTI samples. *Int J Recent Sci Res* 2018;**9**:24479–84.

Reznikoff WS. Transposon Tn 5. *Annu Rev Genet* 2008;**42**:269–86.

Rodrigues AL, Göcke Y, Bolten C *et al.* Microbial production of the drugs violacein and deoxyviolacein: analytical development and strain comparison. *Biotechnol Lett* 2012;**34**:717–20.

Sánchez C, Braña AF, Méndez C *et al.* Reevaluation of the violacein biosynthetic pathway and its relationship to indolocarbazole biosynthesis. *ChemBioChem* 2006;**7**:1231–40.

Sánchez C, Butovich IA, Braña AF *et al.* The biosynthetic gene cluster for the antitumor rebeccamycin: characterization and generation of indolocarbazole derivatives. *Chem Biol* 2002;**9**:519–31.

Sánchez C, Méndez C, Salas JA. Indolocarbazole natural products: occurrence, biosynthesis, and biological activity. *Nat Prod Rep* 2006;**23**:1007–45.

Sánchez C, Zhu L, Braña AF *et al.* Combinatorial biosynthesis of antitumor indolocarbazole compounds. *Proc Natl Acad Sci* 2005;**102**:461–6.

Sánchez-Pascuala A, Fernández-Cabezón L, de Lorenzo V *et al.* Functional implementation of a linear glycolysis for sugar catabolism in *Pseudomonas putida*. *Metab Eng* 2019;**54**:200–11.

Sarovich DS, Pemberton JM. pPSX: a novel vector for the cloning and heterologous expression of antitumor antibiotic gene clusters. *Plasmid* 2007;**57**:306–13.

Sathesh-Prabu C, Tiwari R, Kim D *et al.* Inducible and tunable gene expression systems for *Pseudomonas putida* KT2440. *Sci Rep* 2021;**11**:18079.

Schmidt AW, Reddy KR, Knölker HJ. Occurrence, biogenesis, and synthesis of biologically active carbazole alkaloids. *Chem Rev* 2012;**112**:3193–328.

Schuster LA, Reisch CR. A plasmid toolbox for controlled gene expression across the Proteobacteria. *Nucleic Acids Res* 2021;**49**:7189–202.

Schwanemann T, Otto M, Wierckx N *et al.* *Pseudomonas* as versatile aromatics cell factory. *Biotechnol J* 2020;**15**:1900569.

Schweizer HP. Small broad-host-range gentamycin resistance gene cassettes for site-specific insertion and deletion mutagenesis. *Biotechniques* 1993;**15**:831–3.

Shaner NC, Campbell RE, Steinbach PA *et al.* Improved monomeric red, orange and yellow fluorescent proteins derived from *Discosoma* sp. red fluorescent protein. *Nat Biotechnol* 2004;**22**:1567–72.

Simon R, Priefer U, Pühler A. A broad host range mobilization system for *in vivo* genetic engineering: transposon mutagenesis in Gram negative bacteria. *Nat Biotechnol* 1983;**1**:784–91.

Slager J, Veening J-W. Hard-wired control of bacterial processes by chromosomal gene location. *Trends Microbiol* 2016;**24**:788–800.

Solovyev V, Salamov A. Automatic annotation of microbial genomes and metagenomic sequences. In: Li RW (ed.), *Metagenomics and Its Applications in Agriculture, Biomedicine and Environmental Studies*. New York, USA: Nova Science Publishers, 2011,61–78.

Spiess E, Bestvater F, Heckel-Pompey A *et al.* Two-photon excitation and emission spectra of the green fluorescent protein variants ECFP, EGFP and EYFP. *J Microsc* 2005;**217**:200–4.

Stothard P. The Sequence Manipulation Suite: javaScript programs for analyzing and formatting protein and DNA sequences. *Biotechniques* 2000;**28**:1102–4.

Subach OM, Cranfill PJ, Davidson MW *et al.* An enhanced monomeric blue fluorescent protein with the high chemical stability of the chromophore. *PLoS One* 2011;**6**:e28674.

Subramaniam S, Ravi V, Sivasubramanian A. Synergistic antimicrobial profiling of violacein with commercial antibiotics against pathogenic micro-organisms. *Pharm Biol* 2014;**52**:86–90.

Sutcliffe JG. Complete nucleotide sequence of the *Escherichia coli* plasmid pBR322. *Cold Spring Harb Symp Quant Biol* 1979;**43**:77–90.

Thompson MG, Incha MR, Pearson AN *et al.* Fatty acid and alcohol metabolism in *Pseudomonas putida*: functional analysis using random barcode transposon sequencing. *Appl Environ Microbiol* 2020;**86**:e01665–20.

Thorwall S, Schwartz C, Chartron JW *et al.* Stress-tolerant non-conventional microbes enable next-generation chemical biosynthesis. *Nat Chem Biol* 2020;**16**:113–21.

Tiso T, Ihling N, Kubicki S *et al.* Integration of genetic and process engineering for optimized rhamnolipid production using *Pseudomonas putida*. *Front Bioeng Biotechnol* 2020;**8**:976.

Tiso T, Sabelhaus P, Behrens B *et al.* Creating metabolic demand as an engineering strategy in *Pseudomonas putida* – Rhamnolipid synthesis as an example. *Metab Eng Commun* 2016;**3**:234–44.

Troost K, Loeschcke A, Hilgers F *et al.* Engineered *Rhodobacter capsulatus* as a phototrophic platform organism for the synthesis of plant sesquiterpenoids. *Front Microbiol* 2019;**10**:1998.

Valenzuela-Ortega M, French C. Joint universal modular plasmids (JUMP): a flexible vector platform for synthetic biology. *Synth Biol* 2021;**6**:ysab003

van Dolleweerd CJ, Kessans SA, Van de Bittner KC *et al.* MIDAS: a modular DNA assembly system for synthetic biology. *ACS Synth Biol* 2018;**7**:1018–29.

Verhoef S, Ballerstedt II, Volkers RJM *et al.* Comparative transcriptomics and proteomics of *p*-hydroxybenzoate producing *Pseudomonas putida* S12: novel responses and implications for strain improvement. *Appl Microbiol Biotechnol* 2010;**87**:679–90.

Wang G, Zhao Z, Ke J *et al.* CRAGE enables rapid activation of biosynthetic gene clusters in undomesticated bacteria. *Nat Microbiol* 2019;**4**:2498–510.

Wang H, Wang F, Zhu X *et al.* Biosynthesis and characterization of violacein, deoxyviolacein and oxyviolacein in heterologous host, and their antimicrobial activities. *Biochem Eng J* 2012;**67**:148–55.

Weihmann R, Domröse A, Drepper T *et al.* Protocols for yTREX/Tn5-based gene cluster expression in *Pseudomonas putida*. *Microb Biotechnol* 2020;**13**:250–62.

Weimer A, Kohlstedt M, Volke DC *et al.* Industrial biotechnology of *Pseudomonas putida*: advances and prospects. *Appl Microbiol Biotechnol* 2020;**104**:7745–66.

Yan F, Burgard C, Popoff A *et al.* Synthetic biology approaches and combinatorial biosynthesis towards heterologous lipopeptide production. *Chem Sci* 2018;**9**:7510–9.

Zhang JJ, Tang X, Huan T *et al.* Pass-back chain extension expands multimodular assembly line biosynthesis. *Nat Chem Biol* 2020;**16**:42–9.

Zhang JJ, Tang X, Zhang M *et al.* Broad-host-range expression reveals native and host regulatory elements that influence heterologous antibiotic production in Gram-negative bacteria. *MBio* 2017;**8**:e01291–17.

Zhang L, Veres-Schalnat TA, Somogyi A *et al.* Fatty acid cosubstrates provide β-oxidation precursors for rhamnolipid biosynthesis in *Pseudomonas aeruginosa*, as evidenced by isotope tracing and gene expression assays. *Appl Environ Microbiol* 2012;**78**:8611–22.

Zobel S, Benedetti I, Eisenbach L *et al.* Tn7-based device for calibrated heterologous gene expression in *Pseudomonas putida*. *ACS Synth Biol* 2015;**4**:1341–51.

II.3. Targeted exploitation of a stress response mechanism in a biosynthetic context

PUBLICATION III

Exploring engineered vesiculation by *Pseudomonas putida* KT2440 for natural product biosynthesis

Nora Lisa Bitzenhofer, Carolin Höfel, Stephan Thies, Andrea Jeanette Weiler, Christian Eberlein, Hermann J. Heipieper, Renu Batra-Safferling, Pia Sundermeyer, Thomas Heidler, Carsten Sachse, Tobias Busche, Jörn Kalinowski, Thomke Maren Belthle, Thomas Drepper, Karl-Erich Jaeger, Anita Loeschcke

Microbial Biotechnology (**2023**) 00:1-18.

The online version is available at: 10.1111/1751-7915.14312

Status: published

Supporting Information can be found in the Appendix (**Chapter V.2**)

Own contribution:

Planning and performing the biological experiments, analyzing the data, writing the manuscript.

Received: 4 January 2023 | Accepted: 25 June 2023

DOI: 10.1111/1751-7915.14312

MICROBIAL BIOTECHNOLOGY Applied Microbiology International

RESEARCH ARTICLE

Exploring engineered vesiculation by *Pseudomonas putida* KT2440 for natural product biosynthesis

Nora Lisa Bitzenhofer[1] | Carolin Höfel[1] | Stephan Thies[1] | Andrea Jeanette Weiler[1] | Christian Eberlein[2] | Hermann J. Heipieper[2] | Renu Batra-Safferling[3] | Pia Sundermeyer[4,5] | Thomas Heidler[4,5] | Carsten Sachse[4,5,6] | Tobias Busche[7,8] | Jörn Kalinowski[7] | Thomke Belthle[9,10] | Thomas Drepper[1] | Karl-Erich Jaeger[1,11] | Anita Loeschcke[1]

[1]Institute of Molecular Enzyme Technology (IMET), Heinrich Heine University Düsseldorf, Düsseldorf, Germany
[2]Department of Environmental Biotechnology, Helmholtz Centre for Environmental Research (UFZ), Leipzig, Germany
[3]Institute of Biological Information Processing – Structural Biochemistry (IBI-7: Structural Biochemistry), Forschungszentrum Jülich, Jülich, Germany
[4]Ernst-Ruska Centre for Microscopy and Spectroscopy with Electrons (ER-C-3/Structural Biology), Forschungszentrum Jülich, Jülich, Germany
[5]Institute for Biological Information Processing 6 (IBI-6/ Structural Cellular Biology), Forschungszentrum Jülich, Jülich, Germany
[6]Department of Biology, Heinrich Heine University Düsseldorf, Düsseldorf, Germany
[7]Center for Biotechnology (CeBiTec), Bielefeld University, Bielefeld, Germany
[8]Bielefeld University, Medical School East Westphalia-Lippe, Bielefeld University, Bielefeld, Germany
[9]DWI—Leibniz-Institute for Interactive Materials, Aachen, Germany
[10]Functional and Interactive Polymers, Institute of Technical and Macromolecular Chemistry, RWTH Aachen University, Aachen, Germany
[11]Institute of Bio- and Geosciences IBG-1: Biotechnology, Forschungszentrum Jülich, Jülich, Germany

Correspondence
Anita Loeschcke, Institute of Molecular Enzyme Technology, HHU Düsseldorf, Wilhelm-Johnen-Straße, 52428 Jülich, Germany.
Email: a.loeschcke@fz-juelich.de

Funding information
Bundesministerium für Bildung und Forschung, Grant/Award Number: 031B0837A, 031B0852B, 031B085C and 161B0866A; Deutsche Forschungsgemeinschaft, Grant/Award Number: Project ID 458090666 / CRC1535/1; European Regional Development Fund (EFRE), Grant/Award Number: 34.EFRE-0300095/1703FI04

Abstract

Pseudomonas species have become promising cell factories for the production of natural products due to their inherent robustness. Although these bacteria have naturally evolved strategies to cope with different kinds of stress, many biotechnological applications benefit from engineering of optimised chassis strains with specially adapted tolerance traits. Here, we explored the formation of outer membrane vesicles (OMV) of *Pseudomonas putida* KT2440. We found OMV production to correlate with the recombinant production of a natural compound with versatile beneficial properties, the tripyrrole prodigiosin. Further, several *P. putida* genes were identified, whose up- or down-regulated expression allowed controlling OMV formation. Finally, genetically triggering vesiculation in production strains of the different alkaloids prodigiosin, violacein, and phenazine-1-carboxylic acid, as well as the carotenoid zeaxanthin, resulted in up to three-fold increased product yields. Consequently, our findings suggest that the construction of robust strains by genetic manipulation of OMV formation might be developed into a useful tool which may contribute to improving limited biotechnological applications.

INTRODUCTION

Secondary metabolites of microorganisms exhibit a variety of biological activities which make them applicable as pharmaceuticals, ingredients in cosmetics, and food additives. One approach to accessing these natural products is the biosynthesis in heterologous strains, which are engineered as whole-cell biocatalysts (Lin & Tao, 2017). In the last decades, *Pseudomonas* species have become promising bacterial cell factories for such bioproduction processes. One prominent representative of this group is *Pseudomonas putida*, mainly due to its inherent robustness as reviewed in detail in the last years (Bitzenhofer et al., 2021; Loeschcke & Thies, 2015, 2020; Nikel & de Lorenzo, 2018; Weimer et al., 2020).

The compounds which have been produced in *P. putida* include toxic aromatic acids like *p*-coumarate or cinnamate (Calero et al., 2018; Molina-Santiago et al., 2016; Schwanemann et al., 2020), antimicrobial compounds like violaceins and phenazines (Askitosari et al., 2019; Domröse et al., 2017; Zhang et al., 2017), or prodiginines and glidobactins (Cook et al., 2021; Domröse et al., 2015; Loeschcke & Thies, 2020), as well as different terpenoids including zeaxanthin, β-carotene, and lycopene (Beuttler et al., 2011; Hernandez-Arranz et al., 2019; Sánchez-Pascuala et al., 2019).

Despite these success stories, the high-level production of natural compounds is still challenging, amongst other reasons, due to chemical stress caused by high product and substrate concentrations, respectively, which can damage biomolecules or membranes, ultimately compromising the bioprocess (Nicolaou et al., 2010). It is thus intriguing to understand how bacteria have naturally evolved different strategies to respond and adapt to chemical stress. In Pseudomonads, an active extrusion of a chemical stressor via efflux transporters to avoid its intracellular accumulation or damage recovery/prevention mechanisms (e.g., the use of chaperones or redox enzymes) are prominent strategies to deal with chemical stress (Bitzenhofer et al., 2021; Blanco et al., 2016; Bösl et al., 2006; Hartl et al., 2011; Henderson et al., 2021; Nicolaou et al., 2010; Roca et al., 2008). Further, a *Pseudomonas*-characteristic and quite unique stress response is the conversion of *cis*- unsaturated fatty acids (FA) of the inner membrane (IM) to their *trans*-configuration by the *cis-trans*-isomerase (Cti) (Bitzenhofer et al., 2021; Heipieper et al., 2003; Tan et al., 2016). The Cti exerts an immediate response: The enzyme is described to be constitutively present in the periplasm and as soon as the membrane is sufficiently perturbed, it can access the *cis*-unsaturated FA in the membrane phospholipid bilayer and isomerises them to the corresponding *trans*-configuration (Mauger et al., 2021). Additionally, *P. putida* can also respond by vesiculation to chemical stresses, i.e., releasing outer membrane vesicles (OMVs) into the extracellular space. This can be caused by structural changes in the cell envelope (Juodeikis & Carding, 2022). The two processes, *cis-trans*-isomerisation and OMV release, can be employed synchronously in response to the same stresses, but not obligatory so (Eberlein et al., 2018). The OMVs are mainly composed of phospholipids, lipopolysaccharides (LPS), and proteins (Avila-Calderón et al., 2021). Their release can lead to a more hydrophobic bacterial cell surface and thus enhance biofilm formation, which in turn increases bacterial resistance to chemical stressors (Atashgahi et al., 2018; Baumgarten et al., 2012). In addition, vesiculation can help to bring and/or keep the stressors out of the cell (Eberlein et al., 2019; Mozaheb & Mingeot-Leclercq, 2020) and OMVs may serve as an extracellular reservoir for chemical compounds, effectively reducing the concentration in or surrounding the cell (Domröse et al., 2015; Schwechheimer & Kuehn, 2015). An association of OMV release with natural bacterial export of secondary metabolites has been proposed (Batista et al., 2020; Choi et al., 2020; Mashburn & Whiteley, 2005; Tan et al., 2020). Recently, the engineering of such membrane structures was shown to enhance the recombinant production of hydrophobic metabolites in *Escherichia coli* (Yang et al., 2021).

To alleviate the difficulties of high-level microbial production, the construction of robust cell factories with specifically adapted tolerance features seems to be crucial. Here, we assess OMV formation as a biotechnologically exploitable tolerance trait. We present genetic engineering strategies to increase vesiculation and the production of different secondary metabolites in *Pseudomonas putida* KT2440.

EXPERIMENTAL PROCEDURE

Cultivation of *P. putida*

Pseudomonas putida wild-type KT2440 (Nelson et al., 2002) and the derived strains *P. putida* pig21, vio12, and PCA1 (Domröse et al., 2017), *P. putida* pig-r11, -43, and -r44 (Domröse et al., 2019), as well as *P. putida* crtΔX, which was constructed as previously described (Loeschcke et al., 2013; see Table S4), were cultivated under continuous shaking (130 rpm) at 30°C in 10 mL LB (lysogeny broth) medium (10 g L^{-1} tryptone, 5 g L^{-1} yeast extract, 10 g L^{-1} sodium chloride; Carl Roth®). Antibiotics were added to the culture medium when appropriate to the following final concentrations: 25 μg mL^{-1} kanamycin, 25 μg mL^{-1} irgasan, 25 μg mL^{-1} gentamicin, and 50 μg mL^{-1} tetracycline. For chemical induction of OMV formation, *P. putida* KT2440 was exposed to 1 mM 1-octanol (Acros organics, part of Thermo Fisher Scientific), 50 μM PQS in DMSO

(Biomol GmbH), or 0.6 mM prodigiosin (in DMSO, final concentration 3%; for extraction and purification see Figure S15 and M5 in Appendix S1) after reaching the logarithmic growth phase. To induce gene expression or to manipulate gene expression, respectively, 10 mM L-arabinose was added.

Plasmid and strain construction

Oligonucleotides, plasmids, and strains, which were generated based on *P. putida* KT2440, are summarised in Tables S3 and S4.

All recombinant DNA techniques were essentially performed as described by Sambrook et al. (1989), using *Escherichia coli* strains DH5α (Hanahan, 1983) and Stellar™ cells (Takara Bio, Cat# 636763; see Table S4). Assembly procedures for vectors facilitating overexpression or repression of candidate genes are detailed in M1 in Appendix S1.

Plasmids were introduced into *P. putida* KT2440 by electroporation (Tu et al., 2016). Briefly, 1 mL of overnight cultures of *P. putida* strains was harvested by centrifugation (2 min, 11,000 *g*) and washed with 1 mL H_2O (MilliQ®) twice. The cells were resuspended in 80 μL H_2O (MilliQ®) and supplemented with 50 ng plasmid DNA. Electroporation was performed in a MicroPulser (25 μF, 200 Ω, 4.5–5 ms, 20 kV cm^{-1}; Bio-Budget Technologies GmbH). Cells were incubated in 0.7 mL LB medium under continuous shaking (300 rpm) for 2 h before plating on LB agar plates with an appropriate antibiotic.

Determination of *cis-trans*-isomerase (Cti) activity

Fatty acid extraction and methylation were adapted from previous studies (Bligh & Dyer, 1959; Morrison & Smith, 1964). Briefly, cell samples corresponding to an optical density ($OD_{700\,nm}$) of 1 in 1 mL were harvested from *P. putida* cultures by centrifugation. Fatty acid methyl esters (FAME) were prepared by incubating the samples in 1 mL methanol and 1.75 mL chloroform under continuous shaking (1000 rpm) for 3 min. Then, 0.5 mL dH_2O was added, and the suspension was thoroughly mixed for 30 s. Centrifugation (10 min, 1000 *g*) facilitated clear phase separation. Finally, the chloroform phase was transferred to a new glass vial (CS), and the solvent was removed by evaporation (Concentrator 5301; Eppendorf). For the methylation of fatty acids (FA), samples were incubated in BF3-methanol (Merck) for 15 min at 95°C (Morrison & Smith, 1964). Lastly, FAME were extracted with hexane and stored at 4°C. FAME analysis was performed using gas chromatography with a flame ionisation detector (GC-FID, 6890N Network GC System, 7683B Series Injector; Agilent Technologies). The instrument used a CP-Sil 88 column (CP7488; Varian) in stationary phase and helium as carrier gas. The temperature program was 40°C, 2 min isothermal, followed by a gradient-increase up to 220°C (8°C min^{-1}), and 10 min at 220°C. The FAME peak areas were used to determine their relative amounts. The FA was identified by co-injection of authentic reference compounds obtained from Supelco. *Trans/cis* ratio was calculated taking the sum of the FAME of *cis*-palmitoleic acid (C16:1Δ9*cis*) and *cis*-vaccenic acid (C18:1Δ11*cis*) as divisor and the sum of their corresponding *trans* configuration as dividend (Heipieper et al., 1992).

Isolation of OMVs

Procedures were based on already published protocols by Heipieper and coworkers (Eberlein et al., 2019). After 7 h of cultivation (24 h for some experiments), *P. putida* cells were pelleted by centrifugation (at 5000 *g* and 4°C for 15 min) and to ensure that all cells were removed, the supernatant was filtered through a membrane with 0.45 μm pore size (Sarstedt). As we did not see any cells in either the TEM or the (MA)DLS analyses (see below), we consider the 0.45 μm-filter to be appropriate. For final isolation, OMVs were sedimented by ultracentrifugation (at 100,000 *g* and 4°C for 3 h; rotor 50.2 Ti; Beckman Coulter). The obtained vesicle pellet was resuspended in 100 μL 10 mM HEPES buffer (pH 6.8) and used for characterisation. For TEM analysis, OMVs obtained from one isolation batch were further purified by ultracentrifugation using a density gradient (2%, 15%, 40%, and 50% glucose) at 100,000 *g* and 4°C for 18 h (rotor SW32 Ti; Beckman Coulter). OMV fractions were collected at sugar concentrations of approximately 10% and 30%, respectively (determined with a refractometer (OPTEC, Optimal Technology)). Vesicle bands at higher sugar concentrations (glucose concentration of about 40%–50%) were not collected due to accumulation of other impurities. Here, a larger batch of 50 mL LB medium was used, and the further procedure was applied unchanged.

OMV characterisation

Bradford assay

For an approximation of relative OMV quantity, the amount of proteins within the OMV fraction was determined by the Bradford assay as described before (Eberlein et al., 2019). For this purpose, 75 μL of a 10-fold (or 30-fold) OMV dilution (in 10 mM HEPES buffer, pH 6.8) were mixed with 75 μL Bradford reagent (20 mg Coomassie Brilliant Blue G-250, 10 mL ethanol, 20 mL phosphoric acid, *ad* 200 mL) in a microtiter plate

(MTP), and the absorption was measured at 595 nm using a plate reader (Tecan) after 5 min of incubation. Bovine serum albumin (BSA) solutions were used for calibration (0 to 0.25 mg mL^{-1}). Notably, other large cellular surface structures like flagellar components that co-sediment with OMVs would influence the Bradford results (Bauman & Kuehn, 2006). For prodigiosin-containing OMVs, the Bradford readout was corrected to take the absorption of the red pigment into account (see Figure S1 and M2 in Appendix S1).

Nile red assay

The lipophilic fluorescent dye Nile red was used as an indicator preferentially staining membranes to analyse OMV fractions. In an MTP, 2 µL of a 2% solution of Nile red (in DMSO; Sigma-Aldrich) was mixed with a 10-fold diluted OMV sample in a total volume of 150 µL. Fluorescence was measured using a plate reader (Tecan) with an excitation wavelength λ_{ex} = 543 nm, an emission wavelength λ_{em} of 598 nm, a bandwidth of 5 nm, and a gain of 150.

Biofilm formation assay

Quantification of biofilm formation as an indirect measurement of surface hydrophobicity was conducted according to O'Toole (2011). Cells were cultivated in an MTP in presence of the stressor 1-octanol (1 mM) or inducer for manipulation of gene expression (10 mM L-arabinose) at 30°C for 24 h. The supernatant was used to measure the optical density ($OD_{580\,nm}$) of the planktonic cells. For quantification, the wells were washed, dried, and supplemented with 150 µL of a 0.1% crystal violet (CV) solution. The MTP was incubated at room temperature for 10 min, washed and dried again. To solubilise the CV, 150 µL 40% acetic acid was used and the absorption of the samples was measured at 550 nm in a fresh MTP (diluted with H_2O) using a plate reader (Tecan).

To correct for differences in growth behaviour, the data of all direct or indirect OMV assays were normalised to the respective cell density at 580 nm (or 700 nm in case of prodigiosin-containing samples).

DLS analysis

The average size of isolated OMVs was analysed by dynamic light scattering (DLS) using a SpectroSize 300 (Xtal Concepts) with a 660 nm laser at a fixed angle. Isolated OMVs were diluted to a corresponding optical density ($OD_{580\,nm}$) of 0.2. DLS does not allow straightforward determination of the exact amount of OMVs in a solution. However, the intensity of the scattered light depends on the concentration, diameter, and refractive index of the scatterer in relation to the refractive index of the solution (Makra et al., 2015). As the OMV samples were isolated at the same cultivation time, processed identically and the OMVs had a similar size distribution, the measured intensity of the signal (i.e. count rate in kHz) can be indicative of the vesicle concentration. To test this correlation, the signal intensity of a vesicle sample diluted to different concentrations was determined by DLS and the dilutions were plotted against the signal intensity, which showed a linear correlation (see Figure S7). Hence, DLS data were evaluated as size distribution (diameter in nm) and signal strength (of the count rate in kHz).

For MADLS, a Zetasizer Ultra (Malvern Panalytical GmbH, Herrenberg, Germany) was used, operating at three different scattering angles (θ = 15°, 90°, 175°) and a temperature of 25°C. The isolated vesicle fractions (after 7 or 24 h) were diluted 10-fold in HEPES buffer (10 mM, pH 6.8) for measurements in triplicates and analysed using a DTS0012 cuvette. The software ZSxplorer was used to analyse the results.

TEM analysis

For imaging, isolated OMV samples (3 µL) were added to a glow-discharged Formvar–carbon film, hexagonal, 300-mesh copper grid, washed two times with H_2O (MilliQ®; 15 s) and stained with 2% uranyl acetate solution for 30 s. Surplus uranyl acetate was removed with a filter paper. Prepared grids were analysed using a TALOS L120C G2 transmission electron microscope (ThermoFisher Scientific) operated at 120 keV. Images were taken using the TEM Imaging & Analysis software (TIA; Thermo Fisher Scientific) on a 4 k × 4 k Ceta M16 CEMOS camera.

Transcriptome analysis

For transcriptome analysis, cells were cultivated as described above, the cell pellet was harvested after 7 h, adjusted to an optical density ($OD_{700\,nm}$) of 1 and flash frozen.

Total RNA was isolated from three biological replicates using Quick-RNA Miniprep Plus kit (Zymo Research). The samples were treated with DNAse (Zymo Research), and RNA was again purified with an RNA Clean&Concentrator-5 kit (Zymo Research). Ribosomal rRNA was removed with a riboPOOL for bacteria (siTOOLs Biotech GmbH). The purity of RNA and removal of rRNA was tested with an Agilent RNA Pico 6000 kit and an Agilent 2100 Bioanalyzer (Agilent Technologies). TruSeq Stranded mRNA Sample Preparation guide (Illumina) was then used to construct the cDNA library. The constructed cDNA library was

then sequenced with Illumina NextSeq500 high output mode paired-end using a read length of 75 bases.

Transcriptomics sequencing raw data files are available at the ArrayExpress database (www.ebi.ac.uk/arrayexpress) under accession no. E-MTAB-12470.

The paired-end cDNA reads were mapped to the *P. putida* KT2440 genome sequence (accession number AE015451.2; Belda et al., 2016; Nelson et al., 2002) using bowtie2 v2.2.7 (Langmead & Salzberg, 2012) with default settings for paired-end read mapping. All mapped sequence data were converted from SAM to BAM format with SAMtools v1.3 (Li et al., 2009) and imported to the software ReadXplorer v.2.2 (Hilker et al., 2016). Differential gene expression analysis of three biological replicates was performed using DESeq2 (Love et al., 2014) with ReadXplorer v2.2 (Hilker et al., 2016).

For significance of differentially transcribed genes, we used an adjusted *p*-value cutoff of ≤0.01 and a signal intensity ratio (*M*-value) cutoff of ≥2 or ≤−2.

Natural compound production in *P. putida* KT2440

Pseudomonas putida KT2440-derived previously generated strains, which carried the different biosynthetic gene clusters in the genome under a constitutive promoter (see Table S4), were transformed with plasmids for manipulation of the expression of candidate genes by electroporation. The cells were cultivated in 1 mL LB medium and incubated overnight in FlowerPlates® (Beckman Coulter GmbH (formerly m2p-labs GmbH)) at 30°C and shaking at 1200 rpm in a ThermoMixer® C (Eppendorf AG). For *P. putida* PCA1, Round Well Plates (Beckman Coulter GmbH (formerly m2p-labs GmbH)) were used instead of FlowerPlates® to lower oxygen transfer rates (culture volume: 750 μL). Main cultures were inoculated to an optical density ($OD_{700\,nm}$) of 0.05 in LB medium already containing 10 mM L-arabinose as inducer for gene overexpression or for the implementation of the CRISPRi system. The cells were incubated under above-described conditions for 48 h.

Extraction of natural products

Samples from cultivation of the producers were fractionated into cell pellet and supernatant by centrifugation (at 15,000 *g* and 4°C for 5 min). The pellets were extracted with 1 mL ethanol (p.a.; for prodigiosin: acidified ethanol (4% 1 M HCl) was used). The extracts were cleared by centrifugation (15,000 *g*, 10 min). Additionally, compounds were extracted from the supernatant by two-phase-extraction with ethyl acetate (2 × 500 μL; for PCA, the supernatant was acidified with 100 μL 6 M HCl) and evaporated afterwards (Concentrator 5301; Eppendorf). After evaporation, products (except of PCA samples) were dissolved in 150 μL ethanol (p.a.; for prodigiosin, acidified ethanol was used). As PCA mainly accumulates in the supernatant, extracts from the supernatant were dissolved in 1 mL ethanol (p.a.) after evaporation.

Determination of product titres and analytics

Prodigiosin, (deoxy)violacein, and zeaxanthin were quantified spectrophotometrically based on their molar extinction coefficients (prodigiosin: $\varepsilon_{535\,nm} = 139{,}800\,M^{-1}\,cm^{-1}$; (deoxy)violacein: $\varepsilon_{575\,nm} = 25{,}400\,M^{-1}\,cm^{-1}$; zeaxanthin: $\varepsilon_{450\,nm} = 144{,}500\,M^{-1}\,cm^{-1}$ (Domröse et al., 2015; Loeschcke et al., 2013; Rodrigues et al., 2012)) in acidified (prodigiosin) or pure (zeaxanthin, (deoxy)violacein) ethanol, respectively, using a plate reader (Tecan, Maennedorf, Switzerland).

Phenazine-1-carboxylic acid (PCA) was quantified via HPLC-PDA analysis using an LC-10Ai series (Shimadzu GmbH), equipped with an SPD-M10Avp photodiode array detector (PDA). The column oven temperature and the flow rate were set to 30°C and 1 mL min^{-1}. As mobile phase water (A) and acetonitrile (B), both supplemented with 0.1% formic acid, were used. A C30-reverse-phase HPLC column (250 × 4.6 mm, 5 mm particle size, YMC-Europe GmbH) was applied and 10 μL of extracted samples were injected onto the column. Analyses started at 5% B for 2.5 min, before a gradient was used for 16.5 min to reach 98% B. This ratio was maintained for 2 min and then decreased again to 5% B within 1 min. For re-equilibration, the last condition was again maintained for 5 min (Domröse et al., 2017). Chromatograms were recorded at 366 nm. To identify and quantify the PCA signal, a reference (Apollo Scientific) was used for calibration (0–400 mg L^{-1}). PCA signals were observed at a retention time of 18.1 min.

RESULTS AND DISCUSSION

OMV release is a natural response of *P. putida* KT2440 to chemical stress

To identify a tolerance trait that might provide a useful starting point for the engineering of robust production chassis strains, the native stress response of *P. putida* KT2440 were examined first. We chose to focus on the characteristic membrane adaptation responses of *Pseudomonas* species to environmental stress (i.e., Cti activity and vesiculation), especially triggered by hydrophobic compounds. The established method to assess the activity of Cti relies on the determination of the ratio of *trans*- to *cis*-unsaturated membrane FAs

via GC–MS using common protocols for extraction and derivatisation (Heipieper et al., 1995). One common method to indirectly detect OMV formation is the quantification of proteins in the vesicle fraction which can be obtained by ultracentrifugation of culture supernatants (Eberlein et al., 2019). Positive controls for both assays were derived from previous studies: *P. putida* KT2440 wild type was treated with 1-octanol, which is known to trigger both Cti activity and vesiculation (Baumgarten et al., 2012; Eberlein et al., 2018, 2019; Heipieper et al., 1995), and with the *Pseudomonas* quinolone signal (PQS), a quorum sensing-associated compound that is known to induce vesiculation (Mashburn-Warren et al., 2009). In addition, we analysed the effect of the hydrophobic antimicrobial tripyrrole prodigiosin on the cell envelope stress response since *P. putida* KT2440 has been shown to be especially suitable for the production of this compound (Domröse et al., 2015, 2019). For this, we tested the effects of both, the external addition of prodigiosin to the wild type bacteria and the intrinsic prodigiosin production by *P. putida* pig21, which was previously established by chromosomal integration of the prodigiosin biosynthetic *pig* gene cluster (Domröse et al., 2017).

Cell samples were subjected to analyses regarding changes in the *trans/cis* ratio of unsaturated membrane FA. In addition, vesicle fractions were isolated from the supernatant (see Figure 1A) and their protein content was determined as an estimation of produced vesicles. The untreated wild type was used as reference for the evaluation of all other samples (see Figure 1B,C).

As expected for the positive control, 1-octanol triggered both Cti activity and vesiculation. Interestingly, PQS only caused vesicle formation but no change in the *trans/cis* ratio of FA, while prodigiosin treatment caused the opposite response. External addition of prodigiosin resulted in a significant increase in Cti activity but did not induce hypervesiculation. The production strain *P. putida* pig21, like the PQS-treated wild type, showed again no Cti response but strong vesiculation. Interestingly, the isolated vesicle fraction of this strain exhibited the characteristic bright red colour of prodigiosin, suggesting that the compound had accumulated in these structures (see Figure 1A).

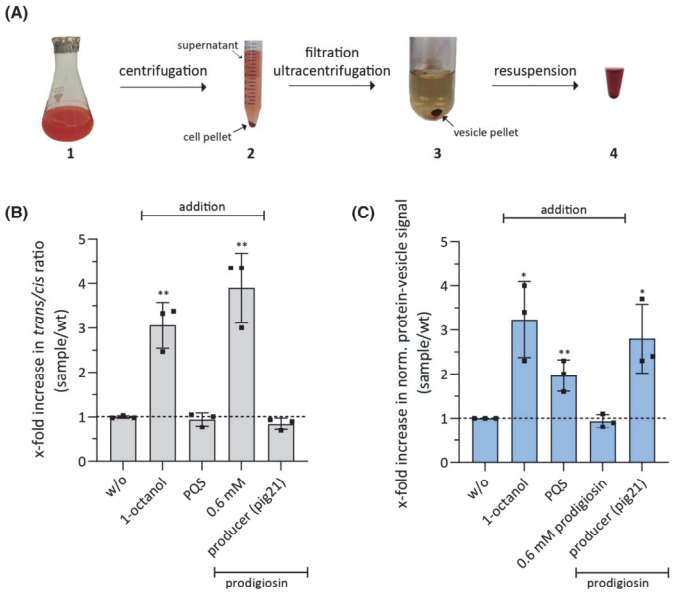

FIGURE 1 Cell envelope stress response of *Pseudomonas putida* after treatment with different stressors. (A) Procedure of OMV isolation using the prodigiosin producing strain *P. putida* pig21 as an example. Starting from a production culture (step 1), cells were harvested (step 2) and the supernatant was filtered (0.45 μm pore size). Vesicle isolation was performed by ultracentrifugation (step 3). Subsequently, the obtained vesicle pellet was resuspended in buffer (step 4). (B) Increase in *trans/cis* ratio of membrane FA (indicative of Cti activity) of different *P. putida* samples. (C) Increase in protein-vesicle signal calculated from Bradford assay of different *P. putida* samples (correction for prodigiosin-containing samples had to be applied (see Figure S1)). The samples are taken after 7 h of cultivation (logarithmic phase) and the data are normalised to the cell density of the cell culture. Data are shown as x-fold increase of values of treated *P. putida* KT2440 wild type cells (1 mM 1-octanol, 50 μM PQS or 0.6 mM prodigiosin) or the prodigiosin producer strain *P. putida* pig21 compared with the wild type sample without any treatment (w/o; indicated by the dashed line). The data are mean values of independent triplicate measurements with their respective standard deviation. Significant differences in comparison to the untreated wild type (w/o) are indicated by asterisks (determined by *T*-test; $*p \leq 0.05$, $**p \leq 0.01$).

Hence, we find that the tested compounds, which share a relatively high value for the partition coefficient logP (1-octanol = 3.0; PQS = 4.74; prodigiosin = 4.07 (calculated using XLOGP3 software (Cheng et al., 2007))) cause a membrane stress response. Interestingly, the quality of membrane adaptation clearly depends on the type of chemical stress. Further, the membrane adaptations appear to be influenced by the compound location and concentration dynamics ("shock treatment" of prodigiosin applied externally as a single full dose application versus steady increase of internally produced compound over the time of cultivation). External "shock treatment" might perturb the membrane to cause fatty acid conversion by Cti, while the production might be accompanied by the general vesiculation stress response which prevents Cti-critical concentrations at the IM. However, the validation of such hypotheses will require further analyses since any potential dynamic responses were not resolved in the end point measurements of the present study. Importantly, our data indicate that the meaningfulness of results obtained from examining cell responses after external application of a chemical stressor as a proxy for a production scenario can be limited and it is useful to analyse production strains themselves.

The observation of enhanced vesiculation in a *P. putida* production strain prompted us to investigate the OMV formation in this context in more detail. The quantification of OMVs by Bradford-based protein quantification as applied here is widely established (Eberlein et al., 2019; Rodriguez & Kuehn, 2020; Roier et al., 2016). However, potential changes in the protein content of OMVs in response to different conditions may influence the results (Bitto et al., 2021). Hence, the vesicle fraction of strain pig21 was additionally subjected to particle analysis by multi angle dynamic light scattering (MADLS), which validated enhanced vesicle formation in comparison to the wild type (see Table S1). We further characterised the OMVs produced by *P. putida* pig21 in comparison to the OMV-triggering controls by fixed angle dynamic light scattering (DLS) and transmission electron microscopy (TEM; see Figure 2). The OMV diameters determined by DLS ranged between 135 and 170 nm (comparable to the MADLS results), which is in the same range as previously described for *P. putida* OMVs (Baumgarten et al., 2012; Roier et al., 2016). Further, qualitative TEM analyses revealed that both OMVs from PQS-treated cells and *P. putida* pig21 producer cells apparently formed clustered agglomerates.

The formation of OMVs thus appears to be a native response of *P. putida* KT2440 to the production of the bioactive compound prodigiosin. We next evaluated whether vesiculation and compound production are quantitatively correlated. To this end, three previously established *P. putida* strains, pig-r43, pig-r11, and pig-r44, which produce prodigiosin at different levels (Domröse et al., 2019), were subjected to OMV characterisation. Here, low, moderate, and strong OMV formation were found to correlate with the low, moderate, and high-level prodigiosin titres of the respective strains (see Figure 3A).

Additionally, the effect of OMV release triggered by chemical treatment with PQS and 1-octanol on the prodigiosin production levels of *P. putida* pig21 was investigated. Here, we also observed a correlation between OMV formation and compound production (see Figure 3B). An effect of the chemical stress on the *pig* gene transcription levels was excluded via RT-qPCR (see Figure S3). Hence, we deduced that the process of vesicle release itself may positively influence prodigiosin production titres and, therefore, both processes appear to influence each other: An increase in the amount of intracellularly produced prodigiosin increases the formation of OMVs and vice versa.

By measuring product concentration in the different fractions (pellet and OMV fraction; Figure 3), we demonstrate prodigiosin accumulation not only in the pellet but also in the vesicles. This confirms our initial visual observation (see Figure 1A). It is also consistent with the compound's hydrophobicity, based on which it was expected that prodigiosin would interact with the OMVs rather than accumulate in the aqueous medium.

Vesiculation can be triggered by genetic manipulation of *P. putida*

As a next step, we aimed to identify candidate genes associated with vesiculation that might allow targeted genetic manipulation of the process.

We first approached this question in an attempt to uncover the specific adaptations in vesiculating strains – based on the above-described observations. To this end, we analysed transcriptomic data of the prodigiosin producing strain *P. putida* pig21 in comparison to the wild type strain and the wild type triggered to form OMVs by addition of PQS or 1-octanol. Interestingly, both prodigiosin production and 1-octanol addition caused higher changes in the overall number of up- or down-regulated genes than PQS addition (see Table 1, see also Figure S4). This observation, along with the finding that PQS treatment did not increase Cti activity, is consistent with the fact that PQS cannot readily cross the outer membrane (OM) (Florez et al., 2017). Among the sample sets of strain pig21 and 1-octanol-treated wild type cells, we identified six common genes, which were highly up- or down-regulated compared to the untreated wild type (PP_2805 (*ethA*), PP_2807, PP_3494, PP_3533, PP_0710, and PP_4524; see Figure 4), which were thus selected as candidate genes presumably associated with OMV formation.

Interestingly, we detected the Cti transcript in all of the samples in comparable copies. It was thus not

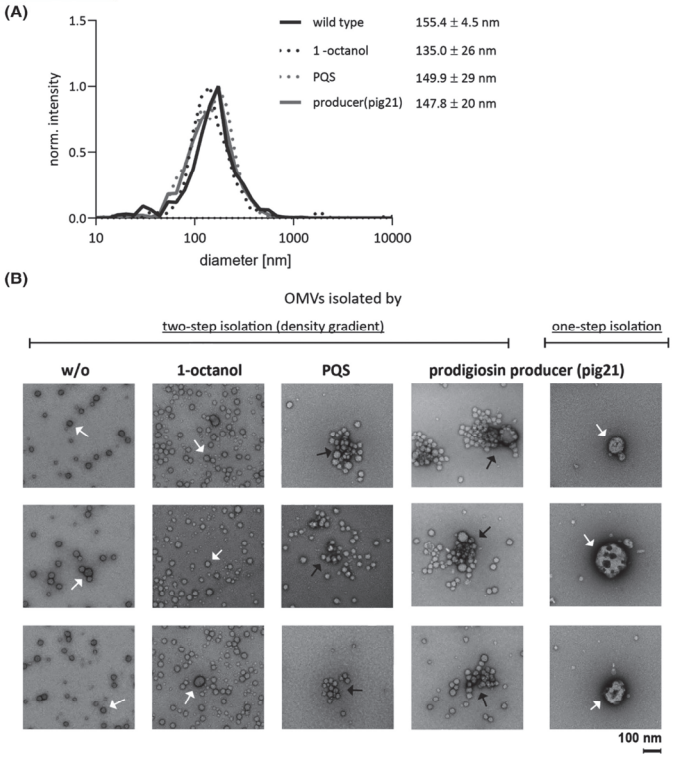

FIGURE 2 *Pseudomonas putida* wild type and prodigiosin producer strain OMVs. (A) Diameter of isolated OMVs of differently treated *P. putida* KT2440 wild type samples (1 mM 1-octanol or 50 μM PQS; w/o: without addition of a stressor) and the prodigiosin producer strain *P. putida* pig21 determined by DLS measurements (diameter plot: intensity is normalised to maximum). Here, OMVs were isolated by a single ultracentrifugation step (one-step isolation). (B) TEM analysis of negatively stained OMVs of the above measured samples. Left side: for higher background purity, the OMV samples were additionally purified using a glucose density gradient (2%–50%) after the first ultracentrifugation step (two-step isolation). Here, only smaller types of vesicles were collected (20–90 nm). Right side: vesicles from the producer *P. putida* pig21 are shown after one-step isolation (identical to DLS sample preparation). Vesicles showed diameters of about ~143.9 ± 45 nm, comparable to the results from DLS measurements (see A and Table S1). White arrows indicate vesicles, black arrows clustered agglomerates. For every OMV sample, TEM images of three different grid squares are shown (see also Figure S2). Magnification: 92,000×. Scale: 100 nm.

regulated, although 1-octanol treatment was shown to enhance the *trans/cis* ratio of unsaturated membrane FA. This is in accordance with previous descriptions of the enzyme being constitutively expressed and constantly present in the periplasm, from where it can slide into a perturbed membrane to reduce fluidity and increase cell stability (Eberlein et al., 2018; Mauger et al., 2021).

As a second approach, additional candidate genes were identified based on existing knowledge. The release of OMVs can be caused by (i) a reduction of local connections between the OM and the peptidoglycan layer (PG), (ii) an increase in local OM curvature, or (iii) an increase in periplasmic pressure (Juodeikis & Carding, 2022). We looked for different genetic targets whose native function is connected to one of the potential OMV generation mechanisms and whose manipulation can thus affect vesiculation. Several genes have been identified as putative candidates involved in OMV formation in Gram-negative bacteria (see Table S2; Avila-Calderón et al., 2021; Juodeikis & Carding, 2022; Kulp & Kuehn, 2010; Schwechheimer & Kuehn, 2015). While *P. putida* features similar genes or respective proteins, which could be identified by sequence homology searches (see M6 in Appendix S1), their role in OMV formation has never been described or examined. Based on the results of the literature- and sequence-based searches as well as transcriptome analysis, we selected a set of 21 candidate genes potentially associated with vesiculation, which encode inner and outer membrane proteins (IMPs and OMPs), regulatory elements, periplasmic proteins, PG-degrading enzymes,

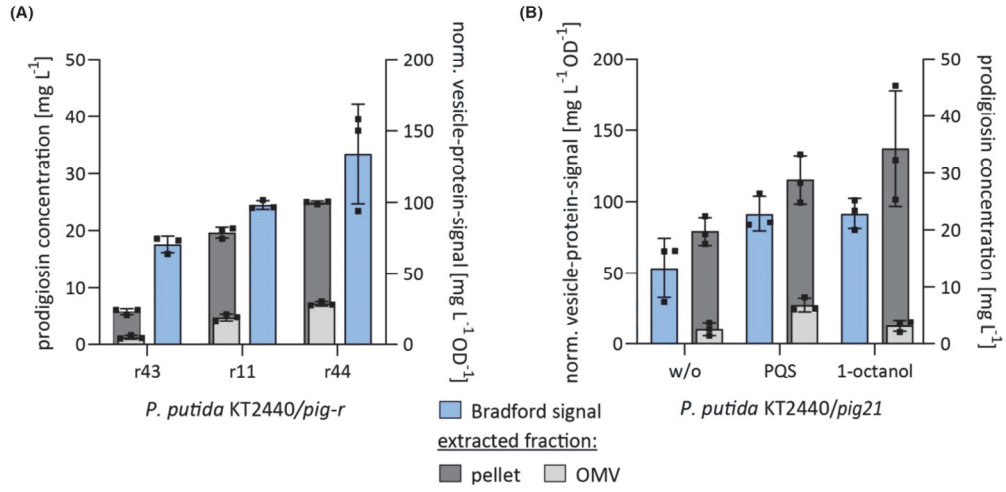

FIGURE 3 Correlation between prodigiosin production and OMV formation in *P. putida* producer strains. (A) Investigation of the effect of prodigiosin production (grey) on vesicle formation (blue) using a low (pig-r43), a moderate (pig-r11), and a high (pig-r44) prodigiosin producer strain. (B) Investigation of the effect of OMV formation (blue) on the prodigiosin titres (grey) of the producer strain *P. putida* pig21. For this, vesiculation is triggered by addition of different vesiculation-inducing stressors (1 mM 1-octanol or 50 μM PQS; w/o: without addition of a stressor). OMV amount was analysed by Bradford assay (correction for prodigiosin containing samples had to be applied (see Figure S1)). The prodigiosin concentration was determined in both fractions, the pellet fraction (dark grey) and the isolated OMV fraction (light grey). All samples were taken after 24 h of cultivation, and the data are normalised to the cell density of the cell culture. The data are mean values of independent triplicate measurements with their respective standard deviation. Bars are sorted in ascending order.

TABLE 1 Overall number of up- or down-regulated genes (identified by transcriptome analysis).

	Pseudomonas Putida KT2440		
Number of regulated genes[a]	Strain pig21	Wild type + 1-octanol	Wild type + PQS
Up	53	29	2
Down	74	7	–

[a]For significance of differentially transcribed genes as compared to the untreated wild type, we used an adjusted *p*-value cutoff of ≤0.01 and a signal intensity ratio (*M*-value) cutoff of ≥2 or ≤−2.

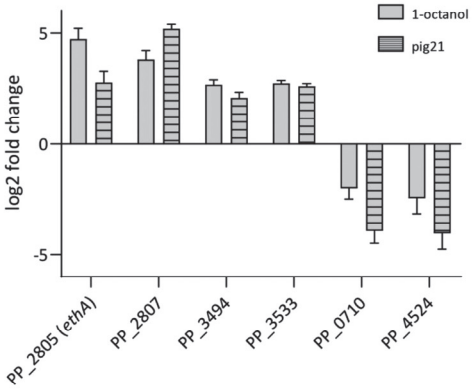

FIGURE 4 Transcriptome analysis of differently stressed *Pseudomonas putida* cells. Highly up- or down-regulated genes of 1-octanol treated *P. putida* KT2440 and *P. putida* pig21 cells as compared to the untreated wild type. Filled bars show M-values for 1-octanol-treated cells, hatched bars the prodigiosin producer. The data are mean values of independent triplicate measurements with their respective standard deviation.

or enzymes involved in iron homeostasis (see Table 2). For each gene, a manipulation strategy to either up- or down-regulate the expression was chosen, depending on the previous findings.

Thus far, knockout strains have been generated and described in the literature for many of the chosen targets. To conveniently test a range of candidate genes in the present study, we chose to implement repression of the target gene expression (i.e., respective protein production) by CRISPR interference (CRISPRi; Batianis et al., 2020; Qi et al., 2013; Tan et al., 2018). With this method, the repression is 'portable on a plasmid' and can be easily implemented and tested in several strain backgrounds, as has been done before to manipulate OMVs (Yu et al., 2023). We further regarded repression advantageous over complete deletion since it should also allow addressing rather essential genes.

TABLE 2 Candidate genes that may affect OMV formation by *Pseudomonas putida* KT2440 (sorted by localisation).

***Pseudomonas putida* protein [Genbank ID]**	**Locus tag (*Pseudomonas* genome DB; Winsor et al., 2016)**	**Product description (*Pseudomonas* genome DB; Winsor et al., 2016)**	**Identification strategy**	**Manipulation strategy (regulation)**
Outer membrane (OM)				
OprI (Lpp) [NP_744471]	PP_2322	OM lipoprotein	Literature, sequence (BLASTp)	Down-regulation (CRISPRi, NT strand)
OprL (Pal) [NP_743383]	PP_1223	Peptidoglycan-associated lipoprotein	Literature, sequence (BLASTp)	Down-regulation (CRISPRi, T strand)
OmpA [NP_743248]	PP_1087	OmpA family OM protein	Literature, sequence (BLASTp)	Down-regulation (CRISPRi, NT strand)
MltA [NP_747074]	PP_4971	Outer membrane-bound lytic murein transglycolase A	Literature, sequence (BLASTp)	Up-regulation (overexpression)
Periplasm (PP)				
Spr [NP_743826]	PP_1669	NLP/P60 family protein	Literature, sequence (BLASTp)	Up-regulation (overexpression)
MrcA [NP_747185]	PP_5084	Penicillin-insensitive transglycosylase/ penicillin-sensitive transpeptidase	Literature, sequence (BLASTp)	Down-regulation (CRISPRi, NT)
PvdQ [NP_745045]	PP_2901	Acyl-homoserine lactone acylase	Literature, sequence (BLASTp)	Down-regulation (CRISPRi, NT strand)
Inner membrane (IM)				
MlaE [NP_743120]	PP_0959	Phospholipid ABC transporter permease	Literature, sequence (BLASTp)	Down-regulation (CRISPRi, NT strand)
PP_0287 (AsmA) [NP_742454]	PP_0287	Hypothetical protein	Literature, sequence (BLASTp)	Up-regulation (overexpression)
WbpL [NP_743959]	PP_1804	Glycosyl transferase	Literature, sequence (BLASTp)	Down-regulation (CRISPRi, NT strand)
TolA [NP_743381]	PP_1221	Colicin S4/filamentous phage transport protein	Literature, sequence (BLASTp)	Down-regulation (CRISPRi, NT strand)
Cytoplasm (CP)				
RpoE [NP_743585]	PP_1427	RNA polymerase sigma E factor	Literature, sequence (BLASTp)	Up-regulation (overexpression)
HldE [NP_4934]	PP_4934	Bifunctional heptose 7-phosphate kinase/heptose 1-phosphate adenylyltransferase	Literature, sequence (BLASTp)	Down-regulation (CRISPRi, NT strand)
WaaC [NP_742509]	PP_0342	ADP-heptose-LPS heptosyltransferase	Literature, sequence (BLASTp)	Down-regulation (CRISPRi, NT strand)
EthA [NP_744949]	PP_2805	FAD-containing monooxygenase	Transcriptomics	Up-regulation (overexpression)
PP_2807 [NP_744951]	PP_2807	Hypothetical protein	Transcriptomics	Up-regulation (overexpression)
Unknown localisation				
PP_0710 [NP_742871]	PP_0710	Hypothetical protein	Transcriptomics	Down-regulation (CRISPRi, NT strand)
PP_3494 [NP_745631]	PP_3494	Hypothetical protein	Transcriptomics	Up-regulation (overexpression)

Therefore, we assembled a broad-host-range CRISPRi vector (pBTBX-2-CRISPRi, see Figure S5A) based on a catalytically inactive variant of the endonuclease Cas9 from *Streptococcus pyogenes* (SpCas9 D10A H840A). We first evaluated the effect of the newly constructed system on both prodigiosin and pyoverdine production. Here, we could verify the functionality of the CRISPRi system in dependence on the guidingRNA (gRNA) target DNA strand (template (T) or non-template (NT)), on the distance from the translational start codon, as well as on the concentration of the inducer L-arabinose (see Figure S5B). Due to the most effective down-regulation, gRNAs targeted to the NT DNA strand close to the translational start codon were selected for down-regulation of the expression of candidate genes. However, the efficiency of down-regulation was dependent on the addressed gene (see Figure S5B). Accepting the limitation that gene-to-gene differences in down-regulation efficiency may occur, we deemed the system applicable to conveniently screen the candidate genes, for which respective gRNA-encoding sequences were cloned.

Candidate genes, whose up-regulation appeared promising, were cloned in the vector pBTBX-2-mcs (Prior et al., 2010), which facilitates L-arabinose-dependent expression (see Figure S6; Hogenkamp et al., 2022). Using both strategies, plasmids for the manipulation of 18 targets could be cloned (for *tonB*, PP_3533, and PP_4524, which were also regarded as promising, cloning was not successful) and introduced into *P. putida* KT2440 to test whether a hypervesiculation phenotype could be implemented.

It is unknow which aspect of vesiculation in terms of quality and quantity might be relevant for supportive effects of natural compound production. Hence, we performed different assays: Bradford and Nile red assay were applied for protein- or lipid-quantification in isolated vesicle fractions as these are also the commonly addressed components for quantifying OMV yields (Klimentová & Stulík, 2015). Further, we analysed the particles via DLS to investigate vesicle sizes; moreover, as the DLS signal intensity may be correlated to the scatterer concentration (see Figure S7), the signal strength was evaluated as potential indicator of relative OMV concentrations. In addition, we measured biofilm formation using crystal violet (CV; Baumgarten et al., 2012; Kulp & Kuehn, 2010) as a measure for vesiculation-induced, increased cell surface hydrophobicity and aggregation (see Figure 5). For all assays, 1-octanol treatment was again used as a positive control. To exclude any effect by d*cas9* expression on the vesiculation response, a CRIPSRi empty vector control (ev (Ci)) was used in all assays.

The different assays for analysis of vesiculation gave comparable results for down- or up-regulated expression of most target genes. Since OMV features may well change upon manipulations, we did not expect to find the exact same outcome in all assays for all strains. Around a third of the manipulations had no or only a minor impact. Notably, in the cases where manipulation relied on CRISPRi, the screening approach cannot distinguish between a manipulation having no effect and a guide RNA failing to implement repression of target gene expression. Around two thirds of the manipulations gave moderately to significantly increased signals. Interestingly, manipulation of OMPs barely caused a change in vesiculation in samples taken from the logarithmic growth phase, however, a stronger effect became apparent after 24 h (see also Figure S8). We also observed differences in the vesiculation phenotype of bacteria examined during the logarithmic and stationary growth phases e.g., upon overexpression of sigma factor *rpoE*, which regulates cell envelope integrity (Rouvière et al., 1995; Schwechheimer et al., 2013). In contrast, the sizes of vesicles produced by differently engineered hypervesiculating strains did not vary significantly (see Figure 5D and Figure S9). In summary, we could identify a range of genes, whose manipulation led to the implementation of hypervesiculation phenotypes in *P. putida* KT2440.

For validation, we aimed to delete the two CRISPRi-downregulated genes, *pvdQ* and *hldE*. However, *hldE* could not be deleted despite several attempts. This underlines the usefulness of a CRISPRi-based down-regulation of genes of interest. The *pvdQ* mutant, which was obtained without difficulties, showed a similarly increased protein and lipid signal in the vesicle fraction as the respective CRISPRi strain (see Figure S10). A limited number of manipulations were chosen for an assessment of tolerance engineering in the generation of robust chassis for natural compound production. We selected the target genes PP_2087 (up), *ethA* (up), *hldE* (down), *mltA* (up), and *pvdQ* (down) because their manipulation led to effects across all assays, which was achieved by both, up- and downregulation approaches. Moreover, these included different types of proteins with different cellular localisations, which are associated with different vesiculation mechanisms.

PP_0287 encodes a protein with sequence-similarity to *E. coli* AsmA, which is predicted to be localised at the IM and to play a role in the assembly of OMPs, LPS biogenesis, OM fluidity, and the tolerance towards hydrophobic antibiotics (Deng & Misra, 1996; Levine, 2019; Misra & Miao, 1995; Xiong et al., 1996). EthA is a cytoplasmatic FAD-containing monooxygenase exhibiting the consensus motifs of Baeyer-Villiger monooxygenases, which was up-regulated in both, 1-octanol-treated and prodigiosin-producing cells and might naturally be involved in the degradation of alkanes and other xenobiotics (Blum et al., 2021; Minerdi et al., 2012; Rehdorf et al., 2007; Van Bogaert et al., 2011; Winsor et al., 2016). However, the association of this monooxygenase with cell envelope properties and vesiculation is unclear.

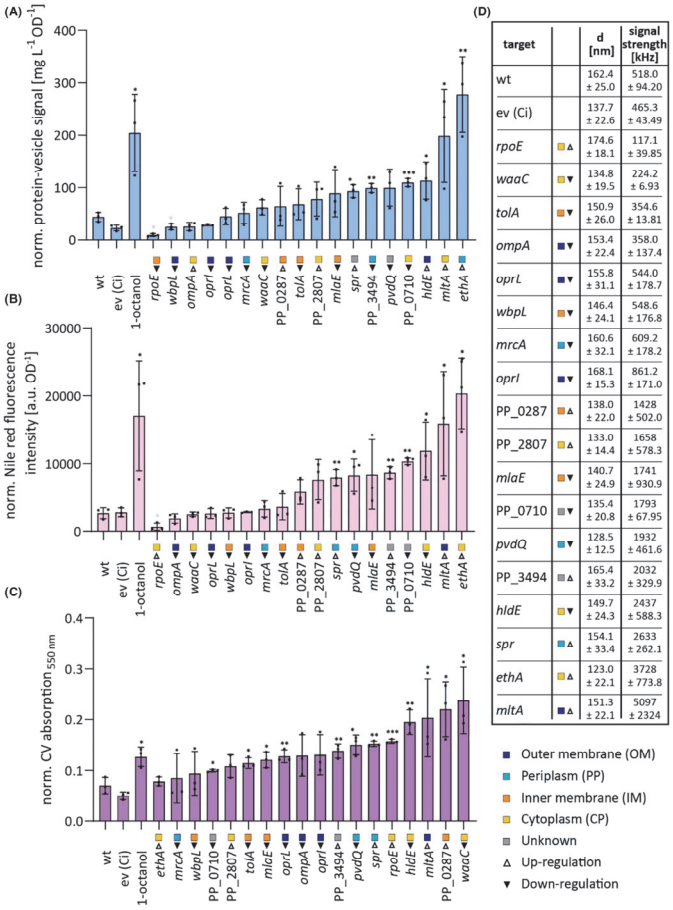

FIGURE 5 Characterisation of OMVs formed by engineered *Pseudomonas putida* strains. (A) Amount of protein in the OMV fraction isolated from engineered *P. putida* strains calculated by Bradford assay (based on λ_{max} = 595 nm) after growth for 7 h (logarithmic phase). The data are normalised to the cell density of the cell culture. (B) Amount of lipid in the OMV fraction formed by engineered *P. putida* strains calculated by Nile red assay (based on λ_{ex} = 543 nm; λ_{em} = 598 nm) after growth for 7 h (logarithmic phase). The data are normalised to the cell density of the cell culture. (C) Quantification of biofilm formation using crystal violet (CV) (based on λ_{max} = 550 nm). The data are normalised to the cell density of the planktonic cells in each sample (after growth for 24 h). (D) Characterisation of OMV particles formed by engineered *P. putida* strains by determination of diameters (d) and the signal strength of count rates with DLS (see also Figure S7 showing a correlation of the sample concentration with signal intensity). Bars and DLS data are sorted in ascending order. Putative cellular localisation of proteins is indicated by different colours (OM: dark blue; PP: light blue; IM: orange; CP: yellow; unknown localisation: grey). Implemented manipulation of gene expression is indicated by arrows (empty arrows: up-regulation; filled arrows: down-regulation). ev (Ci): CRISPRi empty vector control; The data are mean values of independent triplicate measurements with their respective standard deviation. Significant differences in comparison to the untreated wild type are indicated by asterisks (determined by *T*-test; *$p \leq 0.05$, **$p \leq 0.01$, ***$p \leq 0.001$).

HldE is a bifunctional enzyme involved in the biosynthesis of the LPS component L-glycero-D-manno-heptose (L,D-Hep) and localised in the cytoplasm, as reported for *E. coli* (Kneidinger et al., 2002; McArthur et al., 2005; Valvano et al., 2000). In a study with this organism, HldE, together with other enzymes from LPS biosynthesis, was identified as involved in the formation of OMVs (Yang et al., 2021). MltA is a conserved lytic transglycosylase which is presumably anchored in the OM and cleaves linkages between N-acetylglucosamine and N-acetylmuramic acid in the PG layer, thus far described for *E. coli* and *P. aeruginosa* (Chen et al., 2022; Lommatzsch et al., 1997; Mueller & Levin, 2020). PvdQ is a periplasmic (de)acetylase conserved in fluorescent Pseudomonads. In *P. putida* KT2440, it is involved in pyoverdine biosynthesis, where it catalyses the deacylation of the ferribactin precursor in the periplasm as

a maturation step to release the peptide from the IM (Koch et al., 2010; Ringel & Brüser, 2018).

Engineered vesiculation can help to improve the production of diverse natural products

Our results suggested that hypervesiculation could support biosynthetic compound production by *P. putida* KT2440. To verify this hypothesis, we chose the tripyrrolic compound prodigiosin (1), the indolocarbazoles violacein (2), and deoxyviolacein (3) that are co-produced by the respective biosynthetic pathway, phenazine-1-carboxylic acid (PCA) (4), and the carotenoid zeaxanthin (5). These are all relatively hydrophobic but chemically rather diverse bioactive compounds, for which previously characterised *P. putida* KT2440-derived production strains (and product analysis assays) were readily available. The expression vectors to up- or down-regulate the expression of the identified genes PP_2087, *ethA*, *hldE*, *mltA* and *pvdQ* were introduced in the four previously constructed strains *P. putida* pig21, vio12, PCA1, and crtΔX, which carried the respective biosynthetic gene clusters in the genome where they were constitutively expressed (Domröse et al., 2017; Loeschcke et al., 2013). Compound production was assessed by spectrophotometry or HPLC-PDA analyses (see Figure 6).

Production titres of the natural compounds increased to different levels depending on the used engineered producer strain. While for violaceins and zeaxanthin, a smaller increase of titres was observed upon manipulation of some target genes, prodigiosin and PCA titres were more clearly enhanced. Interestingly, this overall trend is not correlated with the hydrophobicity of the compounds (logP values: prodigiosin = 4.07; violacein = 1.88; deoxyviolacein = 2.24; PCA = 1.79; zeaxanthin = 10.91; calculated by XLOGP3 software (Cheng et al., 2007)).

Previous reports on membrane or vesicle association of some compounds might explain the overall trends in parts: It is known that the final reaction of prodigiosin biosynthesis occurs at the membrane, and the release of prodigiosin or related structures by vesicles or unknown mechanisms has been suggested (Domröse et al., 2015; Matsuyama et al., 1986; Schrempf & Merling, 2015; Tan et al., 2020). A transporter has not yet been described. Similarly, release of violacein via OMVs has been described (Batista et al., 2020; Choi et al., 2020). Phenazines also end up in the culture broth of producing bacteria via unknown mechanisms (Bator et al., 2020; Jin et al., 2015; Sakhtah et al., 2016; Schmitz et al., 2015; Sporer et al., 2018). To our knowledge, a membrane association is not known. In contrast, carotenoids like zeaxanthin are thought to be associated with whole cells and to span the lipid double layer (Gruszecki & Strzałka, 2005). In this context, we evaluated the distribution of compounds between

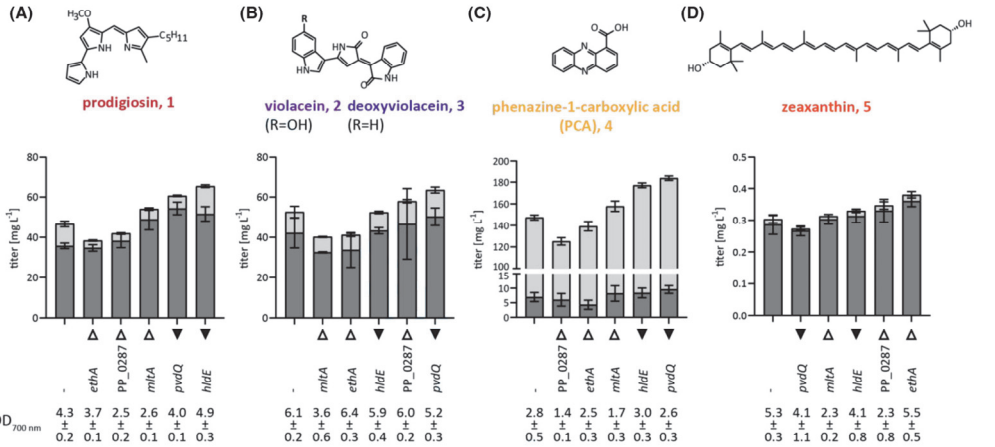

FIGURE 6 Recombinant natural compound production by *Pseudomonas putida* engineered for OMV release. Natural product titres were determined after extraction from both pellet fraction (dark grey) and supernatant (light grey) of the engineered *P. putida* strains (genetic targets addressed by up- (empty arrows) or down-regulation (filled arrows) are indicated) and compared to the respective producer strains (indicated as '-'). (A) Prodigiosin (1) produced by *P. putida* pig21. (B) Violacein (2)/deoxyviolacein (3) produced by *P. putida* vio12. (C) PCA (4) produced by *P. putida* PCA1. (D) Zeaxanthin (5) produced by *P. putida* crtΔX. Implemented manipulation of gene expression is indicated by arrows (empty arrows: up-regulation; filled arrows: down-regulation). Bars are sorted in ascending order. Cell densities reached at the end of the cultivation (after 48 h) are given below graphs. The data are mean values of independent triplicate measurements with their respective standard deviation.

the supernatant and cell pellet fractions. Here, we observed that vesiculation did not exclusively support the accumulation of compounds in the OMV-containing supernatant fraction, but that the engineered strains showed an increase of compound levels also in the cell pellet fraction (see Figure 6). However, we cannot exclude that OMVs may also be present in the cell pellet fraction.

The specific genetic manipulations had rather differential effects: While expression of *ethA* led to enhanced titres only in the zeaxanthin producer, repression of *pvdQ* increased those of all other products. In the prodigiosin producer, *hldE* repression was most effective. An increase in vesiculation upon manipulation of these targets (*hldE*, *pvdQ*, and *ethA*) in the production strains was verified by MADLS analysis (see Figure S11). The effect was not very pronounced in all cases, which might be due to the fact that the production can already cause relatively strong vesiculation (as demonstrated for prodigiosin, see Figure 1 and Table S1). OMV formation might be naturally limited by lipid supply and cellular integrity. Since excessive vesiculation must perturb cell envelope integrity, we tested cell viability by propidium iodide (PI) staining and found the engineered cells to be more damaged (see Figure S12). This indicates that vesiculation engineering may require careful fine-tuning for each case in order to achieve best results.

Notably, some of the engineered strains also did not reach the same cell densities as the parental production strains, which influenced the titres in the cultures (see Figure 6). Therefore, in terms of product yields [mg per gDCW], the manipulations had a higher (by up to 1.5- to 3-fold) and in parts a different effect (see Figure S13).

Our findings did not reveal a single outstanding genetic target which would allow improving production of all compounds. This cannot be expected as also suggested by findings reported for membrane engineering with *E. coli* (Yang et al., 2021). Differential effects may be caused, for example, by the temporal dynamics of vesiculation and biosyntheses. It was interesting to note that the ratio of violacein/deoxyviolacein was slightly changed by the manipulations (see Figure S14). Compared to the parental strain, cell pellet extracts of the manipulated strains showed a decrease of deoxyviolacein relative to violacein (except for *pvdQ* repression). Compared to these samples, supernatant extracts showed an increase in the relative deoxyviolacein levels (except for *ethA* expression). This might indicate that the more hydrophobic compound deoxyviolacein is more amenable to being excreted or to accumulate in vesicles.

Apart from optimising compound release by vesiculation, limitations in the biosynthetic pathways must also be considered. An example is zeaxanthin biosynthesis which is limited by the pool of available precursors (Hernandez-Arranz et al., 2019; Sánchez-Pascuala et al., 2019). Concerted efforts encompassing metabolic engineering and a fine-tuned engineering of the host tolerance shall boost production yields and allow to implement the biosynthetic production of highly toxic compounds which would otherwise be inaccessible.

CONCLUSION

In summary, we show that OMV formation is a natural response of *P. putida* KT2440 not only to external chemical stressors but also to the production of small molecules. Moreover, we demonstrate that this phenotype can be genetically engineered, which can improve production yields. In the future, the engineering of OMV formation may help to create robust chassis strains and serve as a potential tool to improve hitherto limited yields of natural products for biotechnological applications.

AUTHOR CONTRIBUTIONS

Nora Lisa Bitzenhofer: Conceptualisation (equal); data curation (lead); formal analysis (lead); methodology (equal); validation (lead); visualisation (lead); writing – original draft (lead); writing – review and editing (equal). **Carolin Höfel:** Investigation (supporting); writing – review and editing (equal). **Stephan Thies:** Conceptualisation (supporting); funding acquisition (equal); validation (equal); writing – review and editing (equal). **Andrea Jeanette Weiler:** Investigation (supporting); methodology (supporting); resources (supporting); writing – review and editing (equal). **Christian Eberlein:** Data curation (equal); formal analysis (equal); investigation (equal); writing – review and editing (equal). **Hermann J. Heipieper:** Data curation (equal); formal analysis (equal); resources (equal); writing – review and editing (equal). **Renu Batra-Safferling:** Data curation (equal); formal analysis (equal); resources (equal); writing – review and editing (equal). **Pia Sundermeyer:** Investigation (equal); methodology (equal); writing – review and editing (equal). **Thomas Heidler:** Investigation (equal); methodology (equal); writing – review and editing (equal). **Carsten Sachse:** Data curation (equal); formal analysis (equal); resources (equal); writing – review and editing (equal). **Tobias Busche:** Data curation (equal); formal analysis (equal); methodology (equal); writing – review and editing (equal). **Jörn Kalinowski:** Data curation (equal); formal analysis (equal); resources (equal); writing – review and editing (equal). **Thomke Belthle:** Investigation (equal); methodology (equal); writing – review and editing (equal). **Thomas Drepper:** Formal analysis (equal); supervision (equal); writing – review and editing (equal). **Karl-Erich Jaeger:** Funding acquisition (equal); writing – original draft (equal); writing – review and editing (equal). **Anita Loeschcke:** Conceptualisation (equal); data curation (equal); formal analysis (equal); funding acquisition (equal); supervision (lead); validation (equal); writing – original draft (equal); writing – review and editing (equal).

ACKNOWLEDGEMENTS

The authors gratefully acknowledge the support given by Dr. Manuel Banzhaf by discussions about the cell envelope. For support regarding DLS analysis, we acknowledge Dr. Annette Eckhardt from X-Tal Concepts. We thank Esther Knieps-Grünhagen for supporting preparative column chromatography of prodigiosin and Vera Svensson for support in density gradient centrifugation. This work was supported by the German Federal Ministry of Education and Research via the project NO-STRESS under grant numbers 031B0852B (to N.L.B., S.T., A.L. and K.-E.J.) and 031B085C (to C.E. and H.J.H.), as well as the projects GlycoX/161B0866A (to S.T., A.L. and K.-E.J.) and LipoBiocat/031B0837A (to S.T. and K.-E.J.). The authors gratefully acknowledge support by the "European Regional Development Fund (EFRE)" through project "Cluster Industrial Biotechnology (CLIB) Kompetenzzentrum Biotechnologie (CKB)" (34.EFRE-0300095/1703FI04) for T. Busche and J. Kalinowski and by the Deutsche Forschungsgemeinschaft (DFG, German Research Foundation) – Project ID 458090666/CRC1535/1 (A.J.W. and T.D.). Open Access funding enabled and organized by Projekt DEAL.

FUNDING INFORMATION

No funding information provided.

CONFLICT OF INTEREST STATEMENT

The authors declare that there are no competing interests associated with the manuscript.

DATA AVAILABILITY STATEMENT

Transcriptomic data are available at the ArrayExpress database (www.ebi.ac.uk/arrayexpress) under accession no. E-MTAB-12470. All data are available upon request.

ORCID

Nora Lisa Bitzenhofer https://orcid.org/0000-0002-2790-4929
Carolin Höfel https://orcid.org/0000-0002-4230-2942
Stephan Thies https://orcid.org/0000-0003-4240-9149
Christian Eberlein https://orcid.org/0000-0003-4521-8145
Hermann J. Heipieper https://orcid.org/0000-0002-3723-9600
Renu Batra-Safferling https://orcid.org/0000-0002-8597-4335
Thomas Heidler https://orcid.org/0000-0002-5997-3945
Carsten Sachse https://orcid.org/0000-0002-1168-5143
Thomke Belthle https://orcid.org/0000-0001-6802-4189
Thomas Drepper https://orcid.org/0000-0002-0096-8084
Karl-Erich Jaeger https://orcid.org/0000-0002-6036-0708
Anita Loeschcke https://orcid.org/0000-0001-5184-8499

REFERENCES

Askitosari, T.D., Boto, S.T., Blank, L.M. & Rosenbaum, M.A. (2019) Boosting heterologous phenazine production in *Pseudomonas putida* KT2440 through the exploration of the natural sequence space. *Frontiers in Microbiology*, 10, 1–12.

Atashgahi, S., Sánchez-Andrea, I., Heipieper, H.J., van der Meer, J.R., Stams, A.J.M. & Smidt, H. (2018) Prospects for harnessing biocide resistance for bioremediation and detoxification. *Science*, 360, 743–746.

Avila-Calderón, E.D., Ruiz-Palma, M.d.S., Aguilera-Arreola, M.G., Velázquez-Guadarrama, N., Ruiz, E.A., Gomez-Lunar, Z. et al. (2021) Outer membrane vesicles of gram-negative bacteria: an outlook on biogenesis. *Frontiers in Microbiology*, 12, 557902.

Batianis, C., Kozaeva, E., Damalas, S.G., Martín-Pascual, M., Volke, D.C., Nikel, P.I. et al. (2020) An expanded CRISPRi toolbox for tunable control of gene expression in *Pseudomonas putida*. *Microbial Biotechnology*, 13, 368–385.

Batista, J.H., Leal, F.C., Fukuda, T.T.H., Alcoforado Diniz, J., Almeida, F., Pupo, M.T. et al. (2020) Interplay between two quorum sensing-regulated pathways, violacein biosynthesis and VacJ/Yrb, dictates outer membrane vesicle biogenesis in *Chromobacterium violaceum*. *Environmental Microbiology*, 22, 2432–2442.

Bator, I., Wittgens, A., Rosenau, F., Tiso, T. & Blank, L.M. (2020) Comparison of three xylose pathways in *Pseudomonas putida* KT2440 for the synthesis of valuable products. *Frontiers in Bioengineering and Biotechnology*, 7, 1–18.

Bauman, S.J. & Kuehn, M.J. (2006) Purification of outer membrane vesicles from *Pseudomonas aeruginosa* and their activation of an IL-8 response. *Microbes and Infection*, 8, 2400–2408.

Baumgarten, T., Sperling, S., Seifert, J., von Bergen, M., Steiniger, F., Wick, L.Y. et al. (2012) Membrane vesicle formation as a multiple-stress response mechanism enhances *Pseudomonas putida* DOT-T1E cell surface hydrophobicity and biofilm formation. *Applied and Environmental Microbiology*, 78, 6217–6224.

Belda, E., van Heck, R.G.A., José Lopez-Sanchez, M., Cruveiller, S., Barbe, V., Fraser, C. et al. (2016) The revisited genome of *pseudomonas putida* KT2440 enlightens its value as a robust metabolic *chassis*. *Environmental Microbiology*, 18, 3403–3424.

Beuttler, H., Hoffmann, J., Jeske, M., Hauer, B., Schmid, R.D., Altenbuchner, J. et al. (2011) Biosynthesis of zeaxanthin in recombinant *Pseudomonas putida*. *Applied Microbiology and Biotechnology*, 89, 1137–1147.

Bitto, N.J., Zavan, L., Johnston, E.L., Stinear, T.P., Hill, A.F. & Kaparakis-Liaskos, M. (2021) Considerations for the analysis of bacterial membrane vesicles: methods of vesicle production and quantification can influence biological and experimental outcomes. *Microbiology Spectrum*, 9, 1–15.

Bitzenhofer, N.L., Kruse, L., Thies, S., Wynands, B., Lechtenberg, T., Rönitz, J. et al. (2021) Towards robust *Pseudomonas* cell factories to harbour novel biosynthetic pathways. *Essays in Biochemistry*, 65, 319–336.

Blanco, P., Hernando-Amado, S., Reales-Calderon, J., Corona, F., Lira, F., Alcalde-Rico, M. et al. (2016) Bacterial multidrug efflux pumps: much more than antibiotic resistance determinants. *Microorganisms*, 4, 14.

Bligh, E.G. & Dyer, W.J. (1959) A rapid method of total lipid extraction and purification. *Canadian Journal of Biochemistry and Physiology*, 37, 911–917.

Blum, M., Chang, H.-Y., Chuguransky, S., Grego, T., Kandasaamy, S., Mitchell, A. et al. (2021) The InterPro protein families and domains database: 20 years on. *Nucleic Acids Research*, 49, 344–354.

Bösl, B., Grimminger, V. & Walter, S. (2006) The molecular chaperone Hsp104—a molecular machine for protein disaggregation. *Journal of Structural Biology*, 156, 139–148.

Calero, P., Jensen, S.I., Bojanovič, K., Lennen, R.M., Koza, A. & Nielsen, A.T. (2018) Genome-wide identification of tolerance mechanisms toward *p* -coumaric acid in *Pseudomonas putida*. *Biotechnology and Bioengineering*, 115, 762–774.

Chen, Y.-C., Kalawong, R., Toyofuku, M. & Eberl, L. (2022) The role of peptidoglycan hydrolases in the formation and toxicity of *Pseudomonas aeruginosa* membrane vesicles. *microLife*, 3, 1–9.

Cheng, T., Zhao, Y., Li, X., Lin, F., Xu, Y., Zhang, X. et al. (2007) Computation of octanol–water partition coefficients by guiding an additive model with knowledge. *Journal of Chemical Information and Modeling*, 47, 2140–2148.

Choi, S.Y., Lim, S., Cho, G., Kwon, J., Mun, W., Im, H. et al. (2020) *Chromobacterium violaceum* delivers violacein, a hydrophobic antibiotic, to other microbes in membrane vesicles. *Environmental Microbiology*, 22, 705–713.

Cook, T.B., Jacobson, T.B., Venkataraman, M.V., Hofstetter, H., Amador-Noguez, D., Thomas, M.G. et al. (2021) Stepwise genetic engineering of *Pseudomonas putida* enables robust heterologous production of prodigiosin and glidobactin a. *Metabolic Engineering*, 67, 112–124.

Deng, M. & Misra, R. (1996) Examination of AsmA and its effect on the assembly of *Escherichia coli* outer membrane proteins. *Molecular Microbiology*, 21, 605–612.

Domröse, A., Hage-Hülsmann, J., Thies, S., Weihmann, R., Kruse, L., Otto, M. et al. (2019) *Pseudomonas putida* rDNA is a favored site for the expression of biosynthetic genes. *Scientific Reports*, 9, 7028.

Domröse, A., Klein, A.S., Hage-Hülsmann, J., Thies, S., Svensson, V., Classen, T. et al. (2015) Efficient recombinant production of prodigiosin in *Pseudomonas putida*. *Frontiers in Microbiology*, 6, 972.

Domröse, A., Weihmann, R., Thies, S., Jaeger, K.-E., Drepper, T. & Loeschcke, A. (2017) Rapid generation of recombinant *Pseudomonas putida* secondary metabolite producers using yTREX. *Synthetic and Systems Biotechnology*, 2, 310–319.

Eberlein, C., Baumgarten, T., Starke, S. & Heipieper, H.J. (2018) Immediate response mechanisms of gram-negative solvent-tolerant bacteria to cope with environmental stress: *cis-trans* isomerization of unsaturated fatty acids and outer membrane vesicle secretion. *Applied Microbiology and Biotechnology*, 102, 2583–2593.

Eberlein, C., Starke, S., Doncel, Á.E., Scarabotti, F. & Heipieper, H.J. (2019) Quantification of outer membrane vesicles: a potential tool to compare response in *Pseudomonas putida* KT2440 to stress caused by alkanols. *Applied Microbiology and Biotechnology*, 103, 4193–4201.

Florez, C., Raab, J.E., Cooke, A.C. & Schertzer, J.W. (2017) Membrane distribution of the *Pseudomonas* quinolone signal modulates outer membrane vesicle production in *Pseudomonas aeruginosa*. *MBio*, 8, 1–13.

Gruszecki, W.I. & Strzałka, K. (2005) Carotenoids as modulators of lipid membrane physical properties. *Biochimica et Biophysica Acta (BBA) – Molecular Basis of Disease*, 1740, 108–115.

Hanahan, D. (1983) Studies on transformation of *Escherichia coli* with plasmids. *Journal of Molecular Biology*, 166, 557–580.

Hartl, F.U., Bracher, A. & Hayer-Hartl, M. (2011) Molecular chaperones in protein folding and proteostasis. *Nature*, 475, 324–332.

Heipieper, H.J., Diefenbach, R. & Keweloh, H. (1992) Conversion of *cis* unsaturated fatty acids to *trans*, a possible mechanism for the protection of phenol-degrading *Pseudomonas putida* P8 from substrate toxicity. *Applied and Environmental Microbiology*, 58, 1847–1852.

Heipieper, H.J., Loffeld, B., Keweloh, H. & de Bont, J.A.M. (1995) The *cis/trans* isomerisation of unsaturated fatty acids in *Pseudomonas putida* S12: an indicator for environmental stress due to organic compounds. *Chemosphere*, 30, 1041–1051.

Heipieper, H.J., Meinhardt, F. & Segura, A. (2003) The *cis-trans* isomerase of unsaturated fatty acids in *Pseudomonas* and *Vibrio*: biochemistry, molecular biology and physiological function of a unique stress adaptive mechanism. *FEMS Microbiology Letters*, 229, 1–7.

Henderson, P.J.F., Maher, C., Elbourne, L.D.H., Eijkelkamp, B.A., Paulsen, I.T. & Hassan, K.A. (2021) Physiological functions of bacterial "multidrug" efflux pumps. *Chemical Reviews*, 121, 5417–5478.

Hernandez-Arranz, S., Perez-Gil, J., Marshall-Sabey, D. & Rodriguez-Concepcion, M. (2019) Engineering *Pseudomonas putida* for isoprenoid production by manipulating endogenous and shunt pathways supplying precursors. *Microbial Cell Factories*, 18, 152.

Hilker, R., Stadermann, K.B., Schwengers, O., Anisiforov, E., Jaenicke, S., Weisshaar, B. et al. (2016) ReadXplorer 2—detailed read mapping analysis and visualization from one single source. *Bioinformatics*, 32, 3702–3708.

Hogenkamp, F., Hilgers, F., Bitzenhofer, N.L., Ophoven, V., Haase, M., Bier, C. et al. (2022) Optochemical control of bacterial gene expression: novel photocaged compounds for different promoter systems. *Chembiochem*, 23, e202100467.

Jin, K., Zhou, L., Jiang, H., Sun, S., Fang, Y., Liu, J. et al. (2015) Engineering the central biosynthetic and secondary metabolic pathways of *Pseudomonas aeruginosa* strain PA1201 to improve phenazine-1-carboxylic acid production. *Metabolic Engineering*, 32, 30–38.

Juodeikis, R. & Carding, S.R. (2022) Outer membrane vesicles: biogenesis, functions, and issues. *Microbiology and Molecular Biology Reviews*, 86, e0003222.

Klimentová, J. & Stulík, J. (2015) Methods of isolation and purification of outer membrane vesicles from gram-negative bacteria. *Microbiological Research*, 170, 1–9.

Kneidinger, B., Marolda, C., Graninger, M., Zamyatina, A., McArthur, F., Kosma, P. et al. (2002) Biosynthesis pathway of ADP- l-glycero-β-d- *manno* -heptose in *Escherichia coli*. *Journal of Bacteriology*, 184, 363–369.

Koch, G., Jimenez, P.N., Muntendam, R., Chen, Y., Papaioannou, E., Heeb, S. et al. (2010) The acylase PvdQ has a conserved function among fluorescent *Pseudomonas* spp. *Environmental Microbiology Reports*, 2, 433–439.

Kulp, A. & Kuehn, M.J. (2010) Biological functions and biogenesis of secreted bacterial outer membrane vesicles. *Annual Review of Microbiology*, 64, 163–184.

Langmead, B. & Salzberg, S.L. (2012) Fast gapped-read alignment with Bowtie 2. *Nature Methods*, 9, 357–359.

Levine, T.P. (2019) Remote homology searches identify bacterial homologues of eukaryotic lipid transfer proteins, including Chorein-N domains in TamB and AsmA and Mdm31p. *BMC Molecular and Cell Biology*, 20, 43.

Li, H., Handsaker, B., Wysoker, A., Fennell, T., Ruan, J., Homer, N. et al. (2009) The sequence alignment/map format and SAMtools. *Bioinformatics*, 25, 2078–2079.

Lin, B. & Tao, Y. (2017) Whole-cell biocatalysts by design. *Microbial Cell Factories*, 16, 106.

Loeschcke, A., Markert, A., Wilhelm, S., Wirtz, A., Rosenau, F., Jaeger, K-E. et al. (2013) TREX: a universal tool for the transfer and expression of biosynthetic pathways in bacteria. *ACS Synthetic Biology*, 2, 22–33. Available from: https://doi.org/10.1021/sb3000657

Loeschcke, A. & Thies, S. (2015) *Pseudomonas putida*—a versatile host for the production of natural products. *Applied Microbiology and Biotechnology*, 99, 6197–6214.

Loeschcke, A. & Thies, S. (2020) Engineering of natural product biosynthesis in *Pseudomonas putida*. *Current Opinion in Biotechnology*, 65, 213–224.

Lommatzsch, J., Templin, M.F., Kraft, A.R., Vollmer, W. & Höltje, J.V. (1997) Outer membrane localization of murein hydrolases: MltA, a third lipoprotein lytic transglycosylase in *Escherichia coli*. *Journal of Bacteriology*, 179, 5465–5470.

Love, M.I., Huber, W. & Anders, S. (2014) Moderated estimation of fold change and dispersion for RNA-seq data with DESeq2. *Genome Biology*, 15, 550.

Makra, I., Terejánszky, P. & Gyurcsányi, R.E. (2015) A method based on light scattering to estimate the concentration of virus particles without the need for virus particle standards. *MethodsX*, 2, 91–99.

Mashburn, L.M. & Whiteley, M. (2005) Membrane vesicles traffic signals and facilitate group activities in a prokaryote. *Nature*, 437, 422–425.

Mashburn-Warren, L., Howe, J., Brandenburg, K. & Whiteley, M. (2009) Structural requirements of the *Pseudomonas* quinolone signal for membrane vesicle stimulation. *Journal of Bacteriology*, 191, 3411–3414.

Matsuyama, T., Murakami, T., Fujita, M., Fujita, S. & Yano, I. (1986) Extracellular vesicle formation and biosurfactant production by *Serratia marcescens*. *Microbiology*, 132, 865–875.

Mauger, M., Ferreri, C., Chatgilialoglu, C. & Seemann, M. (2021) The bacterial protective armor against stress: the *cis-trans* isomerase of unsaturated fatty acids, a cytochrome-c type enzyme. *Journal of Inorganic Biochemistry*, 224, 111564.

McArthur, F., Andersson, C.E., Loutet, S., Mowbray, S.L. & Valvano, M.A. (2005) Functional analysis of the glycero-manno -heptose 7-phosphate kinase domain from the bifunctional HldE protein, which is involved in ADP- l - glycero - d - *manno* -heptose biosynthesis. *Journal of Bacteriology*, 187, 5292–5300.

Minerdi, D., Zgrablic, I., Sadeghi, S.J. & Gilardi, G. (2012) Identification of a novel Baeyer-Villiger monooxygenase from *Acinetobacter radioresistens*: close relationship to the *Mycobacterium tuberculosis* prodrug activator EtaA. *Microbial Biotechnology*, 5, 700–716.

Misra, R. & Miao, Y. (1995) Molecular analysis of *asmA*, a locus identified as the suppressor of OmpF assembly mutants of *Escherichia coli* K-12. *Molecular Microbiology*, 16, 779–788.

Molina-Santiago, C., Cordero, B.F., Daddaoua, A., Udaondo, Z., Manzano, J., Valdivia, M. et al. (2016) *Pseudomonas putida* as a platform for the synthesis of aromatic compounds. *Microbiology*, 162, 1535–1543.

Morrison, W.R. & Smith, L.M. (1964) Preparation of fatty acid methyl esters and dimethylacetals from lipids with boron fluoride–methanol. *Journal of Lipid Research*, 5, 600–608.

Mozaheb, N. & Mingeot-Leclercq, M.-P. (2020) Membrane vesicle production as a bacterial defense against stress. *Frontiers in Microbiology*, 11, 60221.

Mueller, E.A. & Levin, P.A. (2020) Bacterial cell wall quality control during environmental stress. *MBio*, 11, 1–15.

Nelson, K.E., Weinel, C., Paulsen, I.T., Dodson, R.J., Hilbert, H., Martins dos Santos, V.A.P. et al. (2002) Complete genome sequence and comparative analysis of the metabolically versatile *Pseudomonas putida* KT2440. *Environmental Microbiology*, 4, 799–808.

Nicolaou, S.A., Gaida, S.M. & Papoutsakis, E.T. (2010) A comparative view of metabolite and substrate stress and tolerance in microbial bioprocessing: from biofuels and chemicals, to biocatalysis and bioremediation. *Metabolic Engineering*, 12, 307–331.

Nikel, P.I. & de Lorenzo, V. (2018) *Pseudomonas putida* as a functional *chassis* for industrial biocatalysis: from native biochemistry to *trans*-metabolism. *Metabolic Engineering*, 50, 142–155.

O'Toole, G.A. (2011) Microtiter dish biofilm formation assay. *Journal of Visualized Experiments*, 47, e2437.

Prior, J.E., Lynch, M.D. & Gill, R.T. (2010) Broad-host-range vectors for protein expression across gram negative hosts. *Biotechnology and Bioengineering*, 106, 326–332.

Qi, L.S., Larson, M.H., Gilbert, L.A., Doudna, J.A., Weissman, J.S., Arkin, A.P. et al. (2013) Repurposing CRISPR as an RNA-guided platform for sequence-specific control of gene expression. *Cell*, 152, 1173–1183.

Rehdorf, J., Kirschner, A. & Bornscheuer, U.T. (2007) Cloning, expression and characterization of a Baeyer-Villiger monooxygenase from *Pseudomonas putida* KT2440. *Biotechnology Letters*, 29, 1393–1398.

Ringel, M.T. & Brüser, T. (2018) The biosynthesis of pyoverdines. *Microbial Cell*, 5, 424–437.

Roca, A., Rodríguez-Herva, J.-J., Duque, E. & Ramos, J.L. (2008) Physiological responses of *Pseudomonas putida* to formaldehyde during detoxification. *Microbial Biotechnology*, 1, 158–169.

Rodrigues, A.L., Göcke, Y., Bolten, C., Brock, N.L., Dickschat, J.S. & Wittmann, C. (2012) Microbial production of the drugs violacein and deoxyviolacein: analytical development and strain comparison. *Biotechnology Letters*, 34, 717–720.

Rodriguez, B.V. & Kuehn, M.J. (2020) *Staphylococcus aureus* secretes immunomodulatory RNA and DNA via membrane vesicles. *Scientific Reports*, 10, 18293.

Roier, S., Zingl, F.G., Cakar, F., Durakovic, S., Kohl, P., Eichmann, T.O. et al. (2016) A novel mechanism for the biogenesis of outer membrane vesicles in gram-negative bacteria. *Nature Communications*, 7, 10515.

Rouvière, P.E., De Las Peñas, A., Mecsas, J., Lu, C.Z., Rudd, K.E. & Gross, C.A. (1995) *rpoE*, the gene encoding the second heat-shock sigma factor, sigma E, in *Escherichia coli*. *The EMBO Journal*, 14, 1032–1042.

Sakhtah, H., Koyama, L., Zhang, Y., Morales, D.K., Fields, B.L., Price-Whelan, A. et al. (2016) The *Pseudomonas aeruginosa* efflux pump MexGHI-OpmD transports a natural phenazine that controls gene expression and biofilm development. *Proceedings of the National Academy of Sciences of the United States*, 113, E3538–E3547.

Sambrook, J., Fritsch, E. & Maniatis, T. (1989) *Molecular cloning: a laboratory manual*. New York: Cold Sprin Habor Laboratory Press, p. 545.

Sánchez-Pascuala, A., Fernández-Cabezón, L., de Lorenzo, V. & Nikel, P.I. (2019) Functional implementation of a linear glycolysis for sugar catabolism in *Pseudomonas putida*. *Metabolic Engineering*, 54, 200–211.

Schmitz, S., Nies, S., Wierckx, N., Blank, L.M. & Rosenbaum, M.A. (2015) Engineering mediator-based electroactivity in the obligate aerobic bacterium *Pseudomonas putida* KT2440. *Frontiers in Microbiology*, 6, 1–13.

Schrempf, H. & Merling, P. (2015) Extracellular *Streptomyces lividans* vesicles: composition, biogenesis and antimicrobial activity. *Microbial Biotechnology*, 8, 644–658.

Schwanemann, T., Otto, M., Wierckx, N. & Wynands, B. (2020) *Pseudomonas* as versatile aromatics cell factory. *Biotechnology Journal*, 15, 1900569.

Schwechheimer, C. & Kuehn, M.J. (2015) Outer-membrane vesicles from gram-negative bacteria: biogenesis and functions. *Nature Reviews. Microbiology*, 13, 605–619.

Schwechheimer, C., Sullivan, C.J. & Kuehn, M.J. (2013) Envelope control of outer membrane vesicle production in gram-negative bacteria. *Biochemistry*, 52, 3031–3040.

Sporer, A.J., Beierschmitt, C., Bendebury, A., Zink, K.E., Price-Whelan, A., Buzzeo, M.C. et al. (2018) *Pseudomonas aeruginosa* PumA acts on an endogenous phenazine to promote self-resistance. *Microbiology*, 164, 790–800.

Tan, D., Fu, L., Sun, X., Xu, L. & Zhang, J. (2020) Genetic analysis and immunoelectron microscopy of wild and mutant strains of the rubber tree endophytic bacterium *Serratia marcescens* strain ITBB B5–1 reveal key roles of a macrovesicle in storage and secretion of prodigiosin. *Journal of Agricultural and Food Chemistry*, 68, 5606–5615.

Tan, S.Z., Reisch, C.R. & Prather, K.L.J. (2018) A robust CRISPR interference gene repression system in *Pseudomonas*. *Journal of Bacteriology*, 200, e00575-17.

Tan, Z., Yoon, J.M., Nielsen, D.R., Shanks, J.V. & Jarboe, L.R. (2016) Membrane engineering via *trans* unsaturated fatty acids production improves *Escherichia coli* robustness and production of biorenewables. *Metabolic Engineering*, 35, 105–113.

Tu, Q., Yin, J., Fu, J., Herrmann, J., Li, Y., Yin, Y. et al. (2016) Room temperature electrocompetent bacterial cells improve DNA transformation and recombineering efficiency. *Scientific Reports*, 6, 24648.

Valvano, M.A., Marolda, C.L., Bittner, M., Glaskin-Clay, M., Simon, T.L. & Klena, J.D. (2000) The *rfaE* gene from *Escherichia coli* encodes a bifunctional protein involved in biosynthesis of the lipopolysaccharide core precursor ADP- l - glycero - d - *manno* -heptose. *Journal of Bacteriology*, 182, 488–497.

Van Bogaert, I.N.A., Groeneboer, S., Saerens, K. & Soetaert, W. (2011) The role of cytochrome P450 monooxygenases in microbial fatty acid metabolism. *FEBS Journal*, 278, 206–221.

Weimer, A., Kohlstedt, M., Volke, D.C., Nikel, P.I. & Wittmann, C. (2020) Industrial biotechnology of *Pseudomonas putida*: advances and prospects. *Applied Microbiology and Biotechnology*, 104, 7745–7766.

Winsor, G.L., Griffiths, E.J., Lo, R., Dhillon, B.K., Shay, J.A. & Brinkman, F.S.L. (2016) Enhanced annotations and features for comparing thousands of *Pseudomonas* genomes in the *Pseudomonas* genome database. *Nucleic Acids Research*, 44, D646–D653.

Xiong, X., Deeter, J.N. & Misra, R. (1996) Assembly-defective OmpC mutants of *Escherichia coli* K-12. *Journal of Bacteriology*, 178, 1213–1215.

Yang, D., Park, S.Y. & Lee, S.Y. (2021) Production of rainbow colorants by metabolically engineered *Escherichia coli*. *Advanced Science*, 8, 2100743.

Yu, H., Lu, Y., Lan, F., Wang, Y., Hu, C., Mao, L. et al. (2023) Engineering outer membrane vesicles to increase extracellular electron transfer of *Shewanella oneidensis*. *ACS Synthetic Biology*, 12, 1645–1656.

Zhang, J.J., Tang, X., Zhang, M., Nguyen, D. & Moore, B.S. (2017) Broad-host-range expression reveals native and host regulatory elements that influence heterologous antibiotic production in gram-negative bacteria. *MBio*, 8, e01291-17.

SUPPORTING INFORMATION

Additional supporting information can be found online in the Supporting Information section at the end of this article.

How to cite this article: Bitzenhofer, N.L., Höfel, C., Thies, S., Weiler, A.J., Eberlein, C., Heipieper, H.J. et al. (2023) Exploring engineered vesiculation by *Pseudomonas putida* KT2440 for natural product biosynthesis. *Microbial Biotechnology*, 00, 1–18. Available from: https://doi.org/10.1111/1751-7915.14312

II.4. Bioprocess optimization strategies for increased arcyriaflavin A production

PUBLICATION IV

Biotransformation of L-tryptophan to produce arcyriaflavin A with *Pseudomonas putida* KT2440

Nora Lisa Bitzenhofer, Thomas Classen, Karl-Erich Jaeger, Anita Loeschcke

ChemBioChem (**2023**) 00:e202300576

The online version is available at: 10.1002/cbic.202300576

Status: published

Supporting Information can be found in the Appendix (**Chapter V.3**)

Own contribution:

Planning and performing the experiments, analyzing the data, writing the manuscript.

Check for updates

ChemBioChem

Research Article
doi.org/10.1002/cbic.202300576

Chemistry Europe
European Chemical Societies Publishing

www.chembiochem.org

Biotransformation Of L-Tryptophan To Produce Arcyriaflavin A With *Pseudomonas putida* KT2440

Nora Lisa Bitzenhofer,[a] Thomas Classen,[b] Karl-Erich Jaeger,[a, b] and Anita Loeschcke*[a]

Natural products such as indolocarbazoles are a valuable source of highly bioactive compounds with numerous potential applications in the pharmaceutical industry. Arcyriaflavin A, isolated from marine invertebrates and slime molds, is one representative of this group and acts as a cyclin D1-cyclin-dependent kinase 4 inhibitor. To date, access to this compound has mostly relied on multi-step total synthesis. In this study, biosynthetic access to arcyriaflavin A was explored using recombinant *Pseudomonas putida* KT2440 based on a previously generated producer strain. We used a Design of Experiment approach to analyze four key parameters, which led to the optimization of the bioprocess. By engineering the formation of outer membrane vesicles and using an adsorbent in the culture broth, we succeeded to increase the yield of arcyriaflavin A in the cell-free supernatant, resulting in a nearly eight-fold increase in the overall production titers. Finally, we managed to scale up the bioprocess leading to a final yield of 4.7 mg arcyriaflavin A product isolated from 1 L of bacterial culture. Thus, this study showcases an integrative approach to improve biotransformation and moreover also provides starting points for further optimization of indolocarbazole production in *P. putida*.

Introduction

Indolocarbazole alkaloids are an important class of natural products (NP) due to the potential therapeutic applications based on their biological activities, e.g., antibacterial, antifungal, antitumor, antiviral, and neuroprotective properties.[1] The indolocarbazole bisindoles, belonging to this group consist of an indolo[2,3-*a*]carbazole scaffold (**5**) as a common building block[2,3] (see Figure S1). Several natural compounds with different types of five-membered rings fused to the indolocarbazole (e.g., pyrroles, pyrrolinones, maleimides) have been described, but also variants containing a glycosylation motif attached to either both (e.g., staurosporine (**6**)[4]) or one of the nitrogen atoms (e.g., rebeccamycin (**7**)[5]) in the indolocarbazole backbone.

Arcyriaflavin A (**4**), also known as deschloro-rebeccamycin aglycon, is an example of a maleimide indolocarbazole lacking the sugar moiety, which is biosynthesized from L-tryptophan (**1**). It has been isolated from marine invertebrates and slime molds[6,7] but can also be formed by the implementation of four genes of the rebeccamycin pathway (*rebO*, *rebD*, *rebC*, and *rebP*) from the actinomycete *Lentzea aerocolonigenes* (see Scheme 1).[8–10] In contrast to related compounds such as rebeccamycin (see Figure S1), arcyriaflavin A showed little antimicrobial activity, but appeared to be a potent inhibitor of

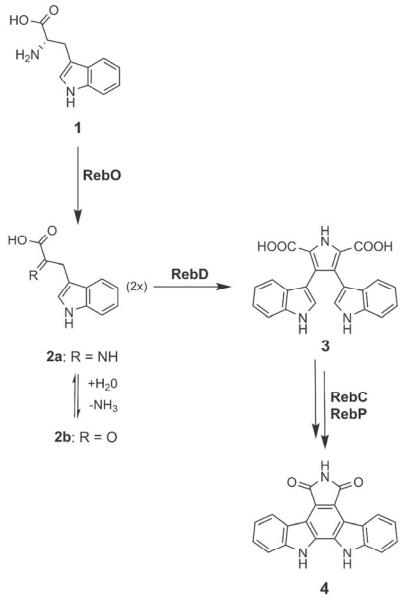

Scheme 1. Arcyriaflavin A (**4**) can be synthesized from L-tryptophan (**1**) by the enzymes RebO, RebD, RebC, and RebP. This pathway is based on the rebeccamycin pathway of *L. aerocolonigenes*. Indole-3-pyruvic acid (IPA) imine (**2a**), which exists in equilibrium with IPA (**2b**), and chromopyrrolic acid (CPA, **3**) are formed as intermediates.[8]

[a] *N. L. Bitzenhofer, Prof. Dr. K.-E. Jaeger, Dr. A. Loeschcke*
Institute of Molecular Enzyme Technology (IMET)
Heinrich Heine University Düsseldorf located at Forschungszentrum Jülich
Stetternicher Forst, Building 15.8, 52426 Jülich (Germany)
E-mail: a.loeschcke@fz-juelich.de

[b] *Dr. T. Classen, Prof. Dr. K.-E. Jaeger*
Institute of Bio- and Geosciences (IBG-1): Biotechnology
Forschungszentrum Jülich GmbH
Stetternicher Forst, Building 15.8, 52426 Jülich (Germany)

Supporting information for this article is available on the WWW under https://doi.org/10.1002/cbic.202300576

ChemBioChem
Research Article
doi.org/10.1002/cbic.202300576
Chemistry Europe
European Chemical Societies Publishing

human cytomegalovirus replication.[11–13] In addition, this compound is an inhibitor of cyclin D1-cyclin-dependent kinase 4 (CDK4), a promising property in the context of endometriosis treatment.[14] To date, arcyriaflavin A and derivatives have mostly been produced by total synthesis.[15–19] As a complement to chemical synthesis, such compounds can be produced by whole-cell biotransformation in a more environmentally friendly process. Some examples of recombinant biosynthetic arcyriaflavin A production have been described in the bacteria *Escherichia coli* and *Streptomyces albus*.[8–10,20] Recently, we reported the construction of a recombinant *Pseudomonas putida* KT2440 strain for the production of arcyriaflavin A using a newly developed toolbox for chromosomal gene integration and expression.[21] However, the biotransformation in *P. putida* resulted in rather low titers of about 500 μg arcyriaflavin A per liter. Since *P. putida* is a promising host for NP synthesis due to its high tolerance to xenobiotics, its low intrinsic NP background, and its versatile metabolism,[22–26] these results prompted us to investigate different strategies to optimize this bioprocess.

Results and Discussion

In our previous study, arcyriaflavin A was produced in the *P. putida* KT2440-derived strain NB04, which carries the genes *rebODCP* from *L. aerocolonigenes* integrated into the chromosome at the *att*Tn7 site and under the control of the salicylic acid-inducible promoter *nagR*-P_{nagAa}.[21] Under standard conditions (30 °C; shaking in 10 mL LB medium; addition of 1 mM L-tryptophan as precursor and 2 mM salicylic acid as inducer after 4 h; total incubation time 48 h), a titer of about 500 $\mu g\,L^{-1}$ was obtained. Since growth of *P. putida* KT2440 is not affected by addition of higher concentrations (up to 33 $mg\,mL^{-1}$) of arcyriaflavin A to the medium (see Figure S2), the production does not appear to be limited by toxicity. To increase the production yield, we first investigated the influence of a set of basic cultivation conditions. For multifactorial, statistics-based optimization, we used the Design of Experiment (DoE) approach. For this purpose, we analyzed the influence of four factors, i.e., temperature (18–33 °C), incubation time (14–48 h), time of L-tryptophan addition (0–34 h), and L-tryptophan concentration (0–5 mM) on the product titer [$mg\,L^{-1}$] and the specific productivity per g dry cell weight (DCW) and hour [$\mu g\,g\,DCW^{-1}\,h^{-1}$] in 10 mL LB medium cultures. The time point for the induction of gene expression (4 h after inoculation of a test culture) and the concentration of the inducer salicylic acid (2 mM) were kept constant over all experiments.[21] The optimization of the bioprocess was done using a four-factor response surface (central composite) design with a quadratic model fit (see Equations S1 and S2). Based on an experimental data set, the production under non-tested conditions could hence be predicted (see Figure 1 and S3).

The obtained design model provided a good prediction of the influence of the selected parameters on the bioprocess (productivity: $R^2 = 0.8707$; titer: $R^2 = 0.9287$) (see Table S1 and S2). The evaluation showed that the temperature and cultivation time had a strong influence on the bioprocess. With regard to the precursor, the time of L-tryptophan addition had a stronger influence on the process than the added concentration (see Figure 1). By applying predicted conditions that would lead to enhanced productivity, a twofold increase in product yield was experimentally obtained. Therefore, optimized cultivation conditions were defined as 30 °C; addition of 4.9 mM L-tryptophan after 18 h; total incubation time of 72 h. In summary, the approach allowed to increase specific productivity and titers, however, the DoE also showed that there appears to be an upper limit for the productivity (see Figure S5), possibly caused by the intracellular accumulation of the product and/or by metabolic limitations.

As excess intracellular accumulation may lead to inhibition of product formation, we first focused on different strategies resulting in removal of the hydrophobic compound from the cell. We investigated (i) co-expression of the RebUT-encoding genes for active transport by a rebeccamycin transporter as well as extracellular accumulation of the compound by (ii) release of outer membrane vesicles (OMVs), and (iii) addition of an extracellular hydrophobic adsorbent to the culture broth (see Figure 2A).

RebU and RebT are putative antibiotic transporters, that share sequence similarities with transporters of the Major Facilitator Superfamily (MFS) (according to a BLASTp analysis[27,28]). The respective genes occur naturally in the rebeccamycin biosynthetic gene cluster of *L. aerocolonigenes*.[5] The transporter genes were also previously implemented in recombinant strains for the production of the rebeccamycin aglycon.[9,10] However, these studies did not compare strains without and with transporter to describe the impact of co-expression of the transporters on the production of rebeccamycin aglycons. Thus, it is unknown if or how well the aglycone or the dechlorinated variants are transported. Applying the adapted cultivation conditions, we tested plasmid-based expression of *rebU* and *rebT* with two different constitutive promoters (P_{tac} and P_{KmR}) (see Figure 2B). This approach of co-expressing *rebUT* did not result in higher specific productivity. We did not further investigate whether the transporter accepts the aglycon as a substrate at all.

The release of OMVs, which are small lipid-particles, by the cells may serve as an alternative mechanism for product release and, in addition, the vesicles may providean extracellular storage space for the product. OMVs are produced by Gram-negative bacteria in adaptation to different types of stress[29,30] and it is known that native producers of hydrophobic compounds, such as prodigiosin or violacein, release these compounds encapsulated in/attached to OMVs.[31–33] It has recently been shown that OMV release by hosts like *E. coli* and *P. putida* can be genetically engineered thereby supporting the recombinant production of hydrophobic natural compounds.[34,35] One approach to such engineering is the downregulation or deletion of genes with an essential function in the formation of the cell envelope.[36–38] Thus, two strains with knocked-out genes *mlaE* and *pvdQ*, respectively, previously identified as suitable targets for engineering of vesiculation (see

ChemBioChem
Research Article
doi.org/10.1002/cbic.202300576
Chemistry Europe
European Chemical Societies Publishing

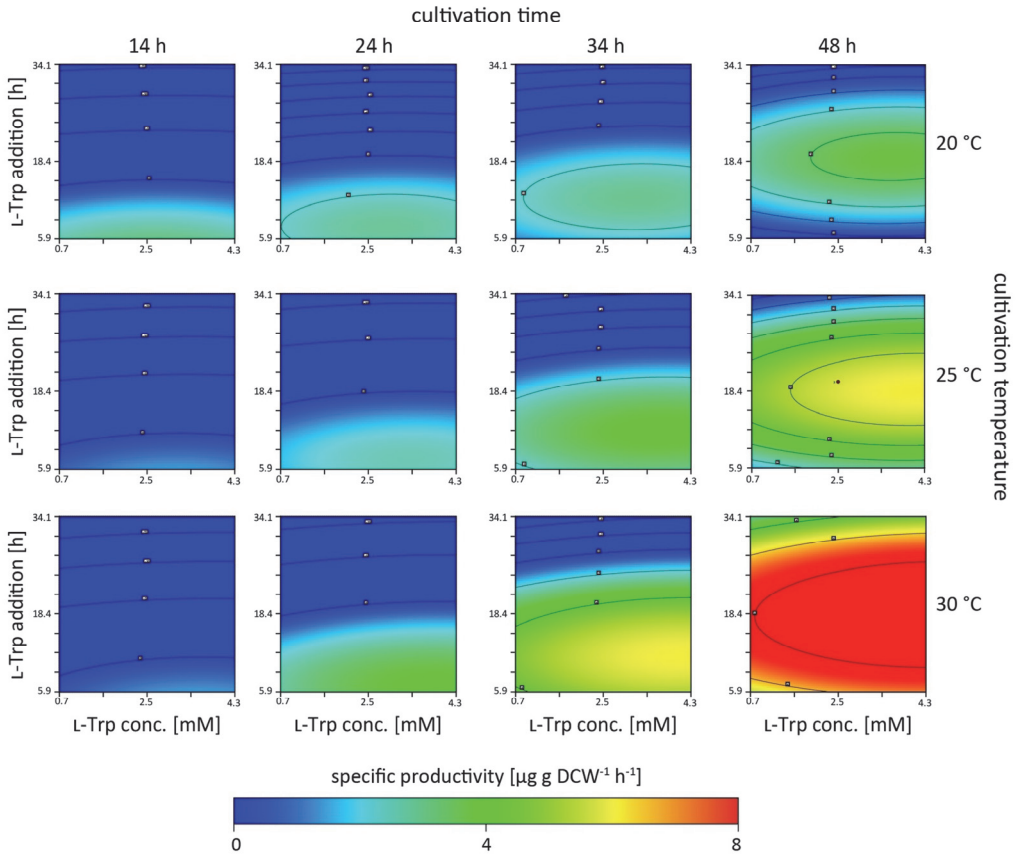

Figure 1. Arcyriaflavin A production in *P. putida* expressing genes *rebODCP* dependent on cultivation conditions and precursor supply. The specific productivity [µg g DCW^{-1} h^{-1}] of *rebODCP* expressing *P. putida* (*P. putida* NB04) for arcyriaflavin A is shown upon L-tryptophan addition (L-Trp addition [h]) at different concentrations (L-Trp conc. [mM]) plotted in contour plots for three different temperatures (20, 25, 30 °C) and four total cultivation times until sampling and analysis (14, 24, 34, 48 h). For statistical analysis of the performed DoE see Figure S4, Tables S1 and S2).

Figure S6),[35] were tested for arcyriaflavin A production (Figure 2C).

The deletion of *mlaE*, which provides a part of the Mla phospholipid transporter system relevant for maintaining outer membrane lipid asymmetry, did not affect arcyriaflavin A production. However, deletion of *pvdQ*, which is essential for pyoverdine release from the inner membrane of *P. putida* KT2440, resulted in an increased production yield.

We next tested the addition of a hydrophobic adsorbent to the culture medium, which was previously shown to effectively bind hydrophobic prodigiosin and elevate product levels in *P. putida*.[39] To this end, we added polyurethane (PU) foam cubes and subsequently extracted the compound from this material, as previously established. This led to an almost complete accumulation of arcyriaflavin A in the PU cubes instead of the cell pellet (see Figure S7).

While the combined use of PU as an adsorbent and the expression of the rebeccamycin transporter did not support production, PU addition and *ΔpvdQ*-based engineering increased productivity by 1.4-fold as compared to the unaltered strain without added PU (Figure 2D).

After optimization of both, culture conditions and physiological framework requirements, we set out to test the potential of precursor availability. To do this, we used the *ΔpvdQ* strain expressing the *rebODCP* genes for cultivation with PU foam and tested the effect of feeding of 4.9 mM L-tryptophan each time after 18 h, and again after 43 h (Figure 3A). We found that productivity tripled with the second feeding compared to single feeding, suggesting that alternative strategies to enhance L-tryptophan uptake or intrinsic biosynthesis may serve to further increase production.[40,41] The fact that the overall productivity was still relatively low despite offering high precursor concentrations may be due to the enzyme RebO having a strong

ChemBioChem
Research Article
doi.org/10.1002/cbic.202300576
Chemistry Europe
European Chemical Societies Publishing

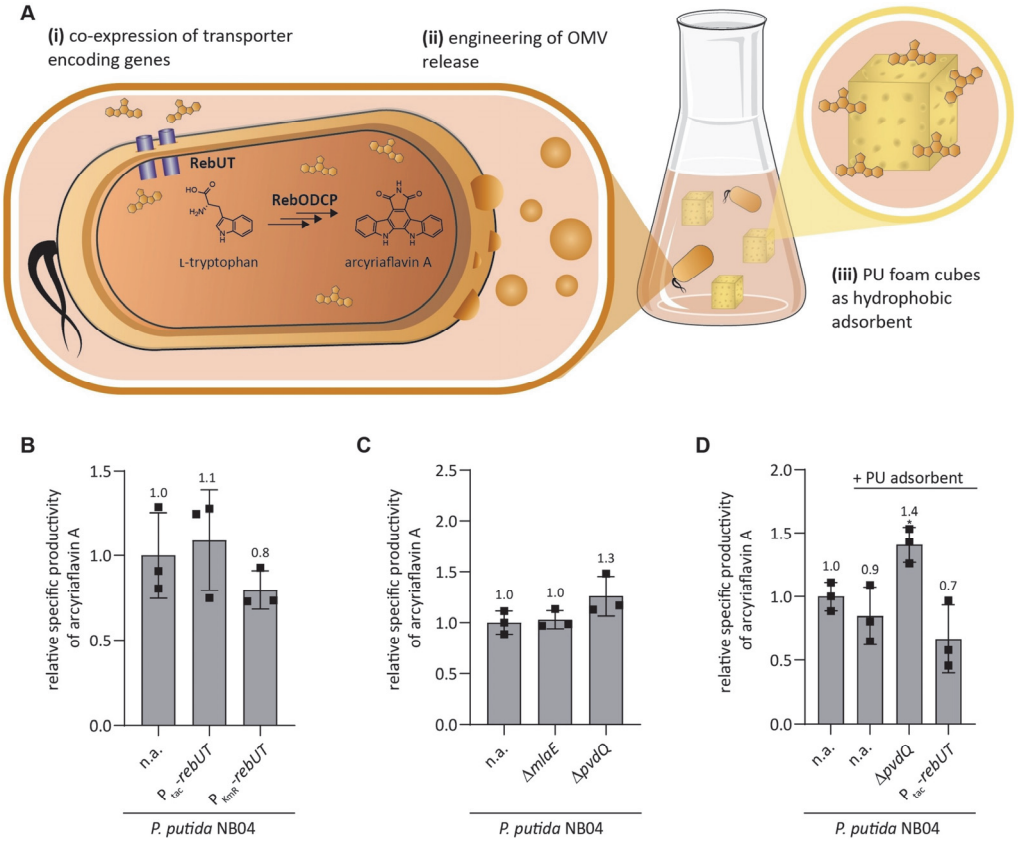

Figure 2. Arcyriaflavin A production in engineered *P. putida* KT2440 producer strains. **A**: Schematic presentation of three strategies for product enrichment outside of the producer cell: (i) co-expression of the transporter encoding genes *rebU* and *rebT*; (ii) engineering of OMV release; (iii) addition of polyurethane (PU) foam cubes as a hydrophobic adsorbent to the culture broth. **B**: Relative specific productivity upon co-expression of *rebUT* transporter genes (using constitutive promoters P_{tac} or P_{KmR}), shown in relation to the result of the unmodified strain *P. putida* NB04 (n.a. = not altered). The product was quantified in the cell pellet and supernatant fraction. **C**: Relative specific productivity of strains with deleted vesiculation-associated genes *mlaE* or *pvdQ*, shown in relation to the unmodified strain *P. putida* NB04 (n.a.). The product was quantified in the cell pellet and supernatant fraction. **D**: Relative specific productivity of *P. putida* NB04 and two engineered strains (P_{tac}-*rebUT* and Δ*pvdQ*) cultivated with PU foam cubes to increase productivity and facilitate the isolation of arcyriaflavin A (see Figure S7), shown in relation to the result of the producer strain *P. putida* NB04 (n.a.) cultivated without PU cubes. The product was quantified in the pellet and PU fraction. The data are means of biological triplicates with their respective standard deviations. Significant differences in comparison to the unmodified strain (n.a.) are indicated by asterisks (determined by T-test; * = $P \leq 0.05$).

preference for C7-substituted tryptophan like its natural substrate 7-chloro-L-tryptophan.[42,43] In the future, it may be interesting to generate hybrid pathways with homologous enzymes (e.g., VioA, VioB) that also produce CPA (**3**) but have a higher preference for L-tryptophan, which could lead to an increased production of arcyriaflavin A.[20] In addition, it could be relevant to investigate the production of arcyriaflavin derivatives by conversion of unnatural substrates (e.g., 5-fluoro-, 5-bromo- or 1-methyl-L-tryptophan[42,44]) in such hybrid pathways. Overall, almost six-fold enhanced productivity (from 5.7 $\mu g\,DCW^{-1}\,h^{-1}$ to 32.2 $\mu g\,DCW^{-1}\,h^{-1}$) and an eight-fold increase in product titer (from 0.49 $mg\,L^{-1}$ to 3.71 $mg\,L^{-1}$) were achieved in the present study (Figure 3B).

Based on these results, the bioprocess was scaled up to yield 4.69 mg of arcyriaflavin from 1 L culture (Figure 3C). Previous studies reported 0.7 $mg\,L^{-1}$ in a recombinant *E. coli* strain for the chlorinated derivative (rebeccamycin aglycon).[10]

Conclusions

Effective recombinant production of a natural product ideally requires the integration of multiple aspects, including gene expression, cultivation conditions, metabolic flux, and product storage or release. DoE can be a powerful tool to address multifactorial optimization approaches, as shown here for the

ChemBioChem
Research Article
doi.org/10.1002/cbic.202300576
Chemistry Europe
European Chemical Societies Publishing

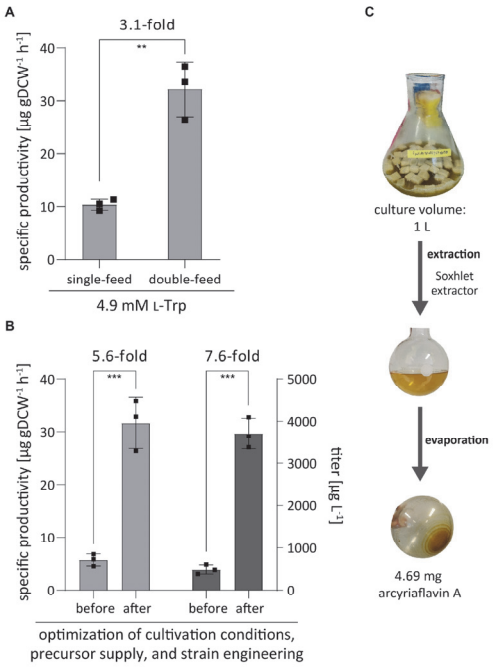

Figure 3. Optimized *P. putida*-based production and isolation of arcyriaflavin A. **A**: Specific productivity of arcyriaflavin A upon double feeding of L-tryptophan (4.9 mM feed each time after 18 h and 43 h) using *P. putida* NB04 (Δ*pvdQ*) as producer strain and PU cubes as hydrophobic adsorbent (cultivation for 72 h at 30 °C). The product was quantified as the sum of product amount in the pellet and in the PU foam cubes. Data are means of biological triplicates with their respective standard deviations. **B**: Total increase in arcyriaflavin A production after all optimization steps. Here, the specific productivity and titer obtained after optimization (cultivation of NB04 (Δ*pvdQ*) for 72 h at 30 °C with PU foam; supplementation of 4.9 mM L-tryptophan each time after 18 h and 43 h) are shown and compared to the productivity and titer of the initial bioprocess before optimization (cultivation of NB04 for 48 h at 30 °C; supplementation of 1 mM L-tryptophan after 4 h).[21] **C**: Schematic presentation of the isolation of arcyriaflavin A in an upscaling approach (cultivation of NB04 (Δ*pvdQ*)). Isolation with PU foam cubes from 1 L culture and extraction with a Soxhlet extractor resulted in the recovery of 4.69 mg arcyriaflavin A calculated based on HPLC-PDA (high performance liquid chromatography with photodiode array detection) analysis. Significant differences are indicated by asterisks (determined by T-test; * = $P \leq 0.05$, ** = $P \leq 0.01$, *** = $P \leq 0.001$).

evaluation of cultivation conditions. Furthermore, the showcase of arcyriaflavin A production in *P. putida* KT2440 presented in this study demonstrates that product release and adsorption can be a key to increased productivity, as this presumably prevents accumulation of the hydrophobic compound at the cell membrane. Comparing the previously reported production titer with the upscaled arcyriaflavin A production in presence of elevated precursor concentrations established here, the combined efforts resulted in an almost ten-fold increase.

Experimental Section

Bacterial strains and cultivation condition

Escherichia coli strains DH5α,[45] DH5α λpir,[46] Stellar (Takara Bio, Cat# 636763), and S17-1,[47] used for cloning and conjugational transfer, were cultivated in LB (lysogeny broth) medium (10 g L^{-1} tryptone, 5 g L^{-1} yeast extract, 10 g L^{-1} sodium chloride; Carl Roth®, Karlsruhe, Germany) under continuous shaking (130 rpm) or on agar plates at 37 °C. Standard conditions for *Pseudomonas putida* KT2440 (wild-type)[48] were 30 °C with continuous shaking (130 rpm) in 10 mL, 50 mL (PU experiments) or 500 mL (upscaling experiment) LB medium respectively. Procedures for online growth monitoring experiments are detailed in **SI-M1**. Antibiotics, if used, were added to the culture medium to the following final concentrations: *E. coli*: 50 µg mL^{-1} kanamycin (Km), 100 µg mL^{-1} ampicillin (Amp); *P. putida*: 25 µg mL^{-1} irgasan (Irg), 25 µg mL^{-1} gentamicin (Gm), 25 µg mL^{-1} kanamycin (Km).

Cloning and strain construction

Oligonucleotides, plasmids, and strains, used or constructed in this study, are summarized in Tables S3 and S4 in the SI.

For the assembly of plasmids for co-expression of the transporter genes, the vector pJT'Tmcs[49] was linearized by XhoI digestion and *rebU* and *rebT* were amplified by PCR using the oligonucleotides **1** to **4** and the *L. aerocolonigenes* (DSM 44217) genome as the template. Backbone and insert were assembled by using InFusion® Snap Assembly (Takara Bio Europe, St Germain en Laye, France) generating pJT'TrebUT. To replace the antibiotic resistance gene, the plasmid pJT'TrebUT was linearized by PCR using oligos **5** and **6** and the *aphII* gene was amplified from pVLT33[50] (using primers **7** and **8**). InFusion® Snap Assembly was again used to construct pJT'TrebUT-KmR.

To generate pBTBX-2-mcs-KmR-rebUT, the empty vector pBTBX-2-mcs (pBTBX-2 was a gift from Ryan Gill, Addgene plasmid # 26068[51]) was amplified by PCR (using primers **9** and **10**). The *rebU* and *rebT* genes were amplified using the previously constructed plasmid as template and oligos **11** and **12**, and both fragments were assembled.

The newly constructed plasmids were confirmed by Sanger sequencing (Eurofins Genomics, Ebersberg, Germany) using the sequencing primers **19** to **21**.

P. putida KT2440 was transformed with the plasmids by plate mating (for genomic integration of *rebODCP*) using *E. coli* S17-1 as donor[21] or by electroporation as previously described.[35,52] Construction of seamless deletion mutants was based on the SacB system using the suicide vector pNTPS138-R6KT.[53] For detailed description see **SI-M2** in the SI.

Arcyriaflavin A production and extraction

For the DoE approach *Design Expert*, (StatEase, Minneapolis, MN, USA) has been used to evaluate the influence of different cultivation parameters (temperature, time, addition time and concentration of the precursor) in 10 mL LB cultures under continuous shaking (130 rpm) (see **SI-M3**). As a result of the DoE prediction, the arcyriaflavin A producer strains were finally cultivated at 30 °C for 72 h and supplemented with 4.9 mM L-tryptophan (stock: 62.5 mM in dH_2O) after 18 h. Gene expression was induced by the addition of 2 mM salicylic acid (1 M stock concentration, prepared in ethanol) in the logarithmic growth phase (after 4 h). PU experiments were performed as previously

ChemBioChem
Research Article
doi.org/10.1002/cbic.202300576
Chemistry Europe
European Chemical Societies Publishing

described.[39] The *P. putida* producer strains were cultivated in 50 mL LB medium in a 500 mL baffled flask, supplemented with 500 mg PU foam cubes (Bornewasser, Göllheim, Germany; softpur, 25 kg m^{-3} density, 4 kPa compression hardness; each approximately 1 cm^3) using the above cultivation parameters. For upscaling, arcyriaflavin A production was performed using two 3 L Fernbach flasks each filled with 500 mL LB medium and 5 g PU foam cubes. Cultures were incubated under the same conditions, with L-tryptophan (4.9 mM) added each time after 18 and 43 hours. All cultures were inoculated to an optical density of $OD_{580\,nm} = 0.05$.

For extraction, samples were fractionated into pellet and supernatant by centrifugation (5000 rpm, 20 min, 4 °C). The pellets were extracted with ethanol (p.a.) using a volume equivalent to 10% (*v*/*v*) of the total culture volume. The extracts were incubated at 45 °C for 10 min and then cleared of cell debris by centrifugation (max speed, 10 min). In addition, arcyriaflavin A was extracted from the supernatant by two-phase extraction (not for DoE). Ethyl acetate (volume = 25% of the culture volume) was added and the mixture was vortexed for 2 min. The extraction was repeated. The organic phases were combined and evaporated under reduced pressure. Arcyriaflavin A was then dissolved in ethanol (volume = 10% of the culture volume). For extraction of PU from 50 mL cultures, the foam cubes were sieved from the culture, washed twice with water (2×50 mL), and extracted with 25 mL ethanol by wringing. The extract was then evaporated under reduced pressure and the residue (approximately 500 µL) was resuspended in 5 mL ethanol. For upscaling, the PU foam cubes were extracted using a Soxhlet extractor.[39] PU foam cubes from both 500 mL cultures were combined. After washing (2×1000 mL water), the PU foam cubes were loaded into a Soxhlet apparatus equipped with a reflux condenser and a 500 mL round bottom flask and filled with 400 mL ethanol. Arcyriaflavin A was continuously extracted by heating overnight.

Analysis of arcyriaflavin A was performed by HPLC-PDA as previously described based on the retention time (6.7 min) and PDA spectrum (λ_{max} = 282 nm, 316 nm).[21] For quantification, a calibration curve (0 to 33 mg mL^{-1}) was measured with a reference (purity ≥ 98% (HPLC); Tocris Bioscience, Bristol, United Kingdom) and specific productivity and titer as well as the yield of upscaled production were calculated from the areas obtained.

Supporting Information

Figure S1: Indolocarbazole basic scaffold and specific examples; Figure S2: Growth of *P. putida* KT2440 in the presence of arcyriaflavin A; Figure S3: DoE contour plots for arcyriaflavin A titers; Figure S4: Statistical analysis of the DoE; Figure S5: DoE model validation; Figure S6: Function of PvdQ and MlaE and their role in OMV formation; Figure S7: Accumulation of arcyriaflavin A; Eq. S1: Equation titer; Eq. S2: Equation specific productivity; Table S1: ANOVA (analysis of variance) and fit statistics for specific productivity; Table S2: ANOVA (analysis of variance) and fit statistics for titer; Table S3: Oligonucleotides used in this study; Table S4: Plasmids and bacterial strains used in this study; Table S5: Cultivation parameters for DoE. The authors have described additional experimental procedures and cited additional references within the Supporting Information.[54–56]

Acknowledgements

The work was supported by the German Federal Ministry of Education and Research within the framework of the NO-STRESS project (grant no. 031B0852B) and by grants from the Bioeconomy Science Center through the NRW Strategieprojekt. The scientific activities of the Bioeconomy Science Center were financially supported by the Ministry of Culture and Science of the German federal state of North Rhine-Westphalia (grant no. 313/323-400-00213). Open Access funding enabled and organized by Projekt DEAL.

Conflict of Interests

The authors declare no conflict of interest.

Data Availability Statement

The data that support the findings of this study are available from the corresponding author upon reasonable request.

Keywords: arcyriaflavin A production · biotransformation · design of experiment · *P. putida* KT2440 · strain engineering

[1] C. Sánchez, C. Méndez, J. A. Salas, *Nat. Prod. Rep.* **2006**, *23*, 1007–1045.
[2] H. Nakano, S. Omura, *J. Antibiot.* **2009**, *62*, 17–26.
[3] G. W. Gribble, *Alkaloids: Chemistry and Biology*, Academic Press Inc. **2012**, pp. 1–165.
[4] A. P. Salas, L. Zhu, C. Sánchez, A. F. Braña, J. Rohr, C. Méndez, J. A. Salas, *Mol. Microbiol.* **2005**, *58*, 17–27.
[5] C. Sánchez, I. A. Butovich, A. F. Braña, J. Rohr, C. Méndez, J. A. Salas, *Chem. Biol.* **2002**, *9*, 519–531.
[6] P. A. Horton, R. E. Longley, O. J. McConnell, L. M. Ballas, *Experientia* **1994**, *50*, 843–845.
[7] W. Steglich, *Pure Appl. Chem.* **1989**, *61*, 281–288.
[8] C. Sánchez, C. Méndez, J. A. Salas, *J. Ind. Microbiol. Biotechnol.* **2006**, *33*, 560–568.
[9] C. Sánchez, L. Zhu, A. F. Braña, A. P. Salas, J. Rohr, C. Méndez, J. A. Salas, *PNAS* **2005**, *102*, 461–466.
[10] A. Casini, F.-Y. Chang, R. Eluere, A. M. King, E. M. Young, Q. M. Dudley, A. Karim, K. Pratt, C. Bristol, A. Forget, A. Ghodasara, R. Warden-Rothman, R. Gan, A. Cristofaro, A. E. Borujeni, M.-H. Ryu, J. Li, Y.-C. Kwon, H. Wang, E. Tatsis, C. Rodriguez-Lopez, S. O'Connor, M. H. Medema, M. A. Fischbach, M. C. Jewett, C. Voigt, D. B. Gordon, *J. Am. Chem. Soc.* **2018**, *140*, 4302–4316.
[11] M. Sancelme, S. Fabre, M. Prudhomme, *J. Antibiot.* **1994**, *47*, 792–798.
[12] M. J. Slater, R. Baxter, R. W. Bonser, S. Cockerill, K. Gohil, N. Parry, E. Robinson, R. Randall, C. Yeates, W. Snowden, A. Walters, *Bioorg. Med. Chem. Lett.* **2001**, *11*, 1993–1995.
[13] M. J. Slater, S. Cockerill, R. Baxter, R. W. Bonser, K. Gohil, C. Gowrie, J. E. Robinson, E. Littler, N. Parry, R. Randall, W. Snowden, *Bioorg. Med. Chem.* **1999**, *7*, 1067–1074.
[14] T. Hirakawa, K. Nasu, Y. Aoyagi, K. Takebayashi, H. Narahara, *Reprod. Biol. Endocrinol.* **2017**, *15*, 53.
[15] D. Alonso, E. Caballero, M. Medarde, F. Tomé, *Tetrahedron Lett.* **2005**, *46*, 4839–4841.
[16] K. Wang, Z. Liu, *Synth. Commun.* **2009**, *40*, 144–150.
[17] S. Lee, K.-H. Kim, C.-H. Cheon, *Org. Lett.* **2017**, *19*, 2785–2788.
[18] M. M. Heravi, S. Rohani, V. Zadsirjan, N. Zahedi, *RSC Adv.* **2017**, *7*, 52852–52887.
[19] G. E. Chambers, A. E. Sayan, R. C. D. Brown, *Nat. Prod. Rep.* **2021**, *38*, 1794–1820.
[20] C. Sánchez, A. F. Braña, C. Méndez, J. A. Salas, *ChemBioChem* **2006**, *7*, 1231–1240.

ChemBioChem | Research Article doi.org/10.1002/cbic.202300576 | Chemistry Europe European Chemical Societies Publishing

[21] R. Weihmann, S. Kubicki, N. L. Bitzenhofer, A. Domröse, I. Bator, L.-M. Kirschen, F. Kofler, A. Funk, T. Tiso, L. M. Blank, K.-E. Jaeger, T. Drepper, S. Thies, A. Loeschcke, *FEMS Microbes* **2023**, *4*, 1–17.
[22] A. Loeschcke, S. Thies, *Curr. Opin. Biotechnol.* **2020**, *65*, 213–224.
[23] A. Loeschcke, S. Thies, *Appl. Microbiol. Biotechnol.* **2015**, *99*, 6197–6214.
[24] N. L. Bitzenhofer, L. Kruse, S. Thies, B. Wynands, T. Lechtenberg, J. Rönitz, E. Kozaeva, N. T. Wirth, C. Eberlein, K.-E. Jaeger, P. I. Nikel, I. J. Heipieper, N. Wierckx, A. Loeschcke, *Essays Biochem.* **2021**, *65*, 319–336.
[25] P. I. Nikel, V. de Lorenzo, *Metab. Eng.* **2018**, *50*, 142–155.
[26] A. Weimer, M. Kohlstedt, D. C. Volke, P. I. Nikel, C. Wittmann, *Appl. Microbiol. Biotechnol.* **2020**, *104*, 7745–7766.
[27] S. McGinnis, T. L. Madden, *Nucleic Acids Res.* **2004**, *32*, 20–25.
[28] S. F. Altschul, W. Gish, W. Miller, E. W. Myers, D. J. Lipman, *J. Mol. Biol.* **1990**, *215*, 403–410.
[29] A. Kulp, M. J. Kuehn, *Annu. Rev. Microbiol.* **2010**, *64*, 163–184.
[30] C. Schwechheimer, M. J. Kuehn, *Nat. Rev. Microbiol.* **2015**, *13*, 605–619.
[31] S. Y. Choi, S. Lim, G. Cho, J. Kwon, W. Mun, H. Im, R. J. Mitchell, *Environ. Microbiol.* **2020**, *22*, 705–713.
[32] D. Tan, L. Fu, X. Sun, L. Xu, J. Zhang, *J. Agric. Food Chem.* **2020**, *68*, 5606–5615.
[33] J. H. Batista, F. C. Leal, T. T. H. Fukuda, J. Alcoforado Diniz, F. Almeida, M. T. Pupo, J. F. da Silva Neto, *Environ. Microbiol.* **2020**, *22*, 2432–2442.
[34] D. Yang, S. Y. Park, S. Y. Lee, *Adv. Sci.* **2021**, *8*, 2100743.
[35] N. L. Bitzenhofer, C. Höfel, S. Thies, A. J. Weiler, C. Eberlein, H. J. Heipieper, R. Batra-Safferling, P. Sundermeyer, T. Heidler, C. Sachse, T. Busche, J. Kalinowski, T. Belthle, T. Drepper, K. Jaeger, A. Loeschcke, *Microb. Biotechnol.* **2023**, 1–18.
[36] M. Toyofuku, N. Nomura, L. Eberl, *Nat. Rev. Microbiol.* **2019**, *17*, 13–24.
[37] S. Roier, F. G. Zingl, F. Cakar, S. Durakovic, P. Kohl, T. O. Eichmann, L. Klug, B. Gadermaier, K. Weinzerl, R. Prassl, A. Lass, G. Daum, J. Reidl, M. F. Feldman, S. Schild, *Nat. Commun.* **2016**, *7*, 10515.
[38] E. D. Avila-Calderón, M. del S Ruiz-Palma, M. G. Aguilera-Arreola, N. Velázquez-Guadarrama, E. A. Ruiz, Z. Gomez-Lunar, S. Witonsky, A. Contreras-Rodríguez, *Front. Microbiol.* **2021**, *12*, 557902.
[39] A. Domröse, A. S. Klein, J. Hage-Hülsmann, S. Thies, V. Svensson, T. Classen, J. Pietruszka, K.-E. Jaeger, T. Drepper, A. Loeschcke, *Front. Microbiol.* **2015**, *6*, 972.
[40] H. Niu, R. Li, Q. Liang, Q. Qi, Q. Li, P. Gu, *J. Ind. Microbiol. Biotechnol.* **2019**, *46*, 55–65.
[41] J. Kuepper, J. Dickler, M. Biggel, S. Behnken, G. Jäger, N. Wierckx, L. M. Blank, *Front. Microbiol.* **2015**, *6*, 1310.
[42] T. Nishizawa, C. C. Aldrich, D. H. Sherman, *J. Bacteriol.* **2005**, *187*, 2084–2092.
[43] C. Schnepel, I. Kemker, N. Sewald, *ACS Catal.* **2019**, *9*, 1149–1158.
[44] H.-E. Lai, A. M. C. Obled, S. M. Chee, R. M. Morgan, R. Lynch, S. V. Sharma, S. J. Moore, K. M. Polizzi, R. J. M. Goss, P. S. Freemont, *ACS Chem. Biol.* **2021**, *16*, 2116–2123.
[45] D. Hanahan, *J. Mol. Biol.* **1983**, *166*, 557–580.
[46] R. Platt, C. Drescher, S.-K. Park, G. J. Phillips, *Plasmid* **2000**, *43*, 12–23.
[47] R. Simon, U. Priefer, A. Pühler, *Bio/Technology* **1983**, *1*, 784–791.
[48] K. E. Nelson, C. Weinel, I. T. Paulsen, R. J. Dodson, H. Hilbert, V. A. P. Martins dos Santos, D. E. Fouts, S. R. Gill, M. Pop, M. Holmes, L. Brinkac, M. Beanan, R. T. DeBoy, S. Daugherty, J. Kolonay, R. Madupu, W. Nelson, O. White, J. Peterson, H. Khouri, I. Hance, P. C. Lee, E. Holtzapple, D. Scanlan, K. Tran, A. Moazzez, T. Utterback, M. Rizzo, K. Lee, D. Kosack, D. Moestl, H. Wedler, J. Lauber, D. Stjepandic, J. Hoheisel, M. Straetz, S. Heim, C. Kiewitz, J. Eisen, K. N. Timmis, A. Dusterhoft, B. Tummler, C. M. Fraser, *Environ. Microbiol.* **2002**, *4*, 799–808.
[49] S. Verhoef, H. Ballerstedt, R. J. M. Volkers, J. H. de Winde, H. J. Ruijssenaars, *Appl. Microbiol. Biotechnol.* **2010**, *87*, 679–690.
[50] V. de Lorenzo, L. Eltis, B. Kessler, K. N. Timmis, *Gene* **1993**, *123*, 17–24.
[51] J. E. Prior, M. D. Lynch, R. T. Gill, *Biotechnol. Bioeng.* **2010**, *106*, 326–332.
[52] Q. Tu, J. Yin, J. Fu, J. Herrmann, Y. Li, Y. Yin, A. F. Stewart, R. Müller, Y. Zhang, *Sci. Rep.* **2016**, *6*, 24648.
[53] J. Lassak, A.-L. Henche, L. Binnenkade, K. M. Thormann, *Appl. Environ. Microbiol.* **2010**, *76*, 3263–3274.
[54] C. Davies, A. J. Taylor, A. Elmi, J. Winter, J. Liaw, A. D. Grabowska, O. Gundogdu, B. W. Wren, D. J. Kelly, N. Dorrell, *Front. Cell. Infect. Microbiol.* **2019**, *9*, 177.
[55] R. Juodeikis, S. R. Carding, *Microbiol Mol Biol* **2022**, *86*, e0003222.
[56] J. R. Elmore, A. Furches, G. N. Wolff, K. Gorday, A. M. Guss, *Metab Eng Commun* **2017**, *5*, 1–8.

Manuscript received: August 16, 2023
Revised manuscript received: September 20, 2023
Accepted manuscript online: September 24, 2023
Version of record online: ■■, ■■

II.5. Combining biosynthetic concepts to produce non-natural prodiginines

II.5.1. Hybrid synthesis of a hydroxylated prodiginine

PUBLICATION V

Production of tailored hydroxylated prodiginine showing combinatorial activity with rhamnolipids against plant-parasitic nematodes

Dorothea Fabiane Kossmann*, Mengmeng Huang*, Robin Weihmann*, Xinghzi Xiao, Florian Gätgens, Tim Moritz Weber, Hannah U. C. Brass, **Nora Lisa Bitzenhofer**, Schinya Ibrahim, Klara Bangert, Leon Rehling, Conrad Müller, Till Tiso, Lars M Blank, Thomas Drepper, Karl-Erich Jaeger, Florian M.W. Grundler, Jörg Pietruszka, A Sylvia S Schleker, Anita Loeschcke

Frontiers in Microbiology (**2023**) 14:1151882.

The online version is available at: 10.3389/fmicb.2023.1151882

Status: published

Supporting Information can be found in the Appendix (**Chapter V.4**)

Own contribution:

Planning and supervising mutasynthesis and RT-PCR experiments, editing the manuscript.

frontiers | Frontiers in Microbiology

TYPE Original Research
PUBLISHED 02 May 2023
DOI 10.3389/fmicb.2023.1151882

OPEN ACCESS

EDITED BY
Monika Prakash Rai,
Amity University, India

REVIEWED BY
Pramod B. Shinde,
Central Salt and Marine Chemicals Research Institute (CSIR), India
Finian Leeper,
University of Cambridge, United Kingdom

*CORRESPONDENCE
J. Pietruszka
j.pietruszka@fz-juelich.de
A. S. S. Schleker
sylvia.schleker@uni-bonn.de
A. Loeschcke
a.loeschcke@fz-juelich.de

†These authors have contributed equally to this work and share first authorship

‡These authors have contributed equally to this work and share last authorship

RECEIVED 26 January 2023
ACCEPTED 03 April 2023
PUBLISHED 02 May 2023

CITATION
Kossmann DF, Huang M, Weihmann R, Xiao X, Gätgens F, Weber TM, Brass HUC, Bitzenhofer NL, Ibrahim S, Bangert K, Rehling L, Mueller C, Tiso T, Blank LM, Drepper T, Jaeger K-E, Grundler FMW, Pietruszka J, Schleker ASS and Loeschcke A (2023) Production of tailored hydroxylated prodiginine showing combinatorial activity with rhamnolipids against plant-parasitic nematodes.
Front. Microbiol. 14:1151882.
doi: 10.3389/fmicb.2023.1151882

Production of tailored hydroxylated prodiginine showing combinatorial activity with rhamnolipids against plant-parasitic nematodes

D. F. Kossmann[1,2†], M. Huang[3†], R. Weihmann[4†], X. Xiao[3], F. Gätgens[4], T. M. Weber[2], H. U. C. Brass[2], N. L. Bitzenhofer[4], S. Ibrahim[4], K. Bangert[4], L. Rehling[3], C. Mueller[5], T. Tiso[5], L. M. Blank[5], T. Drepper[4], K.-E. Jaeger[1,4], F. M. W. Grundler[3], J. Pietruszka[1,2*‡], A. S. S. Schleker[3*‡] and A. Loeschcke[4*‡]

[1]Institute of Bio- and Geosciences (IBG-1): Biotechnology, Forschungszentrum Jülich GmbH, Jülich, Germany, [2]Institute of Bioorganic Chemistry, Forschungszentrum Jülich, Heinrich Heine University Düsseldorf, Jülich, Germany, [3]INRES, Molecular Phytomedicine, University of Bonn, Bonn, Germany, [4]Institute of Molecular Enzyme Technology, Forschungszentrum Jülich, Heinrich Heine University Düsseldorf, Jülich, Germany, [5]iAMB—Institute of Applied Microbiology, ABBt—Aachen Biology and Biotechnology, RWTH Aachen University, Aachen, Germany

Bacterial secondary metabolites exhibit diverse remarkable bioactivities and are thus the subject of study for different applications. Recently, the individual effectiveness of tripyrrolic prodiginines and rhamnolipids against the plant-parasitic nematode *Heterodera schachtii*, which causes tremendous losses in crop plants, was described. Notably, rhamnolipid production in engineered *Pseudomonas putida* strains has already reached industrial implementation. However, the non-natural hydroxyl-decorated prodiginines, which are of particular interest in this study due to a previously described particularly good plant compatibility and low toxicity, are not as readily accessible. In the present study, a new effective hybrid synthetic route was established. This included the engineering of a novel *P. putida* strain to provide enhanced levels of a bipyrrole precursor and an optimization of mutasynthesis, i.e., the conversion of chemically synthesized and supplemented monopyrroles to tripyrrolic compounds. Subsequent semisynthesis provided the hydroxylated prodiginine. The prodiginines caused reduced infectiousness of *H. schachtii* for *Arabidopsis thaliana* plants resulting from impaired motility and stylet thrusting, providing the first insights on the mode of action in this context. Furthermore, the combined application with rhamnolipids was assessed for the first time and found to be more effective against nematode parasitism than the individual compounds. To obtain, for instance, 50% nematode control, it was sufficient to apply 7.8 μM hydroxylated prodiginine together with 0.7 μg/ml (~1.1 μM) di-rhamnolipids, which corresponded to *ca.* ¼ of the individual EC_{50} values. In summary, a hybrid synthetic route toward a hydroxylated prodiginine was established and its effects and combinatorial activity with rhamnolipids on plant-parasitic nematode *H. schachtii* are presented, demonstrating potential application as antinematodal agents.

KEYWORDS

Prodiginines, plant-parasitic nematodes, plant protection, mutasynthesis and semisynthesis, *Pseudomonas putida*, combinatorial activity, rhamnolipids

10.3389/fmicb.2023.1151882

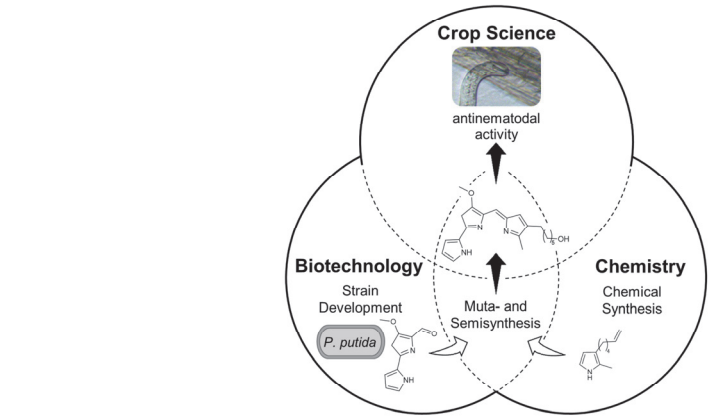

GRAPHICAL ABSTRACT

1. Introduction

Prodiginines are a group of bacterial secondary metabolites with diverse remarkable bioactivities, among which anticancer and antimicrobial effects have perhaps been described in most detail thus far (Fürstner, 2003; Stankovic et al., 2014; Hu et al., 2016; Sakai-Kawada et al., 2019; Yip et al., 2019; Berning et al., 2021; Li et al., 2022). Notably, prodiginine-producing bacteria such as *Streptomyces* and *Serratia* species also dwell in the rhizosphere, the dynamic micro-biosphere around the plant roots and site of manifold chemical interactions between the bacteria and plants (Berg, 2009; Lugtenberg and Kamilova, 2009; Meschke et al., 2012). Here, direct interactions can result in hormonal stimulation, increased stress tolerance and improved nutrient availability and uptake by plant roots. In addition, indirect beneficial effects for the plant can result from the suppression of pathogens. Although the ecophysiological role of prodiginines is still poorly understood, various bioactivities of prodigiosin (**1**) and related tripyrrolic analogs against several plant pathogens have already been reported (Someya et al., 2001; Meschke et al., 2012; Rahul et al., 2014; Roberts et al., 2021). Recently, their effectiveness against the plant-parasitic nematode (PPN) *Heterodera schachtii*, the causative agent of tremendous losses in crop plants, was described (Habash et al., 2020). Moreover, naturally-occurring bacterial secondary metabolites with surfactant properties, namely rhamnolipids, were recently reported to act against *H. schachtii* (Bredenbruch et al., 2023). It has further been shown that prodigiosin (**1**) possesses combinatorial antibacterial activities when applied together with biosurfactants, such as the lipopeptide serrawettin W1 and rhamnolipids (Hage-Hülsmann et al., 2018). It has been postulated that the pigment can only exert its full antimicrobial activity in combination with biosurfactants (Williamson et al., 2008; Roberts et al., 2021).

The aim of the present interdisciplinary study was to facilitate access to the relevant compounds and to investigate their combinatorial activities against *H. schachtii*. *Pseudomonas putida* has become a widely established biotechnological host for natural product biosynthesis (Nikel et al., 2016; Loeschcke and Thies, 2020; Weimer et al., 2020) including heterologous prodigiosin and rhamnolipid production (Domröse et al., 2015; Tiso et al., 2020; Cook et al., 2021). The rhamnolipid bioprocess has already been industrially implemented by Evonik Industries AG while research to improve accessing prodiginine derivatives is ongoing: recent studies showed heterologous expression of the *pig* gene cluster of *Serratia marcescens* via chromosomal integration, which established the biosynthesis of prodigiosin (**1**) (Domröse et al., 2015, 2019; Cook et al., 2021). Further, a mutasynthesis approach enabled the generation of new prodiginines (Klein et al., 2017, 2018). This procedure was based on the partial disruption of the native biosynthesis pathway and feeding of monopyrrole precursor analogs, which were incorporated into new tripyrrolic compounds. A limitation of this mutasynthesis approach was a relatively low product yield of 2–12% (Klein et al., 2017). Therefore, the development of a novel mutasynthesis *chassis* with enhanced bipyrrole production capacity and an optimization of mutasynthesis were identified as promising strategies to obtain target prodiginines more efficiently.

In previous work, a prodiginine bearing a terminal allylalcohol group (**2**) was reported to show remarkable plant growth promoting properties. In addition, it was not toxic for *Caenorhabditis elegans* at concentrations where prodigiosin (**1**) was lethal for this non-target organism (Habash et al., 2020). Based on these findings, the focus of the present study is the development of a feasible synthetic approach to hydroxylated prodiginines for investigations of anti-nematode activity. This study thus reports a mutasynthesis approach in a novel, efficient bipyrrole-producing *P. putida* strain and subsequent chemical conversion, i.e., semisynthesis, toward hydroxylated prodiginine **3** (Figure 1). The mode of action against *H. schachtii* as well as combinatorial activity with di-rhamnolipids (**4**) were investigated for the first time, demonstrating potential application as antinematodal agents.

10.3389/fmicb.2023.1151882

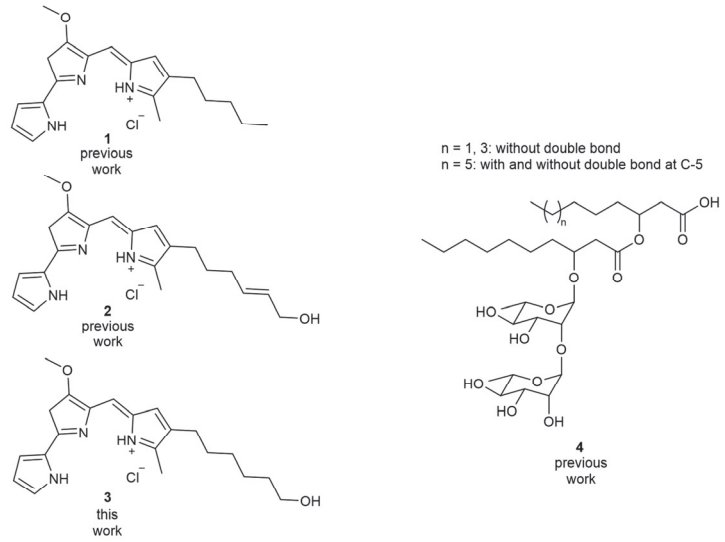

FIGURE 1
Bioactive compounds assessed in this study. The synthesis of prodigiosin **(1)** and hydroxylated derivative **(2)** has been established in previous studies. A synthesis route to hydroxylated prodiginine **(3)** is presented in this study, enabling the compound's application together with di-rhamnolipids **(4)**, which can be obtained via microbial biosynthesis as a mixture of congeners as indicated.

2. Results

2.1. Development of an enhanced *Pseudomonas putida chassis* for optimized mutasynthesis

In natural prodigiosin (**1**) biosynthesis, the monopyrrole MAP (2-methyl-3-amylpyrrole, **5**) and the bipyrrole MBC (4-methoxy-2,2′-bipyrrole-5-carbaldehyde, **6**) are condensed by a ligase (PigC in *S. marcescens*) to a tripyrrolic scaffold. The mutasynthesis approach has previously been established successfully in *P. putida* pig-r2 Δ*pigD* (Klein et al., 2017, 2018). The strain harbored the entire *S. marcescens pig* gene cluster—with the exception of the first MAP biosynthetic gene *pigD*, which was replaced by an antibiotic resistance gene. By feeding chemically synthesized monopyrroles to this MAP-deficient *P. putida* pig-r2 Δ*pigD* strain, the PigC-catalyzed condensation with MBC (**6**) led to novel tripyrrolic compounds in these previous studies.

Since mutasynthesis might be limited by biosynthetic provision of the bipyrrole precursor MBC (**6**), we aimed to establish a streamlined MBC-producing *chassis* preferentially lacking genetic and metabolic burdens. As a new strategy, a truncated *pig* gene cluster specifically designed to facilitate the biosynthesis of the bipyrrole **6** was integrated in the host. To this end, the artificial *pigAFGHIJKLMN* gene cluster (excluding the MAP (**5**) biosynthesis-encoding genes *pigBDE* and the ligase-encoding *pig*C, see Supplementary Figure S1) was assembled by PCR and yeast recombinational cloning into the yTREX vector following established protocols (Domröse et al., 2017; Weihmann et al., 2020). In this process, the promotor-less *lacZ* gene was inserted downstream of *pigN* (Figure 2A). The resulting vector was used for random transposon Tn5-based integration of the recombinant operon in the *P. putida* bacterial chromosome and LacZ was utilized as transcription reporter. Based on that, clones with strong gene expression were indicated by blue coloration as a result of X-gal conversion. Of these clones, 19 were selected and subjected to small scale cultivation, metabolite extraction and LC–MS analysis to verify bipyrrole product accumulation. Results were comparatively evaluated in relation to the previously established mutasynthesis *chassis P. putida* pig-r2 Δ*pigD* (Figure 2B). While four strains did not produce any detectable amounts of MBC (**6**), one clone (MBC17) produced a lower amount of MBC (**6**) than *P. putida* pig-r2 Δ*pigD*, and 14 accumulated the bipyrrole at higher levels (up to 8-fold increased). The best producer (MBC18) showed likewise elevated transcript levels (approx. 4-fold), indicating that a higher expression level could be reached in the new strain, which in turn contributed to higher bipyrrole synthesis. The enhanced MBC (**6**) level was verified for MBC18 in larger scale as applied in preparative mutasynthesis: Both strains, *P. putida* pig-r2 Δ*pigD* and MBC18, were cultivated in TB medium and polyurethane (PU) foam cubes were added as adsorbent for the hydrophobic compound, as previously established for prodigiosin (**1**) recovery (Domröse et al., 2015). Extracts from PU of the cultures with the newly constructed strain MBC18 contained about 12-fold more MBC (**6**) than those of the previously reported strain *P. putida* pig-r2 Δ*pigD* — a promising precondition for mutasynthesis.

The next step was to evaluate the capacity of the new strains for mutasynthesis with MBC17, MBC13, and MBC18 representing a low, an intermediate, and a high MBC level producer, respectively. The ligase PigC was thus introduced into these strains by plasmid-based expression from the IPTG-inducible P_{tac} promoter in pVLT33-pigC

10.3389/fmicb.2023.1151882

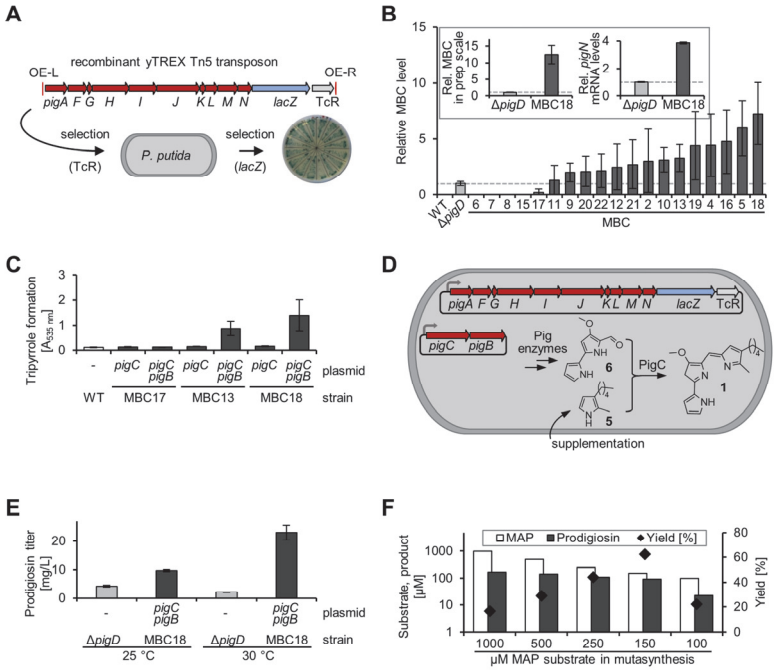

FIGURE 2
Construction of a *Pseudomonas putida* mutasynthesis *chassis*. **(A)** The artificial 4-methoxy-2,2′-bipyrrole-5-carbaldehyde (MBC) biosynthesis-encoding gene cluster was assembled by yeast-cloning and integrated in the bacterial chromosome via Tn5 transposition. After that, expressing clones were selected based on LacZ reporter activity. **(B)** Relative MBC production in small scale cultivation of engineered *P. putida* shown as x-fold increase relative to the signal of *P. putida* pig-r2 Δ*pigD*. Left Inset: Evaluation in preparative mutasynthesis setup (100 ml scale, MBC18 with pVLT33-pigC-pigB). Right inset: Relative *pigN* mRNA levels. **(C)** Dependence of the condensation of biosynthesized MBC (**6**) with supplemented MAP (**5**) on co-expression of PigB in *P. putida* stains MBC17, −13, −18 with plasmids pVLT33-pigC or pVLT33-pigC-pigB, respectively, in small scale cultivation. **(D)** Genetic setup of the new mutasynthesis *chassis* carrying the MBC (**6**) biosynthetic genes in the chromosome and expressing *pigC* and *pigB* from a plasmid. **(E)** Mutasynthesis performance of the newly established *chassis P. putida* MBC18/pVLT33-pigC-pigB in comparison with hitherto used *P. putida* pig-r2 Δ*pigD* in small scale cultivation at 25 or 30°C. The product was detected in extracts via spectrophotometry. Shown are mean values of independently replicated measurements (min. triplicates) with the respective standard deviation. **(F)** Optimization of preparative mutasynthesis in 5x100 ml scale with *P. putida* MBC18/pVLT33-pigC-pigB. The amount of substrate MAP (**5**) was varied from 1.000 µM to 100 µM to optimize conditions with respect to isolated prodigiosin (**1**) and corresponding yields (% mol of product relative to the substance amount of substrate).

(Brands et al., 2020). After small scale cultivation with supplementation of MAP (**5**, 1 mM), cells were extracted and prodigiosin-specific absorption was measured at 535 nm (Figure 2C). However, no noteworthy conversion of the fed monopyrrole to prodigiosin could be detected with either strain (MBC17, MBC13, MBC18/*pigC*).

Since it is known that in *in vitro* assays PigC does not require any additional proteins for functioning (Brass et al., 2019; Brands et al., 2020) it could be excluded that a generally necessary component was missing in the new strains. However, the previous *pigD* deletion mutant *P. putida* pig-r2 Δ*pigD* could facilitate conversion and it additionally contained functional PigB and PigE-encoding genes. This suggested an important role of either one or both of these proteins in the mutasynthesis setup (see Supplementary Figure S1). Based on their localization at the membrane and the proven importance of their membrane-anchoring domains, it may further be speculated that the last precursor-delivering enzymes PigN/F and PigB, as well as PigC could form a membrane-associated protein complex (Williamson et al., 2005; Chawrai et al., 2012; Couturier et al., 2019). This suggested that this complex consisting of PigC and PigN/F, but devoid of PigB might not be functional (see also Supplementary Figures S2, S3). PigB co-expression was therefore tested next by using plasmid pVLT33-pigC-pigB in the new strains (Figures 2C,D). While in the low-level precursor providing strain MBC17, co-expression of PigB did not lead to prodigiosin (**1**) formation, an increased signal was observed with MBC13 and highest levels were found in the high-level MBC-providing strain MBC18 (MBC17, MBC13, MBC18/*pigC-pigB*).

As a next step, mutasynthetic prodigiosin (**1**) production of the newly established *chassis P. putida* MBC18/pVLT33-pigC-pigB was assessed in comparison with hitherto used *P. putida* pig-r2 Δ*pigD*. To this end, small scale cultivation was used to test performance at 25°C as previously established (Klein et al., 2017, 2018) and at the optimal *P. putida* growth temperature 30°C (Figure 2E). At 25°C, 4.2 and 10 mg/L prodigiosin were obtained, while at 30°C, 2.3 and 21 mg/L were produced with *P. putida* pig-r2 Δ*pigD* and MBC18/pVLT33-pigC-pigB, respectively. These results therefore verified enhanced

10.3389/fmicb.2023.1151882

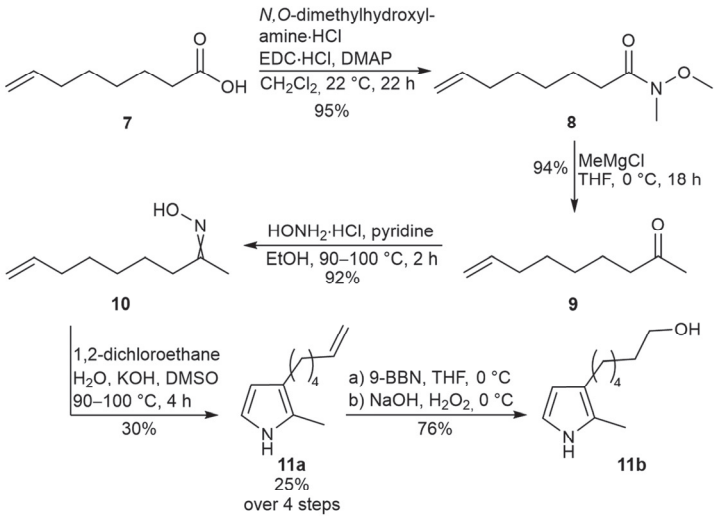

FIGURE 3
Synthesis route toward the 2,3-disubstituted pyrrole precursors **11a** and **11b**.

performance of the newly constructed *chassis*, especially at 30°C, so all following experiments were conducted at this temperature.

Since during small scale cultivation under the applied conditions with excess of MAP (1 mM, **5**), MBC (**6**) was consumed to below limits of quantification, an adjustment of MAP concentrations was tested next. Hence, different MAP (**5**) concentrations were supplemented to *P. putida* MBC18/pVLT33-pigC-pigB in order to potentially match the levels of both precursors in preparative scale experiments and optimize yields (Figure 2F). The best yield of 62% purified product was obtained with 150 µM MAP (**5**). Isolation by soxhlet extraction of PU and column chromatography on silica yielded 17 mg prodigiosin (**1**) from 500 ml mutasynthesis cultures. This outcome corresponding to 34 mg/l represented an improvement to previously reported 17 mg/l, obtained with the same pyrrole via comparable procedures (Klein et al., 2017). Remaining MBC (**6**) was below 2 µM in this experiment (Supplementary Figure S4). This procedure was therefore deemed as suitable for further steps toward accessing the hydroxylated target compound **3**.

2.2. Chemical synthesis of pyrroles, muta- and semisynthesis of hydroxylated prodiginine 3

In order to establish a synthesis route to a hydroxylated prodiginine tripyrrole, a pyrrole with terminal double bond was aimed as precursor to allow a late-stage semisynthetic functionalization. Previously reported prodiginine **2** was synthesized chemically in a condensation reaction of *Boc*-**6** and a pyrrole with allylalcohol function (Habash et al., 2020). With this approach, the functional group is already applied, but further modification and derivatization are less feasible. The here presented mutasynthesis approach is more flexible in terms of late-stage functionalization and allows to functionalize the obtained mutasynthesis product in a variety of ways, such as with a bromination or oxidation. In order to yield the hydroxylated prodiginine **3**, we applied a hydroboration as semisynthetic step.

Starting from carboxylic acid **7**, Weinreb-amide **8** and ketone **9** were obtained in two steps, consecutively. Afterwards, oxime **10** was synthesized to be used as starting material in the Trofimov pyrrole synthesis toward pyrrole **11a**, as previously described (Mikhaleva et al., 1981; Trofimov et al., 2015; Klein et al., 2018). The Trofimov pyrrole synthesis represents the yield-limiting step in this synthesis sequence (Figure 3). This could be explained by the strongly basic reaction conditions, which favor side-product formations as described previously (Ivanov et al., 2014). Observed side-products were a ketoxime diether and an *N*-alkylated pyrrole, which could be removed by flash column chromatography on silica. In a subsequent hydroboration with the organoborane 9-BBN (9-Borabicyclo[3.3.1]nonane), a hydroxylated pyrrole **11b** was obtained as precursor.

Both pyrroles were tested as mutasynthons, but only pyrrole **11a** was converted in *P. putida* MBC18/pVLT33-pigC-pigB (Figure 4A). The hydroxylated group likely prevents the pyrrole **11b** from crossing the cell membrane, since PigC-mediated condensation was observed in experiments with lysate (Figure 4B). Therefore, 150 µM **11a** was applied in a preparative mutasynthesis, yielding 30 mg/L of the corresponding tripyrrole **12** which corresponds to 54% yield.

The hydroxylated prodiginine **3** was synthesized in a final semisynthetic step by hydroboration of the obtained mutasynthesis product **12**, yielding targeted compound **3** in 65% yield (Figure 4C). Notably, for the hydroboration to be successful, the mutasynthesis product had to be purified via reversed phase column chromatography in advance. Overall, a hybrid synthesis route for a

10.3389/fmicb.2023.1151882

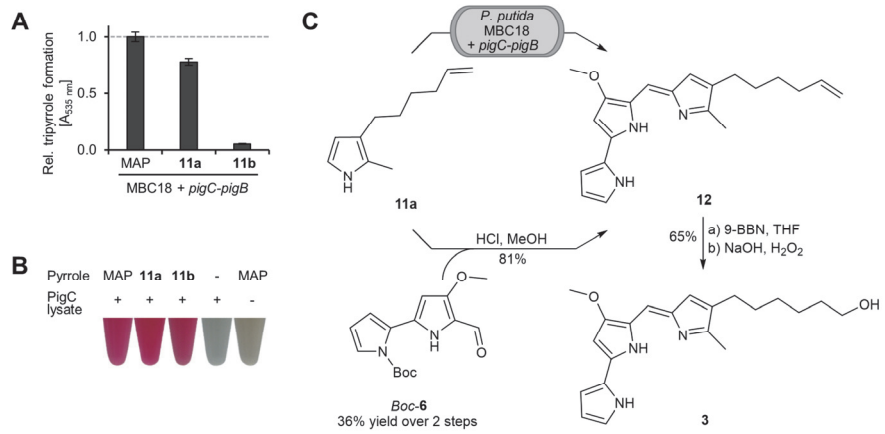

FIGURE 4
Synthetic route toward hydroxylated prodiginine 3. **(A)** Mutasynthetic tripyrrole formation upon feeding of **11a** and **11b**, respectively, in small scale cultivation of *P. putida* MBC18/pVLT33-pigC–pigB. The products were detected spectrophotometrically and quantified relative to the signal upon MAP (**5**) supplementation. Mean values of triplicate measurements with the respective standard deviation are shown. **(B)** Assessment *in vitro* of PigC substrate acceptance, shown as tripyrrole-typical coloration of reaction mixtures after incubation of lysate from PigC-expressing *E. coli* cells with MBC (**6**) and monopyrroles. **(C)** Synthesis scheme of hydroxylated prodiginine **3**. Pyrrole **11a** was supplemented to the MBC producing strain *P. putida* MBC18/pVLT33-pigC–pigB in preparative mutasynthesis to obtain the product **12**. As reference, the compound was also synthesized chemically in a condensation reaction with *Boc*-protected MBC (**6**). By the following semisynthetic hydroboration step, the final hydroxylated prodiginine **3** could be obtained.

hydroxylated prodiginine involving advantageous biosynthesis of the bipyrrole precursor **6** instead of laborious organic synthesis could be established.

2.3. Impact of prodiginines on the plant-parasitic nematode *Heterodera schachtii*

The main focus in this study was on hydroxylated prodiginine **3** for the above mentioned reasons. Additionally, the natural product prodigiosin (**1**) was used as reference in all subsequent assays. The individual effects of the hydroxylated prodiginine **3** and prodigiosin (**1**) against the PPN *H. schachtii* were determined first. To this end, the half maximal effective concentration (EC_{50}) for the reduction of nematode numbers on the model plant *Arabidopsis thaliana* was assessed. Prodiginines were found to inhibit nematode infestation by up to 80%. The EC_{50} (nematode infection) was 31.2 µM for hydroxylated prodiginine **3** and 15.1 µM for prodigiosin (**1**) (Figure 5). Although the synthesis of the previously presented prodiginine **2** is relatively laborious it appeared still interesting to validate its impact on *H. schachtii*. Prodiginine **2** and an alternative prodiginine with a side chain one carbon longer than prodiginine **3** (compound **13**, see Supplementary Information) did not exhibit stronger effects compared to prodiginine **3** (see Supplementary Figure S6) thus justifying our focus on hydroxylated prodiginine **3**.

A next aim was to pinpoint the nematode's life stage(s) and the time during host-pathogen interaction when the effect of prodiginines on the nematode becomes obvious. Therefore a time-resolved analysis of the nematodes' reaction to application of prodigiosin (**1**) and the hydroxylated prodiginine **3** was performed. To this end, fitness parameters of second-stage juveniles of *H. schachtii* (J2), nematode infection of *A. thaliana* and nematode development at the plant were investigated. These parameters were evaluated at different time points during exposure of the parasite to the above determined EC_{50} (nematode infection).

The motility of *H. schachtii* J2, which were exposed to prodigiosin (**1**) and the hydroxylated prodiginine **3** at their EC_{50} concentrations for 1 h, was significantly reduced by 32 and 39%, respectively, compared to the control (Figure 6A). An investigation of *H. schachtii* J2 stylet movement revealed a significant reduction in the frequency of thrusting at *A. thaliana* roots by 19 and 16% upon prodigiosin (**1**) and hydroxylated prodiginine **3** application, respectively (Figure 6B). This could be the reason that the number of nematodes that successfully penetrated the root epidermis (Figure 6C) and established a sedentary interaction with the plant was significantly reduced by prodiginines by 28 to 41% compared to the control (Figure 6D). Finally, the growth of *H. schachtii* females and males developing from J2 that successfully infected the plant despite prodiginine exposure was slightly reduced but not significantly impaired by prodiginines (Figure 6E).

The presented data provides for the first time specific hints to the mode of action of prodiginines and substantiates that prodiginines exert a direct antagonistic effect on *H. schachtii*. In contrast, the antinematodal effect of rhamnolipids has recently been shown to be indirect, i.e., triggering plant defense mechanisms (Bredenbruch et al., 2023). Based on these findings,

10.3389/fmicb.2023.1151882

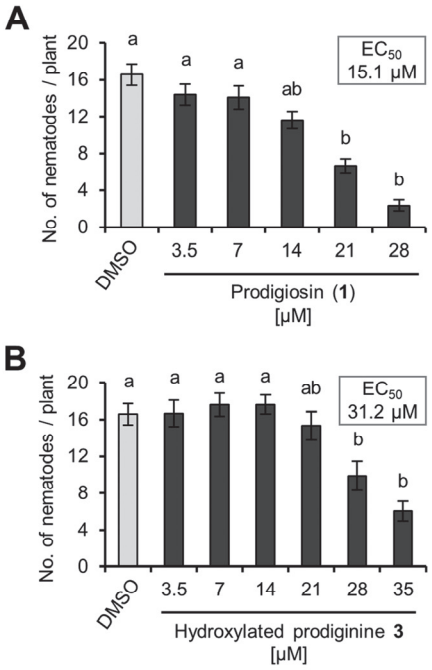

FIGURE 5
EC_{50} determination of prodiginines on the plant-parasitic nematode *Heterodera schachtii*. **(A)** Impact of prodigiosin (**1**) on nematodal plant infestation. **(B)** Impact of hydroxylated prodiginine **3** on nematodal plant infestation. The impact on *H. schachtii* was assessed as reduction of nematode numbers on *Arabidopsis thaliana*. EC_{50} values (effective concentration that causes a reduction of nematode infestation of *A. thaliana* by 50%) were calculated by using 'CompuSyn'. Results are expressed as the mean±standard error of three independent biological replicates ($n \geq 18$). Different letters indicate statistically significant differences among treatments according to Dunn's Method ($p<0.05$).

it is intriguing to assess the combined effects of prodiginines and rhamnolipids as a synergistic activity against nematodes may be hypothesized. For these investigations the previously evaluated and described mixture of di-rhamnolipid congeners (Bredenbruch et al., 2023) was chosen, which revealed an EC_{50} (nematode infection) of 2.8 µg/mL (corresponding to approximately ~ 4.3 µM; Supplementary Figure S7).

Investigations of the combined activities of prodiginines (**1** and **3**) and di-rhamnolipids (**4**) revealed that the combination of the two compounds was more effective against nematode parasitism than the individual compounds, i.e., the combined application reduced the required concentrations for the same effect (Figures 6F,G). To obtain, for instance, 50% nematode control, it was sufficient to apply ¼ the concentration of hydroxylated prodiginine **3** and di-rhamnolipids (**4**) together or prodigiosin (**1**) and di-rhamnolipids (**4**) together instead of the full dose of each compound individually (see Supplementary Figure S8 for dose response curves and combination index plots).

3. Discussion

3.1. Development of hybrid synthesis toward tailored hydroxylated prodiginine

The concept of mutasynthesis is highly attractive for synthetic chemists as a method for structural diversification of natural products by using genetically engineered microorganisms (Kirschning et al., 2007). By using nature's enzymatic biosynthetic machinery for the synthesis of precursor MBC (**6**) this study presents an environmentally friendly way by avoiding heavy metal catalyzed synthesis of *Boc*-**6** (Dairi et al., 2006; Domröse et al., 2015). Furthermore, this approach allows the incorporation of non-native building blocks into new derivatives due to enzyme promiscuity (Sun et al., 2015).

While in our previous studies, prodigiosin (**1**) biosynthesis resulted in titers, e.g., ranging from 60 to 150 mg/L (Domröse et al., 2015, 2017, 2019) depending on the applied conditions, mutasynthetic derivatives were only obtained with 0.6–3.1 mg/L (Klein et al., 2018) or maximally 19.8 mg/L (Klein et al., 2017). In general, this may reflect poor substrate entry into the cells, a low activity of PigC toward unnatural substrates, an insufficient MBC (**6**) supply, or a combination of these factors. In the present study, the MBC (**6**) supply was addressed by implementing expression of MBC (**6**) biosynthetic genes, which successfully led to reaching enhanced titers of 30–34 mg/L. Further improvements are conceivable with alternative ligase enzymes. The new strain setup of *P. putida* MBC18 allows their exchange more easily by use of alternative plasmids, whereas strain *P. putida* pig-r2 Δ*pigD* carried all *pig* genes in the chromosome. In this context, our studies uncovered, that coexpression of *pigB* is essential in this setup. It might be speculated that the enzymes PigN/F and PigB, that naturally deliver the pyrrole precursors, as well as PigC assemble to form a membrane-associated complex (Williamson et al., 2005; Chawrai et al., 2012; Couturier et al., 2019). This may hypothetically ensure fast product release via the membrane. Our findings suggest that an only partial assembly of this putative complex consisting of PigC and PigN/F, but devoid of PigB is not functional. Notably in this context, *Janthinobacterium lividum* appears to contain a *pigCB* fusion in its *pig* gene cluster (Schloss et al., 2010). However, further studies are required to elucidate these interactions.

Previous studies investigated the versatile substrate range of the condensing enzyme PigC (Klein et al., 2017, 2018; Brass et al., 2019). According to these findings, the present study focused on a mutasynthesis approach toward tailored hydroxylated prodiginines by feeding modified pyrroles to the new strain *P. putida* MBC18. In advance, the mutasynthesis experiment was optimized concerning the yields (Figure 2F). Notably, feeding a high amount of MAP (**5**) did not lead to a likewise high amount of prodigiosin (**1**) and thus resulted in relatively low yields up to 17%. Interestingly, by varying the MAP (**5**) concentration in a range of 100–1,000 µM, the prodigiosin (**1**) concentrations obtained (93–167 µM) were relatively constant and did not reflect the magnitude of the fed pyrrole concentration (Figure 2F). This observation could be explained by a substrate inhibition of involved enzymes. A PigC substrate inhibition by MAP (**5**) has been demonstrated in a previous study: conversion assays using different concentrations of MAP (**5**) at a fixed MBC (**6**) concentration suggested an ordered kinetic mechanism in which MBC (**6**) has to bind before MAP (**5**) (Chawrai et al., 2012). In the present study, 62% prodigiosin (**1**), obtained with an adjusted MAP (**5**) concentration, is the highest

10.3389/fmicb.2023.1151882

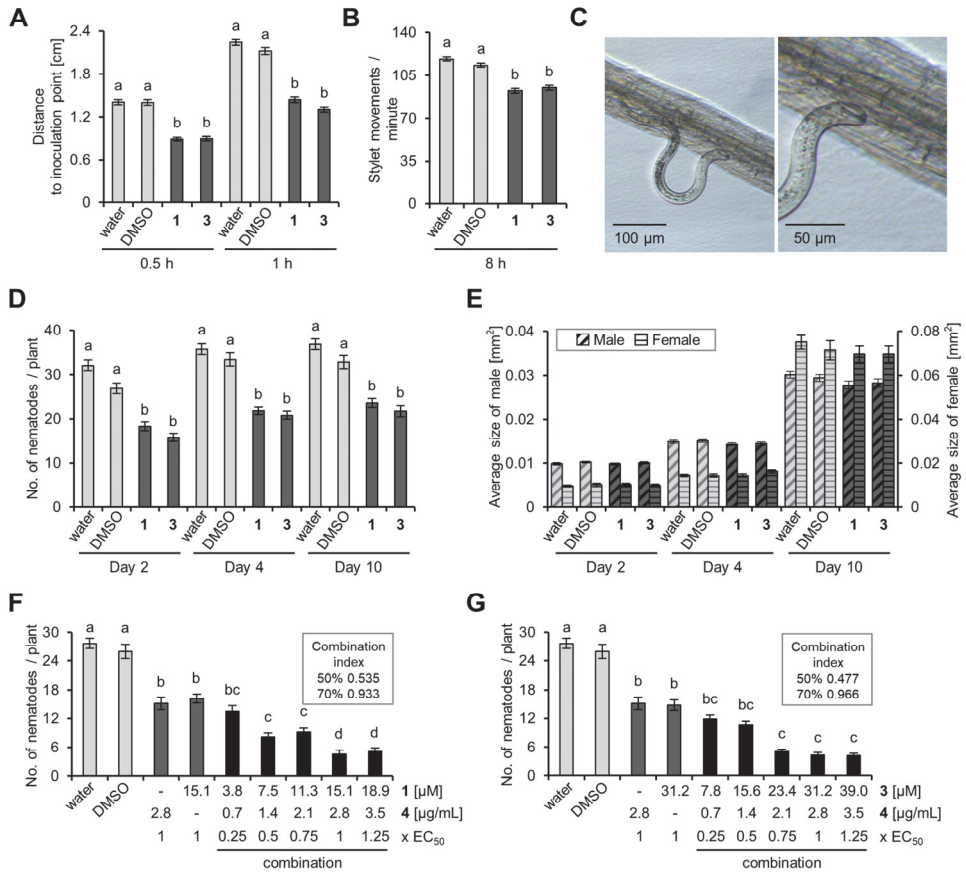

FIGURE 6
Prodiginine impact on *Heterodera schachtii* fitness parameters, plant parasitism, and combined activity with di-rhamnolipids. **(A)** *H. schachtii* J2 motility, assessed as distance to an inoculation point after incubation. **(B)** Stylet thrusting at *Arabidopsis thaliana* roots, assessed as movements/min. **(C)** *A. thaliana* root with an invading J2. **(D)** Nematode infection rate at *A. thaliana*, investigated at different time points after inoculation. **(E)** Nematode size development, evaluated during 10days after inoculation. **(F,G)** The combined effect of prodigiosin (**1**) and di-rhamnolipids (**4**) as well as hydroxylated prodiginine **3** and di-rhamnolipids (**4**), respectively, was assessed at 10days after inoculation. Combination indices were calculated using 'CompuSyn'. Results are expressed as the mean±standard error of at least three biological replicates [n≥614 **(A)**; *n*=40 **(B)**; *n*=56 (D); *n*≥70 **(E)**; *n*≥20 **(F)**; *n*≥22 **(G)**]. Different letters indicate statistically significant differences among treatments according to Dunn's Method ($p<0.05$). EC_{50} is the effective concentration that causes a reduction of nematode infestation of *A. thaliana* by 50%. Prodigiosin (**1**) and hydroxylated prodiginine **3** were used at their EC_{50} concentration in **A**, **B**, **D**.

yield achieved in a preparative scale. However, further investigation and optimization of the mutasynthesis approach may lead to even higher yields, for example by feeding the pyrrole over a period of time to overcome PigC substrate inhibition.

As mentioned above, a strength of mutasynthesis is the substrate promiscuity of the enzymes used. Results of an *in vitro* PigC assay showed acceptance for both pyrroles **11a** and **11b** (Figure 4B). However, using **11b** as mutasynthon in an *in vivo* approach did not result in formation of the targeted hydroxylated prodiginine **3**, rendering an alternative approach necessary. We assume that the hydroxyl group prevents the pyrrole **11b** from crossing the cell membrane. To overcome this issue, pyrrole **11a** was supplemented as mutasynthon to produce prodiginine **12** in a yield of 54%. The hydroxyl group was introduced in a semisynthetic step toward the targeted prodiginine **3**. Notably, the mutasynthesis product **12** had to be purified via reversed-phase column chromatography for the final hydroboration step to succeed. Alternative purification methods, such as aqueous washing steps (sat. NH_4Cl, sat. $NaHCO_3$, sat. Na_2SO_4, sat. NaCl or sat. LiCl) or normal phase column chromatography (silica or alox) led to an apparently inactivated prodiginine, which did not show any conversion to the hydroxylated prodiginine **3**, not even under high excess of the hydroboration agent 9-BBN. Quantitative ^{1}H-NMR spectroscopy showed, that the purity of the mutasynthesis product, which was isolated by normal phase column chromatography

10.3389/fmicb.2023.1151882

increased from 60 ± 3% to 92 ± 5% after an additional reversed-phase column chromatography. This finding was crucial for the success of the hybrid synthesis toward hydroxylated prodiginine **3**, even if the impurities that led to an inactivation of isolated mutasynthesis products could not be identified and further investigations are necessary.

3.2. Prodiginine-induced reduction of the fitness and infectiousness of the plant-parasitic nematode *Heterodera schachtii*

Since PPN mostly inhabit the soil and primarily attack below-surface parts of plants, it is often challenging to control PPN. Microscopic life in the rhizosphere is particularly robust and naturally occurring microbial compounds have been studied and commercialized as potent bioactive ingredients against a diversity of soil-borne pathogens over the past decades (Handelsman and Stabb, 1996; Haas and Défago, 2005; Köhl et al., 2019). Our previous work revealed that prodiginines and rhamnolipids possess activity against the PPN *H. schachtii* (Habash et al., 2020; Bredenbruch et al., 2023). Rhamnolipids exert their activity by triggering plant defense responses effective against nematodes. Unlike that, this current study demonstrated that prodigiosin (**1**) and hydroxylated prodiginine **3** directly antagonize *H. schachtii* J2 by inhibiting motility and stylet thrusting (Figures 6A,B). The J2 is the infective larval stage of *H. schachtii*, which migrates within the soil towards the root. In the natural habitat, *H. schachtii* J2 migrate at the maximum speed when there is no lateral movement and each body part usually follows the movement of its front part (Wallace, 1958). The presence of the investigated prodiginines appears to hinder nematode forward movement.

Stylet thrusting of *H. schachtii* J2 is a prerequisite for destructively invading the host's root tissue and later—after reaching the vascular cylinder—carefully probing plant cells until a suitable cell is found, which becomes the initial syncytial cell (ISC). The frequency of this stylet movement is significantly reduced by prodiginines, as demonstrated in this study. The continuous vigorous stylet thrusting of J2 is an energy consuming process (Wyss and Zunke, 1986; Grundler et al., 1991; Wyss, 1992; Wyss and Grundler, 1992). Since it has been described that prodiginines can uncouple mitochondrial F-ATPases due to their H^+/Cl-symport activity (Konno et al., 1998), their direct effect on the cellular energy metabolism might be one explanation for the lower frequency of J2 stylet movements.

Once *H. schachtii* J2 accomplish the formation of permanent feeding sites, they become immobile and change from a migratory into a sedentary form (Wyss, 1992). Prodiginines were observed to interfere with nematode invasion and infection of *A. thaliana*. However, female and male development at the host plant is not influenced by prodiginines at 2 and 4 days after the inoculation, while it is slightly impaired after 10 days (Figures 6D,E). As stated in our previous study, a significant reduction of female size due to prodigiosin application can be observed after 13 days (Habash et al., 2020). Probably, the impact of prodiginines on the pathogen's development at the root becomes obvious only at later time points after infection. Future studies should investigate this aspect further and additionally determine whether prodiginine exposure interferes with reproduction.

While investigations on the molecular mode of action for the interaction of prodiginines with nematodes are missing, studies of their effects on bacteria document a disturbing impact on biological membranes and reactive oxygen species (ROS) generation (Darshan and Manonmani, 2015, 2016; Suryawanshi et al., 2017; Ravindran et al., 2020; Choi et al., 2021). Whether prodiginines cause disruption of PPN membranes and whether this contributes to the observed effects still needs to be elucidated.

Unlike "single compound - single target" approaches, multicomponent therapeutics enable interactions with multiple targets (Keith et al., 2005; Hopkins, 2007; Yildirim et al., 2007). The discovery of drug–drug combinations offers promising strategies for (1) the improvement of drug treatment efficacy, (2) the reduction of drug dosage to avoid toxicity, and (3) the minimization of drug resistance evolution (Jia et al., 2009; Cheng et al., 2019). Our results demonstrate that, when applying prodiginines and di-rhamnolipids combined, only ¼ of the concentration rather than the full dose of each single agent is required to achieve the same nematode control efficacy (50% reduction of nematode infestation; Figures 6F,G). This validates the two compounds to exert synergistic effects. Intriguingly, by increasing the doses for combinations, the combined effect is diminished and even appears antagonistic. Similar results were reported previously in the analyses of antibacterial effects, which were dependent on the ratio of prodigiosin and rhamnolipids (Hage-Hülsmann et al., 2018).

Synergistic effects between biosurfactants including rhamnolipids and various antibiotics have been described multiple times before (Boonlarppradab et al., 2008; Williamson et al., 2008; Sotirova et al., 2012; Magalhães and Nitschke, 2013; Das et al., 2014; Rossi et al., 2016). On the one hand, rhamnolipids, which exhibit surface-active properties, can increase the solubility of the drug and facilitate its access to target cells (Beal and Betts, 2000; Abdel-Mawgoud et al., 2010). On the other hand, rhamnolipids can perturb the packing of the cell membrane phospholipids by intercalating into the bilayer, which leads to increased permeability of the cell membrane (Dowhan, 1997; Ortiz et al., 2006). As a consequence, the interaction of combined applications facilitates more effective penetration through biological interfaces to better reach the site of action (Bhadoriya et al., 2013; Bnyan et al., 2018; Hage-Hülsmann et al., 2018).

However, the role of rhamnolipids in combined antinematodal activity goes far beyond that. Plants have developed sophisticated defense mechanisms that enhance resistance to their enemies. After perception of rhamnolipids, early events of cell signaling, including calcium influx, MAP kinase activation, ROS accumulation, and defense-related gene stimulation were detected in plants (Garcia-Brugger et al., 2006; Varnier et al., 2009). Besides, rhamnolipids also trigger the activation of a phytohormone-regulated immune signaling network and thus modulate late defense responses to a diversity of phytopathogens (Pieterse et al., 2012; Sanchez et al., 2012). A recent study confirmed that di-rhamnolipids put *A. thaliana* on alert so that the plant responds stronger to *H. schachtii* attack (Bredenbruch et al., 2023). The combined application of rhamnolipids and prodiginines may therefore effectuate molecular structures and processes on multiple levels in both, the plant and the pathogen, and may pose a promising starting point for the development of multicomponent antinematodal agents.

4. Materials and methods

4.1. Engineering and characterization of *Pseudomonas putida* strains, PigC activity assay

4.1.1. Bacterial strains and standard cultivation conditions

Cultivation of *P. putida* KT2440 (Nelson et al., 2002; Belda et al., 2016) was conducted at 30°C, if not stated otherwise, shaking (130 rpm) in Erlenmeyer shake flasks in LB medium (Carl Roth, Karlsruhe, Germany), or on LB agar plates (LB medium completed with 15 g/L Agar). Small scale production tests were conducted in TB medium (Carl Roth, Karlsruhe, Germany) in Flowerplates (m2p-labs GmbH, Baesweiler, Germany). Cultures of *P. putida* pig-r2 Δ*pigD* (Klein et al., 2017) were supplemented with 80 µg/mL streptomycin, MBC strains created in the present study with 50 µg/mL tetracycline, and MBC strains carrying pVLT33 derived plasmids with 25 µg/mL kanamycin. *Escherichia coli* strains S17-1 (Simon et al., 1983; used for conjugation), and DH5α (Hanahan, 1983; used for cloning) were cultivated at 37°C under constant agitation (120 rpm) in shake flasks in liquid LB medium or on LB agar plates.

4.1.2. Cloning of integrative yTREX vector with MBC biosynthetic genes and ligase expression plasmids

The synthetic MBC biosynthesis-encoding *pig* gene cluster was PCR-amplified in three parts for assembly into the yTREX vector (Domröse et al., 2017; Weihmann et al., 2020) which was linearized with endonuclease I-*Sce*I: *pigA* (primers AD142 + 171, 1,239 bp), *pigFGHI* (primers AD172 + 162, 4,867 bp) and *pigJKLMN* (primers AD163 + 164, 5,033 bp) using vector pPIG (Loeschcke et al., 2013) as template. In addition, *lacZ* was amplified as promotorless gene (primers AD124 + 125, 3,127 bp) using vector pRcExpII2-YF1-FixJ-PFixK2-LacZ (Weihmann et al., 2020) as template. All genes were amplified with the respective 5′-UTR sequences including the ribosome binding sites; primers added homology arms to each of the fragments. Assembly of the vector yTREX-MBC-lacZ, carrying the gene cassette *pigA-pigFGHIJKLMN-lacZ*, in *Saccharomyces cerevisiae* VL6-48 was conducted as previously described (Domröse et al., 2017; Weihmann et al., 2020). Plasmid pVLT33-pigC, carrying the *pigC* gene with an adapted codon usage for *P. putida* (Brands et al., 2020), was used for PigC expression. The *pigB* gene was amplified (primers RW144 + 145, 2090 bp) using yTREX-pig (Domröse et al., 2017) as template. The vector and PCR product were hydrolyzed with endonucleases *Hind*III und *Xba*I and ligated to obtain pVLT33-pigC-pigB. All plasmids and oligonucleotides are listed in Supplementary Table S1.

4.1.3. Generation of MBC producing *Pseudomonas putida* strains

To generate *P. putida* production strains, the plasmid yTREX-MBC-lacZ was transformed into *E. coli* S17-1 and further transferred to *P. putida* KT2440 via conjugation as previously described (Weihmann et al., 2020). Since yTREX constructs do not replicate in *P. putida*, positive selection for strains in which Tn5 transposition of the recombinant yTREX transposon occurred, could be conducted by using LB medium supplemented with tetracycline. In addition, 25 µg/mL irgasan was added to prevent *E. coli* growth. Among exconjugants, production strains were identified visually after 16 h of cultivation on agar plates (Weihmann et al., 2020): The selection medium after conjugation was additionally supplemented with 0.3 mM X-gal (stock solution: 50 mM in DMF), and expression strains were identified by blue color due to β-galactosidase activity.

4.1.4. Analysis of MBC biosynthesis in *Pseudomonas putida*

For verification of MBC biosynthesis in small scale cultivation, expression cultures of *P. putida* pig-r2 Δ*pigD* and MBC strains (denoted with 2, 4, 5, 6, 7, 8, 9, 10, 11, 12, 13, 15, 16, 17, 18, 20, 21 or 22) (n = 4, independent biological replicates) were cultivated in Flowerplates. To this end, 1 mL precultures in LB medium were used for inoculation of 1,1 mL main cultures in TB medium to an OD (650 nm) of 0.05. Flowerplates were covered with breathable air sheets (139.7 µm sterile Rayon films, VWR North America Cat.No. 60941-086) and incubated for 24 h (30°C, 1,400 rpm). After that, 700 µL samples were used for cell harvesting (15,000 rpm, 5 min). The pellet was resuspended in 300 µL methanol and subjected to sonication in a water bath (Sonorex RH 100 H) for 10 min. After centrifugation (15,000 rpm, 5 min), the supernatant was dried at 45°C under reduced pressure (in a Concentrator 5,301). For 2-phase extraction, 300 µL DCM und 300 µL MilliQ-water were added and mixed well, before centrifugation (15,000 rpm, 3 min). The organic lower layer was transferred in a fresh reaction tube and the extraction repeated. The resulting pooled DCM was again dried (45°C, Eppendorf Concentrator 5,301). Samples were resuspended in 200 µL methanol, centrifuged (15,000 rpm, 1 min) and finally subjected to LC–MS analysis or stored until that at 4°C. LC–MS analysis was conducted using an HP 1100 Series LC/MSD (Agilent Analytical Instruments) with an Atlantis T3 column (3 µm, 3*100 mm) from Waters. The eluents water (A) and methanol (B), both supplemented with 0.1% formic acid, were used for gradient chromatography at 0.6 mL/min flow rate: Starting at 90% A and 10% B, increasing to 60% B in 4 min, then in further 2 min to 100% B, which was maintained for 4 min. After that, starting conditions were implemented again (10% B) and held for 1 min. Sample volumes of 10 were injected and detection was accomplished with a G1315A DAD-detector and an G1946A mass spectrometer (API-ES, positive ion mode, single quadrupole detector, m/z-range 100–2000). After verification of specific signals corresponding to the ion $[M+H]^+$ of MBC (191 m/z), the UV/Vis signal (364 nm) of the corresponding peaks detected at 6.7 min were evaluated for relative quantification with reference to the values obtained with strain *P. putida* pig-r2 Δ*pigD*. For subsequent routine MBC analysis, HPLC-PDA analysis using an LC-10Ai (Shimadzu Deutschland GmbH, Duisburg, Germany) was also applied with an SPDM10Avp photodiode array detector (PDA), and an Accucore™ C18 HPLC column (2.6 µm, 4.6*50 mm) from Thermo Fisher Scientific (Walkham, United States). At a column oven temperature of 30°C, 10 µL samples were analyzed at 1 mL/min flow rate in a gradient elution using water (A) and acetonitrile (B), both with 0.1% formic acid: Starting at 95%A and 5% B for 0.5 min, increasing to 25% B at 0.9 min, to 55% at 9.5 min, and to 98% at 10 min, which was held for 1 min, before returning to 5% B at 11.5 min, which was maintained for 2 min. Chromatograms were recorded at 360 nm and detected MBC at 4.5 min (λ_{max} 363 nm). To analyze MBC in 100 mL cultures, 1 g polyurethane (PU) foam

cubes were added as described for mutasynthesis conditions, and extracted with 15 mL ethanol.

4.1.5. Quantification of *pig* gene transcript by RT-qPCR

Reverse transcription (RT) followed by quantitative PCR (qPCR) was employed to quantify mRNA levels of *pigN*. Precultures, grown in LB medium, were used to inoculate 1 mL TB main cultures of *P. putida* pig-r2 Δ*pigD* and MBC18 with pVLT33-pigC-pigB to an OD (650 nm) of 0.05 ($n = 3$, independent biological replicates). These were incubated shaking (1,200 rpm) at 30°C for 4 h, before induction of the latter with 0.5 mM IPTG (10 µL of a 50 mM stock solution in water). After additional 4 h incubation, 500 µL of each culture were harvested to extract total RNA with the NucleoSpin® RNA-Kit (Macherey-Nagel, Düren, Germany). DNAse treatment was conducted in three steps with DNase from Macherey-Nagel, Qiagen (Hilden, Germany) and Ambion (Thermo Fisher Scientific). The Maxima Reverse Transcriptase (Thermo Fisher Scientific) was used for reverse transcription of 2000 ng RNA in 20 µL volumes. The qPCR reaction mix contained 9.2 µL of the cDNA solution (diluted to correspond to 50 ng RNA), 0.4 µL containing 4 pmol of each primer (stocks: 10 pmol/µL), and 10 µL Maxima SYBR Green/ROX qPCR Master Mix (2x; Thermo Fisher Scientific). All qPCR reactions were carried out as technical quadruplicates in addition to the biological triplicates. Controls without reverse transcriptase and without template as well as monitoring of PCR product melting curves ensured signal specificity. Calibration with the pPIG plasmid allowed determination of *pigN* copy numbers in *P. putida* pig-r2 Δ*pigD* and MBC18, which were 177×10^4 ($\pm 4 \times 10^4$) and 683×10^4 ($\pm 12 \times 10^4$) per 100 ng total RNA, respectively. For direct comparison, the data was evaluated as expression levels relative to the signal of *P. putida* pig-r2 Δ*pigD*. To corroborate comparability, the transcript levels of *rpoD* were analyzed as internal control, which yielded similar results in both strains as expected [571×10^4 ($\pm 16 \times 10^4$) and 750×10^4 ($\pm 30 \times 10^4$) per 100 ng total RNA].

4.1.6. Mutasynthesis in small scale cultivation

Expression cultures of *P. putida* pig-r2 Δ*pigD* and strains MBC13, −17, −18 with plasmids pVLT33-pigC or pVLT33-pigC-pigB ($n = 3$, independent biological replicates) were cultivated in Flowerplates. Precultures in 1 mL LB medium were used for inoculation of 1 mL main cultures in TB medium to an OD (650 nm) of 0.05. Flowerplates were covered with breathable air sheets and incubated for 4 h (30°C, 1,200 rpm), before 1 mM MAP was supplemented to the cultures (20 µL of a 50 mM stock solution in DMSO) and gene expression in strains with plasmids was induced by addition of 0.5 mM IPTG (10 µL of a 50 mM stock solution in water). Cultivation was subsequently continued for 20 h at 30°C or 25°C. After that, cultures were harvested (12,000 rpm, 2 min). The pellets were pre-resolved with 20 µL milliQ-water and extracted with 500 µL acidified ethanol [4% (*v*/*v*) 1 N HCl in ethanol]. After centrifugation (2 min, 14,000 rpm), 150 µL samples were either diluted by a factor of 10 or directly subjected to spectrophotometric analysis in a microplate reader "Infinite M1000 pro" (Tecan Group LTD., Maennedorf, Switzerland) to measure characteristic absorption spectra from 400 to 700 nm. Plotting the absorption at 535 nm facilitated comparative evaluation. For quantification of prodigiosin formation via the previously published molar extinction coefficient (Domröse et al., 2015), the signal of the Tecan plate reader was calibrated with solutions of known concentration based on ε (535 nm) [M^{-1} cm^{-1}] = 139,800 (Domröse et al., 2015). Prodigiosin titers (expressed in mg/L) were determined by considering the molecular weight of the compound (323.432 g/mol) and the extracted culture volume.

4.1.7. PigC substrate acceptance assay

The *in vitro* assay with cell lysate of *E. coli* BL21 (DE3) pET28a(+)-*pigC* was performed as described previously (Klein et al., 2017; Brass et al., 2019). Accordingly, the heterologous expression of PigC was carried out using *E. coli* BL21 (DE3) pET28a(+)-*pigC* cells, which were stored at −20°C after cultivation and harvesting. Frozen cells (1 g) were thawed and resuspended in potassium phosphate buffer (KP_i buffer, 50 mM, pH 7.0; 5 mL). The cell suspension was disrupted using a SONOPULS Ultrasonic homogenizer (Bandelin, Berlin, Germany) for 2 × 5 min (five cycles, 40% power), to obtain lysed cells which were used for the PigC substrate acceptance assay. The assay solution contained 440 µL of cell lysate in KP_i buffer (50 mM, pH 7.0), 25 µL of a pyrrole **5**, **11a**, **11b** solution in DMSO (20 mM, end concentration: 1 mM), 25 µL of an MBC (**6**) solution in DMSO (20 mM, end concentration: 1 mM) and 10 µL of an ATP•Na_2 solution in water (62.5 mM, end concentration: 1.25 mM). The reaction mixture was shaken in a 1.5 mL tube at 300 rpm and 30°C for 4 h. The supernatant was removed after centrifugation (5 min, 21,100 rcf, 23°C) and the prodiginine pellet was resuspended in 300 µL acidic ethanol [4% (*v*/*v*) 1 N HCl in ethanol]. After centrifugation (5 min, 21,100 rcf, 23°C), the supernatant was transferred in a new 1.5 mL reaction tube and documented photographically.

4.2. Chemical precursor syntheses

4.2.1. General experimental procedures for chemical syntheses

All reactions were carried out under nitrogen atmosphere and magnetic stirring. Used glassware and magnetic stirring bars were dried previously at 110°C. All starting materials were purchased from commercial sources without further purification unless stated otherwise. Dichloromethane, diethyl ether, ethyl acetate (EtOAc) and petroleum ether (PE) were distilled prior to use. Tetrahydrofuran (THF) was used directly. Reactions were monitored by GC–MS, ^{1}H-NMR and thin layer chromatography (TLC; Polygram SIL G/UV254, Macherey-Nagel) using an acidic solution of *p*-anisaldehyde for staining or UV light at 245 nm for visualization. Purification of reaction products was carried out by flash chromatography on silica gel 60 (particle size 0.040–0.063 mm, 230–240 mesh, Macherey-Nagel). Analytics were carried out as described in the Supplementary Information, including Supplementary Tables S2, S3, and Supplementary Figure S5. The precursors 2-methyl-3-*N*-amylpyrrole (MAP, **5**), *tert*-butyloxycarbonyl-5′-formyl-4′-methoxy-1*H*,1′*H*-2,2′-bipyrrole (*boc*-MBC, *Boc*-**6**) and prodigiosin (**1**) as chemical references were synthesized as previously described (Dairi et al., 2006; Domröse et al., 2015).

4.2.2. *N*-methoxy-*N*-methyloct-7-enamide (**8**)

To a solution of 7-octenoic acid (2 mL, 13.0 mmol, 1.0 eq.) in dichloromethane (70 mL) was added *N*,O-dimethylhydroxylamine hydrochloride (1.19 g, 19.5 mmol, 1.50 eq.),

N-(3-dimethylaminopropyl)-*N*′ethylcarbodiimid hydrochloride (3.03 g, 19.5 mmol, 1.5 eq.) and 4-(dimethylamino)pyridine (2.38 g, 19.5 mmol, 1.5 eq.). After stirring for 22 h at 22°C, the reaction mixture was quenched with a saturated solution of NaCl and extracted with dichloromethane (3 × 50 mL). The combined organic layers were first washed with 1 N HCl, afterwards with saturated $NaHCO_3$ solution and dried over $MgSO_4$. After removal of the solvent under reduced pressure *N*-methoxy-*N*-methyloct-7-enamide (**8**, 2.29 g, 12.4 mmol, 95%) was obtained as a yellow oil and was used for the following experiment without further purification. R_f = 0.15 (PE/EtOAc 85:15); **^{1}H-NMR** (600 MHz, $CDCl_3$): δ [ppm] = 1.36 (m_c, 2H, 4-H), 1.41 (m_c, 2H, 5-H), 1.64 (m_c, 2H, 3-H), 2.05 (m_c, 2H, 6-H), 2.41 (t, $^3J_{2,3}$ = 7.7 Hz, 2H, 2-H), 3.18 (s, 3H, 1″-H), 3.68 (s, 3H, 1′-H), 4.93 (dd, $^{cis,3}J_{8a,7}$ = 10.2 Hz, $^2J_{8a,8b}$ = 1.2 Hz, 1H, 8-H_a), 4.99 (ddd, $^{trans,3}J_{8b,7}$ = 17.1 Hz, $^2J_{8b,8a}$ = 1.8 Hz, $^4J_{8b,6}$ = 1.8 Hz, 1H, 8-H_b), 5.80 (ddt, $^{trans,3}J_{7,8b}$ = 17.0 Hz, $^{cis,3}J_{7,8a}$ = 10.2 Hz, $^3J_{7,6}$ = 6.7 Hz, 1H, 7-H); **^{13}C-NMR** (151 MHz, $CDCl_3$): δ [ppm] = 24.6 (C-3), 28.8 (C-4), 29.1 (C-5), 32.0 (C-2), 32.3 (C-1″) 33.8 (C-6) 61.3 (C-1′), 114.5 (C-8), 139.1 (C-7); **IR** (ATR-film): $\tilde{\nu}$ [1/cm] = 3,074, 2,931, 2,855, 1,667, 1,463, 1,415, 1,384, 1,178, 998, 910, 732; **MS** (APCI, positive ion): *m*/*z* = 186 [(M)$^+$], 97, 83, 55.

4.2.3. Non-8-en-2-one (9)

N-methoxy-*N*-methyloct-7-enamide (**8**, 2.29 g, 12.4 mmol, 1.0 eq.) was dissolved in dry THF (100 mL) and methylmagnesium chloride (3 M in diethyl ether, 12.4 mL, 37.1 mmol, 3.0 eq.) was added within 15 min at 0°C. The reaction mixture was stirred for 1.5 h at 0°C and afterwards quenched by the addition of a saturated solution of NH_4Cl at 0°C and extracted with dichloromethane (3 × 60 mL). The combined organic layers were dried over $MgSO_4$ and the solvent was evaporated under reduced pressure to yield non-8-en-2-one (**9**, 1.63 g, 11.6 mmol, 94%) as a yellowish oil without further purification. R_f = 0.40 (PE/EtOAc 85:15); **^{1}H-NMR** (600 MHz, $CDCl_3$): δ [ppm] = 1.25–1.34 (m, 2H, 5-H), 1.35–1.43 (m, 2H, 6-H), 1.58 (tt, $^3J_{4,3}$ = 7.5 Hz, $^3J_{4,5}$ = 7.5 Hz, 2H, 4-H), 2.05 (m, 2H, 7-H), 2.13 (s, 3H, 1-H), 2.42 (t, $^3J_{3,4}$ = 7.5 Hz, 2H, 3-H), 4.93 (ddt, $^{cis,3}J_{9a,8}$ = 10.2 Hz, $^4J_{9a,7}$ = 2.3 Hz, $^2J_{9a,9b}$ = 1.2 Hz, 1H, 9-H_a), 4.99 (dd, $^{trans,3}J_{9b,8}$ = 17.1 Hz, $^2J_{9b,9a}$ = 1.7 Hz, 1H, 9-H_b), 5.79 (ddt, $^{trans,3}J_{8,9b}$ = 17.0 Hz, $^{cis,3}J_{8,9a}$ = 10.2 Hz, $^3J_{8,7}$ = 6.7 Hz, 1H, 8-H); **^{13}C-NMR** (151 MHz, $CDCl_3$): δ [ppm] = 23.8 (C-4), 28.7 (C-5), 28.8 (C-6), 30.0 (C-1), 33.7 (C-7), 43.9 (C-3), 114.6 (C-9), 139.0 (C-8), 209.4 (C-2); **IR** (ATR-film): $\tilde{\nu}$ [1/cm] = 2,928, 2,855, 1738, 1721, 1,443, 1,363, 1,217, 907; **MS** (APCI, positive ion): *m*/*z* = 123.

4.2.4. Dec-9-en-2-one oxime (10)

To a solution of the non-8-en-2-one (**9**, 1.73 g, 12.4 mmol, 1.0 eq.) in ethanol (6.2 mL) was added pyridine (0.78 g, 0.8 mL, 9.89 mmol, 0.8 eq.) and grounded hydroxylamine hydrochloride (1.5 eq.). The reaction mixture was refluxed for 2 h and afterwards extracted with dichloromethane (3 × 25 mL). The combined organic layers were washed with 1 N HCl (3 × 20 mL) and dried over $MgSO_4$. After removal of the solvent under reduced pressure, dec-9-en-2-one oxime (**10**, 1.76 g, 11.3 mmol, 92%) was obtained in a diastereomeric mixture of *E*:*Z* (1:3) without further purification. R_f = 0.34 (PE/EtOAc 80:20); **^{1}H-NMR** (600 MHz, $CDCl_3$): δ [ppm] = 1.28–1.36 (m, 2H, 5-H), 1.37–1.44 (m, 2H, 6-H), 1.51 (tt, $^3J_{4,3}$ = 7.5 Hz, $^3J_{4,5}$ = 7.5 Hz, 2H, 4-H), 1.87 (s, 3H, 1-H), 2.05 (dt, $^3J_{7,6}$ = 6.4 Hz, $^3J_{7,8}$ = 6.4 Hz, 2H, 7-H), 2.18 (t, $^3J_{3,4}$ = 7.5 Hz, 2H, 3-H), 4.94 (ddt, $^{cis,3}J_{9a,8}$ = 10.2 Hz, $^4J_{9a,7}$ = 2.4 Hz, $^2J_{9a,9b}$ = 1.3 Hz, 1H, 9-H_a), 5.00 (dd, $^{trans,3}J_{9b,8}$ = 17.1 Hz, $^2J_{9b,9a}$ = 1.5 Hz, 1H, 9-H_b), 5.80 (ddt, $^{trans,3}J_{8,9b}$ = 17.0 Hz, $^{cis,3}J_{8,9a}$ = 10.4 Hz, $^3J_{8,7}$ = 6.6 Hz, 1H, 8-H); **^{13}C-NMR** (151 MHz, $CDCl_3$): δ [ppm] = 13.4 (C-1), 26.2 (C-4), 28.7 (C-5), 28.8 (C-6), 33.7 (C-7), 35.8 (C-3), 114.4 (C-9), 139.1 (C-8), 159.1 (C-2); **IR** (ATR-film): $\tilde{\nu}$ [1/cm] = 3,074, 2,929, 2,855, 1,637, 1,461, 1,369, 910; **MS** (APCI, positive ion): *m*/*z* = 156 [(M)$^+$], 83; **HRMS** (ESI, positive ion): calculated for $C_9H_{18}NO$ [(M + H)]$^+$ = 156.1383, found = 156.1384.

4.2.5. 3-(hex-5-en-1-yl)-2-methyl-1*H*-pyrrole (11a)

A reaction mixture of dec-9-en-2-one oxime (**10**, 0.72 g, 4.64 mmol, 1.0 eq.), potassium hydroxide (1.30 g, 46.4 mmol, 5.0 eq.), water (62.7 mg, 62.3 µL, 3.48 mmol, 0.75 eq.) and DMSO (8.9 mL) was heated at 90–100°C (using previously degassed DMSO on molecular sieves (3.5 Å) could increase the yield). Over a period of 2 h, a solution of 1,2-dichloroethane (1.38 g, 1.10 mL, 13.9 mmol, 3.5 eq.) in DMSO (1 mL) was added dropwise. After 1 h of 1,2-dichloroethane addition a secondary amount of potassium hydroxide (5.0 eq.) was added. After an overall reaction time of 4 h at 90–100°C the reaction mixture was allowed to reach room temperature and subsequently ice water (20 mL) was added. The mixture was extracted with diethyl ether (3 × 20 mL) and the combined organic layers were dried over $MgSO_4$. After the solvent was evaporated under reduced pressure the crude product was purified by column chromatography on silica gel [PE:dichloromethane (60:40) + 1% trimethylamine (*v*/*v*)] to obtain 3-(hex-5-en-1-yl)-2-methyl-1*H*-pyrrole (**11a**, 228 mg, 1.40 mmol, 30%) as yellowish oil. R_f = 0.37 (PE/dichloromethane 60:40); **^{1}H-NMR** (600 MHz, $CDCl_3$): δ [ppm] = 1.44 (tt, $^3J_{3'',2''}$ = 7.5 Hz, $^3J_{3'',4''}$ = 7.5 Hz, 2H, 3″-H), 1.51–1.59 (m, 2H, 2″-H), 2.02–2.14 (m, 2H, 4″-H), 2.18 (s, 3H, 1′-H), 2.39 (t, $^3J_{1'',2''}$ = 7.6 Hz, 2H, 1″-H), 4.93 (dd, $^{cis,3}J_{6a'',5''}$ = 10.2 Hz, $^2J_{6a'',6b''}$ = 1.2 Hz, 1H, 6″-H_a), 5.00 (dd, $^{trans,3}J_{6b'',5''}$ = 17.1 Hz, $^2J_{6b'',6a''}$ = 1.7 Hz, 1H, 6″-H_b), 5.82 (ddt, $^{trans,3}J_{5'',6b''}$ = 16.9 Hz, $^{cis,3}J_{5'',6a''}$ = 10.2 Hz, $^3J_{5'',4''}$ = 6.7 Hz, 1H, 5″-H), 6.01 (dd, $^4J_{4,1}$ = 2.8 Hz, $^3J_{4,5}$ = 2.8 Hz, 1H, 4-H), 6.59 (dd, $^3J_{5,1}$ = 2.7 Hz, $^3J_{5,4}$ = 2.7 Hz, 1H, 5-H), 7.70 (brs, 1H, 1-NH); **^{13}C-NMR** (151 MHz, $CDCl_3$): δ [ppm] = 11.2 (C-1′), 25.9 (C-1″), 28.9 (C-3″), 31.0 (C-2″), 33.9 (C-4″), 109.0 (C-4), 114.3 (C-6″), 115.0 (C-5), 119.7 (C-3), 123.4 (C-2), 139.4 (C-5″); **IR** (ATR-film): $\tilde{\nu}$ [1/cm] = 3,385, 2,928, 2,855, 1741, 1,467, 1,363, 1,217, 907, 712; **MS** (APCI, positive ion): *m*/*z* = 164 [(M)$^+$]; 121, 108; **HRMS** (ESI, positive ion): calculated for $C_{11}H_{18}N$ [(M + H)]$^+$ = 164.1434, found = 164.1433.

4.2.6. 6-(2-methyl-1*H*-pyrrol-3-yl)hexan-1-ol (11b)

9-BBN (0.5 N in THF, 5.54 g, 3.10 mmol, 2.2 eq.) was added to a solution of 3-(hex-5-en-1-yl)-2-methyl-1*H*-pyrrole (**11a**, 230 mg, 1.41 mmol, 1.0 eq.) in dry THF (11.6 mL) over a period of 15 min at 0°C. After stirring for 1 h at 0°C, the reaction mixture was heated up at 70°C under reflux for 3 h. Subsequently an aqueous solution of 3 N NaOH (2.35 g, 2.35 mL, 7.05 mmol, 5.0 eq.) and 30% H_2O_2 (2.24 g, 2.00 mL, 19.7 mmol, 14.0 eq.) was added at 0°C. After 1 h at 0°C the reaction mixture was allowed to reach room temperature and was stirred for further 15 h at 22°C. Ice water (40 mL) was added and the mixture was extracted with dichloromethane (3 × 50 mL). The combined organic layer was dried over $MgSO_4$, the solvent was evaporated under reduced pressure and the crude product was purified by column chromatography on silica gel [PE:ethyl acetate (70:30 to 50:50) + 1% trimethylamine (*v*/*v*)] to isolate 6-(2-methyl-1*H*-pyrrol-3-yl)hexan-1-ol (**11b**, 193 mg, 1.06 mmol, 76%) as orange oil. R_f = 0.20 (PE/EtOAc 70:30); **^{1}H-NMR** (600 MHz, $CDCl_3$): δ [ppm] = 1.20 (brs, 1H, 1-OH), 1.34–1.42 (m, 4H, 3-H, 4-H), 1.51–1.61 (m, 4H, 2-H, 5-H), 2.18 (s, 3H, 1″-H), 2.39 (t, $^3J_{6,5}$ = 7.7 Hz, 2H, 6-H),

10.3389/fmicb.2023.1151882

3.64 (t, $^{3}J_{1,2}$ = 7.1 Hz, 2H, 1-H), 6.00 (dd, $^{4}J_{4',1'}$ = 2.8 Hz, $^{3}J_{4',5'}$ = 2.8 Hz, 1H, 4′-H), 6.59 (dd, $^{3}J_{5',1'}$ = 2.7 Hz, $^{3}J_{5',4'}$ = 2.7 Hz, 1H, 5′-H), 7.72 (brs, 1H, 1′-NH); **^{13}C-NMR** (151 MHz, $CDCl_3$): δ [ppm] = 11.2 (C-1″), 25.8 (C-4), 26.0 (C-6), 29.4 (C-3), 31.4 (C-5), 33.0 (C-2), 62.7 (C-1), 109.0 (C-4′), 115.0 (C-5′), 119.7 (C-3′), 123.4 (C-2′); **IR** (ATR-film): $\tilde{\nu}$ [1/cm] = 3,373, 2,928, 2,855, 1735, 1,436, 1,363, 1,223, 1,059, 748; **MS** (APCI, positive ion): *m/z* = 182 [(M)$^+$], 164, 108; **HRMS** (ESI, positive ion): calculated for $C_{11}H_{20}NO$ [(M + H)]$^+$ = 182.1539, found = 182.1539.

4.3. Muta- and semisynthetic hydroxylated prodiginine production

4.3.1. General procedure for preparative scale mutasynthesis

A preculture of *P. putida* MBC18 with pVLT33-pigC-pigB in LB medium (25 µg/mL kanamycin) was incubated in a shake flask at 30°C and 130 rpm overnight. Five main cultures of 100 mL each in TB medium (25 µg/mL kanamycin) were inoculated to an OD_{650} of 0.05 and incubated in 1l baffled flask with air-sheet seals for 4 h at 30°C and 130 rpm. The pyrrole precursor was dissolved in DMSO (5–50 mM stock, 10 mL). To each culture 2 mL of pyrrole stock solution was added (final concentration 0.1–1.0 mM). Induction was performed with 0.5 mM IPTG (50 mM stock in dH2O; 1 mL). After an additional hour at 30°C and 130 rpm, 1 g of polyurethane (PU) foam cubes (Soltpur, Göllheim, Germany: Softpur foam, 25 kgm^{-3} density, 4 kPa compression hardness, each cube approximately 1 cm^3) were added to each culture and the cultures were incubated for further 23 h at 30°C and 130 rpm. After a total of 28 h of cultivation, the foam cubes were wrung out, washed with dH_2O, and then extracted with diethyl ether (250–500 mL) in a soxhlet extractor. After evaporation of the solvent, the crude product was dissolved in diethyl ether (20 mL), washed with water, and the aqueous layer was extracted with dichloromethane (3 × 15 mL). The combined organic layers were washed with saturated NaCl (20 mL) and dried over $MgSO_4$. After evaporation of the solvent, the crude product was purified by flash column chromatography on silica gel (CH_2Cl_2 + 1.0–1.5% NH_3 in MeOH). For subsequent hydroboration, the product was further purified by reversed-phase chromatography (column: ISAspher 100–5 C18 AQ, 5 µm, 150*20 mm from ISERA GmbH, Düren, Germany; column oven: 35°C; eluent: 60:40 acetonitrile:water + 0.1% formiate; flow rate 15 mL/min; injection of samples in 1 mL ethanol) to obtain the mutasynthesis product as red solid.

4.3.2. 4-Methoxy-5-[(5-methyl-4-hex-5-en-1-yl-2*H*-pyrrol-2-yliden)methyl]-1*H*,1′*H*-2,2′-bipyrrol (3)

According to the general procedure for preparative mutasynthesis and the use of pyrrole **11a** (12.2 mg, 75.0 µmol, 7.5 mM in DMSO, end concentration in 500 mL culture: 0.15 mm) as precursor prodiginine **12** (15.0 mg, 40.3 µmol, 54%) was obtained as red solid. R_f = 0.15 (dichloromethane); **^{1}H-NMR** (600 MHz, $CDCl_3$): δ [ppm] = 1.43 (tt, $^{3}J_{8'',7''}$ = 7.5 Hz, $^{3}J_{8'',9''}$ = 7.5 Hz, 2H, 8″-H), 1.53–1.59 (m, 2H, 7″-H), 2.08 (dt, $^{3}J_{9'',8''}$ = 7.2 Hz, $^{3}J_{9'',10''}$ = 7.2 Hz, 2H, 9″-H), 2.41 (t, $^{3}J_{6'',7''}$ = 7.6 Hz, 2H, 6″-H), 2.54 (s, 3H, 12″-H), 4.01 (s, 3H, 7-H), 4.95 (dd, $^{cis,3}J_{11a'',10''}$ = 10.2 Hz, $^{2}J_{11a'',11b''}$ = 2.2 Hz, 1H, 11″-H_a), 5.01 (dd, $^{trans,3}J_{11b'',10''}$ = 17.1 Hz, $^{2}J_{11b'',11a''}$ = 1.7 Hz, 1H, 11″-H_b), 5.80 (ddt, $^{trans,3}J_{10'',11b''}$ = 16.9 Hz, $^{cis,3}J_{10'',11a''}$ = 10.2 Hz, $^{3}J_{10'',9''}$ = 6.7 Hz, 1H, 10″-H), 6.08 (d, $^{4}J_{3,1}$ = 2.0 Hz, 1H, 3-H), 6.36 (dd, $^{3}J_{4',5'}$ = 3.7 Hz, $^{4}J_{4',1'}$ = 2.3 Hz, 4′-H), 6.68 (d, ^{3}J = 2.6 Hz), 6.92 (ddd, ^{3}J = 3.9 Hz, ^{3}J = 2.5 Hz, ^{3}J = 1.3 Hz), 6.96 (s, 1H), 7.24 (d, $^{4}J_{3'',1''}$ = 2.7 Hz, 1H, 3″-H), 12.58 (brs, 1H, 1′-NH), 12.75 (brs, 2H, 1-NH, 1″-NH); **^{13}C-NMR** (151 MHz, $CDCl_3$): δ [ppm] = 12.6 (C-12″), 25.3 (C-6″), 28.6 (C-8″), 29.7 (C-7″), 33.7 (C-9″), 58.9 (C-7), 93.0 (C-3), 111.9 (C-4′), 114.7 (C-10″), 116.1 (C-8), 117.2 (C-3′), 120.9 (C-5), 122.4 (C-2′), 125.3 (C-2″), 127.1 (C-5′), 128.3 (C-4″), 128.4 (C-3″), 138.8 (C-9″), 146.9 (C-5″), 147.9 (C-2), 165.9 (C-4); **IR** (ATR-Film): $\tilde{\nu}$ [1/cm] = 3,163, 3,099, 2,974, 2,928, 2,857, 1,630, 1,604, 1,544, 1,512, 1,414, 1,356, 1,261, 1,158, 1,137, 1,044, 993, 960, 838, 756; **MS** (APCI, positive-Ion): *m/z* = 336 [(M)$^+$], 266, 163; **HRMS** (ESI, positive ion): calculated for $C_{21}H_{26}N_3O$ [(M + H)]$^+$ = 336.2070, found = 336.2076.

4.3.3. Semisynthesis toward 6-(2-((4-methoxy-1*H*,1′*H*-(2,2′-bipyrrole)-5-yl) methylene)-5-methyl-2*H*-pyrrole-4-yl)hexan-1-ol (3)

9-BBN (0.5 n in THF, 94.2 mg, 0.05 mmol, 2.2 eq.) was added to a solution of 4-Methoxy-5-((5-methyl-4-hex-5-en-1-yl-2H-pyrrole-2-yliden)methyl)-1*H*,1′*H*-2,2′-bipyrrole (**12**, 9 mg, 0.02 mmol, 1.0 eq.) in dry THF (2 mL) over a period of 15 min at 0°C. After stirring for 1 h at 0°C, the reaction mixture was heated up at 70°C under reflux for 3 h. Subsequently an aqueous solution of 3 N NaOH (39.9 mg, 105 µL, 0.12 mmol, 5.0 eq.) and 30% H_2O_2 (38.0 mg, 34.1 µL, 0.34 mmol, 14.0 eq.) was added at 0°C. After 1 h at 0°C the reaction mixture was allowed to reach room temperature and was stirred for further 15 h at 22°C. Ice water (10 mL) was added and the mixture was extracted with dichloromethane (3 × 15 mL). The combined organic layer was dried over $MgSO_4$, the solvent was evaporated under reduced pressure and the crude product was purified by column chromatography on silica gel [dichloromethane + 0.5–4.0% trimethylamine (*v*/*v*)] to isolate 6-(2-((4-methoxy-1*H*,1′*H*-(2,2′-bipyrrole)-5-yl)methylene)-5-methyl-2*H*-pyrrole-4-yl)hexan-1-ol (**3**, 6.10 mg, 0.02 mmol, 65%) as red solid. R_f = 0.16 (PE/EtOAc 50:50); **^{1}H-NMR** (600 MHz, $CDCl_3$): δ [ppm] = 1.28 (brs, 1H, 12″-OH), 1.37 (m_c, 4H, 8″-H, 9″-H), 1.50–1.63 (m, 4H, 7″-H, 10″-H), 2.40 (t, $^{3}J_{6'',7''}$ = 7.6 Hz, 2H, 6″-H), 2.54 (s, 3 H, 13″-H), 3.64 (t, $^{3}J_{11'',10''}$ = 6.6 Hz, 2H, 11″-H), 4.00 (s, 3H, 7-H), 6.08 (d, $^{4}J_{3,1}$ = 1.9 Hz, 1H, 3-H), 6.35 (dd, $^{3}J_{4',5'}$ = 4.3 Hz, $^{4}J_{4',1'}$ = 2.0 Hz, 1H, 4′-H), 6.67 (d, $^{4}J_{3'',1''}$ = 2.6 Hz, 1H, 3″-H), 6.92 (ddd, $^{3}J_{3',4'}$ = 3.9 Hz, $^{4}J_{3',5'}$ = 2.5 Hz, $^{4}J_{3',1'}$ = 1.4 Hz, 1H, 3′-H), 6.94 (s, 1H, 8-H), 7.23 (dd, $^{3}J_{5',4'}$ = 2.7 Hz, $^{3}J_{5',1'}$ = 1.3 Hz, 1-H, 5′-H), 12.56 (brs, 1H, 1′-NH), 12.72 (brs, 2H, 1-NH, 1″-NH); **^{13}C-NMR** (151 MHz, $CDCl_3$): δ [ppm] = 12.6 (C-13″), 25.0 (C-6″), 25.7 (C-8″), 29.1 (C-9″), 30.2 (C-7″), 32.9 (C-10″), 58.9 (C-7), 63.1 (C-11″), 93.0 (C-3), 111.9 (C-4′), 116.3 (C-8), 117.3 (C-3′), 120.9 (C-5), 122.4 (C-2′), 125.3 (C-2″), 127.2 (C-5′), 128.3 (C-4″), 128.4 (C-3″), 147.0 (C-5″), 148.0 (C-2), 166.0 (C-4); **IR** (ATR-film): $\tilde{\nu}$ [1/cm] = 3,422, 3,172, 2,930, 2,861, 1,630, 1,602, 1,543, 1,511, 1,363, 1,261, 1,137, 960, 748; **MS** (APCI, positive ion): *m/z* = 354 [(M)$^+$], 279, 157; **HRMS** (ESI, positive ion): calculated for $C_{21}H_{28}N_3O_2$ [(M + H)]$^+$ = 354.2176, found = 354.2179.

4.4. Assessment of effects on the plant-parasitic nematode *Heterodera schachtii*

4.4.1. Plant material and nematode culture

Arabidopsis thaliana Columbia (Col-0) seeds were surface-sterilized by soaking in 0.7% sodium hypochlorite for 5 min and

submerging them in 70% (*v*/*v*) ethanol for 1 min. Subsequently, the seeds were rinsed with sterile distilled water 5 times, dried at room temperature for 4 h and stored at 4°C for further experiments. *H. schachtii* cysts were harvested from the roots of mustard (*Sinapsis alba*), which was grown aseptically on modified Knop agar medium, and submerged with sterile 3 mM $ZnCl_2$ in the Baermann funnel (Grundler et al., 1991). After 7 days, the freshly hatched second-stage juveniles (J2s) were collected for subsequent analysis. All preparation procedures were performed under aseptic conditions.

4.4.2. EC_{50} (nematode infection) determination of di-rhamnolipids and prodiginines

EC_{50} determination of selected compounds was performed in an *in vitro* agar system: Petri dishes (90 mm diameter) were filled with modified Knop medium (Sijmons et al., 1991; Matera et al., 2021) supplemented with prodiginines or di-rhamnolipids at different concentrations (Supplementary Table S4). Stock solutions of prodiginines in DMSO were applied to implement a final concentration of 0.5% DMSO. The di-rhamnolipids, which were obtained by microbial production as a congener mixture as previously described (Bredenbruch et al., 2023), were solved in water. Accordingly, modified Knop medium alone or supplemented with 0.5% (v/v) DMSO served as control. On the medium, 2 surface-sterilized *A. thaliana* seeds were germinated aseptically and incubated in a climate chamber under a red/blue light with a 16-h/8-h light/dark photoperiod at 24°C (Sijmons et al., 1991). At 12 days post seeding, each plant was inoculated with approximately 60 *H. schachtii* J2s. At 10 days post inoculation, the total number of males and females on each plant was counted under a Stereo Microscope (Leica, Germany). EC_{50} was determined by using software 'CompuSyn' (Chou and Martin, 2005). Three independent biological replicates of the experiment were performed. Each biological replicate included at least 6 technical replicates (plants) per variant.

4.4.3. Determination of the combinatorial effect of compounds on nematode infection

Assays to measure combinatorial effects were carried out in an analogous experimental set-up as the EC_{50} determination described above. The concentration of compounds alone or in combination is detailed in Supplementary Table S5. The compound combination effects (antagonistic, additive or synergistic) were evaluated according to the Combination Index Plot obtained by the software 'CompuSyn' (Chou and Martin, 2005). The experiments were performed independently in triplicate.

4.4.4. Time-resolved analyses of the compounds' impact on nematodes

The time-resolved analysis consisted of four assays investigating nematode motility, stylet thrusting, infection, and development. Petri dishes (90 mm diameter) were filled with modified Knop medium supplemented with prodigiosin (**1**) or hydroxylated prodiginine **3** at the determined EC_{50}, which is 15.1 and 31.2 µM, respectively. Modified Knop medium alone or supplemented with 0.5% (*v*/*v*) DMSO served as controls.

4.4.4.1. Nematode motility

Approximately 30 *H. schachtii* J2 were inoculated in the center of a Petri dish containing the test compound. The location of J2s was documented after 30 and 60 min and the distance to the inoculation point was measured by Image J (Schneider et al., 2012). The experiment was performed independently in quadruplicate.

4.4.4.2. Nematode stylet thrusting

Two surface-sterilized *A. thaliana* seeds were germinated aseptically on the medium containing the test compound. At 12 days post seeding, approximately 60 *H. schachtii* J2 were inoculated to each plant. At 6 h post inoculation, 10 J2, which successfully penetrated the root epidermis, were tracked under a Stereo Microscope (Leica, Germany) in order to count the number of stylet movements for 5 min. The experiment was performed independently in quadruplicate.

4.4.4.3. Nematode infection and development

Two surface-sterilized *A. thaliana* seeds were germinated aseptically on the medium containing the test compound. At 12 days post seeding, approximately 60 *H. schachtii* J2 were inoculated to each plant. At 2, 4 and 10 days post inoculation, the number of males and females was counted, and the size of male and female nematodes was measured under a LeicaS4E Stereo Microscope (Leica, Germany) equipped with Leica Application Suite (LAS) software. Four independent biological replicates with 14 plants per variant and biological replicate ($n = 56$) were conducted for the nematode infection assay. Three independent biological replicates with in total $n = 70$ technical replicates (nematodes) were performed for the development experiment.

4.4.5. Statistical analysis of bioactivity evaluating data

All data are expressed as mean ± standard error (SE). Statistical analysis was performed by using one-way analysis of variance (ANOVA; $p < 0.05$; SIGMAPLOT 12.5, Systat Software, Inc., San Jose, CA, United States).

Data availability statement

The original contributions presented in the study are included in the article/Supplementary material, further inquiries can be directed to the corresponding authors.

Author contributions

AL, AS, JP, FG, K-EJ, and TD conceived the research concept and designed the experiments. RW, FG, SI, NB, KB, DK, TW, and HB performed microbiological work as well as chemical syntheses and production of prodiginines. CM, TT, and LB provided rhamnolipids. MH, XX, and LR conducted investigations of antinematode activities. DK, RW, and MH drafted the manuscript with input from all the authors. All authors contributed to the article and approved the submitted version.

Funding

The work was supported by grants from the German Bioeconomy Science Center. The scientific activities of the Bioeconomy Science Center were financially supported by the Ministry of Culture and Science within the framework of the NRW Strategieprojekt BioSC (no. 313/323-400-00213). Parts of this work were funded by the state of NRW in the project RhamnoLizer. This

work was supported by the Open Access Publication Fund of the University of Bonn.

Acknowledgments

The authors thank Birgit Henßen for analytical support. We further gratefully acknowledge excellent technical support by Ute Schlee and Stefan Neumann.

Conflict of interest

The authors declare that the research was conducted in the absence of any commercial or financial relationships that could be construed as a potential conflict of interest.

Publisher's note

Supplementary material

The Supplementary material for this article can be found online at: https://www.frontiersin.org/articles/10.3389/fmicb.2023.1151882/full#supplementary-material

References

Abdel-Mawgoud, A. M., Lépine, F., and Déziel, E. (2010). Rhamnolipids: diversity of structures, microbial origins and roles. *Appl. Microbiol. Biotechnol.* 86, 1323–1336. doi: 10.1007/s00253-010-2498-2

Beal, R., and Betts, W. B. (2000). Role of rhamnolipid biosurfactants in the uptake and mineralization of hexadecane in *Pseudomonas aeruginosa*. *J. Appl. Microbiol.* 89, 158–168. doi: 10.1046/j.1365-2672.2000.01104.x

Belda, E., Van Heck, R. G. A., Lopez-sanchez, M. J., Cruveiller, S., Barbe, V., Fraser, C., et al. (2016). The revisited genome of *Pseudomonas putida* KT2440 enlightens its value as a robust metabolic chassis. *Environ. Microbiol.* 18, 3403–3424. doi: 10.1111/1462-2920.13230

Berg, G. (2009). Plant-microbe interactions promoting plant growth and health: perspectives for controlled use of microorganisms in agriculture. *Appl. Microbiol. Biotechnol.* 84, 11–18. doi: 10.1007/s00253-009-2092-7

Berning, L., Schlütermann, D., Friedrich, A., Berleth, N., Sun, Y., Wu, W., et al. (2021). Prodigiosin sensitizes sensitive and resistant urothelial carcinoma cells to cisplatin treatment. *Molecules* 26:1294. doi: 10.3390/molecules26051294

Bhadoriya, S. S., Madoriya, N., Shukla, K., and Parihar, M. (2013). Biosurfactants: a new pharmaceutical additive for solubility enhancement and pharmaceutical development. *Biochem. Pharmacol. Open Access* 2:113. doi: 10.4172/2167-0501.1000113

Bnyan, R., Khan, I., Ehtezazı, T., Saleem, I., Gordon, S., O'Neıll, F., et al. (2018). Surfactant effects on lipid-based vesicle properties. *J. Pharm. Sci.* 107, 1237–1246. doi: 10.1016/j.xphs.2018.01.005

Boonlarppradab, C., Kauffman, C. A., Jensen, P. R., and Fenical, W. (2008). Marineosins a and B, cytotoxic spiroaminals from a marine- derived actinomycete. *Org. Biomol. Chem.* 10, 5505–5508. doi: 10.1021/ol8020644

Brands, S., Brass, H. U. C., Klein, A. S., Pietruszka, J., Ruff, A. J., and Schwaneberg, U. (2020). A colourimetric high-throughput screening system for directed evolution of prodigiosin ligase PigC. *Chem. Commun.* 56, 8631–8634. doi: 10.1039/d0cc02181d

Brass, H. U. C., Klein, A. S., Nyholt, S., Classen, T., and Pietruszka, J. (2019). Condensing enzymes from Pseudoalteromonadaceae for prodiginine synthesis. *Adv. Synth. Catal.* 361, 2659–2667. doi: 10.1002/adsc.201900183

Bredenbruch, S., Mueller, C., Atemnkeng, H., Schroeder, L., Tiso, T., Blank, L. M., et al. (2023). The biological activity of bacterial rhamnolipids is linked to their molecular structure. *bioRxiv* [Epub ahead of preprint], doi: 10.1101/2023.01.23.525263

Chawrai, S. R., Williamson, N. R., Mahendiran, T., Salmond, G. P. C., and Leeper, F. J. (2012). Characterisation of PigC and HapC, the prodigiosin synthetases from *Serratia* sp. and *Hahella chejuensis* with potential for biocatalytic production of anticancer agents. *Chem. Sci.* 3, 447–454. doi: 10.1039/c1sc00588j

Cheng, F., Kovács, I. A., and Barabási, A.-L. (2019). Network-based prediction of drug combinations. *Nat. Commun.* 10:1197. doi: 10.1038/s41467-019-09186-x

Choi, S. Y., Lim, S., Yoon, K., Lee, J. I., and Mitchell, R. J. (2021). Biotechnological activities and applications of bacterial pigments violacein and prodigiosin. *J. Biol. Eng.* 15:10. doi: 10.1186/s13036-021-00262-9

Chou, T., and Martin, N. (2005). *CompuSyn for Drug Combinations: PC Software and User's Guide: A Computer Program for Quantitation of Synergism and Antagonism in Drug Combinations, and the Determination of IC50 and ED50 and LD50 Values.* ComboSyn Inc., Paramus.

Cook, T. B., Jacobson, T. B., Venkataraman, M. V., Hofstetter, H., Amador-Noguez, D., Thomas, M. G., et al. (2021). Stepwise genetic engineering of pseudomonas putida enables robust heterologous production of prodigiosin and glidobactin a. *Metab. Eng.* 67, 112–124. doi: 10.1016/j.ymben.2021.06.004

Couturier, M., Bhalara, H. D., Chawrai, S. R., Monson, R., Williamson, N. R., Salmond, G. P. C., et al. (2019). Substrate flexibility of the flavin-dependent dihydropyrrole oxidases PigB and HapB involved in antibiotic prodigiosin biosynthesis. *Chembiochem* 21, 523–530. doi: 10.1002/cbic.201900424

Dairi, K., Tripathy, S., Attardo, G., and Lavallée, J.-F. (2006). Two-step synthesis of the bipyrrole precursor of prodigiosins. *Tetrahedron Lett.* 47, 2605–2606. doi: 10.1016/j.tetlet.2006.02.035

Darshan, N., and Manonmani, H. K. (2015). Prodigiosin and its potential applications. *J. Food Sci. Technol.* 52, 5393–5407. doi: 10.1007/s13197-015-1740-4

Darshan, N., and Manonmani, H. K. (2016). Prodigiosin inhibits motility and activates bacterial cell death revealing molecular biomarkers of programmed cell death. *AMB Express* 6:50. doi: 10.1186/s13568-016-0222-z

Das, P., Yang, X.-P., and Ma, L. Z. (2014). Analysis of biosurfactants from industrially viable pseudomonas strain isolated from crude oil suggests how rhamnolipids congeners affect emulsification property and antimicrobial activity. *Front. Microbiol.* 5:696. doi: 10.3389/fmicb.2014.00696

Domröse, A., Hage-Hülsmann, J., Thies, S., Weihmann, R., Kruse, L., Otto, M., et al. (2019). Pseudomonas putida rDNA is a favored site for the expression of biosynthetic genes. *Sci. Rep.* 9:7028. doi: 10.1038/s41598-019-43405-1

Domröse, A., Klein, A. S., Hage-Hülsmann, J., Thies, S., Svensson, V., Classen, T., et al. (2015). Efficient recombinant production of prodigiosin in pseudomonas putida. *Front. Microbiol.* 6:972. doi: 10.3389/fmicb.2015.00972

Domröse, A., Weihmann, R., Thies, S., Jaeger, K. E., Drepper, T., and Loeschcke, A. (2017). Rapid generation of recombinant pseudomonas putida secondary metabolite producers using yTREX. *Synth. Syst. Biotechnol.* 2, 310–319. doi: 10.1016/j.synbio.2017.11.001

Dowhan, W. (1997). "The role of phospholipids in cell function" in *Advances in Lipobiology*. ed. R. W. Gross (Amsterdam Niederlande: Elsevier), 79–107.

Fürstner, A. (2003). Chemistry and biology of roseophilin and the prodigiosin alkaloids: a survey of the last 2500 years. *Angew. Chemie - Int. Ed.* 42, 3582–3603. doi: 10.1002/anie.200300582

Garcia-Brugger, A., Lamotte, O., Vandelle, E., Bourque, S., Lecourieux, D., Poinssot, B., et al. (2006). Early signaling events induced by elicitors of plant defenses. *Mol. Plant-Microbe Interact.* 19, 711–724. doi: 10.1094/MPMI-19-0711

Grundler, F. M. W., Schnibbe, L., and Wyss, U. (1991). *In vitro* studies on the behaviour of second-stage juveniles of *Heterodera schachtii* (Nematoda: Heteroderidae) in response to host plant root exudates. *Parasitology* 103, 149–155. doi: 10.1017/S0031182000059394

Haas, D., and Défago, G. (2005). Biological control of soil-borne pathogens by fluorescent pseudomonads. *Nat. Rev. Microbiol.* 3, 307–319. doi: 10.1038/nrmicro1129

Habash, S. S., Brass, H. U. C., Klein, A. S., Klebl, D. P., Weber, T. M., Classen, T., et al. (2020). Novel prodiginine derivatives demonstrate bioactivities on plants, nematodes, and fungi. *Front. Plant Sci.* 11:579807. doi: 10.3389/fpls.2020.579807

Hage-Hülsmann, J., Grünberger, A., Thies, S., Santiago-Schübel, B., Klein, A. S., Pietruszka, J., et al. (2018). Natural biocide cocktails: combinatorial antibiotic effects of prodigiosin and biosurfactants. *PLoS One* 13:e0200940. doi: 10.1371/journal.pone.0200940

Hanahan, D. (1983). Studies on transformation of Escherichia coli with plasmids. *J. Mol. Biol.* 166, 557–580. doi: 10.1016/S0022-2836(83)80284-8

Handelsman, J., and Stabb, E. V. (1996). Biocontrol of soilborne plant pathogens. *Plant Cell* 8, 1855–1869. doi: 10.1105/tpc.8.10.1855

Hopkins, A. L. (2007). Network pharmacology. *Nat. Biotechnol.* 25, 1110–1111. doi: 10.1038/nbt1007-1110

Hu, D. X., Withall, D. M., Challis, G. L., and Thomson, R. J. (2016). Structure, chemical synthesis, and biosynthesis of Prodiginine natural products. *Chem. Rev.* 116, 7818–7853. doi: 10.1021/acs.chemrev.6b00024

Ivanov, A. V., Shcherbakova, V. S., Mikhaleva, A. I., and Trofimov, B. A. (2014). One-pot synthesis of pyrroles from ketones, hydroxylamine, and 1,2-dibromoethane in the system KOH-DMSO. *Russ. J. Org. Chem.* 50, 1775–1778. doi: 10.1134/S1070428014120100

Jia, J., Zhu, F., Ma, X., Cao, Z. W., Li, Y. X., and Chen, Y. Z. (2009). Mechanisms of drug combinations: interaction and network perspectives. *Nat. Rev. Drug Discov.* 8, 111–128. doi: 10.1038/nrd2683

Keith, C. T., Borisy, A. A., and Stockwell, B. R. (2005). Multicomponent therapeutics for networked systems. *Nat. Rev. Drug Discov.* 4, 71–78. doi: 10.1038/nrd1609

Kirschning, A., Taft, F., and Knobloch, T. (2007). Total synthesis approaches to natural product derivatives based on the combination of chemical synthesis and metabolic engineering. *Org. Biomol. Chem.* 5, 3245–3259. doi: 10.1039/b709549j

Klein, A. S., Brass, H. U. C., Klebl, D. P., Classen, T., Loeschcke, A., Drepper, T., et al. (2018). Preparation of cyclic Prodiginines by Mutasynthesis in pseudomonas putida KT2440. *Chembiochem* 19, 1545–1552. doi: 10.1002/cbic.201800154

Klein, A. S., Domröse, A., Bongen, P., Brass, H. U. C., Classen, T., Loeschcke, A., et al. (2017). New Prodigiosin derivatives obtained by Mutasynthesis in pseudomonas putida. *ACS Synth. Biol.* 6, 1757–1765. doi: 10.1021/acssynbio.7b00099

Köhl, J., Kolnaar, R., and Ravensberg, W. J. (2019). Mode of action of microbial biological control agents against plant diseases: relevance beyond efficacy. *Front. Plant Sci.* 10:845. doi: 10.3389/fpls.2019.00845

Konno, H., Matsuya, H., Okamoto, M., Sato, T., Tanaka, Y., Yokoyama, K., et al. (1998). Prodigiosins uncouple mitochondrial and bacterial F-ATPases: evidence for their H^+/cl^- symport activity. *J. Biochem.* 124, 547–556. doi: 10.1093/oxfordjournals.jbchem.a022147

Li, P., He, S., Zhang, X., Gao, Q., Liu, Y., and Liu, L. (2022). Structures, biosynthesis, and bioactivities of prodiginine natural products. *Appl. Microbiol. Biotechnol.* 106, 7721–7735. doi: 10.1007/s00253-022-12245-x

Loeschcke, A., Markert, A., Wilhelm, S., Wirtz, A., Rosenau, F., Jaeger, K.-E., et al. (2013). TREX: a universal tool for the transfer and expression of biosynthetic pathways in bacteria. *ACS Synth. Biol.* 2, 22–33. doi: 10.1021/sb3000657

Loeschcke, A., and Thies, S. (2020). Engineering of natural product biosynthesis in *Pseudomonas putida*. *Curr. Opin. Biotechnol.* 65, 213–224. doi: 10.1016/j.copbio.2020.03.007

Lugtenberg, B., and Kamilova, F. (2009). Plant-growth-promoting Rhizobacteria. *Annu. Rev. Microbiol.* 63, 541–556. doi: 10.1146/annurev.micro.62.081307.162918

Magalhães, L., and Nitschke, M. (2013). Antimicrobial activity of rhamnolipids against listeria monocytogenes and their synergistic interaction with nisin. *Food Control* 29, 138–142. doi: 10.1016/j.foodcont.2012.06.009

Matera, C., Grundler, F. M. W., and Schleker, A. S. S. (2021). Sublethal fluazaindolizine doses inhibit development of the cyst nematode *Heterodera schachtii* during sedentary parasitism. *Pest Manag. Sci.* 77, 3571–3580. doi: 10.1002/ps.6411

Meschke, H., Walter, S., and Schrempf, H. (2012). Characterization and localization of prodiginines from Streptomyces lividans suppressing *Verticillium dahliae* in the absence or presence of *Arabidopsis thaliana*. *Environ. Microbiol.* 14, 940–952. doi: 10.1111/j.1462-2920.2011.02665.x

Mikhaleva, A. I., Trofimov, B. A., Vasilev, A. N., Komarova, G. A., and Skorobogatova, V. I. (1981). Pyrroles from ketoximes and acetylene. Dihaloethanes in place of acetylene in reactions with cyclohexanone oxime. *Acad. Sci. USSR* 9, 1202–1204.

Nelson, K. E., Weinel, C., Paulsen, I. T., Dodson, R. J., Hilbert, H., Santos, V. A. P. M., et al. (2002). Complete genome sequence and comparative analysis of the metabolically versatile *Pseudomonas putida* KT2440. *Environ. Microbiol.* 4, 799–808. doi: 10.1046/j.1462-2920.2002.00366.x

Nikel, P. I., Chavarría, M., Danchin, A., and de Lorenzo, V. (2016). From dirt to industrial applications: pseudomonas putida as a synthetic biology chassis for hosting harsh biochemical reactions. *Curr. Opin. Chem. Biol.* 34, 20–29. doi: 10.1016/j.cbpa.2016.05.0111367-5931/#

Ortiz, A., Teruel, J. A., Espuny, M. J., Marqués, A., Manresa, Á., and Aranda, F. J. (2006). Effects of dirhamnolipid on the structural properties of phosphatidylcholine membranes. *Int. J. Pharm.* 325, 99–107. doi: 10.1016/j.ijpharm.2006.06.028

Pieterse, C. M. J., Van Der Does, D., Zamioudis, C., Leon-Reyes, A., and Van Wees, S. C. M. (2012). Hormonal modulation of plant immunity. *Annu. Rev. Cell Dev. Biol.* 28, 489–521. doi: 10.1146/annurev-cellbio-092910-154055

Rahul, S., Chandrashekhar, P., Hemant, B., Chandrakant, N., Laxmikant, S., and Satish, P. (2014). Nematicidal activity of microbial pigment from *Serratia marcescens*. *Nat. Prod. Res.* 28, 1399–1404. doi: 10.1080/14786419.2014.904310

Ravindran, A., Anishetty, S., and Pennathur, G. (2020). Molecular dynamics of the membrane interation and localisation of prodigiosin. *J. Mol. Graph. Model.* 98:107614. doi: 10.1016/j.jmgm.2020.107614

Roberts, D. P., Selmer, K., Lupitskyy, R., Rice, C., Buyer, J. S., Maul, J. E., et al. (2021). Seed treatment with prodigiosin controls damping-off of cucumber caused by Pythium ultimum. *AMB Express* 11:10. doi: 10.1186/s13568-020-01169-2

Rossi, C. C., Santos-Gandelman, J. F., Barros, E. M., Alvarez, V. M., Laport, M. S., and Giambiagi-deMarval, M. (2016). Staphylococcus haemolyticus as a potential producer of biosurfactants with antimicrobial, anti-adhesive and synergistic properties. *Lett. Appl. Microbiol.* 63, 215–221. doi: 10.1111/lam.12611

Sakai-Kawada, F. E., Ip, C. G., Hagiwara, K. A., and Awaya, J. D. (2019). Biosynthesis and bioactivity of prodiginine analogs in marine bacteria, Pseudoalteromonas: a mini review. *Front. Microbiol.* 10:1715. doi: 10.3389/fmicb.2019.01715

Sanchez, L., Courteaux, B., Hubert, J., Kauffmann, S., Renault, J. H., Clément, C., et al. (2012). Rhamnolipids elicit defense responses and induce disease resistance against biotrophic, hemibiotrophic, and necrotrophic pathogens that require different signaling pathways in Arabidopsis and highlight a central role for salicylic acid. *Plant Physiol.* 160, 1630–1641. doi: 10.1104/pp.112.201913

Schloss, P. D., Allen, H. K., Klimowicz, A. K., Mlot, C., Gross, J. A., Savengsuksa, S., et al. (2010). Psychrotrophic strain of *Janthinobacterium lividum* from a cold Alaskan soil produces prodigiosin. *DNA Cell Biol.* 29, 533–541. doi: 10.1089/dna.2010.1020

Schneider, C. A., Rasband, W. S., and Eliceiri, K. W. (2012). NIH image to ImageJ: 25 years of image analysis. *Nat. Methods* 9, 671–675. doi: 10.1038/nmeth.2089

Sijmons, P., Grundler, F., von Mende, N., Burrows, P. R., and Wyss, U. (1991). Arabidopsis thaliana as a new model host for plant-parasitic nematodes. *Plant J.* 1, 245–254. doi: 10.1111/j.1365-313X.1991.00245.x

Simon, R., Priefer, U., and Pühler, A. (1983). A broad host range mobilization system for *in vivo* genetic engineering: transposon mutagenesis in Gram negative bacteria. *Nat. Biotechnol.* 1, 784–791. doi: 10.1038/nbt1183-784

Someya, N., Nakajima, M., Hirayae, K., Hibi, T., and Akutsu, K. (2001). Synergistic antifungal activity of chitinolytic enzymes and prodigiosin produced by biocontrol bacterium, Serratia marcescens strain B2 against gray mold pathogen. *Botrytis cinerea. J. Gen. Plant Pathol.* 67, 312–317. doi: 10.1007/pl00013038

Sotirova, A., Avramova, T., Stoitsova, S., Lazarkevich, I., Lubenets, V., Karpenko, E., et al. (2012). The importance of rhamnolipid-biosurfactant-induced changes in bacterial membrane lipids of Bacillus subtilis for the antimicrobial activity of thiosulfonates. *Curr. Microbiol.* 65, 534–541. doi: 10.1007/s00284-012-0191-7

Stankovic, N., Senerovic, L., Ilic-Tomic, T., Vasiljevic, B., and Nikodinovic-Runic, J. (2014). Properties and applications of undecylprodigiosin and other bacterial prodigiosins. *Appl. Microbiol. Biotechnol.* 98, 3841–3858. doi: 10.1007/s00253-014-5590-1

Sun, H., Liu, Z., Zhao, H., and Ang, E. L. (2015). Recent advances in combinatorial biosynthesis for drug discovery. *Drug Des. Devel. Ther.* 9, 823–833. doi: 10.2147/DDDT.S63023

Suryawanshi, R. K., Patil, C. D., Koli, S. H., Hallsworth, J. E., and Patil, S. V. (2017). Antimicrobial activity of prodigiosin is attributable to plasma-membrane damage. *Nat. Prod. Res.* 31, 572–577. doi: 10.1080/14786419.2016.1195380

Tiso, T., Ihling, N., Kubicki, S., Biselli, A., Schonhoff, A., Bator, I., et al. (2020). Integration of genetic and process engineering for optimized rhamnolipid production using pseudomonas putida. *Front. Bioeng. Biotechnol.* 8:976. doi: 10.3389/fbioe.2020.00976

Trofimov, B. A., Mikhaleva, A. I., Ivanov, A. V., Shcherbakova, V. S., and Ushakov, I. A. (2015). Expedient one-pot synthesis of pyrroles from ketones, hydroxylamine, and 1,2-dichloroethane. *Tetrahedron* 71, 124–128. doi: 10.1016/j.tet.2014.11.031

Varnier, A. L., Sanchez, L., Vatsa, P., Boudesocque, L., Garcia-Brugger, A., Rabenoelina, F., et al. (2009). Bacterial rhamnolipids are novel MAMPs conferring resistance to *Botrytis cinerea* in grapevine. *Plant Cell Environ.* 32, 178–193. doi: 10.1111/j.1365-3040.2008.01911.x

Wallace, H. R. (1958). Movement of eelworms. The influence of pore size and moisture content of the soil on the migration of larvae of the beet eelworm. *Heterodera schachtii Schmidt. Ann. Appl. Biol.* 46, 74–85. doi: 10.1111/j.1744-7348.1958.tb02179.x

Weihmann, R., Domröse, A., Drepper, T., Jaeger, K. E., and Loeschcke, A. (2020). Protocols for yTREX/Tn5-based gene cluster expression in pseudomonas putida. *Microb. Biotechnol.* 13, 250–262. doi: 10.1111/1751-7915.13402

Weimer, A., Kohlstedt, M., Volke, D. C., Nikel, P. I., and Wittmann, C. (2020). Industrial biotechnology of *Pseudomonas putida*: advances and prospects. *Appl. Microbiol. Biotechnol.* 104, 7745–7766. doi: 10.1007/s00253-020-10811-9

Williamson, N. R., Fineran, P. C., Ogawa, W., Woodley, L. R., and Salmond, G. P. C. (2008). Integrated regulation involving quorum sensing, a two-component system, a GGDEF/EAL domain protein and a post-transcriptional regulator controls swarming and RhlA-dependent surfactant biosynthesis in Serratia. *Environ. Microbiol.* 10, 1202–1217. doi: 10.1111/j.1462-2920.2007.01536.x

Williamson, N. R., Simonsen, H. T., Ahmed, R. A. A., Goldet, G., Slater, H., Woodley, L., et al. (2005). Biosynthesis of the red antibiotic, prodigiosin, in Serratia: identification of a novel 2-methyl-3-n-amyl-pyrrole (MAP) assembly pathway, definition of the terminal condensing enzyme, and implications for undecylprodigiosin biosynthesis in Streptomyces. *Mol. Microbiol.* 56, 971–989. doi: 10.1111/j.1365-2958.2005.04602.x

Wyss, U. (1992). Observations on the feeding behavior of Heterodera schachtii throughout development, including events during moulting. *Fundam. Appl. Nematol.* 15, 75–89.

Wyss, U., and Grundler, F. M. W. (1992). Feeding behavior of sedentary plant parasitic nematodes. *Netherlands J. Plant Pathol.* 98, 165–173. doi: 10.1007/BF01974483

Wyss, U., and Zunke, U. (1986). Observations on the behaviour of second stage juveniles of Heterodera schachtii inside host roots. *Rev. Nématologie* 9, 153–165.

Yildirim, M. A., Goh, K.-I., Cusick, M. E., Barabási, A.-L., and Vidal, M. (2007). Drug-target network. *Nat. Biotechnol.* 25, 1119–1126. doi: 10.1038/nbt1338

Yip, C. H., Yarkoni, O., Ajioka, J., Wan, K. L., and Nathan, S. (2019). Recent advancements in high-level synthesis of the promising clinical drug, prodigiosin. *Appl. Microbiol. Biotechnol.* 103, 1667–1680. doi: 10.1007/s00253-018-09611-z

II.5.2. Production of cycloprodiginines via combinatorial mutasynthesis

PUBLICATION VI

Substrate tolerance of Prub680 and homologous enzymes allows the mutasynthesis of cycloprodiginines in *Pseudomonas putida* KT2440

Nora Lisa Bitzenhofer*, Matthias Bleser*, Anka Siebericchs, Dorothea Fabiane Kossmann, Tim Moritz Weber, Viktoria Warth, Daniel Germes, Robin Weihmann, Karl-Erich Jaeger, Jörg Pietruszka, Anita Loeschcke

Status: manuscript in preparation

Supporting Information can be found in the Appendix (**Chapter V.5**)

Own contribution:

Planning the experiments and performing parts of the biological experiments, analyzing the data, writing the first draft of the manuscript.

Substrate tolerance of Prub680 and homologous enzymes allows the mutasynthesis of cycloprodiginines in *Pseudomonas putida* KT2440

Nora Lisa Bitzenhofer[1‡], Matthias Bleser[2‡], Anka Siebericchs[1], Dorothea F. Kossmann[2], Tim Moritz Weber[2], Viktoria Warth[2], Daniel Germes[2], Robin Weihmann[1], Karl-Erich Jaeger[1,3], Jörg Pietruszka[2,3*], Anita Loeschcke[1*]

[1]Institute of Molecular Enzyme Technology (IMET), Heinrich Heine University Düsseldorf, Düsseldorf, Germany
[2]Institute of Bioorganic Chemistry (IBOC), Heinrich Heine University Düsseldorf, Düsseldorf, Germany
[3]Institute of Bio- and Geosciences (IBG-1): Biotechnology, Forschungszentrum Jülich, Jülich, Germany

KEYWORDS: natural product production, cycloprodiginines, Pseudomonas putida, mutasynthesis

ABSTRACT: Bacterial prodiginines are tripyrrolic compounds with diverse biological activities. Structural differences are associated with differences in the specific effects. For example, cycloprodigiosin, which contains an additional ring structure on one pyrrole, has higher antimicrobial activity than its straight-chain congener prodigiosin.
However, the biological activities of cycloprodigiosin have not been studied in detail, and no structural derivatives have been synthesized for potential further development of this compound. Here, we investigated the mutasynthesis of cycloprodiginines in engineered *Pseudomonas putida* KT2440 strains.
We used *P. putida* strains carrying *pig* genes from *Serratia marcescens* that allow production of the bipyrrole precursor by heterologous biosynthesis and added chemically synthesized monopyrrole mutasynthons. The prodigiosin ligase PigC and candidate cyclases were expressed for pyrrole condensation and cyclization. We evaluated the previously described Prub680 from *Pseudoalteromonas rubra* and four sequence-homologs from cyclic prodiginine producers.
All cyclases facilitated cycloprodigiosin mutasynthesis, with Prub680 showing the best conversion of >90% allowing upscaled production of the compound. The addition of non-natural precursors demonstrated the promiscuity of these enzymes and led to the production of novel derivatives. Mutasynthesis in engineered *P. putida* may therefore provide access to cycloprodigiosin and related structures.

Prodiginines are bright red bacterial tripyrrolic compounds with highly interesting biological activities. These include antibacterial[1–4], antimalaria[5–7], antiphytopathogenic[8,9], immunosuppressive[10,11], and cytostatic bioactivities[2,12,13]. Prodigiosin (**1**) is the most prominent representative biosynthesized e.g., by *Serratia marcescens*[14]. It has a characteristic pentyl chain on the pyrrole C ring[15]. The biosynthesis of cycloprodigiosin (**2**), which contains a hexane ring with a methyl group on this pyrrole ring[16], has been reported in various marine bacteria such as *Pseudoalteromonas rubra*[17,18], *Pseudoalteromonas denitrificans*[19,20], *Vibrio* [21–23] and *Zoochikella* species[24,25]. More recently, *Spartinivicinus ruber* has been described to produce heptylprodigiosin (**3**) and cycloheptylprodigiosin (**4**), which has a seven-membered heterocycle with one ethyl group (**Scheme 1**)[26].

Prodigiosin biosynthesis has been described in several bacteria[27,28]. In a bifurcated pathway, 2-methyl-3-amylpyrrole (MAP) and 4-methoxy-2,2′-bipyrrole-5-carbaldehyde (MBC) are formed as precursors for a final condensation reaction catalyzed by the ligase PigC which yields the tripyrrole prodigiosin (**Figure S1, A**). An enzyme that catalyzes prodigiosin cyclization has also been identified in *P. rubra*[17]. It is a 422 amino acid predicted integral membrane protein that functions as a di-iron oxygenase related to alkylglycerol monooxygenases[17]. Notably, it is not related to Rieske oxygenase-type cyclases from other prodiginine pathways (e.g., *Streptomyces coelicolor* RedG)[29], suggesting a convergent evolution of cyclization and potentially indicating a relevant biological function of cyclic prodiginine derivatives.

Cycloprodigiosin seems to have a different antibacterial and anti-inflammatory activity compared to prodigiosin[23,25,30]. Further, cycloheptylprodigiosin showed a higher antimicrobial activity against Gram-negative bacteria and a higher antifungal activity than heptylprodigiosin[26]. Therefore, access to cycloprodigiosin and related structures seems to be of interest.

Prodiginine mutasynthesis was previously established in *P. putida*. A *P. putida* strain, engineered to carry the entire prodigiosin biosynthetic gene cluster of *S. marcescens*, was adapted for this purpose: The gene *pigD*, which encodes the first enzyme in MAP biosynthesis, was deleted yielding the strain *P. putida* pig-r2 Δ*pigD*[31]. This strain biosynthesized only the MBC precursor and provided the ligase for condensation with fed MAP analogs to prodiginines. In addition, the introduction of only the MBC biosynthetic genes into the chromosome of *P. putida* resulted in strain MBC18, which

provided higher MBC levels than the strain pig-r2 Δ*pigD* and allowed for more efficient mutasynthesis. This strain was complemented by the introduction of the plasmid pVLT33-pigC-pigB to facilitate mutasynthesis[9]. In these studies, the ligase PigC was shown to have relaxed substrate specificity and monopyrrole feeding led to the production of diverse prodiginines[9,31,32]. Since this approach does not yet include an enzymatic cyclization reaction, we focused on the mutasynthetic production of cycloprodiginines in *P. putida* KT2440 strains by using the cyclase Prub680 and interesting sequence-homologous variants.

Scheme 1: Chemical structures of natural prodiginines and their cyclic derivatives.

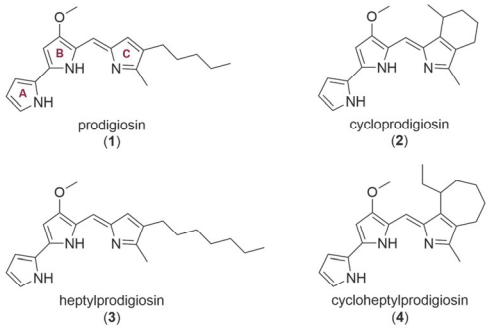

RESULTS AND DISCUSSION

Establishment of a mutasynthesis platform using prodiginine cyclases

Choosing a *P. putida*-based prodiginine mutasynthesis platform. We first aimed to examine if the previously established prodiginine mutasynthesis platforms based on *P. putida* KT2440 may be suitable for enzyme-based production of cyclic prodiginines[9,31,32]. The previously described Prub680 was used as starting point. A codon-usage adapted (c.a.) version of the respective gene was hence cloned. The resulting plasmids enabling P_{tac}-based expression were introduced into the strains *P. putida* pig-r2 Δ*pigD* (pVLT33-Prub680 (c.a.)) and MBC18 (pVLT33-pigCB-Prub680 (c.a.)) (**Figure S1, B**). Both strains were cultivated in LB medium supplemented with 0.25 mM MAP at 30 °C, the standard cultivation temperature for the host. Plasmid-based gene expression was induced by addition of 0.5 mM IPTG. After 24 h, cell pellet samples were extracted and subjected to HPLC-PDA analysis to determine the amount of prodigiosin and cycloprodigiosin using chemically synthesized references for peak identification and calibration (**Figure 1**).

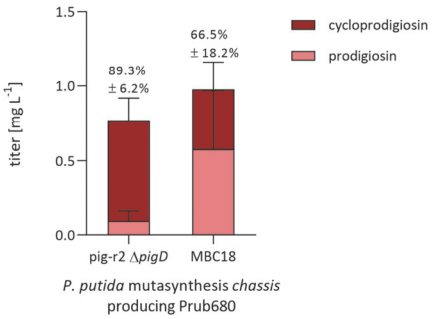

Figure 1: Evaluation of *P. putida* mutasynthesis *chassis* for cycloprodigiosin production.
The enzyme Prub680 was implemented in previously established mutasynthesis strains, resulting in the strains P. *putida* pig-r2 Δ*pigD* pVLT33-Prub680 (c.a.) and *P. putida* MBC18 pVLT33-pigCB-Prub680 (c.a.). Mutasynthesis was performed in LB medium at 30 °C with 0.25 mM MAP. The prodigiosin and cycloprodigiosin titer were calculated based on HPLC-PDA analyses. Percentage of cycloprodigiosin on the total prodiginine amount is given above the bars. The bars of prodigiosin (light red) and cycloprodigiosin (dark red) titers are superimposed. The data are means of biological triplicates with their corresponding standard deviation.

Cycloprodigiosin was observed in both strains. This confirmed that *prub680* can be functionally expressed in the host *P. putida*. Furthermore, it can be used in a mutasynthetic context, which means that prodigiosin built from intrinsically biosynthesized MBC and externally added MAP can be converted to cycloprodigiosin.

While the strain *P. putida* pig-r2 Δ*pigD* produced a high fraction of cycloprodigiosin relative to the total prodiginine titer (hereafter referred to as 'conversion') of approximately 89 ± 6%, the mutasynthesis strain MBC18 showed a higher total prodiginine production and also a higher cycloprodigiosin titer (presented as mg cycloprodigiosin in 1 L culture). However, the conversion to cycloprodigiosin was much lower here (about 67 ± 18%). This strain was selected for our further studies with the aim of increasing the cycloprodigiosin conversion in the culture.

Selection of cyclase candidates. Using Prub680 as starting point (NCBI Accession WP_010386914), we selected further candidate cyclases based on protein sequence similarity (via BLASTp) and based on descriptions about cyclic prodiginine production of the respective bacteria in the literature. Aside from *Pseudoalteromonas rubra*[17,18], other marine bacteria, namely *Pseudoalteromonas denitrificans*[19,20], *Vibrio gazogenes*[21,22], and *Zoochikella ganghwensis*[24,25], were also described to synthesize cycloprodigiosin. In addition, *Spartinivicinus ruber*, in which a protein with 48% identity

to Prub680 is encoded, produces cycloheptylprodigiosin[26] (**Figure S2, Table S1**).

The candidate genes of the four respective prodiginine cyclases were codon usage-adapted and cloned in the expression vector pVLT33-pigC-pigB.[9] HPLC-PDA analyses of the prodiginine extracts revealed that production of all candidate enzymes in *P. putida* led to the formation of cycloprodigiosin (**Figure 2**). This verified their enzymatic functions and that all can be functionally expressed in the host *P. putida* where they can be implemented in a mutasynthesis setup. However, differences in the conversion of prodigiosin to cycloprodigiosin could be observed. Generally, conversion of prodigiosin to cycloprodigiosin was less successful with the enzymes from *P. denitrificans, V. gazogenes, Z. ganghwensis*, or *S. ruber* cyclases than with Prub680 from *P. rubra*.

For the cyclase from *S. ruber*, we observed a small shift in the absorption maximum and in the retention time, which may indicate a structural difference. In contrast to cycloprodigiosin (**2**), which is the product of prodigiosin (**1**) cyclization, the cyclic prodiginine natively produced in *S. ruber* from heptylprodigiosin (**3**) possesses a seven membered ring (**4**). This may indicate functional differences in the enzymes which might thus produce different structures in prodigiosin cyclization. However, further investigation on this was not pursued in the study.

In the future, it may be interesting to expand the enzyme library as BLASTp analysis gave further results on potential homologous enzymes for cycloprodigiosin production in other *Pseudoalteromonas*, *Vibrio*, and *Zooshikella* species, but also in *Comamonas*, *Corallococcus*, and *Myxococcus* species. Some candidate cyclase sequences have already been described together with cycloprodigiosin production[23,25].

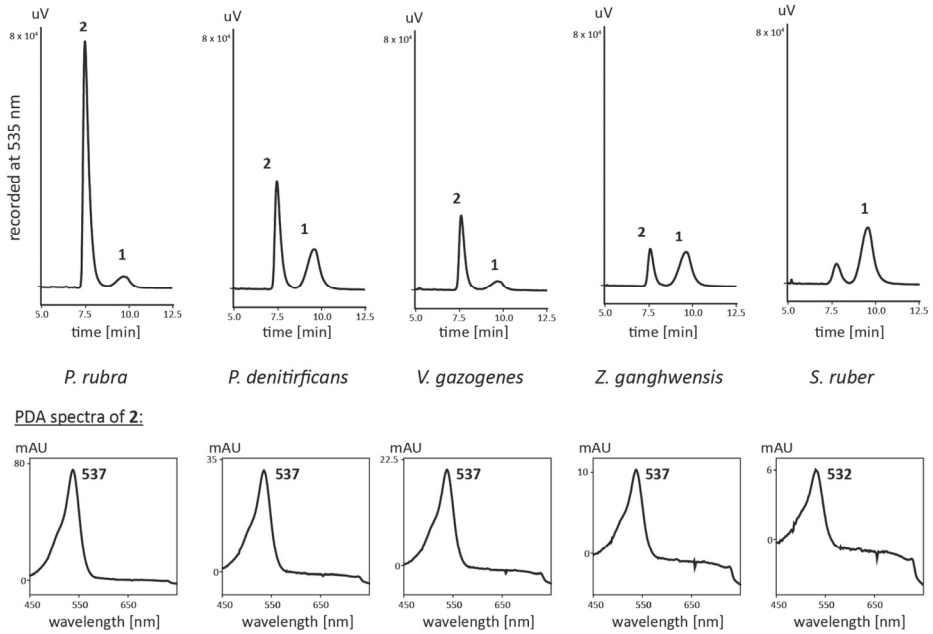

Figure 2: Evaluation of the suitability of homologous enzymes for the mutasynthetic production of cycloprodigiosin.
HPLC-PDA analysis of mutasynthesis extracts for all selected cyclases (using chemically synthesized prodigiosin (**1**) and cycloprodigiosin (**2**) for peak identification). Organisms from which the enzymes are derived are named.

Evaluation of cycloprodigiosin mutasynthesis

Adapting cultivation conditions for cycloprodigiosin mutasynthesis. We next aimed to facilitate production of cycloprodigiosin by analyzing different aspects influencing the production. The use of a richer complex medium has resulted in an increased production of prodiginines in recombinant *P. putida* strains as a higher cell mass is reached[33]. In cycloprodigiosin mutasynthesis approaches, however, the use of LB medium resulted in a 3.3-fold increase in cycloprodigiosin titers compared to richer TB medium (**Figure S3**). Therefore, only LB medium was used for the following experiments. Aside from the amount of the target product in the cultivation broth, the product mixture is of interest here, as the isolation of cycloprodigiosin from prodigiosin is tedious.

Since the cultivation temperature can have a significant influence on recombinant prodiginine production[9,33], we first

assessed cycloprodigiosin formation upon MAP supplementation (0.25 mM) of strain MBC18 with plasmid pVLT33-pigC-pigB-Prub680 (c.a.) at 30, 25, 20, and 15 °C. A temperature influence could be observed as the titers obtained increased with decreasing temperature, showing best results at cultivation temperatures of 25 and 20 °C, with a maximum of 90 ± 1.7% cycloprodigiosin relative to the total prodiginine titer obtained at 20 °C (**Table 1**).

For the cyclases derived from *P. denitrificans*, *V. gazogenes*, *Z. ganghwensis*, or *S. ruber*, similar results could be observed (**Table 1**). Both, a better conversion and an increase in cycloprodigiosin levels compared to cultivation at 30 °C could be detected with decreasing temperatures (except for 15 °C).

It may be worth mentioning that these results do not provide any information about the temperature optimum of Prub680 and the other cyclases, as we analyzed the temperature influence in our mutasynthesis strains where also expression efficiencies play a role, which were not further investigated in this study. However, our observations are consistent with previous studies: Cultivation of prodigiosin producers at lower temperatures has already led to higher prodigiosin production in previous biosynthetic and mutasynthetic approaches[31–33]. Furthermore, a psychrophilic behavior has been described for the enzyme PigC[34].

Table 1: Effect of cultivation temperature on mutasynthetic cycloprodigiosin production

	30 °C	25 °C	20 °C	15 °C	
Pr	60.2% ± 8.0%	66.6% ± 2.0%	90.0% ± 1.2%	96.8% ± 1.7%	conversion[1]
	-	4.2 ± 0.7	3.8 ± 0.2	0.5 ± 0.3	x-fold amount[2]
Pd	23.1% ± 3.9%	27.8% ± 2.1%	56.5% ± 1.4%	80.8% ± 3.0%	conversion[1]
	-	3.7 ± 2.0	3.6 ± 0.6	0.9 ± 0.3	x-fold amount[2]
Vg	26.1% ± 0.6%	33.1% ± 15.0%	77.6% ± 2.4%	84.5% ± 5.3%	conversion[1]
	-	2.6 ± 1.4	3.5 ± 0.7	0.6 ± 0.6	x-fold amount[2]
Zg	12.5% ± 1.2%	13.6% ± 2.5%	34.1% ± 1.0%	79.7% ± 19.8%	conversion[1]
	-	4.5 ± 1.8	4.3 ± 1.3	0.4 ± 0.1	x-fold amount[2]
Sr	6.6% ± 0.8%	8.0% ± 0.2%	21.5% ± 1.8%	68.8% ± 32.6%	conversion[1]
	-	2.2 ± 1.0	2.7 ± 0.5	0.6 ± 0.2	x-fold amount[2]

Cyclases are abbreviated according to the species from which they derive:
Pr (Prub680): *P. rubra*; Pd: *P. denitrificans*; Vg: *V. gazogenes*; Zg: *Z. ganghwensis*; Sr: *S. ruber*;
[1]% of cycloprodigiosin of total prodiginine titer; [2]x-fold amount of cycloprodigiosin titer compared to the experiment with the same cyclase at 30 °C;
mutasynthesis was performed in LB medium with 0.25 mM MAP.

Co-expression of cofactor biosynthetic genes. In previous studies, it could be shown, that the concentration of the fed MAP had only a small influence on the production of prodigiosin (it remained unaffected at concentrations between 250 µM and 1 mM)[9]. Thus, we focused on other factors influencing the production and focused on the cyclization step instead, especially as the other cyclases showed a lower conversion of prodigiosin to cycloprodigiosin than Prub680. For Prub680, a catalytic mechanism has been postulated suggesting that this enzyme uses bridged Fe_2O_2[35] or the cofactor tetrahydropterin, which forms a covalent adduct with O_2[36], for O_2 activation[17]. In some cases, a 4a-hydroxypterin is formed[37,38], in others only the dihydropterin was detectable[39,40]. Supplementation of iron ($Fe(II)SO_4$) to the medium did not influence cycloprodigiosin production (data not shown); we thus aimed to support cofactor availability. We assessed co-expression of PhhB from *P. aeruginosa* (WP_003085898.1) to accelerate the formation of dihydropterin and FolM from *E. coli* (WP_000520804.1), which enables the reduction to tetrahydropterin and shows also low activity for dihydrofolate (**Figure S4**)[41,42]. To this end, the codon-adapted genes were integrated into the *att*Tn7 site of *P. putida* under control of the constitutive synthetic promoter P_{em7} using a vector from the pYT series[43]. This vector carries the gene of the fluorescent protein EYFP as a transcription reporter (**Figure S5, A and B**). Additional expression of *phhB* and *folM* did not result in a higher cycloprodigiosin conversion with Prub680(**Figure S5, C**). Thus, there seems to be no limitation in the availability of the cofactor for Prub680 under the tested conditions. For the other cyclases, there was also no significant increase in cycloprodigiosin titers, but some showed a better conversion (% of cycloprodigiosin of total prodiginine titer) upon *phhB* and *folM* expression (**Figure S5, C**).

After evaluation of different conditions including cultivation and catalytic parameters, a maximum of 3.6 ±0.3 mg L^{-1} cycloprodigiosin was produced with the cyclase Prub680 from *P. rubra* (in strain MBC18/FolM-PhhB at 20 °C). This resulted in a 3.7-fold increase in the production titer compared to the initial titer achieved with strain MBC18 before adapting the conditions.

Cycloprodiginine mutasynthesis with a range of substrates

Next, we investigated the substrate acceptance of Prub680 and whether cycloprodigiosin derivatives could be produced in the established mutasynthesis setup. To this end, we synthesized MAP analogs (**6a – i**) that were differently substituted in the 2-position via a final *Trofimov* reaction (**Scheme 2**). Based on our previous studies on PigC substrate acceptance[31], we prepared monopyrroles with alkyl chains in 2-position of different length (C4-C8), as well as variants with terminal double bonds (chain length C5-C8). These were added to cultures of the *P. putida* mutasynthesis strain MBC18/FolM-PhhB carrying the gene *prub680* at 1 mM final concentration. As a control, *P. putida* MBC18/FolM-PhhB + pVLT33-pigC-pigB, which does not express the cyclase gene, was used to obtain the prodiginines with linear substitutions. As previously established, cell pellet samples were extracted after 24 h cultivation at

20 °C and subjected to HPLC-PDA analysis to evaluate whether Prub680 production resulted in new signals. In addition, samples were analyzed with respect to the expected masses by LC-MS to evaluate prodiginine production and conversion to a cyclic product.

Prodiginine derivatives were obtained upon feeding of monopyrroles in the control mutasynthesis strain (without cyclase gene) as expected. We also observed the conversion of C4 up to C8 chains to presumably new cyclic prodiginines when Prub680 was used (**Figure 3**, see details of HPLC-PDA analyses in **Figure S6**). Conversions were estimated based on the HPLC-PDA analyses (under the assumption of relatively similar extinction coefficients of the compounds). The best conversion was found with **6b** – **6d** (>80%), moderate conversion with **6e** (76%), and the least successful conversion with **6a** (<57%). The 4-pentenyl chain (**6f**) was not converted by the cyclase. Longer alkyl chains with a terminal double bond (**6g** – **6i**) gave moderate to very good conversion (73-93%).

In addition, the conversion of monopyrroles with a terminal double bond (**6g** – **6i**), which allows a further semisynthetic functionalization, such as hydroxylation[9], was investigated with the other four cyclases (**Figure S7 – S10**). As for Prub680, the conversion was estimated based on HPLC-PDA analyses (**Table 2**). The cyclases derived from *P. denitrificans* and *V. gazogenes* accepted the three different mutasynthons, but a lower conversion (40 – 63%) was observed compared to Prub680. The monopyrrole **6h** was also accepted by the cyclases derived from *Z. ganghwensis* and *S. ruber*. The first one also accepted the prodiginine obtained from mutasynthon **6i**. The 5-hexenyl chain (**6g**) was hardly converted by these two enzymes (**Figure S9** and **S10**).

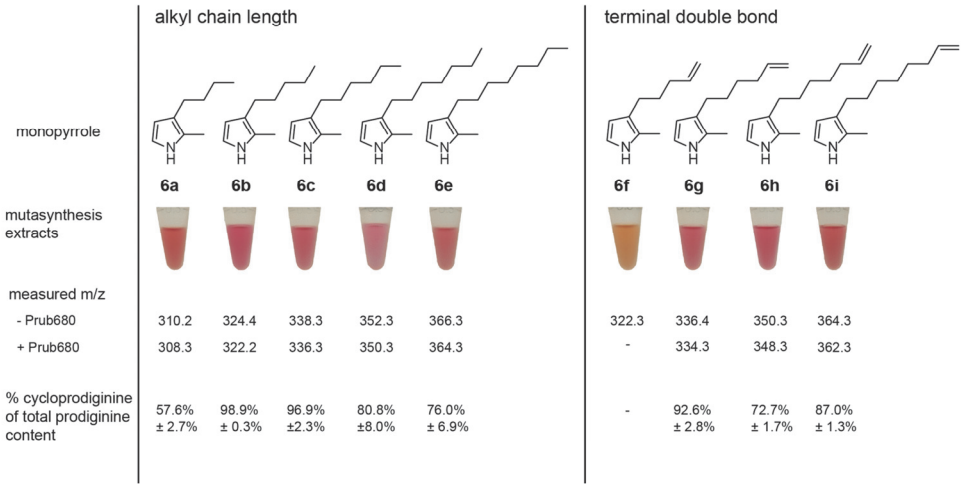

Figure 3: Prub680-based cycloprodiginine mutasynthesis with different monopyrroles.
Ethanolic extracts obtained from mutasynthesis with *P. putida* MBC18/FolM-PhhB pVLT33-pigCB-Prub680 (c.a.) after feeding monopyrroles **6a** – **6l** (1 mM) exhibited different pinkish colors. Mutasynthesis was performed in LB medium at 20 °C. An LC-MS analysis was performed for both, the prodiginines with linear substitutions derived from the control strain (-Prub680) and the assumed cycloprodiginine signal obtained from the mutasynthesis strain producing Prub680 (+Prub680), showing m/z corresponding to the respective expected proton adducts [M+H$^+$]. Cycloprodiginine conversion (% cycloprodigiosin of total prodiginine content) was estimated based on the HPLC-PDA analyses (assuming relatively similar extinction coefficients of the compounds). The conversion is given as the mean with the corresponding standard deviation.

Upscaled mutasynthesis production

For the mutasynthesis products of MAP and the analog carrying a 5-hexenyl chain, we assessed larger scale production in cultures with PU (poly urethane) foam cubes as used before for biosynthetic and mutasynthetic production of prodigiosin[31,33]. PU foam cubes serve as adsorbent for product extraction from the culture broth. First, we tested this experimental setup with MAP in a smaller cultivation volume (50 mL), to evaluate the conversion of prodigiosin to cycloprodigiosin in presence of PU (**Figure S11; A**). Analysis of the cell pellet and PU fractions obtained after extraction showed that binding of cycloprodigiosin to the adsorbent was effective and that a relatively high conversion to cycloprodigiosin (76% cycloprodigiosin of the total prodiginine titer) could be maintained under these conditions. Moreover, almost all produced cycloprodigiosin was found in the PU fraction (96% of total cycloprodigiosin titer), which enables a facilitated isolation (**Figure S11, B and C**). A titer of 2 mg L^{-1} was reached in crude extracts from 50 mL

culture upon feeding of 500 µM MAP. In addition, a mutasynthetic conversion in 1 L culture volume was performed under the same conditions as before. In this scale, we did not only investigate production of cycloprodigiosin upon MAP feeding but also explored the conversion of **6g** to its cyclic product. Feeding of MAP resulted in 1.3 mg L^{-1} cycloprodigiosin with a conversion of 98.5% in the PU fraction. For the cyclic product of **6g**, the titer was estimated to be 1.7 mg L^{-1} in the crude extract based on the calibration for cycloprodigiosin. Here, a similar high conversion (98.8% of the total prodiginine titer) to the cyclic derivative could be observed. In previous studies, feeding of MAP analogs with simple C5 to C12 rings without a stereo centrum led to mutasynthesis of 0.5 – 1.5 mg L^{-1} of the cyclic prodiginine in analytic scale and up to 3.1 mg L^{-1} in preparative scale[32]. The cycloprodiginine titers reached *via* mutasynthesis involving a cyclase in the present work are comparable to those levels.

Table 2: Assessment of different cyclases in cycloprodiginine mutasynthesis with different monopyrroles

Mono-pyrrole	Pr	Pd	Vg	Zg	Sr
6a	**x** (57.6 ±2.7%)	n.d.	n.d.	n.d.	n.d.
6b	**x** (98.9 ±0.3%)	**x** (68.2 ±9.6%)	**x** (85.7 ±2.8%)	**x** (39.7 ±2.5%)	**x** (35.3 ±8.2%)
6c	**x** (96.9 ±2.3%)	n.d.	n.d.	n.d.	n.d.
6d	**x** (80.8 ±8.0%)	n.d.	n.d.	n.d.	n.d.
6e	**x** (76.0 ±6.9%)	n.d.	n.d.	n.d.	n.d.
6f	-	n.d.	n.d.	n.d.	n.d.
6g	**x** (92.6 ±2.8%)	**x** (40.9 ±3.9%)	**x** (55.6 ±1.5%)	**(x)** (5.4% ±1.0%)	**(x)** (13.2 ±7.1%)
6h	**x** (72.7 ±1.7%)	**x** (57.5 ±6.4%)	**x** (56.8 ±14.4%)	**x** (36.7 ±13.4%)	**x** (36.6 ±5.1%)
6i	**x** (87.0 ±1.3%)	**x** (47.3 ±11.7%)	**x** (63.1 ±4.4%)	**x** (56.2 ±31.4%)	**(x)** (5.5 ±1.8%)

Cyclases are abbreviated according to the species from which they derive:
Pd: *P. denitrificans*; Vg: *V. gazogenes*; Zg: *Z. ganghwensis*; Sr: *S. ruber*;
x: addition of the mutasynthon led to a signal of the cyclic variant; **(x)**: very low signals of a cyclic variant; **-**: no signal for the cyclic variant was detected; n.d. not determined;
mutasynthesis was performed in LB medium at 20 °C with 1 mM MAP or analogs.

CONCLUSION

Already established *P. putida*-based mutasynthesis platforms could be extended for cycloprodigiosin production via combinatorial synthesis approaches. The cyclization of prodigiosin was possible with the already well described enzyme Prub680, but also with other sequence-homologs from different organisms. In the Prub680-conversion, cycloprodigiosin could be produced as the major compound (>98%) on a larger scale. Furthermore, a promiscuity of the cyclizing enzymes was described, especially for Prub680, allowing the production of novel cycloprodiginine derivatives.

METHODS

Bacterial strains. For cloning and conjugation, *Escherichia* coli DH5α[44], Stellar™ (Takara Bio, Cat# 636763), and S17.1[45] were cultivated in 10 mL liquid medium (LB (Luria/Miller) (10 g L^{-1} tryptone, 5 g L^{-1} yeast extract, 10 g L^{-1} sodium chloride; Carl Roth, Karlsruhe, Germany) or TB (terrific broth) (12 g L^{-1} casein, 24 g L^{-1} yeast extract, 12.54 g L^{-1} K_2HPO_4, 2.31 g L^{-1} KH_2PO_4, 4 mL L^{-1} glycerol; Carl Roth, Karlsruhe, Germany)) in 100 mL shaking flasks with continuous shaking (130 rpm) or on LB agar plates at 37 °C. Under standard conditions, *P. putida* MBC18[9] and *P. putida* pigr-2 Δ*pigD*[31] were cultivated in FlowerPlates (Beckman Coulter GmbH, Krefeld, Germany) in 1 mL LB medium at 1200 rpm and 30 °C. Antibiotics were added to the following final concentrations: for *E. coli*, 50 µg mL^{-1} kanamycin; for *P. putida*, 25 µg mL^{-1} kanamycin (or 100 µg mL^{-1} for plasmid-based expression in *P. putida* pig-r2 Δ*pigD*); 50 µg mL^{-1} irgasan; 50 µg mL^{-1} tetracycline; 25 µg mL^{-1} gentamicin; 50 µg mL^{-1} streptomycin.

Cloning and strain generation. The oligonucleotides used in this study are listed in **Table S2**. For the generation of the cycloprodigiosin mutasynthesis strains, the genes of the cyclizing enzymes from *P. rubra* (WP_010386914.1), *P. denitrificans* (WP_091980140.1), *V. gazogenes* (WP_072958698.1), *Z. ganghwensis* (WP_212720964.1), and *S. ruber* (WP_163833151.1) were codon-harmonized[46], further manually adapted (e.g., regarding undesired restriction sites, high GC regions), and synthesized (Twist Bioscience, South San Francisco, CA, USA) (**Table S3**). For MBC18-based mutasynthesis, vectors were generated by restriction and ligation cloning. For this purpose, pVLT33-pigCB-Prub680 (not published) and the corresponding synthesis vectors with a cyclase gene were hydrolyzed with *Hind*III and *Xho*I and subsequently ligated.

In addition, pVLT33[47] was linearized with *Eco*RI and *Xba*I and assembled by In-Fusion® cloning (In-Fusion® Snap Assembly, Takara Bio Europe, Saint-Germain-en-Laye, France) with the *prub680* (c.a.) fragment amplified by PCR (primers 1 and 2). For genomic insertion of additional cofactor recycling genes, *phhB* (WP_003085898.1) and *folM* (WP_000520804.1) were codon adapted and synthesized (**Table S3**). First, a promoter exchange was performed using the integration vector pYTNB01K-1G7[43] and the synthetic promoter P_{em7} from pQURE1-II[48,49]. The promoter region was amplified by PCR using oligos 3 and 4 and inserted into the linearized vector (PI-*Sce*I and *Asi*SI) by In-Fusion® cloning yielding vector pYTNB06K-1G7. In the second step, this vector was hydrolyzed with I-*Sce*I. The recycling genes were amplified by PCR (primers 5 and 6) and both fragments were assembled by In-Fusion® cloning resulting in

vector pYTNB07K-1G7. Correct vector assembly was verified by sequencing.

P. putida strains were transformed with the mutasynthesis vectors by electroporation as described previously[50]. Integration into the *att*Tn7 site was also performed as previously described[43]. The integration vector was transferred into *P. putida* MBC18 by conjugative transfer.

Mutasynthesis approaches. For analytical scale, main cultures of *P. putida* mutasynthesis strains pig-r2 Δ*pigD* or MBC18 carrying the respective vectors were inoculated to an optical density ($OD_{580\ nm}$) of 0.05 and incubated in FlowerPlates in 1 mL LB medium at 30 °C and 1200 rpm. At the logarithmic growth phase (after 4 h), gene expression was induced by the addition of 500 µM IPTG (100 mM stock in 70% ethanol). The chemically synthesized monopyrrole precursor (0.25 or 1 mM, final DMSO concentration of 1%) was also added at this time point. Cultivation was continued at 30, 25, 20, or15 °C with continuous shaking (1200 rpm) for 20 h. Changes in medium, temperature, and MAP concentration are indicated where appropriate. Cells were then separated by centrifugation (max. speed, 5 min, RT) and the supernatant was discarded. The cell pellet was extracted with 250 µL acidified ethanol (4% (*v*/*v*) 1 M HCl) as previously described[9,31]. The extracts were cleared by centrifugation and subjected to HPLC-PDA or LC-MS analysis.

PU foam cube experiments were performed in 50 mL and 2x500 mL scale. The culture broth was supplemented with 500 mg or 5 g PU cubes (Softpur foam, 25 kg m^{-3} density, 4 kPa compression hardness, each cube approximately 1 cm^3; Göllheim, Germany)[9]. Cultivation was performed as described for the analytical scale with 0.5 mM monopyrrole (**6b** and **6h**). After 24 h, PU foam cubes from both 500 mL cultures were combined and washed three times with water (in the same volume as the culture volume). For the 50 mL experiment, the PU foam cubes were manually extracted with 50 mL diethyl ether. After evaporation of the solvent, the crude prodiginine extract was resuspended in 12.5 mL acidified ethanol before further analyses.

For extraction from larger scale, the PU-cubes were washed and wrung thoroughly with distilled Et_2O. The solvent was removed under reduced pressure at 40 °C. This process was repeated until the extracted and concentrated solvent showed no further discoloration.

Analysis and quantification of prodiginines. Prodiginine and cycloprodiginine production was monitored by HPLC-PDA analysis (LC-10Ai series, Shimadzu GmbH, Kyoto, Japan; equipped with an SPD-M10Avp photodiode array detector (PDA)). A reversed-phase Accucore™ C18 (4.6 x 50 mm, 2.6 µm particle size, 80 Å pore size, Thermo Fisher Scientific, Waltham, MA, USA) was used at an oven temperature of 30 °C and a flow rate of 1 mL min^{-1}. 20 µL of the ethanol extracts were injected onto the column. The mobile phases used were water (A) and acetonitrile (B), both supplemented with 0.1% formic acid, were used. Analyses started at 5% B for 1.5 min, before a gradient was used for 1 min to reach 40% B. Then, B was increased to 50% within 15 min, followed by another increase to 98% B within 1.5 min. This ratio was maintained for 5 min and then decreased again to 5% B within 1 min. For re-equilibration, the last condition was again maintained for 9 min. The chromatograms were recorded at 535 nm. To identify and quantify the prodiginine signals, chemically synthesized references of prodigiosin[33] and cycloprodigiosin were used (SI-M1). For quantification, both, a prodigiosin calibration curve (using the synthetic reference) and a cycloprodigiosin calibration curve with an isolated sample (SI-M2) were used.

LC-MS analysis (HP 1100 Series LC/MSD, Agilent Technologies, Santa Clara, CA, USA equipped with a G1315A DAD detector) was used for the analysis of different cycloprodiginines produced after the addition of different monopyrrole precursors. The analysis was performed on the Accucore™ C18 column using the same method as described above. In addition, samples were analyzed on an ISQ single quadrupole mass spectrometer (positive mode; m/z range: 100 – 1000). The MS data were analyzed in terms of the (m/z) signals of the expected masses.

Chemical precursor syntheses. The general procedure towards 2-methyl-3-alkenyl-substituted pyrroles is based on previously published syntheses[31,51]. The four-stage synthesis comprises a *Weinrebamid* synthesis, a *Grignard*-reaction, a ketoxim synthesis, and a *Trofimov* reaction (**Scheme 2**).

Scheme 2: General reaction for the production of alkenyl-substituted pyrroles.

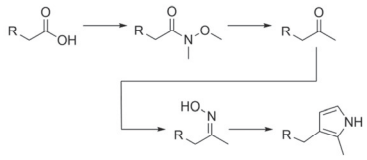

Detailed description of the synthesis of **6f** to **6i** is described in the SI (SI-M3).

ASSOCIATED CONTENT

Supporting Information. **Fig.S1**: *Pseudomonas putida* mutasynthesis *chassis*; **Fig. S2**: Multiple sequence alignment; **Fig. S3**: Evaluation of the cultivation media on the cycloprodigiosin mutasynthesis; **Fig. S4**: Proposed mechanism for cyclization and cofactor recycling; **Fig. S5**: Implementation of cofactor recycling genes in *P. putida* MBC18; **Fig. S6**: HPLC chromatograms for cycloprodiginine mutasynthesis with different monopyrroles; **Fig. S7**: HPLC chromatograms for cycloprodiginine mutasynthesis with the cyclase from *P. denitrificans*; **Fig. S8**: HPLC chromatograms for cycloprodiginine mutasynthesis with the cyclase from *V. gazogenes*; **Fig.S9**: HPLC chromatograms for cycloprodiginine mutasynthesis with the cyclase from *Z. ganghwensis*; **Fig. S10**: HPLC chromatograms for cycloprodiginine mutasynthesis with the cyclase from *S. ruber*; **Fig. S11**: Mutasynthetic production of cycloprodigiosin by supplementation with PU foam cubes; **Tab. S1**: Comparison of different cyclases; **Tab. S2**: Oligonucleotides used in this study; **Tab. S3**: Sequences of synthetic genes. The authors have described additional experimental procedures and cited additional references within the Supporting Information.

AUTHOR INFORMATION

Corresponding Author

*Email: j.pietruszka@fz-juelich.de; a.loeschcke@fz-juelich.de

Author Contributions

‡These authors contributed equally. A.L., K.-E.J., and J.P. conceived the concept. A.S., M.B., R.W., T.M.W., V.W., D.G., and N.L.B. performed the experiments. N.L.B., M.B., A.L., and J.P. drafted the manuscript.

NOTES

The authors declare no competing financial interest.

Funding Sources

The work was supported by the German Federal Ministry of Education and Research within the framework of the BMBF projects NO-STRESS (grant no. 031B0852B) and "Entwicklung der Modellregion BioökonomieREVIER Rheinland", grant number 031 B1134A/ 031 B1134AX.

ACKNOWLEDGMENT

The authors thank Birgit Henßen for analytical support.

ABBREVIATIONS

MAP, 2-methyl-3-amylpyrrole; MBC, 4-methoxy-2,2′bipyrrole-5-carbaldehyde; c.a., codon usage-adapted; PU, poly urethane;

REFERENCES

(1) Sakai-Kawada, F. E.; Ip, C. G.; Hagiwara, K. A.; Awaya, J. D. Biosynthesis and Bioactivity of Prodiginine Analogs in Marine Bacteria, *Pseudoalteromonas*: A Mini Review. *Front. Microbiol.* **2019**, *10*, 1715. https://doi.org/10.3389/fmicb.2019.01715.

(2) Stankovic, N.; Senerovic, L.; Ilic-Tomic, T.; Vasiljevic, B.; Nikodinovic-Runic, J. Properties and Applications of Undecylprodigiosin and Other Bacterial Prodigiosins. *Appl Microbiol Biotechnol* **2014**, *98* (9), 3841–3858. https://doi.org/10.1007/s00253-014-5590-1.

(3) Lapenda, J. C.; Silva, P. A.; Vicalvi, M. C.; Sena, K. X. F. R.; Nascimento, S. C. Antimicrobial Activity of Prodigiosin Isolated from *Serratia Marcescens* UFPEDA 398. *World J Microbiol Biotechnol* **2015**, *31* (2), 399–406. https://doi.org/10.1007/s11274-014-1793-y.

(4) You, Z.; Zhang, S.; Liu, X.; Zhang, J.; Wang, Y.; Peng, Y.; Wu, W. Insights into the Anti-Infective Properties of Prodiginines. *Appl Microbiol Biotechnol* **2019**, *103* (7), 2873–2887. https://doi.org/10.1007/s00253-019-09641-1.

(5) Gerber, N. N. A New Prodiginine (Prodigiosin-like) Pigment from *Streptomyces* - Antimalarial Activity of Several Prodiginines. *J Antibiot (Tokyo)* **1975**, *28* (3), 194–199. https://doi.org/10.7164/antibiotics.28.194.

(6) Marchal, E.; Smithen, D. A.; Uddin, Md. I.; Robertson, A. W.; Jakeman, D. L.; Mollard, V.; Goodman, C. D.; MacDougall, K. S.; McFarland, S. A.; McFadden, G. I.; Thompson, A. Synthesis and Antimalarial Activity of Prodigiosenes. *Org Biomol Chem* **2014**, *12* (24), 4132. https://doi.org/10.1039/c3ob42548g.

(7) Kancharla, P.; Kelly, J. X.; Reynolds, K. A. Synthesis and Structure–Activity Relationships of Tambjamines and B-Ring Functionalized Prodiginines as Potent Antimalarials. *J Med Chem* **2015**, *58* (18), 7286–7309. https://doi.org/10.1021/acs.jmedchem.5b00560.

(8) Habash, S. S.; Brass, H. U. C.; Klein, A. S.; Klebl, D. P.; Weber, T. M.; Classen, T.; Pietruszka, J.; Grundler, F. M. W.; Schleker, A. S. S. Novel Prodiginine Derivatives Demonstrate Bioactivities on Plants, Nematodes, and Fungi. *Front Plant Sci* **2020**, *11*. https://doi.org/10.3389/fpls.2020.579807.

(9) Kossmann, D. F.; Huang, M.; Weihmann, R.; Xiao, X.; Gätgens, F.; Weber, T. M.; Brass, H. U. C.; Bitzenhofer, N. L.; Ibrahim, S.; Bangert, K.; Rehling, L.; Mueller, C.; Tiso, T.; Blank, L. M.; Drepper, T.; Jaeger, K.-E.; Grundler, F. M. W.; Pietruszka, J.; Schleker, A. S. S.; Loeschcke, A. Production of Tailored Hydroxylated Prodiginine Showing Combinatorial Activity with Rhamnolipids against Plant-Parasitic Nematodes. *Front Microbiol* **2023**, *14*. https://doi.org/10.3389/fmicb.2023.1151882.

(10) D'Alessio, R.; Bargiotti, A.; Carlini, O.; Colotta, F.; Ferrari, M.; Gnocchi, P.; Isetta, A.; Mongelli, N.; Motta, P.; Rossi, A.; Rossi, M.; Tibolla, M.; Vanotti, E. Synthesis and Immunosuppressive Activity of Novel Prodigiosin Derivatives. *J Med Chem* **2000**, *43* (13), 2557–2565. https://doi.org/10.1021/jm001003p.

(11) Nakamura, A.; Magae, J.; Tsuji, R. F.; Yamasaki, M.; Nagai, K. Suppression of Cytotoxic T Cell Induction *in Vivo* by Prodigiosin 25-C. *Transplantation* **1989**, *47* (6), 1013–1016. https://doi.org/10.1097/00007890-198906000-00019.

(12) Manderville, R. Synthesis, Proton-Affinity and Anti-Cancer Properties of the Prodigiosin-Group Natural Products. *Current Medicinal Chemistry-Anti-Cancer Agents* **2001**, *1* (2), 195–218. https://doi.org/10.2174/1568011013354688.

(13) Williamson, N. R.; Fineran, P. C.; Gristwood, T.; Chawrai, S. R.; Leeper, F. J.; Salmond, G. P. Anticancer and Immunosuppressive Properties of Bacterial Prodiginines. *Future Microbiol* **2007**, *2* (6), 605–618. https://doi.org/10.2217/17460913.2.6.605.

(14) Hubbard, R.; Rimington, C. The Biosynthesis of Prodigiosin, the Tripyrrylmethene Pigment from *Bacillus Prodigiosus* (*Serratia Marcescens*). *Biochemical Journal* **1950**, *46* (2), 220–225. https://doi.org/10.1042/bj0460220.

(15) Rapoport, H.; Holden, K. G. The Synthesis of Prodigiosin. *J Am Chem Soc* **1962**, *84* (4), 635–642.

(16) Lattasch, H.; Thomson, R. H. A Revised Structure for Cycloprodigiosin. *Tetrahedron Lett* **1983**, *24* (26), 2701–2704. https://doi.org/10.1016/S0040-4039(00)87981-2.

(17) de Rond, T.; Stow, P.; Eigl, I.; Johnson, R. E.; Chan, L. J. G.; Goyal, G.; Baidoo, E. E. K.; Hillson, N. J.; Petzold, C. J.; Sarpong, R.; Keasling, J. D. Oxidative Cyclization of Prodigiosin by an Alkylglycerol Monooxygenase-like Enzyme. *Nat Chem Biol* **2017**, *13* (11), 1155–1157. https://doi.org/10.1038/nchembio.2471.

(18) Johnson, R. E.; de Rond, T.; Lindsay, V. N. G.; Keasling, J. D.; Sarpong, R. Synthesis of Cycloprodigiosin Identifies the Natural Isolate as a Scalemic Mixture. *Org Lett* **2015**, *17* (14), 3474–3477. https://doi.org/10.1021/acs.orglett.5b01527.

(19) Kawauchi, K.; Shibutani, K.; Yagisawa, H.; Kamata, H.; Nakatsuji, S.; Anzai, H.; Yokoyama, Y.; Ikegami, Y.; Moriyama, Y.; Hirata, H. A Possible Immunosuppressant, Cycloprodigiosin Hydrochloride, Obtained from *Pseudoalteromonas Denitrificans*. *Biochem Biophys Res Commun* **1997**, *237* (3), 543–547. https://doi.org/10.1006/bbrc.1997.7186.

(20) Kim, H.-S.; Hayashi, M.; Shibata, Y.; Wataya, Y.; Mitamura, T.; Horii, T.; Kawauchi, K.; Hirata, H.; Tsuboi, S.;

from *Pseudoalteromonas Denitrificans* Is a Potent Antimalarial Agent. *Biol Pharm Bull* **1999**, *22* (5), 532–534. https://doi.org/10.1248/bpb.22.532.

(21) Gerber, N. N. Cycloprodigiosin from *Beneckea Gazogenes*. *Tetrahedron Lett* **1983**, *24* (27), 2797–2798. https://doi.org/10.1016/S0040-4039(00)88026-0.

(22) Allen, G. R.; Reichelt, J. L.; Gray, P. P. Influence of Environmental Factors and Medium Composition on *Vibrio Gazogenes* Growth and Prodigiosin Production. *Appl Environ Microbiol* **1983**, *45* (6), 1727–1732. https://doi.org/10.1128/aem.45.6.1727-1732.1983.

(23) Vitale, G. A.; Sciarretta, M.; Palma Esposito, F.; January, G. G.; Giaccio, M.; Bunk, B.; Spröer, C.; Bajerski, F.; Power, D.; Festa, C.; Monti, M. C.; D'Auria, M. V.; de Pascale, D. Genomics–Metabolomics Profiling Disclosed Marine *Vibrio Spartinae* 3.6 as a Producer of a New Branched Side Chain Prodigiosin. *J Nat Prod* **2020**, *83* (5), 1495–1504. https://doi.org/10.1021/acs.jnatprod.9b01159.

(24) Ramaprasad, E. V. V.; Bharti, D.; Sasikala, Ch.; Ramana, Ch. V. *Zooshikella Marina* Sp. Nov. a Cycloprodigiosin- and Prodigiosin-Producing Marine Bacterium Isolated from Beach Sand. *Int J Syst Evol Microbiol* **2015**, *65* (Pt_12), 4669–4673. https://doi.org/10.1099/ijsem.0.000630.

(25) Lee, J. S.; Kim, Y.-S.; Park, S.; Kim, J.; Kang, S.-J.; Lee, M.-H.; Ryu, S.; Choi, J. M.; Oh, T.-K.; Yoon, J.-H. Exceptional Production of Both Prodigiosin and Cycloprodigiosin as Major Metabolic Constituents by a Novel Marine Bacterium, *Zooshikella Rubidus* S1-1. *Appl Environ Microbiol* **2011**, *77* (14), 4967–4973. https://doi.org/10.1128/AEM.01986-10.

(26) Huang, Z.; Dong, L.; Lai, Q.; Liu, J. *Spartinivicinus Ruber* Gen. Nov., Sp. Nov., a Novel Marine Gammaproteobacterium Producing Heptylprodigiosin and Cycloheptylprodigiosin as Major Red Pigments. *Front Microbiol* **2020**, *11*, 2056. https://doi.org/10.3389/fmicb.2020.02056.

(27) Williamson, N. R.; Fineran, P. C.; Leeper, F. J.; Salmond, G. P. C. The Biosynthesis and Regulation of Bacterial Prodiginines. *Nat Rev Microbiol* **2006**, *4* (12), 887–899. https://doi.org/10.1038/nrmicro1531.

(28) Williamson, N. R.; Simonsen, H. T.; Ahmed, R. A. A.; Goldet, G.; Slater, H.; Woodley, L.; Leeper, F. J.; Salmond, G. P. C. Biosynthesis of the Red Antibiotic, Prodigiosin, in *Serratia*: Identification of a Novel 2-Methyl-3-n-Amyl-Pyrrole (MAP) Assembly Pathway, Definition of the Terminal Condensing Enzyme, and Implications for Undecylprodigiosin Biosynthesis in *Streptomyces*. *Mol Microbiol* **2005**, *56* (4), 971–989. https://doi.org/10.1111/j.1365-2958.2005.04602.x.

(29) Sydor, P. K.; Barry, S. M.; Odulate, O. M.; Barona-Gomez, F.; Haynes, S. W.; Corre, C.; Song, L.; Challis, G. L. Regio- and Stereodivergent Antibiotic Oxidative Carbocyclizations Catalysed by Rieske Oxygenase-like Enzymes. *Nat Chem* **2011**, *3* (5), 388–392. https://doi.org/10.1038/nchem.1024.

(30) Krishna, P. S.; Vani, K.; Prasad, M. R.; Samatha, B.; Bindu, N. S. V. S. S.; Charya, M. A. S.; Reddy Shetty, P. *In –Silico* Molecular Docking Analysis of Prodigiosin and Cycloprodigiosin as COX-2 Inhibitors. *Springerplus* **2013**, *2* (1), 172. https://doi.org/10.1186/2193-1801-2-172.

(31) Klein, A. S.; Domröse, A.; Bongen, P.; Brass, H. U. C.; Classen, T.; Loeschcke, A.; Drepper, T.; Laraia, L.; Sievers, S.; Jaeger, K.; Pietruszka, J. New Prodigiosin Derivatives Obtained by Mutasynthesis in *Pseudomonas Putida*. *ACS Synth Biol* **2017**, *6* (9), 1757–1765. https://doi.org/10.1021/acssynbio.7b00099.

(32) Klein, A. S.; Brass, H. U. C.; Klebl, D. P.; Classen, T.; Loeschcke, A.; Drepper, T.; Sievers, S.; Jaeger, K.; Pietruszka, J. Preparation of Cyclic Prodiginines by Mutasynthesis in *Pseudomonas Putida* KT2440. *ChemBioChem* **2018**, *19* (14), 1545–1552. https://doi.org/10.1002/cbic.201800154.

(33) Domröse, A.; Klein, A. S.; Hage-Hülsmann, J.; Thies, S.; Svensson, V.; Classen, T.; Pietruszka, J.; Jaeger, K.-E.; Drepper, T.; Loeschcke, A. Efficient Recombinant Production of Prodigiosin in *Pseudomonas Putida*. *Front Microbiol* **2015**, *6*, 972. https://doi.org/10.3389/fmicb.2015.00972.

(34) You, Z.; Liu, X.; Zhang, S.; Wang, Y. Characterization of a Prodigiosin Synthetase PigC from *Serratia Marcescens* Jx-1 and Its Application in Prodigiosin Analogue Synthesis. *Biochem Eng J* **2018**, *134*, 1–11. https://doi.org/10.1016/j.bej.2018.01.034.

(35) Banerjee, R.; Proshlyakov, Y.; Lipscomb, J. D.; Proshlyakov, D. A. Structure of the Key Species in the Enzymatic Oxidation of Methane to Methanol. *Nature* **2015**, *518* (7539), 431–434. https://doi.org/10.1038/nature14160.

(36) Roberts, K. M.; Fitzpatrick, P. F. Mechanisms of Tryptophan and Tyrosine Hydroxylase. *IUBMB Life* **2013**, *65* (4), 350–357. https://doi.org/10.1002/iub.1144.

(37) Moran, G. R.; Derecskei-Kovacs, A.; Hillas, P. J.; Fitzpatrick, P. F. On the Catalytic Mechanism of Tryptophan Hydroxylase. *J Am Chem Soc* **2000**, *122* (19), 4535–4541. https://doi.org/10.1021/ja994479a.

(38) Ellis, H. R.; Daubner, S. C.; Fitzpatrick, P. F. Mutation of Serine 395 of Tyrosine Hydroxylase Decouples Oxygen−oxygen Bond Cleavage and Tyrosine Hydroxylation. *Biochemistry* **2000**, *39* (14), 4174–4181. https://doi.org/10.1021/bi9928546.

(39) Daubner, S. C.; Fitzpatrick, P. F. Site-Directed Mutants of Charged Residues in the Active Site of Tyrosine Hydroxylase. *Biochemistry* **1999**, *38* (14), 4448–4454. https://doi.org/10.1021/bi983012u.

(40) Chow, M. S.; Eser, B. E.; Wilson, S. A.; Hodgson, K. O.; Hedman, B.; Fitzpatrick, P. F.; Solomon, E. I. Spectroscopy and Kinetics of Wild-Type and Mutant Tyrosine Hydroxylase: Mechanistic Insight into O_2 Activation. *J Am Chem Soc* **2009**, *131* (22), 7685–7698. https://doi.org/10.1021/ja810080c.

(41) Lin, Y.; Sun, X.; Yuan, Q.; Yan, Y. Engineering Bacterial Phenylalanine 4-Hydroxylase for Microbial Synthesis of Human Neurotransmitter Precursor 5-Hydroxytryptophan. *ACS Synth Biol* **2014**, *3* (7), 497–505. https://doi.org/10.1021/sb5002505.

(42) Pribat, A.; Blaby, I. K.; Lara-Núñez, A.; Gregory, J. F.; de Crécy-Lagard, V.; Hanson, A. D. FolX and FolM Are Essential for Tetrahydromonapterin Synthesis in *Escherichia Coli* and *Pseudomonas Aeruginosa*. *J Bacteriol* **2010**, *192* (2), 475–482. https://doi.org/10.1128/JB.01198-09.

(43) Weihmann, R.; Kubicki, S.; Bitzenhofer, N. L.; Domröse, A.; Bator, I.; Kirschen, L.-M.; Kofler, F.; Funk, A.; Tiso, T.; Blank, L. M.; Jaeger, K.-E.; Drepper, T.; Thies, S.; Loeschcke, A. The Modular PYT Vector Series Employed for Chromosomal Gene Integration and Expression to Produce Carbazoles and Glycolipids in *P. Putida*. *FEMS Microbes* **2023**, *4*, 1–17. https://doi.org/10.1093/femsmc/xtac030.

(44) Hanahan, D. Studies on Transformation of *Escherichia Coli* with Plasmids. *J Mol Biol* **1983**, *166*, 557–580.

(45) Simon, R.; Priefer, U.; Pühler, A. A Broad Host Range Mobilization System for *in Vivo* Genetic Engineering: Transposon Mutagenesis in Gram Negative Bacteria.

Bio/Technology **1983**, *1* (9), 784–791. https://doi.org/10.1038/nbt1183-784.

(46) Claassens, N. J.; Siliakus, M. F.; Spaans, S. K.; Creutzburg, S. C. A.; Nijsse, B.; Schaap, P. J.; Quax, T. E. F.; van der Oost, J. Improving Heterologous Membrane Protein Production in *Escherichia Coli* by Combining Transcriptional Tuning and Codon Usage Algorithms. *PLoS One* **2017**, *12* (9), e0184355. https://doi.org/10.1371/journal.pone.0184355.

(47) de Lorenzo, V.; Eltis, L.; Kessler, B.; Timmis, K. N. Analysis of *Pseudomonas* Gene Products Using *LacIq*/Ptrp-Lac Plasmids and Transposons That Confer Conditional Phenotypes. *Gene* **1993**, *123* (1), 17–24. https://doi.org/10.1016/0378-1119(93)90533-9.

(48) Volke, D. C.; Friis, L.; Wirth, N. T.; Turlin, J.; Nikel, P. I. Synthetic Control of Plasmid Replication Enables Target- and Self-Curing of Vectors and Expedites Genome Engineering of *Pseudomonas Putida*. *Metab Eng Commun* **2020**, *10*, e00126. https://doi.org/10.1016/j.mec.2020.e00126.

(49) Nikel, P. I.; Pérez-Pantoja, D.; de Lorenzo, V. Why Are Chlorinated Pollutants so Difficult to Degrade Aerobically? Redox Stress Limits 1,3-Dichloprop-1-Ene Metabolism by *Pseudomonas Pavonaceae*. *Philosophical Transactions of the Royal Society B: Biological Sciences* **2013**, *368* (1616), 20120377. https://doi.org/10.1098/rstb.2012.0377.

(50) Tu, Q.; Yin, J.; Fu, J.; Herrmann, J.; Li, Y.; Yin, Y.; Stewart, A. F.; Müller, R.; Zhang, Y. Room Temperature Electrocompetent Bacterial Cells Improve DNA Transformation and Recombineering Efficiency. *Sci Rep* **2016**, *6* (1), 24648. https://doi.org/10.1038/srep24648.

(51) Kancharla, P.; Li, Y.; Yeluguri, M.; Dodean, R. A.; Reynolds, K. A.; Kelly, J. X. Total Synthesis and Antimalarial Activity of 2-(*p*-Hydroxybenzyl)-Prodigiosins, Isoheptylprodigiosin, and Geometric Isomers of Tambjamine MYP1 Isolated from Marine Bacteria. *J Med Chem* **2021**, *64* (12), 8739–8754. https://doi.org/10.1021/acs.jmedchem.1c00748.

III. General Discussion and Perspectives

Within this thesis, the potential of the Gram-negative bacterium *Pseudomonas putida* KT2440 was harnessed to generate robust producer strains of different classes of NPs with emphasis on bacterial alkaloids. Various strategies and approaches for genetic and metabolic as well as physiological engineering were evaluated. Additionally, access to non-natural derivatives of the investigated NPs was enabled by combining biosynthetic concepts with chemical approaches.

In the first chapter, the benefits of a robust microbial *chassis* for an efficient, high-level production of NPs have been discussed (**II.1, Publication I**[219]). Here, the hitherto described major stress resistance strategies of *Pseudomonas* species have been reviewed. Opportunities for an exploitation of such traits for producer strain development have been pointed out. Furthermore, approaches for the identification of new tolerance traits along with their potential usefulness to engineer a next-generation *chassis* have been highlighted. The discussion of the current state of research led to the conclusion that an understanding of the exact mechanisms underlying a tolerance is increasing but their targeted exploitation and engineering is only just starting. For example, genetic factors of vesiculation in *Pseudomonas* are for the most part not precisely clear and therefore, biotechnological strain development had not included this aspect thus far. The currently available toolbox for genetic engineering, which will help to unlock tolerance traits for strain engineering, has been presented within this work. Here, a range of different tools was available which facilitate the expression of genes, as well as strain engineering, e.g., via gene deletion. It appears important to utilize standardized tools to spur the developments in the field even more. Besides these aspects, pathway regulation has been identified as another central aspect for the generation of an efficient *chassis*, and hence, effective measures of pathway fine-tuning have been presented.

In the following chapters, the identified requirements for the generation of a robust *P. putida* platform have been put into practice. Here, the basic step of biosynthetic gene expression was addressed first. Namely, a genetic toolbox, the so-called pYT vector series, facilitating genomic integration of biosynthetic genes, was constructed (**II.2**). It allows for customization regarding the integration mode (random, at *att*Tn7, or into the 16S rRNA gene), the promoter, the transcription reporter, as well as the antibiotic resistance marker. The straightforward generation of effective *P. putida*-based producer strains for NPs like rhamnolipids, violacein, and arcyriaflavin A, showcased the suitability of this new standardized and fully modular toolbox.

The influence of physiological engineering strategies on the production of different NPs, especially alkaloids, has been investigated in chapter **II.3**. First, a correlation of vesiculation and NP production in *P. putida* could be demonstrated for the first time for the tripyrrole prodigiosin. This contributes to the understanding why the bacterium appears to have a pronounced resistance to this compound, not only in exposure experiments but also when used as a production host. Following that, a range of genes was verified to be involved in vesiculation.

Finally, OMV formation was exploited as a tolerance strategy and engineering of vesiculation-related gene targets resulted not only in hypervesiculation but supported the recombinant production of NPs. This was evaluated for prodigiosin, (deoxy-)violacein, a phenazine, as well as a carotenoid.

Using a previously generated NP producer and applying the knowledge of the impact of OMV formation on production (from chapter II.2 and II.3), biosynthesis of the bisindole arcyriaflavin A was enhanced (**II.4**). In an integrative approach, which, besides physiological engineering, also considered bioprocess parameters including the cultivation in the presence of an adsorber material for the production, limitations in the biosynthesis of arcyriaflavin A could be overcome.

Lastly, the engineering of new *P. putida* platforms has been pursued to facilitate access to diverse prodiginines (**II.5**). Combining different biosynthetic concepts with chemically prepared building blocks and late-stage chemical conversion (the so-called CHEM-BIO-CHEM strategy) helped to generate a *chassis* for the production of non-natural hydroxylated prodigiosin (**II.5.1**). In a CHEM-BIO-BIO approach, in which the before established mutasynthesis platform (II.5.1) was expanded by further biosynthetic genes, an effective cycloprodigiosin producer was developed for the first time in *P. putida* (**II.5.2**). Here, the desired NP was found to be almost the only product solving the problems previously encountered with whole-cell biosynthesis of cycloprodigiosin in *P. putida* so far[327].

In the following, each section will give a summary of the investigations and gained insights, a classification of the results in the scientific context, and further perspectives in research regarding the aspects discussed. Special emphasis will be put on the following three aspects which affect the potential of *P. putida* as a robust platform for the synthesis of bioactive NPs the most: (i) the generation of stable producer strains (**III.1**), (ii) the provision of access to a diverse portfolio of valuable compounds (**III.2**), (iii) the optimization of the respective bioprocess (**III.3**). Finally, the focus will be shifted towards determining whether a standardized procedure exists for transforming *P. putida* into a robust and highly efficient production platform, which may be applicable for any NP of interest.

III.1. Stable and effective strain development

The possibility to genomically integrate a heterologous BGC in a straightforward way as well as to control and orchestrate its expression is decisive for the generation of stable and effective production platforms. This thought is not at all new in the field of recombinant NP production and has already resulted in the rise of a multitude of cloning and expression strategies[204,256]. Thus, effective tools have been developed for the genomic integration comprising random transposition[99,286] or site-specific integration via transposase-, integrase-, and recombination-based strategies[240,246,289]. Building on previous developments in standardized vector systems[258–260], a fully modular genetic toolbox allowing for a rapid ligase-independent cloning has been constructed (**Publication II**[136]). In the following, the conceptualization, and the modular structure of the so-called pYT toolbox are shortly summarized and biotechnological applications based on this vector series are compared with each other.

The pYT vector series was constructed to facilitate the chromosomal integration and expression of BGCs in *Pseudomonas*. In general, the pYT toolbox is differentiated from its predecessors, the TREX and the yTREX system[99,239], in the realization of a customizable series. The most significant innovation compared to other systems is the flexibility of the chromosomal integration mode. The first option is the random integration via transposon Tn5 yielding strains, in which the target BGC can be integrated downstream of a chromosomal promoter[406]. However, identification of the clones, which actually express the integrated gene cluster, is required. To easily screen a multitude of clones, transcription reporters can be used[226,407]. Previous studies revealed the *rrn* operons as exceptionally suitable for high-level and stable gene expression in *Pseudomonas*[251,408]. Thus, the second option for chromosomal integration is the direct *rrn* targeting into one of the seven 16S rRNA genes[255,409] – enabled by preinstalled landing pads. Site-specific integration at the *att*Tn7 site by the transposase Tn7 has been chosen as the last integration mode. The Tn7 transposon has already been widely used for the fast generation of stable recombinant strains, especially as it allows comparative studies (e.g., of different genes or promoters) without an effect of the genomic position[267,291,410]. These three integration modes define the distinct fundamental vectors of the pYT series.

In addition, the pYT toolbox allows a facilitated and comfortable exchange of the elements of the integrative sequence, referred to as the YT_core, including the antibiotic resistance marker, the used transcription reporter, and the promoter. Regarding the cloning effort, it also enables easy implementation of the desired biosynthetic genes or BGCs. To ensure straightforward adaptability, modularity of the included elements was granted by restriction endonuclease and homing endonuclease recognition sequences which are flanked by randomized sequences (**Figure III-1**). This allows insertion and exchange of the elements at a designated position either by restriction and ligation cloning or by assembly of complementary strands. Due to their

unique sequence, the implementation of homing endonuclease sites allows later adaptations in constructs already carrying a BGC. Although this modular structure offers a wide variety of possible integrable elements based on the user's need, ready-to-use vectors with different combinations of promoter, transcription reporters, and antibiotic markers were built and their functionality was validated (**Publication II**[136] and **VI**, [411,412]). The used promoters (P_{nagAa}, P_{em7}) as well as the fluorescent (eYFP, mTagBFP2, mCherry) and enzymatic transcription reporters (polyester hydrolase (PE-H), β-galactosidase (LacZ), β-glucuronidase (GUS)) were chosen based on their applicability in previous studies[235,284,313,413–416]. For the enzymatic reporters, the availability of an easy screening method was considered a priority in the selection process[226,416–418]. Counting in all ready-to-use pYT vectors available for *P. putida* strain development, 29 vectors have been built for the chromosomal integration and expression of BGCs[136,235,411,412].

Further, the pYT series was proven to be applicable for NP biosynthesis for all three integration modes (random, at *att*Tn7, into the *rrn* operon) in several studies as well as related bachelor and master theses (**Publication II**[136], **IV**[419], and **VI**, [411,412,420]). They explored the development of strains for producing compounds that have already been biosynthesized using *P. putida*, such as (deoxy-)violacein[99] cycloprodigiosin[327], and RLs[234,235,237,303], as well as new-to-*P. putida* NPs (arcyriaflavin A and aurachins) (**Table III-1**).

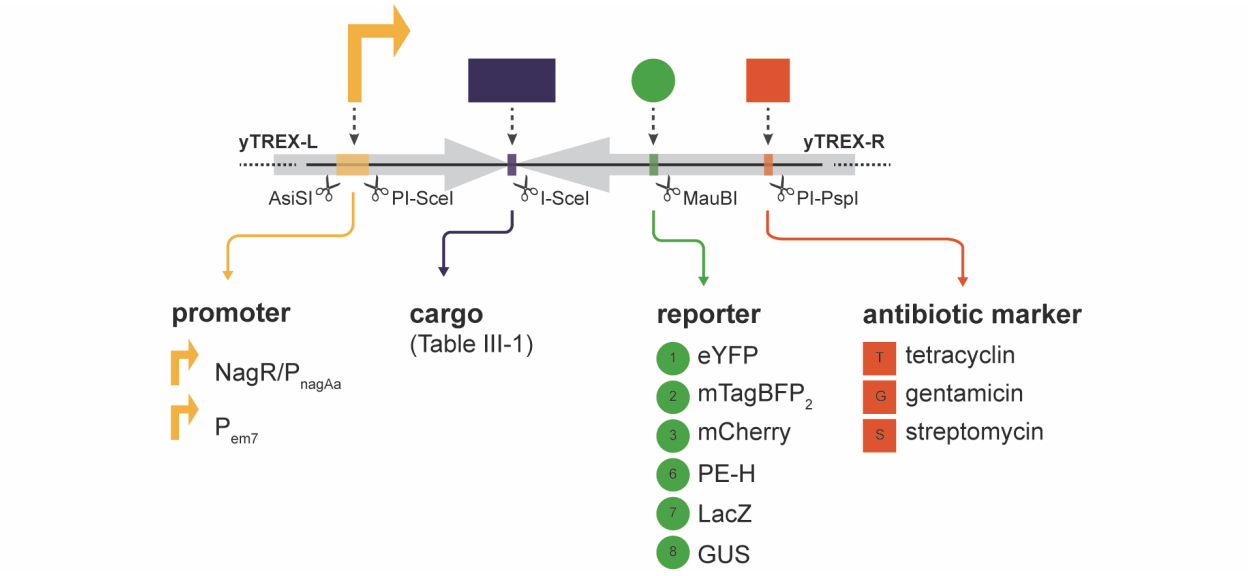

Figure III-1: Schematic integrative YT_core sequence of the modular pYT vector series.
The modular structure of the pYT vectors enable an easy exchange of different promoters (yellow arrow), transcription reporters (green circle), and antibiotic resistance markers (orange square). The integration site for the biosynthetic genes is located between the promoter and reporter element (blue rectangle). Restriction endonuclease and homing endonuclease sites allow for precise integration and exchange. Pre-evaluated and readily available promoters, reporters, and antibiotic markers are presented. Taking together all constructed pYT vectors for random integration, integration at the *att*Tn7 site, and into the *rrn* operon, 29 ready-to-use vectors are available (random (Tn5): 11 vectors; *rrn* operon: 6 vectors; *att*Tn7 site: 10 vectors). These have been primarily generated in **Publication II**[136], but the vector series was extended in the framework of the master theses of Maximilian Spindler and Anka Siebericchs[411,412] and **Publication VI**. Examples of their application on NP production are given in **Table III-1**. PE-H: polyester hydrolase; LacZ: β-galactosidase; GUS: β-glucuronidase.

Table III-1: Summary of pYT-based vectors applied for NP production in *P. putida* KT2440.
[1]parts of *vioD* were deleted/mutated; [2]produced in mutasynthetic approaches; [3]combined with different promoters, integrated directly before these genes; [4]P_{nagAa} promoter was used; [5]genes were used for recycling of cofactors.

integration mode	biosynthetic genes (cargo)	NP production applied for	reference
random (Tn5)	*vioABCDE*	(deoxy-)violacein	**Publication II**[136]
	vioABCE[1]	violacein	
	rebODCP	arcyriaflavin A	
	MVA-*ispA*	β-caryophyllene, aurachin D[2]	[412]
rrn operon	*vioABCE*[1]	deoxyviolacein	**Publication II**[136]
	rebODCP	arcyriaflavin A	
	auaAF	aurachin D[2]	[420]
*att*Tn7	*rhlAB*[3]	RLs	**Publication II**[136]
	rhlABrmlBDAC[4]		
	rhlABrmlBDACalgC[4]		
	rebODCP	arcyriaflavin A	**Publication II**[136] and **IV**[419]
	auaAF	aurachin D[2]	[412]
	folM,phhB	cycloprodigiosin[5]	**Publication VI**, [411]

III.1.1. Advantages of a modular toolbox

In the age of synthetic biology, consistent and customizable vector architecture is a central prerequisite for molecular genetic research[421]. Around the turn of the millennium, progress has been made in this field and since then, further collections of vectors were constructed and continuously expanded[258–260,422–424]. These developments underline the value of modular genetic tools for strain generation.

The design of the pYT series has several advantages. Firstly, it offers the user a flexibility in the integration mode - a capability previously lacking in other collections. On the one hand, it offers a selection of different strategies to choose from, while on the other hand, the same structure enables a facilitated and rapid comparison of different integration and expression strategies between vectors. The influence of the different modes of expression has been shown for arcyriaflavin A production in *P. putida*. Here, integration at the *att*Tn7 site under the control of the inducible P_{nagAa} promoter was found to be the most suitable (**Publication II**[136]).

The implementation of homing endonuclease recognition sites (e.g., for PI-SceI, I-SceI, PI-PspI) is also advantageous compared to other vector collections. As the homing endonucleases recognize longer, asymmetric sequences of 15 to 40 bp[425], the probability of a recognition site occurring in the chosen promoter-, reporter-, or marker sequence is low. Furthermore, it also allows for modification of the pYT vector after insertion of the generally larger biosynthetic genes, as there is a rather low probability for the occurrence of the recognition sequences in BGCs. Classical restriction sites can normally never be used again after this step as they typically occur within the BGC. Within the master theses of Maximilian Spindler and Anka Sieberichs, the homing endonuclease sequences could be used for exchange of the transcription reporter (mCherry → LacZ)[412] and the promoter (P_{nagAa} → P_{em7})[411], respectively.

The adaptation of the reporter provided, for example, vectors for a simultaneous application of two integration modes (random, at *att*Tn7) which allows for implementation of biosynthetic genes and a metabolic engineering module for precursor biosynthesis, respectively. Thus, the modular structure of the toolbox enables an easy and rapid construction *á la carte* by integrating and exchanging elements at will or by the targeted selection of an integration mode.

III.1.2. Is there a favored expression mode?

The advantages of the modular pYT vector series have been described, however the question remains as to whether the conducted studies indicated a favorable integration mode. For recombinant prodigiosin production in *P. putida*, genomic integration into the 16S rRNA genes seemed to be favorable[251]. The observation was made during Tn5 usage and was one reason for pursuing a targeted integration system for 16S rRNA integration. This does not lead to the conclusion that this integration mode should be preferred for any BGC expression and respective NP production. Thus, all three integration modes of the pYT toolbox were applied for production of different NP classes (**Table III-1**). Random integration by transposon Tn5 as well as targeted integration into the 16S rRNA genes facilitated the generation of (deoxy-)violacein producers using the pYT vectors (**Publication II**[136]). Tn5 transposition resulted in comparable titers as previously obtained with the yTREX system (about 120 mg L^{-1})[99]. In one third of the investigated clones, unintended deletions in the *vioD* gene were observed. Site-specific integration into the *rrn* operons, led to unintended deletions in the *vioD* gene during or after genomic integration in all investigated clones. Thus, deoxyviolacein was the only measurable product (**Publication II**[136]). Genetic instability of recombinant violacein producers has already been described before which leads to the assumption that instability might be a violacein-related issue[99,426]. This is also confirmed by the observed high genetic stability of the *rrn*-integration-based prodigiosin producing strains[251]. The high-level expression of a BGC in these loci can therefore not be problematic as such, as for the tripyrrole, strains are stable and productive.

Tn5 transposition enables a rapid integration of biosynthetic genes and provides a large number of clones. However, the lack of information about the integration locus can lead to limitations making it impossible to compare strains. The site-specific integration into the 16S rRNA genes overcomes this restriction of the random approach. Direct *rrn* targeting required preinstallation of landing pad sequences in each 16S gene as the sequences are almost 100% identical[255,409]. The development of *P. putida* strains using integration into the 16S rRNA gene or by Tn5 transposition was hampered by some difficulties for arcyriaflavin A production compared to the related bisindole violacein. For the *rrn* interposon, only clones with a single crossover could be identified. The derived strains produced only low amounts of the desired product (**Publication II**[136]). In contrast, the integration of the biosynthetic genes at the *att*Tn7 site under control of an inducible promoter seemed to be a preferred strategy for arcyriaflavin A

biosynthetic genes since clones could be obtained without any problems (**Publication II**[136] and **IV**[419]). Notably, this observation cannot only be attributed to the impact of the integration site as the used promoter system appears to be crucial. The gene integration under the inducible P_{nagAa} promoter was found to be most suitable most likely because it is not active without the respective inducer. This way, the host is not exposed to expression-related stress until induced. Moreover, the achieved titers by induced gene expression were much higher (about seventyfold after bioprocess optimization[419]) when this strategy was applied. The integration of the biosynthetic genes at the *att*Tn7 site with a strong constitutive promoter may not have led to success. It is worth underlining, that only the Tn7 integration allows to make a conscious decision regarding the used promoter. Including a promoter for Tn5 or *rrn* integration can therefore be deemed unsuitable.

Additionally, the site-specific integration at the *att*Tn7 site enabled rapid strain development for comparative studies of expression modules without having to be concerned about the influence of the genomic position. This was demonstrated by applying the pYT toolbox for optimization of *rhl* expression at the *att*Tn7 site. The strain performance with different expression modules as well as after module expansion for better precursor supply was comparatively assessable (**Publication II**[136]). Comparing both site-specific integration modes, less effort was required and less difficulties were encountered with Tn7 transposition. However, application of this mode in *P. putida* is restricted to this single site. Only a few bacterial genomes, e.g., of *Burkholderia* or *Halopseudomonas* species, have been found to possess more than one copy of the *glmS* gene and respective *att*Tn7 sites [292,427]. In these species, both *att*Tn7 sites could be occupied simultaneously. In addition, successful multicopy integration of two artificial *att*Tn7 sites have already been conducted in *Salmonella* and might also be a promising approach for *P. putida* to enable several rounds of Tn7 transposition[428].

In summary, no clear conclusion can be drawn regarding a preferred integration or expression mode for NP production in *P. putida*. Each strategy has advantages as well as drawbacks and limitations. Moreover, the suitability or benefits of an expression mode significantly depend on the type of NP being produced. These results demonstrate the value of the modular pYT vector series, which facilitates rapid and straightforward experimental testing through integration and expression modes for individual vector design.

III.2. Access to NPs by combining biosynthetic concepts

The use of different biosynthetic concepts in recombinant NP production allows the construction of a high-yield production strain and facilitates access to a variety of derivatives. Depending on the applied concepts, the synthesis of complex mixtures of diverse products can be avoided. Such biosynthetic specificity can decrease the work required for isolation tremendously. These biosynthetic concepts encompass classical and combinatorial biosynthesis as well as strategies

combining biological and chemical approaches, such as PDB, muta- and semisynthesis (**Figure I-9**)[331]. In the last years, *P. putida* has been established as a versatile host for NP production. Most of the biosynthetic pathways investigated for recombinant production are based on classical biosynthesis[204,224]. Within this thesis and in related master theses of Maximilian Spindler and Anka Sieberichs, the production of new-to-*P. putida* compounds, including pyrrole, indole, and quinoline alkaloids, was examined in different biosynthetic approaches (**Publications II**[136], **IV**[419], **V**[429] and **VI**,[411,412]).

III.2.1. The combination of biology and chemistry: valuable for recombinant NP production

Approaching NP production in whole cells requires careful consideration of the planned biochemical or biomimetic steps to identify the most feasible option to maximize yields, purities, and diversification.

First, the already well-established pathway for the synthesis of the tripyrrole prodigiosin was chosen. Prodigiosin was already successfully produced in *P. putida* in different studies using a variety of bio- and mutasynthetic approaches[99,239,408]. Biocatalytic production of prodigiosin derivatives was already conducted *in vitro* using the condensing enzymes PigC, TamQ, and ThreaP for the condensation of MAP and MBC, or analogs, in the final synthesis steps [252,322–324]. Despite the undisputed successes of mutasynthesis, which yielded a range of new compounds (at titers of 0.1 to 34 mg L^{-1}) with adapted bioactivities including autophagy modulation and antibiotic effects, the approach can have some restrictions in the access of certain compound types, as demonstrated for the production of a hydroxylated prodiginine (**Publication V**[429]). To yield the hydroxylated derivative, an alternative synthesis route using late-stage semisynthetic functionalization of a mutasynthesis product was established, as the direct conversion of a hydroxylated mutasynthon was most likely not possible due to a prevented uptake into the cell. The combination of the two biosynthetic concepts in a hybrid synthesis route resulted in a final yield of 65% in a preparative approach, supplying sufficient compound for bioactivity assays against the plant-parasitic nematode *Heterodera schachtii*.

In addition, the recombinant production of cycloprodigiosin was recently investigated as part of Robin Weihmann's doctoral thesis and was continued in the master thesis of Anka Sieberichs[327,411]. For the conversion of prodigiosin to its cyclic derivative, the biosynthetic pathway was extended with the enzyme Prub680 from *P. rubra*, an alkylglycerol monooxygenase-related cyclase [75]. In both studies, production of cycloprodigiosin was detectable, however, prodigiosin still accumulated as the main compound (64% and 59%, respectively). The concurrent production of both variants, the straight-chain and the cyclic derivative, has already been described for native producers[80,81,430]. Thus, for recombinant production in *P. putida*, another strategy was pursued combining the already developed mutasynthesis strains with combinatorial biosynthesis by implementing the cyclase Prub680

and also four other candidate enzymes (**Publication VI**)[76–78,81,82,116]. Following this approach, not only a better conversion to cycloprodigiosin of up to 99% was achieved with Prub680, but also access to seven non-natural cycloprodiginine compounds was enabled upon feeding of mutasynthons which differed in the alkyl chain as well as variants with a terminal double bond. The product titers were in the range of 1 to 4 mg L^{-1} depending on the scale and derivative. While these titers do not reflect a high-level production yet, they are currently representing the only way to access these products. As structural variations of prodiginines have already been demonstrated to expand the bioactivity spectrum[324,429], this new platform offers a promising approach for further research into the biological effect of different functionalization and derivatizations of the prodigiosin family. Physiological evaluation of these new derivatives against cancer cells, nematodes, pathogenic bacteria, or fungi could be conducted as done before[248,324,429,431]. In addition, the findings suggest the potential for testing additional enzyme candidates, particularly those with a previously demonstrated high conversion to cycloprodigiosin[80]. In general, many potential homologs could be identified via BLASTp analysis (Appendix, **Table V-3**). It could be useful to enhance the screening by introducing an automation process which will accelerate the procedure and expand the number of tested enzymes[432].

Arcyriaflavin A is another indole alkaloid besides (deoxy-)violacein which could be successfully produced with *P. putida*. By introducing the truncated *reb* cluster, containing the genes *rebODCP*, into the genome of *P. putida*, it became possible to biosynthetically produce arcyriaflavin A in this organism for the first time (**Publication II**[136]). Additionally, the production could be further optimized by bioprocess adaptations and engineering strategies yielding an almost ten-fold increase of the titer (4.7 mg L^{-1}) and a seven-fold increase in comparison to previously mentioned titers in *E. coli* (rebeccamycin aglycon: 0.7 mg L^{-1}[433]) (**Publication IV**[419]). While many efforts have already been made to diversify prodiginines through feeding of alternative precursors, mutational biosynthesis regarding indole alkaloids is still in its infancy[326]. Within the associated master thesis of Maximilian Spindler, a mutasynthesis platform for indole alkaloid production was built by generation of an L-tryptophan-auxotrophic strain (*P. putida* Δ*trpDC*)[412]. As intrinsic tryptophan biosynthesis is essential for bacterial growth, L-tryptophan feeding is required at a certain level. A two-phase bioprocess was explored starting with an initial growth phase in L-tryptophan supplemented culture medium, followed by later addition of the L-tryptophan analogs in the production phase. Here, the conversion of added L-tryptophan to arcyriaflavin A could be detected in this new platform. In addition, production of the rebeccamycin aglycon (**22**) upon 7-chloro-L-tryptophan feeding was assumed based on the HPLC-PDA results [412]. However, the arcyriaflavin A titer was low compared to the biosynthetic production (0.2 mg L^{-1}), the chlorinated aglycon was only produced together with the native product, arcyriaflavin A, and other tested substrates did not yield any other products.

A more successful access to indolocarbazole derivatives was achieved elsewhere by combinatorial biosynthesis for both arcyriaflavin and violacein compounds[137,326,434]. Based on these initial studies and on the knowledge about the L-AA oxygenases of the *vio* and *reb* cluster[135,435–437], a platform based on combinatorial biosynthesis for the production of chlorinated (**22**, **29** to **31**) and hydroxylated (**32** and **33**) arcyriaflavin compounds might be a potential solution to overcome the insufficient production rates or unfeasible conversion in arcyriaflavin mutasynthesis (**Figure III-2**).

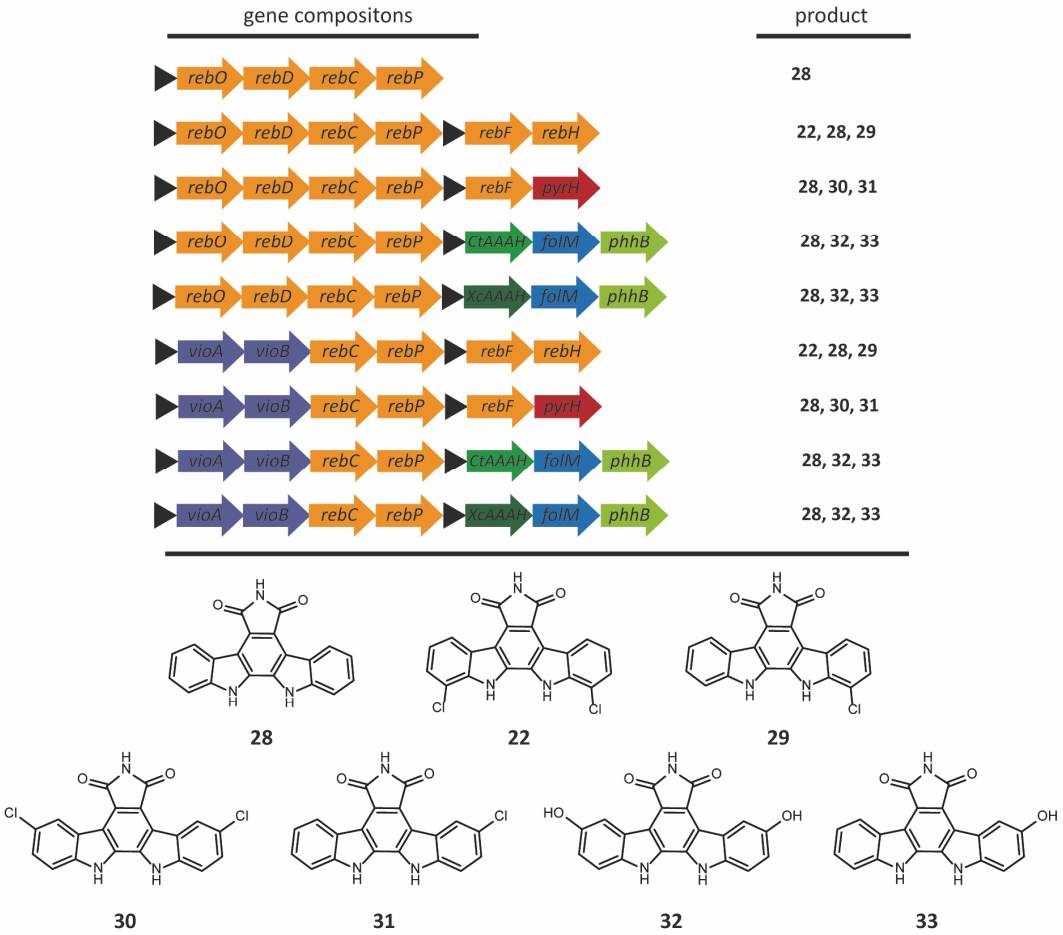

Figure III-2: A combinatorial biosynthesis platform for the production of arcyriaflavin derivatives (based on Sanchez et al. 2005[434]).
The biosynthesis cluster of the indolocarbazole arcyriaflavin A (**28**), which consists of the genes *rebODCP*, can potentially generate arcyriaflavin derivatives by integrating tryptophan halogenases and hydroxylases. Catalysis of L-tryptophan halogenation can be facilitated by RebH (conversion to 7-chloro-L-tryptophan) or PyrH from *Streptomyces rugosporus* (conversion to 5-chloro-L-tryptophan)[438]. Both enzymes are flavin-dependent halogenases requiring the flavin-reductase RebF. Thus, the production of the rebeccamycin aglycon (**22**) and the chlorinated products **29** to **31** might be possible. For hydroxylated arcyriaflavins (**32** and **33**), conversion of L-tryptophan to its 5-hydroxy-derivative could be achieved by the integration of engineered aromatic AA hydroxylases (AAAHs), originally from *Catharanthus roseus* (CtAAAH) or *Xanthomonas campestris* (XcAAAH), which were selected and engineered for the conversion of L-tryptophan[439,440]. A cofactor-recycling system is also required comprising the genes *folM* (*E. coli*) and *phhB* (*P. aeruginosa*). As the violacein biosynthetic enzymes have already been demonstrated to convert substituted L-tryptophan substrates[435] and an exchange of VioAB and RebOD can still maintain biosynthesis[137], combinations of *vio* and *reb* genes could be evaluated for diversification of indole alkaloids.

In comparison to the NPs mentioned above, classical biosynthetic production of aurachins could not be realized in *P. putida*[412,420]. Recently, aurachin D production and generation of its

derivatives was established in *E. coli* by whole-cell biotransformation with the genes *auaA* and *auaF* (**Figure I-5**)[180]. Based on this study, a mutasynthesis approach involving the genomic integration of *auaAF* and feeding of the precursor 4-hydroxy-2-methylquinoline was developed within the master thesis of Maximilian Spindler[412]. Evaluation of the *P. putida* mutasynthesis platform for aurachin production regarding the acceptance of substituted quinolone precursors is as of now missing and might be a good starting point for further investigations, as the substrate flexibility of the respective enzymes as well as the impact of structural modifications in this compound on its bioactivity have been demonstrated recently[175,180].

In summary, the used applications of recombinant NP production in *P. putida* have underlined the value of the different biosynthetic concepts further. While biosynthesis mostly focuses on efficient and high-yield production, the mutasynthesis route allows access to compounds beyond the 'one substrate – one product' concept currently dominating the biosynthesis approaches present in literature. However, mutasynthesis is also associated with specific challenges, as demonstrated, e.g., for the arcyriaflavin MBS platform, where the biosynthetic step to be deleted provides an essential intermediate for the organism's growth. Consequently, it is imperative to provide a variety of biosynthetic concepts and approaches, including (combinatorial) biosynthesis, muta-, and semisynthesis, not only to access novel NPs but also to overcome restrictions and challenges in the production of the respective NP regarding yields and purities.

III.3. From starting *chassis* to robust *chassis* – key strategies for bioprocess optimization

The recombinant production of valuable NPs using *P. putida* as a *chassis* has been proven to be promising in the chapters before. The developments in genetic tools as well as the availability of different strategies of whole-cell conversion contribute to the potential *of P. putida* as a production platform. However, conducting careful adaptations in the bioprocess for an optimization is inevitable for an efficient production. The stages of a bioprocess are (i) the upstream, (ii) the midstream, and (iii) the downstream process[302]. The engineering of the pathway design, the precursor supply, as well as the cell robustness are parts of the first stage. The potential of improving the robustness of *Pseudomonas* by exploiting naturally evolved tolerance strategies has been described in detail before (**Publication I**[219]). In addition, the latest advances in tolerance engineering on microorganisms used for industrial production has been recently reviewed[441]. The aspects affecting production performance including cultivation conditions and parameters, as well as scale-up approaches should be considered in the midstream (fermentation) process. Determinants for the success of the downstream process are the product release, -isolation and -purification, as well as, in a more industrial context, the formulation and packaging procedure[302]. Addressing these aspects was considered to be key for evolving *P. putida* into a more robust *chassis* for NP production and has therefore been

applied to the synthesis of different compounds within this thesis (**Table III-2**). For an evaluation, the product titer (mg product per L culture) was taken into account as a performance indicator and the relative increase compared to the non-engineered *chassis* was considered (indicated as x-fold increase). Besides the impact of the bioprocess strategies, which will be discussed in the following, this summary also provides an overview of all NP classes used for recombinant production in *P. putida* within this work and in associated publications and theses. While NPs that occur naturally in other *Pseudomonas* species, such as phenazines or rhamnolipids[442,443], are particularly well-suited for recombinant production, terpene production appears to be hampered in *P. putida*. This observation is not entirely unexpected, as the toxicity of an intermediate in carotenoid biosynthesis has been reported previously[444]. In addition, several alkaloids, including pyrrole, indole, and quinoline alkaloids, have been studied. Especially promising was the access to new-to-*P. putida* NPs, such as cycloprodigiosin, arcyriaflavin A, and aurachin D, and even to new-to-nature prodiginines.

Table III-2: Bioprocess optimization strategies for efficient NP production in *P. putida*.
[1]these strains were not generated with the newly developed pYT toolbox, but prior generated strains were used to investigate bioprocess optimization in *P. putida* [99,239].

class	NP	investigated bioprocess strategies	x-fold increase	final titer	reference
pyrrole alkaloids	cycloprodigiosin (biosynthesis)	non-natural pathway design, cultivation condition	3.1	5.9 mg L^{-1}	[411]
	cycloprodigiosin (mutasynthesis)	non-natural pathway design, cultivation condition, product release	2.5	2 mg L^{-1}	**Publication VI**
	prodigiosin (mutasynthesis)	strain engineering, cultivation conditions	15	34 mg L^{-1}	**Publication V**[429]
	prodigiosin[1] (biosynthesis)	engineered OMV formation	1.4	65 mg L^{-1}	**Publication III**[445]
indole alkaloids	arcyriaflavin A	strain engineering, cultivation conditions, engineered OMV formation, product release	7.6	4.7 mg L^{-1}	**Publication II**[136] **Publication IV**[419]
	(deoxy-) violacein[1]	engineered OMV formation	1.2	64 mg L^{-1}	**Publication III**[445]
quinoline alkaloids	aurachin D	cultivation conditions, pathway engineering	7.4	7.4 mg L^{-1}	[412]
phenazines	PCA[1]	engineered OMV formation	1.3	184 mg L^{-1}	**Publication III**[445]
rhamnolipids	mono-RL	strain engineering, pathway engineering	1.5	1.5 g L^{-1}	**Publication II**[136]
terpenes	zeaxanthin[1]	engineered OMV formation	1.3	0.4 mg L^{-1}	**Publication III**[445]

The key strategies applied in this thesis addressed the three different stages of a bioprocess mentioned above. In the following chapters, their effects will be discussed in more detail and they will be further divided into product-related (**III.3.1**) and product-unrelated strategies (**III.3.2**).

III.3.1. Product-related strategies

Product-related strategies include engineering the precursor and cofactor availability, improving rate-limiting catalytic steps, or adapting cultivation conditions, specifically to the biosynthesis pathway present.

The performance of a biosynthetic process depends on the conversion of a certain substrate to the respective product. Therefore, the precursor availability directly influences the yields achieved for the desired NP. This effect could be nicely demonstrated for the production of prodigiosin, as an increase in intrinsic MBC biosynthesis (up to eight-fold) in a genetically modified mutasynthesis *chassis* enhanced prodigiosin production by up to nine-fold (**Publication V**[429]). Thus, optimizing precursor supply has become a central aspect of metabolic engineering[446–449]. Within the master thesis of Maximilian Spinder, the mutasynthetic generation of the farnesylated quinoline alkaloid aurachin D was only feasible after the implementation of an additional biosynthetic pathway for FPP production, namely the MVA pathway (**Figure III-3**, A). Here, the synthesis of the sesquiterpene β-caryophyllene was used as a readout for an increased precursor level and could be transferred to the mutasynthetic production of aurachin D, which resulted in successful production in *P. putida* for the first time.

Another pathway engineering strategy, proven successful for mRL production in *P. putida*, is the overexpression of rate-limiting enzymes (**Publication II**[136]). For this purpose, the *rhl* expression module at the *att*Tn7 site was expanded with *rmlBDAC* and *algC* which are genes required for the supply of the precursor dTDP-L-rhamnose. The modification of the biosynthetic genes was facilitated by the modular structure of the pYT vector series. Overexpression of these integrated genes led to an increased mRL titer and simultaneously to a complete prevention of HAA accumulation (**Figure III-3**, B). As the arcyriaflavin A titer showed a dependence on the concentration of externally added L-tryptophan (**Publication IV**[419]), engineering the intrinsic L-tryptophan biosynthesis might be a promising approach for future studies. Following a strategy to increase the anthranilic acid level in *P. putida*, the generation of feedback-inhibition mutants and the deletion of competing pathways may result in an increased L-tryptophan level[225].

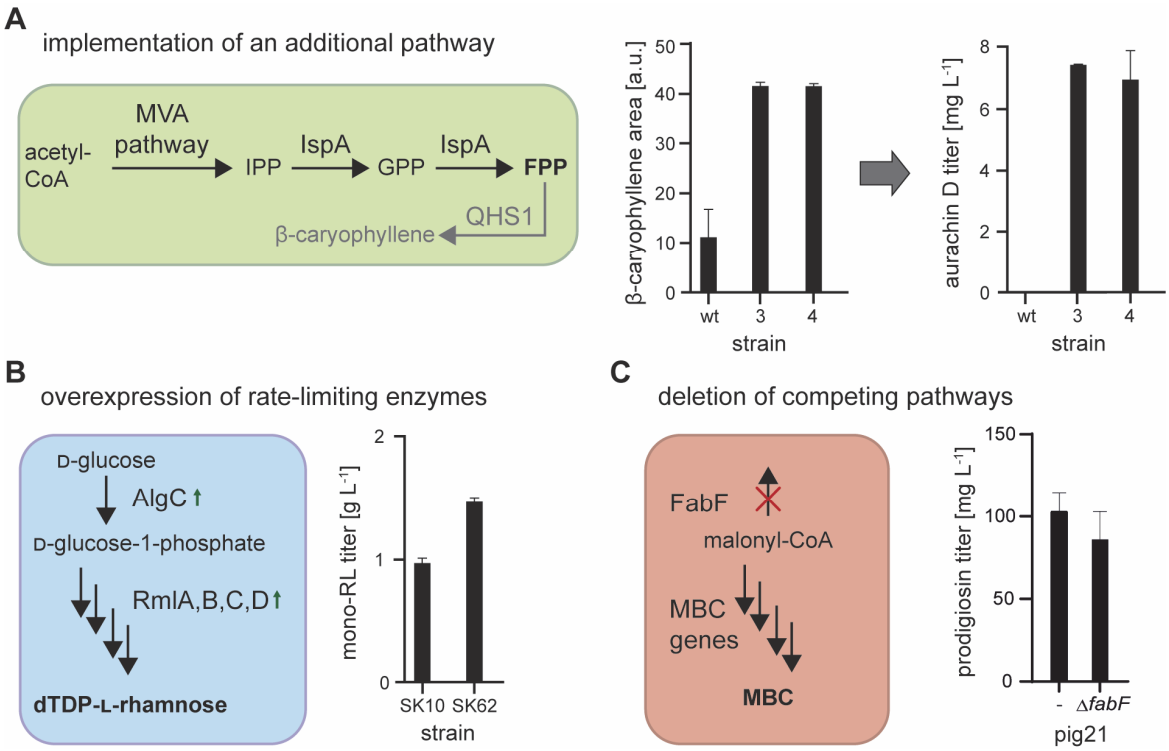

Figure III-3: Pathway engineering strategies for enhancing precursor supply in *P. putida*.
A: For mutasynthetic aurachin D production, FPP and 4-hydroxy-2-methylquinoline are required as precursors. While the quinoline is supplemented to the medium, FPP is produced intrinsically. As the integration of the biosynthetic genes in the *P. putida* KT2440 wild type (wt) did not result in aurachin D formation, the MVA pathway was chromosomally integrated by Tn5 transposition which resulted in two strains (3 and 4) with increased FPP levels (indirectly measured via β-caryophyllene production). The integration of the MVA pathway made aurachin D production possible in both strains. This work was conducted during the master thesis of Maximilian Spindler[412]. **B**: To enhance the production of mRLs and to decrease accumulation of the byproduct HAA, the *rhl* expression module at the *att*Tn7 site was expanded by the genes *rmlBDAC* and *algC*, encoding for potential rate-limiting enzymes for precursor synthesis. This newly developed strain (SK62) showed an increased mono-RL titer (**Publication II**[136]). **C**: The deletion of a competing biosynthetic pathway was applied as a metabolic engineering strategy for prodiginine production. Deletion of the gene *fabF* which has previously been proven to increase malonyl-CoA availability in *P. taiwanensis*[450], did not lead to an increased production of prodigiosin. The data are means of biological triplicates with their corresponding standard deviation. For a detailed description of the additional experiments see **V.6**.

Based on a recently published engineering strategy for increasing malonyl-CoA availability in *P. taiwanensis*, an additional experiment has been conducted within this thesis to evaluate the impact of precursor engineering for platforms with already high product yields. A prodigiosin-producing strain was altered in its fatty acid metabolism by deletion of the β-ketoacyl-ACP synthase II (FabF, PP_1916) (**V.6**). Reducing the metabolic drain on malonyl-CoA may potentially result in higher MBC levels because the precursor may be available in higher amounts for the synthesis of the bipyrrole. For evaluation, the prodigiosin titer was measured but was not positively affected in the engineered strain (**Figure III-3**, C). As the formation of prodigiosin is based on both precursors, MAP and MBC, and MBC biosynthesis is not solely dependent on the malonyl-CoA supply, no clear statement about the impact of *fabF* deletion is possible. Direct measurement of the MBC titer, as done before[429], should ensure a better assessment of the suitability of the applied engineering strategy. The efficacy of pathway engineering strategies and their significant impact on production performance (resulting in a two- to seven-fold increase in titers) is evident from the present studies. However, the attempted

improvement of prodigiosin biosynthesis by adjusting fatty acid metabolism is a good example to show that metabolic engineering not always has an overall positive effect, but rather strongly depends on the NP and the underlying biosynthetic process, classifying it as a product-related strategy.

Metabolic engineering allows for implementation of non-natural biosynthetic pathways as proposed for arcyriaflavin A derivatization (**Figure III-2**) and has already been applied for cycloprodigiosin production (**Publication VI**, [411]). This strategy relies on the implementation of natural enzymes and the combination of their biosynthetic potential. By exploring the substrate repertoire of the enzymes, even access to new-to-nature cycloprodiginines was facilitated. This approach and its potential have already been described by the concept of combinatorial biosynthesis (**III.2**). An alternative strategy for pathway design is the use of non-natural enzymes obtained by protein engineering, as conducted for VioA[135], or *de novo* enzyme design[302]. All these mentioned approaches are strategies for the upstream process.

The determinants which influence the second stage of a bioprocess (midstream process), meaning the cultivation or fermentation, are the cultivation conditions, the culture medium formulations, and the production scale[302]. Although some of these factors are not necessarily directly product- but organism-dependent, they have previously been proven to be crucial factors in bioprocess optimization[250,254]. In the studies presented in this thesis the adjustment of cultivation conditions was also a key strategy to enhance NP production in *P. putida* (**Publication IV**[419], **V**[429], and **VI**, [411,412]). In particular, the achieved titers of the prodiginines and arcyriaflavin A were dependent on the cultivation medium, time and temperature. One similarity between both NPs was observed: in both cases, the most suitable temperature for production deviated from the typical cultivation temperature of *P. putida* (e.g., 20 °C instead of 30 °C for cycloprodigiosin production, **Publication VI**). In general, the examination of cultivation conditions is an essential element in bioprocess engineering and often the starting point for optimizing the recombinant production of new-to-*P. putida* NPs.

III.3.2. Product-unrelated strategies

After the summary of some product-related strategies for developing an efficient producer strain, this chapter emphasizes more general key strategies that are not directly related to the involved biosynthetic enzymes or the metabolic pathway. These aspects could therefore be a promising foundation for the generation of robust microbial cell factories. A useful and feasible strategy, already applied for the construction of an optimal *P. putida chassis* in previous studies, is genome streamlining. The reduction of the bacterial genome boosted growth rates, heterologous gene expression, plasmid stability, as well as enhanced energy metabolism[235,342,451,452].

A further important aspect, which will be discussed here, is the release of the product from the cell to avoid intrinsic accumulation of the NP. Growth inhibition and low production titers may otherwise be the consequence. In addition, extracellular accumulation of the target compound facilitates NP isolation and purification during downstream processing. A commonly applied strategy is the active extrusion by efflux transporters. This aspect has already been discussed as an opportunity for exploiting native tolerance traits before as *Pseudomonas* is well-equipped with different transporter types (**Publication I**[219]). The co-expression of genes, which encode for putative transporters in connection with the desired product, might be a promising approach[453]. The idea was pursued in the integrative approach of bioprocess optimization for arcyriaflavin A production (**Publication IV**[419]). The genes encoding for the rebeccamycin transporter RebUT were integrated into the producer strain using two different constitutive promoters, however, an influence on arcyriaflavin A production in *P. putida* was not detected. The decision for RebUT was based on the desired product being a derivative of rebeccamycin, despite the fact that no association with transportation of arcyriaflavin A was previously reported. The absence of chlorination and the sugar moiety in the arcyriaflavin A scaffold may be hindering the transport compared to the natural substrate.

An almost complete accumulation of the water-insoluble indolocarbazole arcyriaflavin A in the supernatant (>99%) could be achieved by the addition of polyurethane (PU) foam cubes to the medium which serve as a hydrophobic surface, capturing the product in the aqueous environment. Thus, the PU foam cubes are especially suited for the efficient extraction of hydrophobic NPs[250,454]. This approach is based on a study utilizing PU to absorb protochlorophyllides from an aqueous culture medium[455]. A related influence on the tripyrrolic compound was hypothesized due to structural similarities[456]. For prodigiosin production, the use of an external adsorber was very effective and the PU foam cubes were frequently applied for recombinant production in *P. putida* ([250,252], **Publication V**[429], **Publication VI**). The use of a two-phase-system (e.g., using 1-decanol or dodecane as a second phase) for bioproduction of hydrophobic and toxic compounds, which serves as a product sink, has likewise improved the production of different NPs[254,457]. A solid second phase has the advantage that desorption of the enriched product from the PU foam cubes can be achieved relatively easily, which facilitates optimization of the isolation process.

The hydrophobic property of NPs such as prodiginines or arcyriaflavin A, also reflected in their high logP values (prodigiosin: 4.07, arcyriaflavin A: 3.65[458]), demonstrates that the likelihood of accumulation in water or the aqueous supernatant is low. Therefore, the observed presence of prodigiosin in the supernatant in the absence of an adsorber was unexpected and raised the question how the product is released from the cell. Based on this, a correlation of prodigiosin and an intrinsic stress response mechanism, the formation of OMVs, could be revealed for the first time in *P. putida* (**Publication III**[445]). This study did not only show

accumulation of prodigiosin in the vesicles, which is consistent with its hydrophobic character and has already been observed in the native producer[390], but it also showed an increased OMV formation upon recombinant production, and, even more interestingly, an increased prodigiosin titer in chemically triggered hypervesiculation strains. Thus, the exploitation of this stress response for the optimization of a bioprocess was examined. The engineering of OMV formation to support recombinant NP production is not completely new[404], but new to *P. putida* as, so far, potential genetic targets had not been identified.

Within the Bachelor thesis of Carolin Höfel, the focus was laid on the identification of potential genetic targets for engineering vesiculation in *P. putida* based on already described strategies in other Gram-negative bacteria[459]. This provided the fundament for following experimental investigations. By using a plasmid-based system for the manipulation of the expression of these candidate genes (overexpression or CRISPRi-based down-regulation), 18 different targets were analyzed regarding their impact on OMV formation. In fact, a number of genes could be verified to support both, vesiculation and recombinant production of prodigiosin, (deoxy-)violacein, zeaxanthin, PCA and arcyriaflavin A (**Table III-2**) (**Publication III**[445], **Publication IV**[419]).The plasmid-based tools used for the investigation of the candidates were suited for the screening, especially as they allowed for addressing essential genes. In a biotechnological process, however, a stable, genomically engineered strain without any plasmids is important for process stability. Hence, knockout strains were generated for two genes which were shown to cause vesiculation when downregulated (**Publication IV**[419]). This approach not only circumvents possible restrictions of the CRISPRi system, such as off-target effects or insufficient repression, but also facilitates flexibility in terms of resistance marker, expression system, and plasmid-use for recombinant production by using plasmid-less strains.
Within this thesis, additional experiments were conducted to gain a better understanding of the capabilities as well as limitations of engineered vesiculation as an optimization strategy. Firstly, the effect of a combinatorial deletion of two identified target genes was investigated but no clear synergistic effect of the combination on OMV formation was found (Appendix, **Figure V-1**) and, further, only a small impact on the specific productivity of arcyriaflavin A could be observed (Figure III-4, A). A previous study on the generation of hypervesiculation mutants in *E. coli* revealed different effects of combinatorial deletions (i.e., synergistic or non-synergistic) depending on the addressed gene combinations[460]. Overall, the influence of different cellular components on the OMV formation seems to be a highly complex interaction, where the role of each factor as well as combinations of factors, as observed in combinatorial deletions, has to be investigated in depth and a potential effect on NP production needs to be verified. Simultaneous manipulation of different targets may generally be more likely to strongly perturb membrane integrity and will thus require especially careful finetuning in the producer strain.

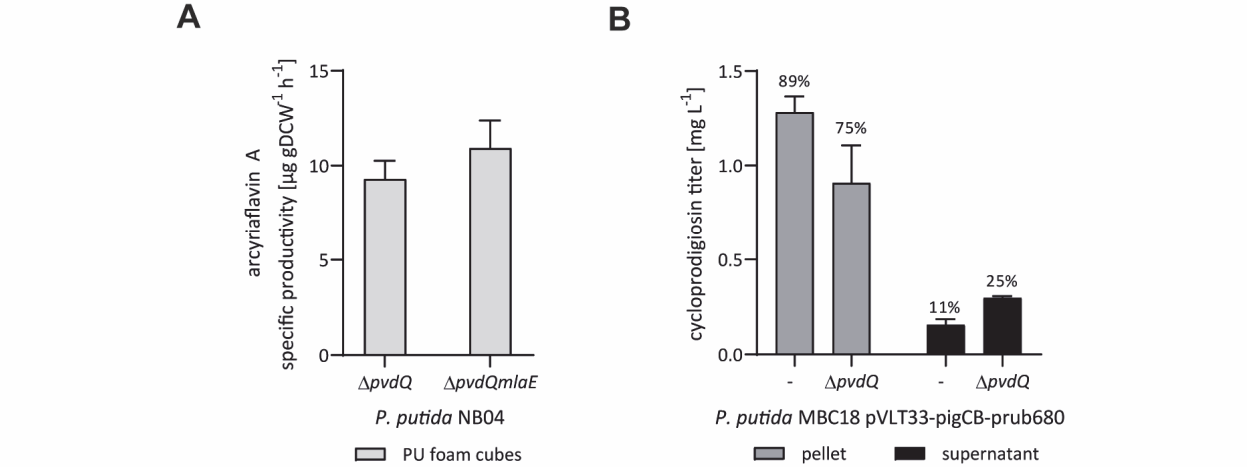

Figure III-4: Applying engineered vesiculation to recombinant NP production in *P. putida*.
A: Combinatorial deletion of identified genetic targets, which affect OMV formation in *P. putida*, was utilized for the recombinant production of arcyriaflavin A. The specific productivity was determined after extraction from the PU foam cubes for both *P. putida* Δ*pvdQ* and *P. putida* Δ*pvdQmlaE* strains carrying the genes *rebODCP,* which are integrated at the *att*Tn7 site under control of an inducible promoter (P_{nagAa}). **B**: Cycloprodigiosin production was carried out using the previously established mutasynthesis platform *P. putida* MBC18 pVLT33-pigCB-prub680 ('-') (**Publication VI**) and an OMV-engineered strain (*'ΔpvdQ'*). Cycloprodigiosin accumulation was analyzed in both the pellet (dark gray) and supernatant fraction (black). The data are means of biological triplicates with their corresponding standard deviation. For a detailed description of the additional experiments see **V.6**.

Another question was whether the OMV approach can be applied for derivatization of NPs. Here, a greater probability that a derivative is extruded effectively may be assumed if the original molecule is already being released from the cell. Therefore, an additional experiment was conducted to engineer OMV formation in the previously developed cycloprodigiosin mutasynthesis platform (Figure III-4, C). The conversion of prodigiosin to cycloprodigiosin was still high (>95%) in both the pellet and supernatant fraction. The same was previously observed for the release of the products in PU foam cubes (**Publication VI**). The overall titer did not change significantly upon engineering, but interestingly a higher amount of cycloprodigiosin accumulated in the supernatant compared to the non-engineered producer. This additional experiment demonstrates that the 'packaging process' of the NP seems not to be a speed-determining factor as the biosynthesis appears to be faster. Thus, the use of OMVs for release and storage of NPs to avoid their intracellular accumulation is also applicable in combinatorial biosynthesis and mutasynthesis.

Considering these recent observations together with previous findings on engineered vesiculation[404,419,445,460], the intricate and multifaceted aspects of engineering OMVs for biotechnological use become clear. However, the findings demonstrate the potential of this strategy and offer a starting point for further exploration of opportunities related to recombinant NP production in *P. putida*. They also contribute to the rather young but versatile field of exploring potential applications of OMVs, which also cover the use of natural and engineered vesicles as carriers in cross-kingdom communication[461], as drug-delivery vehicles[462,463], for extracellular protein secretion[460], as well as for *in vitro* biocatalysis[464].

In general, the product-unrelated strategies discussed here show that the release and adsorption of the NP can be a key factor to increase productivity and titers of whole-cell biotransformation by presumably avoiding the accumulation of the NP at the cell membrane. These approaches would be especially suited for compounds with poor solubility and high hydrophobicity as it has been demonstrated for the prodiginines and arcyriaflavin A (**Publication III**[445], **IV**[419], and **VI**).

In summary, this thesis contributes to the field of recombinant NP production and underlines the potential of *P. putida* as a production platform. Relevant aspects for the efficient production of NPs in *P. putida* as a robust *chassis* organism were discussed which have to be considered for further developments. For the successful production of valuable compounds, several involved determinants could be identified, including (i) the strain stability, (ii) the suitability of the host for diverse compounds, as well as (iii) the productivity of the bioprocess (**Figure III-5**).

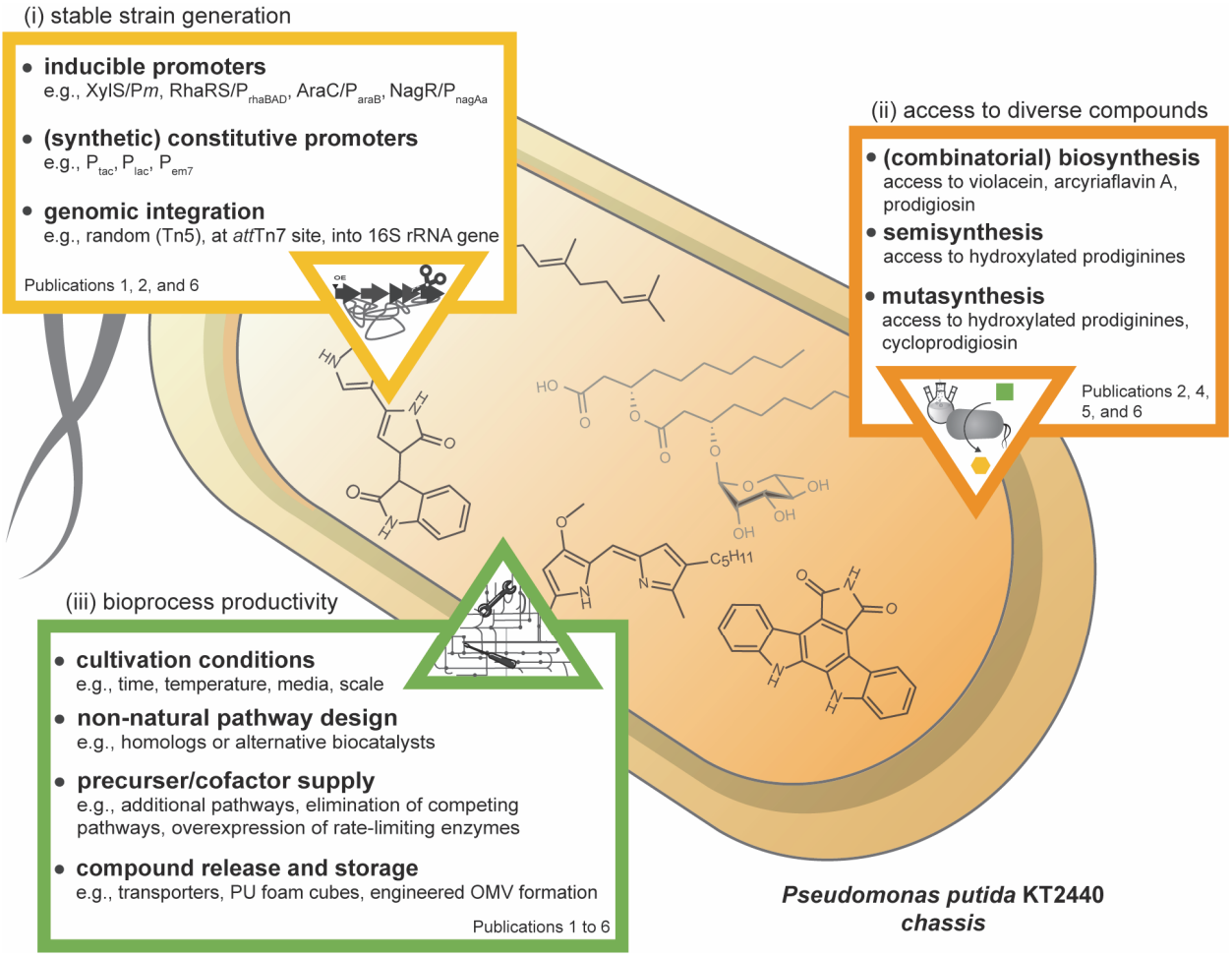

Figure III-5: Overview of the main contributors for efficient NP production in *P. putida*.
Different aspects were addressed within this work which are crucial for developing a robust *chassis* for high-level recombinant NP production. They can be divided into three categories: (**i**) facilitating the generation of stable strains through various expression and integration modes, (**ii**) providing access to diverse products, including new-to-nature compounds by utilizing the capabilities of biology and chemistry in a biosynthetic context, and (**iii**) optimizing the bioprocess productivity by applying engineering strategies directly related to the biosynthetic pathway or more universal strategies for *chassis* generation. The publications which built the framework of this thesis are assigned to the three categories. References: **Publication I**[219], **II**[136], **III**[445], **IV**[419], and **V**[429]. **Publication VI** will be submitted soon.

The here presented thesis investigated the three aspects in the form of expression and integration modules, biosynthesis and biotransformation aspects, as well as bioprocess-related factors. The work revealed that there is no standardized procedure for transforming *P. putida* into an all-round production platform, but every single NP needs individual adjustments on all levels to maximize production of the desired product. Thus, a thorough analysis of the

underlying processes from the strain generation, over biosynthesis to release of the target compound must be performed. This thesis identified several approaches and tools which may be utilized to quickly access the key modulators of NP production in *P. putida*, optimize the (bio-)synthesis as well as facilitate the release. A foundation has been laid to analyze the recombinant production of NPs in greater detail while significantly minimizing the required time and effort to modulate the respective factors using the established modular genetic toolbox. Future research may benefit from the gained insights, as well as the tools established within this thesis, the associated publications as well as the related bachelor and master theses. This could lead to a greater understanding of the various factors influencing such a bioprocess and allow for more in-depth studies regarding different NP production strategies in recombinant hosts.

IV. REFERENCES

[**1**] Cragg GM, Newman DJ (2013) Natural products: A continuing source of novel drug leads. *Biochim Biophys Acta, Gen Sub* **1830**:3670–3695. DOI: 10.1016/j.bbagen.2013.02.008

[**2**] Lewis K (2013) Platforms for antibiotic discovery. *Nat Rev Drug Discov* **12**:371–387. DOI: 10.1038/nrd3975

[**3**] Waksman SA, Schatz A, Reynolds DM (2010) Production of antibiotic substances by *actinomycetes*. *Ann N Y Acad Sci* **1213**:112–124. DOI: 10.1111/j.1749-6632.2010.05861.x

[**4**] Katz L, Baltz RH (2016) Natural product discovery: Past, present, and future. *J Ind Microbiol Biotechnol* **43**:155–176. DOI: 10.1007/s10295-015-1723-5

[**5**] Wright GD (2017) Opportunities for natural products in 21st century antibiotic discovery. *Nat Prod Rep* **34**:694–701. DOI: 10.1039/C7NP00019G

[**6**] Newman DJ, Cragg GM (2020) Natural products as sources of new drugs over the nearly four decades from 01/1981 to 09/2019. *J Nat Prod* **83**:770–803. DOI: 10.1021/acs.jnatprod.9b01285

[**7**] Walesch S, Birkelbach J, Jézéquel G, Haeckl FPJ, Hegemann JD, Hesterkamp T, et al. (2023) Fighting antibiotic resistance—Strategies and (pre)clinical developments to find new antibacterials. *EMBO Rep* **24**:e56033. DOI: 10.15252/embr.202256033

[**8**] Tacconelli E, Pezzani MD (2019) Public health burden of antimicrobial resistance in Europe. *Lancet Infect Dis* **19**:4–6. DOI: 10.1016/S1473-3099(18)30648-0

[**9**] O'Neill J (2014) Antimicrobial resistance: Tackling a crisis for the health and wealth of nations. *Rev Antimicrob Resist* 1–16 [https://amr-review.org/sites/default/files/AMR%20Review%20Paper%20-%20Tackling%20a%20crisis%20for%20the%20health%20and%20wealth%20of%20nations_1.pdf, 26/09/2023]

[**10**] Wencewicz TA (2016) New antibiotics from nature's chemical inventory. *Bioorg Med Chem* **24**:6227–6252. DOI: 10.1016/j.bmc.2016.09.014

[**11**] Rossiter SE, Fletcher MH, Wuest WM (2017) Natural products as platforms to overcome antibiotic resistance. *Chem Rev* **117**:12415–12474. DOI: 10.1021/acs.chemrev.7b00283

[**12**] Genilloud O (2012) Current challenges in the discovery of novel antibacterials from microbial natural products. *Recent Pat Antiinfect Drug Discov* **7**:189–204. DOI: 10.2174/157489112803521968

[**13**] Rodrigues T, Reker D, Schneider P, Schneider G (2016) Counting on natural products for drug design. *Nat Chem* **8**:531–541. DOI: 10.1038/nchem.2479

[**14**] Kossel A (1891) Über die chemische Zusammensetzung der Zelle. *Du Bois-Reymond's Archiv/ Arch Anat Physiol Physiol Abt* **278**:181–186.

[**15**] Hanson JR (2003) Natural Products: The Secondary Metabolites. *Royal Society of Chemistry*; **17**:1-154. DOI: 10.1039/9781847551535

[**16**] Cushnie TPT, Cushnie B, Lamb AJ (2014) Alkaloids: An overview of their antibacterial, antibiotic-enhancing and antivirulence activities. *Int J Antimicrob Agents* **44**:377–386. DOI: 10.1016/j.ijantimicag.2014.06.001

[**17**] Hibbing ME, Fuqua C, Parsek MR, Peterson SB (2010) Bacterial competition: Surviving and thriving in the microbial jungle. *Nat Rev Microbiol* **8**:15–25. DOI: 10.1038/nrmicro2259

[**18**] Gershenzon J, Dudareva N (2007) The function of terpene natural products in the natural world. *Nat Chem Biol* **3**:408–414. DOI: 10.1038/nchembio.2007.5

[**19**] Miethke M, Marahiel MA (2007) Siderophore-based iron acquisition and pathogen control. *MMBR* **71**:413–451. DOI: 10.1128/MMBR.00012-07

[**20**] Keller L, Surette MG (2006) Communication in bacteria: An ecological and evolutionary perspective. *Nat Rev Microbiol* **4**:249–258. DOI: 10.1038/nrmicro1383

[**21**] Walsh CT, Tang Y (2017) Natural Product Biosynthesis. *Royal Society of Chemistry*;

[**22**] Chen Y, de Bruyn Kops C, Kirchmair J (2017) Data resources for the computer-guided discovery of bioactive natural products. *J Chem Inf Model* **57**:2099–2111. DOI: 10.1021/acs.jcim.7b00341

[**23**] Blunt J, Munro M, Upjohn M (2012) The Role of Databases in Marine Natural Products Research. *Springer: Handbook of Marine Natural Products* **1**:389-412. DOI: 10.1007/978-90-481-3834-0_6

[**24**] Gaudêncio SP, Pereira F (2015) Dereplication: Racing to speed up the natural products discovery process. *Nat Prod Rep* **32**:779–810. DOI: 10.1039/C4NP00134F

[**25**] Chassagne F, Cabanac G, Hubert G, David B, Marti G (2019) The landscape of natural product diversity and their pharmacological relevance from a focus on the *Dictionary of Natural Products®*. *Phytochem Rev* **18**:601–622. DOI: 10.1007/s11101-019-09606-2

[**26**] Bérdy J (2012) Thoughts and facts about antibiotics: Where we are now and where we are heading. *J Antibiot* **65**:385–395. DOI: 10.1038/ja.2012.27

[**27**] Huang M, Lu JJ, Huang MQ, Bao JL, Chen XP, Wang YT (2012) Terpenoids: Natural products for cancer therapy. *Expert Opin Investig Drugs* **21**:1801–1818. DOI: 10.1517/13543784.2012.727395

[**28**] Patridge E, Gareiss P, Kinch MS, Hoyer D (2016) An analysis of FDA-approved drugs: Natural products and their derivatives. *Drug Discov Today* **21**:204–207. DOI: 10.1016/j.drudis.2015.01.009

[**29**] Bérdy J (2005) Bioactive microbial metabolites. *J Antibiot* **58**:1–26. DOI: 10.1038/ja.2005.1

[**30**] Baindara P, Mandal SM (2020) Bacteria and bacterial anticancer agents as a promising alternative for cancer therapeutics. *Biochimie* **177**:164–189. DOI: 10.1016/j.biochi.2020.07.020

[**31**] Mohan CD, Rangappa S, Nayak SC, Jadimurthy R, Wang L, Sethi G, et al. (2022) Bacteria as a treasure house of secondary metabolites with anticancer potential. *Semin Cancer Biol* **86**:998–1013. DOI: 10.1016/j.semcancer.2021.05.006

[**32**] Heard SC, Wu G, Winter JM (2021) Antifungal natural products. *Curr Opin Biotechnol* **69**:232–241. DOI: 10.1016/j.copbio.2021.02.001

[**33**] Aldholmi M, Marchand P, Ourliac-Garnier I, Le Pape P, Ganesan A (2019) A decade of antifungal leads from natural products: 2010–2019. *Pharmaceuticals* **12**:182. DOI: 10.3390/ph12040182

[**34**] Al Kassaa I, Hober D, Hamze M, Chihib NE, Drider D (2014) Antiviral potential of lactic acid bacteria and their bacteriocins. *Probiotics Antimicrob Proteins* **6**:177–185. DOI: 10.1007/s12602-014-9162-6

[**35**] Jenab A, Roghanian R, Emtiazi G (2020) Bacterial natural compounds with anti-inflammatory and immunomodulatory properties. *Drug Des Devel Ther* **14**:3787–3801. DOI: 10.2147/DDDT.S261283

[**36**] Gross H, Loper JE (2009) Genomics of secondary metabolite production by *Pseudomonas* spp. *Nat Prod Rep* **26**:1408. DOI: 10.1039/b817075b

[**37**] Haas D, Défago G (2005) Biological control of soil-borne pathogens by fluorescent Pseudomonads. *Nat Rev Microbiol* **3**:307–319. DOI: 10.1038/nrmicro1129

[**38**] Strobel G, Daisy B, Castillo U, Harper J (2004) Natural products from endophytic microorganisms. *J Nat Prod* **67**:257–268. DOI: 10.1021/np030397v

[**39**] Waksman SA (1943) Production and activity of streptothricin. *J Bacteriol* **46**:299–310. DOI: 10.1128/jb.46.3.299-310.1943

[**40**] Waksman SA, Reilly HC, Johnstone DB (1946) Isolation of streptomycin-producing strains of *Streptomyces griseus*. *J Bacteriol* **52**:393–397. DOI: 10.1128/jb.52.3.393-397.1946

[**41**] Tiwari K, Gupta RK (2012) Rare actinomycetes: A potential storehouse for novel antibiotics. *Crit Rev Biotechnol* **32**:108–132. DOI: 10.3109/07388551.2011.562482

[**42**] Lawton EM, Cotter PD, Hill C, Ross RP (2007) Identification of a novel two-peptide lantibiotic, haloduracin, produced by the alkaliphile *Bacillus halodurans* C-125. *FEMS Microbiol Lett* **267**:64–71. DOI: 10.1111/j.1574-6968.2006.00539.x

[**43**] Dischinger J, Josten M, Szekat C, Sahl HG, Bierbaum G (2009) Production of the novel two-peptide lantibiotic lichenicidin by *Bacillus licheniformis* DSM 13. *PLoS One* **4**:e6788. DOI: 10.1371/journal.pone.0006788

[**44**] Stein T (2005) *Bacillus subtilis* antibiotics: Structures, syntheses and specific functions. *Mol Microbiol* **56**:845–857. DOI: 10.1111/j.1365-2958.2005.04587.x

[**45**] Wang J, Zhang L, Teng K, Sun S, Sun Z, Zhong J (2014) Cerecidins, novel lantibiotics from *Bacillus cereus* with potent antimicrobial activity. *Appl Environ Microbiol* **80**:2633–2643. DOI: 10.1128/AEM.03751-13

[**46**] Smanski MJ, Zhou H, Claesen J, Shen B, Fischbach MA, Voigt CA (2016) Synthetic biology to access and expand nature's chemical diversity. *Nat Rev Microbiol* **14**:135–149. DOI: 10.1038/nrmicro.2015.24

[**47**] Martin JF, Liras P (1989) Organization and expression of genes involved in the biosynthesis of antibiotics and other secondary metabolites. *Annu Rev Microbiol* **43**:173–206. DOI: 10.1146/annurev.mi.43.100189.001133

[**48**] Morrison KC, Hergenrother PJ (2014) Natural products as starting points for the synthesis of complex and diverse compounds. *Nat Prod Rep* **31**:6–14. DOI: 10.1039/C3NP70063A

[**49**] Henkel T, Brunne RM, Müller H, Reichel F (1999) Statistical investigation into the structural complementarity of natural products and synthetic compounds. *Angew Chem, Int Ed* **38**:643–647. DOI: 10.1002/(SICI)1521-3773(19990301)38:5<643::AID-ANIE643>3.0.CO;2-G

[**50**] Henkel T, Brunne RM, Müller H, Reichel F (1999) Statistische Untersuchungen zur Strukturkomplementarität von Naturstoffen und synthetischen Substanzen. *Angew Chem* **111**:688–691. DOI: 10.1002/(SICI)1521-3757(19990301)111:5<688::AID-ANGE688>3.0.CO;2-K

[**51**] Lee ML, Schneider G (2001) Scaffold architecture and pharmacophoric properties of natural products and trade drugs: Application in the design of natural product-based combinatorial libraries. *J Comb Chem* **3**:284–289. DOI: 10.1021/cc000097l

[**52**] van Santen JA, Jacob G, Singh AL, Aniebok V, Balunas MJ, Bunsko D, et al. (2019) The Natural Products Atlas: An open access knowledge base for microbial natural products discovery. *ACS Cent Sci* **5**:1824–1833. DOI: 10.1021/acscentsci.9b00806

[**53**] Seo M, Shin HK, Myung Y, Hwang S, No KT (2020) Development of Natural Compound Molecular Fingerprint (NC-MFP) with the Dictionary of Natural Products (DNP) for natural product-based drug development. *J Cheminform* **12**:6. DOI: 10.1186/s13321-020-0410-3

[**54**] Kim HW, Wang M, Leber CA, Nothias LF, Reher R, Kang K Bin, et al. (2021) NPClassifier: A deep neural network-based structural classification tool for natural products. *J Nat Prod* **84**:2795–2807. DOI: 10.1021/acs.jnatprod.1c00399

[**55**] Banerjee P, Erehman J, Gohlke BO, Wilhelm T, Preissner R, Dunkel M (2015) Super Natural II — A database of natural products. *Nucleic Acids Res* **43**:935–939. DOI: 10.1093/nar/gku886

[**56**] Kautsar SA, Blin K, Shaw S, Navarro-Muñoz JC, Terlouw BR, van der Hooft JJJ, et al. (2019) MIBiG 2.0: A repository for biosynthetic gene clusters of known function. *Nucleic Acids Res* **48**:454–458. DOI: 10.1093/nar/gkz882

[**57**] Buckingham J, Baggaley KH, Roberts AD, Szabo LF (2010) Dictionary of Alkaloids with CD-ROM. *CRC Press*

[**58**] Bian C, Wang J, Zhou X, Wu W, Guo R (2020) Recent advances on marine alkaloids from sponges. *Chem Biodivers* **17**:e2000186. DOI: 10.1002/cbdv.202000186

[**59**] Zotchev SB (2013) Alkaloids from Marine Bacteria. *Adv Bot Res* **68**:301-333. DOI: 10.1016/B978-0-12-408061-4.00011-0

[**60**] Willems T, De Mol ML, De Bruycker A, De Maeseneire SL, Soetaert WK (2020) Alkaloids from marine fungi: Promising antimicrobials. *Antibiotics* **9**:340. DOI: 10.3390/antibiotics9060340

[**61**] Bhambhani S, Kondhare KR, Giri AP (2021) Diversity in chemical structures and biological properties of plant alkaloids. *Molecules* **26**:3374. DOI: 10.3390/molecules26113374

[**62**] Matsuura HN, Fett-Neto AG (2015) Plant alkaloids: Main features, toxicity, and mechanisms of action. *Plant Toxins* **2**:1–15. DOI: 10.1007/978-94-007-6728-7_2-1

[**63**] Kittakoop P, Mahidol C, Ruchirawat S (2013) Alkaloids as important scaffolds in therapeutic drugs for the treatments of cancer, tuberculosis, and smoking cessation. *Curr Top Med Chem* **14**:239–252. DOI: 10.2174/15680266136661312161050 49

[**64**] Yan Y, Li X, Zhang C, Lv L, Gao B, Li M (2021) Research progress on antibacterial activities and mechanisms of natural alkaloids: A review. *Antibiotics* **10**:318. DOI: 10.3390/antibiotics10030318

[**65**] Gupta AP, Pandotra P, Kushwaha M, Khan S, Sharma R, Gupta S (2015) Alkaloids: A source of anticancer agents from nature. *Stud Nat Prod Chem* **46**:341–445. DOI: 10.1016/B978-0-444-63462-7.00009-9

[**66**] Song F, Liu D, Huo X, Qiu D (2022) The anticancer activity of carbazole alkaloids. *Arch Pharm* **355**:2100277. DOI: 10.1002/ardp.202100277

[**67**] Roy A (2017) A review on the alkaloids an important therapeutic compound from plants. *IJPB* **3**:1–9.

[**68**] Kohnen-Johannsen K, Kayser O (2019) Tropane alkaloids: Chemistry, pharmacology, biosynthesis and production. *Molecules* **24**:796. DOI: 10.3390/molecules24040796

[**69**] Seipp K, Geske L, Opatz T (2021) Marine pyrrole alkaloids. *Mar Drugs* **19**:514. DOI: 10.3390/md19090514

[**70**] Stankovic N, Senerovic L, Ilic-Tomic T, Vasiljevic B, Nikodinovic-Runic J (2014) Properties and applications of undecylprodigiosin and other bacterial prodigiosins. *Appl Microbiol Biotechnol* **98**:3841–3858. DOI: 10.1007/s00253-014-5590-1

[**71**] Williams RP, Quadri SMH (1980) The Pigment of *Serratia*. *The Genus Serratia*.

[**72**] Tsao SW, Rudd BAM, He XG, Chang CJ, Floss HG (1985) Identification of a red pigment from *Streptomyces coelicolor* A3(2) as a mixture of prodigiosin derivatives. *J Antibiot* **38**:128–131. DOI: 10.7164/antibiotics.38.128

[**73**] Hu DX, Withall DM, Challis GL, Thomson RJ (2016) Structure, chemical synthesis, and biosynthesis of prodiginine natural products. *Chem Rev* **116**:7818–7853. DOI: 10.1021/acs.chemrev.6b00024

[**74**] Lattasch H, Thomson RH (1983) A revised structure for cycloprodigiosin. *Tetrahedron Lett* **24**:2701–2704. DOI: 10.1016/S0040-4039(00)87981-2

[**75**] de Rond T, Stow P, Eigl I, Johnson RE, Chan LJG, Goyal G, et al. (2017) Oxidative cyclization of prodigiosin by an alkylglycerol monooxygenase-like enzyme. *Nat Chem Biol* **13**:1155–1157. DOI: 10.1038/nchembio.2471

[**76**] Kawauchi K, Shibutani K, Yagisawa H, Kamata H, Nakatsuji S, Anzai H, et al. (1997) A possible immunosuppressant, cycloprodigiosin hydrochloride, obtained from *Pseudoalteromonas denitrificans*. *Biochem Biophys Res Commun* **237**:543–547. DOI: 10.1006/bbrc.1997.7186

[**77**] Kim HS, Hayashi M, Shibata Y, Wataya Y, Mitamura T, Horii T, et al. (1999) Cycloprodigiosin hydrochloride obtained from *Pseudoalteromonas denitrificans* is a potent antimalarial agent. *Biol Pharm Bull* **22**:532–534. DOI: 10.1248/bpb.22.532

[**78**] Gerber NN (1983) Cycloprodigiosin from *Beneckea gazogenes*. *Tetrahedron Lett* **24**:2797–2798. DOI: 10.1016/S0040-4039(00)88026-0

[**79**] Allen GR, Reichelt JL, Gray PP (1983) Influence of environmental factors and medium composition on *Vibrio gazogenes* growth and prodigiosin production. *Appl Environ Microbiol* **45**:1727–1732. DOI: 10.1128/aem.45.6.1727-1732.1983

[**80**] Vitale GA, Sciarretta M, Palma Esposito F, January GG, Giaccio M, Bunk B, et al. (2020) Genomics–metabolomics profiling disclosed marine *Vibrio spartinae* 3.6 as a producer of a new branched side chain prodigiosin. *J Nat Prod* **83**:1495–1504. DOI: 10.1021/acs.jnatprod.9b01159

[**81**] Ramaprasad EV V., Bharti D, Sasikala Ch, Ramana Ch V. (2015) *Zooshikella marina* sp. nov. a cycloprodigiosin- and prodigiosin-producing marine bacterium isolated from beach sand. *Int J Syst Evol Microbiol* **65**:4669–4673. DOI: 10.1099/ijsem.0.000630

[**82**] Lee JS, Kim YS, Park S, Kim J, Kang SJ, Lee MH, et al. (2011) Exceptional production of both prodigiosin and cycloprodigiosin as major metabolic constituents by a novel marine bacterium, *Zooshikella rubidus* S1-1. *Appl Environ Microbiol* **77**:4967–4973. DOI: 10.1128/AEM.01986-10

[**83**] Williams RP, Green JA, Rappoport DA (1956) Studies on pigmentation of *Serratia marcescens*. *J Bacteriol* **71**:115–120. DOI: 10.1128/jb.71.1.115-120.1956

[**84**] Casullo de Araújo HW, Fukushima K, Takaki GMC (2010) Prodigiosin production by *Serratia marcescens* UCP 1549 using renewable resources as a low-cost substrate. *Molecules* **15**:6931–6940. DOI: 10.3390/molecules15106931

[**85**] Darshan N, Manonmani HK (2016) Prodigiosin inhibits motility and activates bacterial cell death revealing molecular biomarkers of programmed cell death. *AMB Express* **6**:50. DOI: 10.1186/s13568-016-0222-z

[**86**] Siva R, Subha K, Bhakta D, Ghosh AR, Babu S (2012) Characterization and enhanced production of prodigiosin from the spoiled coconut. *Appl Biochem Biotechnol* **166**:187–196. DOI: 10.1007/s12010-011-9415-8

[**87**] Kim D, Lee JS, Park YK, Kim JF, Jeong H, Oh TK, et al. (2007) Biosynthesis of antibiotic prodiginines in the marine bacterium *Hahella chejuensis* KCTC 2396. *J Appl Microbiol* **102**:937-944. DOI: 10.1111/j.1365-2672.2006.03172.x

[**88**] Kim D, Park YK, Lee JS, Kim JF, Jeong H, Kim BS, et al. (2006) Analysis of a prodigiosin biosynthetic gene cluster from the marine bacterium *Hahella chejuensis* KCTC 2396. *J Microbiol Biotechnol* **16**:1912–1918.

[**89**] Hobbs G, Frazer CM, Gardner DCJ, Flett F, Oliver SG (1990) Pigmented antibiotic production by *Streptomyces coelicolor* A3(2): Kinetics and the influence of nutrients. *J Gen Microbiol* **136**:2291–2296. DOI: 10.1099/00221287-136-11-2291

[**90**] Gerber NN (1975) A new prodiginine (prodigiosin-like) pigment from *Streptomyces*. Antimalarial activity of several prodiginines. *J Antibiot* **28**:194–199. DOI: 10.7164/antibiotics.28.194

[**91**] Kawasaki T, Sakurai F, Hayakawa Y (2008) A prodigiosin from the roseophilin producer *Streptomyces griseoviridis*. *J Nat Prod* **71**:1265–1267. DOI: 10.1021/np7007494

[**92**] Harris AKP, Williamson NR, Slater H, Cox A, Abbasi S, Foulds I, et al. (2004) The *Serratia* gene cluster encoding biosynthesis of the red antibiotic, prodigiosin, shows species- and strain-dependent genome context variation. *Microbiology* **150**:3547–3560. DOI: 10.1099/mic.0.27222-0

[**93**] Williamson NR, Fineran PC, Leeper FJ, Salmond GPC (2006) The biosynthesis and regulation of bacterial prodiginines. *Nat Rev Microbiol* **4**:887–899. DOI: 10.1038/nrmicro1531

[**94**] Williamson NR, Simonsen HT, Ahmed RAA, Goldet G, Slater H, Woodley L, et al. (2005) Biosynthesis of the red antibiotic, prodigiosin, in *Serratia*: Identification of a novel 2-methyl-3-n-amyl-pyrrole (MAP) assembly pathway, definition of the terminal condensing enzyme, and implications for undecylprodigiosin biosynthesis in *Streptomyces*. *Mol Microbiol* **56**:971–989. DOI: 10.1111/j.1365-2958.2005.04602.x

[**95**] Yip CH, Yarkoni O, Ajioka J, Wan KL, Nathan S (2019) Recent advancements in high-level synthesis of the promising clinical drug, prodigiosin. *Appl Microbiol Biotechnol* **103**:1667–1680. DOI: 10.1007/s00253-018-09611-z

[**96**] Chawrai SR, Williamson NR, Mahendiran T, Salmond GPC, Leeper FJ (2012) Characterisation of PigC and HapC, the prodigiosin synthetases from *Serratia* sp. and *Hahella chejuensis* with potential for biocatalytic production of anticancer agents. *Chem Sci* **3**:447–454. DOI: 10.1039/C1SC00588J

[**97**] Couturier M, Bhalara HD, Chawrai SR, Monson R, Williamson NR, Salmond GPC, et al. (2020) Substrate flexibility of the flavin-dependent dihydropyrrole oxidases PigB and HapB involved in antibiotic prodigiosin biosynthesis. *ChemBioChem* **21**:523–530. DOI: 10.1002/cbic.201900424

[**98**] Bitzenhofer NL (2018) Light-driven control of bacterial processes by genetically encoded photosensitizers. *Heinrich Heine University Düsseldorf.* Master thesis

[**99**] Domröse A, Weihmann R, Thies S, Jaeger KE, Drepper T, Loeschcke A (2017) Rapid generation of recombinant *Pseudomonas putida* secondary metabolite producers using yTREX. *Synth Syst Biotechnol* **2**:310–319. DOI: 10.1016/j.synbio.2017.11.001

[**100**] Sakai-Kawada FE, Ip CG, Hagiwara KA, Awaya JD (2019) Biosynthesis and bioactivity of prodiginine analogs in marine bacteria, *Pseudoalteromonas*: A mini review. *Front Microbiol* **10**:1715. DOI: 10.3389/fmicb.2019.01715

[**101**] Cheng MF, Lin CS, Chen YH, Sung PJ, Lin SR, Tong YW, et al. (2017) Inhibitory growth of oral squamous cell carcinoma cancer via bacterial prodigiosin. *Mar Drugs* **15**:224. DOI: 10.3390/md15070224

[**102**] Kavitha R, Aiswariya S, Ratnavali CMG (2010) Anticancer activity of red pigment from *Serratia marcescens* in human cervix carcinoma. *Int J Pharmtech Res* **2**:784–787.

[**103**] Hong B, Prabhu V V., Zhang S, van den Heuvel APJ, Dicker DT, Kopelovich L, et al. (2014) Prodigiosin rescues deficient p53 signaling and antitumor effects via upregulating p73 and disrupting its interaction with mutant p53. *Cancer Res* **74**:1153–1165. DOI: 10.1158/0008-5472.CAN-13-0955

[**104**] Montaner B, Navarro S, Piqué M, Vilaseca M, Martinell M, Giralt E, et al. (2000) Prodigiosin from the supernatant of *Serratia marcescens* induces apoptosis in haematopoietic cancer cell lines. *Br J Pharmacol* **131**:585–593. DOI: 10.1038/sj.bjp.0703614

[**105**] Berning L, Lenz T, Bergmann AK, Poschmann G, Brass HUC, Schlütermann D, et al. (2023) The Golgi stacking protein GRASP55 is targeted by the natural compound prodigiosin. *CCS* **21**:275. DOI: 10.1186/s12964-023-01275-1

[**106**] Davis JT Anion Binding and Transport by Prodigiosin and Its Analogs. *Springer: Anion Recognition in Supramolecular Chemistry* **24**:148-176. DOI: 10.1007/7081_2010_29

[**107**] Nakashima T, Tamura T, Kurachi M, Yamaguchi K, Oda T (2005) Apoptosis-mediated cytotoxicity of prodigiosin-like red pigment produced by γ-proteobacterium and its multiple bioactivities. *Biol Pharm Bull* **28**:2289–2295. DOI: 10.1248/bpb.28.2289

[**108**] Pérez-Tomás R, Montaner B, Llagostera E, Soto-Cerrato V (2003) The prodigiosins, proapoptotic drugs with anticancer properties. *Biochem Pharmacol* **66**:1447–1452. DOI: 10.1016/S0006-2952(03)00496-9

[**109**] Gulani, C., Bhattacharya, S., Das, A. (2012) Assessment of process parameters influencing the enhanced production of prodigiosin from *Serratia marcescens* and evaluation of its antimicrobial, antioxidant and dyeing potentials. *Malays J Microbiol* **8**:116–122. DOI: 10.21161/mjm.03612

[**110**] Ibrahim D, Faridah Nazari T, Kassim J, Lim SH (2014) Prodigiosin - An antibacterial red pigment produced by *Serratia marcescens* IBRL USM 84 associated with a marine sponge *Xestospongia testudinaria*. *J Appl Pharm Sci* **4**:1–6. DOI: 10.7324/JAPS.2014.401001

[**111**] Lapenda JC, Silva PA, Vicalvi MC, Sena KXFR, Nascimento SC (2015) Antimicrobial activity of prodigiosin isolated from *Serratia marcescens* UFPEDA 398. *World J Microbiol Biotechnol* **31**:399–406. DOI: 10.1007/s11274-014-1793-y

[**112**] You Z, Zhang S, Liu X, Zhang J, Wang Y, Peng Y, et al. (2019) Insights into the anti-infective properties of prodiginines. *Appl Microbiol Biotechnol* **103**:2873–2887. DOI: 10.1007/s00253-019-09641-1

[**113**] Kancharla P, Kelly JX, Reynolds KA (2015) Synthesis and structure–Activity relationships of tambjamines and B-ring functionalized prodiginines as potent antimalarials. *J Med Chem* **58**:7286–7309. DOI: 10.1021/acs.jmedchem.5b00560

[**114**] Zhou W, Zeng C, Liu RH, Chen J, Li R, Wang XY, et al. (2016) Antiviral activity and specific modes of action of bacterial prodigiosin against *Bombyx mori* nucleopolyhedrovirus *in vitro*. *Appl Microbiol Biotechnol* **100**:3979–3988. DOI: 10.1007/s00253-015-7242-5

[**115**] D'Alessio R, Bargiotti A, Carlini O, Colotta F, Ferrari M, Gnocchi P, et al. (2000) Synthesis and immunosuppressive activity of novel prodigiosin derivatives. *J Med Chem* **43**:2557–2565. DOI: 10.1021/jm001003p

[**116**] Huang Z, Dong L, Lai Q, Liu J (2020) *Spartinivicinus ruber* gen. nov., sp. nov., a novel marine gammaproteobacterium producing heptylprodigiosin and cycloheptylprodigiosin as major red pigments. *Front Microbiol* **11**:2056. DOI: 10.3389/fmicb.2020.02056

[**117**] Liu Y, Cui Y, Lu L, Gong Y, Han W, Piao G (2020) Natural indole-containing alkaloids and their antibacterial activities. *Arch Pharm* **353**:2000120. DOI: 10.1002/ardp.202000120

[**118**] August PR, Grossman TH, Minor C, Draper MP, MacNeil IA, Pemberton JM, et al. (2000) Sequence analysis and functional characterization of the violacein biosynthetic pathway from *Chromobacterium violaceum*. *J Mol Microbiol Biotechnol* **2**:513–519.

[**119**] Aranda S, Montes-Borrego M, Landa BB (2011) Purple-pigmented violacein-producing *Duganella* spp. inhabit the rhizosphere of wild and cultivated olives in southern spain. *Microb Ecol* **62**:446–459. DOI: 10.1007/s00248-011-9840-9

[**120**] Jiang P, Wang H sheng, Zhang C, Lou K, Xing XH (2010) Reconstruction of the violacein biosynthetic pathway from *Duganella* sp. B2 in different heterologous hosts. *Appl Microbiol Biotechnol* **86**:1077–1088. DOI: 10.1007/s00253-009-2375-z

[**121**] Pantanella F, Berlutti F, Passariello C, Sarli S, Morea C, Schippa S (2006) Violacein and biofilm production in *Janthinobacterium lividum*. *J Appl Microbiol* **102**:992–999. DOI: 10.1111/j.1365-2672.2006.03155.x

[**122**] Agematu H, Suzuki K, Tsuya H (2011) *Massilia* sp. BS-1, a novel violacein-producing bacterium isolated from soil. *Biosci Biotechnol Biochem* **75**:2008–2010. DOI: 10.1271/bbb.100729

[**123**] Thomas T, Evans FF, Schleheck D, Mai-Prochnow A, Burke C, Penesyan A, et al. (2008) Analysis of the *Pseudoalteromonas tunicata* genome reveals properties of a surface-associated life style in the marine environment. *PLoS One* **3**:e3252. DOI: 10.1371/journal.pone.0003252

[**124**] Yang LH, Xiong H, Lee OO, Qi SH, Qian PY (2007) Effect of agitation on violacein production in *Pseudoalteromonas luteoviolacea* isolated from a marine sponge. *Lett Appl Microbiol* **44**:625–630. DOI: 10.1111/j.1472-765X.2007.02125.x

[**125**] Hoshino T (2011) Violacein and related tryptophan metabolites produced by *Chromobacterium violaceum*: biosynthetic mechanism and pathway for construction of violacein core. *Appl Microbiol Biotechnol* **91**:1463–1475. DOI: 10.1007/s00253-011-3468-z

[**126**] Balibar CJ, Walsh CT (2006) *In vitro* biosynthesis of violacein from L-tryptophan by the enzymes VioA−E from *Chromobacterium violaceum*. *Biochemistry* **45**:15444–15457. DOI: 10.1021/bi061998z

[**127**] Sánchez C, Méndez C, Salas JA (2006) Indolocarbazole natural products: Occurrence, biosynthesis, and biological activity. *Nat. Prod. Rep.* **23**:1007–1045. DOI: 10.1039/B601930G

[**128**] Bush JA, Long BH, Catino JJ, Bradner WT (1987) Production and biological activity of rebeccamycin, a novel antitumor agent. *J Antibiot* **40**:668–678. DOI: 10.7164/antibiotics.40.668

[**129**] Long B, Rose W, Vyas D, Matson J, Forenza S (2002) Discovery of antitumor indolocarbazoles: Rebeccamycin, NSC 655649, and fluoroindolocarbazoles. *Curr Med Chem Anticancer Agents* **2**:255–266. DOI: 10.2174/1568011023354218

[**130**] Nouioui I, Carro L, García-López M, Meier-Kolthoff JP, Woyke T, Kyrpides NC, et al. (2018) Genome-based taxonomic classification of the phylum actinobacteria. *Front Microbiol* **22**:2007. DOI: 10.3389/fmicb.2018.02007

[**131**] Sánchez C, Butovich IA, Braña AF, Rohr J, Méndez C, Salas JA (2002) The biosynthetic gene cluster for the antitumor rebeccamycin: Characterization and generation of indolocarbazole derivatives. *Chem Biol* **9**:519–531. DOI: 10.1016/S1074-5521(02)00126-6

[**132**] Pommerehne K, Walisko J, Ebersbach A, Krull R (2019) The antitumor antibiotic rebeccamycin — Challenges and advanced approaches in production processes. *Appl Microbiol Biotechnol* **103**:3627–3636. DOI: 10.1007/s00253-019-09741-y

[**133**] Morohoshi T, Fukamachi K, Kato M, Kato N, Ikeda T (2010) Regulation of the violacein biosynthetic gene cluster by acylhomoserine lactone-mediated quorum sensing in *Chromobacterium violaceum* ATCC 12472. *Biosci Biotechnol Biochem* **74**:2116–2119. DOI: 10.1271/bbb.100385

[**134**] Stauff DL, Bassler BL (2011) Quorum sensing in *Chromobacterium violaceum*: DNA recognition and gene regulation by the CviR receptor. *J Bacteriol* **193**:3871–3878. DOI: 10.1128/JB.05125-11

[**135**] Füller JJ, Röpke R, Krausze J, Rennhack KE, Daniel NP, Blankenfeldt W, et al. (2016) Biosynthesis of violacein, structure and function of L-tryptophan oxidase VioA from *Chromobacterium violaceum*. *Journal of Biological Chemistry* **291**:20068–20084. DOI: 10.1074/jbc.M116.741561

[**136**] Weihmann R, Kubicki S, Bitzenhofer NL, Domröse A, Bator I, Kirschen LM, et al. (2023) The modular pYT vector series employed for chromosomal gene integration and expression to produce carbazoles and glycolipids in *P. putida*. *FEMS Microbes* **4**:xtac030. DOI: 10.1093/femsmc/xtac030

[**137**] Sánchez C, Braña AF, Méndez C, Salas JA (2006) Reevaluation of the violacein biosynthetic pathway and its relationship to indolocarbazole biosynthesis. *ChemBioChem* **7**:1231–1240. DOI: 10.1002/cbic.200600029

[**138**] Spolitak T, Ballou DP (2015) Evidence for catalytic intermediates involved in generating the chromopyrrolic acid scaffold of rebeccamycin by RebO and RebD. *Arch Biochem Biophys* **573**:111–119. DOI: 10.1016/j.abb.2015.03.020

[**139**] Durán N, Menck CFM (2001) *Chromobacterium violaceum*: A review of pharmacological and industiral perspectives. *Crit Rev Microbiol* **27**:201–222. DOI: 10.1080/20014091096747

[**140**] Durán N, Justo GZ, Ferreira C V., Melo PS, Cordi L, Martins D (2007) Violacein: Properties and biological activities. *Biotechnol Appl Biochem* **48**:127–133. DOI: 10.1042/BA20070115

[**141**] Durán N, Nakazato G, Durán M, Berti IR, Castro GR, Stanisic D, et al. (2021) Multi-target drug with potential applications: Violacein in the spotlight. *World J Microbiol Biotechnol* **37**:151. DOI: 10.1007/s11274-021-03120-4

[**142**] Nakamura Y, Sawada T, Morita Y, Tamiya E (2002) Isolation of a psychrotrophic bacterium from the organic residue of a water tank keeping rainbow trout and antibacterial effect of violet pigment produced from the strain. *Biochem Eng J* **12**:79–86. DOI: 10.1016/S1369-703X(02)00079-7

[**143**] Nakamura Y, Asada C, Sawada T (2003) Production of antibacterial violet pigment by psychrotropic bacterium RT102 strain. *Biotechnol Bioprocess Eng* **8**:37–40. DOI: 10.1007/BF02932896

[**144**] Durán M, Ponezi AN, Faljoni-Alario A, Teixeira MFS, Justo GZ, Durán N (2012) Potential applications of violacein: A microbial pigment. *MCRE* **21**:1524–1532. DOI: 10.1007/s00044-011-9654-9

[**145**] Melo P (2003) Violacein and its β-cyclodextrin complexes induce apoptosis and differentiation in HL60 cells. *Toxicology* **186**:217–225. DOI: 10.1016/S0300-483X(02)00751-5

[**146**] Liu L, Lu J, Wang Y, Pang X, Xu M, Zhang S (2017) Antitumor effect of violacein against HT29 by comparative proteomics. *Sci Agric Sin* **50**:1694–1704. DOI: 10.3864/j.issn.0578-1752.2017.09.015

[**147**] Gonçalves PR, Rocha-Brito KJP, Fernandes MRN, Abrantes JL, Durán N, Ferreira-Halder C V. (2016) Violacein induces death of RAS-mutated metastatic melanoma by impairing autophagy process. *Tumor Biology* **37**:14049–14058. DOI: 10.1007/s13277-016-5265-x

[**148**] Mojib N, Nasti TH, Andersen DT, Attigada VR, Hoover RB, Yusuf N, et al. (2011) The antiproliferative function of violacein-like purple violet pigment (PVP) from an antarctic *Janthinobacterium* sp. Ant5-2 in UV-induced 2237 fibrosarcoma. *Int J Dermatol* **50**:1223–1233. DOI: 10.1111/j.1365-4632.2010.04825.x

[**149**] Kodach LL, Bos CL, Durán N, Peppelenbosch MP, Ferreira C V., Hardwick JCH (2006) Violacein synergistically increases 5-fluorouracil cytotoxicity, induces apoptosis and inhibits Akt-mediated signal transduction in human colorectal cancer cells. *Carcinogenesis* **27**:508–516. DOI: 10.1093/carcin/bgi307

[**150**] Platt D, Amara S, Mehta T, Vercuyssee K, Myles EL, Johnson T, et al. (2014) Violacein inhibits matrix metalloproteinase mediated CXCR4 expression: Potential anti-tumor effect

in cancer invasion and metastasis. *Biochem Biophys Res Commun* **455**:107–112. DOI: 10.1016/j.bbrc.2014.10.124

[**151**] Sancelme M, Fabre S, Prudhomme M (1994) Antimicrobial activities of indolocarbazole and bis-indole protein kinase C inhibitors. *J Antibiot* **47**:792–798. DOI: 10.7164/antibiotics.47.792

[**152**] Facompré M, Baldeyrou B, Bailly C, Anizon F, Marminon C, Prudhomme M, et al. (2002) DNA targeting of two new antitumour rebeccamycin derivatives. *Eur J Med Chem* **37**:925–932. DOI: 10.1016/S0223-5234(02)01423-X

[**153**] Nock CJ, Brell JM, Bokar JA, Cooney MM, Cooper B, Gibbons J, et al. (2011) A phase I study of rebeccamycin analog in combination with oxaliplatin in patients with refractory solid tumors. *Invest New Drugs* **29**:126–130. DOI: 10.1007/s10637-009-9322-9

[**154**] Burstein HJ, Overmoyer B, Gelman R, Silverman P, Savoie J, Clarke K, et al. (2007) Rebeccamycin analog for refractory breast cancer: A randomized phase II trial of dosing schedules. *Invest New Drugs* **25**:161–164. DOI: 10.1007/s10637-006-9007-6

[**155**] Schwandt A, Mekhail T, Halmos B, O'Brien T, Ma PC, Fu P, et al. (2012) Phase-II trial of rebeccamycin analog, a dual topoisomerase-I and -II inhibitor, in relapsed "sensitive" small cell lung cancer. *JTO* **7**:751–754. DOI: 10.1097/JTO.0b013e31824abca2

[**156**] Goel S, Wadler S, Hoffman A, Volterra F, Baker C, Nazario E, et al. (2003) A phase II study of rebeccamycin analog NSC 655649 in patients with metastatic colorectal cancer. *Invest New Drugs* **21**:103–107. DOI: 10.1023/A:1022980613420

[**157**] Slater MJ, Baxter R, Bonser RW, Cockerill S, Gohil K, Parry N, et al. (2001) Synthesis of N-alkyl substituted indolocarbazoles as potent inhibitors of human cytomegalovirus replication. *Bioorg Med Chem Lett* **11**:1993–1995. DOI: 10.1016/S0960-894X(01)00352-3

[**158**] Slater MJ, Cockerill S, Baxter R, Bonser RW, Gohil K, Gowrie C, et al. (1999) Indolocarbazoles: Potent, selective inhibitors of human cytomegalovirus replication. *Bioorg Med Chem* **7**:1067–1074. DOI: 10.1016/S0968-0896(99)00032-2

[**159**] Hirakawa T, Nasu K, Aoyagi Y, Takebayashi K, Narahara H (2017) Arcyriaflavin A, a cyclin D1–cyclin-dependent kinase4 inhibitor, induces apoptosis and inhibits proliferation of human endometriotic stromal cells: A potential therapeutic agent in endometriosis. *Reproductive Biology and Endocrinology* **15**:53. DOI: 10.1186/s12958-017-0272-3

[**160**] Shang X, Morris-Natschke SL, Liu Y, Guo X, Xu X, Goto M, et al. (2018) Biologically active quinoline and quinazoline alkaloids part I. *Med Res Rev* **38**:775–828. DOI: 10.1002/med.21466

[**161**] Shang X, Morris-Natschke SL, Yang G, Liu Y, Guo X, Xu X, et al. (2018) Biologically active quinoline and quinazoline alkaloids part II. *Med Res Rev* **38**:1614–1660. DOI: 10.1002/med.21492

[**162**] Wiesner J, Ortmann R, Jomaa H, Schlitzer M (2003) New antimalarial drugs. *Angew Chem, Int Ed* **42**:5274–5293. DOI: 10.1002/anie.200200569

[**163**] Wiesner J, Ortmann R, Jomaa H, Schlitzer M (2003) Neue Antimalaria-Wirkstoffe. *Angew Chem* **115**:5432–5451. DOI: 10.1002/ange.200200569

[**164**] Liu YQ, Li WQ, Morris-Natschke SL, Qian K, Yang L, Zhu GX, et al. (2015) Perspectives on biologically active camptothecin derivatives. *Med Res Rev* **35**:753–789. DOI: 10.1002/med.21342

[**165**] Saalim M, Villegas-Moreno J, Clark BR (2020) Bacterial alkyl-4-quinolones: Discovery, structural diversity and biological properties. *Molecules* **25**:5689. DOI: 10.3390/molecules25235689

[**166**] Kunze B, Höfle G, Reichenbach H (1987) The aurachins, new quinoline antibiotics from myxobacteria : Production, physico-chemical and biological properties. *J Antibiot* **40**:258–265. DOI: 10.7164/antibiotics.40.258

[**167**] Höfle G, Irschik H (2008) Isolation and biosynthesis of aurachin P and 5-nitroresorcinol from *Stigmatella erecta*. *J Nat Prod* **71**:1946–1948. DOI: 10.1021/np800325z

[**168**] Kitagawa W, Tamura T (2008) A quinoline antibiotic from *Rhodococcus erythropolis* JCM 6824. *J Antibiot* **61**:680–682. DOI: 10.1038/ja.2008.96

[**169**] Nachtigall J, Schneider K, Nicholson G, Goodfellow M, Zinecker H, Imhoff JF, et al. (2010) Two new aurachins from *Rhodococcus* sp. Acta 2259. *J Antibiot* **63**:567–569. DOI: 10.1038/ja.2010.79

[**170**] Zhang M, Yang CL, Xiao YS, Zhang B, Deng XZ, Yang L, et al. (2017) Aurachin SS, a new antibiotic from *Streptomyces* sp. NA04227. *J Antibiot* **70**:853–855. DOI: 10.1038/ja.2017.50

[**171**] Pistorius D, Li Y, Sandmann A, Müller R (2011) Completing the puzzle of aurachin biosynthesis in *Stigmatella aurantiaca* Sg a15. *Mol Biosyst* **7**:3308–3315. DOI: 10.1039/c1mb05328k

[**172**] Sandmann A, Dickschat J, Jenke-Kodama H, Kunze B, Dittmann E, Müller R (2007) A type II polyketide synthase from the Gram-negative bacterium *Stigmatella aurantiaca* is involved in aurachin alkaloid biosynthesis. *Angew Chem, Int Ed* **46**:2712–2716. DOI: 10.1002/anie.200603513

[**173**] Sandmann A, Dickschat J, Jenke-Kodama H, Kunze B, Dittmann E, Müller R (2007) Aurachin-Biosynthese im Gram-negativen Bakterium *Stigmatella aurantiaca*: Beteiligung einer Typ-II-Polyketidsynthase. *Angew Chem* **119**:2768–2772. DOI: 10.1002/ange.200603513

[**174**] Kruth S, Nett M (2023) Aurachins, bacterial antibiotics interfering with electron transport processes. *Antibiotics* **12**:1067. DOI: 10.3390/antibiotics12061067

[**175**] Sester A, Stüer-Patowsky K, Hiller W, Kloss F, Lütz S, Nett M (2020) Biosynthetic plasticity enables production of fluorinated aurachins. *ChemBioChem* **21**:2268–2273. DOI: 10.1002/cbic.202000166

[**176**] Li XW, Herrmann J, Zang Y, Grellier P, Prado S, Müller R, et al. (2013) Synthesis and biological activities of the respiratory chain inhibitor aurachin D and new ring versus chain analogues. *Beilstein J Org Chem* **9**:1551–1558. DOI: 10.3762/bjoc.9.176

[**177**] Hoefnagel MHN, Wiskich JT, Madgwick SA, Patterson Z, Oettmeier W, Rich PR (1995) New inhibitors of the ubiquinol oxidase of higher plant mitochondria. *Eur J Biochem* **233**:531–537. DOI: 10.1111/j.1432-1033.1995.531_2.x

[**178**] Oettmeier W, Dostatni R, Majewski C, Höfle G, Fecker T, Kunze B, et al. (1990) The aurachins, naturally occurring inhibitors of photosvnthetic electron flow through photosystem II and the cytochrome b_6/f-complex. *Z Naturforsch C* **45**:322–328. DOI: 10.1515/znc-1990-0503

[**179**] Dejon L, Speicher A (2013) Synthesis of aurachin D and isoprenoid analogues from the myxobacterium *Stigmatella aurantiaca*. *Tetrahedron Lett* **54**:6700–6702. DOI: 10.1016/j.tetlet.2013.09.085

[**180**] Kruth S, Zimmermann CJM, Kuhr K, Hiller W, Lütz S, Pietruszka J, et al. (2023) Generation of aurachin derivatives by whole-cell biotransformation and evaluation of their antiprotozoal properties. *Molecules* **28**:1066. DOI: 10.3390/molecules28031066

[**181**] Mingyar E, Mühling L, Kulik A, Winkler A, Wibberg D, Kalinowski J, et al. (2021) A regulator based “semi-targeted” approach to activate silent biosynthetic gene clusters. *Int J Mol Sci* **22**:7567. DOI: 10.3390/ijms22147567

[**182**] Huo L, Hug JJ, Fu C, Bian X, Zhang Y, Müller R (2019) Heterologous expression of bacterial natural product biosynthetic pathways. *Nat Prod Rep* **36**:1412–1436. DOI: 10.1039/C8NP00091C

[**183**] Luo Y, Li BZ, Liu D, Zhang L, Chen Y, Jia B, et al. (2015) Engineered biosynthesis of natural products in heterologous hosts. *Chem Soc Rev* **44**:5265–5290. DOI: 10.1039/C5CS00025D

[**184**] Newman DJ, Cragg GM (2016) Natural products as sources of new drugs from 1981 to 2014. *J Nat Prod* **79**:629–661. DOI: 10.1021/acs.jnatprod.5b01055

[**185**] Butler MS (2004) The role of natural product chemistry in drug discovery. *J Nat Prod* **67**:2141–2153. DOI: 10.1021/np040106y

[**186**] Locey KJ, Lennon JT (2016) Scaling laws predict global microbial diversity. *PNAS* **113**:5970–5975. DOI: 10.1073/pnas.1521291113

[**187**] Zhang MM, Wang Y, Ang EL, Zhao H (2016) Engineering microbial hosts for production of bacterial natural products. *Nat Prod Rep* **33**:963–987. DOI: 10.1039/C6NP00017G

[**188**] Marienhagen J, Bott M (2013) Metabolic engineering of microorganisms for the synthesis of plant natural products. *J Biotechnol* **163**:166–178. DOI: 10.1016/j.jbiotec.2012.06.001

[**189**] Chemler JA, Koffas MA (2008) Metabolic engineering for plant natural product biosynthesis in microbes. *Curr Opin Biotechnol* **19**:597–605. DOI: 10.1016/j.copbio.2008.10.011

[**190**] Ziemert N, Alanjary M, Weber T (2016) The evolution of genome mining in microbes – A review. *Nat Prod Rep* **33**:988–1005. DOI: 10.1039/C6NP00025H

[**191**] Terlouw BR, Blin K, Navarro-Muñoz JC, Avalon NE, Chevrette MG, Egbert S, et al. (2023) MIBiG 3.0: A community-driven effort to annotate experimentally validated biosynthetic gene clusters. *Nucleic Acids Res* **51**:603–610. DOI: 10.1093/nar/gkac1049

[**192**] Imhoff JF, Labes A, Wiese J (2011) Bio-mining the microbial treasures of the ocean: New natural products. *Biotechnol Adv* **29**:468–482. DOI: 10.1016/j.biotechadv.2011.03.001

[**193**] Blin K, Shaw S, Kloosterman AM, Charlop-Powers Z, van Wezel GP, Medema MH, et al. (2021) antiSMASH 6.0: Improving cluster detection and comparison capabilities. *Nucleic Acids Res* **49**:29–35. DOI: 10.1093/nar/gkab335

[**194**] Mungan MD, Alanjary M, Blin K, Weber T, Medema MH, Ziemert N (2020) ARTS 2.0: Feature updates and expansion of the Antibiotic Resistant Target Seeker for comparative genome mining. *Nucleic Acids Res* **48**:546–552. DOI: 10.1093/nar/gkaa374

[**195**] Skinnider MA, Johnston CW, Gunabalasingam M, Merwin NJ, Kieliszek AM, MacLellan RJ, et al. (2020) Comprehensive prediction of secondary metabolite structure and biological activity from microbial genome sequences. *Nat Commun* **11**:6058. DOI: 10.1038/s41467-020-19986-1

[**196**] Brötz-Oesterhelt H, Hughes C, Sass P, Stegmann E, Ziemert N (2023) Aktuelle Methoden in der antibakteriellen Naturstoffforschung. *BIOspektrum* **6**:599–601. DOI: 10.1007/s12268-023-1998-4

[**197**] Ongley SE, Bian X, Neilan BA, Müller R (2013) Recent advances in the heterologous expression of microbial natural product biosynthetic pathways. *Nat Prod Rep* **30**:1121. DOI: 10.1039/c3np70034h

[**198**] Kang HS, Kim ES (2021) Recent advances in heterologous expression of natural product biosynthetic gene clusters in *Streptomyces* hosts. *Curr Opin Biotechnol* **69**:118–127. DOI: 10.1016/j.copbio.2020.12.016

[**199**] Vickers CE, Williams TC, Peng B, Cherry J (2017) Recent advances in synthetic biology for engineering isoprenoid production in yeast. *Curr Opin Chem Biol* **40**:47–56. DOI: 10.1016/j.cbpa.2017.05.017

[**200**] Moser S, Pichler H (2019) Identifying and engineering the ideal microbial terpenoid production host. *Appl Microbiol Biotechnol* **103**:5501–5516. DOI: 10.1007/s00253-019-09892-y

[**201**] Klaus O, Hilgers F, Nakielski A, Hasenklever D, Jaeger KE, Axmann IM, et al. (2022) Engineering phototrophic bacteria for the production of terpenoids. *Curr Opin Biotechnol* **77**:102764. DOI: 10.1016/j.copbio.2022.102764

[**202**] Park D, Swayambhu G, Pfeifer BA (2020) Heterologous biosynthesis as a platform for producing new generation natural products. *Curr Opin Biotechnol* **66**:123–130. DOI: 10.1016/j.copbio.2020.06.014

[**203**] Nah HJ, Pyeon HR, Kang SH, Choi SS, Kim ES (2017) Cloning and heterologous expression of a large-sized natural product biosynthetic gene cluster in *Streptomyces* species. *Front Microbiol* **8**:394. DOI: 10.3389/fmicb.2017.00394

[**204**] Loeschcke A, Thies S (2020) Engineering of natural product biosynthesis in *Pseudomonas putida*. *Curr Opin Biotechnol* **65**:213–224. DOI: 10.1016/j.copbio.2020.03.007

[**205**] Wackett LP (2003) *Pseudomonas putida* — A versatile biocatalyst. *Nat Biotechnol* **21**:136–138. DOI: 10.1038/nbt0203-136

[**206**] Poblete-Castro I, Becker J, Dohnt K, dos Santos VM, Wittmann C (2012) Industrial biotechnology of *Pseudomonas putida* and related species. *Appl Microbiol Biotechnol* **93**:2279–2290. DOI: 10.1007/s00253-012-3928-0

[**207**] Weimer A, Kohlstedt M, Volke DC, Nikel PI, Wittmann C (2020) Industrial biotechnology of *Pseudomonas putida*: Advances and prospects. *Appl Microbiol Biotechnol* **104**:7745–7766. DOI: 10.1007/s00253-020-10811-9

[**208**] Kampers LFC, Volkers RJM, Martins dos Santos VAP (2019) *Pseudomonas putida* KT2440 is HV1 certified, not GRAS. *Microb Biotechnol* **12**:845–848. DOI: 10.1111/1751-7915.13443

[**209**] Martínez-García E, de Lorenzo V (2011) Engineering multiple genomic deletions in Gram-negative bacteria: Analysis of the multi-resistant antibiotic profile of *Pseudomonas putida* KT2440. *Environ Microbiol* **13**:2702–2716. DOI: 10.1111/j.1462-2920.2011.02538.x

[**210**] Franzetti L, Scarpellini M (2007) Characterisation of *Pseudomonas* spp. isolated from foods. *Ann Microbiol* **57**:39–47. DOI: 10.1007/BF03175048

[**211**] Mozejko-Ciesielska J (2021) *Pseudomonas putida*–based Cell Factories. *Microbial Cell Factories Engineering for Production of Biomolecules*. DOI: 10.1016/B978-0-12-821477-0.00025-8

[**212**] Nikel PI, de Lorenzo V (2018) *Pseudomonas putida* as a functional *chassis* for industrial biocatalysis: From native biochemistry to *trans*-metabolism. *Metab Eng* **50**:142–155. DOI: 10.1016/j.ymben.2018.05.005

[**213**] Nikel PI, Chavarría M, Fuhrer T, Sauer U, de Lorenzo V (2015) *Pseudomonas putida* KT2440 strain metabolizes glucose through a cycle formed by enzymes of the Entner-

Doudoroff, Embden-Meyerhof-Parnas, and pentose phosphate pathways. *J Biol Chem* **290**:25920–25932. DOI: 10.1074/jbc.M115.687749

[**214**] Kim J, Park W (2014) Oxidative stress response in *Pseudomonas putida*. *Appl Microbiol Biotechnol* **98**:6933–6946. DOI: 10.1007/s00253-014-5883-4

[**215**] Ebert BE, Kurth F, Grund M, Blank LM, Schmid A (2011) Response of *Pseudomonas putida* KT2440 to increased NADH and ATP demand. *Appl Environ Microbiol* **77**:6597–6605. DOI: 10.1128/AEM.05588-11

[**216**] Nikel PI, Chavarría M, Danchin A, de Lorenzo V (2016) From dirt to industrial applications: *Pseudomonas putida* as a synthetic biology *chassis* for hosting harsh biochemical reactions. *Curr Opin Chem Biol* **34**:20–29. DOI: 10.1016/j.cbpa.2016.05.011

[**217**] Martinez A, Kolvek SJ, Yip CLT, Hopke J, Brown KA, MacNeil IA, et al. (2004) Genetically modified bacterial strains and novel bacterial artificial chromosome shuttle vectors for constructing environmental libraries and detecting heterologous natural products in multiple expression hosts. *Appl Environ Microbiol* **70**:2452–2463. DOI: 10.1128/AEM.70.4.2452-2463.2004

[**218**] Stephan S, Heinzle E, Wenzel SC, Krug D, Müller R, Wittmann C (2006) Metabolic physiology of *Pseudomonas putida* for heterologous production of myxochromide. *Process Biochemistry* **41**:2146–2152. DOI: 10.1016/j.procbio.2006.06.022

[**219**] Bitzenhofer NL, Kruse L, Thies S, Wynands B, Lechtenberg T, Rönitz J, et al. (2021) Towards robust *Pseudomonas* cell factories to harbour novel biosynthetic pathways. *Essays Biochem* **65**:319–336. DOI: 10.1042/EBC20200173

[**220**] Martins dos Santos VAP, Timmis KN, Tümmler B, Weinel C (2004) Genomic Features of *Pseudomonas putida* strain KT2440. *Pseudomonas*. DOI: 10.1007/978-1-4419-9086-0_3

[**221**] Gross F, Luniak N, Perlova O, Gaitatzis N, Jenke-Kodama H, Gerth K, et al. (2006) Bacterial type III polyketide synthases: Phylogenetic analysis and potential for the production of novel secondary metabolites by heterologous expression in Pseudomonads. *Arch Microbiol* **185**:28–38. DOI: 10.1007/s00203-005-0059-3

[**222**] Gross F, Ring MW, Perlova O, Fu J, Schneider S, Gerth K, et al. (2006) Metabolic engineering of *Pseudomonas putida* for methylmalonyl-CoA biosynthesis to enable complex heterologous secondary metabolite formation. *Chem Biol* **13**:1253–1264. DOI: 10.1016/j.chembiol.2006.09.014

[**223**] Mi J, Becher D, Lubuta P, Dany S, Tusch K, Schewe H, et al. (2014) *De novo* production of the monoterpenoid geranic acid by metabolically engineered *Pseudomonas putida*. *Microb Cell Fact* **13**:170. DOI: 10.1186/s12934-014-0170-8

[**224**] Loeschcke A, Thies S (2015) *Pseudomonas putida*—A versatile host for the production of natural products. *Appl Microbiol Biotechnol* **99**:6197–6214. DOI: 10.1007/s00253-015-6745-4

[**225**] Kuepper J, Dickler J, Biggel M, Behnken S, Jäger G, Wierckx N, et al. (2015) Metabolic engineering of *Pseudomonas putida* KT2440 to produce anthranilate from glucose. *Front Microbiol* **6**:1310. DOI: 10.3389/fmicb.2015.01310

[**226**] Weihmann R, Domröse A, Drepper T, Jaeger K, Loeschcke A (2020) Protocols for yTREX/Tn5-based gene cluster expression in *Pseudomonas putida*. *Microb Biotechnol* **13**:250–262. DOI: 10.1111/1751-7915.13402

[**227**] Askitosari TD, Boto ST, Blank LM, Rosenbaum MA (2019) Boosting heterologous phenazine production in *Pseudomonas putida* KT2440 through the exploration of the natural sequence space. *Front Microbiol* **10**:1990. DOI: 10.3389/fmicb.2019.01990

[**228**] Glandorf DCM, Verheggen P, Jansen T, Jorritsma JW, Smit E, Leeflang P, et al. (2001) Effect of genetically modified *Pseudomonas putida* WCS358r on the fungal rhizosphere microflora of field-grown wheat. *Appl Environ Microbiol* **67**:3371–3378. DOI: 10.1128/AEM.67.8.3371-3378.2001

[**229**] Schmitz S, Nies S, Wierckx N, Blank LM, Rosenbaum MA (2015) Engineering mediator-based electroactivity in the obligate aerobic bacterium *Pseudomonas putida* KT2440. *Front Microbiol* **6**:284. DOI: 10.3389/fmicb.2015.00284

[**230**] Xing X, Peixia Jiang (2014) Recombinant bacteria for producing deoxyviolacein and uses thereof. U.S. Patent No. 8,778,654

[**231**] Müller MM, Kügler JH, Henkel M, Gerlitzki M, Hörmann B, Pöhnlein M, et al. (2012) Rhamnolipids—Next generation surfactants? *J Biotechnol* **162**:366–380. DOI: 10.1016/j.jbiotec.2012.05.022

[**232**] Thum O, Engel P, Gehring C, Schaffer S, Wessel M (2019) Methods of producing rhamnolipids. U.S. Patent No. 10,174,353

[**233**] Abdel-Mawgoud AM, Lépine F, Déziel E (2010) Rhamnolipids: Diversity of structures, microbial origins and roles. *Appl Microbiol Biotechnol* **86**:1323–1336. DOI: 10.1007/s00253-010-2498-2

[**234**] Tiso T, Zauter R, Tulke H, Leuchtle B, Li WJ, Behrens B, et al. (2017) Designer rhamnolipids by reduction of congener diversity: Production and characterization. *Microb Cell Fact* **16**:225. DOI: 10.1186/s12934-017-0838-y

[**235**] Tiso T, Ihling N, Kubicki S, Biselli A, Schonhoff A, Bator I, et al. (2020) Integration of genetic and process engineering for optimized rhamnolipid production using *Pseudomonas putida*. *Front Bioeng Biotechnol* **8**:976. DOI: 10.3389/fbioe.2020.00976

[**236**] Arnold S, Henkel M, Wanger J, Wittgens A, Rosenau F, Hausmann R (2019) Heterologous rhamnolipid biosynthesis by *P. putida* KT2440 on bio-oil derived small organic acids and fractions. *AMB Express* **9**:80. DOI: 10.1186/s13568-019-0804-7

[**237**] Wittgens A, Tiso T, Arndt TT, Wenk P, Hemmerich J, Müller C, et al. (2011) Growth independent rhamnolipid production from glucose using the non-pathogenic *Pseudomonas putida* KT2440. *Microb Cell Fact* **10**:80. DOI: 10.1186/1475-2859-10-80

[**238**] Beuker J, Barth T, Steier A, Wittgens A, Rosenau F, Henkel M, et al. (2016) High titer heterologous rhamnolipid production. *AMB Express* **6**:124. DOI: 10.1186/s13568-016-0298-5

[**239**] Loeschcke A, Markert A, Wilhelm S, Wirtz A, Rosenau F, Jaeger KE, et al. (2013) TREX: A universal tool for the transfer and expression of biosynthetic pathways in bacteria. *ACS Synth Biol* **2**:22–33. DOI: 10.1021/sb3000657

[**240**] Hernandez-Arranz S, Perez-Gil J, Marshall-Sabey D, Rodriguez-Concepcion M (2019) Engineering *Pseudomonas putida* for isoprenoid production by manipulating endogenous and shunt pathways supplying precursors. *Microb Cell Fact* **18**:152. DOI: 10.1186/s12934-019-1204-z

[**241**] Sánchez-Pascuala A, Fernández-Cabezón L, de Lorenzo V, Nikel PI (2019) Functional implementation of a linear glycolysis for sugar catabolism in *Pseudomonas putida*. *Metab Eng* **54**:200–211. DOI: 10.1016/j.ymben.2019.04.005

[**242**] Fidan O, Zhan J (2019) Discovery and engineering of an endophytic *Pseudomonas* strain from Taxus chinensis for efficient production of zeaxanthin diglucoside. *J Biol Eng* **13**:66. DOI: 10.1186/s13036-019-0196-x

[**243**] Cummings M, Breitling R, Takano E (2014) Steps towards the synthetic biology of polyketide biosynthesis. *FEMS Microbiol Lett* **351**:116–125. DOI: 10.1111/1574-6968.12365

[**244**] Gross F, Gottschalk D, Müller R (2005) Posttranslational modification of myxobacterial carrier protein domains in *Pseudomonas* sp. by an intrinsic phosphopantetheinyl transferase. *Appl Microbiol Biotechnol* **68**:66–74. DOI: 10.1007/s00253-004-1836-7

[**245**] Owen JG, Copp JN, Ackerley DF (2011) Rapid and flexible biochemical assays for evaluating 4′-phosphopantetheinyl transferase activity. *Biochem J* **436**:709–717. DOI: 10.1042/BJ20110321

[**246**] Choi KR, Lee SY (2020) Protocols for Rec ET-based markerless gene knockout and integration to express heterologous biosynthetic gene clusters in *Pseudomonas putida*. *Microb Biotechnol* **13**:199–209. DOI: 10.1111/1751-7915.13374

[**247**] Gemperlein K, Hoffmann M, Huo L, Pilak P, Petzke L, Müller R, et al. (2017) Synthetic biology approaches to establish a heterologous production system for coronatines. *Metab Eng* **44**:213–222. DOI: 10.1016/j.ymben.2017.09.009

[**248**] Hage-Hülsmann J, Grünberger A, Thies S, Santiago-Schübel B, Klein AS, Pietruszka J, et al. (2018) Natural biocide cocktails: Combinatorial antibiotic effects of prodigiosin and biosurfactants. *PLoS One* **13**:e0200940. DOI: 10.1371/journal.pone.0200940

[**249**] Danevčič T, Borić Vezjak M, Zorec M, Stopar D (2016) Prodigiosin - A multifaceted *Escherichia coli* antimicrobial agent. *PLoS One* **11**:e0162412. DOI: 10.1371/journal.pone.0162412

[**250**] Domröse A, Klein AS, Hage-Hülsmann J, Thies S, Svensson V, Classen T, et al. (2015) Efficient recombinant production of prodigiosin in *Pseudomonas putida*. *Front Microbiol* **6**:972. DOI: 10.3389/fmicb.2015.00972

[**251**] Domröse A, Hage-Hülsmann J, Thies S, Weihmann R, Kruse L, Otto M, et al. (2019) *Pseudomonas putida* rDNA is a favored site for the expression of biosynthetic genes. *Sci Rep* **9**:7028. DOI: 10.1038/s41598-019-43405-1

[**252**] Klein AS, Domröse A, Bongen P, Brass HUC, Classen T, Loeschcke A, et al. (2017) New prodigiosin derivatives obtained by mutasynthesis in *Pseudomonas putida*. *ACS Synth Biol* **6**:1757–1765. DOI: 10.1021/acssynbio.7b00099

[**253**] Haddix PL, Shanks RMQ (2020) Production of prodigiosin pigment by *Serratia marcescens* is negatively associated with cellular ATP levels during high-rate, low-cell-density growth. *Can J Microbiol* **66**:243–255. DOI: 10.1139/cjm-2019-0548

[**254**] Cook TB, Jacobson TB, Venkataraman M V., Hofstetter H, Amador-Noguez D, Thomas MG, et al. (2021) Stepwise genetic engineering of *Pseudomonas putida* enables robust heterologous production of prodigiosin and glidobactin A. *Metab Eng* **67**:112–124. DOI: 10.1016/j.ymben.2021.06.004

[**255**] Nelson KE, Weinel C, Paulsen IT, Dodson RJ, Hilbert H, Martins dos Santos VAP, et al. (2002) Complete genome sequence and comparative analysis of the metabolically versatile *Pseudomonas putida* KT2440. *Environ Microbiol* **4**:799–808. DOI: 10.1046/j.1462-2920.2002.00366.x

[**256**] Martin-Pascual M, Batianis C, Bruinsma L, Asin-Garcia E, Garcia-Morales L, Weusthuis RA, et al. (2021) A navigation guide of synthetic biology tools for *Pseudomonas putida*. *Biotechnol Adv* **49**:107732. DOI: 10.1016/j.biotechadv.2021.107732

[**257**] Silva-Rocha R, Martínez-García E, Calles B, Chavarría M, Arce-Rodríguez A, de las Heras A, et al. (2013) The Standard European Vector Architecture (SEVA): A coherent platform for the analysis and deployment of complex prokaryotic phenotypes. *Nucleic Acids Res* **41**:666–675. DOI: 10.1093/nar/gks1119

[**258**] Martínez-García E, Aparicio T, Goñi-Moreno A, Fraile S, de Lorenzo V (2015) SEVA 2.0: An update of the Standard European Vector Architecture for de-/re-construction of bacterial functionalities. *Nucleic Acids Res* **43**:1183–1189. DOI: 10.1093/nar/gku1114

[**259**] Martínez-García E, Goñi-Moreno A, Bartley B, McLaughlin J, Sánchez-Sampedro L, Pascual del Pozo H, et al. (2020) SEVA 3.0: An update of the Standard European Vector Architecture for enabling portability of genetic constructs among diverse bacterial hosts. *Nucleic Acids Res* **48**:1164–1170. DOI: 10.1093/nar/gkz1024

[**260**] Damalas SG, Batianis C, Martin-Pascual M, de Lorenzo V, Martins dos Santos VAP (2020) SEVA 3.1: Enabling interoperability of DNA assembly among the SEVA, BioBricks and Type IIS restriction enzyme standards. *Microb Biotechnol* **13**:1793–1806. DOI: 10.1111/1751-7915.13609

[**261**] Zhang JJ, Tang X, Zhang M, Nguyen D, Moore BS (2017) Broad-host-range expression reveals native and host regulatory elements that influence heterologous antibiotic production in Gram-negative bacteria. *mBio* **8**:e01291-17. DOI: 10.1128/mBio.01291-17

[**262**] Jahn M, Vorpahl C, Türkowsky D, Lindmeyer M, Bühler B, Harms H, et al. (2014) Accurate determination of plasmid copy number of flow-sorted cells using droplet digital PCR. *Anal Chem* **86**:5969–5976. DOI: 10.1021/ac501118v

[**263**] Lauritsen I, Porse A, Sommer MOA, Nørholm MHH (2017) A versatile one-step CRISPR-Cas9 based approach to plasmid-curing. *Microb Cell Fact* **16**:135. DOI: 10.1186/s12934-017-0748-z

[**264**] Kolter R, Inuzuka M, Helinski DR (1978) Trans-complementation-dependent replication of a low molecular weight origin fragment from plasmid R6K. *Cell* **15**:1199–1208. DOI: 10.1016/0092-8674(78)90046-6

[**265**] Fernández M, Conde S, de la Torre J, Molina-Santiago C, Ramos JL, Duque E (2012) Mechanisms of resistance to chloramphenicol in *Pseudomonas putida* KT2440. *Antimicrob Agents Chemother* **56**:1001–1009. DOI: 10.1128/AAC.05398-11

[**266**] Meade MJ, Waddell RL, Callahan TM (2001) Soil bacteria *Pseudomonas putida* and *Alcaligenes xylosoxidans* subsp. *denitrificans* inactivate triclosan in liquid and solid substrates. *FEMS Microbiol Lett* **204**:45–48. DOI: 10.1111/j.1574-6968.2001.tb10860.x

[**267**] Zobel S, Benedetti I, Eisenbach L, de Lorenzo V, Wierckx N, Blank LM (2015) Tn7-based device for calibrated heterologous gene expression in *Pseudomonas putida*. *ACS Synth Biol* **4**:1341–1351. DOI: 10.1021/acssynbio.5b00058

[**268**] Calero P, Jensen SI, Nielsen AT (2016) Broad-host-range ProUSER vectors enable fast characterization of inducible promoters and optimization of *p*-coumaric acid production in *Pseudomonas putida* KT2440. *ACS Synth Biol* **5**:741–753. DOI: 10.1021/acssynbio.6b00081

[**269**] Cook TB, Rand JM, Nurani W, Courtney DK, Liu SA, Pfleger BF (2018) Genetic tools for reliable gene expression and recombineering in *Pseudomonas putida*. *J Ind Microbiol Biotechnol* **45**:517–527. DOI: 10.1007/s10295-017-2001-5

[**270**] Salis HM (2011) The Ribosome Binding Site Calculator. *Methods Enzymol* **498**:19–42. DOI: 10.1016/B978-0-12-385120-8.00002-4

[**271**] Amarelle V, Sanches-Medeiros A, Silva-Rocha R, Guazzaroni ME (2019) Expanding the toolbox of broad host-range transcriptional terminators for proteobacteria through metagenomics. *ACS Synth Biol* **8**:647–654. DOI: 10.1021/acssynbio.8b00507

[**272**] Elmore JR, Furches A, Wolff GN, Gorday K, Guss AM (2017) Development of a high efficiency integration system and promoter library for rapid modification of *Pseudomonas putida* KT2440. *Metab Eng Commun* **5**:1–8. DOI: 10.1016/j.meteno.2017.04.001

[**273**] Makart S, Heinemann M, Panke S (2007) Characterization of the AlkS/P_{alkB}-expression system as an efficient tool for the production of recombinant proteins in *Escherichia coli* fed-batch fermentations. *Biotechnol Bioeng* **96**:326–336. DOI: 10.1002/bit.21117

[**274**] Hoffmann L, Sugue MF, Brüser T (2021) A tunable anthranilate-inducible gene expression system for *Pseudomonas* species. *Appl Microbiol Biotechnol* **105**:247–258. DOI: 10.1007/s00253-020-11034-8

[**275**] Prior JE, Lynch MD, Gill RT (2010) Broad-host-range vectors for protein expression across Gram-negative hosts. *Biotechnol Bioeng* **106**:326–332. DOI: 10.1002/bit.22695

[**276**] de Lorenzo V, Eltis L, Kessler B, Timmis KN (1993) Analysis of *Pseudomonas* gene products using *lacIq*/$P_{trp-lac}$ plasmids and transposons that confer conditional phenotypes. *Gene* **123**:17–24. DOI: 10.1016/0378-1119(93)90533-9

[**277**] Graf N, Altenbuchner J (2014) Genetic engineering of *Pseudomonas putida* KT2440 for rapid and high-yield production of vanillin from ferulic acid. *Appl Microbiol Biotechnol* **98**:137–149. DOI: 10.1007/s00253-013-5303-1

[**278**] Hoffmann J, Altenbuchner J (2015) Functional characterization of the mannitol promoter of *Pseudomonas fluorescens* DSM 50106 and its application for a mannitol-inducible expression system for *Pseudomonas putida* KT2440. *PLoS One* **10**:e0133248. DOI: 10.1371/journal.pone.0133248

[**279**] Hüsken LE, Beeftink R, de Bont JAM, Wery J (2001) High-rate 3-methylcatechol production in *Pseudomonas putida* strains by means of a novel expression system. *Appl Microbiol Biotechnol* **55**:571–577. DOI: 10.1007/s002530000566

[**280**] Cebolla A (2001) Rational design of a bacterial transcriptional cascade for amplifying gene expression capacity. *Nucleic Acids Res* **29**:759–766. DOI: 10.1093/nar/29.3.759

[**281**] Martínez-García E, Calles B, Arévalo-Rodríguez M, de Lorenzo V (2011) pBAM1: An all-synthetic genetic tool for analysis and construction of complex bacterial phenotypes. *BMC Microbiol* **11**:38. DOI: 10.1186/1471-2180-11-38

[**282**] Martínez-García E, Aparicio T, de Lorenzo V, Nikel PI (2014) New transposon tools tailored for metabolic engineering of Gram-negative microbial cell factories. *Front Bioeng Biotechnol* **2**:46. DOI: 10.3389/fbioe.2014.00046

[**283**] Dvořák P, de Lorenzo V (2018) Refactoring the upper sugar metabolism of *Pseudomonas putida* for co-utilization of cellobiose, xylose, and glucose. *Metab Eng* **48**:94–108. DOI: 10.1016/j.ymben.2018.05.019

[**284**] Nikel PI, de Lorenzo V (2013) Implantation of unmarked regulatory and metabolic modules in Gram-negative bacteria with specialised mini-transposon delivery vectors. *J Biotechnol* **163**:143–154. DOI: 10.1016/j.jbiotec.2012.05.002

[**285**] Zhang JJ, Tang X, Huan T, Ross AC, Moore BS (2020) Pass-back chain extension expands multimodular assembly line biosynthesis. *Nat Chem Biol* **16**:42–49. DOI: 10.1038/s41589-019-0385-4

[**286**] Martínez-García E, Nikel PI, Aparicio T, de Lorenzo V (2014) *Pseudomonas* 2.0: Genetic upgrading of *P. putida* KT2440 as an enhanced host for heterologous gene expression. *Microb Cell Fact* **13**:159. DOI: 10.1186/s12934-014-0159-3

[**287**] Miyazaki R, van der Meer JR (2013) A new large-DNA-fragment delivery system based on integrase activity from an integrative and conjugative element. *Appl Environ Microbiol* **79**:4440–4447. DOI: 10.1128/AEM.00711-13

[**288**] Wang G, Zhao Z, Ke J, Engel Y, Shi YM, Robinson D, et al. (2019) CRAGE enables rapid activation of biosynthetic gene clusters in undomesticated bacteria. *Nat Microbiol* **4**:2498–2510. DOI: 10.1038/s41564-019-0573-8

[**289**] Bator I, Wittgens A, Rosenau F, Tiso T, Blank LM (2020) Comparison of three xylose pathways in *Pseudomonas putida* KT2440 for the synthesis of valuable products. *Front Bioeng Biotechnol* **7**:1–18. DOI: 10.3389/fbioe.2019.00480

[**290**] Bruckbauer ST, Kvitko BH, Karkhoff-Schweizer RR, Schweizer HP (2015) Tn5/7-lux: A versatile tool for the identification and capture of promoters in Gram-negative bacteria. *BMC Microbiol* **15**:17. DOI: 10.1186/s12866-015-0354-3

[**291**] Choi KH, Gaynor JB, White KG, Lopez C, Bosio CM, Karkhoff-Schweizer RR, et al. (2005) A Tn7-based broad-range bacterial cloning and expression system. *Nat Methods* **2**:443–448. DOI: 10.1038/nmeth765

[**292**] Kruse L, Loeschcke A, De Witt J, Wierckx N, Jaeger KE, Thies S (2023) *Halopseudomonas* species: Cultivation and molecular genetic tools. *Microb Biotechnol* **00**:1-14. DOI: 10.1111/1751-7915.14369

[**293**] Slager J, Veening JW (2016) Hard-wired control of bacterial processes by chromosomal gene location. *Trends Microbiol* **24**:788–800. DOI: 10.1016/j.tim.2016.06.003

[**294**] Chaves JE, Wilton R, Gao Y, Munoz NM, Burnet MC, Schmitz Z, et al. (2020) Evaluation of chromosomal insertion loci in the *Pseudomonas putida* KT2440 genome for predictable biosystems design. *Metab Eng Commun* **11**:e00139. DOI: 10.1016/j.mec.2020.e00139

[**295**] Choi KR, Cho JS, Cho IJ, Park D, Lee SY (2018) Markerless gene knockout and integration to express heterologous biosynthetic gene clusters in *Pseudomonas putida*. *Metab Eng* **47**:463–474. DOI: 10.1016/j.ymben.2018.05.003

[**296**] Volke DC, Friis L, Wirth NT, Turlin J, Nikel PI (2020) Synthetic control of plasmid replication enables target- and self-curing of vectors and expedites genome engineering of *Pseudomonas putida*. *Metab Eng Commun* **10**:e00126. DOI: 10.1016/j.mec.2020.e00126

[**297**] Lassak J, Henche AL, Binnenkade L, Thormann KM (2010) ArcS, the cognate sensor kinase in an atypical Arc system of *Shewanella oneidensis* MR-1. *Appl Environ Microbiol* **76**:3263–3274. DOI: 10.1128/AEM.00512-10

[**298**] Elmore JR, Dexter GN, Salvachúa D, O'Brien M, Klingeman DM, Gorday K, et al. (2020) Engineered *Pseudomonas putida* simultaneously catabolizes five major components of corn stover lignocellulose: Glucose, xylose, arabinose, *p*-coumaric acid, and acetic acid. *Metab Eng* **62**:62–71. DOI: 10.1016/j.ymben.2020.08.001

[**299**] Liang P, Zhang Y, Xu B, Zhao Y, Liu X, Gao W, et al. (2020) Deletion of genomic islands in the *Pseudomonas putida* KT2440 genome can create an optimal *chassis* for synthetic biology applications. *Microb Cell Fact* **19**:70. DOI: 10.1186/s12934-020-01329-w

[**300**] Wirth NT, Kozaeva E, Nikel PI (2020) Accelerated genome engineering of *Pseudomonas putida* by I-*Sce*I—mediated recombination and CRISPR-Cas9 counterselection. *Microb Biotechnol* **13**:233–249. DOI: 10.1111/1751-7915.13396

[**301**] Ko YS, Kim JW, Lee JA, Han T, Kim GB, Park JE, et al. (2020) Tools and strategies of systems metabolic engineering for the development of microbial cell factories for chemical production. *Chem Soc Rev* **49**:4615–4636. DOI: 10.1039/D0CS00155D

[**302**] Fernández-Cabezón L, Nikel PI (2020) Advanced Metabolic Engineering Strategies for the Development of Sustainable Microbial Processes. *New and Future Developments in Microbial Biotechnology and Bioengineering*. DOI: 10.1016/B978-0-444-64301-8.00011-1

[**303**] Tiso T, Sabelhaus P, Behrens B, Wittgens A, Rosenau F, Hayen H, et al. (2016) Creating metabolic demand as an engineering strategy in *Pseudomonas putida* – Rhamnolipid synthesis as an example. *Metab Eng Commun* **3**:234–244. DOI: 10.1016/j.meteno.2016.08.002

[**304**] Qi LS, Larson MH, Gilbert LA, Doudna JA, Weissman JS, Arkin AP, et al. (2013) Repurposing CRISPR as an RNA-guided platform for sequence-specific control of gene expression. *Cell* **152**:1173–1183. DOI: 10.1016/j.cell.2013.02.022

[**305**] Zheng Y, Su T, Qi Q (2019) Microbial CRISPRi and CRISPRa systems for metabolic engineering. *Biotechnol Bioprocess Eng* **24**:579–591. DOI: 10.1007/s12257-019-0107-5

[**306**] Tan SZ, Reisch CR, Prather KLJ (2018) A robust CRISPR interference gene repression system in *Pseudomonas*. *J Bacteriol* **200**:e00575-17. DOI: 10.1128/JB.00575-17

[**307**] Batianis C, Kozaeva E, Damalas SG, Martín-Pascual M, Volke DC, Nikel PI, et al. (2020) An expanded CRISPRi toolbox for tunable control of gene expression in *Pseudomonas putida*. *Microb Biotechnol* **13**:368–385. DOI: 10.1111/1751-7915.13533

[**308**] Kim SK, Yoon PK, Kim S, Woo S, Rha E, Lee H, et al. (2020) CRISPR interference-mediated gene regulation in *Pseudomonas putida* KT2440. *Microb Biotechnol* **13**:210–221. DOI: 10.1111/1751-7915.13382

[**309**] Kiattisewee C, Dong C, Fontana J, Sugianto W, Peralta-Yahya P, Carothers JM, et al. (2021) Portable bacterial CRISPR transcriptional activation enables metabolic engineering in *Pseudomonas putida*. *Metab Eng* **66**:283–295. DOI: 10.1016/j.ymben.2021.04.002

[**310**] Apura P, Saramago M, Peregrina A, Viegas SC, Carvalho SM, Saraiva LM, et al. (2020) Tailor-made sRNAs: A plasmid tool to control the expression of target mRNAs in *Pseudomonas putida*. *Plasmid* **109**:102503. DOI: 10.1016/j.plasmid.2020.102503

[**311**] Calles B, Goñi-Moreno Á, de Lorenzo V (2019) Digitalizing heterologous gene expression in Gram-negative bacteria with a portable ON/OFF module. *Mol Syst Biol* **15**:e8777. DOI: 10.15252/msb.20188777

[**312**] Tan SZ, Prather KL (2017) Dynamic pathway regulation: Recent advances and methods of construction. *Curr Opin Chem Biol* **41**:28–35. DOI: 10.1016/j.cbpa.2017.10.004

[**313**] Volke DC, Turlin J, Mol V, Nikel PI (2020) Physical decoupling of XylS/$_{Pm}$ regulatory elements and conditional proteolysis enable precise control of gene expression in *Pseudomonas putida*. *Microb Biotechnol* **13**:222–232. DOI: 10.1111/1751-7915.13383

[**314**] Gemperlein K, Zipf G, Bernauer HS, Müller R, Wenzel SC (2016) Metabolic engineering of *Pseudomonas putida* for production of docosahexaenoic acid based on a myxobacterial PUFA synthase. *Metab Eng* **33**:98–108. DOI: 10.1016/j.ymben.2015.11.001

[**315**] Wierckx NJP, Ballerstedt H, de Bont JAM, Wery J (2005) Engineering of solvent-tolerant *Pseudomonas putida* S12 for bioproduction of phenol from glucose. *Appl Environ Microbiol* **71**:8221–8227. DOI: 10.1128/AEM.71.12.8221-8227.2005

[**316**] Yu S, Plan MR, Winter G, Krömer JO (2016) Metabolic engineering of *Pseudomonas putida* KT2440 for the production of *para*-hydroxy benzoic acid. *Front Bioeng Biotechnol* **4**:90. DOI: 10.3389/fbioe.2016.00090

[**317**] Wirth NT, Gurdo N, Krink N, Vidal-Verdú À, Donati S, Férnandez-Cabezón L, et al. (2022) A synthetic C2 auxotroph of *Pseudomonas putida* for evolutionary engineering of alternative sugar catabolic routes. *Metab Eng* **74**:83–97. DOI: 10.1016/j.ymben.2022.09.004

[**318**] Banerjee D, Eng T, Lau AK, Sasaki Y, Wang B, Chen Y, et al. (2020) Genome-scale metabolic rewiring improves titers rates and yields of the non-native product indigoidine at scale. *Nat Commun* **11**:5385. DOI: 10.1038/s41467-020-19171-4

[**319**] Bornscheuer UT, Huisman GW, Kazlauskas RJ, Lutz S, Moore JC, Robins K (2012) Engineering the third wave of biocatalysis. *Nature* **485**:185–194. DOI: 10.1038/nature11117

[**320**] Reetz MT (2013) Biocatalysis in organic chemistry and biotechnology: Past, present, and future. *J Am Chem Soc* **135**:12480–12496. DOI: 10.1021/ja405051f

[**321**] Classen T, Pietruszka J (2018) Complex molecules, clever solutions – Enzymatic approaches towards natural product and active agent syntheses. *Bioorg Med Chem* **26**:1285–1303. DOI: 10.1016/j.bmc.2017.06.045

[**322**] Klein AS, Brass HUC, Klebl DP, Classen T, Loeschcke A, Drepper T, et al. (2018) Preparation of cyclic prodiginines by mutasynthesis in *Pseudomonas putida* KT2440. *ChemBioChem* **19**:1545–1552. DOI: 10.1002/cbic.201800154

[**323**] Brass HUC, Klein AS, Nyholt S, Classen T, Pietruszka J (2019) Condensing enzymes from *Pseudoalteromonadaceae* for prodiginine synthesis. *Adv Synth Catal* **361**:2659–2667. DOI: 10.1002/adsc.201900183

[**324**] Weber TM, Leyens A, Berning L, Stork B, Pietruszka J (2023) New prodigiosin derivatives – Chemoenzymatic synthesis and physiological evaluation against cisplatin-resistant cancer cells. *Catal Sci Technol* **13**:6165–6184. DOI: 10.1039/D3CY00913K

[**325**] Floss HG (2006) Combinatorial biosynthesis—Potential and problems. *J Biotechnol* **124**:242–257. DOI: 10.1016/j.jbiotec.2005.12.001

[**326**] Lai HE, Obled AMC, Chee SM, Morgan RM, Lynch R, Sharma S V., et al. (2021) GenoChemetic strategy for derivatization of the violacein natural product scaffold. *ACS Chem Biol* **16**:2116–2123. DOI: 10.1021/acschembio.1c00483

[**327**] Weihmann R (2022) Rekombinante Alkaloidproduktion in *Pseudomonas putida* mit Hilfe modularer Systeme zur Genclusterexpression. *Heinrich Heine University Düsseldorf*. Dissertation

[**328**] Kirschning A, Hahn F (2012) Merging chemical synthesis and biosynthesis: A new chapter in the total synthesis of natural products and natural product libraries. *Angew Chem, Int Ed* **51**:4012–4022. DOI: 10.1002/anie.201107386

[**329**] Kirschning A, Hahn F (2012) Vereinigung von chemischer Synthese und Biosynthese: ein neues Kapitel in der Totalsynthese von Naturstoffen und Naturstoffbibliotheken. *Angew Chem* **124**:4086–4096. DOI: 10.1002/ange.201107386

[**330**] Wong J, Rios-Solis L, Keasling JD (2016) Microbial Production of Isoprenoids. *Consequences of Microbial Interactions with Hydrocarbons, Oils, and Lipids: Production of Fuels and Chemicals*. DOI: 10.1007/978-3-319-31421-1_219-1

[**331**] Vollmann DJ, Winand L, Nett M (2022) Emerging concepts in the semisynthetic and mutasynthetic production of natural products. *Curr Opin Biotechnol* **77**:102761. DOI: 10.1016/j.copbio.2022.102761

[**332**] Winand L, Sester A, Nett M (2021) Bioengineering of anti-inflammatory natural products. *ChemMedChem* **16**:767–776. DOI: 10.1002/cmdc.202000771

[**333**] Kirschning A, Taft F, Knobloch T (2007) Total synthesis approaches to natural product derivatives based on the combination of chemical synthesis and metabolic engineering. *Org Biomol Chem* **5**:3245. DOI: 10.1039/b709549j

[**334**] Rinehart KL (1977) Mutasynthesis of new antibiotics. *Pure Appl Chem* **49**:1361–1384. DOI: 10.1351/pac197749091361

[**335**] Weist S, Süssmuth RD (2005) Mutational biosynthesis—A tool for the generation of structural diversity in the biosynthesis of antibiotics. *Appl Microbiol Biotechnol* **68**:141–150. DOI: 10.1007/s00253-005-1891-8

[**336**] Wang CL, Ozuna SC, Clark DS, Keasling JD (2002) A deep-sea hydrothermal vent isolate, *Pseudomonas aeruginosa* CW961, requires thiosulfate for Cd tolerance and precipitation. *Biotechnol Lett* **24**:637–641. DOI: 10.1023/A:1015043324584

[**337**] Vyas P, Rahi P, Gulati A (2009) Stress tolerance and genetic variability of phosphate-solubilizing fluorescent *Pseudomonas* from the cold deserts of the trans-Himalayas. *Microb Ecol* **58**:425–434. DOI: 10.1007/s00248-009-9511-2

[**338**] Craig K, Johnson BR, Grunden A (2021) Leveraging *Pseudomonas* stress response mechanisms for industrial applications. *Front Microbiol* **12**:660134. DOI: 10.3389/fmicb.2021.660134

[**339**] Kim J, Park W (2014) Oxidative stress response in *Pseudomonas putida*. *Appl Microbiol Biotechnol* **98**:6933–6946. DOI: 10.1007/s00253-014-5883-4

[**340**] Ramos JL, Sol Cuenca M, Molina-Santiago C, Segura A, Duque E, Gómez-García MR, et al. (2015) Mechanisms of solvent resistance mediated by interplay of cellular factors in *Pseudomonas putida*. *FEMS Microbiol Rev* **39**:555–566. DOI: 10.1093/femsre/fuv006

[**341**] Liu H, Li S, Xie X, Shi Q (2021) *Pseudomonas putida* actively forms biofilms to protect the population under antibiotic stress. *Environ Pollut* **270**:116261. DOI: 10.1016/j.envpol.2020.116261

[**342**] Martínez-García E, Nikel PI, Chavarría M, de Lorenzo V (2014) The metabolic cost of flagellar motion in *Pseudomonas putida* KT2440. *Environ Microbiol* **16**:291–303. DOI: 10.1111/1462-2920.12309

[**343**] An BC, Lee SS, Lee EM, Lee JT, Wi SG, Jung HS, et al. (2011) Functional switching of a novel prokaryotic 2-Cys peroxiredoxin (PpPrx) under oxidative stress. *Cell Stress Chaperones* **16**:317–328. DOI: 10.1007/s12192-010-0243-5

[**344**] Yeom J, Lee Y, Park W (2012) ATP-dependent RecG helicase is required for the transcriptional regulator OxyR function in *Pseudomonas* species. *J Biol Chem* **287**:24492–24504. DOI: 10.1074/jbc.M112.356964

[**345**] Santos PM, Benndorf D, Sá-Correia I (2004) Insights into *Pseudomonas putida* KT2440 response to phenol-induced stress by quantitative proteomics. *Proteomics* **4**:2640–2652. DOI: 10.1002/pmic.200300793

[**346**] Tavita K, Mikkel K, Tark-Dame M, Jerabek H, Teras R, Sidorenko J, et al. (2012) Homologous recombination is facilitated in starving populations of *Pseudomonas putida* by phenol stress and affected by chromosomal location of the recombination target. *Mutat Res-Fundam Mol Mech Mutagen* **737**:12–24. DOI: 10.1016/j.mrfmmm.2012.07.004

[**347**] Nikel PI, Chavarría M, Martínez-García E, Taylor AC, de Lorenzo V (2013) Accumulation of inorganic polyphosphate enables stress endurance and catalytic vigour in *Pseudomonas putida* KT2440. *Microb Cell Fact* **12**:50. DOI: 10.1186/1475-2859-12-50

[**348**] Yeom J, Imlay JA, Park W (2010) Iron homeostasis affects antibiotic-mediated cell death in *Pseudomonas* species. *J Biol Chem* **285**:22689–22695. DOI: 10.1074/jbc.M110.127456

[**349**] Ramos JL, Krell T, Daniels C, Segura A, Duque E (2009) Responses of *Pseudomonas* to small toxic molecules by a mosaic of domains. *Curr Opin Microbiol* **12**:215–220. DOI: 10.1016/j.mib.2009.02.001

[**350**] Wijte D, van Baar BLM, Heck AJR, Altelaar AFM (2011) Probing the proteome response to toluene exposure in the solvent tolerant *Pseudomonas putida* S12. *J Proteome Res* **10**:394–403. DOI: 10.1021/pr100401n

[**351**] Rojas A, Duque E, Mosqueda G, Golden G, Hurtado A, Ramos JL, et al. (2001) Three efflux pumps are required to provide efficient tolerance to toluene in *Pseudomonas putida* DOT-T1E. *J Bacteriol* **183**:3967–3973. DOI: 10.1128/JB.183.13.3967-3973.2001

[**352**] Otero-Asman JR, Wettstadt S, Bernal P, Llamas MA (2019) Diversity of extracytoplasmic function sigma (σ^{ECF}) factor-dependent signaling in *Pseudomonas*. *Mol Microbiol* **112**:356–373. DOI: 10.1111/mmi.14331

[**353**] Welsh DT (2000) Ecological significance of compatible solute accumulation by microorganisms: from single cells to global climate. *FEMS Microbiol Rev* **24**:263–290. DOI: 10.1111/j.1574-6976.2000.tb00542.x

[**354**] Mikkat S, Galinski EA, Berg G, Minkwitz A, Schoor A (2000) Salt adaptation in Pseudomonads: Characterization of glucosylglycerol-synthesizing isolates from brackish coastal waters and the rhizosphere. *Syst Appl Microbiol* **23**:31–40. DOI: 10.1016/S0723-2020(00)80043-0

[**355**] Kurz M, Burch AY, Seip B, Lindow SE, Gross H (2010) Genome-driven investigation of compatible solute biosynthesis pathways of *Pseudomonas syringae* pv. *syringae* and their contribution to water stress tolerance. *Appl Environ Microbiol* **76**:5452–5462. DOI: 10.1128/AEM.00686-10

[**356**] Freeman BC, Chen C, Beattie GA (2010) Identification of the trehalose biosynthetic loci of *Pseudomonas syringae* and their contribution to fitness in the phyllosphere. *Environ Microbiol* **12**:1486–1497. DOI: 10.1111/j.1462-2920.2010.02171.x

[**357**] Sandhya V, Ali SkZ, Grover M, Reddy G, Venkateswarlu B (2010) Effect of plant growth promoting *Pseudomonas* spp. on compatible solutes, antioxidant status and plant growth of maize under drought stress. *Plant Growth Regul* **62**:21–30. DOI: 10.1007/s10725-010-9479-4

[**358**] Maslowska KH, Makiela-Dzbenska K, Fijalkowska IJ (2019) The SOS system: A complex and tightly regulated response to DNA damage. *Environ Mol Mutagen* **60**:368–384. DOI: 10.1002/em.22267

[**359**] Lawless C, Hubbard SJ (2014) Analysis of Chaperone Network Throughput. *The Molecular Chaperones Interaction Networks in Protein Folding and Degradation*. DOI: 10.1007/978-1-4939-1130-1_1

[**360**] Hartl FU, Bracher A, Hayer-Hartl M (2011) Molecular chaperones in protein folding and proteostasis. *Nature* **475**:324–332. DOI: 10.1038/nature10317

[**361**] Singh B, Gupta RS (2009) Conserved inserts in the Hsp60 (GroEL) and Hsp70 (DnaK) proteins are essential for cellular growth. *MGG* **281**:361–373. DOI: 10.1007/s00438-008-0417-3

[**362**] Ito F, Tamiya T, Ohtsu I, Fujimura M, Fukumori F (2014) Genetic and phenotypic characterization of the heat shock response in *Pseudomonas putida*. *Microbiologyopen* **3**:922–936. DOI: 10.1002/mbo3.217

[**363**] Bittner L, Arends J, Narberhaus F (2016) Mini review: ATP-dependent proteases in bacteria. *Biopolymers* **105**:505–517. DOI: 10.1002/bip.22831

[**364**] Henderson PJF, Maher C, Elbourne LDH, Eijkelkamp BA, Paulsen IT, Hassan KA (2021) Physiological functions of bacterial “multidrug” efflux pumps. *Chem Rev* **121**:5417–5478. DOI: 10.1021/acs.chemrev.0c01226

[**365**] Jayakody LN, Johnson CW, Whitham JM, Giannone RJ, Black BA, Cleveland NS, et al. (2018) Thermochemical wastewater valorization via enhanced microbial toxicity tolerance. *Energy Environ Sci* **11**:1625–1638. DOI: 10.1039/C8EE00460A

[**366**] Xu Q, Zheng Z, Zou L, Zhang C, Yang F, Zhou K, et al. (2020) A versatile *Pseudomonas putida* KT2440 with new ability: Selective oxidation of 5-hydroxymethylfurfural to 5-hydroxymethyl-2-furancarboxylic acid. *Bioprocess Biosyst Eng* **43**:67–73. DOI: 10.1007/s00449-019-02205-7

[**367**] Wehrmann M, Billard P, Martin-Meriadec A, Zegeye A, Klebensberger J (2017) Functional role of lanthanides in enzymatic activity and transcriptional regulation of pyrroloquinoline quinone-dependent alcohol dehydrogenases in *Pseudomonas putida* KT2440. *mBio* **8**:e00570-17. DOI: 10.1128/mBio.00570-17

[**368**] Zheng Z, Xu Q, Tan H, Zhou F, Ouyang J (2020) Selective biosynthesis of furoic acid from furfural by *Pseudomonas putida* and identification of molybdate transporter involvement in furfural oxidation. *Front Chem* **8**:587456. DOI: 10.3389/fchem.2020.587456

[**369**] Adewunmi Y, Namjilsuren S, Walker WD, Amato DN, Amato D V., Mavrodi O V., et al. (2019) Antimicrobial activity of, and cellular pathways targeted by, *p*-anisaldehyde and epigallocatechin gallate in the opportunistic human pathogen *Pseudomonas aeruginosa*. *Appl Environ Microbiol* **86**:e02482-19. DOI: 10.1128/AEM.02482-19

[**370**] de Bont JAM, Kieboom J (2001) Identification and molecular characterization of an efflux system involved in *Pseudomonas putida* S12 multidrug resistance. *Microbiology* **147**:43–51. DOI: 10.1099/00221287-147-1-43

[**371**] Helmann TC, Ongsarte CL, Lam J, Deutschbauer AM, Lindow SE (2019) Genome-wide transposon screen of a *Pseudomonas syringae mexB* mutant reveals the substrates of efflux transporters. *mBio* **10**:e02614-19. DOI: 10.1128/mBio.02614-19

[**372**] Nie L, Grell E, Malviya VN, Xie H, Wang J, Michel H (2016) Identification of the high-affinity substrate-binding site of the multidrug and toxic compound extrusion (MATE) family transporter from *Pseudomonas stutzeri*. *J Biol Chem* **291**:15503–15514. DOI: 10.1074/jbc.M116.728618

[**373**] García V, Godoy P, Daniels C, Hurtado A, Ramos JL, Segura A (2009) Functional analysis of new transporters involved in stress tolerance in *Pseudomonas putida* DOT-T1E. *Environ Microbiol Rep* **2**:389–395. DOI: 10.1111/j.1758-2229.2009.00093.x

[**374**] Roca A, Rodríguez-Herva JJ, Duque E, Ramos JL (2008) Physiological responses of *Pseudomonas putida* to formaldehyde during detoxification. *Microb Biotechnol* **1**:158–169. DOI: 10.1111/j.1751-7915.2007.00014.x

[**375**] Shivaji S, Prakash JSS (2010) How do bacteria sense and respond to low temperature? *Arch Microbiol* **192**:85–95. DOI: 10.1007/s00203-009-0539-y

[**376**] Sandoval NR, Papoutsakis ET (2016) Engineering membrane and cell-wall programs for tolerance to toxic chemicals: Beyond solo genes. *Curr Opin Microbiol* **33**:56–66. DOI: 10.1016/j.mib.2016.06.005

[**377**] Heipieper HJ, Diefenbach R, Keweloh H (1992) Conversion of *cis* unsaturated fatty acids to *trans*, a possible mechanism for the protection of phenol-degrading *Pseudomonas putida* P8 from substrate toxicity. *Appl Environ Microbiol* **58**:1847–1852. DOI: 10.1128/AEM.58.6.1847-1852.1992

[**378**] Heipieper HJ, Meinhardt F, Segura A (2003) The *cis-trans* isomerase of unsaturated fatty acids in *Pseudomonas* and *Vibrio*: biochemistry, molecular biology and physiological function of a unique stress adaptive mechanism. *FEMS Microbiol Lett* **229**:1–7. DOI: 10.1016/S0378-1097(03)00792-4

[**379**] Atashgahi S, Sánchez-Andrea I, Heipieper HJ, van der Meer JR, Stams AJM, Smidt H (2018) Prospects for harnessing biocide resistance for bioremediation and detoxification. *Science* **360**:743–746. DOI: 10.1126/science.aar3778

[**380**] Mann EE, Wozniak DJ (2012) *Pseudomonas* biofilm matrix composition and niche biology. *FEMS Microbiol Rev* **36**:893–916. DOI: 10.1111/j.1574-6976.2011.00322.x

[**381**] Chung J, Eisha S, Park S, Morris AJ, Martin I (2023) How three self-secreted biofilm exopolysaccharides of *Pseudomonas aeruginosa*, Psl, Pel, and alginate, can each be exploited for antibiotic adjuvant effects in cystic fibrosis lung infection. *Int J Mol Sci* **24**:8709. DOI: 10.3390/ijms24108709

[**382**] Baumgarten T, Sperling S, Seifert J, von Bergen M, Steiniger F, Wick LY, et al. (2012) Membrane vesicle formation as a multiple-stress response mechanism enhances *Pseudomonas putida* DOT-T1E cell surface hydrophobicity and biofilm formation. *Appl Environ Microbiol* **78**:6217–6224. DOI: 10.1128/AEM.01525-12

[**383**] Mozaheb N, Mingeot-Leclercq MP (2020) Membrane vesicle production as a bacterial defense against stress. *Front Microbiol* **11**:60221. DOI: 10.3389/fmicb.2020.600221

[**384**] MacDonald IA, Kuehn MJ (2013) Stress-induced outer membrane vesicle production by *Pseudomonas aeruginosa*. *J Bacteriol* **195**:2971–2981. DOI: 10.1128/JB.02267-12

[**385**] Eberlein C, Baumgarten T, Starke S, Heipieper HJ (2018) Immediate response mechanisms of Gram-negative solvent-tolerant bacteria to cope with environmental stress: *cis-trans* isomerization of unsaturated fatty acids and outer membrane vesicle secretion. *Appl Microbiol Biotechnol* **102**:2583–2593. DOI: 10.1007/s00253-018-8832-9

[**386**] Avila-Calderón ED, Ruiz-Palma M del S, Aguilera-Arreola MG, Velázquez-Guadarrama N, Ruiz EA, Gomez-Lunar Z, et al. (2021) Outer membrane vesicles of Gram-negative bacteria: An outlook on biogenesis. *Front Microbiol* **12**:557902. DOI: 10.3389/fmicb.2021.557902

[**387**] Kulp A, Kuehn MJ (2010) Biological functions and biogenesis of secreted bacterial outer membrane vesicles. *Annu Rev Microbiol* **64**:163–184. DOI: 10.1146/annurev.micro.091208.073413

[**388**] Jan AT (2017) Outer membrane vesicles (OMVs) of Gram-negative bacteria: A perspective update. *Front Microbiol* **8**:1053. DOI: 10.3389/fmicb.2017.01053

[**389**] Schwechheimer C, Kuehn MJ (2015) Outer-membrane vesicles from Gram-negative bacteria: Biogenesis and functions. *Nat Rev Microbiol* **13**:605–619. DOI: 10.1038/nrmicro3525

[**390**] Tan D, Fu L, Sun X, Xu L, Zhang J (2020) Genetic analysis and immunoelectron microscopy of wild and mutant strains of the rubber tree endophytic bacterium *Serratia marcescens* strain ITBB B5–1 reveal key roles of a macrovesicle in storage and secretion of prodigiosin. *J Agric Food Chem* **68**:5606–5615. DOI: 10.1021/acs.jafc.0c00078

[**391**] Choi SY, Lim S, Cho G, Kwon J, Mun W, Im H, et al. (2020) *Chromobacterium violaceum* delivers violacein, a hydrophobic antibiotic, to other microbes in membrane vesicles. *Environ Microbiol* **22**:705–713. DOI: 10.1111/1462-2920.14888

[**392**] Mashburn LM, Whiteley M (2005) Membrane vesicles traffic signals and facilitate group activities in a prokaryote. *Nature* **437**:422–425. DOI: 10.1038/nature03925

[**393**] Salvachúa D, Werner AZ, Pardo I, Michalska M, Black BA, Donohoe BS, et al. (2020) Outer membrane vesicles catabolize lignin-derived aromatic compounds in *Pseudomonas putida* KT2440. *PNAS* **117**:9302–9310. DOI: 10.1073/pnas.1921073117

[**394**] Manning AJ, Kuehn MJ (2011) Contribution of bacterial outer membrane vesicles to innate bacterial defense. *BMC Microbiol* **11**:258. DOI: 10.1186/1471-2180-11-258

[**395**] Juodeikis R, Carding SR (2022) Outer membrane vesicles: Biogenesis, functions, and issues. *MMBR* **86**:e0003222. DOI: 10.1128/mmbr.00032-22

[**396**] Schwechheimer C, Sullivan CJ, Kuehn MJ (2013) Envelope control of outer membrane vesicle production in Gram-negative bacteria. *Biochemistry* **52**:3031–3040. DOI: 10.1021/bi400164t

[**397**] Singh SK, SaiSree L, Amrutha RN, Reddy M (2012) Three redundant murein endopeptidases catalyse an essential cleavage step in peptidoglycan synthesis of *Escherichia coli* K12. *Mol Microbiol* **86**:1036–1051. DOI: 10.1111/mmi.12058

[**398**] Kulp AJ, Sun B, Ai T, Manning AJ, Orench-Rivera N, Schmid AK, et al. (2015) Genome-wide assessment of outer membrane vesicle production in *Escherichia coli*. *PLoS One* **10**:e0139200. DOI: 10.1371/journal.pone.0139200

[**399**] Roier S, Zingl FG, Cakar F, Durakovic S, Kohl P, Eichmann TO, et al. (2016) A novel mechanism for the biogenesis of outer membrane vesicles in Gram-negative bacteria. *Nat Commun* **7**:10515. DOI: 10.1038/ncomms10515

[**400**] Toyofuku M, Nomura N, Eberl L (2019) Types and origins of bacterial membrane vesicles. *Nat Rev Microbiol* **17**:13–24. DOI: 10.1038/s41579-018-0112-2

[**401**] Schwechheimer C, Kulp A, Kuehn MJ (2014) Modulation of bacterial outer membrane vesicle production by envelope structure and content. *BMC Microbiol* **14**:324. DOI: 10.1186/s12866-014-0324-1

[**402**] McBroom AJ, Kuehn MJ (2007) Release of outer membrane vesicles by Gram-negative bacteria is a novel envelope stress response. *Mol Microbiol* **63**:545–558. DOI: 10.1111/j.1365-2958.2006.05522.x

[**403**] Tashiro Y, Sakai R, Toyofuku M, Sawada I, Nakajima-Kambe T, Uchiyama H, et al. (2009) Outer membrane machinery and alginate synthesis regulators control membrane vesicle production in *Pseudomonas aeruginosa*. *J Bacteriol* **191**:7509–7519. DOI: 10.1128/JB.00722-09

[**404**] Yang D, Park SY, Lee SY (2021) Production of rainbow colorants by metabolically engineered *Escherichia coli*. *Adv Sci* **8**:2100743. DOI: 10.1002/advs.202100743

[**405**] Batista JH, Leal FC, Fukuda TTH, Alcoforado Diniz J, Almeida F, Pupo MT, et al. (2020) Interplay between two quorum sensing-regulated pathways, violacein biosynthesis and VacJ/Yrb, dictates outer membrane vesicle biogenesis in *Chromobacterium violaceum*. *Environ Microbiol* **22**:2432–2442. DOI: 10.1111/1462-2920.15033

[**406**] Reznikoff WS (2008) Transposon Tn5. *Annu Rev Genet* **42**:269–286. DOI: 10.1146/annurev.genet.42.110807.091656

[**407**] Nazareno ES, Acharya B, Dumenyo CK (2021) A mini-Tn5-derived transposon with reportable and selectable markers enables rapid generation and screening of insertional mutants in Gram-negative bacteria. *Lett Appl Microbiol* **72**:283–291. DOI: 10.1111/lam.13423

[**408**] Otto M, Wynands B, Drepper T, Jaeger KE, Thies S, Loeschcke A, et al. (2019) Targeting 16S rDNA for stable recombinant gene expression in *Pseudomonas*. *ACS Synth Biol* **8**:1901–1912. DOI: 10.1021/acssynbio.9b00195

[**409**] Belda E, van Heck RGA, José Lopez-Sanchez M, Cruveiller S, Barbe V, Fraser C, et al. (2016) The revisited genome of *Pseudomonas putida* KT2440 enlightens its value as a robust metabolic *chassis*. *Environ Microbiol* **18**:3403–3424. DOI: 10.1111/1462-2920.13230

[**410**] Damron FH, McKenney ES, Barbier M, Liechti GW, Schweizer HP, Goldberg JB (2013) Construction of mobilizable mini-Tn7 vectors for bioluminescent detection of Gram-negative bacteria and single-copy promoter *lux* reporter analysis. *Appl Environ Microbiol* **79**:4149–4153. DOI: 10.1128/AEM.00640-13

[**411**] Sieberichs A (2023) Biocatalytic production of cycloprodiginines using heterologous cyclases in *Pseudomonas putida*. *Heinrich Heine University Düsseldorf*. Master thesis

[**412**] Spindler MC (2023) Engineering of *Pseudomonas putida* KT2440 as a mutasynthesis platform for indole and quinoline alkaloids. *Heinrich Heine University Düsseldorf*. Master thesis

[**413**] Hogenkamp F, Hilgers F, Bitzenhofer NL, Ophoven V, Haase M, Bier C, et al. (2022) Optochemical control of bacterial gene expression: Novel photocaged compounds for different promoter systems. *ChemBioChem* **23**:e202100467. DOI: 10.1002/cbic.202100467

[**414**] Murillo-Roos M, Abdullah HSM, Debbar M, Ueberschaar N, Agler MT (2022) Cross-feeding niches among commensal leaf bacteria are shaped by the interaction of strain-level diversity and resource availability. *ISME J* **16**:2280–2289. DOI: 10.1038/s41396-022-01271-2

[**415**] Bollinger A, Thies S, Katzke N, Jaeger K (2020) The biotechnological potential of marine bacteria in the novel lineage of *Pseudomonas pertucinogena*. *Microb Biotechnol* **13**:19–31. DOI: 10.1111/1751-7915.13288

[**416**] Bollinger A, Thies S, Knieps-Grünhagen E, Gertzen C, Kobus S, Höppner A, et al. (2020) A novel polyester hydrolase from the marine bacterium *Pseudomonas aestusnigri* – Structural and functional insights. *Front Microbiol* **11**:114. DOI: 10.3389/fmicb.2020.00114

[**417**] Molitor R, Bollinger A, Kubicki S, Loeschcke A, Jaeger K, Thies S (2020) Agar plate-based screening methods for the identification of polyester hydrolysis by *Pseudomonas* species. *Microb Biotechnol* **13**:274–284. DOI: 10.1111/1751-7915.13418

[**418**] Horwitz JP, Chua J, Curby RJ, Tomson AJ, Da Rooge MA, Fisher BE, et al. (1964) Substrates for cytochemical demonstration of enzyme activity. I. Some substituted 3-indolyl-*β*-D-glycopyranosides. *J Med Chem* **7**:574–575. DOI: 10.1021/jm00334a044

[**419**] Bitzenhofer NL, Classen T, Jaeger K, Loeschcke A (2023) Biotransformation of L-tryptophan to produce arcyriaflavin A with *Pseudomonas putida* KT2440. *ChemBioChem* **0**:e202300576. DOI: 10.1002/cbic.202300576

[**420**] Zube C (2020) Expression von *Stigmatella*-Biosynthesegenen zur Aurachin-Mutasynthese in *Pseudomonas putida*. Bachelor thesis

[**421**] Nora LC, Westmann CA, Martins-Santana L, Alves L de F, Monteiro LMO, Guazzaroni M, et al. (2019) The art of vector engineering: Towards the construction of next-generation genetic tools. *Microb Biotechnol* **12**:125–147. DOI: 10.1111/1751-7915.13318

[**422**] Lutz R, Bujard H (1997) Independent and tight regulation of transcriptional units in *Escherichia coli* via the LacR/O, the TetR/O and AraC/I1-I2 regulatory elements. *Nucleic Acids Res* **25**:1203–1210. DOI: 10.1093/nar/25.6.1203

[**423**] Baldwin CY, Clark KB (2000) Design Rules: The Power of Modularity. *MIT Press*;

[**424**] Shetty RP, Endy D, Knight TF (2008) Engineering BioBrick vectors from BioBrick parts. *J Biol Eng* **2**:5. DOI: 10.1186/1754-1611-2-5

[**425**] Stoddard BL (2011) Homing endonucleases: From microbial genetic invaders to reagents for targeted DNA modification. *Structure* **19**:7–15. DOI: 10.1016/j.str.2010.12.003

[**426**] Sarovich DS, Pemberton JM (2007) pPSX: A novel vector for the cloning and heterologous expression of antitumor antibiotic gene clusters. *Plasmid* **57**:306–313. DOI: 10.1016/j.plasmid.2006.11.004

[**427**] Choi KH, DeShazer D, Schweizer HP (2006) mini-Tn7 insertion in bacteria with multiple *glmS*-linked *att*Tn7 sites: Example *Burkholderia mallei* ATCC 23344. *Nat Protoc* **1**:162–169. DOI: 10.1038/nprot.2006.25

[**428**] Roos K, Werner E, Loessner H (2015) Multicopy integration of mini- Tn7 transposons into selected chromosomal sites of a *Salmonella* vaccine strain. *Microb Biotechnol* **8**:177–187. DOI: 10.1111/1751-7915.12187

[**429**] Kossmann DF, Huang M, Weihmann R, Xiao X, Gätgens F, Weber TM, et al. (2023) Production of tailored hydroxylated prodiginine showing combinatorial activity with rhamnolipids against plant-parasitic nematodes. *Front Microbiol* **14**:1151882. DOI: 10.3389/fmicb.2023.1151882

[**430**] Johnson RE, de Rond T, Lindsay VNG, Keasling JD, Sarpong R (2015) Synthesis of cycloprodigiosin identifies the natural isolate as a scalemic mixture. *Org Lett* **17**:3474–3477. DOI: 10.1021/acs.orglett.5b01527

[**431**] Habash SS, Brass HUC, Klein AS, Klebl DP, Weber TM, Classen T, et al. (2020) Novel prodiginine derivatives demonstrate bioactivities on plants, nematodes, and fungi. *Front Plant Sci* **11**:579807. DOI: 10.3389/fpls.2020.579807

[**432**] Tenhaef N, Stella R, Frunzke J, Noack S (2021) Automated rational strain construction based on high-throughput conjugation. *ACS Synth Biol* **10**:589–599. DOI: 10.1021/acssynbio.0c00599

[**433**] Casini A, Chang FY, Eluere R, King AM, Young EM, Dudley QM, et al. (2018) A pressure test to make 10 molecules in 90 days: External evaluation of methods to engineer biology. *J Am Chem Soc* **140**:4302–4316. DOI: 10.1021/jacs.7b13292

[**434**] Sánchez C, Zhu L, Braña AF, Salas AP, Rohr J, Méndez C, et al. (2005) Combinatorial biosynthesis of antitumor indolocarbazole compounds. *PNAS* **102**:461–466. DOI: 10.1073/pnas.0407809102

[**435**] Wilkinson MD, Lai HE, Freemont PS, Baum J (2020) A biosynthetic platform for antimalarial drug discovery. *Antimicrob Agents Chemother* **64**:e02129-19. DOI: 10.1128/AAC.02129-19

[**436**] Schnepel C, Kemker I, Sewald N (2019) One-pot synthesis of D-halotryptophans by dynamic stereoinversion using a specific L-amino acid oxidase. *ACS Catal* **9**:1149–1158. DOI: 10.1021/acscatal.8b04944

[**437**] Nishizawa T, Aldrich CC, Sherman DH (2005) Molecular analysis of the rebeccamycin L-amino acid oxidase from *Lechevalieria aerocolonigenes* ATCC 39243. *J Bacteriol* **187**:2084–2092. DOI: 10.1128/JB.187.6.2084-2092.2005

[**438**] Zehner S, Kotzsch A, Bister B, Süssmuth RD, Méndez C, Salas JA, et al. (2005) A regioselective tryptophan 5-halogenase is involved in pyrroindomycin biosynthesis in *Streptomyces rugosporus* LL-42D005. *Chem Biol* **12**:445–452. DOI: 10.1016/j.chembiol.2005.02.005

[**439**] Lin Y, Sun X, Yuan Q, Yan Y (2014) Engineering bacterial phenylalanine 4-hydroxylase for microbial synthesis of human neurotransmitter precursor 5-hydroxytryptophan. *ACS Synth Biol* **3**:497–505. DOI: 10.1021/sb5002505

[**440**] Mora-Villalobos JA, Zeng AP (2018) Synthetic pathways and processes for effective production of 5-hydroxytryptophan and serotonin from glucose in *Escherichia coli*. *J Biol Eng* **12**:3. DOI: 10.1186/s13036-018-0094-7

[**441**] Gao S, Liao Y, He H, Yang H, Yang X, Xu S, et al. (2023) Advance of tolerance engineering on microbes for industrial production. *Synth Syst Biotechnol* **8**:697–707. DOI: 10.1016/j.synbio.2023.10.004

[**442**] Mavrodi D V., Bonsall RF, Delaney SM, Soule MJ, Phillips G, Thomashow LS (2001) Functional analysis of genes for biosynthesis of pyocyanin and phenazine-1-carboxamide from *Pseudomonas aeruginosa* PAO1. *J Bacteriol* **183**:6454–6465. DOI: 10.1128/JB.183.21.6454-6465.2001

[**443**] Tiso T, Thies S, Müller M, Tsvetanova L, Carraresi L, Bröring S, et al. (2017) Rhamnolipids: Production, Performance, and Application. *Consequences of Microbial Interactions with Hydrocarbons, Oils, and Lipids: Production of Fuels and Chemicals*. DOI: 10.1007/978-3-319-50436-0_388

[**444**] Beuttler H, Hoffmann J, Jeske M, Hauer B, Schmid RD, Altenbuchner J, et al. (2011) Biosynthesis of zeaxanthin in recombinant *Pseudomonas putida*. *Appl Microbiol Biotechnol* **89**:1137–1147. DOI: 10.1007/s00253-010-2961-0

[**445**] Bitzenhofer NL, Höfel C, Thies S, Weiler AJ, Eberlein C, Heipieper HJ, et al. (2023) Exploring engineered vesiculation by *Pseudomonas putida* KT2440 for natural product biosynthesis. *Microb Biotechnol* **00**:1–18. DOI: 10.1111/1751-7915.14312

[**446**] Li J, Ye BC (2021) Metabolic engineering of *Pseudomonas putida* KT2440 for high-yield production of protocatechuic acid. *Bioresour Technol* **319**:124239. DOI: 10.1016/j.biortech.2020.124239

[**447**] Wynands B, Kofler F, Siebericht A, da Silva N, Wierckx N (2023) Engineering a *Pseudomonas taiwanensis* 4-coumarate platform for production of *para*-hydroxy aromatics with high yield and specificity. *Metab Eng* **78**:115–127. DOI: 10.1016/j.ymben.2023.05.004

[**448**] Otto M, Wynands B, Lenzen C, Filbig M, Blank LM, Wierckx N (2019) Rational engineering of phenylalanine accumulation in *Pseudomonas taiwanensis* to enable high-yield production of *trans*-cinnamate. *Front Bioeng Biotechnol* **7**:312. DOI: 10.3389/fbioe.2019.00312

[**449**] Wynands B, Lenzen C, Otto M, Koch F, Blank LM, Wierckx N (2018) Metabolic engineering of *Pseudomonas taiwanensis* VLB120 with minimal genomic modifications

for high-yield phenol production. *Metab Eng* **47**:121–133. DOI: 10.1016/j.ymben.2018.03.011

[**450**] Schwanemann T, Otto M, Wynands B, Marienhagen J, Wierckx N (2023) A *Pseudomonas taiwanensis* malonyl-CoA platform strain for polyketide synthesis. *Metab Eng* **77**:219–230. DOI: 10.1016/j.ymben.2023.04.001

[**451**] Lieder S, Nikel PI, de Lorenzo V, Takors R (2015) Genome reduction boosts heterologous gene expression in *Pseudomonas putida*. *Microb Cell Fact* **14**:23. DOI: 10.1186/s12934-015-0207-7

[**452**] Liang P, Zhang Y, Xu B, Zhao Y, Liu X, Gao W, et al. (2020) Deletion of genomic islands in the *Pseudomonas putida* KT2440 genome can create an optimal *chassis* for synthetic biology applications. *Microb Cell Fact* **19**:70. DOI: 10.1186/s12934-020-01329-w

[**453**] Zhu Y, Zhou C, Wang Y, Li C (2020) Transporter engineering for microbial manufacturing. *Biotechnol J* **15**:1900494. DOI: 10.1002/biot.201900494

[**454**] Hilgers F (2016) Light-controlled production of bacterial secondary metabolites. *Heinrich Heine University Düsseldorf*. Master thesis

[**455**] Heyes DJ, Ruban A V., Hunter CN (2003) Protochlorophyllide oxidoreductase: “Dark” reactions of a light-driven enzyme. *Biochemistry* **42**:523–528. DOI: 10.1021/bi0268448

[**456**] Klein AS (2017) Methoden zur Herstellung von Prodigininen als Wirkstoffe - Eine farbenfrohe Brücke zwischen Chemie und Biologie. *Heinrich Heine University Düsseldorf*. Dissertation

[**457**] Verhoef S, Wierckx N, Westerhof RGM, de Winde JH, Ruijssenaars HJ (2009) Bioproduction of *p*-hydroxystyrene from glucose by the solvent-tolerant bacterium *Pseudomonas putida* S12 in a two-phase water-decanol fermentation. *Appl Environ Microbiol* **75**:931–936. DOI: 10.1128/AEM.02186-08

[**458**] Cheng T, Zhao Y, Li X, Lin F, Xu Y, Zhang X, et al. (2007) Computation of octanol−water partition coefficients by guiding an additive model with knowledge. *J Chem Inf Model* **47**:2140–2148. DOI: 10.1021/ci700257y

[**459**] Höfel C (2021) Genetic control of outer membrane vesicle formation in *Pseudomonas putida* KT2440. *Heinrich Heine University Düsseldorf*. Bachelor thesis

[**460**] Ojima Y, Sawabe T, Konami K, Azuma M (2020) Construction of hypervesiculation *Escherichia coli* strains and application for secretory protein production. *Biotechnol Bioeng* **117**:701–709. DOI: 10.1002/bit.27239

[**461**] Gao H, Jiang Y, Wang L, Wang G, Hu W, Dong L, et al. (2023) Outer membrane vesicles from a mosquito commensal mediate targeted killing of *Plasmodium* parasites via the phosphatidylcholine scavenging pathway. *Nat Commun* **14**:5157. DOI: 10.1038/s41467-023-40887-6

[**462**] Gujrati V, Kim S, Kim SH, Min JJ, Choy HE, Kim SC, et al. (2014) Bioengineered bacterial outer membrane vesicles as cell-specific drug-delivery vehicles for cancer therapy. *ACS Nano* **8**:1525–1537. DOI: 10.1021/nn405724x

[**463**] Qing G, Gong N, Chen X, Chen J, Zhang H, Wang Y, et al. (2019) Natural and engineered bacterial outer membrane vesicles. *Biophys Rep* **5**:184–198. DOI: 10.1007/s41048-019-00095-6

[**464**] Thakur M, Dean SN, Caruana JC, Walper SA, Ellis GA (2023) Bacterial membrane vesicles for *in vitro* catalysis. *Bioengineering* **10**:1099. DOI: 10.3390/bioengineering10091099

V. APPENDIX

V.1. Supporting Information for chapter II.2

Supplementary Material

The modular pYT vector series employed for chromosomal gene integration and expression to produce carbazoles and glycolipids in *P. putida*

Robin Weihmann[1,2,#], Sonja Kubicki[1,2,#], Nora Lisa Bitzenhofer[1], Andreas Domröse[1], Isabel Bator[2,3], Lisa-Marie Kirschen[1], Franziska Kofler[1], Aileen Funk[1], Till Tiso[2,3], Lars M. Blank[2,3], Karl-Erich Jaeger[1,2,4], Thomas Drepper[1,2], Stephan Thies[1,2,*], Anita Loeschcke[1,2,*]

[1]Institute of Molecular Enzyme Technology, Heinrich Heine University Düsseldorf at Forschungszentrum Jülich GmbH, Jülich, Germany
[2]Bioeconomy Science Center (BioSC), Forschungszentrum Jülich GmbH, Jülich, Germany
[3]iAMB - Institute of Applied Microbiology, ABBt - Aachen Biology and Biotechnology, RWTH Aachen University, Aachen, Germany
[4]Institute of Bio-and Geosciences IBG-1: Biotechnology, Forschungszentrum Jülich GmbH, Jülich, Germany
[#]equally contributed

*** Correspondence:**
a.loeschcke@fz-juelich.de; Tel. +(49) 2461 613790
s.thies@fz-juelich.de; Tel. +(49) 2461 613790

Content **Page**

Supplementary Material

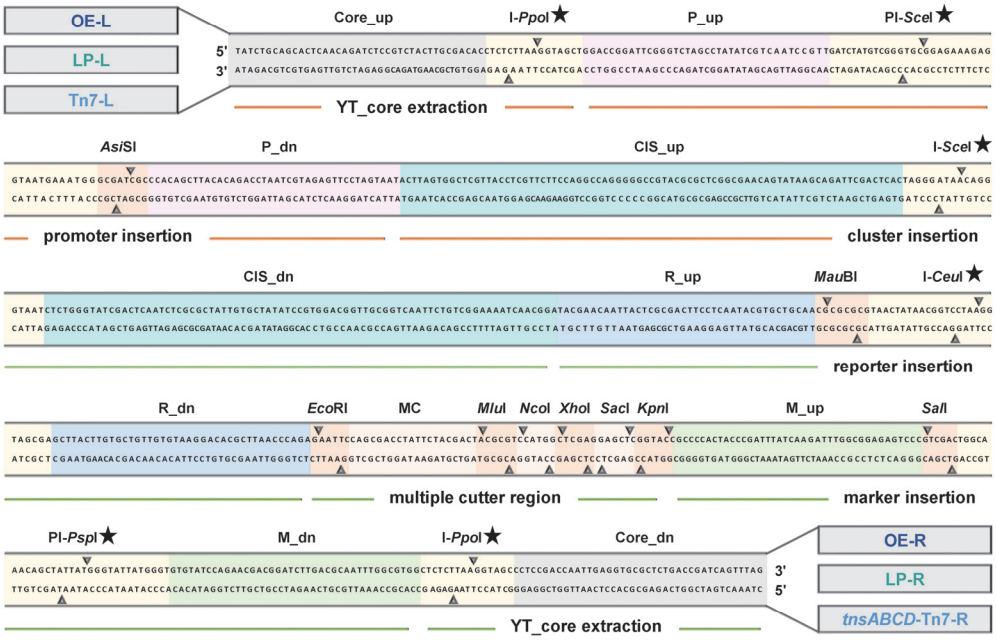

Supplementary Figure S1. Gene sequence and labeled elements of the YT_core sequence.
The CIS (cluster integration site, I-*Sce*I) is the central position for insertion of target genes. Orange and green regions denote sequences framing the target genes. Depending on the integration mode, there are different outer ends around the YT_core sequence (OE-L/R for Tn5 transposition, LP-L/R for integration in preinstalled landing pads within 16S rRNA-encoding genes and Tn7-L/R for Tn7 transposition). The recombination regions (Core_up/dn, P_up/dn, CIS_up/dn, R_up/dn and M_up/dn) are shown in grey, pink, green, and blue, respectively. Restriction endonuclease sites are marked in orange, homing endonuclease sites in yellow and by black asterisks.

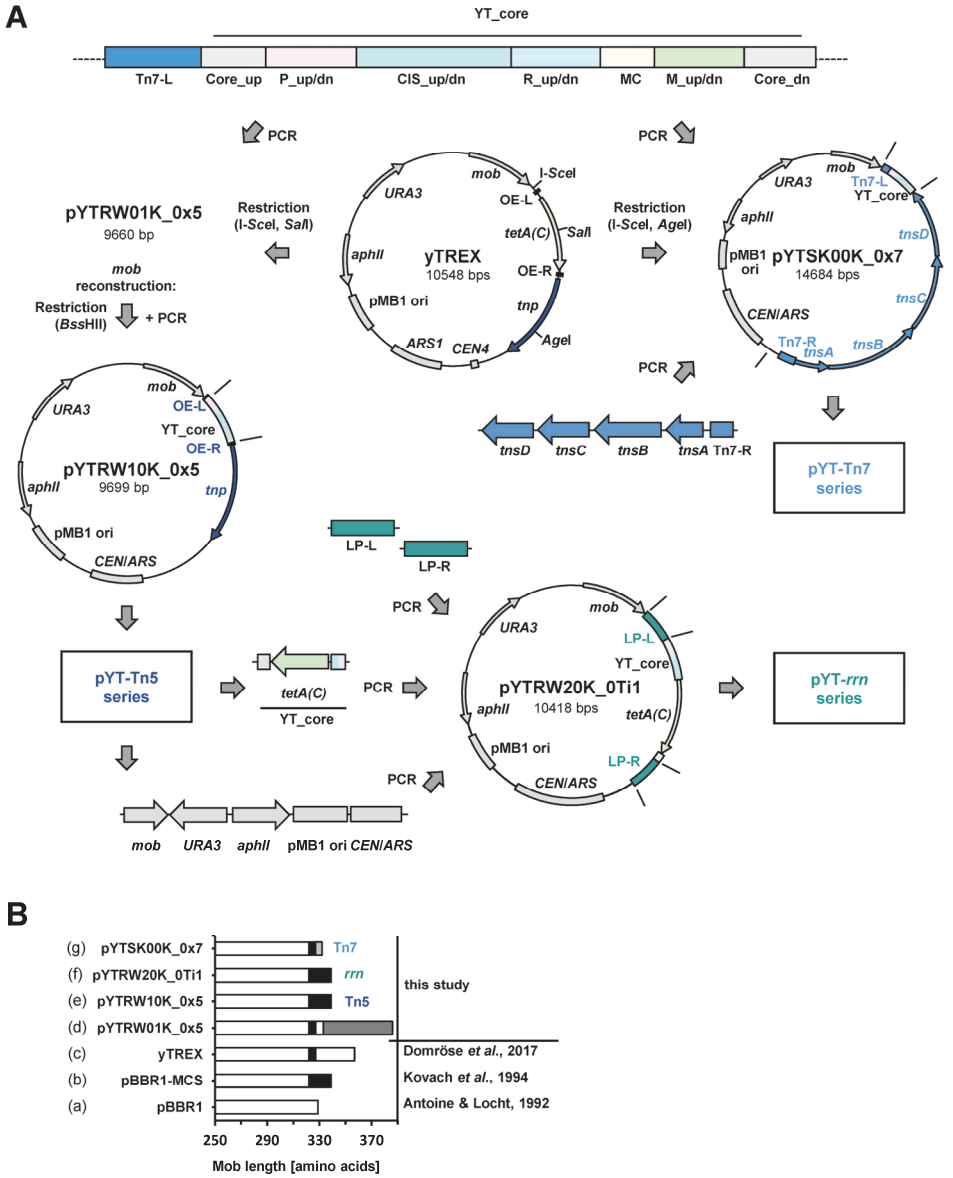

Supplementary Figure S2. Construction of pYTRW10K_0x5, pYTRW28K_0Ti1, and pYTSK00K_0x7.
See caption on the following page.

Supplementary Material

See Figure on the previous page.

Supplementary Figure S2. Construction of pYTRW10K_0x5, pYTRW28K_0Ti1, and pYTSK00K_0x7.

(A) Vector construction scheme:

pYTRW10K_0x5: For construction of the pYT vector version facilitating Tn5 transposition, the YT_core sequence (detailed in **Figure S1**), which was obtained as a gene synthesis fragment, was first PCR-amplified (with primers RW001/002) and assembled in yeast with the backbone of the I-*Sce*I/*Sal*I hydrolysed yTREX vector. Since this caused an extension of the *mob* ORF in the resulting pYTRW01K_0x5 (please see further details under **(B)**) and placed the stop codon downstream of the PI-*Sce*I and *Asi*SI site within the YT_core, making use of the "slot" for e.g. promoter insertion, may introduce further changes to the *mob* gene and interfere with functionality. We therefore reconstructed the *mob* gene as it occurs in the widely used pBBR1-MCS series (Kovach *et al.* 1994, 1995). To this end, a small fragment containing the *mob* 3' end was released from the vector pYTRW01K_0x5 using *Bss*HII; the same fragment was amplified by PCR (with primers RW100/101), during which the *mob* sequence was completed, and inserted into the vector by In-Fusion® cloning to obtain vector pYTRW10K_0x5, from which all further constructs for Tn5 integration were derived.

pYTRW28K_0Ti1: For construction of the pYT vector version facilitating gene integration into the 16S gene of an *rrn* operon (in the *P. putida* strains RW1-7), the backbone of the vector pYTRW09K_0T5 was amplified (with primers RW157/159), as well as the YT_core (with primers RW159/160), leaving out the Tn5 *tnp* and OE sequences. The synthetic landing pad sequence (see **Figure S3**) was used as template to amplify LP-L and LP-R (with primers RW158/147 and RW148/149, respectively), which were introduced *via* In-Fusion® cloning on both ends of the YT_core to yield pYTRW20K_0Ti1. The vector and landing pad were designed so that a gene cluster of interest, which was cloned in the I-*Sce*I site of the vector, would be integrated into a 16S gene 1395 bp downstream of the 16S promoter P1. Since the cassette flanked by LP-L/R would be integrated into the bacterial chromosome by homologous recombination, we additionally cloned the *sacB* gene (amplified with RW194/195) in the *Spe*I-site of the vector backbone to enable counter-selection if necessary, creating pYTRW28K_1Ti1.

pYTSK00K_0x7: For construction of the pYT vector version facilitating Tn7 transposition, the YT_core was amplified together with the Tn7-L insertion element (with primers fw_SynSK and rv_KleSK). The transposase genes *tnsABCD* were amplified together with the Tn7-R insertion element (using primers fw_HMR_tnsD and rv_Tn7R_HBy). These fragments were assembled in yeast with the backbone of the I-*Sce*I/*Age*I hydrolysed yTREX vector. The resulting pYTSK00K_0x7 served as basic vector for all further constructs enabling Tn7 integration.

(B) History of the *mob* gene:

For the initiation of conjugational plasmid transfer, the pYT series relies on the *mob*/oriT derived from vector pBBR1 (Antoine and Locht 1992) **(a)**: The *mob* gene encodes a DNA relaxase; the *mob* promoter sequence includes the oriT sequence, at which the relaxase causes a *nick* by phosphodiester bond cleavage. Through the cloning steps of the pBBR1-MCS series (Kovach *et al.* 1994) **(b)** and, in the following, of the yTREX vector (Domröse *et al.* 2017) **(c)**, the stop codon of the *mob* gene has been truncated, which led to an elongation of the ORF in the new constructs. New C-terminal regions are shown in black and white. In the named cases, this did not render the protein non-functional. However, our initial cloning step to construct the pYT vector for Tn5 integration caused another significant extension **(d)** (shown in dark-grey), which led to the stop codon being positioned downstream of the PI-*Sce*I and *Asi*SI site within the YT_core sequence (see **Figure S1**). In this case, making use of the "slot" for e.g. promoter insertion, may introduce further changes to the *mob* gene and interfere with functionality. Therefore, the 3'-end of the *mob* gene was reconstructed in pYTRW10K_0x5 **(e)** as present in the widely used as it occurs in widely used pBBR1-MCS series (Kovach *et al.* 1994, 1995). The pYT vectors for integration in the 16S gene of the *rrn* operons of *P. putida* RW1-7 were derived from Tn5 versions and thus likewise possess the reconstructed *mob* gene **(f)**. The *mob* gene in pYT vectors for Tn7 integration was not reconstructed, since the elongation was moderate here **(g)** and the *mob* stop codon is positioned within Tn7-L (*i.e.* upstream of the YT_core) so that no further changes can occur by using the respective cloning slots.

Supplementary Methods S1. Construction of ready-to-use pYT vectors.

Vector set for Tn5-based chromosomal gene integration: Four versions carrying resistance markers Gm^R (pYTRW07K_0G5), Cm^R (pYTRW08K_0C5), Tc^R (pYTRW09K_0T5) and Sm^R (pYTRW11K_0S5) in the integron were cloned by introduction of the respective PCR-amplified genes together with the respective promoters (primers were Fw_HMF_Gm/Rv_Gm_HMR, yTT_CmRM_fw AF neu/yTT_CmRM_rev AF; yTT_TcRM_fw AF neu/yTT_TcRM_rev AF, and yTT Sm RM fw/yTT Sm RM rev, respectively) at the designated marker position (*Sal*I site) of pYTRW010K_0x5 (**Figure S2**). The *Sal*I recognition site was regenerated at the 3' end of the genes. The latter cloning steps were realised by recombination in yeast, while we used In-Fusion cloning for the following steps. The vector pYTRW07K_0G5, which carries Gm^R, was additionally equipped at the reporter position (*Mau*BI site) with the promoterless genes encoding the yellow fluorescent protein (eYFP), its red and blue derivatives mCherry and mTagBFP2, the enzymes β-galactosidase (LacZ) or polyester hydrolase (PE-H), creating pYTRW16K_1G5, pYTRW13K_3G5, pYTRW15K_2G5, pYTRW14K_7G5 and pYTRW17K_6G5, respectively. Used primers were: RW108/109, InFusion mCherry fw/InFusion mCherry rev, RW106/107, RW110/111, and RW127/128, respectively. In addition, mCherry was analogously cloned in the vector pYTRW09K_0T5, which carries Tc^R, generating pYTRW18K-3T5.

Vector set for integration into a 16S gene: The vectors pYTRW20K_0Ti1 and pYTRW028K_1Ti1 (**Figure S2**), which carry the LP-L and LP-R sequences for integration (the latter additionally carries *sacB*) were equipped at the reporter position (*Mau*BI) with the promoterless *eYFP* reporter gene (amplified with RW108/109), creating pYTRW21K_1Ti1 and pYTRW26K_1Ti1, respectively. The *lacZ* gene (amplified with RW110/111) was likewise cloned in the two basic vectors, creating pYTRW22K_7Ti1 and pYTRW27K_7Ti1, respectively. These cloning steps were realised by In-Fusion® cloning.

Vector set for Tn7-based chromosomal gene integration:
The version pYTSK01_0G7 (Tiso *et al.* 2020), which carries the Gm^R marker, represents a formal derivative of the basic vector pYTSK00K_0x7 (**Figure S2**) but was generated likewise in a one-step assembly: Here, the PCR-amplified *tnsABCD* and Tn7-R (primers fw_HMR_tnsD/rv_Tn7R_HBy) and the I-*Sce*I/*Age*I-hydrolysed yTREX vector were assembled with the YT_core, which was PCR-amplified in two sections (primers fw_SynSK/rv_SynSK and fw_KleSK/rv_KleSK), and the Gm^R cassette (primers fw_HMF_Gm/rv_Gm_HMR). The alternative basic vector pYTSK02A_0G7, which offers Ap^R as backbone resistance marker and Gm^R as integron marker, was assembled from the PCR-amplified YT_core and Tn7-L (primers fw_SynSK/rv_KleSK), the transposase genes *tnsABCD* and the Tn7-R (primers fw_HMR_tnsD/rv_Tn7R_HBy), and the I-*Sce*I/*Age*I-hydrolysed yTREX-Amp vector. The yTREX-Amp vector was previously assembled from the PCR-amplified Ap^R cassette (primers Amp fw/Amp rev) and the *Sac*I/*Pvu*I-hydrolysed yTREX vector by yeast homologous recombination.
In addition, the vector pYTSK01_0G7 (backbone Km^R, integron Gm^R) was further equipped at the reporter position (*Mau*BI site) with different promoterless genes encoding fluorescent proteins eYFP, mCherry, mTagBFP2, or the enzymes LacZ GUS or PE-H, accordingly creating pYTSK31K_1G7, pYTSK56K_3G7, pYTSK55K_2G7, pYTSK54K_7G7, pYTSK65K_8G7 and pYTSK58K_6G7 (used primers were fw_CIS II_eYFP/rv_eYFP_HB-R-rv, fw_CIS II_mtagBFP2/rv_mtagBFP2_HB-R-rv, fw_CIS II_mCherry/ rv_mCherry_HB-R-rv, fw_CIS I_LacZ/rv_LacZ_HB-R-rv, fw_CIS I_GUS/rv_GUS_HB-R-rv, and fw_CIS I_PE-H/ rv_PE-H_HB-R-rv, respectively). These cloning steps were realised by recombination in yeast.
Finally, the promoter module *nagR*-P_{nagAa} (amplified with primers IF_PI-SceI-nagR_fw/IF_nagAa-AsiSI_rev) was cloned in the respective position (PI-*Sce*I/*Asi*SI site) of the vector pYTSK31K_1G7, which carries the integron marker Gm^R and the *eYFP* reporter gene using In-Fusion® cloning. The PI-*Sce*I and *Asi*SI recognition sites were regenerated at the 3' end of the promoter module.

Supplementary Material

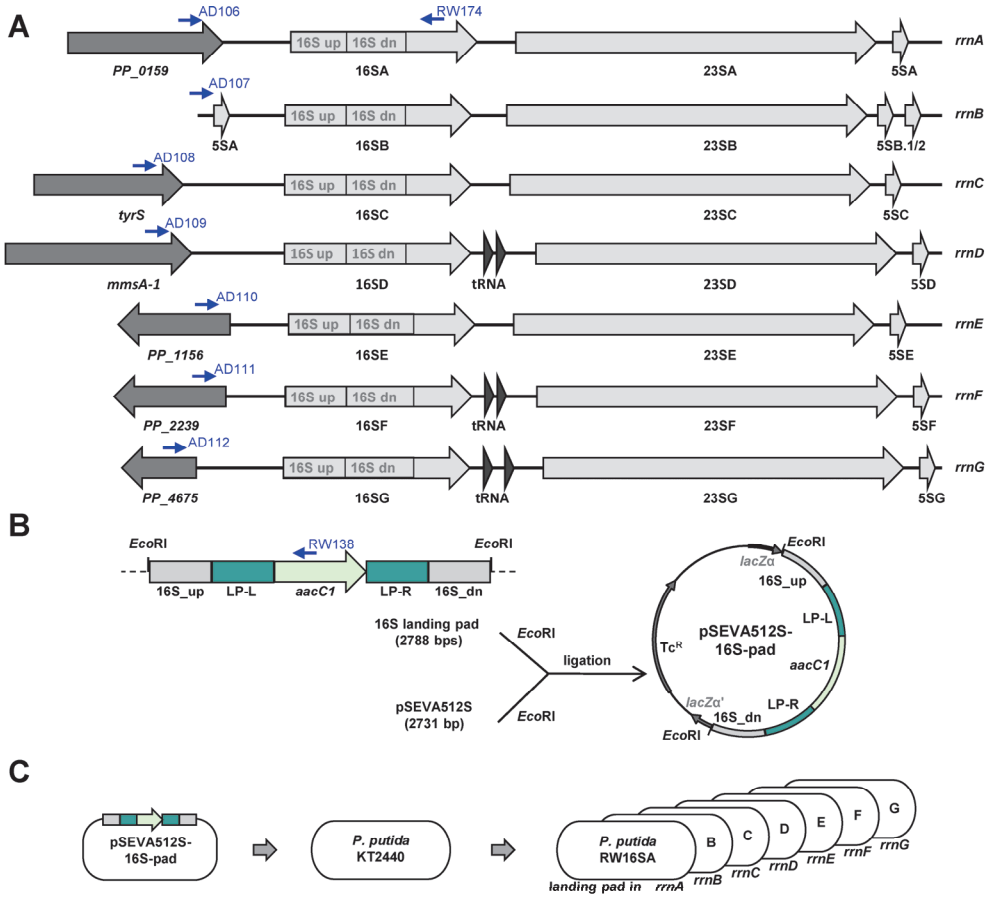

Supplementary Figure S3. Construction of *P. putida* strains carrying pYT landing pads in 16S genes of *rrn* operons.
(A) *Pseudomonas putida* KT2440 possesses seven highly conserved *rrn* operons. Each is composed of a 16S, a 23S and one or two 5S genes. The operons *rrnD*, *rrnF*, *rrnG* additionally include tRNA coding regions. Individual upstream regions are shown; 16S up and dn sequences, which are relevant for strain construction are indicated (grey font). **(B)** To facilitate targeted pYT integration in one of these, "landing pads" were integrated in each operon to provide unique sequences for recombination of a pYT integron specifically into the 16S gene of *rrnA*, *rrnB*, *rrnC* etc. To this end, a synthetic DNA cassette was designed and obtained by commercial synthesis that was composed of 500 bp sequences corresponding to the 16S gene sequence of *P. putida* KT2440 on both ends (16S up, 16S dn), in between which two 500 bp random DNA sequences (denoted as LP-L and LP-R – short for left and right arm of the landing pad) again flanked a central Gm^R cassette (the *aacC1* gene with its promoter (Wohlleben *et al.* 1989; Schweizer 1993)). The 16S sequences were included for integration of the cassette into the bacterial chromosome, while the LP-L/R sequences would serve as pYT interposon target sequences. The selected 16S sequences were identical in all rDNA operons with the exception of *rrnD*, where recombination with the integron would lead to a cytosine to thymine exchange. The landing pad was designed to begin 630 bp downstream of the 16S promoter P1 (Domröse *et al.* 2019). **(C)** Using plasmid

pSEVA512S-16S-pad, the landing pad was introduced into the genome of *P. putida* KT2440, where correct integration in the seven different 16S genes was verified by analyses of the antibiotic resistance phenotype (*i.e.* gentamicin resistance, tetracycline sensitivity, which indicated a double crossover integration), PCR analyses (using primers AD106-112, which bind as forward primers specifically in one of the seven upstream regions, together with RW138, which binds in reverse in the *aacC1* gene of the landing pad, to indicate the *rrn* operon), and sequencing of PCR products (obtained with one of the primers AD106-112 together with RW174, which binds in the 16S sequence downstream of the integrated landing pad). Seven strains, each carrying the landing pad in one of the *rrn* operons A, B, C, D, E, F, and G were thus generated and denoted as *P. putida* RW-16SA, B, C, D, E, F, and G.

7

Supplementary Material

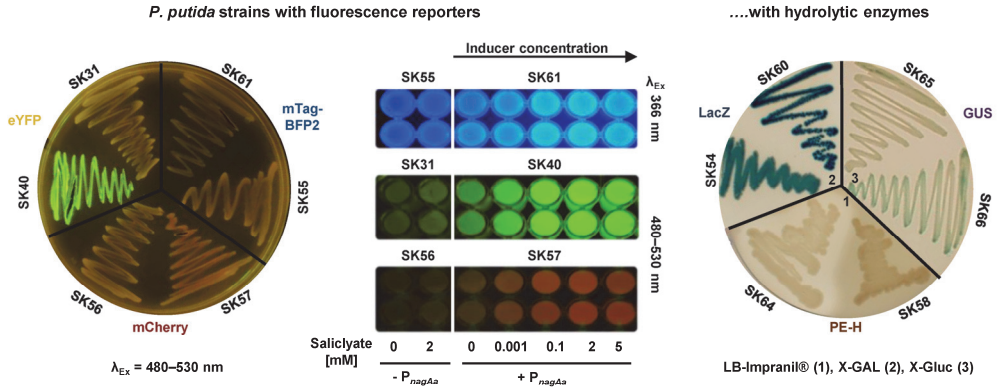

Supplementary Figure S4. Qualitative comparison of different reporter systems integrated in the *att*Tn7-site.
Qualitative analyses of NagR/P_{nagAa}-induced expression of the different reporter genes were conducted after integration of respective pYT constructs into the *att*Tn7 site of *P. putida* KT2440. For each reporter, a strain with an expression cassette (*nagR*-P_{nagAa}-*rhlAB*; SK40, SK61, SK57, SK60, SK66, SK64) and without an expression cassette (SK31, SK55, SK56, SK54, SK65, SK58) were analysed in comparison to show low basal expression levels, which arise due to the integration in the genomic context of the *att*Tn7 site. **Left:** Strains were cultured on LB agar plates containing 25 µg mL^{-1} gentamicin and 5 mM salicylic acid. The plate was photographed under illumination with 480-530 nm. **Middle:** After overnight incubation of liquid cultures in FlowerPlates containing LB medium with 12 mg L^{-1} $FeSO_4$ and different inducer concentrations (0, 0.001, 0.1, 2 and 5 mM), cells were washed in Tris-HCl buffer before fluorescence of mTagBFP2 was photo-documented in samples in a microtiter plate under illumination with λ_{Ex}= 366 nm (blue); for eYFP (green) and mCherry (red), λ_{Ex}= 480-530 nm was applied. **Right:** For visualisation of LacZ, GUS, and PE-H expression, X-Gal, X-Gluc, and Impranil® DLN were used as substrates in agar plates. LacZ and GUS activity on X-Gal and X-Gluc led to blue pigment formation, while PE-H activity on Impranil became apparent as clearing zone around grown cells.

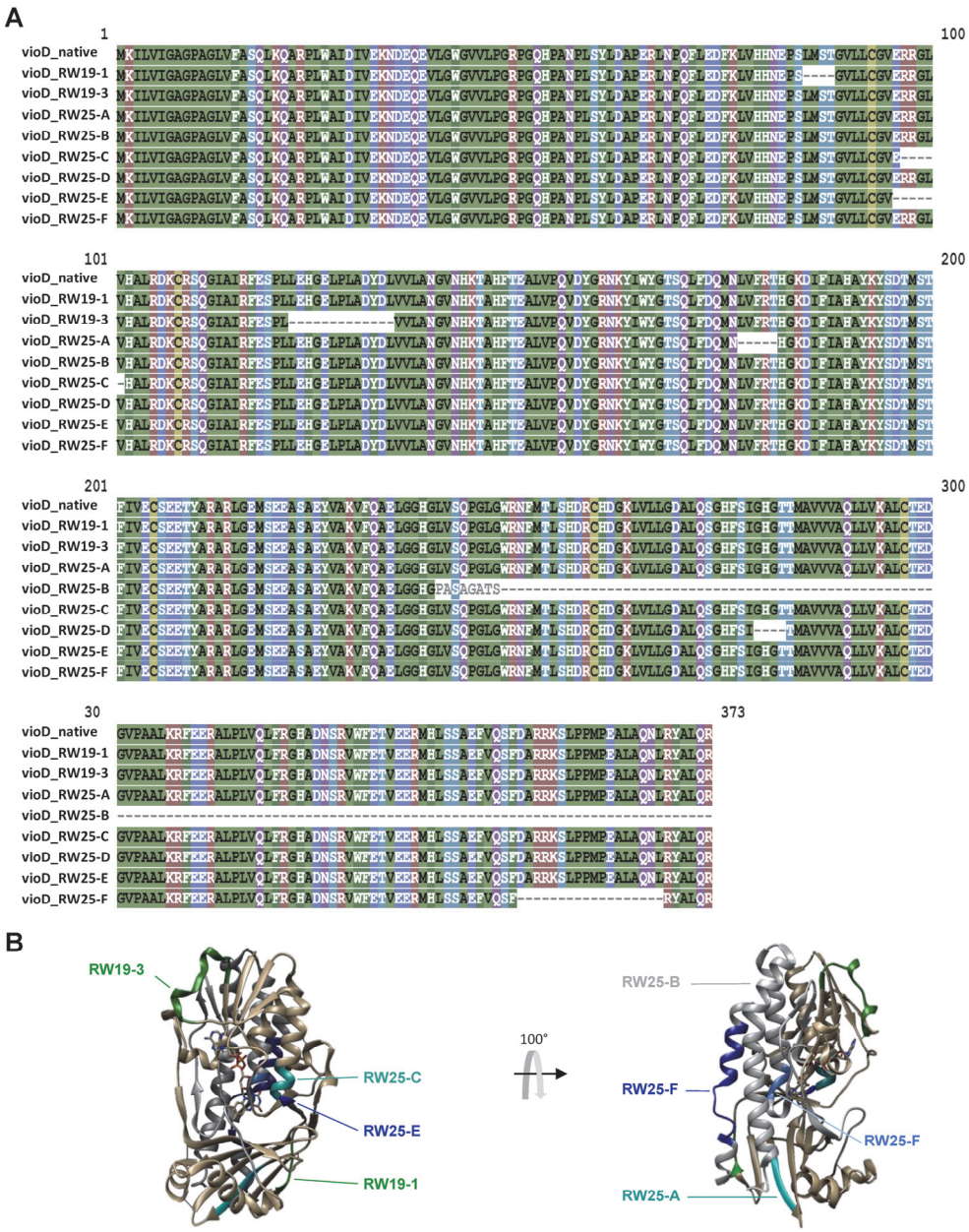

Supplementary Figure S5. Deletions in *vioD*-encoded protodeoxyviolaceinate monooxygenase.
(A) The amino acid sequence of the native VioD enzyme from *Chromobacterium violaceum* ATCC 12472 (UniProtKB - Q9S3U8) was aligned as reference with VioD sequences, which were encoded in deletion variants after chromosomal gene integration in *P. putida via* CLUSTAL Omega (1.2.4) multiple sequence alignment

Supplementary Material

(Sievers *et al.* 2011) and visualised with mView (Madeira *et al.* 2019). Deletions are marked with "-", identical amino acids are indicated by the color shading. **(B)** Crystal structure of VioD of *C. violaceum* (pdb 3C4A, protein as ribbon presentation, bound cofactor FAD as stick representation). Areas deleted in the respective variants are highlighted indicating that the deletions would probably evoke pronounced disturbances of the protein structure in the Rossman fold domain (upper part) or the reactive center (lower part).

10

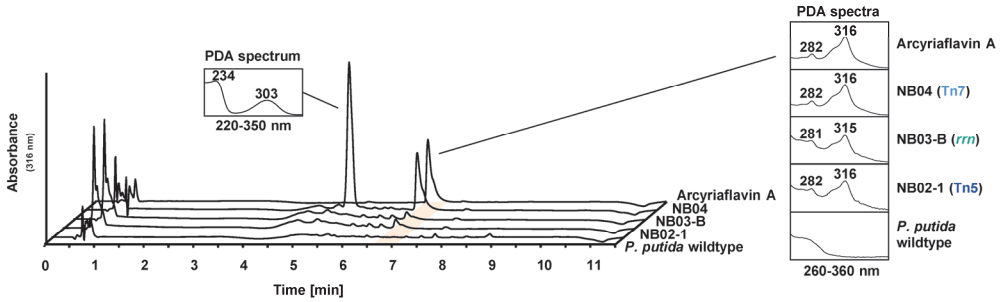

Supplementary Figure S6. HPLC-PDA analysis of arcyriaflavin A in recombinant *P. putida* strains.
The genes *rebODCP* were expressed in *P. putida* in three different modi, relying on Tn5 transposition, integration into the 16S gene of *rrnB*, or at *att*Tn7. One representative chromatogram (recorded at 316 nm) is shown for each modus – in comparison to a commercial arcyriaflavin A reference and the *P. putida* KT2440 wild type. In all extracts of expression strains, a peak was detected at 6.7 min, which exhibited the characteristic PDA spectrum of arcyriaflavin A and did not occur in wild type samples. The peak at 5.3 min, which occurred in the extracts of NB04, which carries the *rebODCP* genes in the *att*Tn7 site under control of NagR/P_{nagAa} and was accordingly supplemented with sodium salicylate, was assigned to the inducer.

Supplementary Material

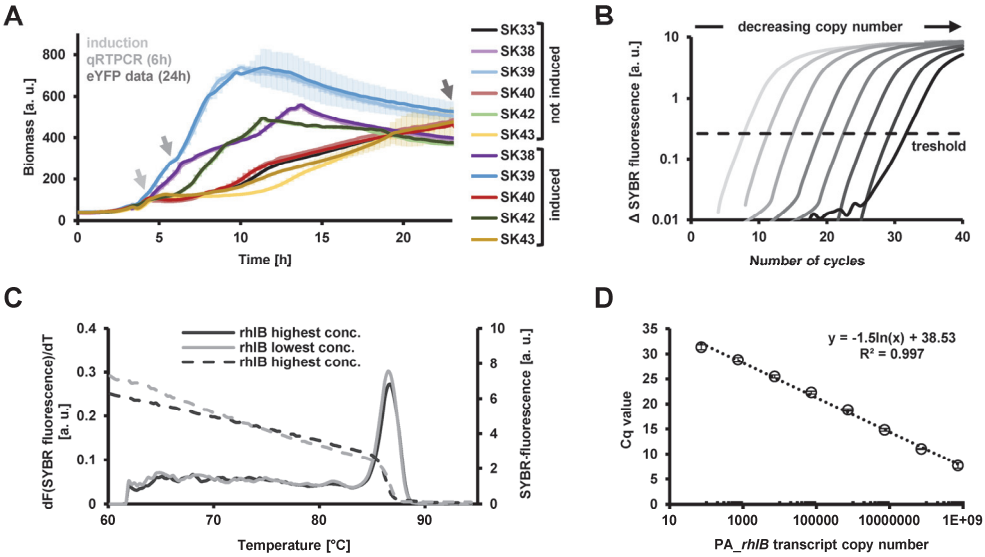

Supplementary Figure S7. Calibration and quality control of RT-qPCR after induced *rhl* expression. **(A)** Cultures of the *P. putida* strains SK33, SK38, SK39, SK40, SK42, and SK43, which carry the *rhlAB* genes under control of different promoters (P_{lac}, *araC*-P_{BAD}, *rhaRS-rha*P_{BAD}, *nagR*-P_{nagAa}, *mtlR*-P_{mtlE}, and *tetR*-P_{TetA}, respectively), were inoculated in 1.2 mL LB medium supplemented with 10 g L^{-1} glucose with an $OD_{580\ nm}$= 0.05, cultured shaking at 1200 rpm for 24 h at 30 °C. After 3.5 h, inducers were added: SK38, 10 mM L-arabinose; SK39, 10 mM L-rhamnose; SK40, 2 mM salicylate; SK42, 2 mM D-mannitol; SK43, 0.5 mM anhydrotetracycline). The data of the non-induced cultures (lighter color) are also shown. Growth was monitored *via* a BioLector system as scattered light at 620 nm (20 min intervals). For RT-qPCR, samples were taken after 6 h and eYFP fluorescence was analysed at 24 h. **(B)** Courses of normalised SYBR Green fluorescence (ΔRn) during the qPCR with the different template dilutions. **(C)** Validation of the PCR specificity using the primers PA-*rhlB*_fw-RT, PA-*rhlB*_rv-RT and the template pYTSK40K_1G7. Depicted are exemplary dissociation curves and their first derivatives for the reactions with the highest applied template concentration (ca. 70,000,000 copies) as well as for the lowest (ca. 700 copies). **(D)** Calibration plot of the Cq value (number of cycles at threshold fluorescence) versus template copy number. The equation derived from the regression (y = -1.5ln(x)+38.53, with R^2= 0.997) was used for the determination of *rhlB* transcript copy numbers in the biological samples.

Supplementary Table S1. Occurrence of endonuclease sites of the YT_core sequence within other pYT elements.
Endonuclease sites in the YT_core sequence that occur in pYT vector backbone elements or YT_core components (M, markers; R, reporters, P, promoters) used in this study are marked ("cuts"). Homing endonucleases are highlighted by bold font. Vector elements which are not co-integrated into the genome are marked with an asterisk (*). If sites occur in chosen elements, attention should be paid to the order of integration of the necessary genes or alternative endonuclease sites for further modifications should be considered.

	Purpose			YT_ core extrac -tion	element addition			target genes	reporter insertion		marker insertion		multiple cutters				
	restriction site			I-*Ppo*I	PI-*Sce*I	*Asi*SI	*Eco*RI	I-*Sce*I	*Mau*BI	I-*Ceu*I	*Sal*I	PI-*Psp*I	*Mlu*I	*Nco*I	*Xho*I	*Sac*I	*Kpn*I
backbone elements	pYT-backbone*		yCP	-	-	-	-	-	-	-	-	-	-	cuts	cuts	cuts	-
	*tnp**		Tn5	-	-	-	-	-	-	-	-	-	-	-	cuts	-	-
	landing pads		rrn	-	-	-	-	-	-	-	-	-	-	-	-	-	-
	sacB marker*		SacB	-	-	-	-	-	-	-	-	-	-	-	-	-	cuts
	tnsABCD		Tn7	-	-	-	-	-	-	-	-	-	-	cuts	-	cuts	cuts
	P_{bla}-*bla**		Ap^R	-	-	-	-	-	-	-	-	-	-	-	-	-	-
	P_{aphII}-*aphII**		Km^R	-	-	-	-	-	-	-	-	-	-	cuts	-	-	-
variable YT_core components	M	P_{aacC1}-*aacC1*	Gm^R	-	-	-	-	-	-	-	-	-	-	-	-	-	-
		P_{tet}-*tetA(C)*	Tc^R	-	-	-	-	-	-	-	cuts	-	-	-	-	-	-
		P_{aphII}-*aphII*	Km^R	-	-	-	-	-	-	-	-	-	-	cuts	-	-	-
		P_{aadA}-*aadA*	Sm^R	-	-	-	-	-	-	-	-	-	-	-	-	-	-
		P_{cat}-*cat*	Cm^R	-	-	-	cuts	-	-	-	-	-	-	cuts	-	-	-
	R	*eYFP*	YFP	-	-	-	-	-	-	-	-	-	-	cuts	-	-	-
		mCherry	RFP	-	-	-	-	-	-	-	-	-	-	cuts	-	-	-
		mTagBFP2	BFP	-	-	-	-	-	-	-	-	-	-	-	cuts	-	-
		lacZ	LacZ	-	-	-	-	-	cuts	-	-	-	cuts	-	-	cuts	-
		uidA	GUS	-	-	-	-	-	-	-	-	-	cuts	-	-	-	-
		pe-h	PE-H	-	-	-	-	-	-	-	-	-	-	-	-	-	-
	P	*nagR*-P_{nagAa}	P_{nagAa}	-	-	-	-	-	-	-	-	-	-	-	-	cuts	cuts

Supplementary Table S2. Proteins encoded by the genes utilizes for the pYT vector series.

Gene	Encoded protein
mob	Mob relaxase (from pBBR1)
URA3	*Saccharomyces cerevisiae* orotidine 5'-phosphate decarboxylase
Tn5 *tnp*	Transposon Tn5 transposase
sacB	*Bacillus subtilis* levansucrase
tnsA	Transposon Tn7 transposase subunit
tnsB	Transposon Tn7 transposase subunit
tnsC	Transposon Tn7 regulator/connector protein
tnsD	Transposon Tn7 recognition protein of the *att*Tn7 site
bla	beta-lactamase TEM (from pBBR322)
aphII	aminoglycoside 3'-phosphotransferase (from transposon Tn5)
aacC1	*Pseudomonas aeruginosa* gentamicin 3-N-acetyltransferase
tetA(C)	*Salmonella* sp. tetracycline efflux pump
aadA	*Shigella* spc. aminoglycoside (3") (9) adenylyltransferase
cat	*Shigella flexneri* chloramphenicol O-acetyltransferase
eYFP	*Aequorea victoria* yellow fluorescent protein
mCherry	*Discosoma* sp. red fluorescent protein
mTagBFP2	*Entacmaea quadricolor* blue fluorescent protein
lacZ	*Escherichia coli* beta-galactosidase
uidA	*Escherichia coli* beta-glucuronidase
pe-h	*Pseudomonas aestusnigri* polyester hydrolase (B7O88_RS11490)
nagR	*Comamonas testosterone* LysR type transcriptional regulator of P_{nagAa}

Supplementary Material

Supplementary Table S3. Nomenclature of the pYT vectors.
Fluorescent reporters **1-3**: eYFP (Spiess *et al.* 2005); mTagBFP2 (Subach *et al.* 2011), mCherry (Shaner *et al.* 2004). Enzymes **6-8**: P-EH (Bollinger *et al.* 2020); LacZ (Miller 1972); GUS (Jefferson, Burgess and Hirsh 1986).

pYT nomenclature follows the scheme: pYTUVX^{b}_WX^{c}Z					
W = reporter		**X = marker (^{b} = backbone; ^{c} = core)**		**Z = integration mode**	
0	no reporter	**x**	no marker	**5**	transposon Tn5
1	eYFP	**A**	ampicillin	**7**	transposon Tn7
2	mTagBFP2	**T**	tetracyclin	**i1**	interposon into landing pad in 16S RNA genes
3	mCherry	**C**	chloramphenicol		
6	PE-H	**K**	kanamycin	**U = creator initials (2-letter code)**	
7	LacZ	**G**	gentamicin		
8	GUS	**S**	spectinomycin/streptomycin	**V = consecutive number (01, 02, 03, …)**	

Table S4. List of plasmids and gDNA templates. Relevant biosynthetic genes are denoted with prefixes indicating the original organisms (CV, *Chromobacterium violaceum*; PA, *Pseudomonas aeruginosa*; LA, *Lentzea aerocolonigenes*). Relevant elements of vectors used for cloning are marked in bold font.

Vectors and templates used for cloning		
Vector / template	**Information**	**Reference**
Vectors used for the construction of pYT backbones		
YCp50-poly-Km^R	*CEN4/ARS1*, pMB1 ori, Km^R, *URA3*,	(Domröse *et al.* 2017)
YCp50-poly	*CEN4/ARS1*, pMB1 ori, Ap^R, *URA3*, P$_{lac}$	(Wang and Stillman 1993)
yTREX	**YCp50-poly-Km^R**, **oriT-*mob***, OE-L, P$_{T7}$, CIS, P$_{T7}$, Tc^R, **Tn5 *tnp*, OE-R**	(Domröse *et al.* 2017)
yTREX-Ap^R	**YCp50-poly-Ap^R**, **oriT-*mob***, OE-L, P$_{T7}$, CIS, P$_{T7}$, Tc^R, Tn5 *tnp*, OE-R	This study
pYTRW01K_0x5	YCp50-poly-Km^R, oriT-***mob*** (with altered 3' end), OE-L, CIS, OE-R, Tn5 *tnp*	This study
pMK-RQ-YT_core	ColE1 ori, Km^R, **Tn7-L, YT_core, Tn7-R** (gene synthesis)	This study
pTNS1	R6K ori, *Ap^R*, **Tn7 *tnsA-D***	(Choi *et al.* 2005)
pSEVA512S	R6K ori, oriT, *lacZ*α. I-*Sce*I sites, Tc^R	(Aparicio, de Lorenzo and Martínez-García 2017)
pSEVA512S-16S-pad	pSEVA512S carrying gene synthesis **16S_up, LP-L, Gm^R, LP-R, 16S_dn**	This study
pK19-mobSacB	pBR322 ori, oriT-mob, Km^R, *lacZ*α-MCS, ***sacB***	(Schäfer *et al.* 1994)
templates for resistance markers, transcriptional reporters and promoters		
pUC18-mini-Tn7-Gm	Template for **Gm^R** pMB1 ori, Ap^R, *lacZ*α, FRT-L, Tn7-L, Gm^R, Tn7-R, FRT-L	(Choi *et al.* 2005)
pRhotHi-2	Template for **Cm^R** pBBR1 ori, oriT-*mob*, Km^R, Cm^R, P$_{T7}$-MCS	(Katzke *et al.* 2010)
pHP45Ω	Template for **Sm^R** pBR322 ori, Ap^R, omega element: Sm^R/Spc^R	(Prentki and Krisch 1984)
yTREX vector	Template for **Tc^R** YCp50-poly-Km^R oriT-*mob*, OE-L, P$_{T7}$, CIS, P$_{T7}$, Tc^R, Tn5 *tnp*, OE-R	(Domröse *et al.* 2017)
pRhon5Hi-2-eyfp	Template for **eYFP**, pBBR1 ori, oriT-*mob*, Km^R, Cm^R, P$_{nil}$-*eYFP*	(Troost *et al.* 2019)
pAra-mCherry	Template for **mCherry** pBR322 ori, oriT, Km^R, P$_{tac}$-*araE* , *araC*-P$_{BAD}$-*mCherry*	Jaeger Lab, unpublished
pRhotHi-2-mTagBFP2	Template for **mTagBFP2**, pBBR1 ori, oriT-*mob*, Km^R, Cm^R, P$_{T7}$-*mTagBFP2*, pelB	Jaeger Lab, unpublished
yTREX-phzA-G-lacZ	Template for ***lacZ*** yTREX vector carrying PA_*phzABCDEFG*-EC_*lacZ*	(Weihmann *et al.* 2020)
Strain: *Escherichia coli* BL21(DE3)	Template for ***uidA***	(Studier and Moffatt 1986)
pET22b_PE-H$_{c6H}$	Template for ***pe-h*** pBR322 ori, Ap^R, *lacI*, P$_{T7}$, *Pseudomonas aestusnigri* PE-H (B7O88_RS11490)	(Bollinger *et al.* 2020)
pSK02	Template for **P$_{lac}$-BCD2** R6K ori, oriT, Km^R, Gm^R, Tn7-L, P$_{ffg}$-BCD2-PA_*rhlAB*, Tn7-R	(Bator *et al.* 2020)
pAra-final	Template for **P$_{tac}$-*araE, araC*-P$_{BAD}$** pMB1 ori, oriT, Km^R, *araC*-P$_{tac}$-*araE*, P$_{BAD}$-*GFPmut3*	(Binder *et al.* 2016)
Strain: *Escherichia coli* DH5α	Template for **P$_{tac}$-*rhaT*, *rhaRS*-*rha*P$_{BAD}$**	(Grant *et al.* 1990)
pBNTmcs(t)Km	Template for ***nagR*-P$_{nagAa}$** pBBR1 ori, Km^R, *nagR*-P$_{nagAa}$	(Verhoef *et al.* 2010)
Strain: *Pseudomonas protegens* Pf-5	Template for ***mtlR*-P$_{mtlE}$**	(Loper, Kobayashi and Paulsen 2007)
pASKINt110	Template for ***tetR*-P$_{tetA}$** pColE1 ori, F1 ori, Cm^R, *tetR*-P$_{tetA}$-*eaeA*	(Adams, Wentzel and Kolmar 2005; Becker *et al.* 2005)
templates for biosynthetic genes		
pAra-Vio	Template for **CV_*vioABCDE*** pMB1 ori, oriT, Km^R, *araC*-P$_{BAD}$-CV_*vioABCDE*	(Binder *et al.* 2016)
pVLT33-PA_*rhlABC*	Template for **PA_*rhlAB*** pRSF1010 ori, oriT-*mob*, Km^R, *lacI*-P$_{tac}$_PA_*rhlABC*	(Wittgens *et al.* 2017)
pVLT33-PA_*rmlBADC*	Template for **PA_*rmlBADC*** pRSF1010 ori, oriT-*mob*, Km^R, *lacI*-P$_{tac}$_PA_*rmlBADC*	Jaeger Lab, unpublished
pLO03	Template for **PA_*algC*** pBR322 ori, oriT, Sm^R, Spc^R, PA_*algC_full*	Blank Lab, unpublished
Strain: *Lentzea aerocolonigenes* ATCC 39243	Template for **LA_*rebODCP***	(Bush *et al.* 1987)
Integrative pYT vectors		
pYT vectors for Tn5, *rrn*, and Tn7 integration		

Supplementary Material

pYTRW10K_0x5	YCp50-poly-Km^R, oriT-*mob*, OE-L, CIS, OE-R, Tn5 *tnp*	This study
pYTRW07K_0G5	YCp50-poly-Km^R, oriT-*mob*, OE-L, CIS, Gm^R, OE-R, Tn5 *tnp*	This study
pYTRW08K_0C5	YCp50-poly-Km^R, oriT-*mob*, OE-L, CIS, Cm^R, OE-R, Tn5 *tnp*	This study
pYTRW09K_0T5	YCp50-poly-Km^R, oriT-*mob*, OE-L, CIS, Tc^R, OE-R, Tn5 *tnp*	This study
pYTRW11K_0S5	YCp50-poly-Km^R, oriT-*mob*, OE-L, CIS, Sm^R, OE-R, Tn5 *tnp*	This study
pYTRW14K_7G5	YCp50-poly-Km^R, oriT-*mob*, OE-L, CIS, *lacZ*, Gm^R, OE-R, Tn5 *tnp*	This study
pYTRW17K_6G5	YCp50-poly-Km^R, oriT-*mob*, OE-L, CIS, *pe-h*, Gm^R, OE-R, Tn5 *tnp*	This study
pYTRW16K_1G5	YCp50-poly-Km^R, oriT-*mob*, OE-L, CIS, *eYFP*, Gm^R, OE-R, Tn5 *tnp*	This study
pYTRW13K_3G5	YCp50-poly-Km^R, oriT-*mob*, OE-L, CIS, *mCherry*, Gm^R, OE-R, Tn5 *tnp*	This study
pYTRW20K_0Ti1	YCp50-poly-Km^R, oriT-*mob*, LP-L, CIS, Tc^R, LP-R	This study
pYTRW28K_0Ti1	YCp50-poly-Km^R, oriT-*mob*, LP-L, CIS, Tc^R, LP-R, *sacB*	This study
pYTRW21K_1Ti1	YCp50-poly-Km^R, oriT-*mob*, LP-L, CIS, *eYFP*,Tc^R, LP-R	This study
pYTRW26K_1Ti1	YCp50-poly-Km^R, oriT-*mob*, LP-L, CIS, *eYFP*, Tc^R, LP-R, *sacB*	This study
pYTRW22K_7Ti1	YCp50-poly-Km^R, oriT-*mob*, LP-L, CIS, *lacZ*,Tc^R, LP-R	This study
pYTRW27K_7Ti1	YCp50-poly-Km^R, oriT-*mob*, LP-L, CIS, *lacZ*, Tc^R, LP-R, *sacB*	This study
pYTSK00K_0x7	YCp50-poly-Km^R, oriT-*mob*, Tn7-L, CIS, Tn7 *tnsA-D*, Tn7-R	This study
pYTSK01K_0G7	YCp50-poly-Km^R, oriT-*mob*, Tn7-L, CIS, Gm^R, Tn7 *tnsA-D*, Tn7-R	Genbank MT522186
pYTSK02A_0G7	YCp50-poly-Km^R, oriT-*mob*, Tn7-L, CIS, Gm^R, Tn7 *tnsA-D*, Tn7-R	This study
pYTSK31K_1G7	YCp50-poly-Km^R, oriT-*mob*, Tn7-L, CIS, *eYFP*, Gm^R, Tn7 *tnsA-D*, Tn7-R	This study
pYTSK56K_3G7	YCp50-poly-Km^R, oriT-*mob*, Tn7-L, CIS, *mCherry*, Gm^R, Tn7 *tnsA-D*, Tn7-R	This study
pYTSK55K_2G7	YCp50-poly-Km^R, oriT-*mob*, Tn7-L, CIS, *mTagBFP2*, Gm^R, Tn7 *tnsA-D*, Tn7-R	This study
pYTSK54K_7G7	YCp50-poly-Km^R, oriT-*mob*, Tn7-L, CIS, *lacZ*, Gm^R, Tn7 *tnsA-D*, Tn7-R	This study
pYTSK65K_8G7	YCp50-poly-Km^R, oriT-*mob*, Tn7-L, CIS, *uidA*, Gm^R, Tn7 *tnsA-D*, Tn7-R	This study
pYTSK58K_6G7	YCp50-poly-Km^R, oriT-*mob*, Tn7-L, CIS, *pe-h*, Gm^R, Tn7 *tnsA-D*, Tn7-R	This study
pYTNB01K_1G7	YCp50-poly-Km^R, oriT-*mob*, Tn7-L, CIS, *nagR*-P$_{nagAa}$-*eYFP*, Gm^R, Tn7 *tnsA-D*, Tn7-R	This study
YT vectors with biosynthetic genes - for Tn5, *rrn*, and Tn7 integration		
pYTRW19K_0T5	YCp50-poly-Km^R, oriT-*mob*, OE-L, CV_*vioABCDE*, Tc^R, OE-R, Tn5 *tnp*	This study
pYTNB02K_3T5	YCp50-poly-Km^R, oriT-*mob*, OE-L, LA_*rebODCP*, Tc^R, *mCherry*, OE-R, Tn5 *tnp*	This study
pYTRW24K_1Ti1	YCp50-poly-Km^R, oriT-*mob*, LP-L, CV_*vioABCDE*, Tc^R, eYFP, LP-R	This study
pYTRW25K_1Ti1	YCp50-poly-Km^R, oriT-*mob*, LP-L, CV_*vioABCDE*, Tc^R, eYFP, LP-R, *sacB*	This study
pYTNB03K_1Ti1	YCp50-poly-Km^R, oriT-*mob*, LP-L, LA_*rebODCP*, Tc^R, eYFP, LP-R, *sacB*	This study
pYTSK03K_0G7	YCp50-poly-Km^R, oriT-*mob*, Tn7-L, P$_{lac}$-BCD2-PA_*rhlAB*, Gm^R, Tn7 *tnsA-D*, Tn7-R	This study
pYTSK08K_0G7	YCp50-poly-Km^R, oriT-*mob*, Tn7-L, P$_{tac}$-*araE*, *araC*-P$_{BAD}$-BCD2-PA_*rhlAB*, Gm^R, Tn7 *tnsA-D*, Tn7-R	This study
pYTSK09K_0G7	YCp50-poly-Km^R, oriT-*mob*, Tn7-L, P$_{tac}$-*rhaT*, *rhaRS*-rhaP$_{BAD}$-BCD2-PA_*rhlAB*, Gm^R, Tn7 *tnsA-D*, Tn7-R	This study
pYTSK10K_0G7	YCp50-poly-Km^R, oriT-*mob*, Tn7-L, *nagR*-P$_{nagAa}$-BCD2-PA_*rhlAB*, Gm^R, Tn7 *tnsA-D*, Tn7-R	(Tiso *et al.* 2020)
pYTSK12K_0G7	YCp50-poly-Km^R, oriT-*mob*, Tn7-L, *mtlR* P$_{mtlE}$-BCD2-PA_*rhlAB*, Gm^R, Tn7 *tnsA-D*, Tn7-R	This study
pYTSK13K_0G7	YCp50-poly-Km^R, oriT-*mob*, Tn7-L, *tetR*-P$_{tetA}$-BCD2-PA_*rhlAB*, Gm^R, Tn7 *tnsA-D*, Tn7-R	This study
pYTSK33K_1G7	YCp50-poly-Km^R, oriT-*mob*, Tn7-L, P$_{lac}$-BCD2-PA_*rhlAB*, *eYFP*, Gm^R, Tn7 *tnsA-D*, Tn7-R	This study
pYTSK38K_1G7	YCp50-poly-Km^R, oriT-*mob*, Tn7-L, P$_{tac}$-*araE*, *araC*-P$_{BAD}$-BCD2-PA_*rhlAB*, *eYFP*, Gm^R, Tn7 *tnsA-D*, Tn7-R	This study
pYTSK39K_1G7	YCp50-poly-Km^R, oriT-*mob*, Tn7-L, P$_{tac}$-*rhaT*, *rhaRS*-rhaP$_{BAD}$-BCD2-PA_*rhlAB*, *eYFP*, Gm^R, Tn7 *tnsA-D*, Tn7-R	This study
pYTSK40K_1G7	YCp50-poly-Km^R, oriT-*mob*, Tn7-L, *nagR*-P$_{nagAa}$-BCD2-PA_*rhlAB*, *eYFP*, Gm^R, Tn7 *tnsA-D*, Tn7-R	(Tiso *et al.* 2020)
pYTSK42K_1G7	YCp50-poly-Km^R, oriT-*mob*, Tn7-L, *mtlR*-P$_{mtlE}$-BCD2-PA_*rhlAB*, *eYFP*, Gm^R, Tn7 *tnsA-D*, Tn7-R	This study
pYTSK43K_1G7	YCp50-poly-Km^R, oriT-*mob*, Tn7-L, *tetR*-P$_{tetA}$-BCD2-PA_*rhlAB*, *eYFP*, Gm^R, Tn7 *tnsA-D*, Tn7-R	This study
pYTSK57K_3G7	YCp50-poly-Km^R, oriT-*mob*, Tn7-L, *nagR*-P$_{nagAa}$-BCD2-PA_*rhlAB*, *mCherry*, Gm^R, Tn7 *tnsA-D*, Tn7-R	This study
pYTSK61K_2G7	YCp50-poly-Km^R, oriT-*mob*, Tn7-L, *nagR*-P$_{nagAa}$-BCD2-PA_*rhlAB*, *mTagBFP2*, Gm^R, Tn7 *tnsA-D*, Tn7-R	This study
pYTSK60K_7G7	YCp50-poly-Km^R, oriT-*mob*, Tn7-L, *nagR*-P$_{nagAa}$-BCD2-PA_*rhlAB*, *lacZ*, Gm^R, Tn7 *tnsA-D*, Tn7-R	This study

pYTSK66K_8G7	YCp50-poly-Km^R, oriT-*mob,* Tn7-L, *nagR*-P$_{nagAa}$-BCD2-PA_*rhlAB, uidA,* Gm^R, Tn7 *tnsA-D*, Tn7-R	This study
pYTSK64K_6G7	YCp50-poly-Km^R, oriT-*mob,* Tn7-L, *nagR*-P$_{nagAa}$-BCD2-PA_*rhlAB, pe-h,* Gm^R, Tn7 *tnsA-D*, Tn7-R	This study
pYTSK51K_0G7	YCp50-poly-Km^R, oriT-*mob*, Tn7-L, *nagR*-P$_{nagAa}$-BCD2-PA_*rhlAB* +PA_*rmlBDAC*, Gm^R, Tn7 *tnsA-D*, Tn7-R	This study
pYTSK62K_0G7	YCp50-poly-Km^R, oriT-*mob*, Tn7-L, *nagR*-P$_{nagAa}$-BCD2-PA_*rhlAB* +PA_*rmlBDAC* +PA_*algC_full*, Gm^R, Tn7 *tnsA-D*, Tn7-R	This study
pYTNB04K_1G7	YCp50-poly-Km^R, oriT-*mob*, Tn7-L, *nagR*-P$_{nagAa}$-*rebODCP*, *eYFP*, Gm^R, Tn7 *tnsA-D*, Tn7-R	This study

Supplementary Material

Supplementary Table S5. List of oligonucleotides.
Sequences designated as overhangs for yeast recombination or In-Fusion cloning are underlined. Endonuclease recognition sites are highlighted in italic font. Special sequences are marked in colour (*mob* 3' end, orange; promoters, blue; BCD2 and RBS regions, green).

Name	Nucleotide sequence (5'→3')	Amplicon (template) / Info
Cloning of vectors pYTWR10K_0x5, pYTRW20K_0Ti1, RW28K_0Ti1, pYTSK00K_0x7, pYTSK01K_0G7, and pYTSK02A_0G7		
RW001	ATTTCCCCGAACTGACTCTTATACACAAGTTATCTGCAGCACTCAACAGATC	YT_core (for Tn5) (pMK-RQ-YT_core)
RW002	TTCAGGACGCTCTGACTCTTATACACAAGTCTAAACTGATCGGTCAGAGCGC ACCTC	
RW100	CAGCAGGAACGCGGG*CGCGC*ACATTTCCCCGAAAAGTGCCACCTGACGTCT AAGAAACCATTATTATCA**TGA**CTGACTCTTATACACAAGT	*mob* reconstruction (*pYTRW01K_0x5*)
RW101	TTATAGTTAC*GCGCGCG*TTGCAGCACGTATTGAG	
RW156	ACGTTCGATCGCGTGGCGTCTCATGATAATAATGGTTTCTTAGACGTCAGG	pYT backbone (pYTRW10K_0x5)
RW157	CGGTGATCAATATAGTGGTTGACATGCTGGCTAGTCAACATTG	
RW159	CACGACAGGGTGCGTGTACCTATCTGCAGCACTCAACAG	YT_core (for *rrn*) (pYTRW10K_0x5)
RW160	TCAAGATCCGTCGTTCTGGATACACACCCATAATACCCATAATAG	
RW158	GACGCCACGCGATCGAACG	LP-L (pSEVA512S-16S-pad)
RW164	GGTACACGCACCCTGTCGTG	
RW148	TCCAGAACGACGGATCTTGACGCAATTTGGCGTGG*CTCTCTTAAGGTAGCCC* TCCGACCAATTGAGGTGCGCTCTGACCGATCAGTTTAGGGTGAGCCAACCC GGCCGATC	LP-R (pSEVA512S-16S-pad)
RW149	AACCACTATATTGATCACCGATATATGGACTTCCACACCAGTTTACCAGCGGC TAGTC	
RW194	ATTTATTGTCATATTACTAGCACGTGCCCATCACATATACCTGCCGTTC	*sacB* (pK19-mobSacB)
RW195	ATATGTGGACCCGGGACTAGTTTATTTGTTAACTGTTAATTGTCCTTGTTC	
fw_HMR_tnsD	CTCTGACCGATCAGTTTAGTCACTCTTCCCCATAAACCATTTCCAAGAA	*tnsABCD* (pTNS1)
rv_Tn7R_HBy	ATTGATCACCGATATATGGACTTCCACACCAACTAGTCCCGGGTCGAGATGC CGCATGTG	
Fw_SynSK	CAGGAACGCGGGCGCGCACATTTCCCCGAATGTGGGCGGACAAAATAG	YT_core (for Tn7) (pMK-RQ-YT_core)
Rv_SynSK	AACCGAACAGGCTTATGTCAATGGGACTCTCCGCCAAATC	
Fw_KleSK	GACCCAAGTACCGCCACCTAA*GTCGAC*TGGCAAACAGCTATTATG	
Rv_KleSK	TTCTTGGAAATGGTTTATGGGGAAGAGTGACTAAACTGATCGGTCAGAG	
Amp fw	ATCCGTTAGCGAGGTGCCGCCGGCTTCCAT*CGATCG*GTGCGCGGAACCCCT ATTTG	YCp50-poly
Amp rev	AAGTATATATGAGTAAACTTGGTCTGACAG*GAGCTC*TTACCAATGCTTAATCA GTG	
Cloning of promoters		
fw_CIS I_lac_BCD2	CGGCGAACAGTATAAGCAGATTCGACTCACTTTACACTTTATGCTTCCGGCTC GTATAATGCCCAAGTTCACTTAAAAAGG	P_{lac}-BCD2 (pSK02)
rv_BCD2	TAGAAAACCTCCTTAGCATGATTAAGAT	
fw_CIS I_AraEC	CGGCGAACAGTATAAGCAGATTCGACTCACTCAGACGCCGATATTTCTC	P_{tac}-*araE*, *araC*-P_{BAD} (pAra-final)
rv_PBADara_BCD2	TAGAAAACCTCCTTAGCATGATTAAGATGTTTCAGTACGAAAATTGCTTTCATT GTTGATCTCCTTTTTAAGTGAACTTGGGCAGCCCAAAAAACGGGTAT	
fw_CIS I_PtacRhaT	CGGCGAACAGTATAAGCAGATTCGACTCACTGACAATTAATCATCGGCTCGT ATAATGTCATCTCGTCGGAGATGTG	P_{tac}-*rhaT*, *rhaRS*-*rha*P_{BAD} (*E. coli* DH5α)
rv_PBADrha_BCD2	TAGAAAACCTCCTTAGCATGATTAAGATGTTTCAGTACGAAAATTGCTTTCATT GTTGATCTCCTTTTTAAGTGAACTTGGGCGCTGAATTTCATTACGACCAGTCT	
fw_CIS I_NagR	CGGCGAACAGTATAAGCAGATTCGACTCACCAGTCAATATGGGTTTGCTGGA AGCTTATG	*nagR*-P_{nagAa} (pBNTmcs(t)Km)
rv_PnagAa_BCD2	TAGAAAACCTCCTTAGCATGATTAAGATGTTTCAGTACGAAAATTGCTTTCATT GTTGATCTCCTTTTTAAGTGAACTTGGGCCGGTACCTCCTGTTTCC	
IF_PI-SceI-nagR_fw	*GTTGATCTATGTCGGGTGCGGAGAAAGAGGTAATGAAATGGCAGTCAATATG* GGTTTGCTGGAAGCTTATGCTTCAG	*nagR*-P_{nagAa} (pBNTmcs(t)Km)
IF_nagAa-AsiSI_rev	TGTAAGCTGTGG*GCGATCG*CCGGTACCTCCTGTTTCCTGTGG	
fw_CIS I_TetR	CGGCGAACAGTATAAGCAGATTCGACTCACTTAAGACCCACTTTCACAT	*tetR*-P_{tetA} (pASKINt110)
rv_TetR	CAATAACCCTGATAAATGCTTCAA	
fw_TetR_PtetA	ATATTATTGAAGCATTTATCAGGGTTATTGCCATCGAATGGCCAGATG	
rv_PtetA_BCD2	TAGAAAACCTCCTTAGCATGATTAAGATGTTTCAGTACGAAAATTGCTTTCATT GTTGATCTCCTTTTTAAGTGAACTTGGGCTTTTTGCCCTCGTTATCTAG	
fw_CIS I_mtlR	CGGCGAACAGTATAAGCAGATTCGACTCACTCAGCCGAGGTTCTGTTC	*mtlR*-P_{mtlE} (*P. protegens* Pf-5)
rv_mtlR	GGGCGCCAACCCTGAGAAC	
fw_mtlR_PmtlE	CCAGAGAAGGCGTTCTCAGGGTTGGCGCCCGACCGGGAAAAAGCCAGTG	
rv_PmtlE_BCD2	TAGAAAACCTCCTTAGCATGATTAAGATGTTTCAGTACGAAAATTGCTTTCATT GTTGATCTCCTTTTTAAGTGAACTTGGGCCGTTCACTCCTGTCCTGCGCCGG TGAG	
Cloning of markers		
fw_HMF_Gm	CAAGATTTGGCGGAGAGTCCCATTGACATAAGCCTGTTCGGTTC	P_{aacC1}-*aacC1* (pUC18-mini-Tn7-Gm)
rv_Gm_HMR	AGATCCGTCGTTCTGGATACACACCCATAATACCCATAATAGCTGTTTGCCA*G TCGAC*TTAGGTGGCGGTACTTGGGTCG	
yTT_CmRM_fw AF neu	CCGATTTATCAAGATTTGGCGGAGAGTCCCCACGAGGCCCTTTCGTCTTC	P_{cat}-*cat*

yTT_CmRM_rev AF	ACCCATAATACCCATAATAGCTGTTTGCCA*GTCGAC*CGGCCAACGCGCGGGGAGAG	(pRhotHi-2)
yTT_TcRM_fw AF neu	CCGATTTATCAAGATTTGGCGGAGAGTCCCTCATGTTTGACAGCTTATCA	*P*$_{tet}$-*tetA(C)* (yTREX vector)
yTT_TcRM_rev AF	ACCCATAATACCCATAATAGCTGTTTGCCA*GTCGAC*TCAGGTCGAGGTGGCCCGGCTC	
yTT Sm RM fw	CCGATTTATCAAGATTTGGCGGAGAGTCCCCGCACACCGTGGAAACGGAT	P$_{aadA}$-*aadA* (pHP45Ω)
yTT Sm RM rev	ACCCATAATACCCATAATAGCTGTTTGCCA*GTCGAC*TTATTTGCCGACTACCTTGG	
Cloning of reporters		
fw_CIS II_eYFP	CAATTACTCGCGACTTCCTCAATACGTGCTGCAAAACTTTAGAAGGAGATATACCATGGTGAGCAAGGGCGAGGAG	*eYFP* (pRhon5-eYFP)
rv_eYFP_HB-R-rv	TCTGGGTTAAGCGTGTCCTTACACAACAGCACAAGTAAGCTTACTTGTACAGCTCGTCCATG	
RW108	GTGCTGCAA*CGCGCGCG*AACTTTAGAAGGAGATATACCATGGTGAGCAAGGGCGAGGAG	
RW109	TTATAGTTA*CGCGCGCG*TTACTTGTACAGCTCGTCCATGCC	
fw_CIS II_mtagBFP2	CAATTACTCGCGACTTCCTCAATACGTGCTGCAAAACTTTAGAAGGAGATATACCATGAGCGAGCTGATTAAG	*mTagBFP2* (pRhotHi-2 mTagBFP2)
rv_mtagBFP2_HB-R-rv	CTCGCTACCTTAGGACCGTTATAGTTA*CGCGCGCG*TCACTCGAGATTAAGCTTGTGCCCCAGTTTG	
RW106	GTGCTGCAA*CGCGCGCG*AACTTTAGAAGGAGATATACCATGAGCGAGCTGATTAAG	
RW107	TTATAGTTA*CGCGCGCG*TTACTCGAGATTAAGCTTGTGC	
fw_CIS II_mCherry	TACTCGCGACTTCCTCAATACGTGCTGCAAAACTTTAGAAGGAGATATACCATGGTGAGCAAGGGCGAGG	*mCherry* (pAra-mCherry)
rv_mCherry_HB-R-rv	CTCGCTACCTTAGGACCGTTATAGTTA*CGCGCGCG*TTACTTGTACAGCTCGTCCA	
RW108	GTGCTGCAA*CGCGCGCG*AACTTTAGAAGGAGATATACCATGGTGAGCAAGGGCGAGG	
InFusion mCherry rev	TTATAGTTA*CGCGCGCG*TTACTTGTACAGCTCGTCC	
fw_CIS I_LacZ	CAATTACTCGCGACTTCCTCAATACGTGCTGCAAAACTTTAGAAGGAGATATACCATGACCATGATTACGGATTCACT	*lacZ* (yTREX-phzA-G-lacZ)
rv_LacZ_HB-R-rv	TCGCTACCTTAGGACCGTTATAGTTA*CGCGCGCGCGGCG*CTTATTTTTGACACCAGACCAAC	
RW110	GTGCTGCAA*CGCGCGCG*AACTTTAGAAGGAGATATACCATGACCAATTACGGATTC	
RW111	TTATAGTTA*CGCGCGCG*TTATTTTTGACACCAGACCAAC	
fw_CIS I_GUS	CAATTACTCGCGACTTCCTCAATACGTGCTGCAAAACTTTAGAAGGAGATATACCATGTTACGTCCTGTAGAAACC	*uidA* (*E. coli* BL21(DE3))
rv_GUS_HB-R-rv	CTCGCTACCTTAGGACCGTTATAGTTA*CGCGCG*CGTCATTGTTTGCCTCCCTGCTGCGGTTT	
fw_CIS I_PE-H	CAATTACTCGCGACTTCCTCAATACGTGCTGCAAAACTTTAGAAGGAGATATACCATGCCATTTAACAAGAAAAGC	*pe-h* (pET22b_PE-H$_{c6H}$)
rv_PE-H_HB-R-rv	CTCGCTACCTTAGGACCGTTATAGTTA*CGCGCG*CGTTAGTACGGGCAGTTGC	
RW127	GTGCTGCAA*CGCGCG*CGAACTTTAGAAGGAGATATACCATGCCATTTAACAAGAAAAGCGTTC	
RW128	TTATAGTTA*CGCGCG*CGTTATTAGTACGGGCAGTTGCC	
Cloning of biosynthetic genes		
RW 170	GCAGATTCGACTCACTAGGGGGGCTAACAGGAGGAATTAACC	*vioABCDE* (pAra-Vio)
RW 171	GATACCCAGAG*ATTACCCTGTTATCCCTA*CTAGCGCTTGGCGGCGAAGAC	
fw_BCD2_PA-rhlAB	ACATCTTAATCATGCTAAGGAGGTTTTCTAATGCGGCGCGAAAGTCTG	*rhlAB* (pVLT33-PA_*rhlABC*)
rv_PA-rhlAB_I-SceI_CIS II	AATAGCGCGAGATTGAGTCGATACCCAGAG*ATTACCCTGTTATCCCTA*TCAGGACGCAGCCTTC	
fw_rhlB_rmlB	AGGGGGATGCTCGATGGCTGAAGGCTGCGTCCTGAACGGACAACCACTGCTTGAAC	*rmlBADC* (pVLT33-PA_*rmlBADC*)
rv_rmlC_ISceI_CIS I	AATAGCGCGAGATTGAGTCGATACCCAGAG*ATTACCCTGTTATCCCTA*TCAGGGGAAGCAGTC	
rv_algC_ISceI_CIS I	AATAGCGCGAGATTGAGTCGATACCCAGAG*ATTACCCTGTTATCCCTA*TCAGAAGGGCACGGGCAGCGAG	*algC* (pLO03)
fw_rmlC_algC_full	GCAAGGCATTCGCCGACGCCGACTGCTTCCCCTGAAGACGCCGAGGAGACGCGGCATGAAGCTTTTCCAGCGCACCGCCAA	
IF_rebODCP_fw	GCAGATTCGACTCACTAGGGCACGCGGGGTCAGGC	*rebODCP* (*L. aerocolonigenes*)
IF_rebODCP_I-SceI_rev	GATACCCAGAG*ATTACCCTGTTATCCCTA*GTCAACGTGTCAGCATCGGC	
Determination of gene integration at *att*Tn7		
PTn7L_rv	ATTAGCTTACGACGCTACACCC	Tn7-recombinant *P. putida* KT2440
PTn7R_fw	CACAGCATAACTGGACTGATTTC	
Pput-glmS_fw	AGTCAGAGTTACGGAATTGTAGG	
Pput-glmS_rv	TTACGTGGCCGTGCTAAAGGG	
Verification of landing pad integration in *rrn* operons of *P. putida* KT2440		
AD106	TACGGTTGTCGGAGACGCCAGTGGAGTATC	binds forward upstream of *rrnA*
AD107	CCCATCCCGAACTCAGTAGTGAAACGATGC	binds forward upstream of *rrnB*
AD108	AAGAAGTCGTTTGGCCGGGTTACCCTCAAG	binds forward upstream of *rrnC*
AD109	CATGAAGCGTCGCAGTTTGCATTCCCTAGC	binds forward upstream of *rrnD*
AD110	AGGATCACTGCAAGAAAGCCCGCACTGTAG	binds forward upstream of *rrnE*
AD111	AGCAGCATGATGATGCTGGCGAAGATCAGG	binds forward upstream of *rrnF*

Supplementary Material

AD112	CTTGGGTTGGGCTTGTTGCATTTCCTGTGG	binds forward upstream of *rrnG*
RW138	GCGACTGCCCTGCTGCGTAACATC	binds reverse in *aacC1*
RW174	CTTGCACCCTCTGTATTACC	binds reverse in 16S
RW196	CCGCGCTCATCAATC	Sequencing of LP-L
RW197	TAACGCGCTTGCTGCTTG	Sequencing of LP-R
Sequencing of elements after cloning into pYT vectors		
Seq_yTREX_Reporter_fw	CTCAATCTCGCGCTATTGTG	Reporter
Seq_yTREX_Reporter_rv	CCATGGACGCGTAGTCGTAG	
Seq_yTREX_Marker_fw	TACGACTACGCGTCCATGGC	Marker
Seq_yTREX_Marker_rv	GCCAAATTGCGTCAAGATCC	
Seq_yTREX_Cluster_fw	AGTGGCTCGTTACCTCGTTC	Cluster (CIS)
Seq_yTREX_Cluster_rv	GAGGAAGTCGCGAGTAATTG	
Seq_yTREX_Promoter_fw	CTAGCCTATATCGTCAATCCG	Promoter
Verification of *vio* gene integration in landing pad and sequencing of *vioD*		
RW217	CAGGCCGAACTCCTCGTCCAGGAAATG	binds reverse in *vio* cluster
RW220	CTTTACCCGCCGGACATGG	Sequencing of *vioD*
RW221	CAGATGAACCTGGTGTTCCG	
RW223	CTTGCAGGGCGATATG	
RW232	GCTTGGCGGCGAAGAC	
RW233	CGACCAGGGATTGAAC	
RT-qPCR primers		
PA-rhlB_fw-RT	CGCTGTTCGACGGCAGTATC	*rhlB* transcript
PA-rhlB_rv-RT	AGGGCCATGGCGTAGAAGTC	

Supplementary Table S6. *P. putida* strains used for expression studies.

Strain name	Features	Reference
KT2440	Wildtype, derivative of mt-2	(Bagdasarian *et al.* 1981)
	Strains carrying a landing pad for pYT integrons	
RW-16SA	landing pad (Gm^R) in the 16S gene of *rrnA*	This study
RW-16SB	landing pad (Gm^R) in the 16S gene of *rrnB*	This study
RW-16SC	landing pad (Gm^R) in the 16S gene of *rrnC*	This study
RW-16SD	landing pad (Gm^R) in the 16S gene of *rrnD*	This study
RW-16SE	landing pad (Gm^R) in the 16S gene of *rrnE*	This study
RW-16SF	landing pad (Gm^R) in the 16S gene of *rrnF*	This study
RW-16SG	landing pad (Gm^R) in the 16S gene of *rrnG*	This study
	Strains carrying a pYT Tn5 transposon	
RW16-1	*eYFP*, Gm^R	This study
RW14-1	*lacZ*, Gm^R	This study
RW19-1	CV_*vioABCDE*, Tc^R	This study
RW19-2	CV_*vioABCDE*, Tc^R	This study
RW19-3	CV_*vioABCDE*, Tc^R	This study
RW19-4	CV_*vioABCDE*, Tc^R	This study
RW19-5	CV_*vioABCDE*, Tc^R	This study
RW19-6	CV_*vioABCDE*, Tc^R	This study
NB02-1	LA_*rebODCP*, *mCherry*, Tc^R	This study
NB02-2	LA_*rebODCP*, *mCherry*, Tc^R	This study
NB02-3	LA_*rebODCP*, *mCherry*, Tc^R	This study
NB02-4	LA_*rebODCP*, *mCherry*, Tc^R	This study
NB02-5	LA_*rebODCP*, *mCherry*, Tc^R	This study
	Strains carrying a pYT integron in a 16S gene	
RW25-A	in *rrnA*: CV_*vioABCDE*, *eYFP*, Tc^R	This study
RW25-B	in *rrnB*: CV_*vioABCDE*, *eYFP*, Tc^R	This study
RW25-C	in *rrnC*: CV_*vioABCDE*, *eYFP*, Tc^R	This study
RW25-D	in *rrnD*: CV_*vioABCDE*, *eYFP*, Tc^R	This study
RW25-E	in *rrnE*: CV_*vioABCDE*, *eYFP*, Tc^R	This study
RW25-F	in *rrnF*: CV_*vioABCDE*, *eYFP*, Tc^R	This study
NB03-B	in *rrnB*: LA_*rebODCP*, *eYFP*, Tc^R, Km^R	This study
	Strains carrying a pYT Tn7 transposon at *att*Tn7	
SK31	*eYFP*, Gm^R, *tnsA-D*	This study
SK55	*mTagBFP2*, Gm^R, *tnsA-D*	This study
SK56	*mCherry*, Gm^R, *tnsA-D*	This study
SK54	*lacZ*, Gm^R, *tnsA-D*	This study
SK65	*uidA*, Gm^R, *tnsA-D*	This study
SK58	*pe-h*, Gm^R, *tnsA-D*	This study
SK33	P_{lac}-BCD2-PA_*rhlAB*, *eYFP*, Gm^R, *tnsA-D*	This study
SK38	P_{tac}-*araE, araC*-P_{BAD}-BCD2-PA_*rhlAB*, *eYFP*, Gm^R, *tnsA-D*	This study
SK39	P_{tac}-*rhaT*, *rhaRS*-*rha*P_{BAD}-BCD2-PA_*rhlAB*, *eYFP*, Gm^R, *tnsA-D*	This study
SK40	*nagR*-P_{nagAa}-BCD2-PA_*rhlAB*, *eYFP*, Gm^R, *tnsA-D*	(Tiso *et al.* 2020)
SK42	*mtlR*-P_{mtlE}-BCD2-PA_*rhlAB*, *eYFP*, Gm^R, *tnsA-D*	This study
SK43	*tetR*-P_{TetA}-BCD2-PA_*rhlAB*, *eYFP*, Gm^R, *tnsA-D*	This study
SK60	*nagR*-P_{nagAa}-BCD2-PA_*rhlAB*, *lacZ*, Gm^R, *tnsA-D*	This study
SK66	*nagR*-P_{nagAa}-BCD2-PA_*rhlAB*, *uidA*, Gm^R, *tnsA-D*	This study
SK64	*nagR*-P_{nagAa}-BCD2-PA_*rhlAB*, *pe-h*, Gm^R, *tnsA-D*	This study
SK57	*nagR*-P_{nagAa}-BCD2-PA_*rhlAB*, *mCherry*, Gm^R, *tnsA-D*	This study
SK61	*nagR*-P_{nagAa}-BCD2-PA_*rhlAB*, *mTagBFP2*, Gm^R, *tnsA-D*	This study
SK10	*nagR*-P_{nagAa}-BCD2-PA_*rhlAB*, Gm^R, *tnsA-D*	(Tiso *et al.* 2020)
SK51	*nagR*-P_{nagAa}-BCD2-PA_*rhlAB*+PA_*rmlBDAC*, Gm^R, *tnsA-D*	This study
SK62	*nagR*-P_{nagAa}-BCD2-PA_*rhlAB*+PA_*rmlBDAC*+PA_*algC_full*, Gm^R, *tnsA-D*	This study
NB04	*nagR*-P_{nagAa}-LA_*rebODCP*, *eYFP*, Gm^R, *tnsA-D*	This study

Supplementary Material

References

Adams TM, Wentzel A, Kolmar H. Intimin-mediated export of passenger proteins requires maintenance of a translocation-competent conformation. *J Bacteriol* 2005;**187**:522–33.

Antoine R, Locht C. Isolation and molecular characterization of a novel broad-host-range plasmid from *Bordetella bronchiseptica* with sequence similarities to plasmids from Gram-positive organisms. *Mol Microbiol* 1992;**6**:1785–99.

Aparicio T, de Lorenzo V, Martínez-García E. Broadening the SEVA plasmid repertoire to facilitate genomic editing of Gram-negative bcteria. In: McGenity TJ, Timmis KN, Nogales B (eds.). *Hydrocarbon and Lipid Microbiology Protocols, Springer Protocols Handbooks*. Berlin Heidelberg: Springer-Verlag, 2017, 9–27.

Bagdasarian M, Lurz R, Rückert B *et al.* Specific-purpose plasmid cloning vectors II. Broad host range, high copy number, RSF1010-derived vectors, and a host-vector system for gene cloning in *Pseudomonas*. *Gene* 1981;**16**:237–47.

Bator I, Wittgens A, Rosenau F *et al.* Comparison of three xylose pathways in *Pseudomonas putida* KT2440 for the synthesis of valuable products. *Front Bioeng Biotechnol* 2020;**7**:480.

Becker S, Theile S, Heppeler N *et al.* A generic system for the *Escherichia coli* cell-surface display of lipolytic enzymes. *FEBS Lett* 2005;**579**:1177–82.

Binder D, Bier C, Grünberger A *et al.* Photocaged arabinose: A novel optogenetic switch for rapid and gradual control of microbial gene expression. *ChemBioChem* 2016;**17**:296–9.

Bollinger A, Thies S, Knieps-Grünhagen E *et al.* A Novel Polyester Hydrolase From the Marine Bacterium *Pseudomonas aestusnigri* – Structural and Functional Insights. *Front Microbiol* 2020;**11**:114.

Bush JA, Long BH, Catino JJ *et al.* Production and biological activity of rebeccamycin, a novel antitumor agent. *J Antibiot (Tokyo)* 1987;**40**:668–78.

Choi K-H, Gaynor JB, White KG *et al.* A Tn7-based broad-range bacterial cloning and expression system. *Nat Methods* 2005;**2**:443–8.

Domröse A, Hage-Hülsmann J, Thies S *et al. Pseudomonas putida* rDNA is a favored site for the expression of biosynthetic genes. *Sci Rep* 2019;**9**:7028.

Domröse A, Weihmann R, Thies S *et al.* Rapid generation of recombinant *Pseudomonas putida* secondary metabolite producers using yTREX. *Synth Syst Biotechnol* 2017;**2**:310–9.

Grant SGN, Jessee J, Bloom FR *et al.* Differential plasmid rescue from transgenic mouse DNAs into *Escherichia coli* methylation-restriction mutants. *Proc Natl Acad Sci* 1990;**87**:4645–9.

Jefferson RA, Burgess SM, Hirsh D. β-Glucuronidase from *Escherichia coli* as a gene-fusion marker. *Proc Natl Acad Sci* 1986;**83**:8447–51.

Katzke N, Arvani S, Bergmann R *et al.* A novel T7 RNA polymerase dependent expression system for high-level protein production in the phototrophic bacterium *Rhodobacter capsulatus*. *Protein Expr Purif* 2010;**69**:137–46.

Kovach ME, Elzer PH, Hill DS *et al.* Four new derivatives of the broad-host-range cloning vector pBBR1MCS, carrying different antibiotic-resistance cassettes. *Gene* 1995;**166**:175–6.

Kovach ME, Phillips RW, Elzer PH *et al.* pBBR1MCS: A broad-host-range cloning vector. *Biotechniques* 1994;**16**:800–2.

Loper JE, Kobayashi DY, Paulsen IT. The genomic sequence of *Pseudomonas fluorescens* Pf-5: Insights into biological control. *Phytopathology* 2007;**97**:233–8.

Madeira F, Park YM, Lee J *et al.* The EMBL-EBI search and sequence analysis tools APIs in 2019. *Nucleic Acids Res* 2019;**47**:W636–41.

Miller JH. Assay of β-Galactosidase. In: Experiments in Molecular Genetics. *Cold Spring Harb Lab Cold Spring Harb New York* 1972:352–5.

Prentki P, Krisch HM. *In vitro* insertional mutagenesis with a selectable DNA fragment. *Gene* 1984;**29**:303–13.

Schäfer A, Tauch A, Jäger W *et al.* Small mobilizable multi-purpose cloning vectors derived from the *Escherichia coli* plasmids pK18 and pK19: selection of defined deletions in the chromosome of *Corynebacterium glutumicum*. *Gene* 1994;**145**:69–73.

Schweizer HP. Small broad-host-range gentamycin resistance gene cassettes for site-specific insertion and deletion mutagenesis. *Biotechniques* 1993;**15**:831–3.

Shaner NC, Campbell RE, Steinbach PA *et al.* Improved monomeric red, orange and yellow fluorescent proteins derived from *Discosoma* sp. red fluorescent protein. *Nat Biotechnol* 2004;**22**:1567–72.

Sievers F, Wilm A, Dineen D *et al.* Fast, scalable generation of high-quality protein multiple sequence alignments using Clustal Omega. *Mol Syst Biol* 2011;**7**:539.

Spiess E, Bestvater F, Heckel-Pompey A *et al.* Two-photon excitation and emission spectra of the green fluorescent protein variants ECFP, EGFP and EYFP. *J Microsc* 2005;**217**:200–4.

Studier FW, Moffatt BA. Use of bacteriophage T7 RNA polymerase to direct selective high-level expression of cloned genes. *J Mol Biol* 1986;**189**:113–30.

Subach OM, Cranfill PJ, Davidson MW *et al.* An enhanced monomeric blue fluorescent protein with the high chemical stability of the chromophore. *PLoS One* 2011;**6**:e28674.

Tiso T, Ihling N, Kubicki S *et al.* Integration of genetic and process engineering for optimized rhamnolipid production using *Pseudomonas putida*. *Front Bioeng Biotechnol* 2020;**8**:976.

Troost K, Loeschcke A, Hilgers F *et al.* Engineered *Rhodobacter capsulatus* as a phototrophic platform organism for the synthesis of plant sesquiterpenoids. *Front Microbiol* 2019;**10**:1998.

Verhoef S, Ballerstedt H, Volkers RJM *et al.* Comparative transcriptomics and proteomics of *p*-hydroxybenzoate producing *Pseudomonas putida* S12: novel responses and implications for strain improvement. *Appl Microbiol Biotechnol* 2010;**87**:679–90.

Wang H, Stillman DJ. Transcriptional repression in *Saccharomyces cerevisiae* by a SIN3-LexA fusion protein. *Mol Cell Biol* 1993;**13**:1805–14.

Weihmann R, Domröse A, Drepper T *et al.* Protocols for yTREX/Tn5-based gene cluster expression in *Pseudomonas putida*. *Microb Biotechnol* 2020;**13**:250–62.

Wittgens A, Kovacic F, Müller MM *et al.* Novel insights into biosynthesis and uptake of rhamnolipids and their precursors. *Appl Microbiol Biotechnol* 2017;**101**:2865–78.

Wohlleben W, Arnold W, Bissonnette L *et al.* On the evolution of Tn21-like multiresistance transposons: Sequence analysis of the gene (*aacC1*) for gentamicin acetyltransferase-3-I(AAC(3)-I), another member of the Tn 21-based expression cassette. *MGG Mol Gen Genet* 1989;**217**:202–8.

V.2. Supporting Information for chapter II.3

Supplementary Information

Exploring engineered vesiculation by *Pseudomonas putida* KT2440 for natural product biosynthesis

Nora Lisa Bitzenhofer[1], Carolin Höfel[1], Stephan Thies[1], Andrea Jeanette Weiler[1], Christian Eberlein[2], Hermann J. Heipieper[2], Renu Batra-Safferling[3], Pia Sundermeyer[4,5], Thomas Heidler[4.5], Carsten Sachse[4,5,6], Tobias Busche[7,8], Jörn Kalinowski[7], Thomke Belthle[9,10], Thomas Drepper[1], Karl-Erich Jaeger[1,11], Anita Loeschcke**,[1]

[1]Institute of Molecular Enzyme Technology (IMET), Heinrich Heine University Düsseldorf, Düsseldorf, Germany
[2]Department of Environmental Biotechnology, Helmholtz Centre for Environmental Research (UFZ), Leipzig, Germany
[3]Institute of Biological Information Processing – Structural Biochemistry (IBI-7: Structural Biochemistry), Forschungszentrum Jülich, Jülich, Germany
[4]Ernst-Ruska Centre for Microscopy and Spectroscopy with Electrons (ER-C-3/Structural Biology), Forschungszentrum Jülich, Jülich, Germany
[5]Institute for Biological Information Processing 6 (IBI-6/ Structural Cellular Biology), Forschungszentrum Jülich, Jülich, Germany [6]Department of Biology, Heinrich Heine University Düsseldorf, Düsseldorf, Germany
[7]Center for Biotechnology (CeBiTec), Bielefeld University, Bielefeld, Germany
[8]Bielefeld University, Medical School East Westphalia-Lippe, Bielefeld University, Bielefeld, Germany
[9]DWI–Leibniz-Institute for Interactive Materials, Aachen, Germany
[10]Functional and Interactive Polymers, Institute of Technical and Macromolecular Chemistry, RWTH Aachen University, Aachen, Germany
[11]Institute of Bio- and Geosciences IBG-1: Biotechnology, Forschungszentrum Jülich, Jülich, Germany

** corresponding author

Correspondence: Anita Loeschcke (a.loeschcke@fz-juelich.de), Natural product biosynthesis, Institute of Molecular Enzyme Technology, HHU Düsseldorf, Wilhelm-Johnen-Straße, 52428 Jülich, Germany, phone: +49 2461 613790

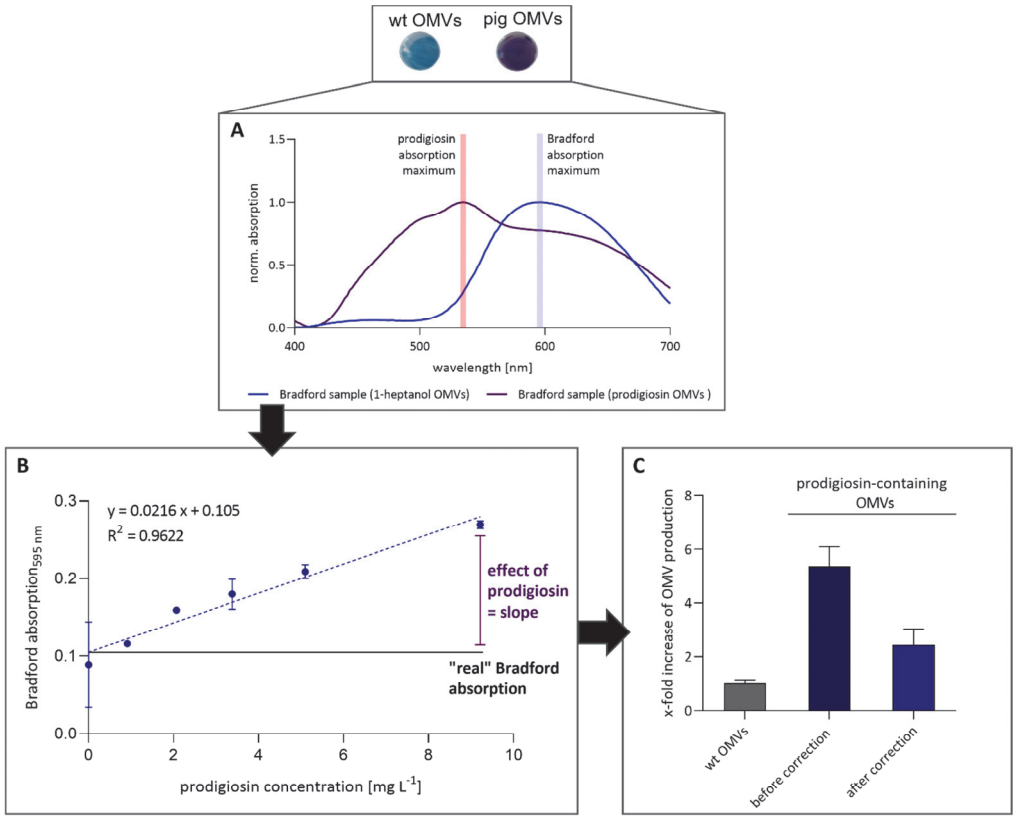

Figure S1: Correction of Bradford assay for prodigiosin-containing vesicles.
For Bradford measurements with prodigiosin-containing OMVs (pig OMVs), a mock test was performed to determine a correction factor for the Bradford absorption. Since the prodigiosin and the Bradford absorption interferes (**A**), the effect of prodigiosin has to be subtracted from the Bradford absorption. For this purpose, a correction factor was determined by adding different prodigiosin concentrations to OMVs from *P. putida* KT2440 wild type cells and measuring the Bradford absorption at 595 nm (**B**). Thus, the effect of prodigiosin corresponds to the slope of the measured absorptions. To calculate the 'actual' Bradford absorption of the prodigiosin-containing OMVs, the prodigiosin concentration in the vesicles was determined by Lambert-Beer law (ε(prodigiosin) = 139 800 M^{-1} cm^{-1}; M(prodigiosin) = 323.432 g mol^{-1}), multiplied by the slope and subtracted from the measured absorption (**C**). For detailed description of methodical procedure see **SI-M2**.

Table S1: MADLS for validation of vesicle formation in *P. putida* pig21.

Cultivation time	OMVs derived from	Population size [d. nm][1]			Count of particles [particles mL^{-1} OD^{-1}]*[1]
		1	2	3	
7 h	*P. putida* KT2440	39.2 ± 2.40	132.3 ± 1.77	431.5 ± 19.4	$2.89 \cdot 10^8 \pm 6.81 \cdot 10^7$
	P. putida pig21		130.3 ± 3.52	255.1 ± 12.7	$2.56 \cdot 10^{10} \pm 7.45 \cdot 10^9$
24 h	*P. putida* KT2440	41.9 ± 7.36	151.3 ± 12.5	401.5 ± 0.0	$1.43 \cdot 10^9 \pm 2.05 \cdot 10^9$
	P. putida pig21		154.5 ± 6.29		$3.99 \cdot 10^9 \pm 7.70 \cdot 10^8$

* particle counts refer to the main population (~ 130 – 150 nm); particle counts are specified per mL bacterial culture, normalised to the cell density ($OD_{700\ nm}$)
[1] measured with Zetasizer Ultra (Malvern Panalytical GmbH)

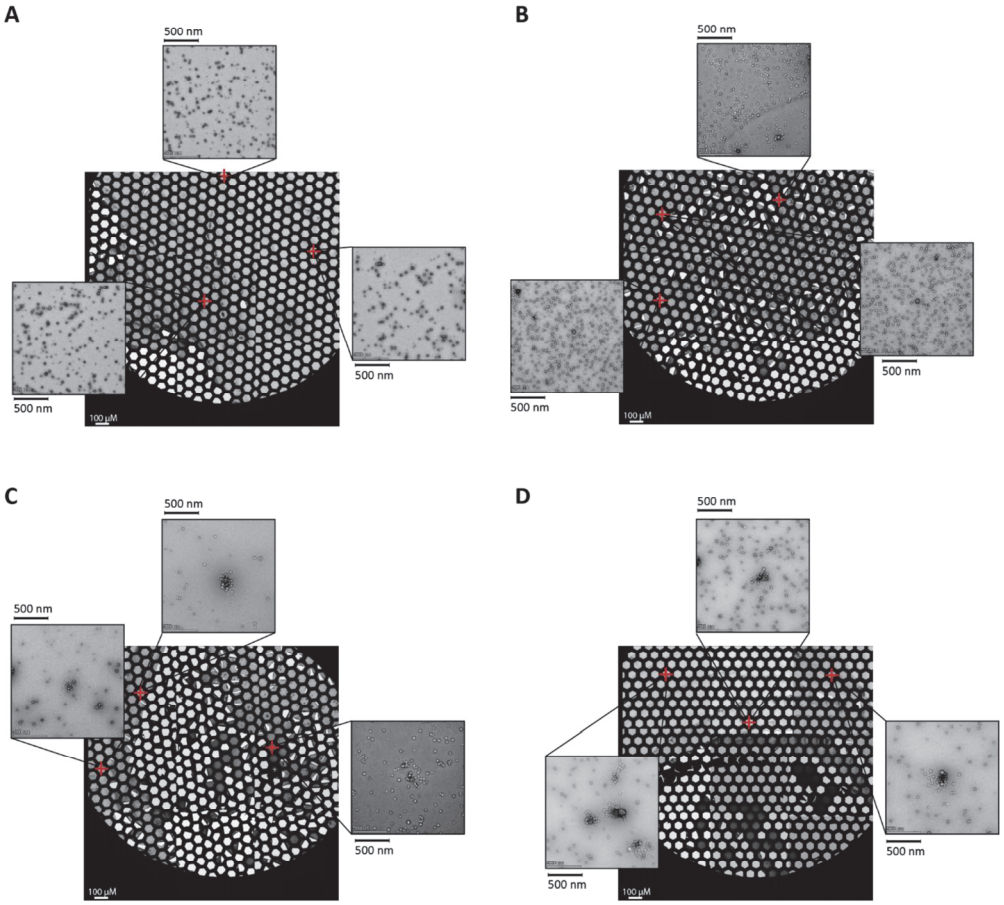

Figure S2: TEM analysis of isolated OMV fractions.
Overview of negatively stained grids and examined squares for TEM analysis. Analysed squares are indicated by a red reticle. The enlarged views (magnification 36 000x; scale: 500 nm) correspond to the sections in **Figure 2** (left side, two-step isolation) in the manuscript (scale bar: 500 nm). **A**: *P. putida* KT2440 wild type (wt) OMVs; **B**: 1-octanol-treated wt OMVs; **C**: PQS-treated wt OMVs; **D**: *P. putida* pig21 OMVs.

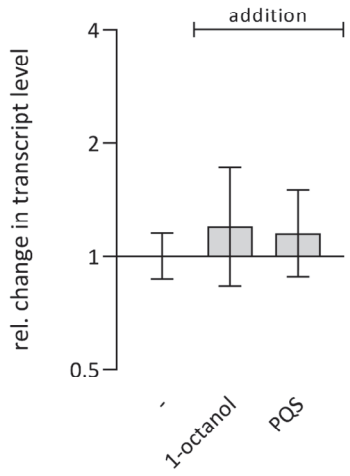

Figure S3: Transcript levels of *pigN* in differently treated prodigiosin producer strains.
To exclude an influence of the environmental stress (here: addition of 1 mM 1-octanol or 50 µM PQS) on the transcription of the *pig* gene cluster, the transcript levels of *pigN*, the last gene in the *pig* gene cluster, was determined by RT-qPCR. The data are mean values of independent triplicate measurements with their respective standard deviation. For detailed description of methodical procedure see **SI-M3**.

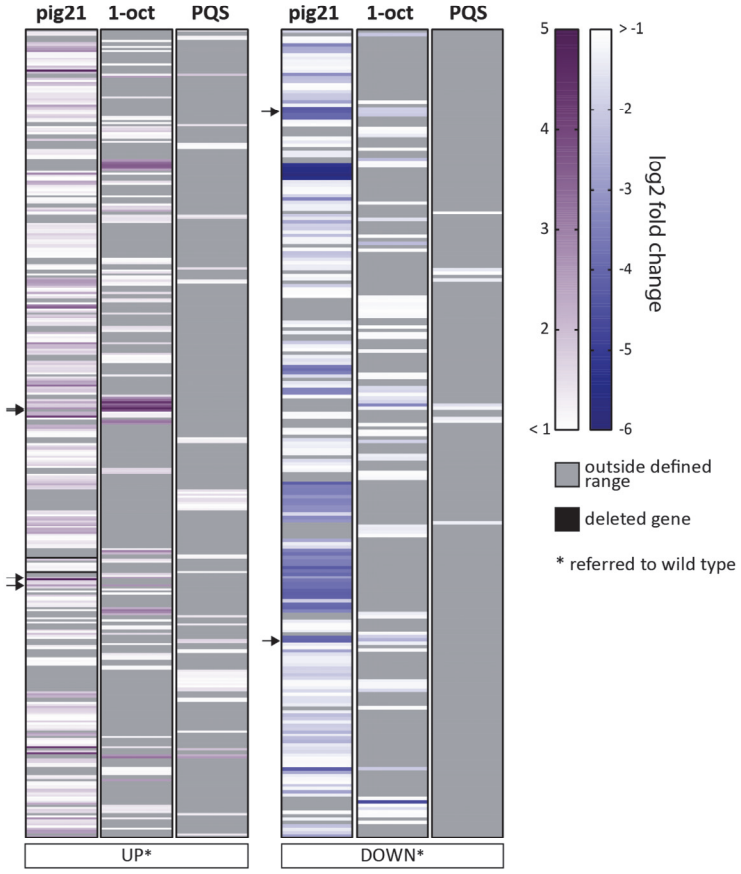

Figure S4: Heat-mapped log2 fold change of transcriptome data from *P. putida* KT2440.
For transcriptome analysis, *P. putida* KT2440 cells treated with 1 mM 1-octanol (1-oct) or 50 µM *Pseudomonas* quinolone signal (PQS), respectively, as well as *P. putida* pig21 cells were used. All samples were compared to *P. putida* KT2440 without addition of a stressor. Up-regulated genes are shown in purple shades. Down-regulated genes are shown in blue shades. Light grey colour indicates genes whose M-values are not in the log2 fold change area (M-value cutoff of ≥2 or ≤−2). The black wells represent the genes which are deleted in the prodigiosin producer strain *P. putida* pig21. Overall, 78 genes are deleted in this strain: PP_0025, PP_0035, PP_3849-3852, PP_3854-3867, PP_3869-3871, PP_3873-3884, PP_3886-3917, PP_3919-3920, PP_5637-5641, and PP_5649-5647. Genes that are up- or down-regulated in the prodigiosin producer pig21 as well as in one of the treated wild type cell samples are indicated by an arrow. The data are mean values of independent triplicate measurements. Transcriptomics sequencing raw data files are available at the ArrayExpress database (www.ebi.ac.uk/arrayexpress) under accession no. E-MTAB-12470.

Table S2: Known genetically encoded targets allowing modulation of OMV formation in Gram-negative bacteria.

Element[1]	Organism	Reference	Function[2]
Outer and inner membrane proteins (OMPs and IMPs)			
Lpp	*E. coli*	(Inouye *et al.*, 1972; Inouye, 1974; Kulp and Kuehn, 2010; Schwechheimer and Kuehn, 2015)	`Linkage´: stabilises OM, OM lipoprotein with hydrophobic head, linked by covalent bonds to PG, evenly distributed throughout membrane
Tol-Pal system	*E. coli* *C. crescentus* *Bordetella*	(Bernadac *et al.*, 1998; Schwechheimer *et al.*, 2013; Schwechheimer and Kuehn, 2015)	`Linkage´: lipoprotein Pal of the OM, binds non-covalently to PG, interacts with IMPs (TolA, TolQ, TolB, TolR), confers envelope stability, supports OM invagination during constriction phase of cell division, interacts with OmpA and Lpp, localised at cell poles
OmpA	*E. coli* *A. baumanii* *Salmonella* species *V. cholerae*	(Sonntag *et al.*, 1978; Kulp and Kuehn, 2010; Schwechheimer and Kuehn, 2015)	`Linkage´: OM porin, interacts with Pal, stabilises envelope, binds PG with periplasmic binding site for diaminopimelic acid (DAP)
NlpI[3]	*E. coli*	(McBroom *et al.*, 2006; Schwechheimer and Kuehn, 2015; Toyofuku *et al.*, 2019; Banzhaf *et al.*, 2020)	`Linkage´: OM lipoprotein, involved in cell division, controls Spr/ MepS peptidase activity leading to reduction in LPP-PG cross-linking
Mla system[3] (VacJ-Yrb system)	*E. coli* *H. influenza* *Bordetella* species	(Malinverni and Silhavy, 2009; Roier *et al.*, 2016; Yeow *et al.*, 2018; Toyofuku *et al.*, 2019)	`Membrane maintenance´: ATP-binding cassette (MlaA, MlaB, MlaC, MlaD, MlaE, MlaF), phospholipid transporter, maintains membrane asymmetry, MlaB-F/Yrb proteins are in the IM, MlaA/VacJ protein is located at the OM
Regulating elements			
σ^E/RpoE	*E. coli*	(Rouvière *et al.*, 1995; Schwechheimer *et al.*, 2013)	Transcription factor, activated by envelope stress such as accumulation of misfolded OMPs in the envelope, regulates cell envelope integrity
MicA (VrrA)	*E. coli* *V. cholerae*	(Udekwu and Wagner, 2007; Song *et al.*, 2008; Schwechheimer *et al.*, 2013)	Small RNA, down-regulates expression of *ompA*, regulated by σ^E
Reg26	*E. coli*	(Gogol *et al.*, 2011; Schwechheimer *et al.*, 2013)	Small RNA, down-regulates cellular Lpp levels and is under positive σ^E control
AsmA	*E. coli*	(Misra and Miao, 1995; Deng and Misra, 1996; Xiong *et al.*, 1996; Levine, 2019)	Putative outer membrane protein assembly factor (OmpF/OmpC)
Periplasmatic protein „quality control“			
DegP[3] (HtrA)	*E. coli* *H. pylori* *S. enterica* *P. aeruginosa* *V. fischeri* *S. flexneri* *C. jejuni*	(Strauch *et al.*, 1989; Spiess *et al.*, 1999; Schwechheimer *et al.*, 2013; Schwechheimer and Kuehn, 2015)	`Cleaning´: periplasmic chaperone at low temperatures and serine protease at high temperatures, ensures bacterial survival in the event of increased protein accumulation
Peptidoglycan (PG) metabolism			
MepS (Spr)	*E. coli*	(Singh *et al.*, 2012; Schwechheimer and Kuehn, 2015; Avila-Calderón *et al.*, 2021)	`Cleavage´: DD-endopeptidase, cleaves peptide cross-links in PG, activity is regulated by NlpI, essential role in membrane renewal
MltA	*E. coli*	(Mueller and Levin, 2020)	`Cleavage´: lytic transglycosylase, cleaves glycosidic bonds in PG,
PBP1a (MrcA)	*E. coli*		`Synthesis´: DD-transpeptidase and glycosyltransferase (bifunctional), catalyses both glycan polymerisation and peptide cross-linking
Lipopolysaccharide (LPS) biosynthesis			
RfaE (WaaE/ HldE)	*E. coli*	(Yang *et al.*, 2021)	Bifunctional protein, catalyses phosphorylation of D-glycero-D-manno-heptose 7-phosphate, catalyses ADP transfer from ATP to D-glycero-D-manno-heptose 7-phosphate

RfaC (WaaC)	*E. coli*		Lipopolysaccharide heptosyltransferase, catalyses heptose transfer to LPS core
RfaG (WaaG)	*E. coli*		Glycosyltransferase, involved in the addition of the first glucose residue to the LPS core
RffD (WecC)	*E. coli*		UDP-N-acetyl-D-mannosamine dehydrogenase, catalyses oxidation of UDP-ManNAc, releases UDP-ManNAcA
RfaI (WaaI)	*E. coli*		Lipopolysaccharide 1,3-galactosyltransferase, adds the galactose group to the glucose of LPS
PagL-1	*S. typhimurium*	(Avila-Calderón *et al.*, 2021)	Lipid A deacylase, hydrolyses the ester bond of lipid A (at position 3)
Iron homeostasis			
PvdQ	*P. putida*	(Koch *et al.*, 2010; Ringel and Brüser, 2018)	'Pyoverdine biosynthesis': acyl-homoserine lactone acylase
TonB	*A. baumannii*	(Dhurve *et al.*, 2022)	'Nutrient uptake': transporter, crucial role in transporting nutrients (e.g., iron, nickel, copper, complex carbohydrates)
Virulence factors			
VirD4	*H. pylori*	(Schwechheimer and Kuehn, 2015)	Type IV secretion system component, associated with induction of proinflammatory host responses
PQS biosynthetic enzymes	*P. aeruginosa*	(Kulp and Kuehn, 2010; Schwechheimer and Kuehn, 2015; Toyofuku *et al.*, 2019)	*Pseudomonas* quinolone signal (PQS), curvature-inducing metabolite, intercalates into the OM, increases anionic repulsion between LPS molecules

UDP-ManNAc: UDP-N-acetyl-D-mannosamine; UDP-ManNAcA: UDP-N-acetylmannosaminuronic acid

[1]Commonly used names of genetic elements refer to those in *E. coli* wherever applicable. Alternative designations for *E. coli* elements are separated by a forward slash. Names of prominently studied elements from other organisms are given in brackets, in the same line as the corresponding organism.

[2]The diverse functions are summarised in short keywords where appropriate (in quotation marks). To generate hypervesiculation mutants, proteins involved in `linkage´, `cleaning´, `synthesis´ or `membrane maintenance´ are generally down-regulated or deleted. In contrast, regulating elements and proteins involved in `cleavage´ are overexpressed in this context.

[3]Combinatorial effects on OMV formation in *E. coli* have been described for these targets (Ojima *et al.*, 2020): Cumulative gene knockout in the Mla pathway (*mlaE* and *mlaA*) had no further effect on vesiculation (non-synergistic effect). Double knockout strains of unrelated targets (e.g., Δ*degP*Δ*mlaE*, Δ*degP*Δ*mlaA*, Δ*degP*Δ*nlpI*, Δ*nlpI*Δ*mlaE*, or Δ*nlpI*Δ*mlaA*) significantly increased OMV formation compared to single gene deletions (synergistic effect).

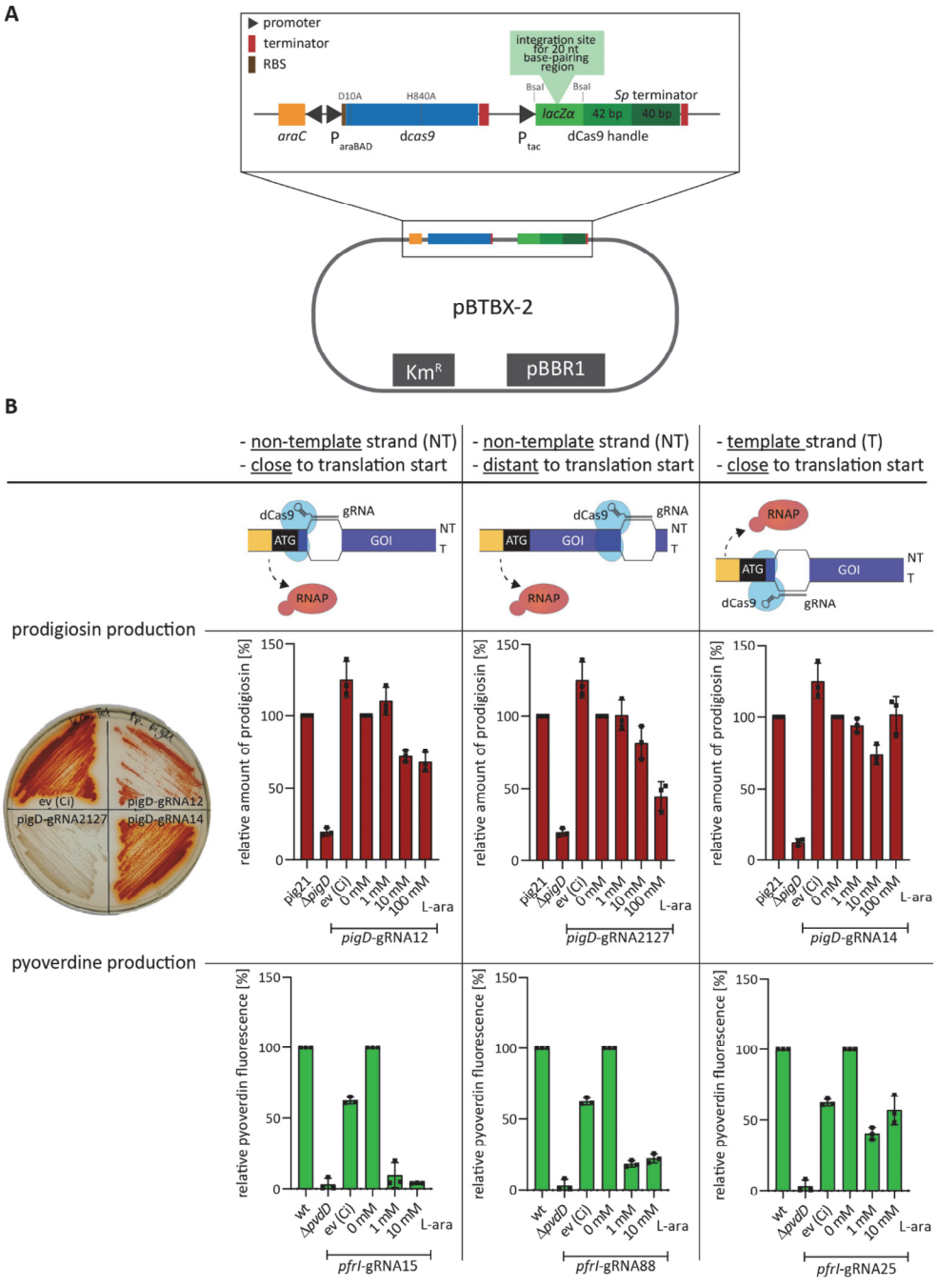

Figure S5: Evaluation of the CRISPRi system in *P. putida* KT2440.
A: Architecture of the broad-host CRISPRi-plasmid for different Gram-negative bacteria (e.g., *E. coli*, *P. putida*). **B**: P_{araBAD}-dependent down-regulation of prodigiosin production (red) and pyoverdine synthesis (green) for evaluation of the CRISPR

interference (CRISPRi) system in *P. putida* pig21 and *P. putida* KT2440, respectively. For prodigiosin, the integrated base-pairing region targets the gene *pigD* of the prodigiosin biosynthesis gene cluster. It is known that a knockout of *pigD* results in a complete loss of prodigiosin production (Klein *et al.*, 2017). For pyoverdine, the integrated base-pairing region targets the *pfrI* gene, a sigma factor for pyoverdine production. For comparison, both a prodigiosin and a pyoverdine null mutant (*P. putida* KT2440 pig-r2 Δ*pigD* and *P. putida* KT2440 Δ*pvdD*, respectively) were used. To stimulate pyoverdine production, an iron chelator (2,2'-dipyridyl (DIP)) was added to the LB medium (see **SI-M7**). For evaluation, the designed gRNAs bind the template (T) or non-template (NT) DNA strand at different distances to the translation start codon. Data are mean values of independent triplicate measurements with their respective standard deviation. The relative amounts refer to the wild type and producer for the null mutant and empty vector, respectively, and to the uninduced sample for the induced CRISPRi approaches. RBS: ribosome binding site; RNAP: DNA-dependent RNA polymerase; NT: non-template; T: template; L-ara: L-arabinose, GOI: gene of interest. ev (Ci): CRISPRi empty vector control.

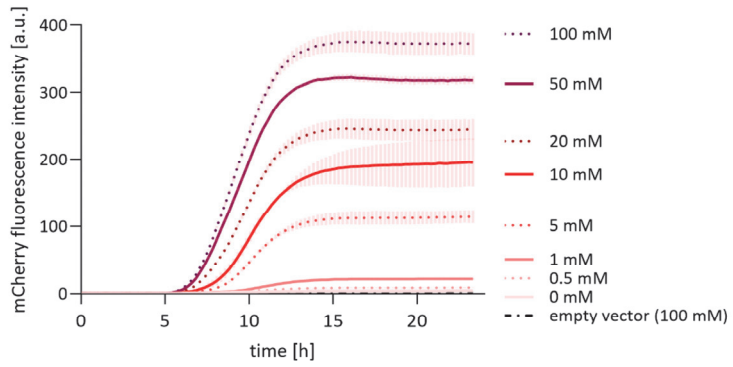

Figure S6: Expression profile of pBTBX-2-mCherry in *P. putida* KT2440.
mCherry fluorescence intensities of *P. putida* KT2440 pBTBX-2-mCherry expression cultures were measured, to assess the system regarding the inducer-dependent up-regulation of target genes. For determination of the expression profile, different L-arabinose concentrations (0 to 100 mM) as well as an "induced" empty vector control (ev) were used. Data are mean values of independent triplicate measurements. Data are obtained from online measurements using a BioLector with an mCherry/RFP filter module. For detailed description of methodical procedure see **SI-M8**.

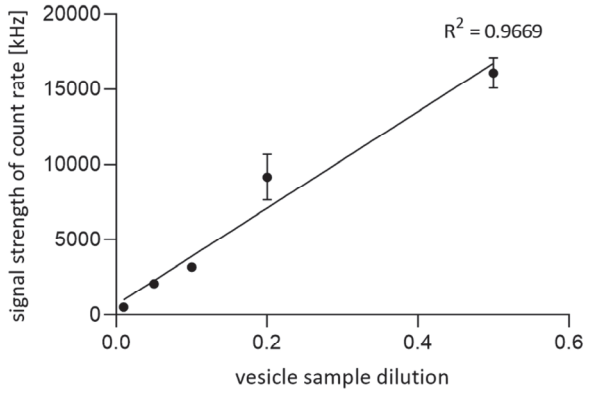

Figure S7: Correlation of DLS signal intensity and particle concentration of isolated OMVs.
To validate the correlation between DLS signal intensity and sample concentration, a dilution series was prepared using isolated OMVs from *P. putida* KT2440 pBTBX-2-mltA and subjected to measurement of the DLS signal intensity (signal strength of count rate) using a SpectroSize 300 (Xtal Concepts). The protein-vesicle signal of the undiluted sample was measured by the Bradford assay (195.7 mg L^{-1}) and the dilutions were plotted against the signal strength of count rate.

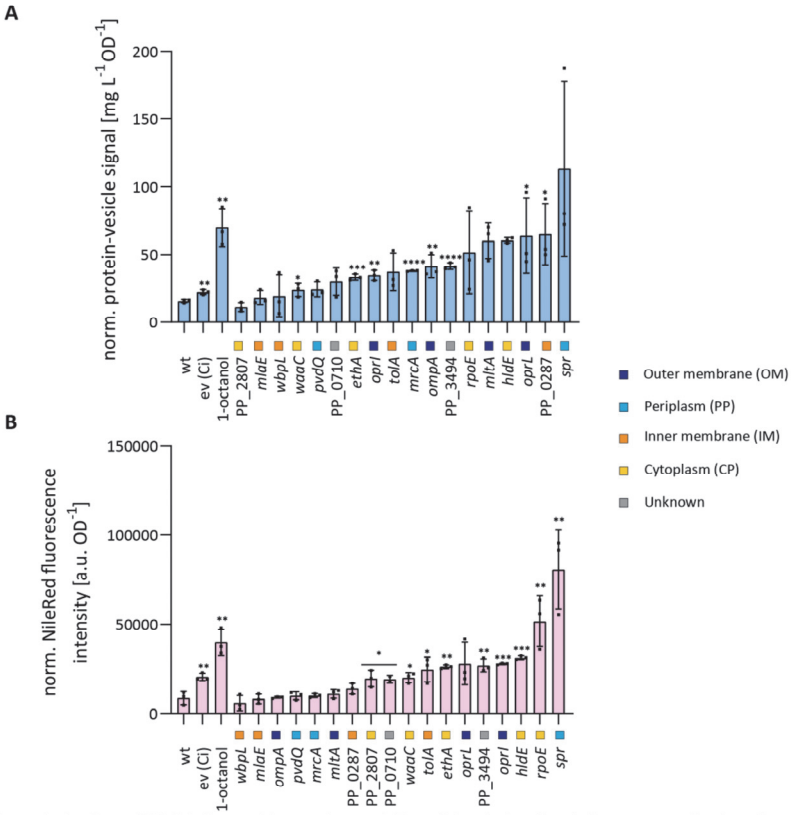

Figure S8: Characterisation of OMVs formed by engineered *P. putida* strains (in stationary growth phase).
A: Amount of protein in the OMV fraction isolated from engineered *P. putida* strains calculated by Bradford assay (based on λ_{max} = 595 nm) after growth for 24 h (stationary phase). The data are normalised to the cell density of the cell culture. **B**: Amount of lipid in the OMV fraction formed by engineered *P. putida* strains assessed with the Nile red assay (based on λ_{ex} = 543 nm; λ_{em} = 598 nm) after growth for 24 h (stationary phase). The data are normalised to the cell density of the cell culture. The data are mean values of independent triplicate measurements with their respective standard deviation. Significant differences ware indicated by asterisks (determined by T-test; * = p≤0.05, ** = p≤0.01, *** = p≤0.001, **** = p≤0.0001). Bars are sorted in ascending order. Putative cellular localisation of proteins is indicated by different colours (OM: dark blue; PP: light blue; IM: orange; CP: yellow; unknown localisation: grey). ev (Ci): CRISPRi empty vector control.

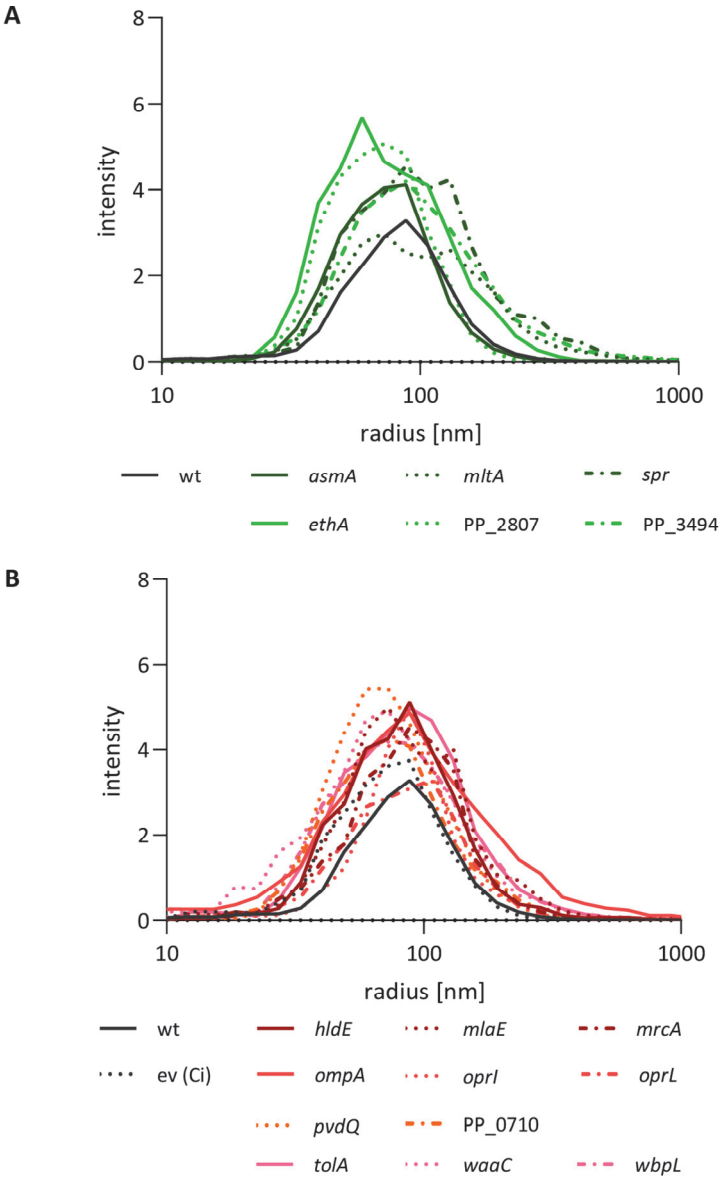

Figure S9: Vesicle sizes of OMVs formed by engineered *P. putida* strains.
Sizes of isolated OMVs (radius) formed by manipulated *P. putida* KT2440 strains (**A**: L-arabinose-dependent overexpression; **B**: CRISPRi-based down-regulation) after growth for 7 h. The radius is calculated from data obtained by DLS measurements. Data are mean values of independent triplicate measurements and isolation procedures. As the *rpoE* mutant showed barely OMV formation within 7 h, determination of vesicle size was not possible. ev(Ci): CRISPRi empty vector control.

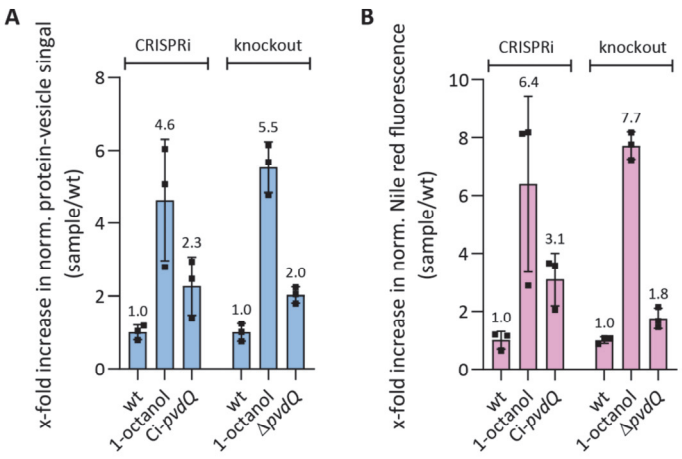

Figure S10: Characterisation of vesicle formation in a CRISPRi engineered strain and a deletion mutant.
For confirmation of the effect of CRISPRi-dependent down-regulation on vesiculation, a clean deletion of the gene *pvdQ* was done in *P. putida* KT2440, resulting in the knockout strain *P. putida* Δ*pvdQ* (see **SI-M9**). The effect of CRISPRi-based down-regulation of *pvdQ* (Ci-*pvdQ*) as well as the complete deletion (Δ*pvdQ*) on OMV formation was determined by analysing the protein content (Bradford assay) (**A**) and lipid content (Nile red assay) (**B**) in isolated OMV fractions. For reference, the *P. putida* wild type (wt) and a 1-octanol-treated wt sample were used. The samples were taken after 7 h of cultivation (logarithmic phase) and the data are normalised to the cell density of the cell culture. Data are shown as x-fold increase compared to the *P. putida* wt sample (mean values are additionally shown above the bars). The data are mean values of independent triplicate measurements with their respective standard deviation.

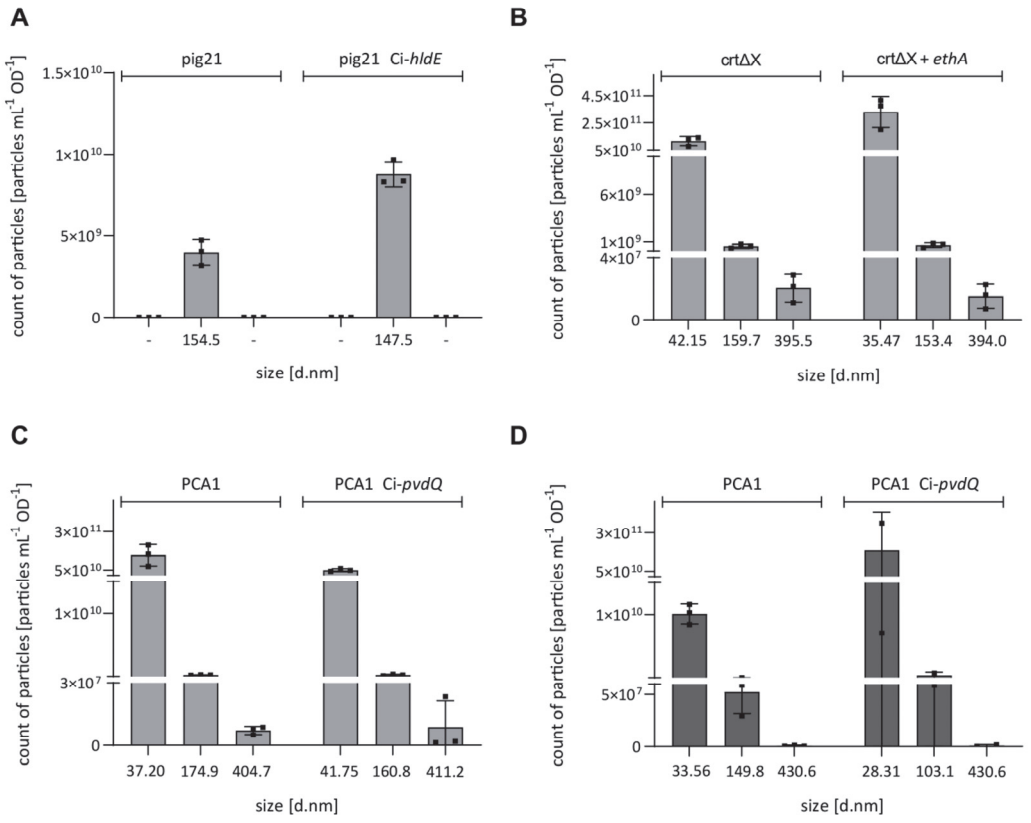

Figure S11: Validation of enhanced vesiculation in selected engineered producer strains.
To determine the amount of vesicles during the production of different natural compounds, mutli-angle dynamic light scattering (MADLS) measurements were performed. The prodigiosin producer *P. putida* pig21 (**A**), the zeaxanthin producer *P. putida* crtΔX (**B**), and the PCA producer *P. putida* PCA1 (**C**) were used (strain vio12 was excluded due to interference of the pigment with the measurement). Additionally, selected engineered strains of these three producers were analysed. The selection was based on the highest production titres in **Figure 6**. OMVs were isolated after 24 h of cultivation. As there was no clear increase detected upon manipulation of *P. putida* PCA1 at this time point, we additionally analysed the amount of OMVs in *P. putida* PCA1 after 7 h of cultivation (**D**). The previous results on the characterisation of OMVs (**Figure 5**, **Figure S8**) already showed that strains with manipulated *pvdQ* expression showed lower signals after 24 h compared to an earlier growth phase. The data are mean values of independent triplicate measurements with their respective standard deviation. Measurements of each biological sample were performed as technical triplicates. Particle counts are specified per mL bacterial culture, normalised to the cell density ($OD_{700\,nm}$). For PCA1 Ci-*pvdQ* (after 7 h), only two biological replicates were measurable.

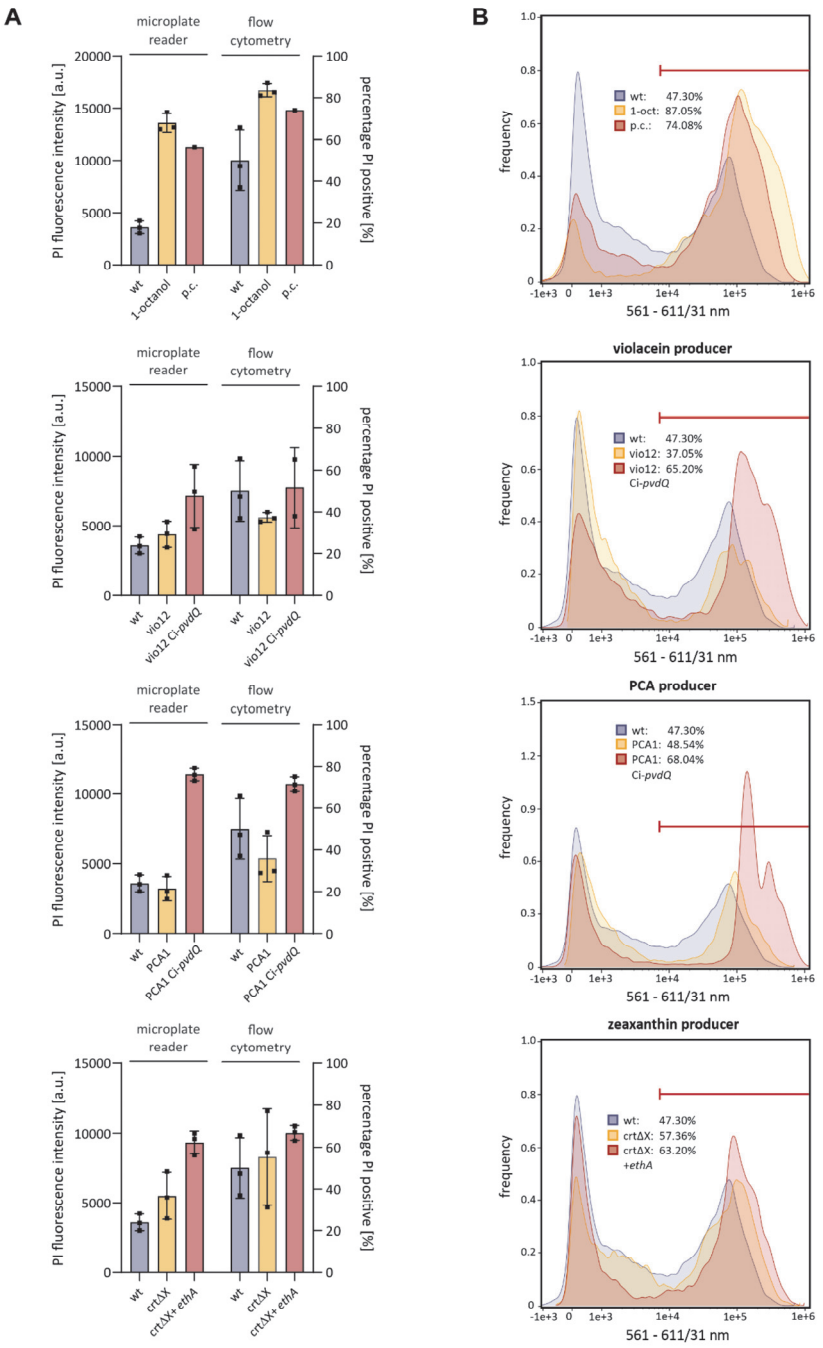

Figure S12: PI assay for determination of membrane integrity in selected engineered producer strains.
A: A propidium iodide (PI) assay was performed to determine the membrane integrity of different producer strains and selected manipulations regarding *pvdQ* and *ethA* expression. Cells were used after 7 h of cultivation and treated as

described in the methods section (**SI-M10**). PI fluorescence was measured using a Tecan Infinite microplate reader. In addition, PI fluorescence was analysed on a single cell level by flow cytometry (FCM). For both quantification methods, a positive control (p.c.), i.e. ultrasonic bath-treated cells (see **SI-M10**) and a sample treated with 1-octanol were used for reference (upper graphs). The data are mean values of independent triplicate measurements with their respective standard deviation. **B**: Histograms of example FCM data sets are shown for the different producers and engineered strains. The red line indicates the gated region for PI positive events. The prodigiosin producer *P. putida* pig21 could not be measured in the PI assay as the pigment prodigiosin interfered with the PI fluorescence.

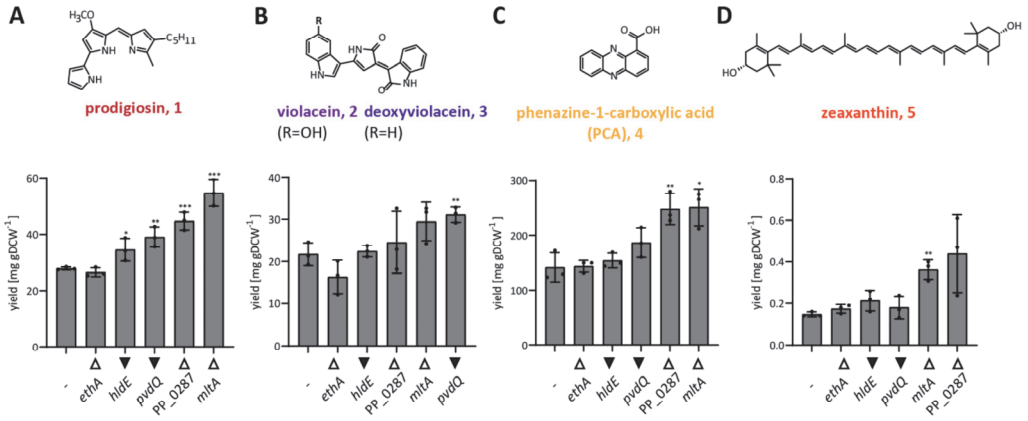

Figure S13: Recombinant natural compound production by *P. putida* engineered for OMV release.
Total yields were determined after extraction from both, the pellet fraction and supernatant of engineered *P. putida* strains and compared to the respective producer strains (indicated as '-'). **A**: Prodigiosin (**1**) produced by *P. putida* pig21. **B**: Violacein (**2**)/deoxyviolacein (**3**) produced by *P. putida* vio12. **C**: PCA (**4**) produced by *P. putida* PCA1. **D**: Zeaxanthin (**5**) produced by *P. putida* crtΔX. Bars are sorted in ascending order. The data are mean values of independent triplicate measurements with their respective standard deviation. Significant differences are indicated by asterisks (determined by T-test; * = p≤0.05, ** = p≤0.01, *** = p≤0.001). While *ethA* expression and *hldE* repression led to lowest yields of all products, *mltA* expression elevated them. Expression of PP_2087 enhanced yields of all products except violacein, and repression of *pvdQ* increased those of violacein and prodigiosin.

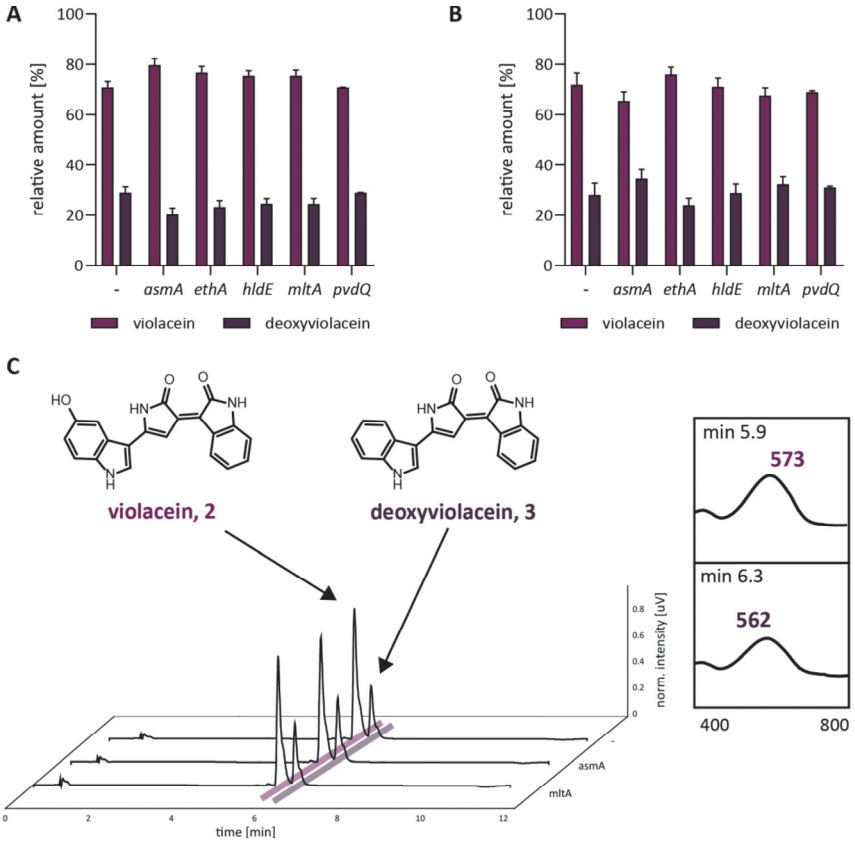

Figure S14: Relative amount of violacein and deoxyviolacein in *P. putida* vio12-based strains.
Relative amount of violacein (**2**) and deoxyviolacein (**3**) in the pellet fraction (**A**) or supernatant (**B**) of *P. putida* vio12 upon different manipulations regarding *asmA*, *ethA*, *hldE* or *pvdQ* expression (measured by HPLC at 569 nm). The data are mean values of independent triplicate measurements with their respective standard deviation. **C**: Exemplary HPLC chromatograms at 569 nm of selected *P. putida* KT2440 vio12-based strains (supernatant fraction) and corresponding PDA spectra to analyse the composition of violacein (**2**) (5.9 min) and deoxyviolacein (**3**) (6.3 min). For detailed description of methodical procedure see **SI-M4**.

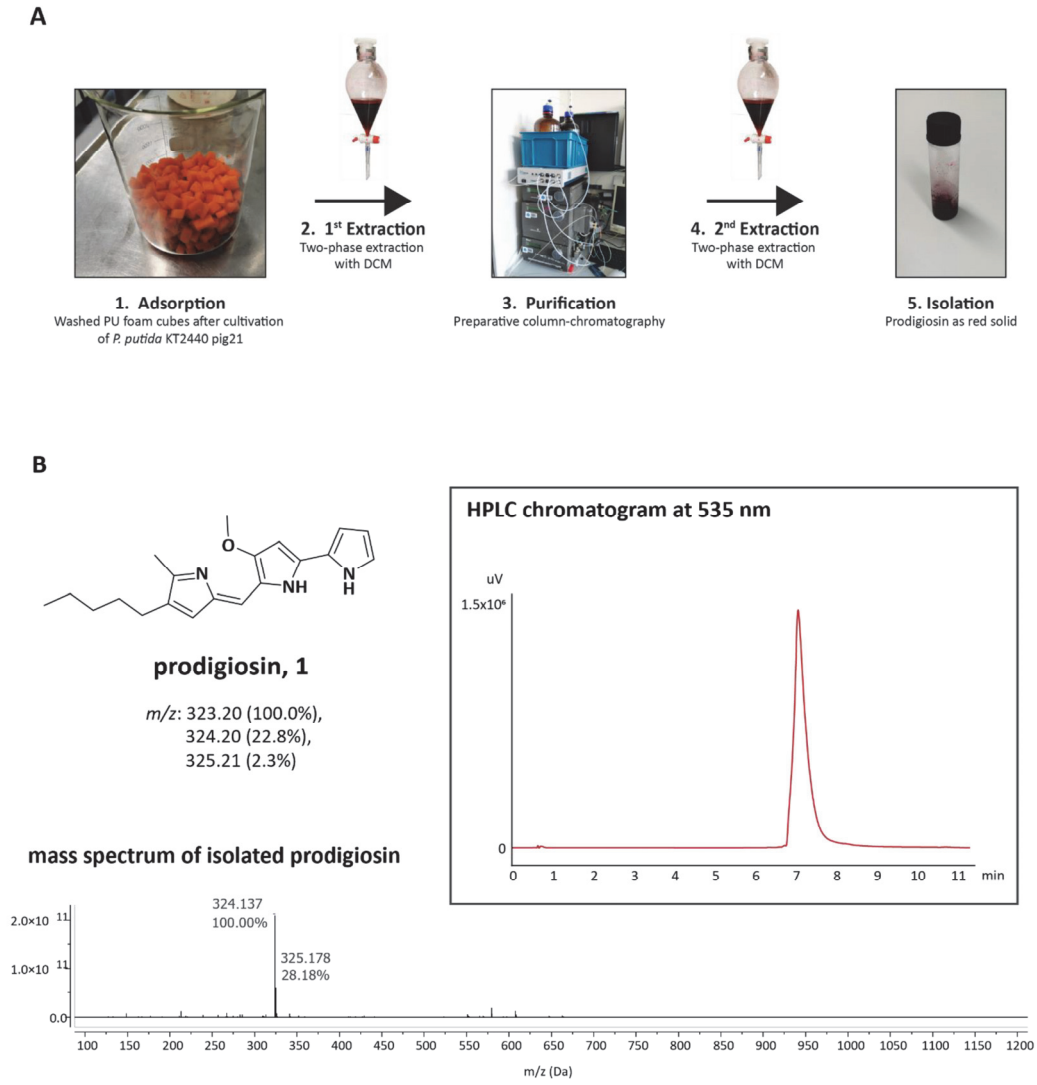

Figure S15: Extraction and purification of prodigiosin.
A: Prodigiosin (**1**) was extracted out of polyurethane (PU) foam cubes with ethanol (step **1**). A two-phase extraction and subsequent preparative column-chromatography were used for further isolation of prodigiosin (steps **2**, **3** and **4**). Using this extraction and isolation procedure, prodigiosin was obtained as a red solid (step **5**). **B**: For verification and monitoring of purification, the isolate was analysed by HPLC-PDA (at 535 nm) (prodigiosin signal at 7.188 min) and mass spectrometry ([prodigiosin + H^+]: *m/z* = 324.137). For detailed description of methodical procedure see **SI-M5**. PU: polyurethane; DCM: dichloromethane.

SI Methods

Table S3: Oligonucleotides, gRNAs used for CRISPRi in this study.

Oligonucleotides				
#	name	sequence (5' → 3')	Tm [°C]	application
1	IF_pBTBX_ fw	GTTCTAGAAAATTCGTCAACGAATTCAAGCT	60	backbone PCR
2	IF_pBTBX_ rev	GGTATATCTCCTTCTTAAAGTTCGTATCTCCG	59	
3	IF_PP_0287_ fw	GTTGACGAATTTTCTAGAACTCATCGGTTGAACAGCCCC	67	construction of expression plasmids for target screening
4	IF_PP_0287_ rev	CTTTAAGAAGGAGATATACCATGAAAGCGTTCGGCAAAA	64	
5	IF_ethA_ fw	GTTGACGAATTTTCTAGAACTCATCGGCGGCTACCTT	67	
6	IF_ethA_ rev	CTTTAAGAAGGAGATATACCATGTCCTCTCACACTGCTCTTCC	65	
7	IF_mltA__fw	CTTTAAGAAGGAGATATACCCATGTTCGCTCATGACAGGAAT	65	
8	IF_mltA__rev	GTTGACGAATTTTCTAGAACTCAAGGTACCTTGGGTACCTCAGG	67	
9	IF_PP_2807_fw	CTTTAAGAAGGAGATATACCATGGATACACGAGCGCTCT	65	
10	IF_PP_2807_rev	GTTGACGAATTTTCTAGAACTCAGAAGCCTTTACCCGGCTCG	68	
11	IF_PP_3494_fw	CTTTAAGAAGGAGATATACCATGAAACGCTCGATCGCC	65	
12	IF_PP_3494_rev	GTTGACGAATTTTCTAGAACTCACTGCTGCGAGCAG	66	
13	IF_rpoE__fw	CTTTAAGAAGGAGATATACCATGCTAACCCAGGAAGAGGATCAG	65	
14	IF_rpoE__rev	GTTGACGAATTTTCTAGAACTCAGGTTTCCTGCAACAACGGCTG	68	
15	IF_spr__fw	CTTTAAGAAGGAGATATACCGTGCCCATGCTGAAGCGC	68	
16	IF_spr__rev	GTTGACGAATTTTCTAGAACTCAGTTGCGCGC	64	
17	IF-dCas9-1-H840A_fw	TTTGTGGAACAATCGCATCGACATCATAATCACTTAAACG	64	construction of CRISPRi plasmids
18	IF-dCas9-1-D10A_rev	CTTTAAGAAGGAGATATACCATGGATAAGAAATACTCAATAGGCTTA	59	
19	IF-dCas9-2_fw	GTTGACGAATTTTCTAGAACTCAGTCACCTCCTAGCTGACTC	65	
20	IF-dCas9-2-H840A_rev	TGTCGATGCGATTGTTCCACAAAGTTTCCTTAAAG	63	
21	IF-Mut_Cas9-D10A_fw	GGCTTAGCCATCGGCACAAATAGCGTC	65	
22	IF-Mut_Cas9-D10A_rev	GCCGATGGCTAAGCCTATTGAGTATTTCTTATC	62	
23	IF_SoxT_Ptac_fw	AGGAGGTGACTGAGTTCTAGAAAACAAACTAAAGCGCCCTTGTGGCGCTTTAGTTTTGTCAACGTAAATGCCGCTTCG	75	
24	IF-Ptac_rev	CGCGTAGGTAGTGAAATTGTTATCCGCTCACAATTCC	66	
25	IF_lacZ-gRNA_fw	ACAATTTCACTACCTACGCGAGACCTCATTCG	65	
26	IF_lacZ-gRNA_rev	TTCGTTGACGAATTTTCTAGAAAAAAGCACCGACTCGGTG	66	
27	pBTBX-2_araBAD prom fw	CACGGCGTCACACTTTGCTATG	66	sequencing primers
28	pBTBX-2_ori_rv	GCTTGTCCAGCAGGGTTGTC	65	
29	Seq_pNPTS-lacZmcs_fw	CACAGGAAACAGCTATGAC	52	
30	Seq_pNPTS-lacZmcs_rev	GTTTTCCCAGTCACGACG	56	
31	Ci_pigD_gRNA12_fw	tacgGCGACGGTCTCTGCAGGCGG	67	oligonucleotides for hybridisation of spacer sequences (CRISPRi vector construction)
32	Ci_pigD_gRNA12_rev	aaacCCGCCTGCAGAGACCGTCGC	66	
33	Ci_pigD_gRNA14_fw	tacgGCCGCCTGCAGAGACCGTCG	67	
34	Ci_pigD_gRNA14_rev	aaacCGACGGTCTCTGCAGGCGGC	66	
35	Ci_pigD_gRNA2127_fw	tacgCAGGGCGCGGCCATACCAGC	67	
36	Ci_pigD_gRNA2127_rev	aaacGCTGGTATGGCCGCGCCCTG	67	
37	Ci_pfrI_gRNA15_fw	tacgTGGTGAATCGCACTTACTTG	53	
38	Ci_pfrI_gRNA15_rev	aaacCAAGTAAGTGCGATTCACCA	55	

39	Ci_pfrI_gRNA25_fw	tacgGTGCGATTCACCATTACTGC	56	
40	Ci_pfrI_gRNA25_rev	aaacGCAGTAATGGTGAATCGCAC	56	
41	Ci_pfrI_gRNA88_fw	tacgGTGAACGGCAGCCTGTGATA	56	
42	Ci_pfrI_gRNA88_rev	aaacTATCACAGGCTGCCGTTCAC	57	
43	Ci_hldE_gRNA1095_fw	tacgACCCGCAGCTTGACGATAGT	61	
44	Ci_hldE_gRNA1095_rev	aaacACTATCGTCAAGCTGCGGGT	60	
45	Ci_mlaE_gRNA15_fw	tacgCAGGCGGACACGCTCGAGTA	63	
46	Ci_mlaE_gRNA15_rev	aaacTACTCGAGCGTGTCCGCCTG	62	
47	Ci_mrcA_gRNA101_fw	tacgCTTCTGAGGGACTCGACCGA	59	
48	Ci_mrcA_gRNA101_rev	aaacTCGGTCGAGTCCCTCAGAAG	58	
49	Ci_ompA_gRNA1148_fw	tacgGGCTCAGACGACACTCGAAC	59	
50	Ci_ompA_gRNA1148_rev	aaacGTTCGAGTGTCGTCTGAGCC	59	
51	Ci_oprI_gRNA191_fw	tacgGCAACCGGTAGCCAGAACTG	60	
52	Ci_oprI_gRNA191_rev	aaacCAGTTCTGGCTACCGGTTGC	60	
53	Ci_oprL_gRNA56_fw	tacgGTAGGTTGCTCCTCGAAGGG	58	
54	Ci_oprL_gRNA56_rev	aaacCCCTTCGAGGAGCAACCTAC	58	
55	Ci_PP_0710_gRNA361_fw	tacgCTTGCCGCACTTGAAGTGTC	59	
56	Ci_PP_0710_gRNA361_rev	aaacGACACTTCAAGTGCGGCAAG	58	
57	Ci_pvdQ_gRNA3_fw	tacgGGGACGGCAAAATGGAAACA	58	
58	Ci_pvdQ_gRNA3_rev	aaacTGTTTCCATTTTGCCGTCCC	57	
59	Ci_tolA_gRNA21_fw	tacgGGGCCAGAAGTAGCTTTCCG	59	
60	Ci_tolA_gRNA21_rev	aaacCGGAAAGCTACTTCTGGCCC	59	
61	Ci_wbpL_gRNA92_fw	tacgGTATGCGAGCTACGCGCATT	60	
62	Ci_wbpL_gRNA92_rev	aaacAATGCGCGTAGCTCGCATAC	60	
63	Ci_waaC_gRNA91_fw	tacgCTTCCACCACCCAATCGAAA	57	
64	Ci_waaC_gRNA91_rev	aaacTTTCGATTGGGTGGTGGAAG	55	
65	qPCR-pigN_fw	TACCTGATAGGCACGCTGTT	57	RT-qPCR[1] (Domröse *et al.*, 2019)
66	qPCR-pigN-rev	TTGTTCGGATCCTGTTTGAA	53	
67	qPCR-rpoD_fw	TCGCCAAGAAGTACACCAAC	56	
68	qPCR-rpoD_rev	TTTCATCAGACCGATGTTGC	54	
69	pvdQ-up-fw	CGGAATTCCGGGTTGAGCCTGTAGCACTTGTC	75	Generation of knockout strains
70	pvdQ-up-rv	CGACGCGTCGTCCTCGGGTTCGGGGGTCATC	80	
71	pvdQ-dw-fw	CGACGCGTCGGGCGTCAGCCTGCGCCGGCCCATTC	86	
72	pvdQ-dw-rv	GCTCTAGAGCTGGCACGGCCATCTACCTGATGCATG	77	
73	pvdD-up-fw	CGGAATTCCGTGGCGTATTGCTGGTAG	58	
74	pvdD-up-rv	CGACGCGTCGGCTTTCGGGGCCGCCAGCGCGGCCCCTCTGGA GAATCGAACG	84	
75	pvdD-dw-fw	CGACGCGTCGTTGAACATCTCCTACCAGGGCACCGGTCTTTG	74	
76	pvdD-dw-rv	GCTCTAGAGCTATCTGCGTGCCAGCCTTC	64	
77	pvdQ-sequencing_up	AACCTTGAGGCGGATCAG	61	
78	pvdQ-sequencing_dw	TCGGCCAGCGATTCACAAG	65	
79	pvdD-sequencing_up	TGGTCAACGAAAGGTCGCTG	61	
80	pvdD-sequencing_dw	GGTTGAGCAGGTCGGTATC	65	
guiding RNAs for CRISPRi[2]				
#	**name**	**sequence**	**PAM**	**target**
1	pigD-gRNA12	GCGACGGTCTCTGCAGGCGG	CGG	*pigD*
2	pigD-gRNA14	GCCGCCTGCAGAGACCGTCG	CGG	
3	pigD-gRNA2127	CAGGGCGCGGCCATACCAGC	CGG	

4	pfrI-gRNA15	TGGTGAATCGCACTTACTTG	TGG	*pfrI*
5	pfrI-gRNA25	GTGCGATTCACCATTACTGC	AGG	
6	pfrI-gRNA88	GTGAACGGCAGCCTGTGATA	CGG	
7	hldE-gRNA1095	ACCCGCAGCTTGACGATAGT	CGG	*hldE*
8	mlaE-gRNA15	CAGGCGGACACGCTCGAGTA	AGG	*mlaE*
9	mrcA-gRNA101	CTTCTGAGGGACTCGACCGA	CGG	*mrcA*
10	ompA-gRNA1148	GGCTCAGACGACACTCGAAC	TGG	*ompA*
11	oprI-gRNA191	GCAACCGGTAGCCAGAACTG	AGG	*oprI*
12	oprL-gRNA56	GTAGGTTGCTCCTCGAAGGG	CGG	*oprL*
13	PP_0710-gRNA361	CTTGCCGCACTTGAAGTGTC	TGG	PP_0710
14	pvdQ-gRNA3	GGGACGGCAAAATGGAAACA	CGG	*pvdQ*
15	tolA-gRNA21	GGGCCAGAAGTAGCTTTCCG	AGG	*tolA*
16	wbpL-gRNA92	GTATGCGAGCTACGCGCATT	CGG	*wbpL*
17	waaC-gRNA91	CTTCCACCACCCAATCGAAA	CGG	*waaC*

[1]designed using the Primer3Web suite (Untergasser *et al.*, 2012)

[2]identified using CRISPy-Web (Blin *et al.*, 2016)

Table S4: Plasmids and bacterial strains used in this study.

Plasmids			
name	**genotype**	**application**	**reference**
pBTBX-2-mcs	*araC*, P_{araBAD}, Km^R, pBBR1 ori,	empty vectors	(Prior *et al.*, 2010)
pBTBX-2-CRISPRi	*araC*, P_{araBAD}→d*cas9*, P_{tac}→*lacPOZ*, gRNA, Km^R, pBBR1 ori,		This study
pBTBX-2-mCherry	*araC*, P_{araBAD}→mCherry, Km^R, pBBR1 ori,	expression profile	(Hogenkamp *et al.*, 2022)
pBTBX-2-PP_0287	*araC*, P_{araBAD}→PP_0287, Km^R, pBBR1 ori,	expression plasmids for target screening	This study
pBTBX-2-ethA	*araC*, P_{araBAD}→*ethA*, Km^R, pBBR1 ori,		
pBTBX-2-mltA	*araC*, P_{araBAD}→*mltA*, Km^R, pBBR1 ori,		
pBTBX-2-PP_2807	*araC*, P_{araBAD}→PP_2807, Km^R, pBBR1 ori,		
pBTBX-2-PP_3494	*araC*, P_{araBAD}→PP_3494, Km^R, pBBR1 ori,		
pBTBX-2-rpoE	*araC*, P_{araBAD}→*rpoE*, Km^R, pBBR1 ori,		
pBTBX-2-spr	*araC*, P_{araBAD}→*spr*, Km^R, pBBR1 ori,		
pBTBX-2-Cas9-H840A	*araC*, P_{araBAD}→*cas9* H840A, Km^R, pBBR1 ori,	CRISPRi vectors	This study
pBTBX-2-dCas9	*araC*, P_{araBAD}→d*cas9*, Km^R, pBBR1 ori,		
pBTBX-2-Ci_pigD-gRNA12	pBTBX-2-CRISPRi with integrated gRNA for *pigD* locus (see #1)		
pBTBX-2-Ci_pigD-gRNA14	pBTBX-2-CRISPRi with integrated gRNA for *pigD* locus (see #2)		
pBTBX-2-Ci_pigD-gRNA2127	pBTBX-2-CRISPRi with integrated gRNA for *pigD* locus (see #3)		
pBTBX-2-Ci_pfrI-gRNA15	pBTBX-2-CRISPRi with integrated gRNA for *pfrI* locus (see #4)		
pBTBX-2-Ci_pfrI-gRNA25	pBTBX-2-CRISPRi with integrated gRNA for *pfrI* locus (see #5)		
pBTBX-2-Ci_pfrI-gRNA88	pBTBX-2-CRISPRi with integrated gRNA for *pfrI* locus (see #6)		
pBTBX-2-Ci_hldE-gRNA1095	pBTBX-2-CRISPRi with integrated gRNA for *hldE* locus (see #7)		

pBTBX-2-Ci-mlaE-gRNA15	pBTBX-2-CRISPRi with integrated gRNA for *mlaE* locus (see #8)		
pBTBX-2-Ci_mrcA-gRNA101	pBTBX-2-CRISPRi with integrated gRNA for *mrcA* locus (see #9)		
pBTBX-2-Ci_ompA-gRNA1148	pBTBX-2-CRISPRi with integrated gRNA for *ompA* locus (see #10)		
pBTBX-2-Ci_oprI-gRNA191	pBTBX-2-CRISPRi with integrated gRNA for *oprI* locus (see #11)		
pBTBX-2-Ci_oprL-gRNA56	pBTBX-2-CRISPRi with integrated gRNA for *oprL* locus (see #12)		
pBTBX-2-Ci_PP_0710-gRNA361	pBTBX-2-CRISPRi with integrated gRNA for PP_0710 locus (see #13)		
pBTBX-2-Ci_pvdQ-gRNA3	pBTBX-2-CRISPRi with integrated gRNA for *pvdQ* locus (see #14)		
pBTBX-2-Ci_tolA-gRNA21	pBTBX-2-CRISPRi with integrated gRNA for *tolA* locus (see #15)		
pBTBX-2-Ci_wbpL-gRNA92	pBTBX-2-CRISPRi with integrated gRNA for *wbpL* locus (see #16)		
pBTBX-2-Ci_waaC-gRNA91	pBTBX-2-CRISPRi with integrated gRNA for *waaC* locus (see #17)		
pJOE8999	pUC ori, *rep pE194ts*, *cas9*, Km^R, sgRNA, *lacPOZ*	template plasmids	(Altenbuchner, 2016)
pVLT33	lacIq, P_{tac}, Km^R, RSF1010 ori, *mob*, *repABC*,		(de Lorenzo *et al.*, 1993)
pSNW2-pvdQ	suicide vector with up-/down-stream region of *pvdQ* for deletion in *P. putida* KT2440; oriT, *traJ*, ori(R6K), P_{14g}(BCD2)→msfGFP; Km^R	knockout strain	This study
pSNW2-pvdD	suicide vector with up-/down-stream region of *pvdD* for deletion in *P. putida* KT2440; oriT, *traJ*, ori(R6K), P_{14g}(BCD2)→msfGFP; Km^R		This study
pQure6-high	oriV(RK2), XylS/P_m→*trfA*, XylS/P_m→I-SceI, P_{14g}(BCD2)→mRFP, Gm^R		(Volke *et al.*, 2020)
Strains			
name	**features**	**application**	**reference**
E. coli DH5α	F-Φ80*lac*ZΔM15 Δ(*lac*ZYA-argF) U169 deoR recA1 endA1 hsdR17 (rk-, mk+) phoA glnV44 thi-1 gyrA96 relA1	cloning	(Hanahan, 1983)
E. coli DH5α λpir	λpir lysogen derivative of strain DH5α		(Platt *et al.*, 2000)
E. coli Stellar™	*E. coli* HST08 strain (F-Φ80d *lac*ZΔM15 Δ(*lacZYA-argF*) U169 recA1 endA1 phoA glnV44 thi-1 gyrA96 relA1 , , Δ(*mrr-hsdRMS-mcrBC*), Δ*mcrA*, λ-); provides high transformation efficiency		(Takara Bio, Cat# 636763)
P. putida KT2440	wild type, derivative of mt-2		(Nelson *et al.*, 2002)
P. putida KT2440 pig-r2 Δ*pigD*	*P. putida* KT2440::TREX-L*pig*R, Δ*pigD* Sm^R,	CRISPRi	(Klein *et al.*, 2017)
P. putida KT2440 Δ*pvdD*	*P. putida* KT2440 with seamless deletion of *pvdD* gene		This study

P. putida KT2440 pig-r11	*P. putida* KT2440::TREX-L*pig*R, Gm^R	producer strains for natural compounds	(Domröse *et al.*, 2019)
P. putida KT2440 pig-r43			
P. putida KT2440 pig-r44			
P. putida KT2440 pig21	*P. putida* KT2440::yTREX-*pig*, Tc^R		(Domröse *et al.*, 2017)
P. putida KT2440 vio12	*P. putida* KT2440::yTREX-*vio*, Tc^R		
P. putida KT2440 crtΔ*X*	*P. putida* KT2440::TREX-L-*crtE(ΔX)YIBZ* -R, Gm^R		(Loeschcke *et al.*, 2013)
P. putida KT2440 PCA1	*P. putida* KT2440::yTREX-*pca, lacZ*, Tc^R		(Domröse *et al.*, 2017)
P. putida KT2440 Δ*pvdQ*	*P. putida* KT2440 with seamless deletion of *pvdQ* gene		This study

M1. Plasmid construction

For the construction of vectors for overexpression of candidate genes, the vector pBTBX-2-mcs (pBTBX-2 was a gift from Ryan Gill, Addgene plasmid # 26068) (Prior *et al.*, 2010) was amplified by PCR using oligonucleotides **1** and **2**. Candidate genes were amplified *via* PCR using the *P. putida* KT2440 genome as template and oligonucleotides **3** to **16**, which contained homologous sequences for integration into the amplified vector backbone. Backbone and insert fragments were assembled using InFusion® Snap Assembly (Takara Bio Europe, St Germain en Laye, France).

The CRIPSRi vector was constructed in several steps using InFusion® Snap Assembly (Takara Bio Europe, St Germain en Laye, France). First, the backbone of pBTBX-2-mcs was amplified as described above (using primers **1** and **2**). The “dead Cas” devoid of nucleolytic activity was implemented as follows: The *cas9* gene was amplified in two segments using the vector pJOE8999 (Altenbuchner, 2016) as template and a H840A mutation was introduced *via* the PCR primers IF_dCas9-1-H840A_fw, IF_dCas9-1-D10A_rev, IF-dCas9-2_fw, IF-dCas9-2-H840A_rev (**17** to **20)**. Assembly of *cas9*-H840A fragments and the backbone resulted in the plasmid pBTBX-2-Cas9-H840A. Then, for introduction of the second mutation (D10A), the newly constructed vector was amplified using the oligos IF-Mut_Cas9-D10A_fw and IF-Mut_Cas9-D10A_rev (**21** and **22**) and the resulting linear fragment was circularised using InFusion® Snap Assembly (Takara Bio Europe, St Germain en Laye, France). The resulting plasmid was designated as pBTBX-2-dCas9. To complete the CRISPRi plasmid, a constitutive *tac* promoter (P_{tac}) as well as the *lacZα*, the Cas9 handle, and terminator sequences were incorporated. Using the plasmid pVLT33 (de Lorenzo *et al.*, 1993) as

template DNA, the promoter sequence was amplified by PCR using oligonucleotides **23** and **24**. The second fragment (*lacZα*, Cas9 handle, terminator (from *Streptococcus pyogenes*)) was amplified using pJOE8999 (Altenbuchner, 2016) as template and oligos **25** and **26**. Finally, the plasmid pBTBX-2-dCas9 was linearised by XbaI digestion and assembled with both amplified fragments to construct the plasmid pBTBX-2-CRISPRi.

In the CRISPRi plasmid, the *lacZα* is located between two BsaI sites, which enables both a fast exchange of the DNA base-pairing region (spacer sequence) *via* oligonucleotides fitted between the BsaI sites, and a facilitated cloning based on blue-white-screen. For construction of the pBTBX-2-CRISPRi plasmid series for down-regulating the expression of candidate genes, the respective spacer sequences were identified using CRISPy-Web (Blin *et al.*, 2016) (**see Table S3**). For all targets, base-pairing sequences complementary to the non-template (NT) strand were selected except for *oprL*, here, the template strand (T) was targeted because transfer of the other construct into *P. putida* KT2440 failed to yield clones. Oligonucleotides were designed following scheme **1** introducing complementary overhangs for BsaI restriction sites:

5'-**tacg**-*20 nt base-pairing region*
20 nt base-pairing region-**caaa**-5'

The designed oligonucleotides are listed in **Table S3** (oligos **31** to **64**). For hybridisation of the complementary oligonucleotides, they were mixed in a 1:1 molar ratio (20 µL), incubated at 99 °C for 10 min, and then cooled at 1 °C min^{-1}. Finally, the hybridised fragments were ligated into the vector backbone pBTBX-2-CRISPRi (before BsaI hydrolysed).

All newly constructed vectors were confirmed by Sanger sequencing (Eurofins Genomics, Ebersberg, Germany) using oligonucleotides **27** to **30**.

M2. Correction term for prodigiosin OMVs

To evaluate a correction factor for prodigiosin-containing vesicles, OMVs isolated from *P. putida* KT2440 wild type were supplemented with different concentrations (0 to 9 mg L^{-1}) of extracted prodigiosin (for extraction and isolation, see **SI-M5** and **Figure S15**) and measured by Bradford assay. The absorption of the Bradford reagent (and prodigiosin) at 595 nm was plotted against the used

prodigiosin concentration (**Figure S1**). As the amount of OMVs was the same in every sample, differences in the absorption were caused by prodigiosin. For correction of the Bradford absorption in prodigiosin-containing vesicle fractions, the prodigiosin concentration was determined. Further, the slope (**Figure S1**) was used as a correction term, multiplied with the measured prodigiosin concentration in the, and subtracted from the absorption of the Bradford reagent.

M3. RT-qPCR

For measurement of the *pig* transcript levels, *P. putida* pig21 cells were cultivated and stressed as described in the manuscript. After 7 h, cells were harvested by centrifugation (2 min, max. speed) from 1 mL culture samples and the RNA was isolated using the NucleoSpin® RNA kit (Macherey-Nagel GmbH & Co. KG, Düren, Germany) as recommended by the supplier. Additionally, a DNA digestion step using RNAse-free DNAse (Qiagen GmbH, Hilden, Germany) was performed. After elution with nuclease-free water (Qiagen GmbH, Hilden, Germany), samples were treated with the DNA-free DNA Removal kit (Thermo Fisher Scientific, Waltham, MA, USA). RT (reverse transcription) was performed with the Maxima First Strand cDNA Synthesis Kit for RT-qPCR (Thermo Fisher Scientific, Waltham, MA, USA). Here, 2000 ng of total RNA were used as template. As controls, noRT (no addition of the reverse transcriptase) and NTC (no template control) samples were also run. For qPCR (quantitative PCR), 9.2 µL cDNA (diluted to correspond to 50 ng total RNA), 0.4 µL of each primer (stocks: 10 pmol μL^{-1}, oligos **59** and **60**), and 10 µL Maxima SYBR Green/ROX qPCR Master Mix (2x) (Thermo Fisher Scientific, Waltham, MA, USA) were mixed. Additionally, the transcript level of the sigma factor *rpoD* was analysed as internal control using oligonucleotides **65** and **68**. Further, all qPCR reactions, including the noRT and NTC controls, were measured as technical quadruplicates in addition to the biological triplicates, running 35 cycles in a 7900HT Fast Real-Time PCR System (Thermo Fisher Scientific, Waltham, MA, USA).

M4. HPLC-PDA analysis of (deoxy)violacein and prodigiosin

For (deoxy)violacein and prodigiosin, HPLC-PDA analysis was performed to analyse the composition of samples in differently manipulated strains. Here, 10 µL of the extracted samples were injected onto an Accucore^{TM} C18 column (50 x 4.6 mm, 2.6 µm particle size, 80 Å pores, Thermo Fisher Scientific, Waltham, MA, USA) using an LC-10Ai series (Shimadzu GmbH; Duisburg, Germany), equipped with an SPD-M10Avp photodiode array detector (PDA). The column oven temperature was 30 °C and a flowrate of 1 mL min^{-1} was used. As mobile phase, water (**A**) and acetonitrile (**B**), both supplemented with 0.1% formic acid, were used starting at 5% **B** for 1.5 min, followed by a gradient to 98% **B** over 5.5 min. For 2 min, this condition was maintained, before returning to 5% **B** within 0.5 min and again maintaining this condition for another 2 min. Chromatograms were recorded at 569 nm to identify signals of deoxyviolacein (at 5.9 min) and violacein (at 6.3 min), which were assigned based on published data (Sánchez *et al.*, 2006; Lee *et al.*, 2013; Domröse *et al.*, 2017). For prodigiosin, chromatograms were recorded at 535 nm.

M5. Extraction and purification of prodigiosin

Prodigiosin was extracted from polyurethane (PU) foam cubes as described before (Domröse *et al.*, 2015). For production of prodigiosin, *P. putida* KT2440-derived strain pig21 was cultivated in 500 mL TB medium (Carl Roth GmbH + Co.KG, Karlsruhe, Germany) in a 3 L Fernbach flask supplemented with 5 g PU foam cubes (Bornewasser, Göllheim, Germany: softpur, 25 kg m^{-3} density,4 kPa compression hardness, cube size approx. 1 cm^3). The culture was incubated for 48 h at 20 °C. Afterwards, the PU cubes were isolated from the culture by sieving, wrung out and washed with H_2O (500 mL) twice (**Figure S15A-1**). Acidified ethanol (supplemented with 4% 1 M HCl) was used to extract prodigiosin from the PU foam cubes. For this purpose, the PU foam cubes were mixed four times with 250 mL of solvent, wrung out and sieved. The extracts were pooled in a round bottom flask and the solvent was removed under reduced pressure by rotatory evaporation. For the removal of water-soluble impurities, the product was washed with water and dichloromethane (30 mL x 180 mL) twice (**Figure S15A-2**). The organic layers were combined, dried over $MgSO_4$ and the solvent was again removed under reduced pressure. Residual material was resolved in acidified ethanol and

prodigiosin was isolated by preparative column-chromatography (**Figure S15A-3**). Preparative column-chromatography was realised as reversed-phase chromatography with a column from ISERA GmbH (Düren, Germany) (ISAspher 100-5 C18 AQ, 5 µm, 150 x 20 mm), using a column oven temperature of 35 °C and 40:60 acetonitrile:water (supplemented with 0.1% formic acid) as eluent at a flowrate of 15 mL min^{-1}. Samples were solved in 1 mL ethanol for injection. Prodigiosin eluted around min 15 (total run time: 60 min). Respective fractions of several runs were collected for further isolation steps. Finally, the collected fractions were again extracted with water and dichloromethane, dried over $MgSO_4$ and the solvent was evaporated under reduced pressure yielding the isolated prodigiosin as a red solid (**Figure S15A-4**). For verification, the isolate was analysed by HPLCPDA (prodigiosin signal at 7.188 min) (for HPLC-PDA procedure see **SI-M4**) and mass spectrometry ([prodigiosin + H^+]: *m/z* = 324.137) (Advion Expression-L CMS, Ithaca, USA) (**Figure S15B**).

M6. Sequence homology search for putative *P. putida* homologues

Reference sequences of the selected targets were obtained from the Uniprot database (https://www.uniprot.org) or the NCBI nucleotide database (https://www.ncbi.nlm.nih.gov/nucleotide/) using existing genomes of the described organisms. For sequence homology search, the NCBI protein BLAST (Basic Local Alignment Search Tool) (https://blast.ncbi.nlm.nih.gov/Blast.cgi?PAGE=Proteins) was used and the search was restricted to the organism *Pseudomonas putida* KT2440 (taxid:160488). For more detailed information (localisation, function, locus), the Pseudomonas Genome Database was used (Winsor *et al.*, 2016).

M7. Pyoverdine production

To stimulate pyoverdine production in *P. putida* KT2440, cells were cultivated in LB medium supplemented with 700 µM of the iron chelator 2,2'-dipyridyl (DIP) overnight at 30 °C and 1200 rpm in FlowerPlates® (Beckman Coulter GmbH (formerly m2p-labs GmbH), Baesweiler, Germany). Afterwards, the cells were separated by centrifugation (5 min, 15000x*g*) and the supernatant was analysed regarding pyoverdine fluorescence using a plate reader (Tecan, Maennedorf, Switzerland) with the following settings: λ_{ex} =398 nm, λ_{em} = 455, $bandwidth_{ex/em}$ = 5 nm, gain = 150.

M8. Expression profile of pBTBX-2

To analyse the expression profile of the L-arabinose-dependent gene expression with vector pBTBX-2, a plasmid with integrated mCherry gene was used (pBTBX-2-mCherry) (Hogenkamp *et al.*, 2022). *P. putida* KT2440 pBTBX-2-mCherry was cultivated in LB medium at 30 °C and 1200 rpm in FlowerPlates® (Beckman Coulter GmbH (formerly m2p-labs GmbH), Baesweiler, Germany) using a microbioreactor system for online monitoring (BioLector I, Beckman Coulter GmbH (formerly m2p-labs GmbH), Baesweiler, Germany). After 4 h of cultivation, L-arabinose was added to the culture at different concentrations (0 to 100 mM), and mCherry fluorescence was detected using an mCherry/RFP filter module (Gain: 100).

M9. Construction of knockout strains

Knockout mutants of *P. putida* KT2440 (*P. putida* Δ*pvdQ and P. putida* Δ*pvdD*) were constructed using a previously established I-SceI-based engineering system (Volke *et al.*, 2020). To construct the suicide vector pSNW2-pvdQ, the up-stream (545 bp) and down-stream (621 bp) regions of the target gene were amplified using the *P. putida* KT2440 genome as template and primers **69** to **72**. For the suicide vector pSNW2-pvdD, primers **73** to **76** were used for amplification of the up-stream (747 bp) and down-stream (642 bp) region. The PCR products were hydrolysed with EcoRI/MluI (up-stream fragment) and MluI/XbaI (down-stream fragment). The suicide vector pSNW2 was hydrolysed with EcoRI and XbaI, and both fragments were ligated into the linearised vector.

P. putida KT2440 was transformed with the generated suicide vectors by electroporation and cells were grown on selective agar plates with 25 µg mL^{-1} kanamycin. Successful genomic integration of the vector was confirmed by detection of green fluorescence under blue light using a Blue/Green LED Transilluminator XL (Nippon Genetics Europe GmbH, Düren, Germany). A positive clone was grown overnight in liquid culture and transformed by electroporation with the plasmid pQure6-high. The transformation suspension was plated on LB agar plates containing 2 mM 3-methylbenzoate (3-*m*Bz) and 25 µg mL^{-1} gentamicin. Red fluorescent clones were checked for double-crossover (Km-sensitivity, msfGFP$^-$) and target gene deletion was confirmed by colony PCR (using oligos **77** and **78** (for *pvdQ* knockout) and oligos **79** and **80** (for *pvdD* knockout)) and DNA sequencing. To cure cells

from the plasmid pQure6-high, the confirmed knockout strain was streaked onto LB agar plates without the antibiotics (only irgasan was used). Gentamicin-sensitivity and loss of red fluorescence were used to confirm plasmid loss.

M10. Propidium iodide (PI) assay

To determine the effect of manipulations on the membrane integrity, a PI assay was performed as described previously (Endres *et al.*, 2018). Cells were grown in 10 mL LB medium at 30 °C and 130 rpm for 7 h. Strains harbouring plasmid DNA were additionally supplemented with the inducer. For this purpose, 10 mM L-arabinose was added at the beginning of the cultivation. After 7 h, the cells were washed in 1xPBS (pH 7.4) buffer and adjusted to an $OD_{700\ nm}$ of 0.5 in PI assay buffer (5 µM propidium iodide, 100 µM EDTA, 1xPBS, pH 7.4). As a positive control, cells of *P. putida* KT2440 (in PI assay buffer) were placed in an ultrasonic bath for 5 min.

For analysis, 100 µL of the cell suspensions were transferred to an MTP (flat bottom, Greiner Bio-One GmbH, Frickenhausen, Germany) and the PI fluorescence was measured using a microplate reader (Infinite® M1000 Pro, Tecan Group LTD., Maennedorf, Switzerland) (λ_{ex} = 535 nm; λ_{em} = 617 nm; bandwidth: 5 nm; gain: 150). In addition, the cells were analysed for PI fluorescence at the single cell level by flow cytometry (FCM). The FCM was performed as described previously using the Amnis® CellStreamTM System (Luminex Corporation, Austin, USA) (Hilgers *et al.*, 2019). To this end, prepared samples were diluted tenfold in PI assay buffer and the fluorescence was analysed using a 561 nm-laser (laser power: 150 mW) and a 611/31 nm (red) bandpass filter. Front scatter (FSC) was measured using a FSC laser at 30% laser power (456/51 nm bandpass filter). Side scatter (SSC) was measured using the laser with 100% laser power (773/56 nm bandpass filter). On the basis of the scatter plots, bacterial cells were gated for fluorescence analysis. Flow cytometric data were analysed using the CellStreamTM Analysis Software (Luminex Corporation, Austin, TX, USA).

SI References

Altenbuchner, J. (2016) Editing of the *Bacillus subtilis* genome by the CRISPR-Cas9 system. *Appl Environ Microbiol* **82**: 5421–5427.

Avila-Calderón, E.D., Ruiz-Palma, M. del S., Aguilera-Arreola, M.G., Velázquez-Guadarrama, N., Ruiz, E.A., Gomez-Lunar, Z., et al. (2021) Outer membrane vesicles of Gram-negative bacteria: An outlook on biogenesis. *Front Microbiol* **12**: 557902.

Banzhaf, M., Yau, H.C., Verheul, J., Lodge, A., Kritikos, G., Mateus, A., et al. (2020) Outer membrane lipoprotein NlpI scaffolds peptidoglycan hydrolases within multi-enzyme complexes in *Escherichia coli*. *EMBO J* **39**: 1–20.

Bernadac, A., Gavioli, M., Lazzaroni, J.-C., Raina, S., and Lloubès, R. (1998) *Escherichia coli tol-pal* mutants form outer membrane vesicles. *J Bacteriol* **180**: 4872–4878.

Blin, K., Pedersen, L.E., Weber, T., and Lee, S.Y. (2016) CRISPy-web: An online resource to design sgRNAs for CRISPR applications. *Synth Syst Biotechnol* **1**: 118–121.

Deng, M. and Misra, R. (1996) Examination of AsmA and its effect on the assembly of *Escherichia coli* outer membrane proteins. *Mol Microbiol* **21**: 605–612.

Dhurve, G., Madikonda, A.K., Jagannadham, M.V., and Siddavattam, D. (2022) Outer membrane vesicles of *Acinetobacter baumannii* DS002 are selectively enriched with TonB-dependent transporters and play a key role in iron acquisition. *Microbiol Spectr* **10**: e0029322.

Domröse, A., Hage-Hülsmann, J., Thies, S., Weihmann, R., Kruse, L., Otto, M., et al. (2019) *Pseudomonas putida* rDNA is a favored site for the expression of biosynthetic genes. *Sci Rep* **9**: 7028.

Domröse, A., Klein, A.S., Hage-Hülsmann, J., Thies, S., Svensson, V., Classen, T., et al. (2015) Efficient recombinant production of prodigiosin in *Pseudomonas putida*. *Front Microbiol* **6**: 972.

Domröse, A., Weihmann, R., Thies, S., Jaeger, K.-E., Drepper, T., and Loeschcke, A. (2017) Rapid generation of recombinant *Pseudomonas putida* secondary metabolite producers using yTREX. *Synth Syst Biotechnol* **2**: 310–319.

Endres, S., Wingen, M., Torra, J., Ruiz-González, R., Polen, T., Bosio, G., et al. (2018) An optogenetic toolbox of LOV-based photosensitizers for light-driven killing of bacteria. *Sci Rep* **8**: 15021.

Gogol, E.B., Rhodius, V.A., Papenfort, K., Vogel, J., and Gross, C.A. (2011) Small RNAs endow a transcriptional activator with essential repressor functions for single-tier control of a global stress regulon. *Proceedings of the National Academy of Sciences* **108**: 12875–12880.

Hanahan, D. (1983) Studies on transformation of *Escherichia coli* with plasmids. *J Mol Biol* **166**: 557–580.

Hilgers, F., Bitzenhofer, N.L., Ackermann, Y., Burmeister, A., Grünberger, A., Jaeger, K.-E., and Drepper, T. (2019) Genetically Encoded Photosensitizers as Light-Triggered Antimicrobial Agents. *Int J Mol Sci* **20**: 4608.

Hogenkamp, F., Hilgers, F., Bitzenhofer, N.L., Ophoven, V., Haase, M., Bier, C., et al. (2022) Optochemical control of bacterial gene expression: Novel photocaged compounds for different promoter systems. *ChemBioChem* **23**: e202100467.

Inouye, M. (1974) A three-dimensional molecular assembly model of a lipoprotein from the *Escherichia coli* outer membrane. *Proceedings of the National Academy of Sciences* **71**: 2396–2400.

Inouye, M., Shaw, J., and Shen, C. (1972) The assembly of a structural lipoprotein in the envelope of *Escherichia coli*. *Journal of Biological Chemistry* **247**: 8154–8159.

Klein, A.S., Domröse, A., Bongen, P., Brass, H.U.C., Classen, T., Loeschcke, A., et al. (2017) New prodigiosin derivatives obtained by mutasynthesis in *Pseudomonas putida*. *ACS Synth Biol* **6**: 1757–1765.

Koch, G., Jimenez, P.N., Muntendam, R., Chen, Y., Papaioannou, E., Heeb, S., et al. (2010) The acylase PvdQ has a conserved function among fluorescent *Pseudomonas* spp. *Environ Microbiol Rep* **2**: 433–439.

Kulp, A. and Kuehn, M.J. (2010) Biological functions and biogenesis of secreted bacterial outer membrane vesicles. *Annu Rev Microbiol* **64**: 163–184.

Lee, M.E., Aswani, A., Han, A.S., Tomlin, C.J., and Dueber, J.E. (2013) Expression-level optimization of a multi-enzyme pathway in the absence of a high-throughput assay. *Nucleic Acids Res* **41**: 10668–10678.

Levine, T.P. (2019) Remote homology searches identify bacterial homologues of eukaryotic lipid transfer proteins, including chorein-N domains in TamB and AsmA and Mdm31p. *BMC Mol Cell Biol* **20**: 43.

Loeschcke, A., Markert, A., Wilhelm, S., Wirtz, A., Rosenau, F., Jaeger, K.E., and Drepper, T. (2013) TREX: A universal tool for the transfer and expression of biosynthetic pathways in bacteria. *ACS Synth Biol* **2**: 22–33.

de Lorenzo, V., Eltis, L., Kessler, B., and Timmis, K.N. (1993) Analysis of *Pseudomonas* gene products using *lacIq*/Ptrp-lac plasmids and transposons that confer conditional phenotypes. *Gene* **123**: 17–24.

Malinverni, J.C. and Silhavy, T.J. (2009) An ABC transport system that maintains lipid asymmetry in the Gram-negative outer membrane. *Proceedings of the National Academy of Sciences* **106**: 8009–8014.

McBroom, A.J., Johnson, A.P., Vemulapalli, S., and Kuehn, M.J. (2006) Outer membrane vesicle production by *Escherichia coli* is independent of membrane instability. *J Bacteriol* **188**: 5385–5392.

Misra, R. and Miao, Y. (1995) Molecular analysis of *asmA*, a locus identified as the suppressor of OmpF assembly mutants of *Escherichia coli* K-12. *Mol Microbiol* **16**: 779–788.

Mueller, E.A. and Levin, P.A. (2020) Bacterial cell wall quality control during environmental stress. *mBio* **11**: 1–15.

Nelson, K.E., Weinel, C., Paulsen, I.T., Dodson, R.J., Hilbert, H., Martins dos Santos, V.A.P., et al. (2002) Complete genome sequence and comparative analysis of the metabolically versatile *Pseudomonas putida* KT2440. *Environ Microbiol* **4**: 799–808.

Ojima, Y., Sawabe, T., Konami, K., and Azuma, M. (2020) Construction of hypervesiculation *Escherichia coli* strains and application for secretory protein production. *Biotechnol Bioeng* **117**: 701–709.

Platt, R., Drescher, C., Park, S.-K., and Phillips, G.J. (2000) Genetic system for reversible integration of DNA constructs and *lacZ* gene fusions into the *Escherichia coli* chromosome. *Plasmid* **43**: 12–23.

Prior, J.E., Lynch, M.D., and Gill, R.T. (2010) Broad-host-range vectors for protein expression across Gram negative hosts. *Biotechnol Bioeng* **106**: 326–332.

Ringel, M.T. and Brüser, T. (2018) The biosynthesis of pyoverdines. *Microbial Cell* **5**: 424–437.

Roier, S., Zingl, F.G., Cakar, F., Durakovic, S., Kohl, P., Eichmann, T.O., et al. (2016) A novel mechanism for the biogenesis of outer membrane vesicles in Gram-negative bacteria. *Nat Commun* **7**: 10515.

Rouvière, P.E., De Las Peñas, A., Mecsas, J., Lu, C.Z., Rudd, K.E., and Gross, C.A. (1995) *rpoE*, the gene encoding the second heat-shock sigma factor, sigma E, in *Escherichia coli*. *EMBO J* **14**: 1032–1042.

Sánchez, C., Braña, A.F., Méndez, C., and Salas, J.A. (2006) Reevaluation of the violacein biosynthetic pathway and its relationship to indolocarbazole biosynthesis. *ChemBioChem* **7**: 1231–1240.

Schwechheimer, C. and Kuehn, M.J. (2015) Outer-membrane vesicles from Gram-negative bacteria: biogenesis and functions. *Nat Rev Microbiol* **13**: 605–619.

Schwechheimer, C., Sullivan, C.J., and Kuehn, M.J. (2013) Envelope control of outer membrane vesicle production in Gram-negative bacteria. *Biochemistry* **52**: 3031–3040.

Singh, S.K., SaiSree, L., Amrutha, R.N., and Reddy, M. (2012) Three redundant murein endopeptidases catalyse an essential cleavage step in peptidoglycan synthesis of *Escherichia coli* K12. *Mol Microbiol* **86**: 1036–1051.

Song, T., Mika, F., Lindmark, B., Liu, Z., Schild, S., Bishop, A., et al. (2008) A new *Vibrio cholerae* sRNA modulates colonization and affects release of outer membrane vesicles. *Mol Microbiol* **70**: 100–111.

Sonntag, I., Schwarz, H., Hirota, Y., and Henning, U. (1978) Cell envelope and shape of *Escherichia coli*: multiple mutants missing the outer membrane lipoprotein and other major outer membrane proteins. *J Bacteriol* **136**: 280–285.

Spiess, C., Beil, A., and Ehrmann, M. (1999) A temperature-dependent switch from chaperone to protease in a widely conserved heat shock protein. *Cell* **97**: 339–347.

Strauch, K.L., Johnson, K., and Beckwith, J. (1989) Characterization of *degP*, a gene required for proteolysis in the cell envelope and essential for growth of *Escherichia coli* at high temperature. *J Bacteriol* **171**: 2689–2696.

Toyofuku, M., Nomura, N., and Eberl, L. (2019) Types and origins of bacterial membrane vesicles. *Nat Rev Microbiol* **17**: 13–24.

Udekwu, K.I. and Wagner, E.G.H. (2007) Sigma E controls biogenesis of the antisense RNA MicA. *Nucleic Acids Res* **35**: 1279–1288.

Untergasser, A., Cutcutache, I., Koressaar, T., Ye, J., Faircloth, B.C., Remm, M., and Rozen, S.G. (2012) Primer3—new capabilities and interfaces. *Nucleic Acids Res* **40**: e115–e115.

Volke, D.C., Friis, L., Wirth, N.T., Turlin, J., and Nikel, P.I. (2020) Synthetic control of plasmid replication enables target- and self-curing of vectors and expedites genome engineering of *Pseudomonas putida*. *Metab Eng Commun* **10**: e00126.

Winsor, G.L., Griffiths, E.J., Lo, R., Dhillon, B.K., Shay, J.A., and Brinkman, F.S.L. (2016) Enhanced annotations and features for comparing thousands of *Pseudomonas* genomes in the *Pseudomonas* genome database. *Nucleic Acids Res* **44**: D646–D653.

Xiong, X., Deeter, J.N., and Misra, R. (1996) Assembly-defective OmpC mutants of *Escherichia coli* K-12. *J Bacteriol* **178**: 1213–1215.

Yang, D., Park, S.Y., and Lee, S.Y. (2021) Production of rainbow colorants by metabolically engineered *Escherichia coli*. *Advanced Science* **8**: 2100743.

Yeow, J., Tan, K.W., Holdbrook, D.A., Chong, Z.-S., Marzinek, J.K., Bond, P.J., and Chng, S.-S. (2018) The architecture of the OmpC–MlaA complex sheds light on the maintenance of outer membrane lipid asymmetry in *Escherichia coli*. *Journal of Biological Chemistry* **293**: 11325–11340.

V.3. Supporting Information for chapter II.4

ChemBioChem

Supporting Information

Biotransformation Of L-Tryptophan To Produce Arcyriaflavin A With *Pseudomonas putida* KT2440

Nora Lisa Bitzenhofer, Thomas Classen, Karl-Erich Jaeger, and Anita Loeschcke*

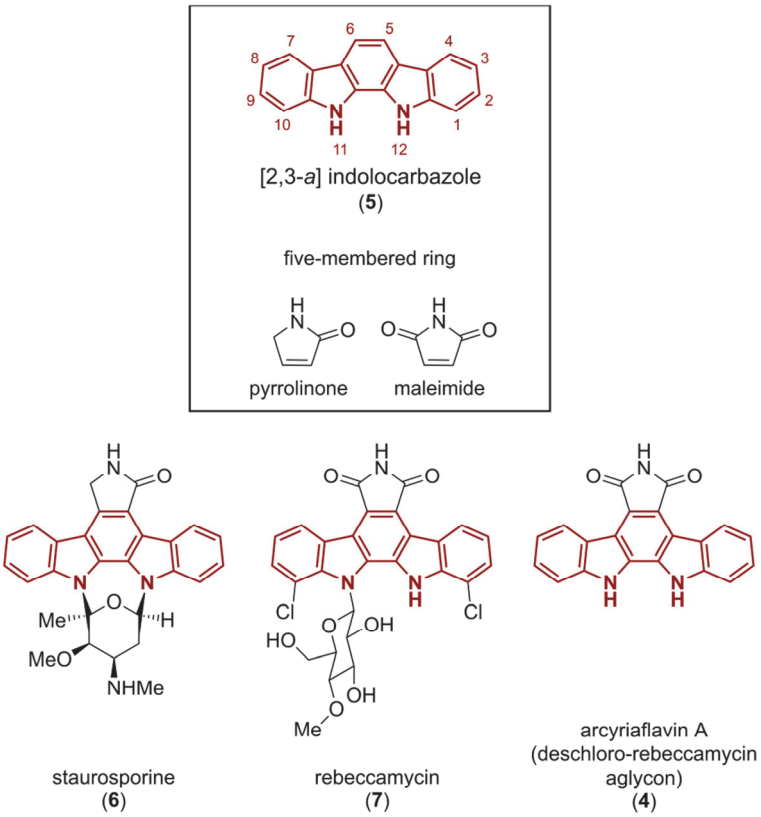

Figure S1: Indolocarbazole basic scaffold and specific examples.
11,12-Dihydroindolo[2,3-*a*]-carbazole scaffold (**5**) and two different types of the five-membered ring fused to the indolocarbazole (pyrrolinone and maleimide).[1] Staurosporine (**6**), rebeccamycin (**7**), and arcyriaflavin A (**4**) are shown as examples of this class of compounds. The indolocarbazole scaffold is highlighted in red.

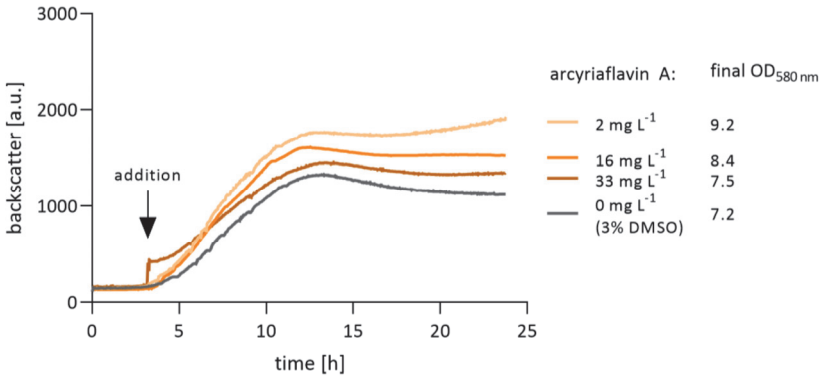

Figure S2: Growth of *P. putida* KT2440 in the presence of arcyriaflavin A.
A potential toxicity effect of arcyriaflavin A on the growth of *P. putida* KT2440 wild type was analyzed by addition of different concentrations to the culture. Additionally, a reference sample only supplemented with the corresponding concentration of DMSO (3%) was analyzed. Growth was measured as backscatter using the Cell Growth Quantifier (CGQ) system (aquila biolabs, now Scientific Bioprocessing, Inc. (SBI), Baesweiler, Germany). The observed shift in backscatter after adding 33 mg L^{-1} arcyriaflavin A is due to a color shift of the culture. Final cell densities (after 24 h) given as OD (optical density) – here, $OD_{580\ nm}$ values – refer to measurements of liquid cultures in a Spectrophotometer (Genesys 20, ThermoFisher Scientific, Waltham, MA, USA) using 1 mL samples in cuvettes with 1 cm path length. The data are mean values of biological triplicates. For detailed description of the experimental procedure, see **SI-M1**.

Equation 1 for quadratic model:

Titer [µg L^{-1}]	=	
+1129.902	µg L^{-1}	
-68.183	µg L^{-1} °C^{-1}	Temperature [°C]
-56.848	µg L^{-1} h^{-1}	Time [h]
+40.899	µg L^{-1} h^{-1}	L-Trp add. [h]
-17.404	µg L^{-1} mM^{-1}	L-Trp conc. [mM]
+2.131	µg L^{-1} °C^{-1} h^{-1}	Temperature [°C] · Time [h]
-1.253	µg L^{-1} °C^{-1} h^{-1}	Temperature [°C] · L-Trp add. [h]
+3.225	µg L^{-1} °C^{-1} mM^{-1}	Temperature [°C] · L-Trp conc. [mM]
+1.944	µg L^{-1} h^{-2}	Time [h] · L-Trp add. [h]
+1.373	µg L^{-1} h^{-1} mM^{-1}	Time [h] · L-Trp conc. [mM]
-0.095	µg L^{-1} h^{-1} mM^{-1}	L-Trp add. [h] · L-Trp conc. [mM]
+0.787	µg L^{-1} °C^{-2}	Temperature² [°C^2]
-0.016	µg L^{-1} h^{-2}	Time² [h^2]
-2.865	µg L^{-1} h^{-2}	L-Trp add.² [h^2]
-16.705	µg L^{-1} mM^{-2}	L-Trp conc.² [mM^2]

Equation 2 for quadratic model:

Specific productivity [µg $gDCW^{-1}$ h^{-1} = Φ]	=	
+28.923	Φ	
-1.817	Φ °C^{-1}	Temperature [°C]
-0.518	Φ h^{-1}	Time [h]
-0.048	Φ h^{-1}	L-Trp add. [h]
+0.082	Φ mM^{-1}	L-Trp conc. [mM]
+0.023	Φ °C^{-1} h^{-1}	Temperature [°C] · Time [h]
-0.004	Φ °C^{-1} h^{-1}	Temperature [°C] · L-Trp add. [h]
+0.019	Φ °C^{-1} mM^{-1}	Temperature [°C] · L-Trp conc. [mM]
+0.018	Φ h^{-2}	Time [h] · L-Trp add. [h]
+0.005	Φ h^{-1} mM^{-1}	Time [h] · L-Trp conc. [mM]
+0.004	Φ h^{-1} mM^{-1}	L-Trp add. [h] · L-Trp conc. [mM]
+0.026	Φ °C^{-2}	Temperature² [°C^2]
-0.002	Φ h^{-2}	Time² [h^2]
-0.020	Φ h^{-2}	L-Trp add.² [h^2]
-0.106	Φ mM^{-2}	L-Trp conc.² [mM^2]

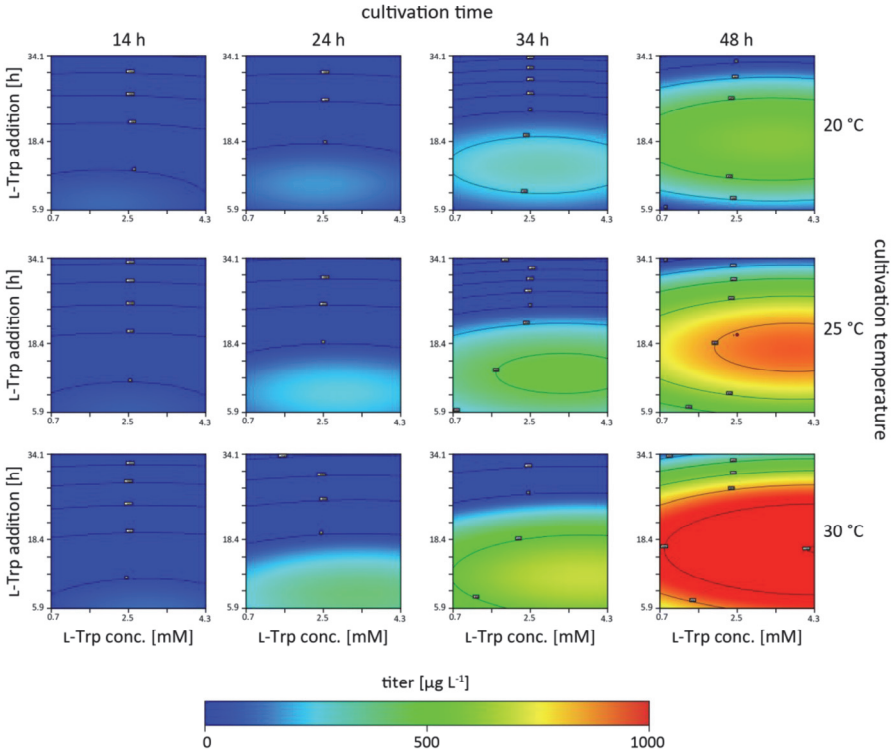

Figure S3: DoE contour plots for arcyriaflavin A titers.
Arcyriaflavin A titer [µg L^{-1}] reached in *rebODCP* expressing *P. putida* (*P. putida* NB04) cultures depending on L-Trp addition [h] and L-Trp concentration [mM] is plotted in contour plots for three different temperatures (20, 25, 30 °C) and four cultivation times (14, 24, 34, 48 h).

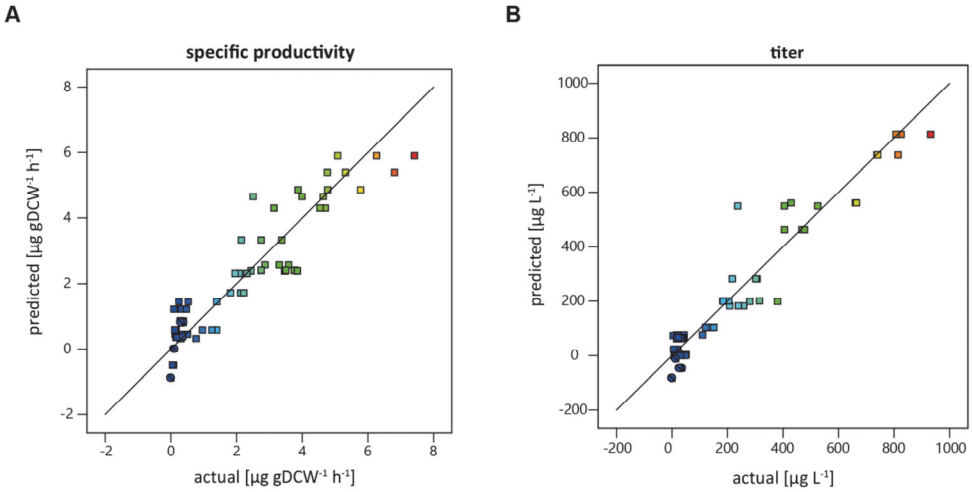

Figure S4: Statistical analysis of the DoE.
The predicted specific productivity [µg gDCW^{-1} h^{-1}] (**A**) and titer [µg L^{-1}] (**B**), respectively, are plotted against the actually obtained values to make a statement about the distribution of the measured data and, thus, about the reliability of the DoE. Overall, 69 experimental runs with varying conditions were performed for deducing the fit (for detailed description see **SI-M3** and **Table S5**). The data are presented for two different outputs (i.e. specific productivity and titer) based on the same measurements. For specific productivity, dry cell weight (DCW) and cultivation time (in hours) were included. For titer, the amount of the product arcyriaflavin A was related to 1 L of culture.

Table S1: ANOVA (analysis of variance) and fit statistics for specific productivity

specific productivity	DF	Sum of squares	Mean squares	F	p
Model	14	225.58	16.11	24.54	< 0.0001
Cor. total	65	259.06			
Residual	51	33.49	0.6566		
Lack of Fit (Model error)	6	18.89	3.15	9.71	< 0.0001
Pure error (Replicate error)	45	14.59	0.3243		
Fit statistics	N = 66	R^2 = 0.8707 R^2 adj. = 0.8353 R^2 pred. = 0.7818	SD = 0.8103 Mean = 2.08 C.V. % = 38.93	Adeq. Precision	= 16.5510

Table S2: ANOVA (analysis of variance) and fit statistics for titer

concentration	DF	Sum of squares	Mean squares	F	p
Model	14	$3.934 \cdot 10^6$	$2.810 \cdot 10^5$	47.44	< 0.0001
Cor. total	65	$4.236 \cdot 10^6$			
Residual	51	$3.021 \cdot 10^5$	5922.84		
Lack of Fit (Model error)	6	$1.664 \cdot 10^5$	27735.87	9.20	< 0.0001
Pure error (Replicate error)	45	$1.356 \cdot 10^5$	3014.43		
Fit statistics	N = 66	R^2 = 0.9287 R^2 adj. = 0.9091 R^2 pred. = 0.8915	SD = 76.96 Mean = 207.84 C.V. % = 37.03	Adeq. Precision	= 22.2426

Cor. Total: corrected total sum of squares;
Model error: difference between observed vs. predicted;
Replicate error: variation between the repeats;
DF: degrees of freedom, used to compute the F-statistic and subsets of the model;
Sum of squares: the sum of the squared deviations from the mean due to the effect of this term;
Mean squares: sum of squares/degrees of freedom (variance);
F-value: ration between explained variation and unexplained variation; the higher the better;
p-value: less than 0.05 indicates model terms are significant;
Adeq. Precision: measures the signal to noise ratio, greater than 4 is desirable;
N: runs; SD: standard deviation; C.V.: coefficient of variation;

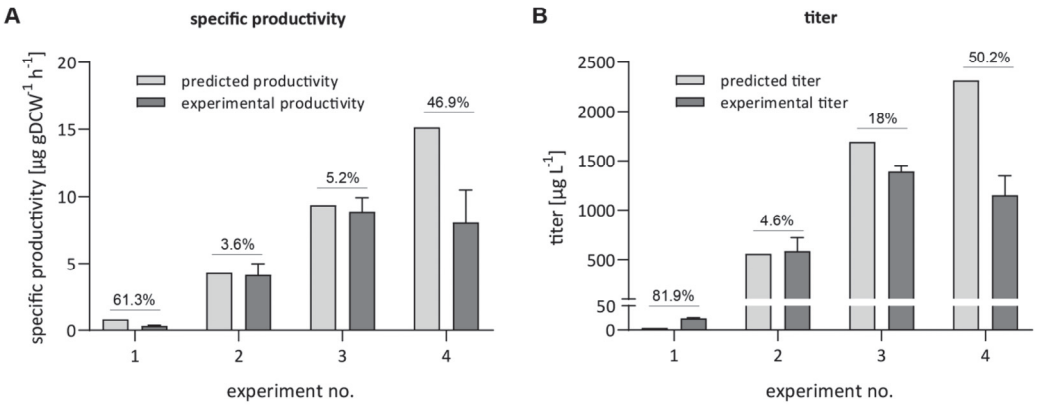

Figure S5: DoE model validation.
To validate the DoE model, four experiments differing in the four parameters (temperature, time, precursor addition and concentration) were performed and the predicted values were compared with the experimentally obtained values for specific productivity and titer, respectively. Experiments were performed that should result in low, medium, and high titers and productivity. Experiment number (no.) indicates the validation experiment performed. These differed in the cultivation temperature, cultivation time, time point of L-Trp addition, and L-Trp concentration as follows: **1**: 18 °C, 28 h, 20 h, 2.5 mM; **2**: 30 °C, 48 h, 4 h, 1 mM; **3**: 30 °C, 72 h, 9 h, 3.7 mM; **4**: 30 °C, 72 h, 18 h, 4.9 mM (see also **Table S5**). Discrepancies between predicted and experimental values are given as percentages above the bars. Significant differences are indicated by asterisks (determined by T-test; ns: no significance, * = P≤0.05, ** = P≤0.01, *** = P≤0.001, **** = P≤0.0001).

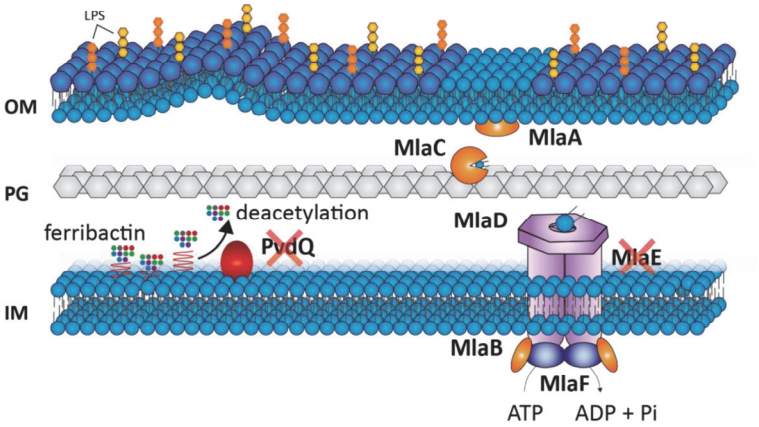

Figure S6: Function of PvdQ and MlaE and their role in OMV formation.
Schematic illustration of the PvdQ-catalyzed deacetylation in pyoverdine biosynthesis and of the maintenance of lipid asymmetry (Mla) system in *P. putida* KT2440. Manipulation of these targets (proteins targeted for knockout are marked with a red cross) affects outer membrane vesicle (OMV) formation.[2–4] In general, several local mechanisms have been described which led to OMV formation in Gram-negative bacteria ((i) a reduction of the connections between the outer membrane (OM) and the peptidoglycan layer (PG), (ii) an increase in OM curvature, or (iii) an increase in periplasmic pressure.[5] The targets addressed here may be assigned to two different mechanisms. For PvdQ, we hypothesize that accumulation of the precursor molecule ferribactin in the inner membrane (IM) of a *pvdQ* knockout strain causes periplasmic pressure and thus activates OMV formation. Deletion of *mlaE* leads to an accumulation of phospholipids in the outer leaflet of the OM, modifying the asymmetric bilayer and inducing membrane curvature, which can lead to OMV formation.[4,6,7]

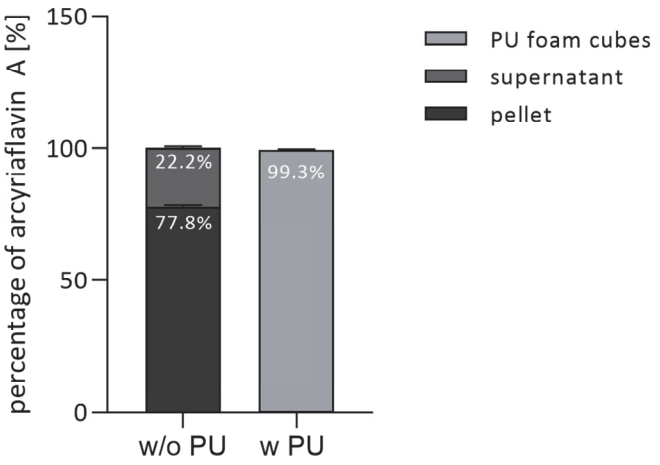

Figure S7: Accumulation of arcyriaflavin A.
To study the distribution of arcyriaflavin A by addition of extracellular hydrophobic components during cultivation with the *rebODCP* expressing *P. putida* KT2440 strain (NB04), cultivation without (w/o) and with (w) polyurethane (PU) foam cubes is compared. For analysis, the pellet (black), the supernatant (dark gray) and the PU fraction (light gray) were extracted and subjected to HPLC-PDA analysis. For each of these fractions, the percentage of arcyriaflavin A in the total amount was calculated. An almost complete accumulation in the PU foam cubes was observed when using the hydrophobic adsorbent. Only 0.7% of the amount of arcyriaflavin A was found in the pellet fraction. Arcyriaflavin A was not measurable in the supernatant fraction. The data are means of biological duplicates with their corresponding standard deviation.

SI Experimental Section

Table S3: Oligonucleotides in this study.

Oligonucleotides				
#	name	sequence (5' → 3')	Tm [°C]	application
1	IF_rebT_in pJT_fw	GCATGCTCCTCTAGACTCGATCACTCGTGTGGTGTCGT	70	cloning pJT'TrebUT-KmR
2	IF_rebT_in pJT_rev	CAAGATTGACGCCAGGACCAAGGAGCAAG	66	
3	IF_rebU_fw	GGAGGTACCGAATTCCTCGAATGAGCGTGCACATCGAG	70	
4	IF_rebU_rev	TGGTCCTGGCGTCAATCTTGCCGGACATGAAACG	70	
5	IF_pJT_AbR_fw	CAATTCGTTCAAGCCGAGATCGG	60	
6	IF_pJT_AbR_rev	CGTTGCTGCTCCATAACATCAAAC	60	
7	IF-KmR-in pJT_fw	GATGTTATGGAGCAGCAACGATGATTGAACAAGATGGATTGCACG	69	
8	IF-KmR-in pJT_rev	ATCTCGGCTTGAACGAATTGTCAGAAGAACTCGTCAAGAAGGCGATAGAA	70	
9	IF-PCR_pBTBX-KmR_fw	GGATCCCCCTCAAGTCAAAAGCC	61	cloning pBTBX-2-mcs-KmR-rebUT
10	IF-PCR_pBTBX-KmR_rev	GCCCTCAGAAAAACTCATCGAGCA	61	
11	IF-PCR_rebUT_in pBTBX_fw	CGATGAGTTTTTCTGAGGGCACACAGGAAACAGGAGGTACC	70	
12	IF-PCR_rebUT_pBTBX_rev	TTTTGACTTGAGGGGGATCCTCACTCGTGTGGTGTCGTCG	71	
13	IF_pNPTS-R6KT_fw	TCTCCGGATGTACAGGCATGCGT	64	mlaE knockout
14	IF_pNPTS-R6KT_rev	TGGCGCCAGCCGGCT	64	
15	IF_mlaE-up_fw	ATTGAAGCCGGCTGGCGCCAGGCGTCCATTAGGACGAGGCTGC	78	
16	IF_mlaE-up_rev	CGGTTTTGCATCAACGCGCCCCCAGCAG	71	
17	IF_mlaE-down_fw	GGCGCGTTGATGCAAAACCGCACCCTGGAAATCG	72	
18	IF_mlaE-down_rev	CATGCCTGTACATCCGGAGAACAGTGATGCCCTGGTTATTGTATTCGAG	70	
19	M13 rev (-49) (from Eurofins Genomics)	GAGCGGATAACAATTTCACACAGG	59	sequencing primers
20	pEX-For (from Eurofins Genomics)	GGAGCAGACAAGCCCGTCAGG	63	
21	Seq-KmR-rebUT_fw	TTGATGCTCGATGAGTTTTTC	52	
22	Seq_pNPTS-lacZmcs_fw	CACAGGAAACAGCTATGAC	52	
23	Seq_pNPTS-lacZmcs_rev	GGTTTTCCCAGTCACGAC	54	
24	Seq_mlaE_fw	GGTGCGCCTGATTCGC	59	
25	Seq_mlaE_rev	CTGCAACGTCACCCGAC	57	

Table S4: Plasmids and bacterial strains used in this study.

Plasmids			
name	characteristics	application	reference
pYTNB04K_1G7	Km^R, oriT-mob, Tn7-L, nagR-P_{nagAa}→*rebODCP*, eYFP, Gm^R, Tn7 tnsA-D, Tn7-R	integration vector into *att*Tn7 site	[8]
pJT'Tmcs	Amp^R, Gm^R, P_{tac}, colE1 ori, pRO1600 Rep, pRO1600 oriV	empty vectors	[9]
pVLT33	Km^R, lacIq, P_{tac}, RSF1010 ori, *mob*, *repABC*,		[10]
pBTBX-2-mcs	Km^R, araC, P_{araBAD}, pBBR1 ori		[11]
pNPTS138-R6KT	Km^R, mobRP4, ori-R6K, *sacB*, P_{lac}→*lacZα*; suicide plasmid for in-frame deletions;		[12]
pJT'T-rebUT	Amp^R, Gm^R, P_{tac}→*rebUT*, colE1 ori, pRO1600 Rep, pRO1600 oriV	co-expression of transporter genes	This study
pJT'T-rebUT-KmR	Amp^R, Km^R, P_{tac}→*rebUT*, colE1 ori, pRO1600 Rep, pRO1600 oriV		This study
pBTBX-2-mcs-KmR-rebUT	Km^R, araC, P_{araBAD}, P_{KmR}→*rebUT*, pBBR1 oris		This study

pNPTS138-R6KT-mlaE-up/down	suicide vector pNTPS with up-/down-stream region of *mlaE* (for deletion in *P. putida* KT2440); cloned into *lacZα* gene	knockout strain	This study
Strains			
name	**features**	**application**	**reference**
E. coli DH5α	F-Φ80*lac*ZΔM15 Δ(*lac*ZYA-argF) U169 deoR recA1 endA1 hsdR17 (rk-, mk+) phoA glnV44 thi-1 gyrA96 relA1	cloning	[13]
E. coli DH5α λpir	λpir lysogen derivative of strain DH5α		[14]
E. coli Stellar™	*E. coli* HST08 strain (F-Φ80d *lacZ*ΔM15 Δ(*lacZYA-argF*) U169 recA1 endA1 phoA glnV44 thi-1 gyrA96 relA1, , Δ(*mrr-hsdRMS-mcrBC*), Δ*mcrA*, λ-); provides high transformation efficiency		(Takara Bio, Cat# 636763)
E. coli S17-1	Ec294::[RP4-2 (Tc^R::Mu)(Km^R::Tn7)] *recA*, *thi*, *pro*, *hsdR*$^-$ *hsdM*$^+$ Tp^R, Sm^R	conjugation	[15]
P. putida KT2440	wild type, derivative of mt-2		[16]
P. putida KT2440 Δ*pvdQ*	*P. putida* KT2440 with seamless deletion of *pvdQ* gene	knockout strains	[2]
P. putida KT2440 Δ*mlaE*	*P. putida* KT2440 with seamless deletion of *mlaE* gene		This study
P. putida KT2440/Tn7- P_{nagAa}-*rebODCP* (NB04)	*nagR*-P_{nagAa}-*rebODCP*, eYFP, Gm^R, tnsA-D	arcyriaflavin A producer strains	[8]
P. putida KT2440 Δ*pvdQ*/Tn7-P_{nagAa}-*rebODCP*	*P. putida* KT2440 with seamless deletion of *pvdQ* gene; *nagR*-P_{nagAa}→*rebODCP*, eYFP, Gm^R, tnsA-D		This study
P. putida KT2440 Δ*mlaE*/Tn7-P_{nagAa}-*rebODCP*	*P. putida* KT2440 with seamless deletion of *mlaE* gene; *nagR*-P_{nagAa}→*rebODCP*, eYFP, Gm^R, tnsA-D		This study

M1. Growth of treated *P. putida* samples

To analyze the effect of arcyriaflavin A supplementation on the bacterial growth, *P. putida* KT2440 was cultured under standard conditions in 10 mL LB medium. Growth was measured as backscatter using the Cell Growth Quantifier (CGQ) system (aquila biolabs, now Scientific Bioprocessing, Inc. (SBI), Baesweiler, Germany). Arcyriaflavin A was added in the logarithmic phase (after 4 h) at different concentrations (stock: 3.1 mM in DMSO): 0 µM, 5 µM (2 mg L^{-1}), 50 µM (16 mg L^{-1}), and 100 µM (33 mg L^{-1}). All cultures were supplemented with DMSO to a final concentration of 3% (*v*/*v*). Cultures were incubated for 24 h and the optical density $OD_{580\ nm}$ was measured using a Spectrophotometer (Genesys 20, ThermoFisher Scientific, Waltham, MA, USA) using 1 mL samples in cuvettes with 1 cm path length.

M2. Construction of an *mlaE* knockout strain

The deletion mutant *P. putida* KT2440 Δ*mlaE* was constructed using a SacB-based engineering system.[12] The suicide vector pNPTS138-R6KT was linearized by PCR using the primers **13** and **14**. Additionally, the upstream (880 bp) and downstream (880 bp) regions of *mlaE* were amplified using

the *P. putida* KT2440 genome as template and oligonucleotides **15** to **18**. The backbone and the two fragments were assembled by InFusion® Snap Assembly (Takara Bio Europe, St Germain en Laye, France) using *E. coli* DH5α λpir for cloning. The new plasmid was confirmed by Sanger sequencing (Eurofins Genomics, Ebersberg, Germany) using the sequencing primers **22** and **23**.

To delete *mlaE*, *P. putida* KT2440 was transformed with the new suicide vector pNPTS138-R6KT-mlaE-up/down by electroporation. For single-crossover selection, the cells were plated on LB agar plates with 25 µg mL^{-1} irgasan and 25 µg mL^{-1} kanamycin and incubated overnight at 30 °C.[17] For SacB counter-selection, single colonies were then streaked onto YT+25% (*w*/*v*) sucrose plates (10 g L^{-1} yeast extract, 20 g L^{-1} tryptone, 36 g L^{-1} agar; sucrose (stock: 50% (*w*/*v*) was added after autoclaving) and incubated at 30 °C for one to two days. The resulting clones were again streaked onto a fresh YT+25% (*w*/*v*) sucrose plate. Grown clones were then screened for deletion by kanamycin sensitivity and colony PCR (cPCR) (using oligos **24** and **25**). The cPCR products were sequenced for final confirmation. The newly constructed knockout strain was named *P. putida* KT2440 Δ*mlaE*.

M3. Design of Experiment (DoE)

Experiments for the Design of Experiment approach were conducted with different cultivation conditions. The conditions are listed in the following **Table S5**. The time point of induction of the gene expression, as well as the inducer concentration were kept constant (2 mM, 4 h after inoculation).

Table S5: Cultivation parameters for DoE

initial DoE experiments				
run	**temperature**	**cultivation time**	**L-Trp concentration**	**L-Trp addition time**
1	20 °C	14 h	4.3 mM	6 h
2	25 °C	28 h	2.5 mM	20 h
3	20 °C	14 h	0.73 mM	6 h
4	30 °C	42 h	4.3 mM	28 h
5	32 °C	28 h	2.5 mM	20 h
6	20 °C	42 h	4.3 mM	28 h
7	20 °C	42 h	4.3 mM	6 h
8	30 °C	42 h	0.73 mM	6 h
9	30 °C	42 h	0.73 mM	28 h
10	30 °C	42 h	4.3 mM	6 h
11	25 °C	48 h	2.5 mM	20 h
12	18 °C	28 h	2.5 mM	20 h
13	30 °C	42 h	4.3 mM	6 h
14	32 °C	28 h	2.5 mM	20 h
15	30 °C	42 h	4.3 mM	28 h
16	20 °C	42 h	4.3 mM	28 h
17	25 °C	28 h	2.5 mm	20 h
18	20 °C	14 h	0.73 mM	6 h
19	25 °C	28 h	5 mM	20 h
20	20 °C	42 h	4.3 mM	28 h
21	30 °C	42 h	0.73 mM	28 h
22	25 °C	28 h	2.5 mM	20 h
23	18 °C	28 h	2.5 mM	20 h
24	30 °C	42 h	4.3 mM	6 h
25	25 °C	48 h	2.5 mM	20 h
26	20 °C	14 h	4.3 mM	6 h
27	20 °C	42 h	0.73 mM	28 h
28	20 °C	42 h	4.3 mM	6 h
29	30 °C	14 h	4.3 mM	6 h
30	20 °C	14 h	4.3 mM	6 h
31	25 °C	28 h	2.5 mM	20 h
32	30 °C	14 h	4.3 mM	6 h
33	30 °C	42 h	0.73 mM	28 h
34	20 °C	42 h	4.3 mM	6 h
35	25 °C	48 h	2.5 mM	20 h
36	18 °C	28 h	2.5 mM	20 h
37	30 °C	14 h	0.73 mM	6 h
38	25 °C	28 h	2.5 mM	20 h
39	30 °C	42 h	4.3 mM	28 h
40	20 °C	42 h	0.73 mM	28 h
41	30 °C	42 h	0.73 mM	6 h
42	20 °C	14 h	0.73 mM	6 h
43	30 °C	14 h	0.73 mM	6 h
44	25 °C	28 h	5 mM	20 h
45	30 °C	42 h	0.73 mM	6 h
46	30 °C	14 h	4.3 mM	6 h
47	30 °C	14 h	0.73 mM	6 h
48	20 °C	42 h	0.73 mM	28 h
49	25 °C	28 h	2.5 mM	20 h
50	32 °C	28 h	2.5 mM	20 h
51	25 °C	28 h	5 mM	20 h
52	30 °C	48 h	1 mM	4 h
53	30 °C	48 h	1 mM	4 h
54	30 °C	48 h	1 mM	4 h
55	25 °C	24 h	1 mM	4 h

run	temperature	cultivation time	L-Trp concentration	L-Trp addition time
56	25 °C	24 h	1 mM	4 h
57	25 °C	24 h	1 mM	4 h
58	25 °C	48 h	1 mM	4 h
59	25 °C	48 h	1 mM	4 h
60	25 °C	48 h	1 mM	4 h
61	30 °C	24 h	0 mM	4 h
62	30 °C	24 h	0 mM	4 h
63	30 °C	24 h	0 mM	4 h
64	30 °C	24 h	1 mM	4 h
65	30 °C	24 h	1 mM	4 h
66	30 °C	24 h	1 mM	4 h
67	25 °C	28 h	2.5 mM	20 h
68	32 °C	28 h	2.5 mM	20 h
69	25 °C	28 h	5 mM	20 h
validation experiments				
run	temperature	cultivation time	L-Trp concentration	L-Trp addition time
1	18 °C	28 h	2.5 mM	20 h
2	30 °C	48 h	1.0 mM	4 h
3	30 °C	72 h	3.7 mM	9 h
4	30 °C	72 h	4.9 mM	18 h

References

[1] G. E. Chambers, A. E. Sayan, R. C. D. Brown, *Nat Prod Rep* **2021**, *38*, 1794–1820.

[2] N. L. Bitzenhofer, C. Höfel, S. Thies, A. J. Weiler, C. Eberlein, H. J. Heipieper, R. Batra-Safferling, P. Sundermeyer, T. Heidler, C. Sachse, T. Busche, J. Kalinowski, T. Belthle, T. Drepper, K. Jaeger, A. Loeschcke, *Microb Biotechnol* **2023**, 1–18.

[3] C. Davies, A. J. Taylor, A. Elmi, J. Winter, J. Liaw, A. D. Grabowska, O. Gundogdu, B. W. Wren, D. J. Kelly, N. Dorrell, *Front Cell Infect Microbiol* **2019**, *9*, 177.

[4] S. Roier, F. G. Zingl, F. Cakar, S. Durakovic, P. Kohl, T. O. Eichmann, L. Klug, B. Gadermaier, K. Weinzerl, R. Prassl, A. Lass, G. Daum, J. Reidl, M. F. Feldman, S. Schild, *Nat Commun* **2016**, *7*, 10515.

[5] R. Juodeikis, S. R. Carding, *Microbiol Mol Biol* **2022**, *86*, e0003222.

[6] M. Toyofuku, N. Nomura, L. Eberl, *Nat Rev Microbiol* **2019**, *17*, 13–24.

[7] E. D. Avila-Calderón, M. del S. Ruiz-Palma, M. G. Aguilera-Arreola, N. Velázquez-Guadarrama, E. A. Ruiz, Z. Gomez-Lunar, S. Witonsky, A. Contreras-Rodríguez, *Front Microbiol* **2021**, *12*, 557902.

[8] R. Weihmann, S. Kubicki, N. L. Bitzenhofer, A. Domröse, I. Bator, L.-M. Kirschen, F. Kofler, A. Funk, T. Tiso, L. M. Blank, K.-E. Jaeger, T. Drepper, S. Thies, A. Loeschcke, *FEMS Microbes* **2023**, *4*, 1–17.

[9] S. Verhoef, H. Ballerstedt, R. J. M. Volkers, J. H. de Winde, H. J. Ruijssenaars, *Appl Microbiol Biotechnol* **2010**, *87*, 679–690.

[10] V. de Lorenzo, L. Eltis, B. Kessler, K. N. Timmis, *Gene* **1993**, *123*, 17–24.

[11] J. E. Prior, M. D. Lynch, R. T. Gill, *Biotechnol Bioeng* **2010**, *106*, 326–332.

[12] J. Lassak, A.-L. Henche, L. Binnenkade, K. M. Thormann, *Appl Environ Microbiol* **2010**, *76*, 3263–3274.

[13] D. Hanahan, *J Mol Biol* **1983**, *166*, 557–580.

[14] R. Platt, C. Drescher, S.-K. Park, G. J. Phillips, *Plasmid* **2000**, *43*, 12–23.

[15] R. Simon, U. Priefer, A. Pühler, *Bio/Technology* **1983**, *1*, 784–791.

[16] K. E. Nelson, C. Weinel, I. T. Paulsen, R. J. Dodson, H. Hilbert, V. A. P. Martins dos Santos, D. E. Fouts, S. R. Gill, M. Pop, M. Holmes, L. Brinkac, M. Beanan, R. T. DeBoy, S. Daugherty, J. Kolonay, R. Madupu, W. Nelson, O. White, J. Peterson, H. Khouri, I. Hance, P. C. Lee, E. Holtzapple, D. Scanlan, K. Tran, A. Moazzez, T. Utterback, M. Rizzo, K. Lee, D. Kosack, D. Moestl, H. Wedler, J. Lauber, D. Stjepandic, J. Hoheisel, M. Straetz, S. Heim, C. Kiewitz, J. Eisen, K. N. Timmis, A. Dusterhoft, B. Tummler, C. M. Fraser, *Environ Microbiol* **2002**, *4*, 799–808.

[17] J. R. Elmore, A. Furches, G. N. Wolff, K. Gorday, A. M. Guss, *Metab Eng Commun* **2017**, *5*, 1–8.

V.4. Supporting Information for chapter II.5.1

Supplementary Material

Production of tailored hydroxylated prodiginine showing combinatorial activity with rhamnolipids against plant parasitic nematodes

D. F. Kossmann[†,1], M. Huang[†,2], R. Weihmann[†,3], X. Xiao[2], F. Gätgens[3], T. M. Weber[1], H. U. C. Brass[1], N. L. Bitzenhofer[3], S. Ibrahim[3], K. Bangert[3], L. Rehling[2], C. Mueller[4], T. Tiso[4], L. M. Blank[4], T. Drepper[3], K.-E. Jaeger[3,5], F. M. W. Grundler[2], J. Pietruszka*[‡,1,5], A. S. S. Schleker*[‡,2], A. Loeschcke*[‡,3]

[1] Institute of Bioorganic Chemistry, Heinrich Heine University Düsseldorf, Forschungszentrum Jülich, Jülich, Germany.
[2] INRES Molecular Phytomedicine, University of Bonn, Bonn, Germany.
[3] Institute of Molecular Enzyme Technology, Heinrich Heine University Düsseldorf, Forschungszentrum Jülich, Jülich, Germany.
[4] iAMB – Institute of Applied Microbiology, ABBt – Aachen Biology and Biotechnology, RWTH Aachen University, Aachen, Germany
[5] Institute of Bio- and Geosciences (IBG-1): Biotechnology, Forschungszentrum Jülich GmbH, Jülich, Germany
*** Correspondence:** J. Pietruszka, j.pietruszka@fz-juelich.de; A. S. S. Schleker, sylvia.schleker@uni-bonn.de; A. Loeschcke, a.loeschcke@fz-juelich.de.
[†] These authors have contributed equally to this work and share first authorship.
[‡] These authors have contributed equally to this work and share last authorship.

Content

Supplementary Material

I Development of an enhanced *P. putida* mutasynthesis chassis and optimization of mutasynthesis

Supplementary Table S1. Used plasmids and oligonucleotides.

Plasmids		
Name	Relevant characteristics	Reference
pPIG	pUC19, AmpR, *S. marcescens* W838 *pig* gene cluster	(Loeschcke et al., 2013)
pRcExpII2-YF1-FixJ-PFixK2-LacZ	pRcExpII-2, *yf1-fixJ*, P_{fixK2}, *lacZ*, KmR, CmR	(Weihmann et al., 2020)
yTREX	yCP50-poly derived, pMB1 ori, KmR, URA3, mob/oriT, *CEN4*/ARS1, transposon Tn5 *tnp*, OE-L/R, TcR	(Domröse et al., 2017)
yTREX-MBC-lacZ	yTREX, KmR, *pigAFGHIJKLMN-lacZ*, TcR	This study
yTREX-HBC-pigC-lacZ	yTREX, KmR, *pigACGHIJKLM-lacZ*, TcR	This study
pVLT33-pigC	pVLT33 (de Lorenzo et al., 1993), KmR, $LacI^q/P_{tac}$, *pigC*	(Brands et al., 2020)
pVLT33-pigC-pigB	pVLT33, KmR, $LacI^q/P_{tac}$, *pigC-pigB*	This study

Oligonucleotides		
Name	Sequence	Application
Cloning of yTREX-MBC-lacZ		
AD142	AGAAATATTAGCTAATTTAATCTCTCAACCCGATGGCGGAGTTCGTCATGG	PCR *pigA*
AD171	CATTGCTGGCTCCCTAGTCTAAAAAGGTGGAGAGTCATGCGCCTCCCCGCAGAC	PCR *pigA*
AD172	GTCTGCGGGGAGGCGCATGACTCTCCACCTTTTTAGACTAGGGAGCCAGCAATG	PCR *pigFGHI*
AD162	GTTGGACAGATCGATACGATCGATGCCGGGCAGTGCGCAG	PCR *pigFGHI*
AD163	CTGCGCACTGCCCGGCATCGATCGTATCGATCTGTCCAAC	PCR *pigJKLMN*
AD164	GTAATCATGGTCATAGCTGTTTCCTGTGTGTTACAGCACGAAAGGAATGAAACATTTAAC	PCR *pigJKLMN*
AD124	CACACAGGAAACAGCTATGACCATGATTACGGATTCACTGGCCGTCGTTTTAC	PCR *lacZ*
AD125	GAAACAGCTATGACCATGATTACGCCAAGCTAGCGCTTATTTTTGACACCAGACC	PCR *lacZ*
Cloning of yTREX-HBC-pigC-lacZ		
AD142	AGAAATATTAGCTAATTTAATCTCTCAACCCGATGGCGGAGTTCGTCATGG	PCR *pigA*
AD143	CATCACCTCCGCAGGCGTAACGGGCATTGCTCATGCGCCTCCCCGCAGAC	PCR *pigA*
AD144	GTCTGCGGGGAGGCGCATGAGCAATGCCCGTTACGCCTGCGGAGGTGATG	PCR *pigC*
AD145	TGCGAGCTCCCGTTGCTAACTGGTCTAGTTCTAGCCATCGGCACGTTCTCCGCGTTG	PCR *pigC*
AD146	CGCGGAGAACGTGCCGATGGCTAGAACTAGACCAGTTAGCAACGGGAGCTCG	PCR *pigGHIJKLM*
AD158	GTAATCATGGTCATAGCTGTTTCCTGTGTGTCCTCAGCGGATTAGGGGGAATCG	PCR *pigGHIJKLM*
AD124	CACACAGGAAACAGCTATGACCATGATTACGGATTCACTGGCCGTCGTTTTAC	PCR *lacZ*
AD125	GAAACAGCTATGACCATGATTACGCCAAGCTAGCGCTTATTTTTGACACCAGACC	PCR *lacZ*
Cloning of pVLT33-pigC-pigB		
RW144	GTCTGCGGGGAGGCGCATGAGCAATGCCCGTTACGCCTGCGGAGGTGATG	PCR *pigB*
RW145	TGCGAGCTCCCGTTGCTAACTGGTCTAGTTCTAGCCATCGGCACGTTCTCCGCGTTG	PCR *pigB*
qPCR primers		
AD153	TACCTGATAGGCACGCTGTT	PCR *pigN*
AD154	TTGTTCGGATCCTGTTTGAA	PCR *pigN*
AD155	TCGCCAAGAAGTACACCAAC	PCR *rpoD*
AD156	TTTCATCAGACCGATGTTGC	PCR *rpoD*

2

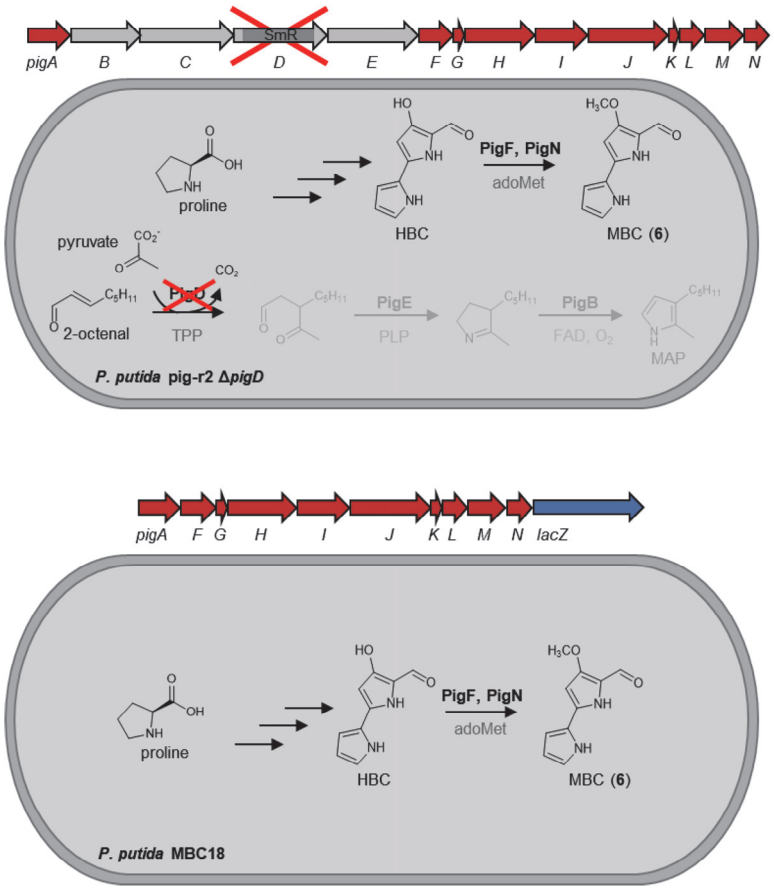

Supplementary Figure S1. Schematic comparison of the MBC-providing *P. putida* chassis pig-r2 Δ*pigD* and MBC18. Chromosomally integrated genes are shown above cells; precursor biosynthetic pathways are schematically shown in cells. **Upper part, *P. putida* pig-r2 Δ*pigD*:** MBC biosynthetic genes are shown in red, MAP biosynthetic genes and ligase-encoding *pigC* are marked in grey. The deletion of *pigD* by integration of a resistance cassette (Klein et al., 2017) is indicated. **Lower part, *P. putida* MBC18:** MBC biosynthetic genes are shown in red, β-galactosidase-encoding *lacZ* is marked in blue. Note that *P. putida* pig-r2 Δ*pigD* is a readily functional mutasynthesis chassis as it also expresses PigC (not shown in the cell), while in MBC18, an additional plasmid for expression of *pigC* and *pigB* has to be introduced.

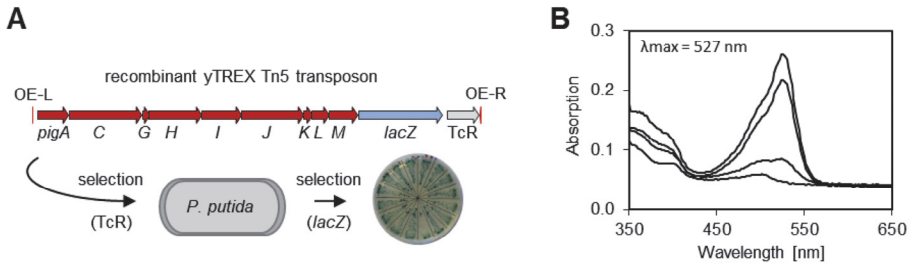

Supplementary Figure S2. Mutasynthesis of norprodigiosin from biosynthesized HBC and supplemented MAP.
(A) The HBC-pigC strain was generated via an analogous procedure to MBC strain construction: *pigA*, *pigC*, and *pigGHIJKLM* were PCR-amplified (primers AD142+AD143, AD144+AD145 and AD146+AD158, respectively) using vector pPIG (Loeschcke et al., 2013) as template. Thereby, *pigNF* and all MAP biosynthetic genes were excluded. In addition, *lacZ* was amplified as promotorless gene (primers AD124+125, 3127 bp) using vector pRcExpII2-YF1-FixJ-PFixK2-LacZ (Weihmann et al., 2020) as template. All genes were amplified with the respective 5'-UTR sequences including the ribosome binding sites; primers added homology arms to each of the fragments. The synthetic gene cluster was assembled into the yTREX vector, which was used for conjugational transfer into *P. putida* KT2440. Clones with integrated recombinant yTREX transposon were selected on LB agar plates containing 50 µg/mL tetracycline. Expressing clones were identified by blue color due to X-gal conversion by *lacZ*-encoded β-galactosidase.
(B) Precultures (1 mL LB medium in Flowerplates) were used to inoculate 1 mL test cultures with an OD_{650} of 0.05 in LB medium. After a 5 h incubation (30 °C, 1200 rpm), 150 µL samples were transferred to a microtiter plate, supplemented with 50 µM MAP, and incubated for 18 h (30 °C, 600 rpm), before metabolites were extracted with acidified ethanol (4% 1 M HCL) and absorption spectra were measured with a plate reader (infinite M1000 PRO, Tecan). Results of quadruplicate measurements showed orange coloration and a characteristic prodiginine absorption (λmax = 527 nm) with extremely varying intensity, which we assigned to norprodigiosin based on previously published data (Mody et al., 1990; Williamson et al., 2005). Samples were additionally analysed via LC-MS as described for MBC strains, which showed specific signals corresponding to the ion [M+H]+ of norprodigiosin (310 m/z), at 8,0 min (data not shown). Since the results were difficult to reproduce, this strategy, which aimed at obtaining norprodigiosin derivatives via mutasynthesis, was not further pursued. However, results were of interest because they indicated that a conversion of HBC and MAP is generally possible in the HBC strain by expression of PigC. Since HBC strains only lack PigN/F compared to MBC strains, this finding pointed to PigN/F completely prohibiting PigC-mediated condensation of MBC and MAP in the MBC strains.

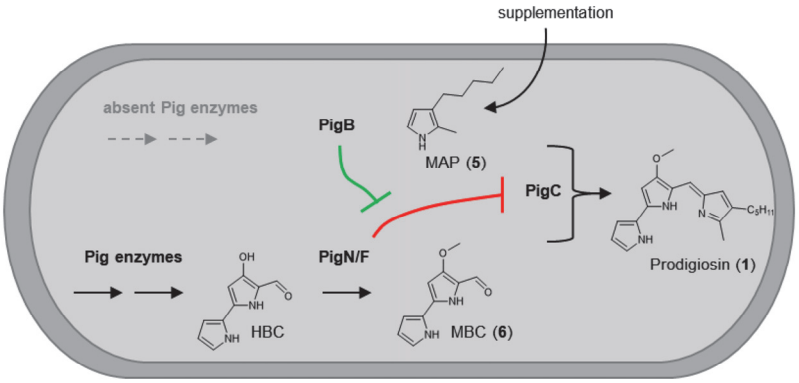

Protein	Function	Putative membrane association*
PigB	Flavin-dependent amine oxidase	3 predicted TMHs, experimental indication (Couturier et al., 2019)
PigC	prodigiosin synthesizing transferase	no predicted TMHs, experimental indication (Chawrai et al., 2012; Brands et al., 2020)
FigF	SAM-dependent O-methyl transferase	no predicted TMHs, potential association to membrane via PigN (Williamson et al., 2005)
PIgN	Unknown function in HBC → MBC conversion (Williamson et al., 2005)	6 predicted TMHs, experimental indication (Williamson et al., 2005)

Supplementary Figure S3. Hypothetical interplay of late prodigiosin biosynthetic Pig enzymes of *S. marcescens* W838. Depicted are our summarized results in this regard: **(i)** PigC by itself is sufficient for condensation of MAP and MBC to prodigiosin. **(ii)** In the absence of MAP biosynthetic enzymes, we supplemented MAP (or analoga) for mutasynthesis (indicated in purple). In this setup, we found the presence of PigN/F to prohibit condensation (indicated in red). **(iii)** In the depicted scenario, only the additional expression of PigB restored condensation (abolishment of the PigN/F-associated inhibition is indicated in green).

Both, the last precursor biosynthetic enzymes and the final ligase PigC are thought to be membrane-associated: While PigC lacks sequence features allowing transmembrane domain prediction, activity is often investigated by utilization of membrane fractions from expression cultures (Chawrai et al., 2012; Brands et al., 2020). PigN has predicted transmembrane helices and mutations in these regions are particularly detrimental to pigment formation (Williamson et al., 2005). Its involvement in the conversion of HBC to MBC by a methyl transfer has been shown and since the actual methyl transferase is clearly PigF (which has no predicted transmembrane domains), a function in protein assembly at the membrane was postulated (Williamson et al., 2005, 2006). Another study recently showed that in a Δ*pigB* mutant of *Serratia* sp. ATCC 39006, the pigmentation phenotype could not be recovered by expression of a PigB version with truncated membrane anchor (Couturier et al., 2019). Only faint recovery was observed with HapB complementation, which is the functional equivalent of PigB in *Hahella chejuensis* but lacks the membrane anchor. This could further point to an essential interplay of the late prodigiosin biosynthetic Pig enzymes of *Serratia* that takes place at the membrane.

Supplementary Material

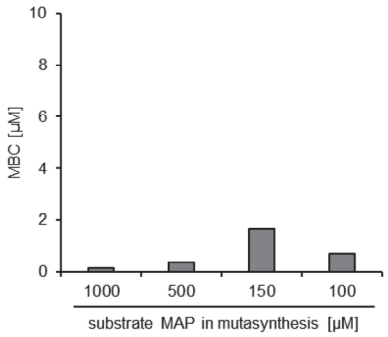

Supplementary Figure S4. Remaining MBC in MBC18/pVLT33-pigC-pigB in mutasynthesis with different MAP concentrations. MBC levels in mutasynthesis cultures were estimated by analysis of crude extracts from PU foam cubes (after recovery from preparative mutasynthesis cultures) via HPLC-PDA.

II Chemical synthesis of pyrroles and preparation of prodiginines

1 General methods and analytics

Mass spectrometry: The reactions were monitored by GS-MS on a Thermo Scientific Frace 1310 Gas Chromatography (*Thermo Scientific,* Waltham, MA, USA) coupled to an ISQ™ QD Single Quadrupole Mass Spectrometer (*Thermo Scientific*, Waltham, MA, USA). For chromatographic separation, an Optima 5MS column (30 m x 0.25 mm, 0.25 µm; *Macherey-Nagel*, Düren, Germany) was used as stationary phase and helium as carrier gas. The measurement followed the following temperature program: 60 °C (1 min), 60−185 °C (15 °C/min), 185−280 °C (120 °C/min), 280 °C (5 min); temperature injector: 250 °C; temperature detector: 230 °C. The ionization method used was electron impact ionization at 70 eV. Fractionation patterns were measured on an Atmospheric Solid Analysis Probe (ASAP) Mass Spectrometer (Model: *Expression Compact*, Advion, New York, USA). Atmospheric pressure chemical ionization (APCI) was used as the ionization method. High-resolution mass spectra (HRMS) were measured at Heinrich Heine University Düsseldorf on a UHR-QTOF maXis 4G (*Bruker*, Massachusetts, USA) using electron spray ionization (ESI).

NMR spectroscopy: For structural elucidation, an NMR data set of all chemical compounds was recorded on the Advance/DRX 600 NMR spectrometer (*Bruker*, Massachusetts, USA). The samples were measured at ambident temperature in $CDCl_3$ at 600 MHz and 151 MHz, respectively. The chemical shift is given in ppm relative to tetramethylsilane [^{1}H: $\delta(SiMe_4) = 0.00$ ppm] as an internal standard or relative to the solvent reference signal [^{1}H: $\delta(CDCl_3) = 7.26$ ppm; ^{13}C: $\delta(CDCl_3) = 77.16$ ppm]. The multiplicities were given as follows: singlet (s), doublet (d), triplet (t), quartet (q), multiplet (m), centred multiplet (m_c) and broad singlet (brs). Quantitative NMR analysis was performed in triplicates with 1,3,5-trimethoxybenzene (*Sigma-Aldrich*) as internal standard.

IR spectroscopy: IR date were recorded on a *SpectrumTwo* ATR-IR instrument (*Perkin Elmer*, Hamburg, Germany). Liquids were measured in pure form. Solids were dissolved in chloroform or dichloromethane and measured after evaporation of the solvent. Absorbance frequencies are reported in cm^{-1}.

2 Synthesis of 2,3-disubstituted pyrroles (11)

The pyrroles **11** were synthesised in a four-step synthesis sequence starting from the according carboxylic acid. The synthesis conditions were adapted from literature (Klein et al., 2017).

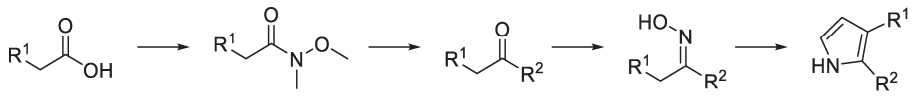

7 **8** **9** **10** **11**

***N*-Methoxy-*N*-methylhept-6-enamid (8b)**

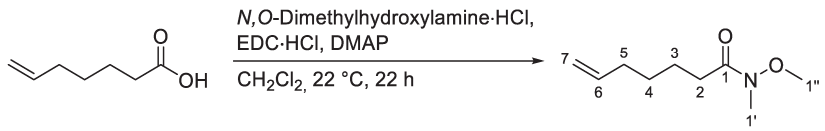

7b **8b**

To a solution of 6-heptenoic acid (3.30 g, 25.8 mmol, 1.0 eq.) in dichloromethane (90.3 mL, 3.5 mL/mmol carboxylic acid) were added *N*,O-dimethylhydroxylamine hydrochlorid (2.36 g, 38.6 mmol, 1.50 eq.), *N*-(3-dimethylaminopropyl)-*N*′ethylcarbodiimid hydrochlorid (6.00 , 38.6 mmol, 1.5 eq.) and 4-(dimethylamino)pyridine (4.72 g, 38.6 mmol, 1.5 eq.). After stirring for 22 h at 22 °C, the reaction mixture was quenched with a saturated solution of NaCl and extracted with dichloromethane (3 x 50 mL). The combined organic layers were first washed with 1 N HCl, afterwards with saturated $NaHCO_3$ solution and dried over $MgSO_4$. After removal of the solvent under reduced pressure *N*-Methoxy-*N*-methylhept-6-enamide (**8b**, 4.20 g, 24.5 mmol, 95%) was obtained as a yellow oil and was used for the following experiment without further purification. **^{1}H-NMR** (600 MHz, $CDCl_3$): δ [ppm] = 1.44 (m_c, 2H, 4-H), 1.65 (m_c, 2H, 3-H), 2.08 (m_c, 2H, 5-H), 2.42 (t, $^3J_{2,3}$ = 7.6 Hz, 2H, 2-H), 3.18 (s, 3H, 1″-H), 3.68 (s, 3H, 1′-H), 4.94 (dd, $^{cis,3}J_{7a,6}$ = 10.2 Hz, $^2J_{7a,7b}$ = 1.2 Hz, 1H, 7-H$_a$), 5.01 (dd, $^{trans,3}J_{7b,6}$ = 17.2 Hz, $^2J_{7b,7a}$ = 1.7 Hz, 1H, 7-H$_b$), 5.81 (ddt, $^{trans,3}J_{6,7b}$ = 16.9 Hz, $^{cis,3}J_{6,7a}$ = 10.2 Hz, $^3J_{6,5}$ = 6.7 Hz, 1H, 6-H); **^{13}C-NMR** (151 MHz, $CDCl_3$): δ [ppm] = 24.2 (C-3), 28.8 (C-4), 31.7 (C-2), 31.8 (C-1″) 33.6 (C-5) 61.3 (C-1′), 114.6 (C-7), 138.7 (C-6). **IR** (ATR-film): $\tilde{\nu}$ [1/cm] = 3074, 2936, 2861, 1663, 1414, 1384, 1177, 1118, 993, 910, 497; **MS** (APCI): *m*/*z* = 172 [$(M)^+$], 123, 83, 55.

Oct-7-en-2-one (9b)

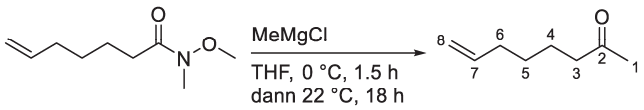

8b **9b**

N-Methoxy-*N*-methylhept-6-enamide (**8b**, 2.80 g, 16.4 mmol, 1.0 eq.) was dissolved in dry THF (100 mL) and methylmagnesium chloride (3 M in diethyl ether, 16.4 mL, 49.1 mmol, 3.0 eq.) was added within 15 min at 0 °C. The reaction mixture was stirred for 1.5 h at 0 °C and afterwards quenched by the addition of a saturated solution of NH_4Cl at 0 °C and extracted with dichloromethane (3 x 60 mL). The combined organic layers were dried over $MgSO_4$ and the solvent was evaporated under reduced pressure to yield oct-7-en-2-one (**8b**, 1.63 g, 11.6 mmol, 94%) as a yellowish oil without further purification. **^{1}H-NMR** (600 MHz, $CDCl_3$): δ [ppm] = 1.39 (tt, $^3J_{5,4}$ = 9.5 Hz, $^3J_{5,6}$ = 6.8 Hz, 2H, 5-H), 1.56–1.62 (m, 2H, 4-H), 2.06 (dt, $^3J_{6,5}$ = 7.3 Hz, $^3J_{6,7}$ = 7.0 Hz, 2H, 6-H), 2.13 (s, 3H, 1-H), 2.43 (t, $^3J_{3,4}$ = 7.4 Hz, 2H, 3-H), 4.95 (dd, $^{cis,3}J_{8a,7}$ = 10.2 Hz, $^2J_{8a,8b}$ = 1.2 Hz, 1H, 8-H$_a$), 5.01 (dd, $^{trans,3}J_{8b,7}$ = 17.1 Hz, $^2J_{8b,8a}$ = 1.7 Hz, 1H, 8-H$_b$), 5.79 (ddt, $^{trans,3}J_{7,8b}$ = 17.0 Hz, $^{cis,3}J_{7,8a}$ = 10.2 Hz, $^3J_{7,6}$ = 6.7 Hz, 1H, 7-H); **^{13}C-NMR** (151 MHz, CDCl3): δ [ppm] = 23.4 (C-4), 28.5 (C-5), 30.0 (C-6), 33.5 (C-1), 43.7 (C-3), 114.8 (C-8), 138.6 (C-7), 209.2 (C-2); **IR** (ATR-film): $\tilde{\nu}$ [1/cm] = 3074, 2934, 2861, 1717, 1601, 1363, 1217, 992, 913; **MS** (APCI): *m*/*z* = 123, 109.

General synthesis procedure for oximes (10)

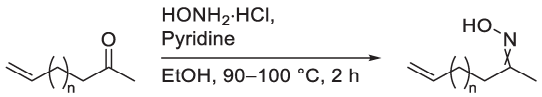

9b,c **10b,c**

To a solution of the ketone (9b,c, 1.0 eq.) in undenatured EtOH (0.5 mL/mmol ketone) was added pyridine (0.8 eq.) and ground hydroxylamine hydrochloride (1.5 eq.). The reaction mixture was heated for 2 h at 90−100 °C under reflux and afterwards extracted with dichloromethane (3 x 25 mL). The combined organic layers were washed with 1 N HCl (3 x 20 mL) and then dried over $MgSO_4$. After removal of the solvent under reduced pressure, the oxime (**10b,c**) was obtained as *E*/*Z* isomer mixture without further purification.

Oct-7-enone oxime (10b)

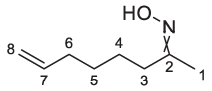

10b

According to the general procedure for the synthesis of oximes, the oxime **10b** was prepared from oct-7-en-2-one (**9b**, 1.42 g, 11.3 mmol) and hydroxylamine hydrochloride (1.17 g, 16.9 mmol) and was obtained as a yellow oil (1.40 g, 10.1 mmol, 88%). **^{1}H-NMR** (600 MHz, $CDCl_3$): δ [ppm] = 1.38−1,44 (m, 2H, 5-H), 1.50−1.60 (m, 2H, 4-H), 1.91 (s, 3H, 1-H), 2.07 (dt, $^3J_{6,5}$ = 7.8 Hz, $^3J_{6,7}$ = 7.8 Hz, 2H, 6-H), 2.24 (t, $^3J_{3,4}$ = 7.5 Hz, 2H, 3-H), 4.93−4.97 (m, 1H, 8-H_a), 5.01 (dd, $^{trans,3}J_{8b,7}$ = 17.1 Hz, $^2J_{8b,8a}$ = 1.7 Hz, 1H, 8-H_b), 5.78 (m, 1H, 7-H); **^{13}C-NMR** (151 MHz, $CDCl_3$): δ [ppm] = 13.6 (C-1), 25.8 (C-4), 28.4 (C-5), 33.5 (C-6), 35.4 (C-3), 114.8 (C-8), 138.6 (C-7); **IR** (ATR-Film): $\tilde{\nu}$ [1/cm] = 2971, 2922, 2861, 1735, 1443, 1363, 1217, 901, 748; **MS** (APCI): *m*/*z* = 142 [$(M)^+$], 115, 109.

Dec-9-enone oxime (10c)

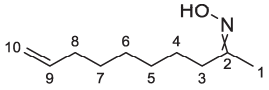

10b

According to the general procedure for the synthesis of oximes, oxime **10c** was prepared from commercial available dec-9-en-2-one (**9c**, 4.34 g, 28.1 mmol) and hydroxylamine hydrochloride (2.93 g, 42.2 mmol) and was obtained as a yellow oil (4.70 g, 27.7 mmol, 99%). **^{1}H-NMR** (600 MHz, $CDCl_3$): δ [ppm] = 1.31−1.37 (m, 4H, 6-H, 7-H), 1.37−1.43 (m, 2H, 5-H), 1.49−1.57 (m, 2H, 4-H), 1.89 (s, 3H, 1-H), 2.06 (dt, $^3J_{8,7}$ = 7.1 Hz, $^3J_{8,9}$ = 7.1 Hz, 2H, 8-H), 2.19 (t, $^3J_{3,4}$ = 7.6 Hz, 2H, 3-H), 4.91−4.97 (m, 1H, 10-H_a), 5.01 (dd, $^{trans,3}J_{10b,9}$ = 17.2 Hz, $^2J_{10b,10a}$ = 1.7 Hz, 1H, 10-H_b), 5.83 (ddt, $^{trans,3}J_{9,10b}$ = 16.9 Hz, $^{cis,3}J_{9,10a}$ = 10.0 Hz, $^3J_{9,8}$ = 6.7 Hz, 1H, 9-H); **^{13}C-NMR** (151 MHz, $CDCl_3$): δ [ppm] = 13.4 (C-1), 26.3 (C-4), 28.9 (C-5), 29.0 (C-6), 29.2 (C-7), 33.9 (C-8), 35.9 (C-3), 114.4 (C-10), 139.2 (C-9), 159.1 (C-2); **IR** (ATR-film): $\tilde{\nu}$ [1/cm] = 3081, 2927, 1641, 1463, 1368, 993, 909; **MS** (APCI): *m*/*z* = 170 [$(M)^+$], 168, 152. **HRMS** (ESI, positive ion): calculated for $C_{10}H_{20}NO$ $(M + H)^+$ = 170.1539, found = 170.1540.

General synthesis procedure for pyrroles (11)

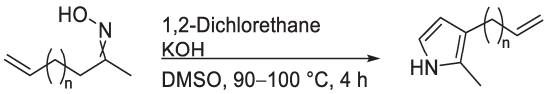

10b,c **11c,d**

To a solution of oxime (**10b,c**, 1.0 eq.) in DMSO (2.14 mL/mmol oxime) was added ground KOH (5.0 eq.) and water (0.75 eq.). A solution of 1,2-dichloroethane (3.5 eq.) in DMSO (0.21 mL/mmol oxime) was added at 95 °C over a period of 2 h by a syringe pump. After 1 h addition, again KOH (5.0 eq.) was added. After a total reaction time of 4 h at 90−100 °C, the reaction was cooled to 23 °C, ice water (20 mL) was added and extracted with diethyl ether (3 x 20 mL). The combined organic layers were dried over $MgSO_4$ and the solvent evaporated under reduced pressure. Subsequent column chromatographic separation [silica gel, PE/AcOEt (80:20) + 1% (*v*/*v*) trimethylamine] allowed excess starting material to be removed and the pyrrole (**11b,c**) was subsequently isolated as a colourless oil via a ball tube distillation (1 mbar, 70−80 °C). The reaction was monitored via thin layer chromatography, GC-MS and ^{1}H NMR. The product was stored under argon atmosphere at −20 °C.

2-Methyl-3-(pent-4-en-1-yl)-1*H*-pyrrole (11c)

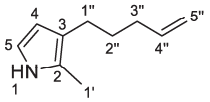

11c

According to the general procedure for the synthesis of pyrroles, the pyrrole **11c** was prepared from oct-7-ene-2-one oxime (**10b**, 1.59 g, 11.2 mmol) and obtained as a colourless oil (863.0 mg, 5.78 mmol, 51%). In addition the side products *N*-vinyl pyrrole (207 mg, 1.18 mmol, 11%) and oxime diether (217 mg, 0.70 mmol, 6%) were isolated. **^{1}H-NMR** (600 MHz, $CDCl_3$): δ [ppm] = 1.63 (tt, $^3J_{2'',1''}$ = 7.6 Hz, $^3J_{2'',3''}$ = 7.6 Hz, 2H, 2″-H), 2.02−2.14 (m, 2H, 3″-H), 2.18 (s, 3H, 1′-H), 2.40 (t, $^3J_{1'',2''}$ = 7.8 Hz, 2H, 1″-H), 4.95 (dd, $^{cis,3}J_{5a'',4''}$ = 10.2 Hz, $^2J_{5a'',5b''}$ = 1.3 Hz, 1H, 5″-H$_a$), 5.02 (dd, $^{trans,3}J_{5b'',4''}$ = 17.1 Hz, $^2J_{5b'',5a''}$ = 1.8 Hz, 1H, 5″-H$_b$), 5.85 (ddt, $^{trans,3}J_{4'',5b''}$ = 16.9 Hz, $^{cis,3}J_{4'',5a''}$ = 10.2 Hz, $^3J_{4'',3''}$ = 6.6 Hz, 1H, 4″-H), 6.01 (dd, $^4J_{4,1}$ = 2.8 Hz, $^3J_{4,5}$ = 2.8 Hz, 1H, 4-H), 6.59 (dd, $^3J_{5,1}$ = 2.7 Hz, $^3J_{5,4}$ = 2.7 Hz, 1H, 5-H), 7.71 (brs, 1H, 1-NH); **^{13}C-NMR** (151 MHz, $CDCl_3$): δ [ppm] = 11.2 (C-1′), 25.5 (C-1″), 30.6 (C-2″), 33.7 (C-3″), 109.0 (C-4), 114.4 (C-5″), 115.0 (C-5), 119.4 (C-3), 123.5 (C-2), 139.3 (C-4″); **IR** (ATR-film): $\tilde{\nu}$ [1/cm] = 3381, 3074, 2971, 2928, 2855, 1637, 1443, 1108, 992, 907, 712; **MS** (APCI): *m*/*z* = 150 [(M)$^+$], 108.

2-Methyl-3-(hept-6-en-1-yl)-1*H*-pyrrole (11d)

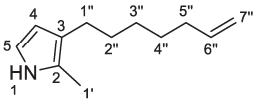

11d

According to the general procedure for the synthesis of pyrroles, the pyrrole **11d** was prepared from dec-9-ene-2-one oxime (**10c**, 3.00 g, 17.7 mmol) and was obtained as a colorless oil (935 mg, 5.3 mmol, 30%). **^{1}H-NMR** (600 MHz, $CDCl_3$): δ [ppm] = 1.44 (tt, $^3J_{3'',2''}$ = 7.5 Hz, $^3J_{3'',4''}$ = 7.5 Hz, 2H, 3″-H), 1.51−1.59 (m, 2H, 2″-H), 2.02−2.14 (m, 2H, 4″-H), 2.18 (s, 3H, 1′-H), 2.39 (t, $^3J_{1'',2''}$ = 7.6 Hz, 2H, 1″-H), 4.93 (dd, $^{cis,3}J_{6a'',5''}$ = 10.2 Hz, $^2J_{6a'',6b''}$ = 1.2 Hz, 1H, 6″-H_a), 5.00 (dd, $^{trans,3}J_{6b'',5''}$ = 17.1 Hz, $^2J_{6b'',6a''}$ = 1.7 Hz, 1H, 6″-H_b), 5.82 (ddt, $^{trans,3}J_{5'',6b''}$ = 16.9 Hz, $^{cis,3}J_{5'',6a''}$ = 10.2 Hz, $^3J_{5'',4''}$ = 6.7 Hz, 1H, 5″-H), 6.01 (dd, $^4J_{4,1}$ = 2.8 Hz, $^3J_{4,5}$ = 2.8 Hz, 1H, 4-H), 6.59 (dd, $^3J_{5,1}$ = 2.7 Hz, $^3J_{5,4}$ = 2.7 Hz, 1H, 5-H), 7.70 (brs, 1H, 1-NH); **^{13}C-NMR** (151 MHz, $CDCl_3$): δ [ppm] = 11.2 (C-1′), 25.9 (C-1″), 28.9 (C-3″), 31.0 (C-2″), 33.9 (C-4″), 109.0 (C-4), 114.3 (C-6″), 115.0 (C-5), 119.7 (C-3), 123.4 (C-2), 139.4 (C-5″); **IR** (ATR-film): $\tilde{\nu}$ [1/cm] = 3385, 2928, 2855, 1741, 1467, 1363, 1217, 907, 712; **MS** (APCI): *m*/*z* = 164 [$(M)^+$], 121, 108; **HRMS** (ESI, positive ion): calculated for $C_{11}H_{18}N$ $(M + H)^+$ = 164.1434, found = 164.1433.

3 Procedure for hydroxylation of pyrroles with terminal double bond

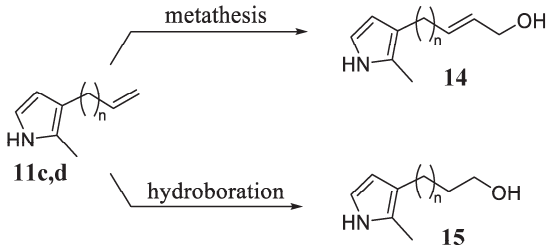

To synthesis pyrrole **14** with allyl alcohol function, a modified metathesis procedure was used(Taber and Frankowski, 2006; Habash et al., 2020). The hydroboration towards pyrrole **15** was performed following the method previously described (Aldrich, 2012).

(*E*)-6-(2-methyl-1*H*-pyrrole-3-yl)hex-2-en-1-ol (14)

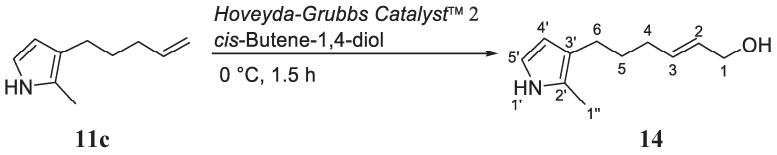

11c **14**

2-Methyl-3-(pent-4-en-1-yl)-1*H*-pyrrole **(11c**, 53.0 mg, 0.36 mmol, 1.0 eq.**)** and *cis*-butene-1,4-diol (125 mg, 1,41 mmol, 4.0 eq.) were dissolved in dry dichloromethane (2.5 mL). At 0 °C, *Hoveyda-Grubbs Catalyst*™ 2nd Generation (7.69 mg, 12.3 µmol, 3 mol-%) was added and the reaction was stirred for 1.5 h at 0 °C. After removal of the solvent under reduced pressure, the crude product was purified by column chromatography [silica gel; PE/AcOEt (70:30, 30−60% AcOEt gradient) + 1% (*v*/*v*) trimethylamine] to give (*E*)-6-(2-methyl-1*H*-pyrrol-3-yl)hex-2-en-1-ol (**14**, 30.0 mg, 0.17 mmol, 47%) as yellow oil. The reaction was monitored by thin layer chromatography, GC-MS and ^{1}H NMR. The products were stored under argon atmosphere at −20 °C. 0.36 mmol). **^{1}H-NMR** (600 MHz, $CDCl_3$): δ [ppm] = 1.2 (brs, 1H, 1-OH), 1.6−1.7 (m, 2H, 5-H), 2.05−2.14 (m, 2H, 4-H), 2.18 (s, 3H, 1″-H), 2.40 (t, $^3J_{6,5}$ = 7.6 Hz, 2H, 6-H), 4.09 (d, $^3J_{1,2}$ = 5.7 Hz, 2H, 1-H), 5.69 (m_c,

2H, 3-H, 2-H), 6.00 ($^4J_{4',1'}$ = 2.8 Hz, $^3J_{4',5'}$ = 2.8 Hz, 1H, 4′-H), 6.59 (dd, $^3J_{5',1'}$ = 2.7 Hz, $^3J_{5',4'}$ = 2.7 Hz, 1H, 5′-H), 7.72 (brs, 1H, 1′-NH); **^{13}C-NMR** (151 MHz, $CDCl_3$): δ [ppm] = 11.2 (C-1″), 25.5 (C-6), 30.7 (C-5), 32.1 (C-4), 64.0 (C-1), 109.0 (C-4′), 115.0 (C-5′), 119.1 (C-3′), 123.3 (C-2′), 129.1 (C-3), 133.7 (C-2); **IR** (ATR-film): $\tilde{\nu}$ [1/cm] = 3373, 2922, 2855, 1741, 1443, 1363, 1089, 974, 706; **MS** (APCI): *m/z* = 180 [$(M)^+$], 162, 120; **HRMS** (ESI, positive ion): calculated for $C_{11}H_{18}NO$ $(M + H)^+$ = 180.1383, found = 180.1382.

7-(2-methyl-1*H*-pyrrole-3-yl)heptan-1-ol (15)

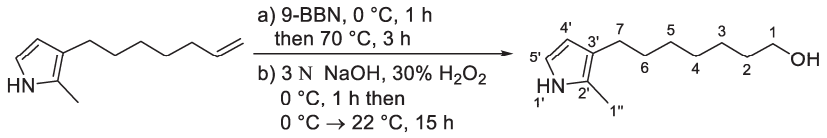

11d **15**

9-BBN (0.5 N in THF, 2.02 g, 1.13 mmol, 2.2 eq.) was added to a solution of 3-(hept-6-en-1-yl)-2-methyl-1*H*-pyrrole (**11d**, 91.0 mg, 0.51 mmol, 1.0 eq.) in dry THF (4.2 mL) over a period of 15 min at 0 °C. After stirring for 1 h at 0 °C, the reaction mixture was heated up at 70 °C under reflux for 3 h. Subsequently an aqueous solution of 3 N NaOH (866 mg, 855 µL, 2.57 mmol, 5.0 eq.) and 30% H_2O_2 (815 mg, 731 µL, 7.19 mmol, 14.0 eq.) was added at 0 °C. After 1 h at 0 °C the reaction mixture was allowed to reach room temperature and was stirred for further 15 h at 22 °C. Ice water (40 mL) was added and the mixture was extracted with dichloromethane (3 x 50 mL). The combined organic layers were dried over $MgSO_4$, the solvent was evaporated under reduced pressure and the crude product was purified by column chromatography on silica gel [PE:ethyl acetate (70:30 to 50:50) + 1% (*v/v*) trimethylamine] to isolate 7-(2-methyl-1*H*-pyrrole-3-yl)heptan-1-ol (**15**, 49 mg, 0.25 mmol, 50%) as orange oil. **^{1}H-NMR** (600 MHz, $CDCl_3$): δ [ppm] = 1.18 (brs, 1H, 1-OH), 1.30−1.35 (m, 6H, 3-H, 4-H, 5-H), 1.48−1.60 (m, 4H, 2-H, 6-H), 2.18 (s, 3H, 1″-H), 2.38 (t, $^3J_{7,6}$ = 7.6 Hz, 2H, 7-H), 3.63 (t, $^3J_{1,2}$ = 7.6 Hz, 2H, 1-H), 6.00 (dd, $^4J_{4',1'}$ = 2.9 Hz, $^3J_{4',5'}$ = 2.8 Hz, 1H, 4′-H), 6.59 (dd, $^3J_{5',1'}$ = 2.7 Hz, $^3J_{5',4'}$ = 2.7 Hz, 1H, 5′-H), 7.72 (brs, 1H, 1′-NH); **^{13}C-NMR** (151 MHz, $CDCl_3$): δ [ppm] = 11.2 (C-1″), 25.8 (C-7), 26.0 (C-5), 29.5 (C-4), 29.6 (C-3), 31.4 (C-6), 33.0 (C-2), 63.3 (C-1), 109.0 (C-4′), 115.0 (C-5′), 119.8 (C-3′), 123.3 (C-2′); **IR** (ATR-film): $\tilde{\nu}$ [1/cm] = 3373, 2927, 2855, 1741, 1686, 1467, 1369, 1053, 712; **MS** (APCI, positive ion): *m/z* = 196 [$(M)^+$], 178; **HRMS** (ESI, positive ion): calculated for $C_{12}H_{22}NO$ $(M + H)^+$ = 196.1696, found = 196.1697.

4 General synthesis procedure of prodiginines

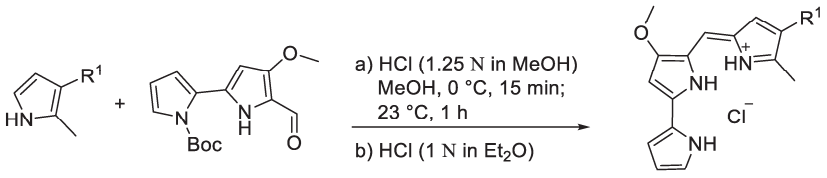

14, 15 *Boc*-**6** **2, 13**

The chemical condensation reaction towards the prodiginines **2** and **13** was performed in a modified reaction procedure (Brass et al., 2019).

To a solution of *Boc*-**6** (1.0 eq.) in dry methanol (20 mL/mmol *Boc*-**6**) was added a solution of the corresponding pyrrole (**14**, **15**, 1.0 eq.) in dry methanol (6 mL/mmol *Boc*-MBC), as well as a HCl in methanol solution (1.25 M, 1.3 eq.) at 0 °C in parallel via two syringes. After stirring for 15 min at 0 °C, the dark red reaction mixture was stirred at 23 °C for 1 h. The reaction was quenched by adding an aqueous ammonia solution [25% (*w*/*w*)] until the reaction solution showed an orange color. The mixture was extracted with dichloromethane (3 x 10 mL), the combined organic layers were washed with saturated NaCl solution and dried over $MgSO_4$. The solvent was evaporated under reduced pressure and the crude product was purified by column chromatography [silica gel; dichloromethane/ammonia in MeOH (7 N)-gradient; then aluminium oxide; *n*-pentane/AcOEt-gradient]. A few drops of HCl solution (1 M in diethyl ether) were added to the product and after evaporation of the solvent, prodiginines (**2**, **13**) were obtained in their hydrochloride form as dark red solids. The products were coated with argon and stored at −20 °C.

(*E*)-6-((*Z*)-2-((4-methoxy-1*H*,1'*H*-[2,2'-bipyrrol]-5-yl)methylene)-5-methyl-2*H*-pyrrol-4-yl)hex-2-en-1-ol hydrochloride (2)

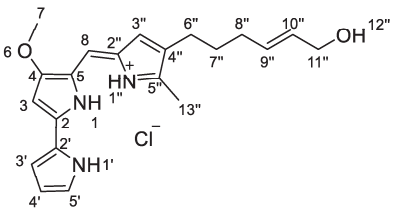

2

Following the general procedure for the synthesis of prodiginines, prodiginine **2** was prepared from *Boc*-**6** (68.0 mg, 0.23 mmol, 1.0 eq.) and the pyrrole **13** (42.0 mg, 0.23 mmol, 1.0 eq.). After purification by column chromatography [silica gel; dichloromethane/ammonia in MeOH (7 N, 0.5-4% gradient); then alumina; *n*-pentane/AcOEt (10-100% gradient; then 1-6% MeOH gradient] and precipitation as hydrochloride, **2** (39.6 mg, 0.10 mmol, 44%) was obtained as dark red solid. **^{1}H-NMR** (600 MHz, $CDCl_3$): δ [ppm] = 1.63 (tt, $^3J_{7'',6''}$ = 7.6 Hz, $^3J_{7'',8''}$ = 7.6 Hz, 2H, 7″-H), 2.08 (dt, $^3J_{8'',7''}$ = 6.9 Hz, $^3J_{8'',9''}$ = 6.9 Hz, 2H, 8″-H), 2.40 (t, $^3J_{6'',7''}$ = 7.6 Hz, 2H, 6″-H), 2.53 (s, 3H, 13″-H), 4.00 (s, 3H, 7-H), 4.10 (d, $^3J_{11'',10''}$ = 5.0 Hz, 2H, 11′-H), 5.67 (ddt, $^3J_{9'',10''}$ = 15.6 Hz, $^3J_{9'',8''}$ = 10.3 Hz, $^3J_{10'',11''}$ = 5.7 Hz, 2H, 9″-H, 10″-H), 6.07 (d, $^4J_{3,1}$ = 1.9 Hz, 1H, 3-H), 6.34 (dd, $^3J_{4',5'}$ = 4.3 Hz, $^4J_{4',1'}$ = 2.3 Hz, 1H, 4′-H), 6.66 (d, $^4J_{3'',1''}$ = 2.7 Hz, 1H, 3″-H), 6.92 (m_c, 1H, 3′-H), 6.93 (s, 1H, 8-H), 7.22 (dd, $^3J_{5',4'}$ = 2.8 Hz, $^3J_{5',1'}$ = 1.4 Hz, 1-H, 5′-H), 12.55 (brs, 1H, 1′-NH), 12.71 (brs, 2H, 1-NH, 1″-NH); **^{13}C-NMR** (151 MHz, $CDCl_3$): δ [ppm] = 12.6 (C-13″), 25.0 (C-6″), 29.6 (C-7″), 31.8 (C-8″), 58.9 (C-7), 63.8 (C-11″), 93.0 (C-3), 111.9 (C-4′), 116.1 (C-3′), 117.4 (C-8), 121.0 (C-5), 122.4 (C-2′), 125.3 (C-2″), 127.2 (C-5′), 127.9 (C-4″), 128.3 (C-3″), 129.7 (C-10″), 132.6 (C-9″), 146.8 (C-5″), 148.1 (C-2), 166.0 (C-4); **IR** (ATR-film): $\tilde{\nu}$ [1/cm] = 3166, 3106, 2932, 2854, 1734, 1630, 1603, 1548, 1509, 1358, 1258, 1140, 1118, 1043, 993, 960, 835, 745; **MS** (APCI, positiv-Ion): *m*/*z* = 352 [$(M)^+$], 334, 163; **HRMS** (ESI, positive ion): calculated for $C_{21}H_{26}N_3O_2$ $(M + H)^+$ = 352.2020, found = 352.2018.

(*Z*)-7-(2-((4-methoxy-1*H*,1'*H*-[2,2'-bipyrrol]-5-yl)methylene)-5-methyl-2*H*-pyrrol-4-yl)heptan-1-ol hydrochloride (13)

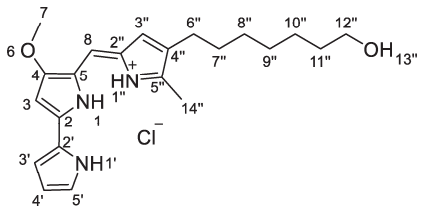

13

Following the general procedure for the synthesis of prodiginines, prodiginine **13** was prepared from *Boc*-**6** (100 mg, 0.34 mmol, 1.0 eq.) and the pyrrole **15** (67 mg, 0.34 mmol, 1.0 eq.). After purification by column chromatography [silica gel; dichloromethane/ammonia in MeOH (7 N, 0.5−4% gradient); then alumina; *n*-pentane/AcOEt (10−100% gradient; then 1−8% MeOH gradient] and precipitation as hydrochloride, **13** (89.8 mg, 0.22 mmol, 65%) was obtained as a dark red solid. **^{1}H-NMR** (600 MHz, $CDCl_3$): δ [ppm] = 1.35 (m_c, 6H, 8″-H, 9″-H, 10″-H), 1.50−1.59 (m, 4H, 7″-H, 11″-H), 2.38 (t, $^3J_{6'',7''}$ = 7.3 Hz, 2H, 6″-H), 2.53 (s, 3H, 14″-H), 3.63 (t, $^3J_{12'',11''}$ = 6.5 Hz, 2H, 12″-H), 3.99 (s, 3H, 7-H), 6.07 (dd, $^4J_{3,1}$ = 3.0 Hz, 1H, 3-H), 6.34 (1H, $^3J_{4',5'}$ = 2.5 Hz, $^4J_{4',1'}$ = 2.5 Hz, 4′-H), 6.66 (s, 1H, 3″-H), 6.91 (s, 1H, 3′-H), 9.94 (s, 1H, 8-H), 7.22 (s, 1H, 5′-H), 12.55 (brs, 1H, 1′-NH), 12.71 (brs, 1H, 1-NH, 1″-NH); **^{13}C-NMR** (151 MHz, $CDCl_3$): δ [ppm] = 12.6 (C-14″), 25.5 (C-6″), 25.8 (C-8″), 29.3 (C-9″), 29.4 (C-10″), 30.2 (C-11″), 32.9 (C-7″), 58.9 (C-7), 63.1 (C-12″), 93.0 (C-3), 111.9 (C-4′), 116.1 (C-8), 117.2 (C-3′), 120.9 (C-5), 122.4 (C-2′), 125.3 (C-2″), 127.0 (C-5′), 127.1 (C-4″), 128.5 (C-3″), 147.0 (C-5″), 147.9 (C-2), 165.9 (C-4); **IR** (ATR-film): $\tilde{\nu}$ [1/cm] = 3007, 2965, 2928, 2855, 1735, 1607, 1540, 1369, 1217, 961; **MS** (APCI, positive ion): *m*/*z* = 368 [$(M)^+$], 341, 313, 267; **HRMS** (ESI, positive ion): calculated for $C_{22}H_{30}N_3O_2$ $(M + H)^+$ = 368.2333, found = 368.2336.

5 Optimization of preparative mutasynthesis

Supplementary Table S2. Optimization of preparative mutasynthesis. The mutasynthesis was performed according to the general procedure for preparative scale mutasynthesis. The final concentration of MAP (**5**) varied from 0.1−1.0 mM resulting in yields between 17% and 62%.

c(MAP) in 500 mL culture [mM]	*n*(MAP) [mmol]	*m*(Prodigiosin) [mg]	*n*(Prodigiosin) [µmol]	yield [%]
1.00	0.50	30.0	83.4	17
0.50	0.25	26.0	72.2	29
0.25	0.125	19.8	55.0	44
0.15	0.075	16.8	46.7	62
0.10	0.05	4.00	11.1	22

6 Calculation of molar extinction coefficient

The determination of the molar extinction coefficients ε of the prodiginines **2**, **3**, **12** and **13** was carried out on a UV photometer (*Shimadzu*, Duisburg, Germany). In a triplicate determination, three 4 mM stock solutions were prepared in acidic ethanol [4% (*v*/*v*) 1 N HCl in ethanol] and a 40 µM working solution was prepared in each case by dilution with acidic ethanol. A dilution series was prepared with all three working solutions, resulting in 3 x 6 samples in the concentration range of 1−6 µM for three-fold determination. The volumes used to prepare the dilution series are listed in the following table:

Supplementary Table S3. Dilution series for determination of molar extinction coefficients.

dilution series / µM	added volume of 40 µM stock solution / µL	added volume of acidic ethanol / µL
1	25	975
2	50	950
3	75	925
4	100	900
5	125	875
6	150	850

The absorbances of the dilution series were measured at a wavelength λ of 535 nm. According to *Lambert-Beer's* law, with a linear dependence of absorption A and concentration c, the molecular extinction coefficient ε corresponds to the slope through the layer thickness of the cuvette (polystyrene cuvettes, d = 1 cm):

$$\varepsilon = \frac{A}{c \cdot d} = \frac{\text{slope}}{d} \qquad (1)$$

The respective graphs are shown in **Supplementary Figure S5**.

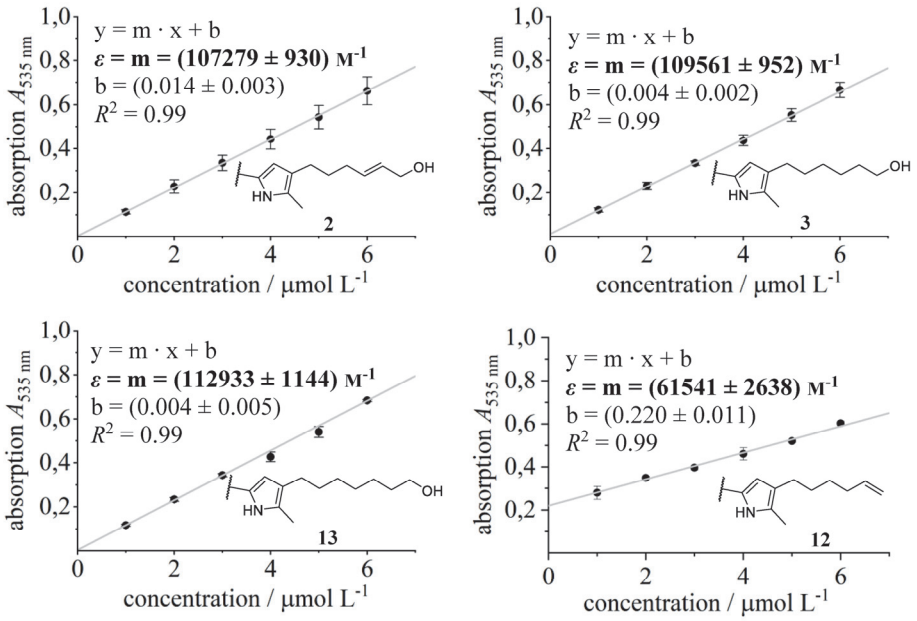

Supplementary Figure S5. Calculation of molar extinction coefficients *ε*. The measurement is carried out in acidic ethanol [4% (*v*/*v*) 1 N HCl] at a wavelength of 535 nm in a three-fold determination. The absorbance values were plotted against the concentrations and linear regression by *OriginPro* 2021 (*OriginLap Corp.*) was used to determine the slopes, which were equated to the molar extinction coefficients *ε*. Chemical structures show the C-pyrrole ring of the measured prodiginine derivatives.

7 Analytical data

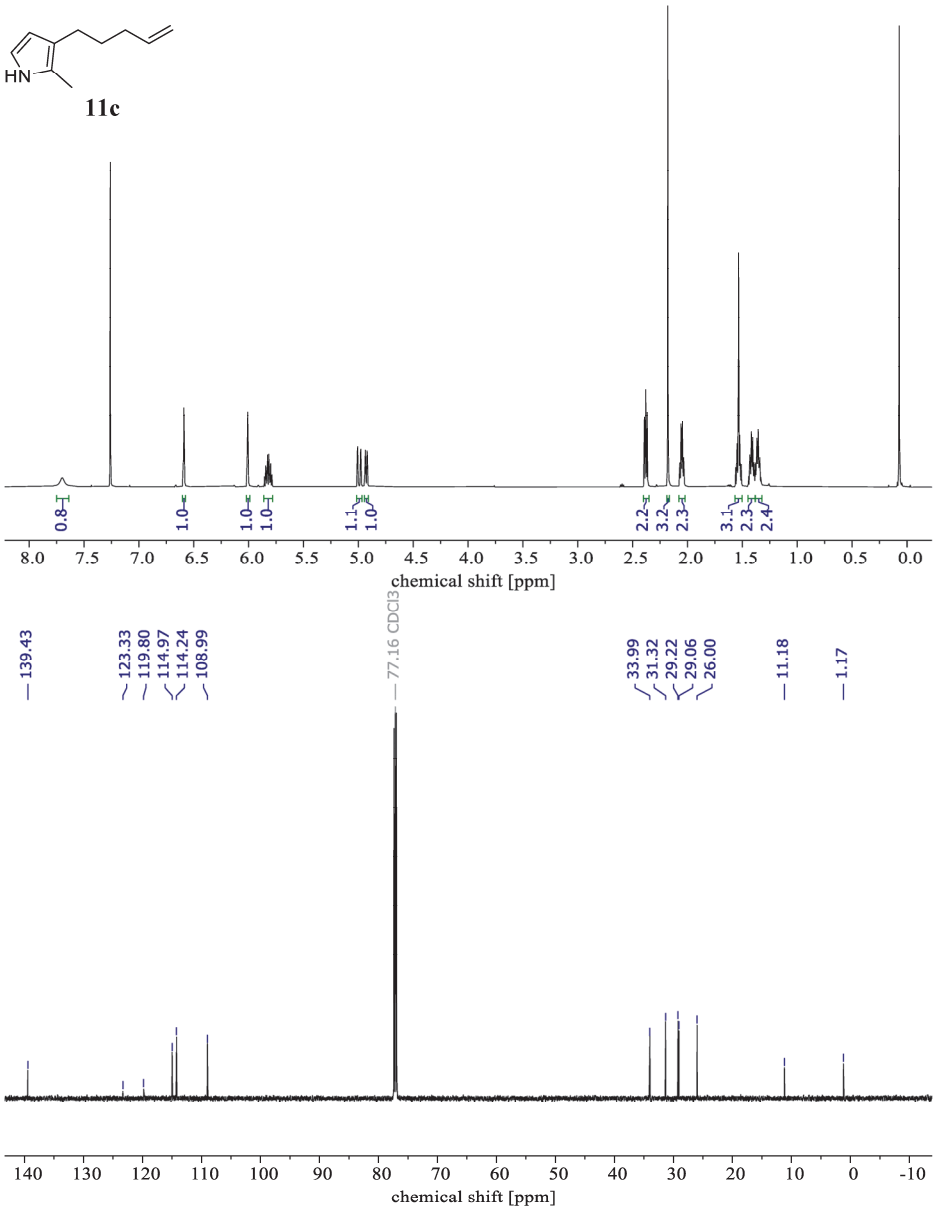

17

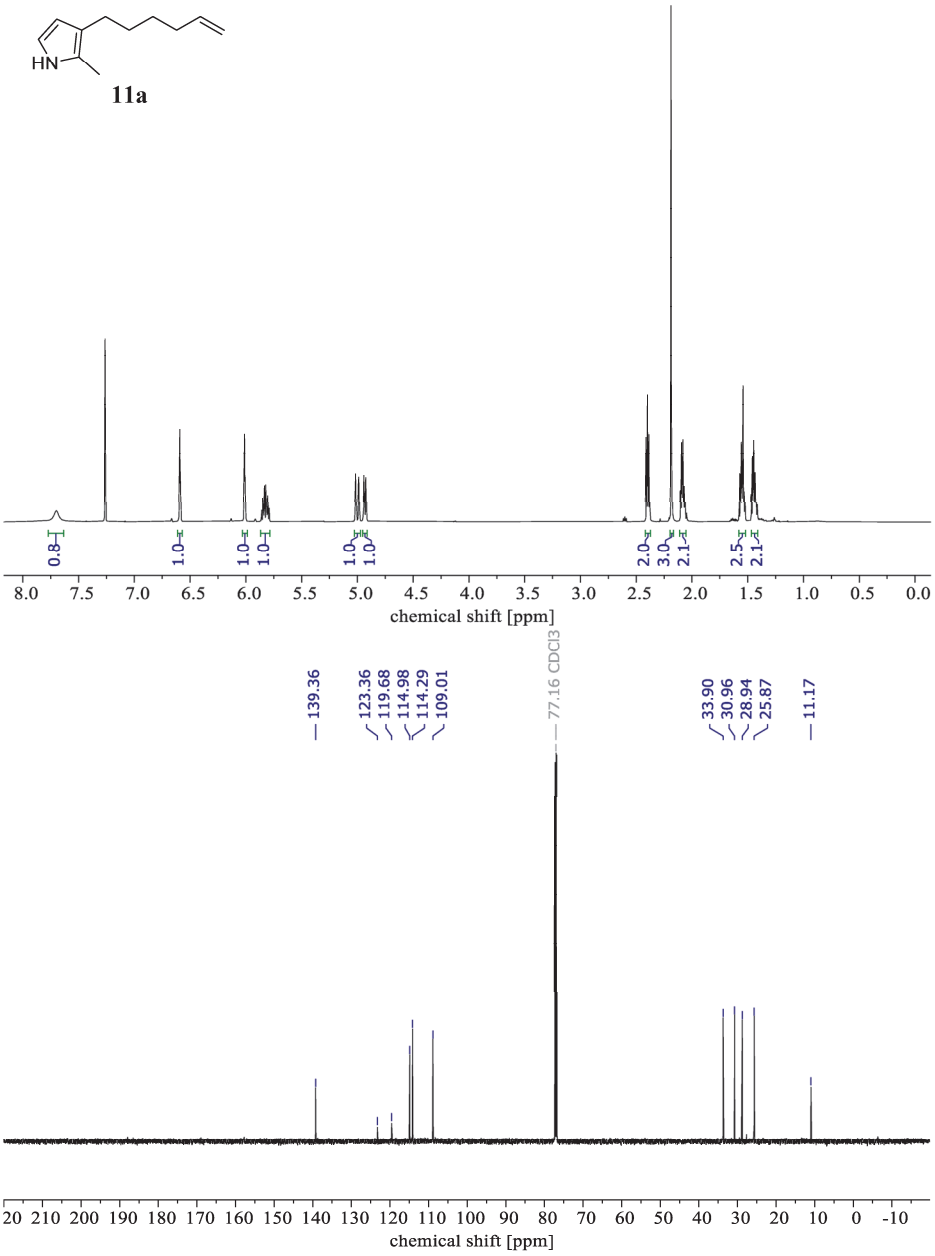
HN
11a
0.8
1.0
1.0
1.0
1.0
1.0
2.0
3.0
2.1
2.5
2.1
8.0 7.5 7.0 6.5 6.0 5.5 5.0 4.5 4.0 3.5 3.0 2.5 2.0 1.5 1.0 0.5 0.0
chemical shift [ppm]
139.36
123.36
119.68
114.98
114.29
109.01
77.16 CDCl3
33.90
30.96
28.94
25.87
11.17
20 210 200 190 180 170 160 150 140 130 120 110 100 90 80 70 60 50 40 30 20 10 0 -10
chemical shift [ppm]

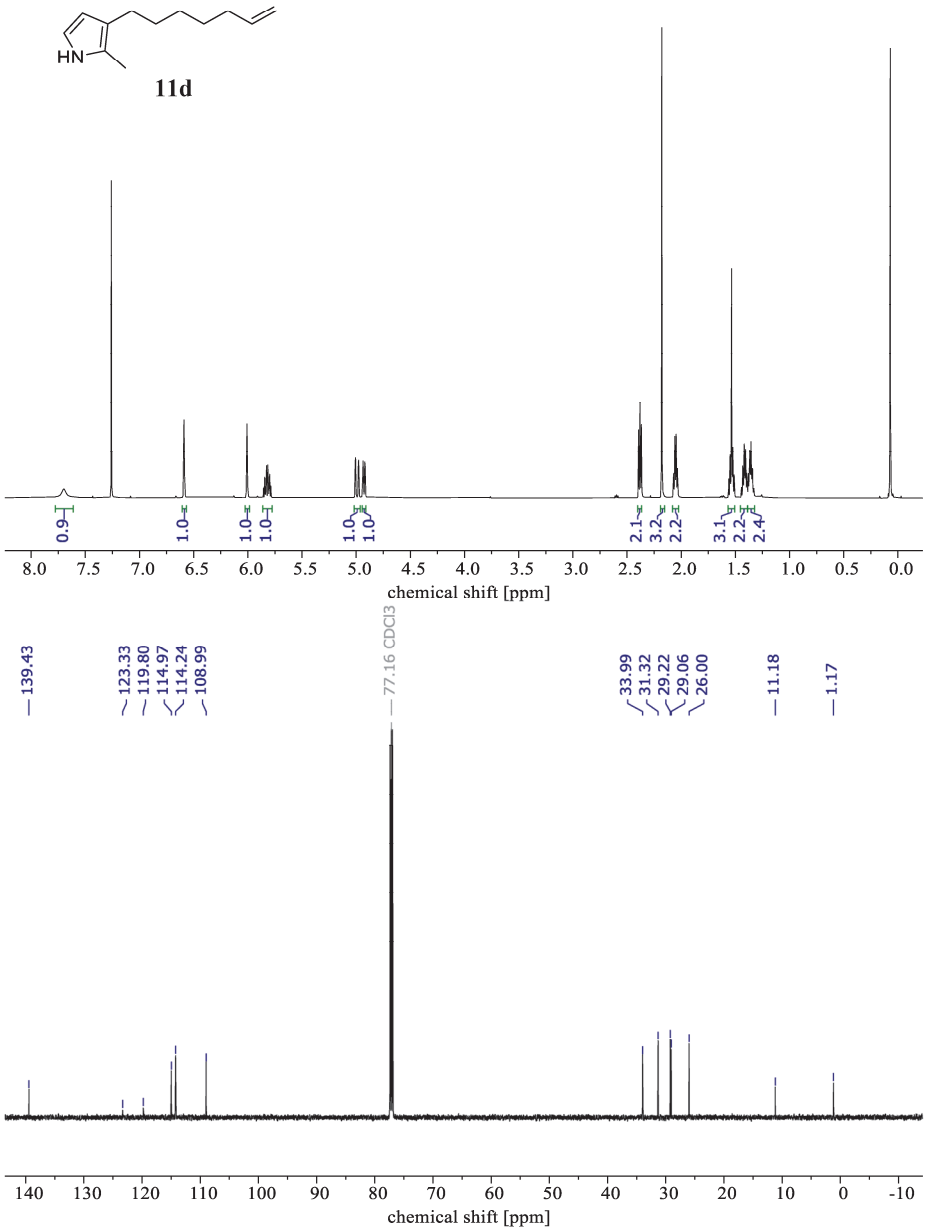
HN
11d
0.9
1.0
1.0
1.0
1.0
1.0
2.1
3.2
2.2
3.1
2.2
2.4
8.0 7.5 7.0 6.5 6.0 5.5 5.0 4.5 4.0 3.5 3.0 2.5 2.0 1.5 1.0 0.5 0.0
chemical shift [ppm]
139.43
123.33
119.80
114.97
114.24
108.99
77.16 CDCl3
33.99
31.32
29.22
29.06
26.00
11.18
1.17
140 130 120 110 100 90 80 70 60 50 40 30 20 10 0 -10
chemical shift [ppm]

19

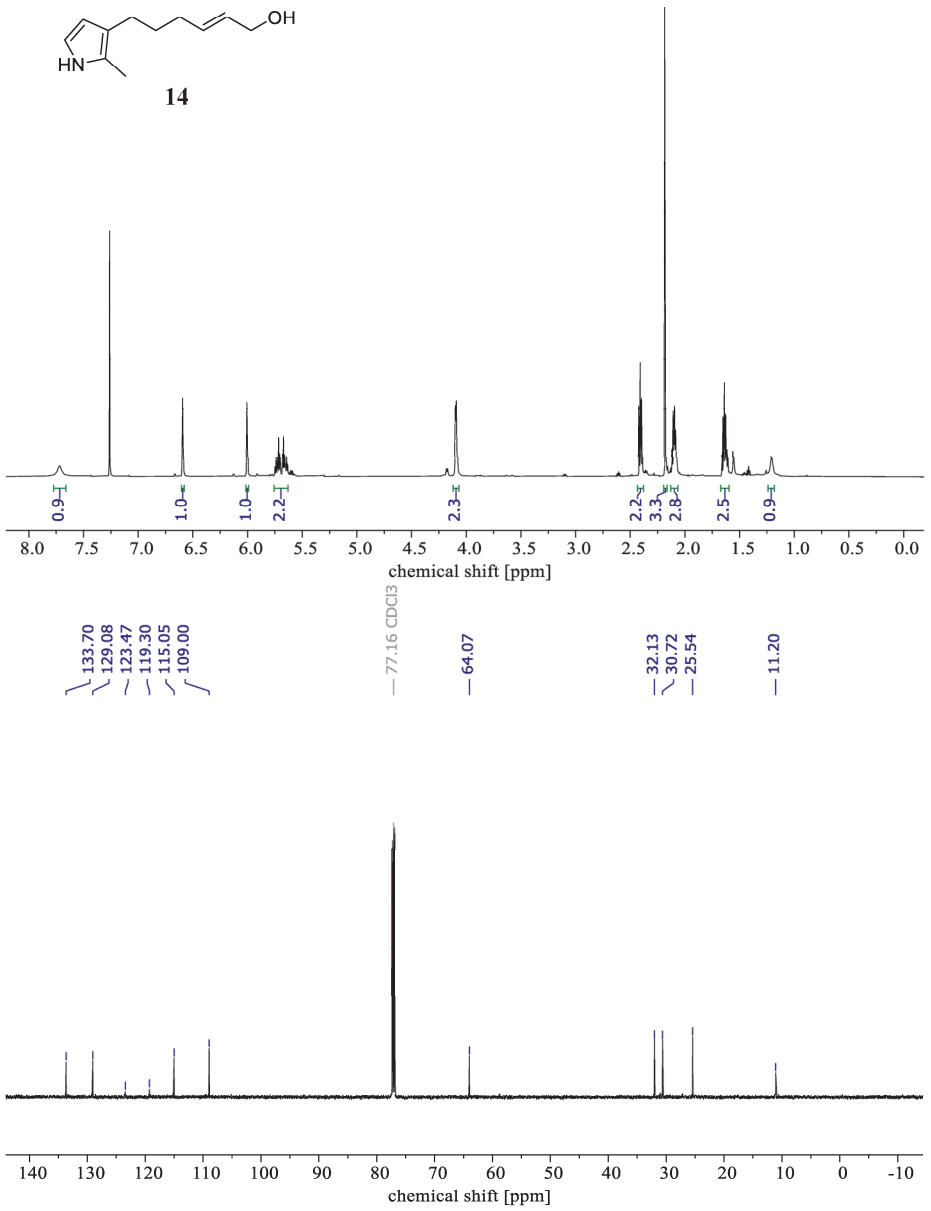
OH
HN
14
0.9
1.0
1.0
2.2
2.3
2.2
3.3
2.8
2.5
0.9
8.0 7.5 7.0 6.5 6.0 5.5 5.0 4.5 4.0 3.5 3.0 2.5 2.0 1.5 1.0 0.5 0.0
chemical shift [ppm]
133.70
129.08
123.47
119.30
115.05
109.00
77.16 CDCl3
64.07
32.13
30.72
25.54
11.20
140 130 120 110 100 90 80 70 60 50 40 30 20 10 0 -10
chemical shift [ppm]

20

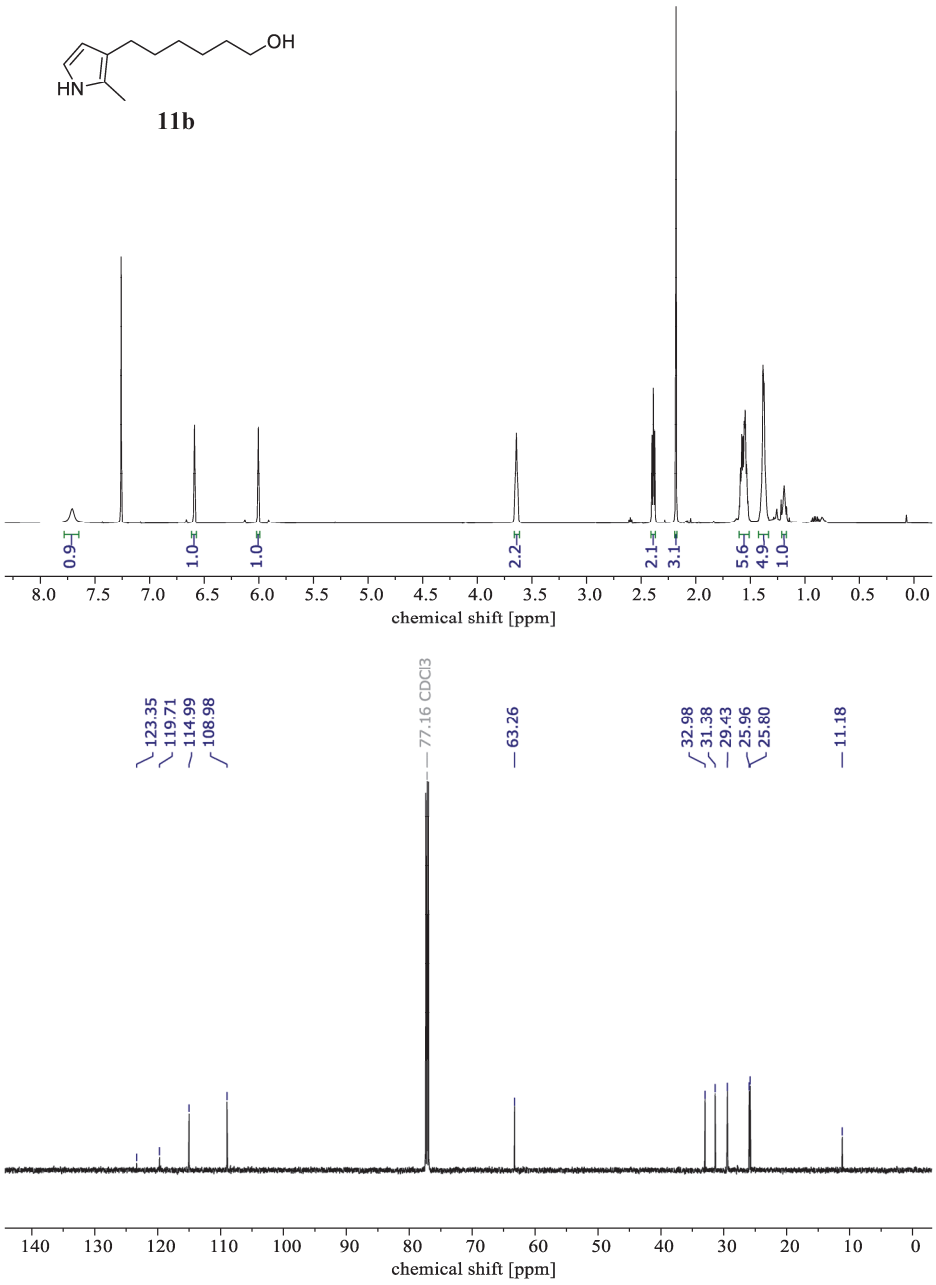
OH
HN
11b
0.9
1.0
1.0
2.2
2.1
3.1
5.6
4.9
1.0
chemical shift [ppm]
123.35
119.71
114.99
108.98
77.16 CDCl3
63.26
32.98
31.38
29.43
25.96
25.80
11.18
chemical shift [ppm]

21

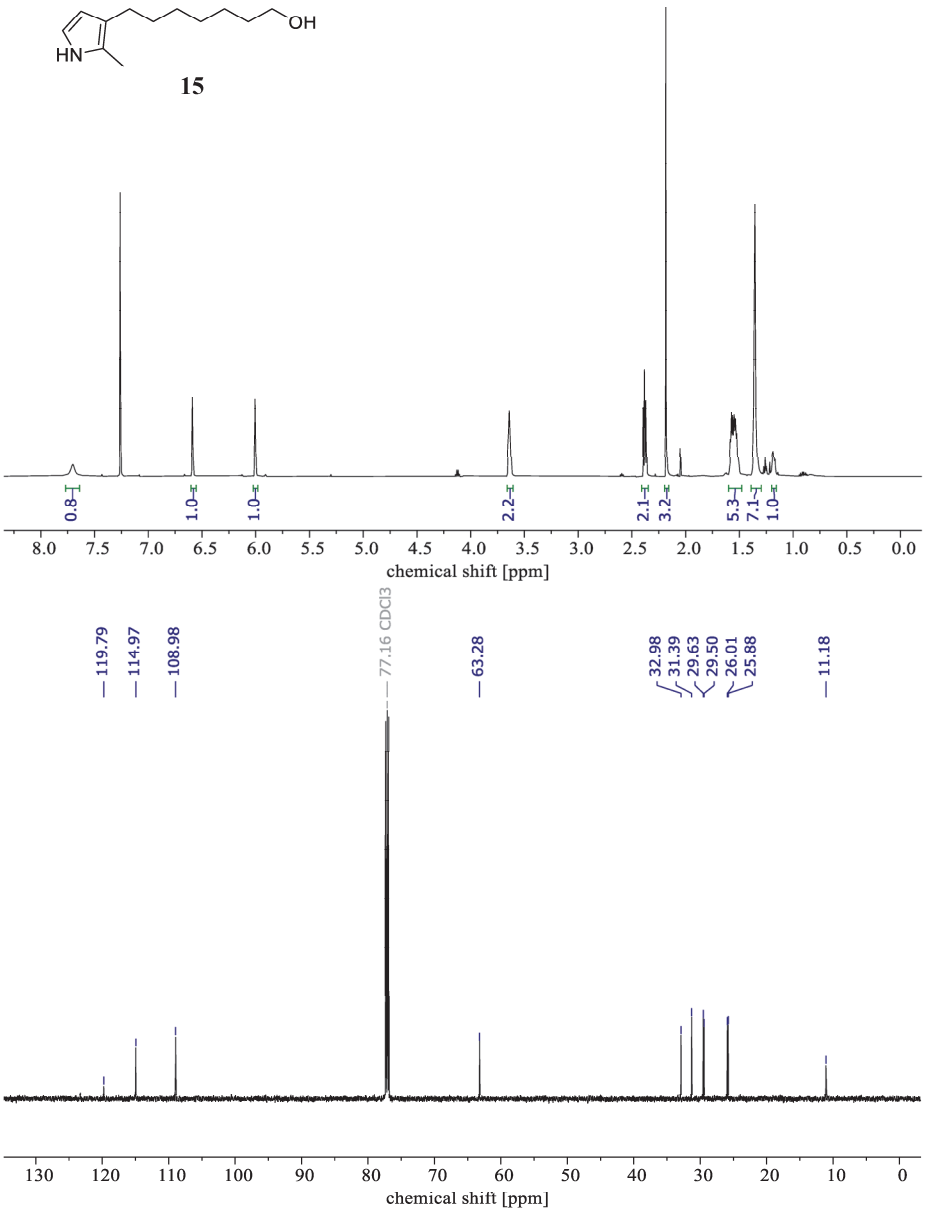
OH
HN
15
0.8
1.0
1.0
2.2
2.1
3.2
5.3
7.1
1.0
8.0 7.5 7.0 6.5 6.0 5.5 5.0 4.5 4.0 3.5 3.0 2.5 2.0 1.5 1.0 0.5 0.0
chemical shift [ppm]
119.79
114.97
108.98
77.16 CDCl3
63.28
32.98
31.39
29.63
29.50
26.01
25.88
11.18
130 120 110 100 90 80 70 60 50 40 30 20 10 0
chemical shift [ppm]

22

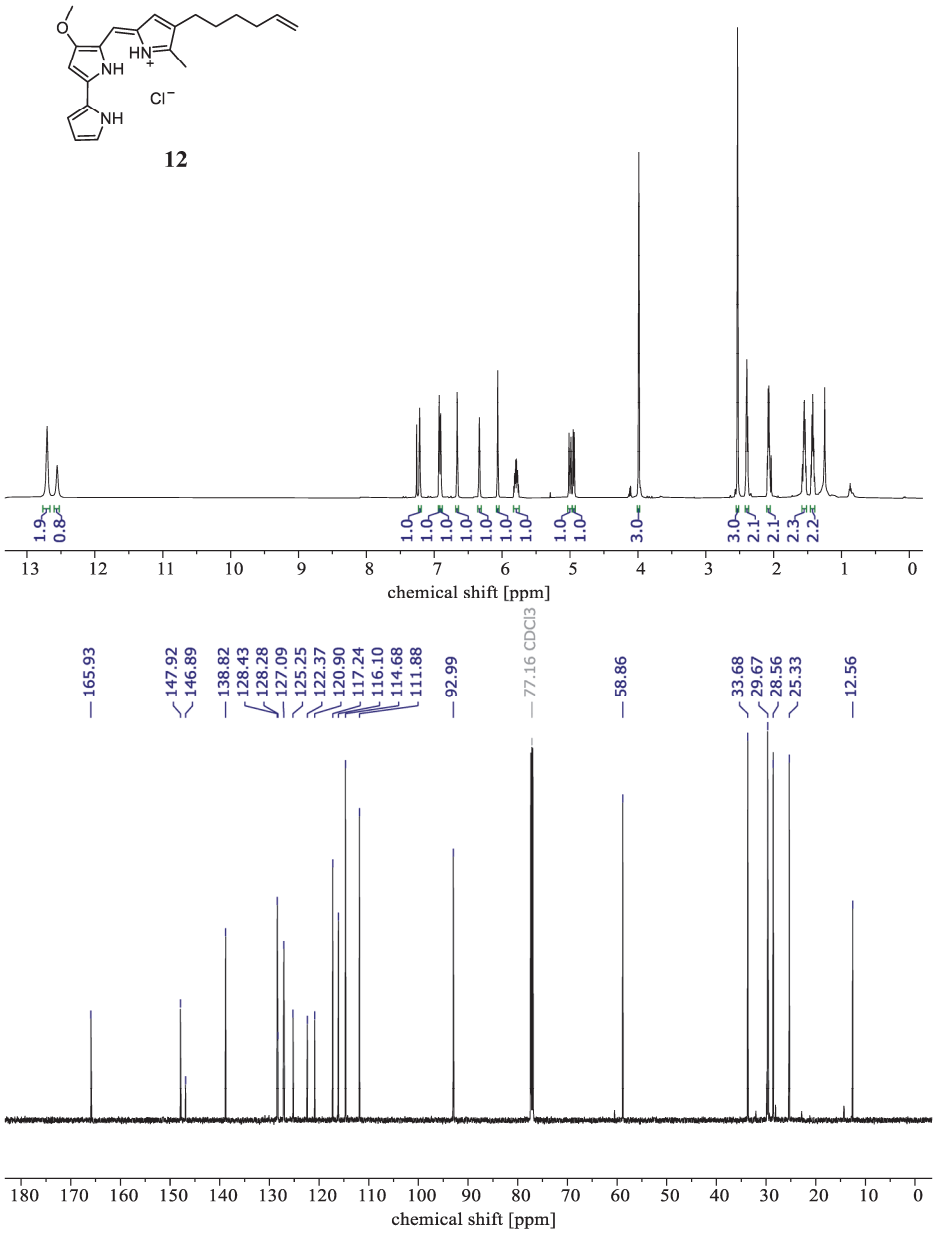
O
HN
NH
NH
Cl⁻
12
1.9
0.8
1.0
1.0
1.0
1.0
1.0
1.0
1.0
1.0
3.0
3.0
2.1
2.1
2.3
2.2
chemical shift [ppm]
165.93
147.92
146.89
138.82
128.43
128.28
127.09
125.25
122.37
120.90
117.24
116.10
114.68
111.88
92.99
77.16 CDCl3
58.86
33.68
29.67
28.56
25.33
12.56
chemical shift [ppm]

23

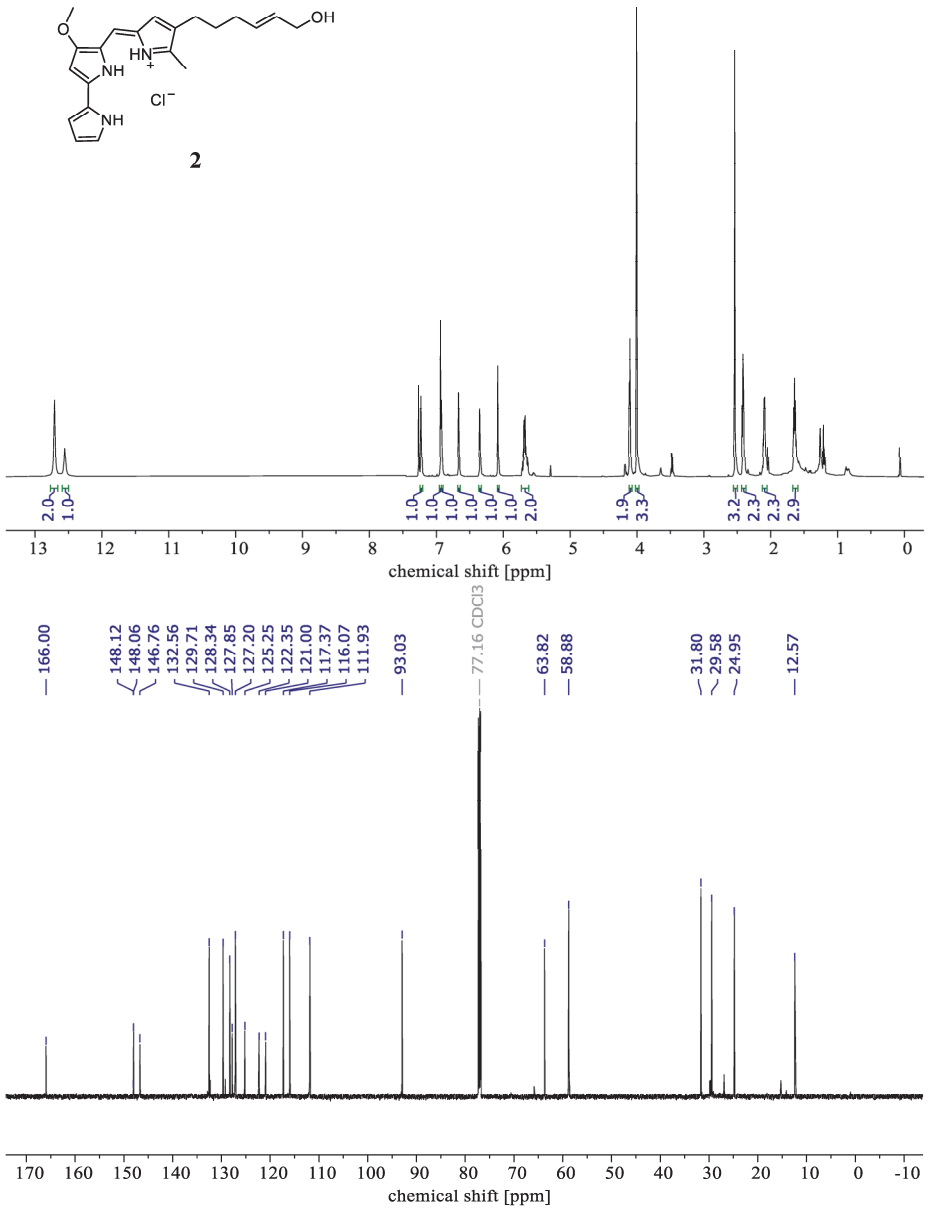
OH
NH
HN+
Cl−
NH
2
2.0
1.0
1.0
1.0
1.0
1.0
1.0
2.0
1.9
3.3
3.2
2.3
2.3
2.9
chemical shift [ppm]
166.00
148.12
148.06
146.76
132.56
129.71
128.34
127.85
127.20
125.25
122.35
121.00
117.37
116.07
111.93
93.03
77.16 CDCl3
63.82
58.88
31.80
29.58
24.95
12.57
chemical shift [ppm]

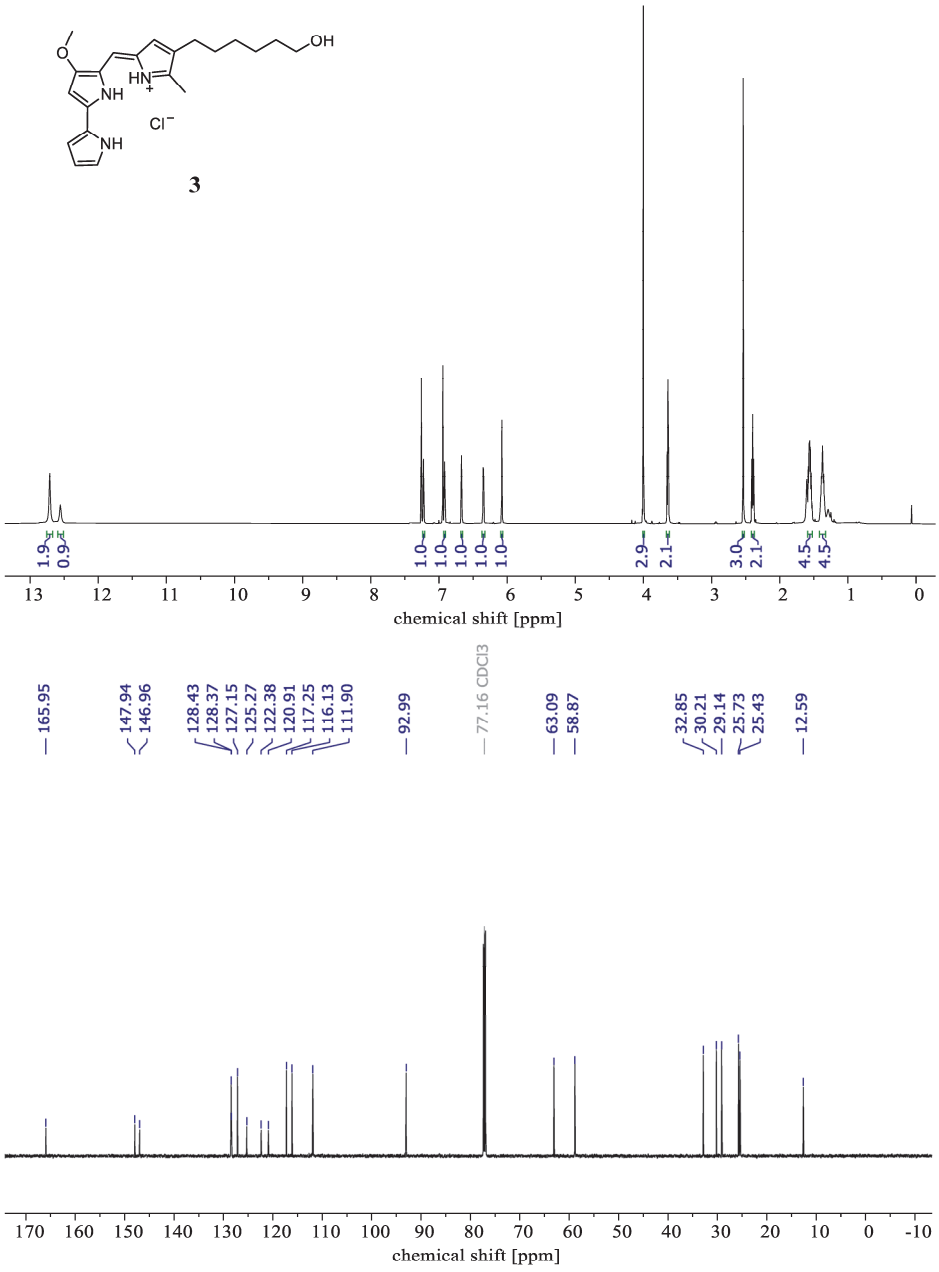
OH
O
HN
NH
NH
Cl⁻
3
1.9
0.9
1.0
1.0
1.0
1.0
2.9
2.1
3.0
2.1
4.5
4.5
chemical shift [ppm]
165.95
147.94
146.96
128.43
128.37
127.15
125.27
122.38
120.91
117.25
116.13
111.90
92.99
77.16 CDCl3
63.09
58.87
32.85
30.21
29.14
25.73
25.43
12.59
chemical shift [ppm]

25

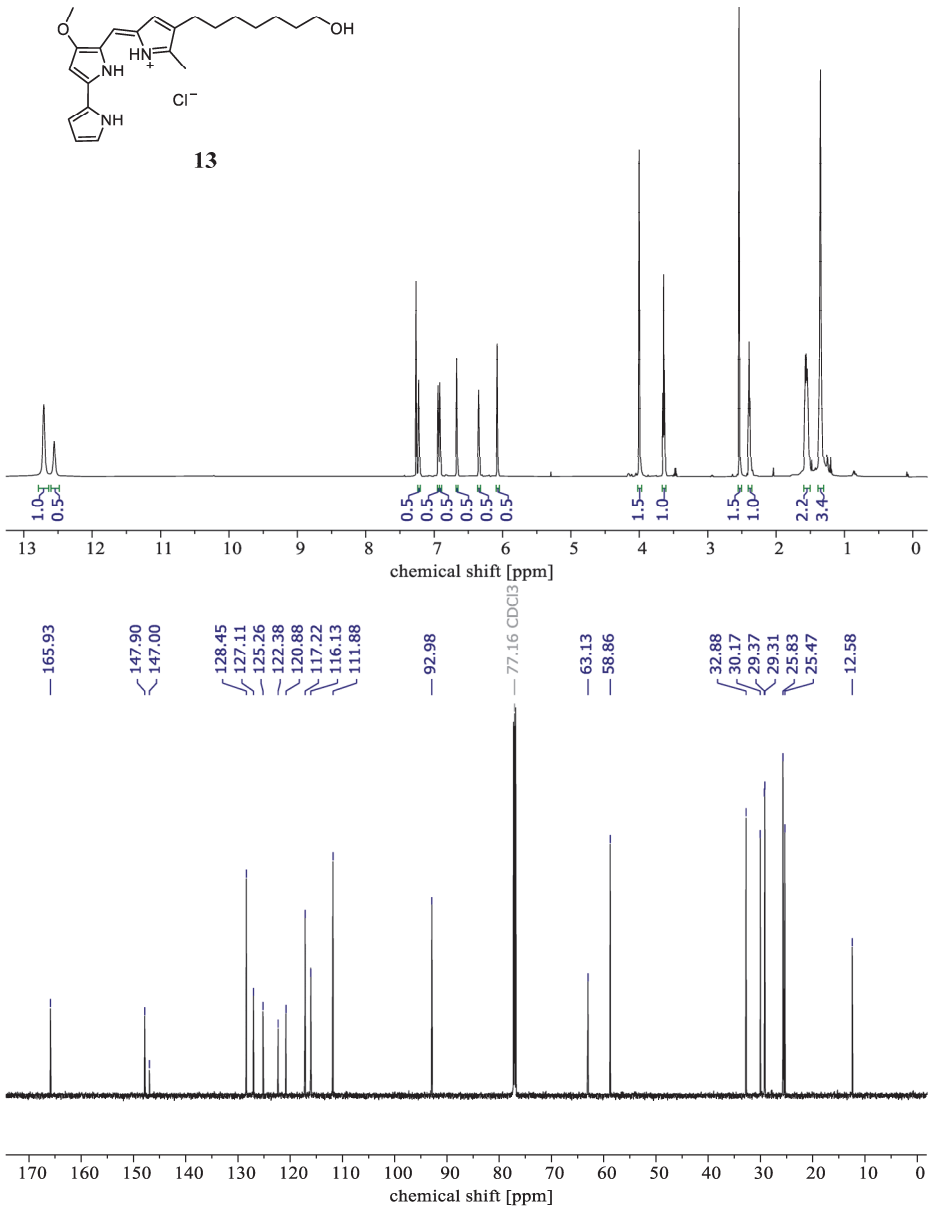
OH
HN
NH
NH
Cl⁻
13
1.0
0.5
0.5
0.5
0.5
0.5
0.5
1.5
1.0
1.5
1.0
2.2
3.4
chemical shift [ppm]
165.93
147.90
147.00
128.45
127.11
125.26
122.38
120.88
117.22
116.13
111.88
92.98
77.16 CDCl3
63.13
58.86
32.88
30.17
29.37
29.31
25.83
25.47
12.58
chemical shift [ppm]

III Impact of prodiginines on the plant parasitic nematode *Heterodera schachtii*

Supplementary Table S4. List of concentrations used for treatments.

Treatment	Concentration (µg/mL)					
Di-rhamnolipid (**4**)	1.125	2.500	5.000	7.500	10.000	-
Prodigiosin (**1**)	1.260	2.519	5.039	7.558	10.077	-
Hydroxylated prodiginine **3**	1.365	2.729	5.459	8.188	10.918	13.647
Hydroxylated prodiginine **2**	1.358	2.715	5.431	8.146	10.861	13.577
Hydroxylated prodiginine **13**	1.414	2.828	5.655	8.483	11.311	14.138

All prodiginines were obtaines as hydrochlorides. Accordingly, all given weights and concentrations refer to the respective molecular weights.

Supplementary Table S5. List of treatments and concentrations used in the combinatorial assay.

Treatment	Concentration (µg/mL)		
	Di-rhamnolipid (**4**)	Prodigiosin (**1**)	Hydroxylated prodiginine **3**
Compound alone (EC_{50})	2.77	-	-
	-	5.43	-
	-	-	12.16
Compound combination (0.25x, 0.5x, 0.75x, 1x, 1.25x of EC_{50})	0.69	1.36	-
	1.39	2.72	-
	2.08	4.07	-
	2.77	5.43	-
	3.46	6.79	-
	0.69	-	3.04
	1.39	-	6.08
	2.08	-	9.12
	2.77	-	12.16
	3.46	-	15.20

All prodiginines were obtaines as hydrochlorides. Accordingly, all given weights and concentrations refer to the respective molecular weights.

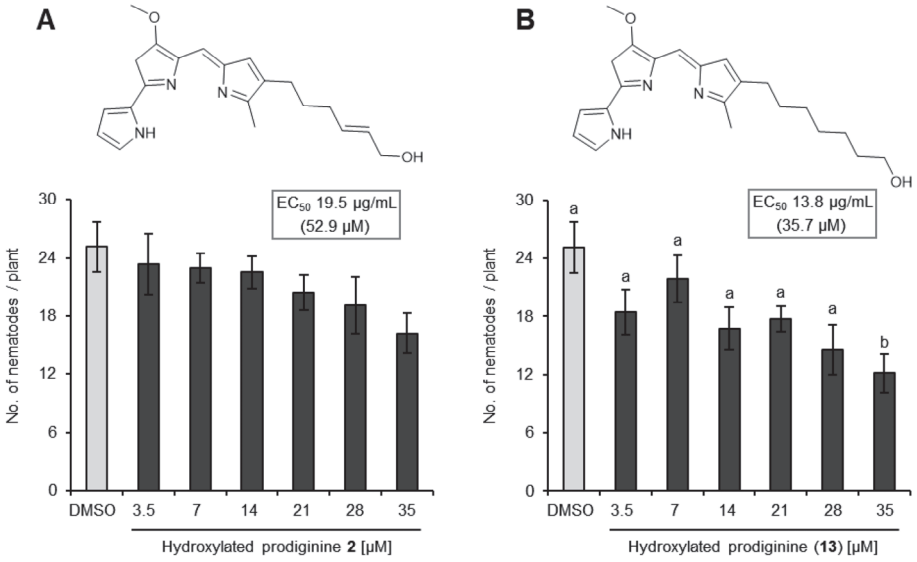

Supplementary Figure S6. EC_{50} determination of hydroxylated prodiginines 2 and 13 on the plant-parasitic nematode *Heterodera schachtii*. Effects of hydroxylated prodinines **2 (A)** and **13 (B)** were assessed as reduction of nematode numbers on *A. thaliana*. EC_{50} values (effective concentration that causes a reduction of nematode infestation of *A. thaliana* by 50%) were calculated by using software 'CompuSyn'. Results are expressed as the mean ± standard error of two independent biological replicates (n≥16; at least 8 plants/treatment were evaluated per biological replicate). Different letters indicate statistically significant differences among treatments according to Dunn's Method (p<0.05). No significant differences were found for treatments with different concentrations of prodiginine **2**.

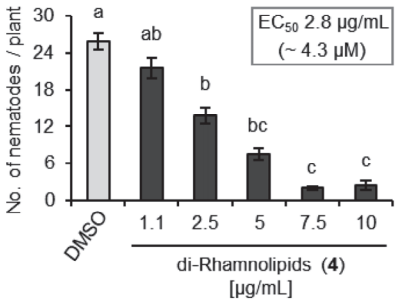

Supplementary Figure S7. EC_{50} determination of di-rhamnolipids (4) on the plant-parasitic nematode *Heterodera schachtii*. The effect of di-rhamnolipids (**4**) was assessed as reduction of nematode numbers on *A. thaliana*. The EC_{50} value (effective concentration that causes a reduction of nematode infestation of *A. thaliana* by 50%) was calculated by using software 'CompuSyn'. Results are expressed as the mean ± standard error of three independent biological replicates (n≥20). Different letters indicate statistically significant differences among treatments according to Dunn's Method (p<0.05).

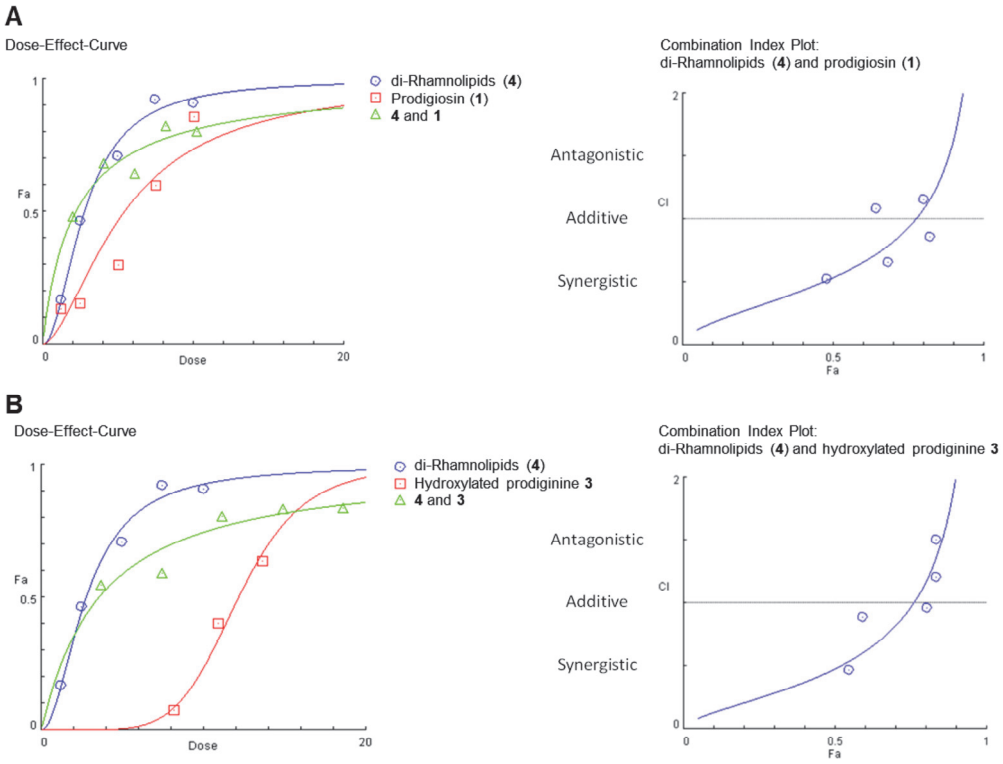

Supplementary Figure S8. Dose-effect curves and combination index plots of prodiginines and di-rhamnolipids. Effects of the compound combinations were assessed as reduction of *Heterodera schachtii* numbers on *Arabidopsis thaliana*. The schematic representation was generated by software 'CompuSyn' (Chou and Martin, 2005) based on five concentrations (0.25x, 0.5x, 0.75x, 1x, 1.25x of before determined EC_{50} (see Tables S4 and S5)) of prodigiosin (**1**) **(A)** or hydroxylated prodiginine **3** **(B)** applied alone or in combination with di-rhamnolipids (**4**). Dose – total compound dose in µg/mL; Fa – fraction affected; CI – combination index (determined using 'CompuSyn'(Chou and Martin, 2005)).

Supplementary References

Aldrich, L. N. (2012). Progress toward the total synthesis of marineosins A & B; total synthesis of tambjamine K and unnatural analogs with improved anticancer activity, and discovery of selective M1 antagonists.

Brands, S., Brass, H. U. C., Klein, A. S., Pietruszka, J., Ruff, A. J., and Schwaneberg, U. (2020). A colourimetric high-throughput screening system for directed evolution of prodigiosin ligase PigC. *Chem. Commun.* 56, 8631–8634. doi:10.1039/d0cc02181d.

Brass, H. U. C., Klein, A. S., Nyholt, S., Classen, T., and Pietruszka, J. (2019). Condensing enzymes from *Pseudoalteromonadaceae* for prodiginine synthesis. *Adv. Synth. Catal.* 361, 2659–2667.

Chawrai, S. R., Williamson, N. R., Mahendiran, T., Salmond, G. P. C., and Leeper, F. J. (2012). Characterisation of PigC and HapC, the prodigiosin synthetases from *Serratia* sp. and *Hahella chejuensis* with potential for biocatalytic production of anticancer agents. *Chem. Sci.* 3, 447–454. doi:10.1039/c1sc00588j.

Chou, T., and Martin, N. (2005). CompuSyn for drug combinations: PC software and user's guide: A computer program for quantitation of synergism and antagonism in drug combinations, and the determination of IC50 and ED50 and LD50 values. *ComboSyn Inc, Paramus,*.

Couturier, M., Bhalara, H. D., Chawrai, S. R., Monson, R., Williamson, N. R., Salmond, G. P. C., et al. (2019). Substrate flexibility of the flavin-dependent dihydropyrrole oxidases PigB and HapB involved in antibiotic prodigiosin biosynthesis. *ChemBioChem* 21, 523–530. doi:10.1002/cbic.201900424.

de Lorenzo, V., Eltis, L., Kessler, B., and Timmis, K. N. (1993). Analysis of *Pseudomonas* gene products using *lacI*q/*Ptrp-lac* plasmids and transposons that confer conditional phenotypes. *Gene* 123, 17–24. doi:10.1016/0378-1119(93)90533-9.

Domröse, A., Weihmann, R., Thies, S., Jaeger, K. E., Drepper, T., and Loeschcke, A. (2017). Rapid generation of recombinant *Pseudomonas putida* secondary metabolite producers using yTREX. *Synth. Syst. Biotechnol.* 2, 310–319. doi:10.1016/j.synbio.2017.11.001.

Habash, S. S., Brass, H. U. C., Klein, A. S., Klebl, D. P., Weber, T. M., Classen, T., et al. (2020). Novel prodiginine derivatives demonstrate bioactivities on plants, nematodes, and fungi. *Front. Plant Sci.* 11, 579807. doi:10.3389/fpls.2020.579807.

Klein, A. S., Domröse, A., Bongen, P., Brass, H. U. C., Classen, T., Loeschcke, A., et al. (2017). New Prodigiosin Derivatives Obtained by Mutasynthesis in *Pseudomonas putida*. *ACS Synth. Biol.* 6, 1757–1765. doi:10.1021/acssynbio.7b00099.

Loeschcke, A., Markert, A., Wilhelm, S., Wirtz, A., Rosenau, F., Jaeger, K.-E., et al. (2013). TREX: A universal tool for the transfer and expression of biosynthetic pathways in bacteria. *ACS Synth. Biol.* 2, 22–33. doi:10.1021/sb3000657.

Mody, R. S., Heidarynejad, V., Patel, A. M., and Dave, P. J. (1990). Isolation and characterization of

Serratia marcescens mutants defective in prodigiosin biosynthesis. *Curr. Microbiol.* 20, 95–103. doi:10.1007/BF02092880.

Taber, D. F., and Frankowski, K. J. (2006). Grubbs's cross metathesis of eugenol with *cis*-2-butene-1,4-diol to make a natural product. An organometallic experiment for the undergraduate lab. *J. Chem. Educ.* 83, 283–284. doi:10.1021/ed083p283.

Weihmann, R., Domröse, A., Drepper, T., Jaeger, K. E., and Loeschcke, A. (2020). Protocols for yTREX/Tn*5*-based gene cluster expression in *Pseudomonas putida*. *Microb. Biotechnol.* 13, 250–262. doi:10.1111/1751-7915.13402.

Williamson, N. R., Fineran, P. C., Leeper, F. J., and Salmond, G. P. C. (2006). The biosynthesis and regulation of bacterial prodiginines. *Nat. Rev. Microbiol.* 4, 887–99. doi:10.1038/nrmicro1531.

Williamson, N. R., Simonsen, H. T., Ahmed, R. A. A., Goldet, G., Slater, H., Woodley, L., et al. (2005). Biosynthesis of the red antibiotic, prodigiosin, in *Serratia*: Identification of a novel 2-methyl-3-n-amyl-pyrrole (MAP) assembly pathway, definition of the terminal condensing enzyme, and implications for undecylprodigiosin biosynthesis in <i>Strep. *Mol. Microbiol.* 56, 971–989. doi:10.1111/j.1365-2958.2005.04602.x.

V.5. Supporting Information for chapter II.5.2

Supporting Information

Substrate tolerance of Prub680 and homologous enzymes allows the mutasynthesis of cycloprodiginines in *Pseudomonas putida* KT2440

Nora Lisa Bitzenhofer[1*‡], Matthias Bleser[2‡], Anka Sieberichs[1], Dorothea F. Kossmann[2], Tim Moritz Weber[2], Viktoria Warth[2], Daniel Germes[2], Robin Weihmann[1], Karl-Erich Jaeger[1,3], Jörg Pietruszka[2,3*], Anita Loeschcke[1*]

[1]Institute of Molecular Enzyme Technology (IMET), Heinrich Heine University Düsseldorf, Düsseldorf, Germany
[2]Institute of Bioorganic Chemistry (IBOC), Heinrich Heine University Düsseldorf, Düsseldorf, Germany
[3]Institute of Bio- and Geosciences IBG-1: Biotechnology, Forschungszentrum Jülich, Jülich, Germany

‡ these authors contributed equally

Correspondence: Prof. Dr. Jörg Pietruszka (j.pietruszka@fz-juelich.de); Dr. Anita Loeschcke (a.loeschcke@fz-juelich.de)

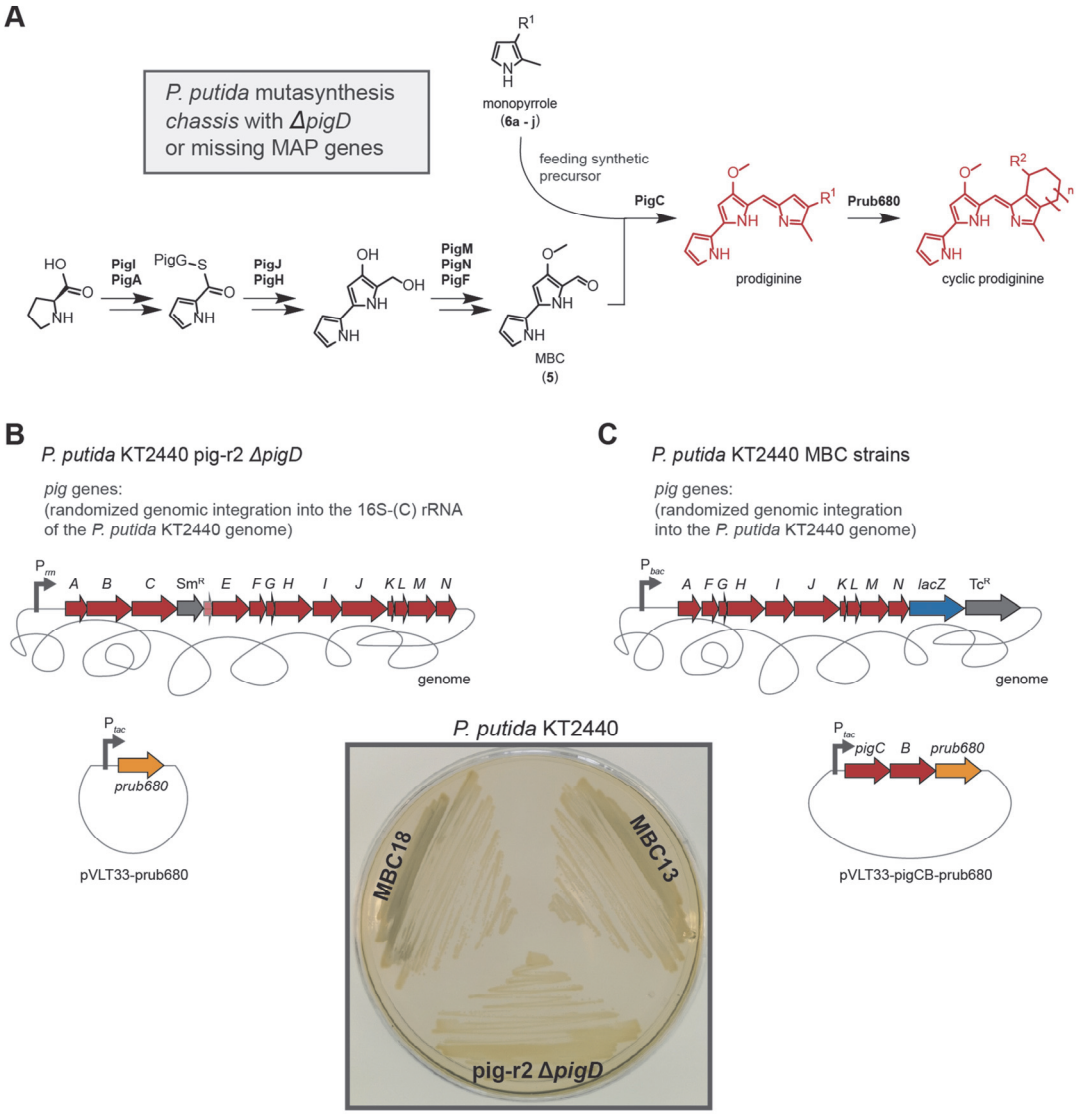

Figure S1: *Pseudomonas putida* mutasynthesis *chassis*.
A: Cycloprodiginine mutasynthesis scheme by implementation of the enzyme Prub680 from *P. rubra*. **B**: In *P. putida* pig-r2 Δ*pigD*, the *pig* genes from *S. marcescens* are integrated into the 16S rRNA (operon C). MAP synthesis is blocked in the first step by *pigD* knockout[1]. For the mutasynthetic production of cycloprodiginines, the *prub680* gene from *P. rubra* is placed under the control of the inducible promoter P_{tac} on a plasmid. **C**: The cycloprodigiosin mutasynthesis *chassis*, based on the previously generated *P. putida* MBC strains[2], carrying only the genes relevant for MBC biosynthesis in the chromosome under a constitutive bacterial promoter. To restore prodiginine production upon MAP addition, the *pigC* and *pigB* genes (expressed on a plasmid under the control of the inducible promoter P_{tac}) are also required. For cyclization, the *prub680* gene is also integrated on the plasmid.

```
S.ruber             MDIEFHEIILYTLPSLFLPLFFDAGIDYIKKTHRYRLNDTITNLSISLANLGASFIILTA      60
Z.ganghwensis       MSTDFSEQLLFTLPLYLGPLFIFALIDFVRSTRGYRVNDTLTNATIALGNLGFTFILVAG      60
V.gazogenes         MNLDFSDEVMYTLPFYLGPLFILSILSYLKKHKNYRFNDTLTNASIALGNLGFSFIMLLG      60
P.rubra             MDLNFTEEVMYTLPFYLGPLFILATINFLRKQKNYRLNDTLTNATIALGNLGLSFIFLLA      60
P.denitrificans     MDLNFTEEIMYTLPFYLGPLFLLASINFFRKQKNYRLNDTLTNASIALGNLGLSFIFLLA      60
                    *. :* : :::***  : ***: : :.:.:. : **.***:** :*:*.*** :**:: .

S.ruber             VLAVYSYTYSNFSQFQLNQTELSTWLLAFILYDFCYYWNHRLHHKIGILWADHIVHHSGE      120
Z.ganghwensis       IIAMYNYLYSNFSLFTLDQTSVTTWLIAFIFYDFCFYWNHRVHHAIGIFWVDHIVHHTAE      120
V.gazogenes         VVAAYSYVYKEFRIFELDQSSPLTYILAFFAYDFCYYWNHRIHHMIGLFWTDHLVHHTAE      120
P.rubra             VVALYTLVYNEYRLVDLDQSNPLIYLLAFLVYDFLYYWNHRFHHMIGLFWADHLVHHTAE      120
P.denitrificans     VVAVYSLVYSEYKFFDLDQSDPLTYVLAFLLYDFLYYWNHRFHHMIGLFWADHLVHHTAE      120
                    ::* *.  *.::  . *:*:.   :::**: *** :*****.** **::*.**:***:.*

S.ruber             EMNFGVSIRQSFLTELTMWPLFLLMALVGISIEVFLITSYIQATWAFLIHTKCLKNTRWL      180
Z.ganghwensis       NFNFGVSIRNSYFMEVTMWLTFIPMALAGISIEVFLAVSYTQMTWAFLIHHKKLKHTPRL      180
V.gazogenes         NFNFGVSIRISYFTELTMWMSFIVMAFLGISLEVFLVASYIQVLWAFCIHTKYLKNTPRL      180
P.rubra             NFNFGVSIRISYFTELTMWMTFIPMAFMGISLEVFLAASYTQIIWAFCIHTKYLKKTPRA      180
P.denitrificans     NFNFGVSIRISYFTELTMWMTFIPMAFLGISLEVFLIASYAQIVWAFCIHTKWFKSTPIA      180
                    ::******* *:: *:***  *: **: ***:**** .** *  *** ** * :* *

S.ruber             DNILNTPSLHRVHHATNQMYIDKNFGGILVVWDQIFGTYQNELADSPVKYGIMESFASFS      240
Z.ganghwensis       DKVFNTPSLHRVHHARNTKYIDKNFGGIFIIWDRLFGTYQTESESVPVTYGVRESIQSFS      240
V.gazogenes         DKFVNTPSLHRVHHARNGKYIDKNFGGILVVWDQLFGTYQRELEEEPVVYGVRESYPSFS      240
P.rubra             DKIFNTPSLHRVHHARNRQYIDKNYGGILIIWDRLFGTYQRELESDPVVYGVRESYPSFS      240
P.denitrificans     DKLLNTPSLHRVHHARNTKYIDKNFGGIFIIWDRLFGTYQTELNDNPVTFGVRESFPSFS      240
                    *:..********** *  *****:***:::**::***** *  . ** :*: **  ***

S.ruber             PVSINLQYYKVILKKIAYSHSISEMLKSIFASPGWVPKAISAKKFYAEISNLSARQHVSS      300
Z.ganghwensis       PLMINIQYLKVIIKKFTHSKTLIDKLKSIFYSPGWLPAGLTKTECLGKIADIPCKYFKPK      300
V.gazogenes         PFVINSYYLKTIWKKIQLSHSPWEIFCSVFASPGWLPKGVERRHFYSDVARIPCSQFKPR      300
P.rubra             PLVINSYYLKTIWQKIKCSRSVFEVLCSVFAPPAWLPKNANKADFYSLTAKVKSKDFKPK      300
P.denitrificans     PLIINSYYLKTIAKKIRLSSSLFEVVCSIFGPPVWLPKKANKSTFYSKTCKIDSKNFKAK      300
                    *. **  * *.* :*:  * :  : . *:*  * *:*         .  . : .  .

S.ruber             RGEISVNARKSCIIRFILTLSVFILLMWNFALLGWWQIANLAVLFFWLCHYNGLAFDGVK      360
Z.ganghwensis       NSPLTATMKLSCILRFIVILVVFTYLMWNFYDLPWLQTTALSCLFFWLCHYNGIVFDGVK      360
V.gazogenes         DPYISLRTKLTTLVRFFVTLILFCYLMSYFGDFPILPVTALSLLFLWLSHYNGIVLDGRN      360
P.rubra             DPYICKRTKWTAFVRFSSIVVLFTYLMSYFGELPTLPLVSLSLLFFWLCHFNGLVFDGAK      360
P.denitrificans     DPYLSTKTKWTCFNRFICIIVVFCYLMMNFGALPVLPLIILSVLFFWLCHYNGIVFDGFK      360
                       :    : : : **   : :*  **  *  :       *: **:**.*:**:.:** :

S.ruber             LTWKIEAISQFLIILVGGVVVYNNQPGHLLILVLIASITSLSCYIVYQNPPIKPETDALT      420
Z.ganghwensis       ITWKSEVLSQFLIILSGITGLGYT---SVNIVSAAIIFTSFVSFICYTLHHSPPSHSRKN      417
V.gazogenes         VGWGAEIISQGFAGIFLYWAVSTEQNHLLIISTVILMVITLLNYIIYRQGRELKGR----      416
P.rubra             LGLPMEAVTQVLYGLILYWAIETDQAAWITIGTATLALISLCNYVIYRTRPAAPVE----      416
P.denitrificans     IGWTTEIITQILFISFLSWAITSKQPEYLILSTGILACLSLVNYLIYSNKKSQYEE----      416
                    :    * ::* :       :       : :       ::  :: *

S.ruber             KALVE----  425
Z.ganghwensis       RLLSALTE-  425
V.gazogenes         -LLPQSETL  424
P.rubra             -LSAELQ--  422
P.denitrificans     -NNLDIQQQ  424
```

Figure S2: Multiple sequence alignment.
Sequence alignment of the protein Prub680 from *P. rubra* and the four chosen homologs from *P. denitrificans*, *V. gazogenes*, *Z. ganghwensis*, and *S. ruber* performed with Clustal Omega[3].

Table S1: Comparison of different cyclases.

enzyme name[1]	organism	description	NCBI accession	pers. identity
Prub680 (Pr)	*P. rubra*	sterol desaturase family protein	WP_010386914.1	(reference sequence)
Pd	*P. denitrificans*	sterol desaturase family protein	WP_091980140.1	72.04%
Vg	*V. gazogenes*	sterol desaturase family protein	WP_072958698.1	68.38%
Zg	*Z. ganghwensis*	sterol desaturase family protein	WP_212720964.1	54.59%
Sr	*S. r uber*	sterol desaturase family protein	WP_163833151.1	48.07%

[1]or abbreviation referring to the species from which the proteins derive.

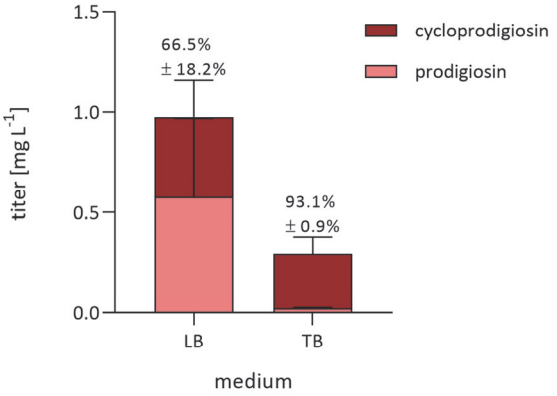

Figure S3: Evaluation of the cultivation media on the cycloprodigiosin mutasynthesis.
Cultivation of *P. putida* MBC18 pVLT33-pigCB-Prub680 (c.a.) at 30 °C in LB and TB medium. MAP (0.25 mM) and IPTG (0.5 mM) were added after 4 h of cultivation. Mutasynthesis was performed in different media at 30 °C with 0.25 mM MAP. Extracts were analyzed by HPLC-PDA analyses. Percentage of cycloprodigiosin on the total prodiginine amount is given above the bars. The bars of prodigiosin (light red) and cycloprodigiosin (dark red) titers are superimposed. The data are means of biological triplicates with their corresponding standard deviation.

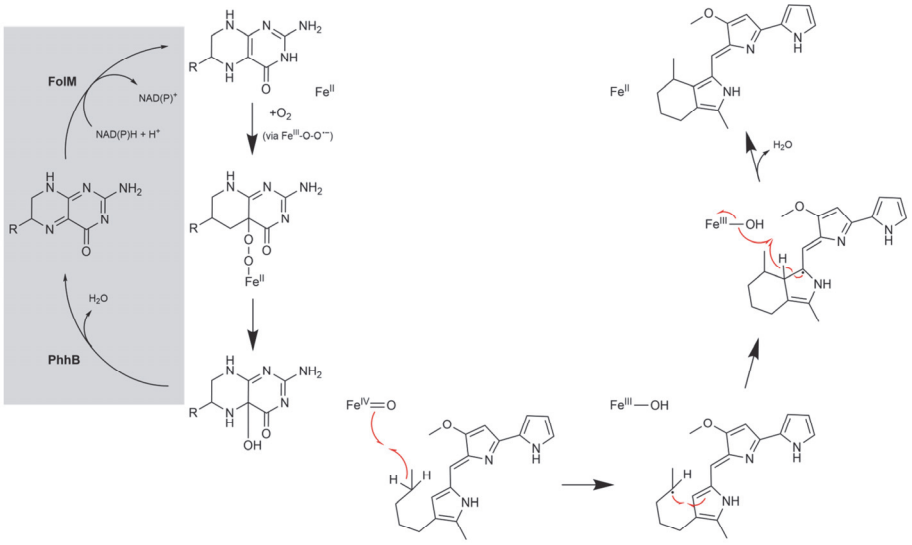

Figure S4:Proposed mechanism for cyclization and cofactor recycling.
The catalytic mechanism for the cyclization of prodigiosin is shown based on the mechanism proposed by de Rond and coworkers[4]. They suggested that O_2 can be activated either by bridged Fe_2O_2 or by the tetrahydropterin cofactor which can form an adduct with the oxygen. The latter is known from several amino acid hydroxylases, such as the tetrahydropterin-dependent tryptophan or tyrosine hydroxylase. Here, the oxygen first reacts with the active site iron to form an Fe^{III} superoxide intermediate, which would then react with the cofactor. This new intermediate can then be cleaved to the 4a-hydroxypterin and a $Fe^{IV}O$ intermediate[5,6]. For the recycling of 4a-hydroxypterin to the tetrahydropterin cofactor in amino acid hydroxylases, an artificial recycling system has been established for *E. coli* (gray box)[7]. The enzymes FolM (from *E. coli*) and PhhB (from *P. aeruginosa*) were integrated. These enzymes share 40% (FolM) and 86% (PhhB) sequence identity with homologs from *P. putida* KT2440. To support cofactor availability, additional copies of both genes were integrated into the *P. putida* genome under the control of a strong synthetic promoter (P_{em7})[8].

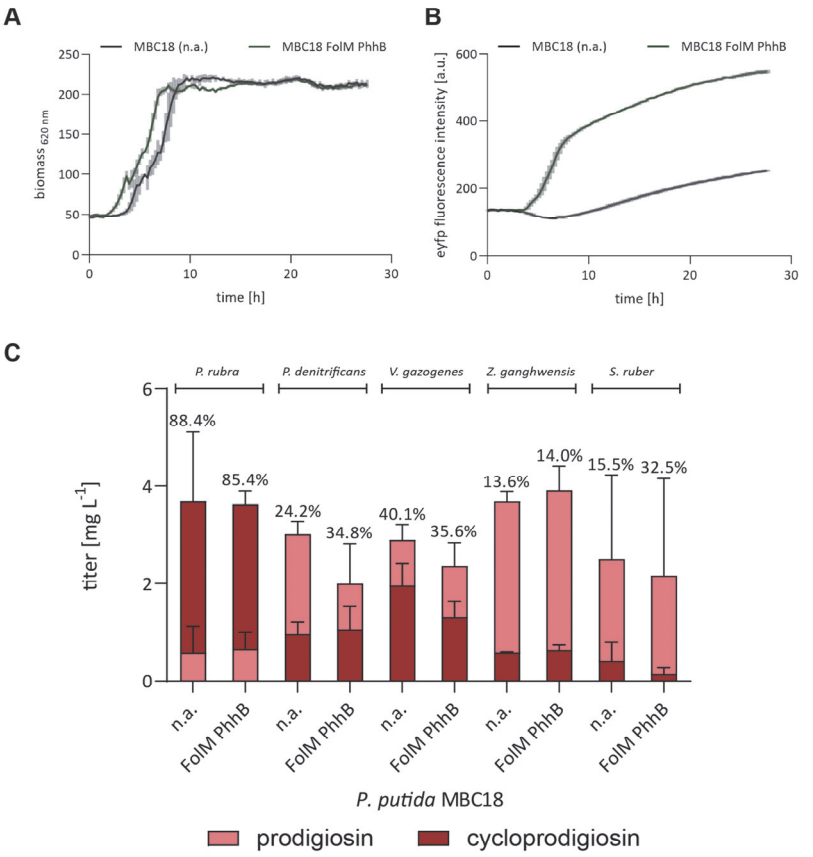

Figure S5: Implementation of cofactor recycling genes in *P. putida* MBC18.
The *folM* and *phhB* genes were integrated into the *att*Tn7 site of *P. putida* MBC18 using the integration vector pYT-Tn7-P_{em7}-folM-phhB-eyfp possessing an *eyfp*-based transcription control. Transcription of the cofactor recycling genes as well as the *eyfp* gene was investigated by cultivation in a BioLector system (Beckman Coulter, Krefeld, Germany). For this, *P. putida* MBC18 (black) and *P. putida* MBC18/FolM-PhhB (green) were cultivated in FlowerPlates under standard conditions. The biomass (**A**) and EYFP fluorescence (**B**) of both strains was measured. **C**: Mutasynthetic cycloprodigiosin production in *P. putida* MBC18 without (n.a.) and with the expression of cofactor recycling genes (FolM PhhB). Mutasynthesis was performed in LB medium at 20 °C with 1 mM MAP. Extracts were analyzed by HPLC-PDA analyses. Percentage of cycloprodigiosin on the total prodiginine amount is given above the bars. The bars of prodigiosin (light red) and cycloprodigiosin (dark red) titers are superimposed. The data are means of biological triplicates with their corresponding standard deviation. n.a.: not altered.

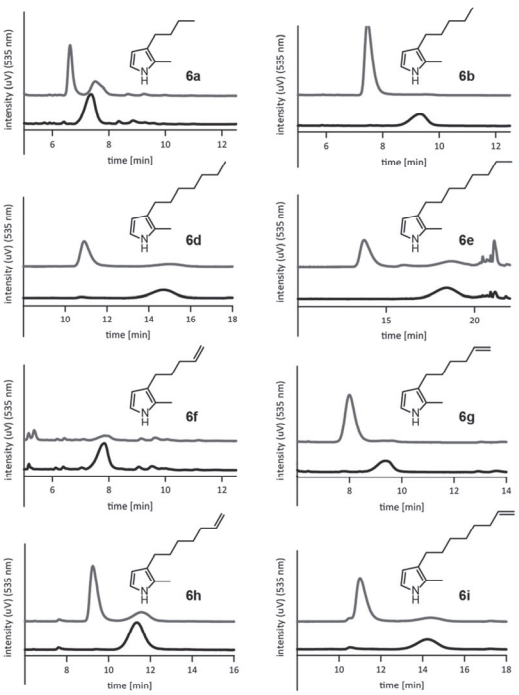

muta-synthon	pVLT33-pigCB	pVLT33-pigCB-Prub680 (c.a)	
	linear variant	linear variant	cyclic variant
6a	**7.4 min**	7.5 min	6.6 min
6b	**9.3 min**	9.1 min	7.5 min
6c	**11.5 min**	12.0 min	8.7 min
6d	**14.7 min**	15.1 min	10.9 min
6e	**18.5 min**	18.7 min	13.8 min
6f	**7.9 min**	8.0 min	-
6g	**9.4 min**	9.6 min	8.0 min
6h	**11.4 min**	11.7 min	9.3 min
6i	**14.3 min**	14.5 min	11.0 min

Figure S6: HPLC chromatograms for cycloprodiginine mutasynthesis with different monopyrroles.
Chromatograms (recorded at 535 nm) of extracts from *P. putida* MBC18 carrying the *prub680* gene (gray) and a control strain without the cyclase (black) were used to assign the signals of the cyclic derivative after the addition of monopyrroles **6a** – **6i**. The box shows the retention times for the linearly substituted and cyclic variants, respectively. Mutasynthesis was performed in LB medium at 20 °C with 1 mM MAP.

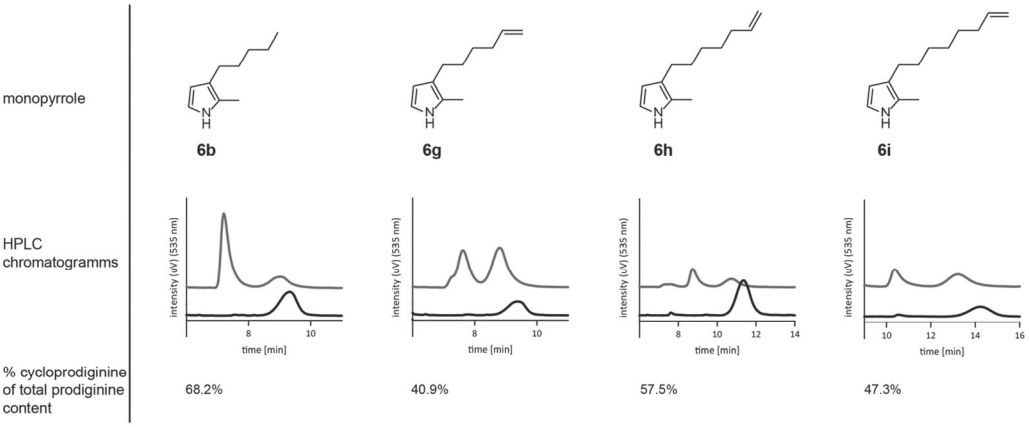

Figure S7: HPLC chromatograms for cycloprodiginine mutasynthesis with the cyclase from *P. denitrificans*.
Chromatograms (recorded at 535 nm) for the conversion of the monopyrroles **6a**, **6h** – **6j** in *P. putida* MBC18 carrying the cyclase gene from *P. denitrificans* (gray) and a control strain without the cyclase (black) were used to assign the signals of the cyclic derivative. Mutasynthesis was performed in LB medium at 20 °C with 1 mM MAP.

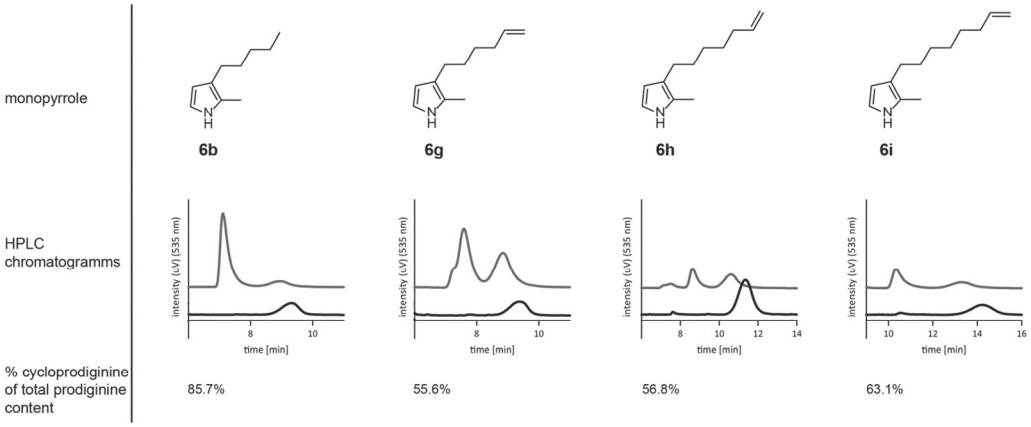

Figure S8: HPLC chromatograms for cycloprodiginine mutasynthesis with the cyclase from *V. gazogenes*.
Chromatograms (recorded at 535 nm) for the conversion of the monopyrroles **6a**, **6h** – **6j** in *P. putida* MBC18 carrying the cyclase gene from *V. gazogenes* (gray) and a control strain without the cyclase (black) were used to assign the signals of the cyclic derivative. Mutasynthesis was performed in LB medium at 20 °C with 1 mM MAP.

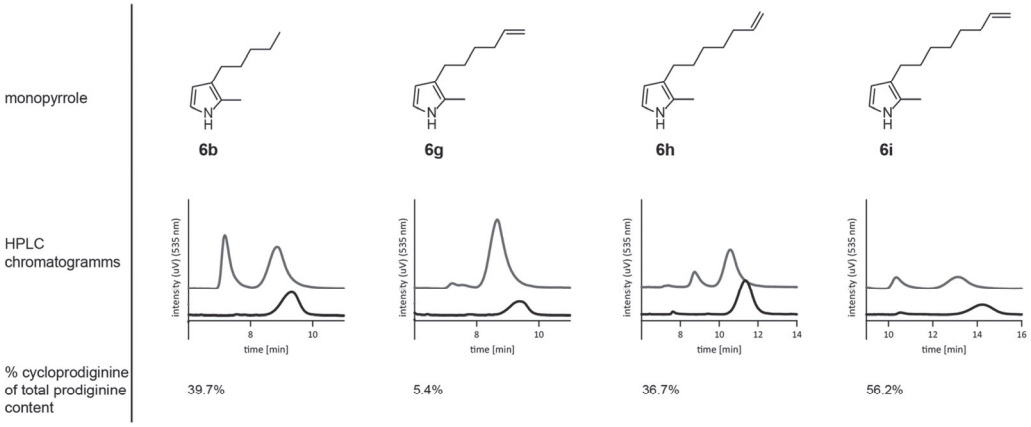

Figure S9: HPLC chromatograms for cycloprodiginine mutasynthesis with the cyclase from *Z. ganghwensis* .
Chromatograms (recorded at 535 nm) for the conversion of the monopyrroles **6a**, **6h** – **6j** in *P. putida* MBC18 carrying the cyclase gene from *Z. ganghwensis* (gray) and a control strain without the cyclase (black) were used to assign the signals of the cyclic derivative. Mutasynthesis was performed in LB medium at 20 °C with 1 mM MAP.

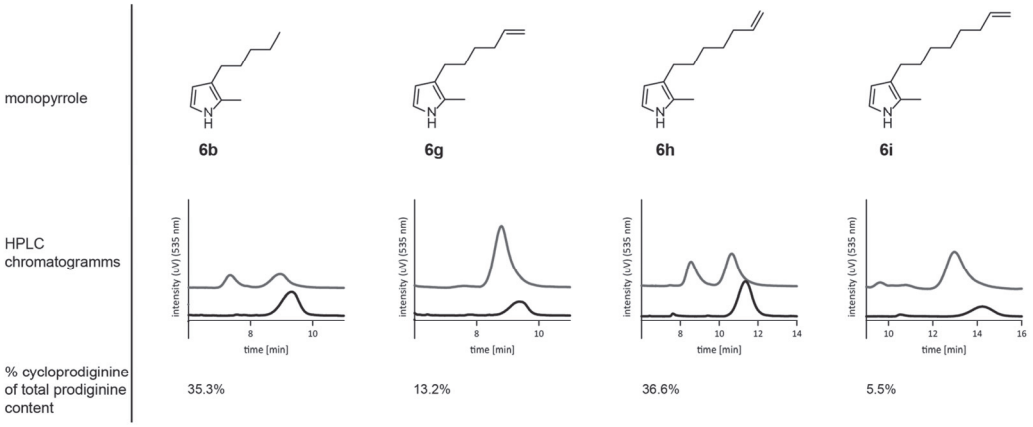

Figure S10: HPLC chromatograms for cycloprodiginine mutasynthesis with the cyclase from *S. ruber*.
Chromatograms (recorded at 535 nm) for the conversion of the monopyrroles **6a**, **6h** – **6j** in *P. putida* MBC18 carrying the cyclase gene from *S. ruber* (gray) and a control strain without the cyclase (black) were used to assign the signals of the cyclic derivative. Mutasynthesis was performed in LB medium at 20 °C with 1 mM MAP.

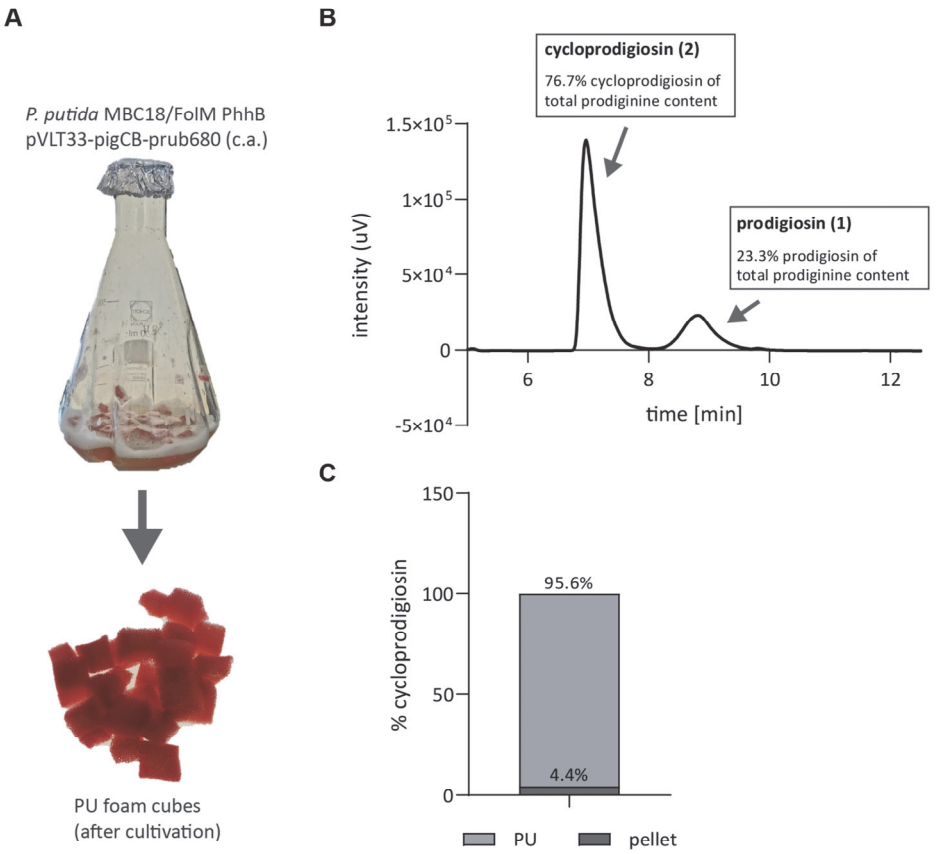

Figure S11: Mutasynthetic production of cycloprodigiosin by supplementation with PU foam cubes.
A: Cultivation of *P. putida* MBC18/FolM-PhhB pVLT33-pigCB-prub680 (c.a.) in 50 mL LB medium at 20 °C with 0.5 mM MAP. The culture broth was supplemented with PU foam cubes. Isolated PU cubes are shown below the shake flask. The PU cubes showed a red color which is typical for prodiginines. **B**: HPLC chromatogram (at 535 nm) of extracts from the PU foam cubes. Prodigiosin (**1**) and cycloprodigiosin (**2**) signals were assigned based on chemically synthesized references. The amount of prodigiosin and cycloprodigiosin, respectively, relative to the total prodiginine content is given in the boxes. **C**: The amount of cycloprodigiosin in the pellet (dark gray) and in the PU cubes (light gray) (given as fraction of the total cycloprodigiosin content in the culture) was quantified based on HPLC-PDA analysis.

SI Methods

Table S2: Oligonucleotides used in this study.

oligonucleotides				
#	name	sequence (5' → 3')	Tm [°C]	application
1	IF-BS_Pr-h_fw	TTCACACAGGAAACAGAATTCATGGACTTGAACTTCACC GAAGAG	67	cloning mutasynthesis vector
2	IF-BS_Pr-h_rev	TGCCTGCAGGTCGACTCTAGACTACTGCAATTCAGCAGA GAGCT	71	
3	IF-pEM7_fw	AATCCGTTGATCTATGTCGGTTCGAGCTCGGTACCCGG G	71	cofactor recycling
4	IF-pEM7_rev	GTCTGTGTAAGCTGTGGGCGCTCTAGTAGTGCTCAGTG GTTTAGT	71	
5	IF_folM_phhB_fw	ATTCGACTCACTAGGGATAAGATACCGAAGACATCTGAG ATACG	66	
6	IF_folM_phhB_rev	GATACCCAGAGATTACCCTGTCATTTGCGCCCCTCGGC G	71	

sequence of *prub680* (from *P. rubra*)

ATGGACTTGAACTTCACCGAAGAGGTCATGTATACGTTGCCGTTCTATCTCGGGCCCCTCTTTATTCTGGCCACTATCAACTTCCTGCGCAAACAGAA
GAACTACCGGCTGAACGACACCTTGACCAACGCGACCATCGCACTGGGCAATCTGGGTCTGAGCTTCATCTTCCTGCTCGCCGTAGTGGCCCTGTAT
ACCCTCGTCTACAACGAGTACCGCCTCGTGGATCTCGATCAGAGCAACCCGCTGATCTATCTGCTGGCCTTCCTCGTGTATGACTTCCTGTACTATTG
GAACCACCGTTTCCACCATATGATCGGCTTGTTCTGGGCCGATCACCTCGTTCACCATACGGCCGAAAACTTCAATTTTGGCGTCAGCATCCGGATCA
GCTACTTCACCGAGCTGACAATGTGGATGACGTTCATTCCGATGGCTTTCATGGGGATTAGCCTGGAAGTGTTTCTGGCCGCCTCGTATACGCAAATC
ATCTGGGCCTTCTGTATCCACACCAAATACCTGAAAAAGACGCCGCGGGCCGACAAGATCTTTAACACACCGAGCCTGCACCGCGTCCACCACGCG
CGCAACCGCCAGTACATCGACAAGAACTACGGCGGCATCCTGATCATCTGGGACCGCCTGTTCGGCACGTACCAGCGTGAGCTGGAGTCCGACCCT
GTCGTGTACGGGGTCCGCGAGAGCTACCCATCCTTCAGCCCGCTGGTGATCAACAGCTATTACCTGAAGACCATTTGGCAAAAAATCAAGTGCAGCC
GCAGCGTGTTCGAGGTGCTGTGCTCAGTGTTCGCCCCGCCGGCCTGGCTCCCAAAGAACGCTAACAAGGCCGATTTCTACTCCCTGACCGCTAAGG
TCAAGTCGAAGGATTTCAAACCGAAAGATCCTTACATCTGTAAACGCACCAAGTGGACCGCGTTCGTTCGTTTTAGCTCAATCGTGGTTCTGTTCACCT
ACCTCATGTCCTACTTTGGCGAGCTCCCCACGTTGCCTCTCGTCTCGCTGTCACTGCTGTTCTTCTGGCTCTGCCATTTTAACGGCCTGGTATTTGAC
GGCGCCAAACTGGGTCTCCCGATGGAAGCTGTCACCCAGGTGCTGTACGGCCTGATCCTGTATTGGGCGATCGAGACCGACCAGGCAGCCTGGAT
CACCATTGGTACAGCGACCCTCGCCCTGATCAGCCTCTGCAACTATGTGATTTACCGTACCCGGCCCGCGGCCCCTGTAGAGCTCTCTGCTGAATTG
CAGTAG

sequence of cyclase from *P. denitrificans*

ATGGACCTGAACTTTACGGAGGAAATCATGTATACCCTGCCGTTCTACTTGGGCCCGCTGTTCCTGCTGGCATCAATCAACTTTTTTCGGAAGCAGAA
GAACTACCGCCTGAACGACACGCTCACCAACGCTAGTATTGCCCTCGGGAATTTGGGTCTGAGCTTCATTTTCCTCCTGGCGGTAGTGGCGGTCTAC
TCGTTGGTGTACTCCGAATATAAATTTTTCGATCTGGACCAGAGCGACCCGTTGACTTATGTCCTGGCCTTCTTGCTGTACGATTTCCTGTATTATTGG
AACCACCGCTTCCATCACATGATCGGCTTGTTCTGGGCGGACCACTTGGTCCATCACACCGCAGAAAACTTTAACTTCGGCGTCTCGATCCGTATCAG
CTACTTCACGGAATTGACAATGTGGATGACCTTCATCCCAATGGCATTCCTGGGTATTAGTCTGGAAGTGTTCCTGATCGCCAGCTACGCGCAGATCG
TGTGGGCCTTCTGTATTCACACTAAGTGGTTCAAATCAACGCCGATCGCCGATAAACTCCTGAATACCCCTAGCCTGCACCGCGTGCACCATGCCCG
CAACACCAAGTACATCGATAAAAACTTCGGCGGCATCTTCATCATTTGGGACCGCCTGTTCGGGACTTACCAGACCGAACTGAACGACAACCCGGTG
ACCTTTGGGGTGCGCGAATCCTTCCCTAGCTTCAGCCCGCTCATCATCAATAGCTACTACCTCAAGACTATCGCCAAGAAGATCCGTCTGTCGAGCA
GCCTGTTCGAAGTTGTTTGCAGCATCTTCGGCCCACCCGTGTGGTTGCCGAAGAAGGCCAATAAGTCCACTTTCTATTCTAAGACCTGCAAAATCGAT
AGCAAAAACTTCAAAGCGAAGGACCCCTATCTGTCCACCAAGACCAAGTGGACCTGCTTCAACCGCTTCATTTGCATCATCGTGGTGTTCTGCTACCT
CATGATGAACTTCGGCGCCCTGCCGGTCCTGCCTCTGATTATTCTGAGCGTACTCTTCTTCTGGCTGTGCCACTACAACGGTATTGTTTTTGATGGGT
TCAAGATCGGCTGGACCACGGAGATCATCACTCAAATCCTGTTCATTTCGTTCCTGTCCTGGGCGATCACCTCGAAGCAGCCCGAATACCTGATCCTC
TCGACCGGCATTCTGGCTTGCCTGTCGCTGGTAAATTATCTGATCTACTCGAACAAGAAGTCGCAGTATGAAGAAAATAACTTGGACATTCAACAGCA
GTAG

sequence of cyclase from *V. gazogenes*

ATGAACCTGGACTTCAGCGACGAGGTAATGTACACCCTCCCCTTCTACCTCGGCCCACTGTTCATCCTGAGCATCCTGAGCTACCTCAAAAAGCACAA
AAACTACCGTTTCAACGATACGCTGACCAACGCGTCCATCGCGCTGGGCAACTTGGGCTTCAGCTTTATCATGCTGTTGGGGGTTGTGGCCGCCTAC
AGCTACGTGTACAAGGAGTTTCGGATTTTTGAGCTGGACCAGAGCTCGCCGCTGACATACATCTTGGCCTTCTTCGCGTACGACTTTTGTTACTACTG
GAACCACCGCATTCACCATATGATCGGCCTCTTCTGGACGGACCACCTCGTCCACCACACCGCAGAGAACTTCAATTTCGGTGTCTCGATCCGCATC
AGCTACTTTACGGAGCTGACCATGTGGATGAGCTTTATCGTGATGGCTTTCCTGGGCATTAGCCTGGAGGTTTTTTTGGTGGCTAGCTACATTCAGGT
CTTGTGGGCCTTCTGTATTCACACCAAGTACCTCAAAAACACTCCCCGCCTGGACAAGTTCGTCAATACCCCGTCCCTCCACCGCGTGCATCATGCTC
GTAACGGTAAGTATATCGACAAGAATTTTGGCGGTATTCTGGTCGTTTGGGACCAGCTGTTCGGCACCTACCAGCGCGAACTGGAGGAAGAACCAGT
GGTCTACGGCGTACGTGAAAGCTACCCCAGCTTCAGCCCATTCGTGATTAATAGCTATTACCTCAAAACCATTTGGAAAAAGATCCAACTGAGTCATT
CCCCCTGGGAAATCTTCTGCAGTGTGTTCGCCTCGCCGGGTTGGCTGCCGAAGGGGGTGGAACGCCGTCACTTCTACAGTGACGTAGCCCGGATCC
CGTGCAGCCAATTCAAGCCTCGGGACCCATACATCAGCCTGCGCACCAAGCTGACCACCCTGGTGCGGTTTTTCGTAACCCTGATTCTGTTTTGTTAC
CTCATGAGCTATTTCGGCGATTTCCCCATCCTCCCGGTCACCGCCCTGAGCCTGCTGTTTCTCTGGTTGTCGCACTACAACGGGATCGTGCTGGACG
GGCGGAATGTTGGCTGGGGCGCCGAGATTATTAGCCAGGGCTTCGCGGGCATCTTCCTCTATTGGGCGGTCAGCACCGAACAGAACCACCTGCTGA
TCATTAGCACCGTCATCCTGATGGTTATCACCCTGCTGAACTATATCATCTATCGCCAGGGGCGTGAACTGAAGGGCCGGTTGCTCCCACAGTCTGA
AACCCTCTAG

sequence of cyclase from *Z. ganghwensis*

ATGTCTACCGACTTCTCGGAACAGCTGCTCTTTACCTTGCCGCTGTACTTGGGTCCGCTGTTCATCTTCGCGTTGATCGACTTCGTTCGCTCCACCCG
CGGCTACCGCGTGAATGACACCCTGACTAACGCCACCATTGCGCTGGGCAACCTGGGGTTCACCTTCATCCTGGTCGCCGGTATTATCGCCATGTAC
AATTACCTGTATTCTAATTTTTCCCTCTTCACGCTGGACCAGACGTCCGTCACCACCTGGCTGATCGCCTTCATTTTTTATGACTTTTGCTTCTACTGGA
ACCATCGCGTGCACCACGCCATCGGCATCTTCTGGGTGGATCACATCGTGCATCATACTGCCGAGAACTTCAACTTCGGTGTGAGCATCCGCAACTC
TTACTTCATGGAAGTGACTATGTGGCTGACTTTCATTCCGATGGCCCTGGCGGGCATCAGCATCGAAGTCTTCCTGGCAGTCTCATACACGCAGATGA
CCTGGGCATTTCTCATCCACCACAAGAAGCTGAAACATACCCCGCGTCTCGATAAGGTGTTCAACACCCCGTCGTTGCACCGGGTGCATCATGCCCG
GAACACGAAATATATCGATAAGAACTTCGGCGGCATTTTTATCATTTGGGACCGTCTGTTTGGCACCTACCAGACCGAATCGGAATCCGTGCCGGTGA
CCTACGGCGTCCGCGAGTCGATCCAATCGTTCAGCCCCCTGATGATCAACATCCAGTACCTGAAGGTGATCATCAAGAAATTTACCCACTCGAAGAC
CCTGATTGACAAGCTGAAGTCCATTTTCTACAGTCCGGGCTGGTTGCCGGCCGGCCTGACTAAAACCGAATGCCTGGGCAAGATCGCCGATATCCCC
TGTAAATATTTCAAGCCCAAGAACAGCCCGCTCACCGCGACCATGAAGCTGAGCTGTATTCTGCGCTTCATCGTGATCCTGGTCGTCTTCACCTACCT
CATGTGGAACTTCTATGACTTGCCTTGGTTGCAGACGACGGCGCTCTCTTGCCTCTTCTTTTGGCTGTGCCACTATAATGGCATCGTGTTCGACGGCG
TTAAGATCACGTGGAAGAGCGAAGTGTTGTCGCAGTTCCTGATCATTCTGTCGGGCATCACGGGTCTGGGCTACACCAGCGTCAACATTGTAAGTGC
CGCCATCATTTTCACCTCCTTCGTGAGCTTTATTTGCTACACGCTGCATCACAGCCCGCCGAGCCACTCCCGGAAGAACCGCCTCCTGTCAGCTCTC
ACCGAGTAG

sequence of cyclase from *S. ruber*

ATGGATATTGAGTTCCACGAAATCATCCTCTACACGCTGCCCTCGCTGTTTCTGCCCTTGTTCTTTGACGCCGGCATCGACTACATTAAGAAAACGCA
CCGCTACCGCCTGAACGACACGATTACCAATCTCTCCATCTCGCTGGCTAACCTCGGCGCCTCCTTCATTATCCTGACCGCCGTGCTGGCCGTCTAT
AGTTACACGTATTCCAACTTTTCTCAGTTCCAACTGAACCAAACGGAGCTGAGCACGTGGCTCCTGGCATTCATCCTGTACGACTTTTGCTACTACTG
GAATCATCGCCTGCACCACAAGATCGGTATTCTCTGGGCCGACCATATCGTGCACCACTCGGGCGAAGAAATGAATTTCGGGGTCAGCATCCGCCA
GAGCTTCCTCACCGAGCTGACCATGTGGCCCCTCTTCCTCCTGATGGCGTTGGTGGGGATCTCCATAGAGGTGTTTCTGATCACCAGCTATATTCAA
GCCACCTGGGCATTTCTCATTCATACTAAGTGCCTCAAAAACACCCGGTGGCTGGACAATATCCTGAACACCCCGTCCCTGCATCGCGTGCACCACG
CGACCAATCAGATGTACATCGACAAGAACTTCGGCGGCATCCTGGTCGTTTGGGATCAAATCTTCGGCACCTACCAGAACGAGCTGGCCGACTCGCC
CGTCAAGTACGGCATCATGGAGTCATTCGCCAGCTTCAGTCCCGTGTCGATCAATTTGCAGTACTACAAAGTGATTCTGAAGAAGATCGCCTATAGTC
ACTCCATCTCCGAAATGCTGAAGTCGATCTTTGCCAGCCCTGGTTGGGTGCCCAAGGCTATCTCCGCAAAAAAGTTCTACGCGGAGATCAGCAACCT
CAGCGCCCGCCAGCACGTGTCGAGCCGCGGCGAGATCTCGGTGAACGCGCGCAAGAGCTGCATCATCCGGTTCATTCTGACTCTGAGCGTGTTCAT
CCTGCTGATGTGGAATTTCGCGCTCTTGGGCTGGTGGCAGATCGCAAACCTGGCCGTGCTCTTCTTCTGGTTGTGCCATTACAACGGCCTGGCATTC
GATGGTGTAAAGCTGACCTGGAAAATCGAGGCCATCAGCCAATTTCTGATCATCTTGGTGGGCGGTGTGGTGGTGTATAATAATCAGCCAGGCCACC
TGCTGATCCTGGTGCTGATCGCGAGTATTACCTCGCTCAGCTGCTATATCGTGTACCAGAACCCCCCTATCAAACCCGAAACCGACGCCCTGACGAA
GGCCCTGGTCGAGTAG

sequence of *phhB* (from *P. aeruginosa*)

ATGACCGCTTTGACCCAAGCCCATTGCGAAGCCTGCCGCGCTGACGCCCCGCACGTGAGCGACGAAGAACTGCCCGTGCTGCTGCGGCAGATCCC
GGATTGGAACATCGAAGTGCGCGACGGCATCATGCAGTTAGAGAAGGTGTACCTGTTCAAGAACTTCAAGCATGCCCTGGCCTTCACCAATGCCGTG
GGCGAGATATCCGAGGCCGAAGGCCACCATCCGGGCCTGCTGACCGAGTGGGGCAAAGTGACCGTGACCTGGTGGAGCCACTCGATCAAGGGCCT
GCACCGCAACGATTTCATCATGGCGGCGCGCACCGATGAGGTTGCGAAAACCGCCGAGGGGCGCAAATGA

sequence of *folM* (from *E. coli*)
ATGGGCAAGACCCAGCCTTTGCCAATTTTGATCACGGGCGGGGGCCGCCGCATCGGCTTGGCCTTGGCGTGGCACTTCATCAACCAAAAACAACCG
GTGATCGTCAGCTACCGGACGCACTACCCAGCCATCGACGGGCTGATCAACGCGGGCGCCCAGTGCATCCAGGCGGACTTCTCGACCAACGATGG
CGTGATGGCCTTCGCCGACGAGGTCCTCAAGAGCACCCACGGCCTGCGCGCGATCTTGCACAACGCCTCGGCCTGGATGGCCGAGAAGCCGGGC
GCCCCACTGGCCGATGTCCTGGCGTGCATGATGCAGATCCACGTCAACACCCCATACCTGTTGAACCACGCCCTGGAGCGATTGCTGCGCGGTCAC
GGGCACGCCGCCAGCGACATCATCCACTTCACCGACTACGTGGTGGAACGCGGCAGCGATAAGCACATCGCCTACGCGGCGAGCAAGGCCGCGCT
GGACAACATGACCCGCTCGTTCGCCCGCAAACTGGCGCCGGAGGTGAAGGTGAACTCGATCGCCCCATCGCTGATCCTGTTCAACGAGCACGACGA
CGCCGAGTACCGGCAACAGGCCCTGAACAAGTCCCTGATGAAGACCGCCCCAGGCGAAAAGGAGGTGATCGATCTGGTCGACTACTTGCTCACCTC
GTGCTTCGTCACCGGGCGCTCGTTCCCACTCGACGGCGGCCGCCACCTGCGCTGA

SI-M1: Total synthesis of cycloprodigiosin

(*Z*)-*N*-((5-bromo-3-methoxy-2*H*-pyrrol-2-ylidene)methyl)-*N*-ethylethanamine (**11**)

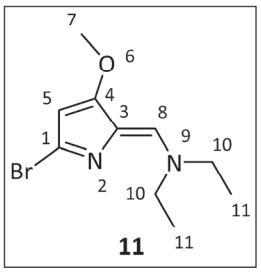

11

At 0 °C, $POBr_3$ (12.8 g, 44.2 mmol, 2.5 eq.) was dissolved in dry dichloromethane (60.0 mL, 0.3 M), to which diethylformamide (5.9 g, 53 mmol, 3.0 eq.) was added and stirred for 30 min. A solution of 4-methoxy-3-pyrroline-2-on (**12**, 2.00 g, 17.7 mmol, 1 eq.) in dichloromethane (30 mL) was added slowly at 0 °C. The reaction was stirred for 3 h at 50 °C, then for 16 h at 22 °C. After quenching with 200 mL ice water and neutralization with 1 M NaOH, the reaction was diluted with 40 mL EE and the precipitated salt was filtered off. The aqueous phase was extracted three times with 40 mL EE, washed twice with 50 mL saturated sodium chloride solution, dried over $MgSO_4$, filtered off and concentrated. The crude product was purified by column chromatography (PE/EE, 8:2 + 1% NEt_3) to give the product as a yellow solid (2.00 g, 7.73 mmol, 60%).

^{1}H-NMR (600 MHz, $CDCl_3$) δ [ppm] = 1.30 (m, 6H, 11-H), 3.41 (m, 2H, 10-H), 3.77 (s, 3H, 7-H), 4.12 (m, 2H, 10-H), 5.62 (s, 1H, 5-H), 7.02 (s, 1H, 8-H).

^{13}C-NMR (151 MHz, $CDCl_3$): δ [ppm] = 12.7 (C-11), 14.7 (C-11), 44.8 (C-10), 51.4 (C-10), 58.2 (C-7), 96.8 (C-4), 120.4 (C-3), 133.6 (C-1), 138.8 (C-8), 165.4 (C-4).

MS (APCI): m/z = 260 [$M+H^+$].

tert-Butyloxycarbonyl-5'-formyl-4'-methoxy-1*H*,1'*H*-(2,2'-bipyrrole) (**13**, Boc-MBC)

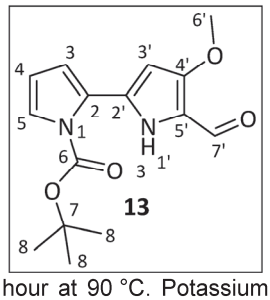

A mixture of 1,4-dioxane and water (9:1 (*v*/*v*), 37 mL 1,4-dioxane: 4.1 mL water) was degassed. Tetrakis(triphenylphosphine)palladium(0) (**14**, 301 mg, 0.52 mmol, 1.5 eq.) was dissolved in, degassed toluene (2.25 mL) to which pyrrole (**11**, 1.35 g, 5.17 mmol, 1 eq.) and N-Boc-pyrrole MIDA ester (2.50 g, 7.75 mmol, 1.5 eq.) were added. The solution was diluted with the dioxane/water mixture (41 mL) and stirred for one hour at 90 °C. Potassium phosphate (2.20 g, 10.3 mmol, 2 eq.) was added and stirred at 90 °C for one hour. After repeated tetrakis(triphenylphosphine)palladium(0) addition (301 mg, 0.52 mmol, 0.05 eq.), the solution was stirred at 90 °C for 3 h. The reaction was stopped with 50 mL water and 6 mL 2 M HCl, extracted three times with CH_2Cl_2, dried over magnesium sulfate, filtered off and concentrated. The crude product was loaded onto Celite and purified by column chromatography (PE/EE, 7.5:2.5 + 1% TEA). The product was obtained as a yellow solid (688 mg, 2.37 mmol, 48%).

^{1}H-NMR (600 MHz, $CDCl_3$) δ [ppm] = 1.62 (s, 9H, 8-H), 3.91 (s, 3H, 6'-H), 6.10 (d, *J* = 2.7 Hz, 1H, 3'-H), 6.27 (t, *J* = 3.5 Hz, 1H, 4-H), 6.77 (dd, *J* = 3.6, 1.8 Hz, 1H, 3-H), 7.32 - 7.39 (m, 1H, 5-H), 9.28 (s, 1H, 7'-H), 11.09 (s, 1H, 1'-H).

^{13}C-NMR (151 MHz, $CDCl_3$): δ [ppm] = 28.1 (8-C), 58.2 (6'-C), 86.1 (7-C), 95.2 (3'-C), 111.8 (4-C), 118.0 (3-C), 118.4 (5'-C), 125.3 (5-C), 127.0 (2-C), 130.7 (2'-C), 144.4 (6-C), 149.7 (4'-C), 172.1 (7'-C).

MS (APCI): m/z = 291.3 [$M+H^+$].

6-Methylcyclohex-1-en-1-yl acetate (**15**)

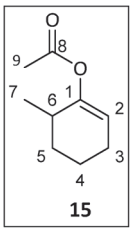

Diisopropylamine (9.77 ml, 69.5 mmol, 1,3 eq.) was dissolved in dry THF (217 ml) and cooled to -78 °C. *n*-Butyllithium (25.7 ml, 2.5 M, 1.2 eq.) was added dropwise over 15 min followed by 2-methylcyclohexanone (6.49 ml, 53.49 mmol, 1 eq.), acetic anhydride (50 mL, 535 mmol, 10 eq.) and Montmorillonite KSF (2.6 g). The reaction mixture was warmed to 21 °C over 3 h. The reaction was quenched using saturated NH_4Cl, filtered through Celite, extracted with EtOAc, dried over $MgSO_4$ and the solvent was evaporated. The crude product was isolated by two step column chromatography using 15:1 PE/EE

and in the second column 20:1 PE/EE as mobile phase. The product was gained as characteristic smelling colorless oil (6.42 g, 41.6 mmol, 78%).

^{1}H-NMR (600 MHz, $CDCl_3$) δ [ppm] = 0.99 (d, *J* = 7.0 Hz, 3H, 7-H), 1.36-1.44 (m, 1H, 5-H), 1.55-1.61 (m, 1H, 4-H), 1.62-1.69 (m, 1H, 4-H), 1.85-1.91 (m, 1H, 5-H), 2.07-2.12 (m, 2H, 3-H), 2.13 (s, 3H, 9-H), 2.43-2.49 (m, 1H, 6-H), 5.32 (t, *J* = 4.0 Hz, 1H, 2-H).

^{13}C-NMR (151 MHz, $CDCl_3$): *δ* [ppm] = 18.2 (7-C), 20.1 (4-C), 20.9 (9-C), 24.3 (3-C), 31.4 (6-C), 31.5 (5-C), 114.4 (2-C), 152.0 (1-C), 169.7 (8-C).

MS (APCI): *m/z* = 155.1 [M+H$^+$].

5-Methyl-2-nitrocyclohexan-1-on (**16**)

The acetate (**15**, 1.10 g, 7.13 mmol, 1 eq) was dissolved in chloroform (7.13 mL) and fine ground ammonium nitrate (1.10 g, (78%) 10.7 mmol, 1.5 eq.) was added. Trifluoroacetic anhydride (7.13 mL, 94.5 mmol, 13.2 eq.) was added to the solution in a water bath and stirred at 22 °C for one hour. The solution was diluted with CH_2Cl_2 and washed with water. The organic phase was washed with cold potassium bicarbonate solution (1%), dried over $MgSO_4$, filtered and concentrated. After column chromatographic isolation (PE/EE, 8:2 + 0.5% AcOH), the product was obtained as yellow oil (407 mg, 2,59 mmol, 36%).

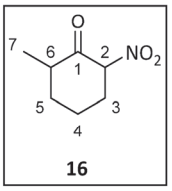

16

^{1}H-NMR (600 MHz, $CDCl_3$) δ [ppm] = 1.12 (d, *J* = 6.4 Hz, 3H, 7-H), 1.50 (qd, *J* = 3.79, 13.20 Hz, 1H, 5-H), 1.81 (qt, *J* = 3.70, 13.80 Hz, 2H, 4-H), 2.05 (dqin, 1H, 4-H), 2.09 - 2.21 (m, 1H, 5-H), 2.36 - 2.46 (m, 1H, 3-H), 2.51 (dq, *J* = 12.7 Hz, *J* = 6.4 Hz, 1H, 6-H), 2.55 - 2.61 (m, 1H, 3-H), 5.28 (dd, *J* = 13.3 Hz, *J* = 5.7 Hz, 1H, 2-H).

^{13}C-NMR (151 MHz, $CDCl_3$): *δ* [ppm] = 14.2 (7-C), 22.7 (4-C), 32.3 (3-C), 35.6 (5-C), 45.4 (5-C), 92.4 (2-C), 200.4 (1-C).

MS (APCI): *m/z* = 158.1 [M+H$^+$].

2-Methyl-6-nitrocyclohexan-1-ol (**17**)

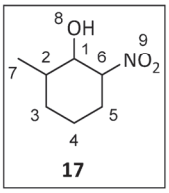

17

Compound **16** (407 mg, 2.59 mmol, 1 eq.) was dissolved in dry THF (67.7 mL, 0.15 M), cooled to 0 °C, and sodium borohydride (48 mg, 1.27 mmol, 1.5 eq.) was added. After 1 h, the reaction was quenched with water, extracted with EE, dried with $MgSO_4$, filtered off, and concentrated. The product was isolated on SiO_2 with (PE/EE, 8:2 + 0.5% AcOH) and obtained as yellow oil (164 mg, 1.03 mmol, 40%).

^{1}H-NMR (600 MHz, $CDCl_3$) δ [ppm] = 1.05 (d, *J* = 6.97 Hz, 3H, 7-H), 1.14-1.21 (m, 1H, 5-H), 1.58 (m, 2H, 4-H), 1.82-1.94 (m, 2H, 3,5-H), 2.0-2.12 (m, 1H, 6-H), 2.29-2.41 (m, 2H, 3-H), 3.80 (m, 1H, 1-H), 4.64 (quin, *J* = 3.85 Hz, 1H, 2-H).

^{13}C-NMR (151 MHz, $CDCl_3$): *δ* [ppm] = 17.3 (7-C), 19.7 (4-C), 27.3 (3-C), 28.9 (5-C), 34.9 (6-C), 73.9 (1-C), 85.3 (2-C).

MS (APCI): *m/z* = 160.0 [M+H$^+$].

3-Methyl-1-nitrocyclohex-1-ene (**18**)

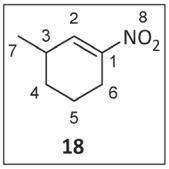

18

The alcohol (**17**, 470 mg, 2.95 mmol, 1 eq.) was dissolved in acetic anhydride (**19**, 18 mL, 19 mmol, 6.5 eq.). DMAP (**20**, 364 mg, 2.95 mmol, 1.0 eq.) was added and the reaction was stirred for 1.5 h at 50 °C. The bulk of the acetic anhydride was evaporated under reduced pressure and the crude product isolated by two consecutive column chromatographic steps (PE/EE, 8:2 + 0.5% AcOH). The product (**18**, 135 mg, 0.95 mmol, 32%) was obtained as a colorless to slight yellow oil.

^{1}H-NMR (600 MHz, $CDCl_3$) δ [ppm] = 1.14 (d, *J* = 7.1 Hz, 3H, 7-H), 1.21 (m, 1H, 5-H), 1.59-1.69 (m, 1H, 4-H), 1.83 (dtd, *J* = 2.8, 5.9, 12.9 Hz, 1H, 5-H), 1.87 - 1.96 (m, 1H, 4-H), 2.44 - 2.51 (m, 2H, 3,6-H), 2.56 - 2.65 (m, 1H, 6-H), 7.16 (dd, *J* = 3.2, 1.8 Hz, 1H, 2-H).

^{13}C-NMR (151 MHz, $CDCl_3$): *δ* [ppm] = 20.4 (7-C), 20.9 (4-C), 24.1 (6-C), 29.5 (5-C), 30.6 (3-C), 139.2 (2-C), 149.4 (1-C).

MS (APCI): *m/z* = 142.0 [M+H$^+$].

Ethyl 7-methyl-4,5,6,7-tetrahydro-2*H*-isoindole-1-carboxylate (**21**)

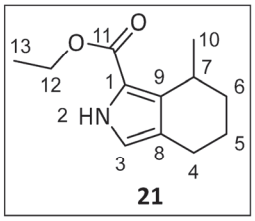

21

Compound (**18**, 485 mg, 3.44 mmol) was dissolved in dry THF (4.3 mL, 0.8 M) and isocyanoacetic acid ethyl ester (**22**, 400 µL, 3.44 mmol, 1.0 eq.). DBU (534 µL, 3.44 mmol, 1.0 eq.) was added and stirred for 16 h at 22 °C. The solution was washed with saturated sodium chloride solution, extracted three times with EE, dried with magnesium sulfate, filtered off and concentrated. The crude product was purified by column chromatography (dichloromethane). The product (587 mg, 2.83 mmol, 82%) crystallized as a white solid.

^{1}H-NMR (600 MHz, $CDCl_3$) δ [ppm] = 1.25 (d, *J* = 6.93 Hz, 3H, 10-H), 1.35 (t, *J* = 7.03 Hz, 3H, 13-H), 1.63-1.82 (m, 4H, 5,6-H), 2.44 (m, 1H, 4-H), 2.60 (m, 1H, 4-H), 3.28 (m, 1H, 7-H), 4.31 (m, 2H, 12-H), 6.62 (d, *J* = 2.51 Hz, 1H, 3-H), 8.86 (s, 1H, 2-H).

^{13}C-NMR (151 MHz, $CDCl_3$): *δ* [ppm] = 14.6 (13-C), 18.8 (6-C), 21.9 (10-C), 22.1 (4-C), 26.8 (7-C), 31.0 (5-C), 59.9 (12-C), 117.7 (1-C), 118.5 (3-C), 121.6 (8-C), 133.7 (9-C), 161.4 (11-C).

MS (APCI): *m/z* = 208.1 [M+H$^+$].

Ethyl 3-bromo-7-methyl-4,5,6,7-tetrahydro-2*H*-isoindole-1-carboxylate (**23**)

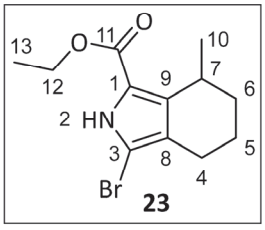

23

The pyrrole (**21**, 587 mg, 2.83 mmol, 1 eq.) was dissolved in dry THF (14.15 mL, 0.2 M). In a room temperature water bath, NBS (555 mg, 3.12 mmol, 1.1 eq.) was added over 10 min. The reaction was stirred for one hour at 22 °C, diluted with dichloromethane and the organic phase was washed three times with water and once with $NaCl_{sat.\ aq.}$, dried over $MgSO_4$, filtered and concentrated. The crude product was purified by column chromatography (*PE/EE*, *4:1*). The product was obtained as red crystals (693 mg, 2.42 mmol, 86%).

^{1}H-NMR (600 MHz, $CDCl_3$) δ [ppm] = 1.22 (d, *J*=7.02 Hz, 3H, 10-H), 1.36 (t, *J*=7.02 Hz, 2H, 13-H), 1.59-1.78 (m, 4H, 5,6-H), 2.23-2.30 (m, 1H, 4-H), 2.45 (m, 1H, 4-H), 3.25 (m, 1H, 7-H), 4.31 (m, 2H, 12-H), 8.92 (s, 1H, 2-H).

^{13}C-NMR (151 MHz, $CDCl_3$): *δ* [ppm] = 14.6 (13-C), 18.1 (6-C), 21.6 (10-C), 21.9 (4-C), 26.9 (7-C), 30.6 (5-C), 60.2 (12-C), 102.0 (3-C), 118.8 (7-C), 121.5 (8-C), 135.1 (9-C), 160.4 (11-C).

MS (APCI): *m/z* = 285.9/287.9 [M+H$^+$].

N-Boc-ethyl 3-bromo-7-methyl-4,5,6,7-tetrahydro-2*H*-isoindole-1-carboxylate (**24**)

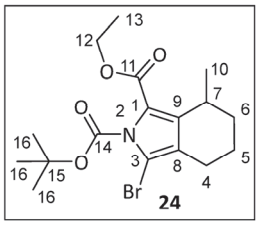

24

Pyrrole (**23**, 685 mg, 2.39 mmol, 1 eq.) was dissolved in acetonitrile (15.9 mL, 0.15 M), mixed with DMAP (40, 56 mg, 0.46 mmol, 0.2 eq.) and di-*tert*-butyl dicarbonate (**25**, 697 mg, 3.11 mmol, 1.3 eq.), and then stirred for 12 h at 22 °C. The solution was diluted with CH_2Cl_2, washed twice with saturated sodium bicarbonate solution and once with water, dried with magnesium sulfate, filtered off and concentrated. The crude product was purified by column chromatography (PE/EE, 4:1), yielding product as orange oil (710 mg, 1.84 mmol, 77%).

^{1}H-NMR (600 MHz, $CDCl_3$) δ [ppm] = 1.19 (d, *J*=7.03 Hz, 3H, 10-H), 1.34 (t, *J*=7.14 Hz, 4H, 13-H), 1.61 (s, 9H, 16-H), 1.63-1.77 (m, 4H, 5,6-H), 2.24 (m, *J* = 16.5, 8.9 Hz, 1H, 4-H), 2.46 (m, 1H, 4-H), 3.23 (m, 1H, 7-H), 4.30 (m, 2H, 12-H).

^{13}C-NMR (151 MHz, $CDCl_3$): *δ* [ppm] = 14.5 (13-C), 17.8 (6-C), 21.6 (6-C), 22.1 (4-C), 26.9 (7-C), 27.7 (16-C), 30.5 (5-C), 60.6 (12-C), 85.7 (15-C), 104.5 (3-C), 121.0 (1-C), 122.4 (8-C), 136.8 (9-C), 148.8 (14-C), 160.3 (11-C).

MS (APCI): *m/z* = 387.2/ 389.2 [$M+H^+$].

2-(Tert-butyl) 1-ethyl 3,7-dimethyl-4,5,6,7-tetrahydro-2*H*-isoindole-1,2-dicarboxylate (**26**)

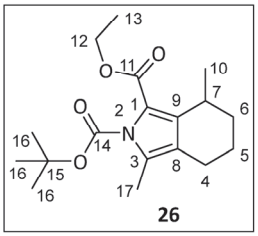

26

Pyrrole (**24**, 647 mg, 1.67 mmol, 1 eq.) was dissolved in 1,4-dioxane/water (93:7, 0.07 M) to which was added potassium carbonate (439 mg, 3.18 mmol, 1.9 eq.) and tetrakis(triphenylphosphine)palladium(0) (**14**, 195 mg, 0.17 mmol, 0.1 eq.). The solution was degassed with three cycles of freeze, pump, thaw, trimethylboroxine (**27**, 1.2 mL (50% solution in THF), 4.19 mmol, 2.5 eq.) was added and stirred for 18 h at 110 °C. The solvent was concentrated, the mixture dissolved in EE, washed three times with water, dried with $MGSO_4$, filtered, and concentrated. The crude product was isolated by column chromatography (PE/EE, 4:1) and the product was obtained as an orange colored oil (436 mg, 1.36 mmol, 81%).

^{1}H-NMR (600 MHz, $CDCl_3$) δ [ppm] = 1.19 (d, *J*=7.01 Hz, 3H, 10-H), 1.34 (t, *J*=7.09 Hz, 3H, 13-H), 1.56 (s, 9H, 16-H), 1.58 - 1.78 (m, 1H, 5-H), 1.71 (ddd, *J* = 2.9, 6.3, 9.9 Hz, 3H, 5,6-H), 2.22 (s, 3H, 17-H), 2.23 - 2.30 (m, 1H, 4-H), 2.47 (m, 1H, 4-H), 3.18 (m, 1H, 7-H), 4.28 (q, *J*=7.14 Hz, 2H, 12-H).

^{13}C-NMR (151 MHz, $CDCl_3$): *δ* [ppm] = 11.6 (17-C), 14.5 (13-C), 18.4 (6-C), 21.4 (4-C), 21.8 (10-C), 26.7 (7-C), 27.8 (16-C), 30.7 (5-C), 60.3 (12-C), 84.2 (15-C), 118.9 (3-C), 120.8 (1-C), 130.9 (8-C), 137.1 (9-C), 150.2 (14-C), 161.5 (11-C).

MS (APCI): *m/z* = 322.2 [M+H$^+$].

1,4-Dimethyl-4,5,6,7-tetrahydro-2*H*-isoindole (**28**)

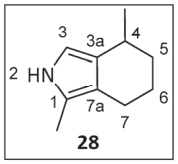

28

Monopyrrole (**26**, 15 mg, 70 µmol, 1 eq.) and NaOH (23 mg, 0.68 mmol, 10 eq.) were suspended in water (122 µl, 6.78 mmol, 100 eq.) and ethylene glycol (6 ml), degassed in vacuum at 70 mbar for 10 min and in an ultrasonic bath with Argon blown through the suspension for another 10 min. This suspension was heated to 200 °C for one hour, cooled to room temperature, extracted with CH_2Cl_2 and concentrated. The product was isolated by column chromatography (PE/EE, 8+2) and the product was obtained as an orange colored oil (approximately: 3.7 mg, 25 µmol, 35%). Due tue low yield and purity and the high sensitivity of the product toward oxidative polymerisation only MS-analysis was done. The success of the reaction was proven by the following reaction.

MS (APCI): m/z = 291.3 [M+H$^+$].

Cycloprodigiosin (**2**)

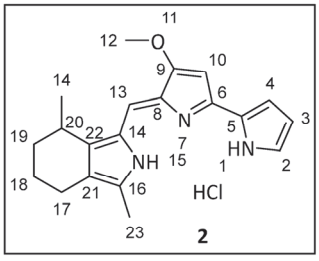

2

Boc-MBC (**13**, 7.19 mg, 20 µmol, 1 eq.) and the monopyrrole (**28**, 3.7 mg, 20 µmol, 1 eq.) were dissolved in dry MeOH (1.5 ml) and AcCl (1.76 µl, 20 µmol, 1 eq.) was added under argon atmosphere. After 1 h at room temperature, the bright red product was concentrated under reduced pressure and purified by a series of column chromatographic steps (2%/1,5%/1,25% (7N NH_3 in MeOH) in CH_2Cl_2). The product was identified by ^{1}H-NMR spectroscopy and literature comparison of the respective spectra[9].

^{1}H-NMR (600 MHz, $CDCl_3$) δ [ppm] = 1.29 (d, 3H, *J* = 7.05 Hz, 14-H), 1.66-1.84 (m, 4H), 1.97-2.52 (m, 5H), 3.12 (s, 1H), 4.01 (s, 1H), 6.09 (s, 1H), 6.33 (m, 1H), 6.87 (s, 1H), 7.20 (s, 1H), 12.48 (br.s, 1H), 12.60 (br.s, 1H).

MS (APCI) *m/z* = 322.4 [$M+H^+$].

SI-M2: Isolation and purification of cycloprodigiosin

Cycloprodigiosin extract, isolated from the PU cube cultivation of 1 L cell culture, gave 108.9 mg of crude sample. The product was enriched on SiO_2 using column chromatography with a stepwise gradient of 1, 2, and 3% methanol in CH_2Cl_2. The elution was tracked by TLC. The cycloprodigiosin containing fractions were pooled, and concentrated. For preparative reversed-phase column-chromatography, we used an ISAspher 100-5 C18 AQ column (5 µm, 150 x 20 mm) from ISERA GmbH (Düren, Germany) and 40:60 acetonitrile:water (both supplemented with 0.1% formic acid) as eluent for isocratic elution. The column oven temperature was kept at 35 °C and a flowrate of 12-14 mL min^{-1} was implemented after injection of samples. The cycloprodigiosin sample was solved in 2 mL ethanol (p.a.) and injected in two portions à 1 mL. Chromatograms were recorded at 535 nm. Cycloprodigiosin eluted around min 14 (total run time was 60 min). In both runs, fractions à 10 mL, which corresponded to the respective signal, were collected and the solvent was removed under reduced pressure.

The purity of the isolated product was determined by q-NMR using trimethoxybenzene as standard: (40 mg), purity: 23.7%. The majority of the impurities were due to inseparable grease from the used PU-cubes. The NMR-spectra were in accordance with literature[9].

^{1}H-NMR (600 MHz, $CDCl_3$) δ [ppm] = 1.29 (d, *J* = 7.13 Hz), 1.66-2.66 (m), 3.12 (s, 1H), 4.0 (s, 3H), 6.08 (s, 1H), 6.33 (s, 1H), 6.87 (s, 1H), 7.01 (s, 1H), 7.19 (s, 1H), 12.48 (brs, 1H), 12.60 (brs, 1H).

MS (APCI): m/z = 322 [$M+H^+$].

SI-M3: Precursor synthesis

The four-stage synthesis is based on previously published reactions[1,10]. Here, a detailed description is given for the new pyrroles **6f** to **6i**.

***Weinrebamid* synthesis:**

To a solution of the carboxylic acid (1.0 eq.) in CH_2Cl_2 (3.5 mL/mmol), *N*,*O*-dimethylhydroxylamine·HCl (1.5 eq.), EDC·HCl (1.5 eq.) and DMAP (1.5 eq.) were added and stirred at room temperature for 22 h. The reaction solution was quenched with saturated NaCl solution and extracted with CH_2Cl_2. The combined organic phases were washed with 1 M HCl and followed by a saturated $NaHCO_3$ solution, dried over $MgSO_4$ and concentrated. The crude product was obtained in quantitative yield as a colorless to pale yellow oil and used for further synthetic steps without purification.

N-Methoxy-*N*-methylhept-6-enamid (**29**)

According to the general procedure for the *Weinrebamid* synthesis, hept-6-enoic acid (**30**, 4.00 g, 31.2 mmol, 1 eq.) was converted to the regarding *Weinrebamid* **29** in 95% yield.

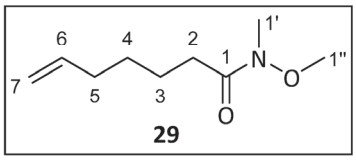

29

^{1}H-NMR (600 MHz, $CDCl_3$) δ [ppm] = = 1.44 (m, 2H, 4-H), 1.65 (m, 2H, 3-H), 2.08 (m, 2H, 5-H), 2.42 (t, *J* = 7.6 Hz, 2H, 2-H), 3.18 (s, 3H, 1''-H), 3.68 (s, 3H, 1'-H), 4.94 (dd, *J* = 1.2, 10.2 Hz, 1H, 7-H), 5.01 (dd, J = 1.7, 17.2 Hz 1H, 7-H), 5.81 (ddt, *J* = 6.7, 10.2, 16.9 Hz, 1H, 6-H).

^{13}C-NMR (151 MHz, $CDCl_3$): *δ* [ppm] = 24.2 (C-3), 28.8 (C-4), 31.7 (C-2), 31.8 (C-1'') 33.6 (C-5) 61.3 (C-1'), 114.6 (C-7), 138.7 (C-6).

MS (APCI): m/z = 172 [M+H$^+$].

N-Methoxy-*N*-methyloct-7-enamid (**31**)

According to the general procedure for the *Weinrebamid* synthesis, oct-7-enoic acid (**32**, 2.84 g, 20.0 mmol, 1 eq.) was converted to the regarding *Weinrebamid* **31** in 78% yield.

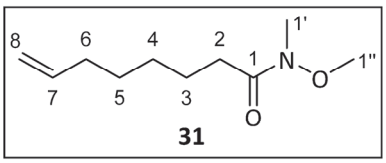

31

^{1}H-NMR (600 MHz, $CDCl_3$) δ [ppm] = 1.36 (m, 2H, 4-H), 1.41 (m, 2H, 5-H), 1.64 (m, 2H, 3-H), 2.05 (m, 2H, 6-H), 2.41 (t, *J* = 7.7 Hz, 2H, 2-H), 3.18 (s, 3H, 1''-H), 3.68 (s, 3H, 1'-H), 4.93 (dd, *J* = 1.2, 10.2 Hz, 1H, 8-H), 4.99 (ddd, *J* = 1.8, 1.8, 17.1 Hz, 1H, 8-H), 5.80 (ddt, *J* = 6.7, 10.2, 17.0 Hz, 1H, 7-H).

^{13}C-NMR (151 MHz, $CDCl_3$): *δ* [ppm] = 24.6 (C-3), 28.8 (C-4), 29.1 (C-5), 32.0 (C-2), 32.3 (C-1'') 33 8 (C-6) 61.3 (C-1'), 114.5 (C-8), 139.1 (C-7).

MS (APCI): m/z = 186 [M+H$^+$].

N-methoxy-*N*-methylnon-8-enamide (**33**)

According to the general procedure for the *Weinrebamid* synthesis, non-8-enoic acid (**34**, 2.00 g, 12.8 mmol, 1 eq.) was converted to the regarding *Weinrebamid* **33** in 97% yield.

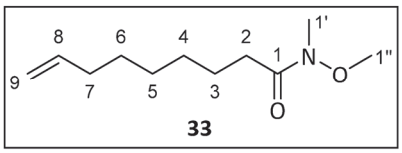

33

^{1}H-NMR (600 MHz, $CDCl_3$) δ [ppm] = 2.33 (m, 4H, 4-H, 5-H), 1.38 (quin, *J* = 6.48 Hz, 2H, 6-H), 1.63 (quin, *J* = 7.46 Hz, 2H, 3-H), 2.41 (t, *J* = 7.31 Hz, 2H, 7-H), 3.17 (s, 3H, 1''), 3.67 (s, 3H, 1'), 4.92 (ddt, *J* = 1.2, 2.3, 10.2 Hz, 1H, 9-H), 4.98 (dq, *J* = 1.7, 17.1 Hz, 1H, 9-H), 5.80 (ddt, *J* = 6.6, 10.2, 17.0 Hz, 8-H).

MS (APCI): m/z = 200 [M+H$^+$].

N-methoxy-*N*-methyldec-9-enamide (**35**)

According to the general procedure for the *Weinrebamid* synthesis, dec-9-enoic acid (**36**, 6.00 g, 35.2 mmol, 1.0 eq.) was converted to the regarding *Weinrebamid* **35** in 91% yield.

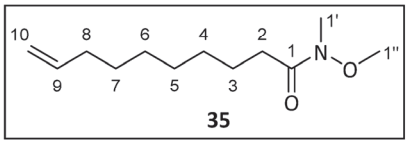

35

^{1}H-NMR (600 MHz, $CDCl_3$) δ [ppm] = 1.34 (m, 6H, 7-H, 6-H, 5-H, 4-H), 1.63 (m, 2H, 3-H), 2.04 (m, 2 H, 8-H), 2.40 (t, *J* = 7.6 Hz, 2H, 2-H), 3.17 (s, 3H, 1''-H), 3.67 (s, 3H, 1'- H), 4.92 (dd, *J* = 1.2, 10.2 Hz, 1H, 10-H), 4.98 (dd, *J* = 1.8, 17.1 Hz, 10-H), 5.80 (ddt, *J* = 6.7, 10.2, 17.0 Hz, 1H, 9-H).

^{13}C-NMR (151 MHz, $CDCl_3$): *δ* [ppm] = 24.8 (C-3), 29.0 (C-5), 29.1 (C-7), 29.4 (C-4), 29.5 (C-6), 32.0 (C-2), 32.3 (C-1''), 33.9 (C-8), 61.3 (C-1'), 114.3 (C-10), 139.3 (C-9).

MS (APCI): m/z = 214 200 [M+H$^+$].

Grignard-reaction:

Methylmagnesium chloride (3 M in THF, 3.0 eq.) was added to a solution of *Weinrebamide* (1 eq.) in dry THF (6.6 mL/mmol Weinreb amide) within 15 min at 0 °C. The reaction mixture was stirred at 0 °C for 1.5 h. After further stirring for 18 h at room temperature, the reaction solution was slowly quenched at 0 °C with saturated ammonium chloride solution and extracted with CH_2Cl_2. The combined organic phases were dried over $MgSO_4$ and the solvent was evaporated on a rotary evaporator. Ketone was obtained as a pale yellow oil in quantitative yield and used for further synthetic steps without purification.

Oct-7-en-2-one (**37**)

According to the general procedure for the *Grignard*-reaction, *Weinrebamid* **29** (2.80 g, 16.4 mmol, 1 eq.) was converted to the regarding ketone **37** in 94% yield.

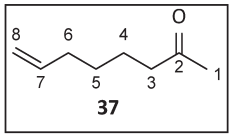

37

^{1}H-NMR (600 MHz, $CDCl_3$) δ [ppm] = 1.39 (tt, *J* = 6.8, 9.5 Hz, 2H, 5-H), 1.56–1.62 (m, 2H, 4-H), 2.06 (dt, *J* = 7.0, 7.3 Hz, 2H, 6-H), 2.13 (s, 3H, 1-H), 2.43 (t, *J* = 7.4 Hz, 2H, 3-H), 4.95 (dd, *J* = 1.2, 10.2 Hz, 1H, 8-H), 5.01 (dd, *J* = 1.7, 17.1 Hz, 1H, 8-H), 5.79 (ddt, *J* = 6.7, 10.2, 17.0 Hz, 1H, 7-H).

^{13}C-NMR (151 MHz, $CDCl_3$): *δ* [ppm] = 23.4 (C-4), 28.5 (C-5), 30.0 (C-6), 33.5 (C-1), 43.7 (C-3), 114.8 (C 8), 138.6 (C-7), 209.2 (C-2).

MS (APCI): m/z = 123 [M+H$^+$].

Non-8-en-2-one (**38**)

According to the general procedure for the *Grignard*-reaction, *Weinrebamid* **31** (2.80 g, 15.1 mmol, 1 eq.) was converted to the regarding ketone **38** in 92% yield.

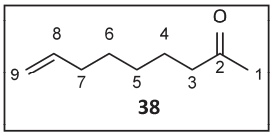

38

^{1}H-NMR (600 MHz, $CDCl_3$) δ [ppm] = 1.25−1 34 (m, 2H, 5-H), 1.35−1 43 (m, 2H, 6-H), 1.58 (tt, *J* = 7.5, 7.5 Hz, 2H, 4-H), 2.05 (m, 2H, 7-H), 2.13 (s, 3H, 1-H), 2.42 (t, *J* = 7.5 Hz, 2H, 3-H), 4.93 (ddt, *J* = 1,2, 2.3, 10.2 Hz, 1H, 9-H), 4.99 (dd, *J* = 1.7, 17.1 Hz, 1H, 9-H), 5.79 (ddt, *J* = 6.7, 10.2, 17.0 Hz, 1H, 8-H).

^{13}C-NMR (151 MHz, $CDCl_3$): *δ* [ppm] = 23.8 (C-4), 28.7 (C-5), 28.8 (C-6), 30.0 (C-1), 33.7 (C-7), 43.9 (C-3), 114.6 (C-9), 139.0 (C-8), 209.4 (C-2).

MS (APCI): m/z = 141 [M+H$^+$].

Dec-9-en-2-one (**39**)

According to the general procedure for the *Grignard*-reaction, Weinrebamid **33** (2.40 g, 10.4 mmol, 1 eq.) was converted to the regarding ketone **39** in quantitative yield.

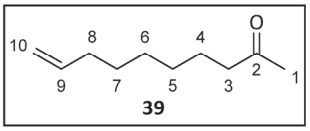

39

^{1}H-NMR (600 MHz, $CDCl_3$) δ [ppm] = 1.29 (m, 4H, 5-H, 6-H), 1.38 (quint, 2H, *J* = 7.20 Hz, 7-H), 1.57 (quint., 2H, *J* = 7.03 Hz, 4-H), 2.03 (q, 2H, *J* = 7.14 Hz, 8-H), 2.13 (s, 3H, 1-H), 2.41 (t, 2H, *J* = 7.43 Hz, 3-H), 4.93 (d, *J* = 10.6 Hz, 1H, 10-H), 4.98 (dd, *J* = 1.8, 17.1 Hz, 1H, 10-H), 5.80 (ddt, *J* = 6.7, 10.2, 17.0 Hz, 1H, 9-H).

^{13}C-NMR (151 MHz, $CDCl_3$): *δ* [ppm] = 23.9 (4-C), 28.8 (7-C), 29.0, 29.1 (5-C/6-C), 30.0 (1-C), 33.8 (8-C), 43.9 (3-C), 114.4 (10-C), 139.2 (9-C), 209.4 (2-C).

MS (APCI): m/z = 155 [M+H$^+$].

Undec-10-en-2-one (**40**)

According to the general procedure for the *Grignard*-reaction, Weinrebamid **35** (2.40 g, 10.4 mmol, 1 eq.) was converted to the regarding ketone **40** in quantitative yield.

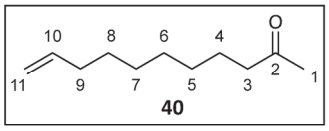

40

^{1}H-NMR (600 MHz, $CDCl_3$) δ [ppm] = 1.18-1.40 (m, 8H, 8-H, 7-H, 6-H, 5-H), 1.56 (tt, *J* = 7.3, 7.3 Hz, 2H, 4-H), 2.02 (m, 2 H, 9-H), 2.12 (s, 3H, 1-H), 2.41 (t, *J* = 7.5 Hz, 2H, 3-H), 4.92 (dd, *J* = 1.2, 10.2 Hz, 1H, 11-H), 4.98 (dd, *J* = 1.7, 17.1 Hz, 1H, 11-Hb), 5.79 (ddt, *J* = 6.7, 10.2, 16.9 Hz, 1H, 10-H).

^{13}C-NMR (151 MHz, $CDCl_3$): *δ* [ppm] = 24.0 (C-4), 29.0 (C-6), 29.1 (C-8), 29.3 (C-5), 29.4 (C-7), 30.0 (C-1), 33.9 (C-9), 44.0 (C-3), 114.3 (C-11), 139.3 (C-10) 209.5 (C-2).

Ketoxim synthesis:

The ketone (1 eq.) was dissolved in undenatured EtOH (0.5 mL/mmol ketone) and mixed with pyridine (0.8 eq.) and ground hydroxylamine hydrochloride (1.5 eq.). The reaction mixture was heated for 2 h at 90 °C under reflux, extracted with CH_2Cl_2, the combined organic phases were washed with 1 M HCl and then dried over $MgSO_4$. After concentration of the solvent, ketoxime was obtained as an E/Z isomer mixture and used for further synthetic steps without purification.

(*Z*)-Oct-7-en-2-one oxime (**41**)

According to the general procedure for the ketoxime synthesis, ketone **37** (1.42 g, 11.3 mmol, 1 eq.) was converted to the regarding ketoxime **41** in 88% yield.

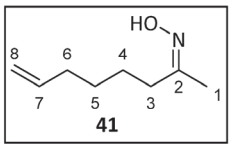

41

^{1}H-NMR (600 MHz, $CDCl_3$) δ [ppm] = 1.38−1,44 (m, 2H, 5-H), 1.50−1 60 (m, 2H, 4-H), 1.91 (s, 3H, 1-H), 2.07 (dt, *J* = 7.8, 7.8 Hz, 2H, 6-H), 2.24 (t, *J* = 7.5 Hz, 2H, 3-H), 4.93−4 97 (m, 1H, 8-H), 5.01 (dd, *J* = 1.7, 17.1 Hz, 1H, 8-H), 5.78 (m, 1H, 7-H).

^{13}C-NMR (151 MHz, $CDCl_3$): *δ* [ppm] = 13.6 (C-1), 25.8 (C-4), 28.4 (C-5), 33.5 (C-6), 35.4 (C-3), 114.8 (C-8), 138.6 (C-7).

MS (APCI): m/z = 142 [$M+H^+$].

(*Z*)-Non-8-en-2-one oxime (**42**)

According to the general procedure for the ketoxime synthesis, ketone **38** (1.90 g, 13.6 mmol, 1 eq.) was converted to the regarding ketoxime **42** in 86% yield.

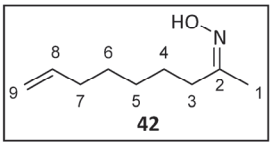

42

^{1}H-NMR (600 MHz, $CDCl_3$) δ [ppm] = 1.28−1.36 (m, 2H, 5-H), 1.37−1.44 (m, 2H, 6-H), 1.51 (tt, *J* = 7.5, 7.5 Hz, 2H, 4-H), 1.87 (s, 3H, 1-H), 2.05 (dt, *J* = 6.4, 6.4 Hz, 2H, 7-H), 2.18 (t, *J* = 7.5 Hz, 2H, 3-H), 4.94 (ddt, *J* = 1.3, 2.4, 10.2 Hz, 1H, 9-H), 5.00 (dd, J = 1.5, 17.1 Hz, 1H, 9-H), 5.80 (ddt, *J* = 6.6, 10.4, 17.0 Hz, 1H, 8-H).

^{13}C-NMR (151 MHz, $CDCl_3$): *δ* [ppm] = 13.4 (C-1), 26.2 (C-4), 28.7 (C-5), 28.8 (C-6), 33.7 (C-7), 35.8 (C-3), 114.4 (C-9), 139.1 (C-8), 159.1 (C-2).

MS (APCI): m/z = 156 [$M+H^+$].

(*Z*)-Dec-9-en-2-one oxime (**43**)

According to the general procedure for the ketoxime synthesis, ketone **39** (4.34 g, 28.1 mmol, 1 eq.) was converted to the regarding ketoxime **43** in 99% yield.

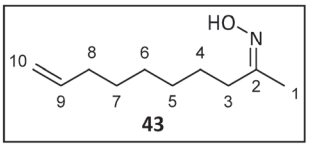

43

^{1}H-NMR (600 MHz, $CDCl_3$) δ [ppm] = 1 31−1 37 (m, 4H, 6-H, 7-H), 1 37−1 43 (m, 2H, 5-H), 1 49−1 57 (m, 2H, 4-H), 1.89 (s, 3H, 1-H), 2.06 (dt, *J* = 7.1, 7.1 Hz, 2H, 8-H), 2.19 (t, *J* = 7.6 Hz, 2H, 3-H), 4 91−4 97 (m, 1H, 10-H), 5.01 (dd, *J* = 1.7, 17.2 Hz, 1H, 10-H), 5.83 (ddt, *J* = 6.7, 10.0, 16.9 Hz, 1H, 9-H).

^{13}C-NMR (151 MHz, $CDCl_3$): *δ* [ppm] = 13.4 (C-1), 26.3 (C-4), 28.9 (C-5), 29.0 (C-6), 29.2 (C-7), 33.9 (C-8), 35.9 (C-3), 114.4 (C-10), 139.2 (C-9), 159.1 (C-2).

(*Z*)-Undec-10-en-2-one oxime (**44**)

According to the general procedure for the ketoxime synthesis, ketone **40** (5.75 g, 34.3 mmol, 1 eq.) was converted to the regarding ketoxime **44** in 84% yield.

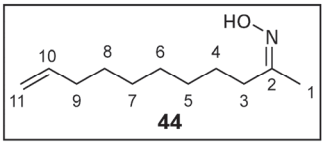

44

^{1}H-NMR (600 MHz, $CDCl_3$) δ [ppm] = 1.18-1.42 (m, 8H, 8-H, 7-H, 6-H, 5-H), 1.42-1.55 (m, 2H, 4-H), 1.90 (d, *J* = 5.9 Hz, 2H, 9-H), 2.03 (dt, *J* = 1.4, 6.6 Hz, 2H, 9-H), 2.20 (t, *J* = 7.5 Hz, 2H, 3-H), 2.38 (t, *J* = 7.9 Hz, 2H, 3-H), 4.92 (dd, J = 1.3, 10.2 Hz, 1H, 11-H), 4.98 (dd, *J* = 1.8, 17.1 Hz, 1H, 11-H), 5.79 (ddt, *J* = 1.6, 6.7, 16.9 Hz, 1H, 10-H);

^{13}C-NMR (151 MHz, $CDCl_3$): *δ* [ppm] = 13.6 (C-1), 26.4 (C-4), 28.9 (C-5), 29.0 (C-6), 29.1 (C-7), 29.2 (C-8), 34.0 (C-9), 35.8 (C-3), 114.3 (C-11), 139.3 (C-10), 159.4 (C-2).

HRMS (ESI): m/z = 184.17 [$M+H^+$].

Trofimov-reaction:

All solvents and liquid reagents were degassed before the reaction and work was carried out under oxygen-free conditions. To a solution of the ketoxime (1.0 eq.) in DMSO (2.14 mL/mmol ketoxime) ground KOH (5.0 eq.) and water (0.75 eq.) were added. At 95 °C, a solution of 1,2-dichloroethane (3.5 eq.) in DMSO (0.21 mL/mmol ketoxime) was added over 2 h using a syringe pump. After 1 h reaction time, a second batch of KOH (5.0 eq.) was added. After a total of 4 h at 90-100 °C, the reaction was cooled, ice water (20 mL) was added and extracted with diethyl ether. The combined organic phases were dried over $MgSO_4$ and the solvent was removed. The crude product was purified by column chromatography (PE/EE, 80:20 + 1% TEA) followed by vacuum distillation (1 mbar, 70-80 °C). The pyrrole was obtained as a colorless oil.

2-Methyl-3-(pent-4-en-1-yl)-1*H*-pyrrole (**6f**)

According to the general procedure for the Trofimov-reaction, ketoxime **41** (1.00 g, 7.08 mmol, 1 eq.) was converted to the regarding pyrrole **6f** in 38% yield.

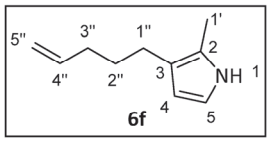

^{1}H-NMR (600 MHz, $CDCl_3$) δ [ppm] = 1.63 (tt, *J* = 7.6, 7.6 Hz, 2H, 2''-H), 2 02−2 14 (m, 2H, 3''-H), 2.18 (s, 3H, 1'-H), 2.40 (t, *J* = 7.8 Hz, 2H, 1''-H), 4.95 (dd, *J* = 1.3, 10.2 Hz, 1H, 5''-Ha), 5.02 (dd, *J* = 1.8, 17.1 Hz, 1H, 5''-Hb), 5.85 (ddt, *J* = 6.6, 10.2, 16.9 Hz, 1H, 4''-H), 6.01 (dd, *J* = 2.8, 2.8 Hz, 1H, 4-H), 6.59 (dd, *J* = 2.7, 2.7 Hz, 1H, 5-H), 7.71 (brs, 1H, 1-NH).

^{13}C-NMR (151 MHz, $CDCl_3$): *δ* [ppm] = 11.2 (C-1'), 25 5 (C-1''), 30 6 (C-2''), 33 7 (C-3''), 109 0 (C-4), 114.4 (C-5''), 115.0 (C-5), 119.4 (C-3), 123.5 (C-2), 139.3 (C-4'').

MS (APCI): m/z = 150 [M+H$^+$].

3-(Hex-5-en-1-yl)-2-methyl-1*H*-pyrrole (**6g**)

According to the general procedure for the Trofimov-reaction, ketoxime **42** (0.50 g, 3.22 mmol, 1 eq.) was converted to the regarding pyrrole **6g** in 39% yield.

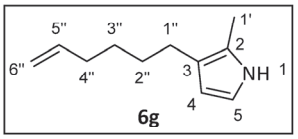

^{1}H-NMR (600 MHz, $CDCl_3$) δ [ppm] = 1.44 (tt, J = 7.5, 7.5 Hz, 2H, 3''-H), 1.51−1.59 (m, 2H, 2''-H), 2.02−2.14 (m, 2H, 4''-H), 2.18 (s, 3H, 1'-H), 2.39 (t, *J* = 7.6 Hz, 2H, 1''-H), 4.93 (dd, *J* = 1.2, 10.2 Hz, 1H, 6''-H), 5.00 (dd, *J* = 1.7, 17.1 Hz, 1H, 6''-H), 5.82 (ddt, *J* = 6.7, 10.2, 16.9 Hz, 1H, 5''-H), 6.01 (dd, *J* = 2.8, 2.8 Hz, 1H, 4-H), 6.59 (dd, *J* = 2.7, 2.7 Hz, 1H, 5-H), 7.70 (brs, 1H, 1-NH).

^{13}C-NMR (151 MHz, $CDCl_3$): *δ* [ppm] = 11.2 (C-1'), 25 9 (C-1''), 28.9 (C-3''), 31.0 (C-2''), 33 9 (C-4''), 109.0 (C-4), 114.3 (C-6''), 115.0 (C-5), 119.7 (C-3), 123.4 (C-2), 139.4 (C-5'').

MS (APCI): m/z = 164 [M+H$^+$].

4-(Hept-6-en-1-yl)-2-methyl-1*H*-pyrrole (**6h**)

According to the general procedure for the Trofimov-reaction, ketoxime **43** (0.50 g, 3.22 mmol, 1 eq.) was converted to the regarding pyrrole **6h** in 39% yield.

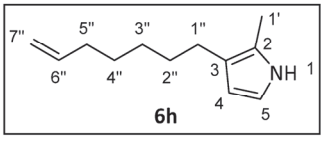

^{1}H-NMR (600 MHz, $CDCl_3$) δ [ppm] = 1 31−1 38 (m, 2H, 3''-H), 1.39−1.45 (m, 2H, 4''-H), 1 49−1 58 (m, 2H, 2''-H) 2.05 (dt, *J* = 7.1, 7.1 Hz, 2H, 5''-H), 2.18 (s, 3H, 1'-H), 2.38 (t, *J* = 7.7 Hz, 2H, 1''-H), 4.93 (dd, *J* = 1.2, 10.2 Hz, 1H, 7''-H), 4.99 (dd, *J* = 1.7, 17.1 Hz, 1H, 7''-H), 5.82 (ddt, *J* = 6.7, 10.2, 16.9 Hz, 1H, 6''-H), 6.01 (dd, *J* = 2.8, 2.8 Hz, 1H, 4-H), 6.59 (dd, J = 2.7, 2.7 Hz, 1H, 5-H), 7.70 (brs, 1H, 1-NH).

^{13}C-NMR (151 MHz, $CDCl_3$): *δ* [ppm] = 11.2 (C-1'), 26 0 (C-1''), 29.0 (C-4''), 29 2 (C-3''), 31 3 (C-2''), 34 0 (C-5''), 109 0 (C-4), 114.2 (C-7''), 115 0 (C-5), 119.8 (C-3), 123.3 (C--2), 139.4 (C-6'').

MS (APCI): m/z = 178 [M+H$^+$].

5-(Oct-7-en-1-yl)-2-methyl-1*H*-pyrrole **(6i)**

According to the general procedure for Trofimov-reaction, ketoxime **44** (2.56 g, 14.0 mmol, 1 eq.) was converted to the regarding pyrrole **6i** in 39% yield.

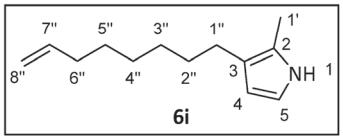

6i

^{1}H-NMR (600 MHz, $CDCl_3$) δ [ppm] = 1.35 (m, 6H, 3'', 4'', 5''-H), 1.54 (m, 2H, 2''-H), 2.05 (m, 2H, 6''-H), 2.19 (s, 3H, 1'-H), 2.39 (t, *J* = 7.8 Hz, 2H, 1''-H), 4.94 (dd, *J* = 1.2, 10.2 Hz, 1H, 8''-H), 5.00 (dd, *J* = 1.7, 17.1 Hz, 1H, 8''-H), 5.82 (ddt, *J* = 6.7, 10.2, 16.9 Hz, 1H, 7''-H), 6.02 (dd, *J* = 2.8 Hz, 1H, 4-H), 6.59 (dd, *J* = 2.7 Hz, 1H, 5-H), 7.70 (s, 1H, 1-H).

^{13}C-NMR (151 MHz, $CDCl_3$): *δ* [ppm] = 11.2 (C-6), 26.0 (C-7), 29.1 (C-11), 29.2 (C-10), 29.5 (C-9), 29.7 (C-8), 31.4 (C-7), 34-0 (C-12), 109.0 (C-4), 114.2 (C-14), 115.0 (C-5), 119.9 (C-3); 123.3 (C-2), 139.4 (C-13)

HRMS (ESI): m/z = 192.17 [M+H$^+$].

SI References

[1] A. S. Klein, A. Domröse, P. Bongen, H. U. C. Brass, T. Classen, A. Loeschcke, T. Drepper, L. Laraia, S. Sievers, K. Jaeger, J. Pietruszka, *ACS Synth Biol* **2017**, *6*, 1757–1765.
[2] D. F. Kossmann, M. Huang, R. Weihmann, X. Xiao, F. Gätgens, T. M. Weber, H. U. C. Brass, N. L. Bitzenhofer, S. Ibrahim, K. Bangert, L. Rehling, C. Mueller, T. Tiso, L. M. Blank, T. Drepper, K.-E. Jaeger, F. M. W. Grundler, J. Pietruszka, A. S. S. Schleker, A. Loeschcke, *Front Microbiol* **2023**, *14*, DOI 10.3389/fmicb.2023.1151882.
[3] H. McWilliam, W. Li, M. Uludag, S. Squizzato, Y. M. Park, N. Buso, A. P. Cowley, R. Lopez, *Nucleic Acids Res* **2013**, *41*, W597–W600.
[4] T. de Rond, P. Stow, I. Eigl, R. E. Johnson, L. J. G. Chan, G. Goyal, E. E. K. Baidoo, N. J. Hillson, C. J. Petzold, R. Sarpong, J. D. Keasling, *Nat Chem Biol* **2017**, *13*, 1155–1157.
[5] K. M. Roberts, P. F. Fitzpatrick, *IUBMB Life* **2013**, *65*, 350–357.
[6] A. J. Panay, M. Lee, C. Krebs, J. M. Bollinger, P. F. Fitzpatrick, *Biochemistry* **2011**, *50*, 1928–1933.
[7] Y. Lin, X. Sun, Q. Yuan, Y. Yan, *ACS Synth Biol* **2014**, *3*, 497–505.
[8] P. I. Nikel, D. Pérez-Pantoja, V. de Lorenzo, *Philosophical Transactions of the Royal Society B: Biological Sciences* **2013**, *368*, 20120377.
[9] R. E. Johnson, T. de Rond, V. N. G. Lindsay, J. D. Keasling, R. Sarpong, *Org Lett* **2015**, *17*, 3474–3477.
[10] P. Kancharla, Y. Li, M. Yeluguri, R. A. Dodean, K. A. Reynolds, J. X. Kelly, *J Med Chem* **2021**, *64*, 8739–8754.

V.6. Experimental procedure of additional experiments

In the following, a description of the experiments, which have been additionally conducted within this thesis, is given. **Table V-1** and **Table V-2** summarize the used oligonucleotides, constructed plasmids, and generated strains.

Table V-1: Oligonucleotides used for additional experiments in this thesis.

#	name	sequence (5' → 3')	Tm [°C]	application
1	NBi_IF-fabF-ko_TS1_fw	ATAACAGGGTAATCTGAATTTTCGCGTGGTATCACCGTCA	67	Pathway engineering for prodiginine production
2	NBi_IF-fabF-ko_TS1_rev	CAGCTGTGCAAGTACTCTCCTTTTCTAAT AACAGAGTCTCTTG	65	
3	NBi_IF-fabF-ko_TS2_fw	GGAGAGTACTTGCACAGCTGGATCGACG	65	
4	NBi_IF-fabF-ko_TS2_rev	TGCCTGCAGGTCGACTCTAGTTTCCAGCAACAGC AGGAATTTACGT	72	

Table V-2: Plasmids and strains used for additional experiments in this thesis.

plasmids			
name	**features**	**application**	**reference**
pSNW2	oriT, traJ, ori(R6K), $P_{14g(BCD2)}$→msfGFP; KmR	cloning	[296]
pSNW2-fabF-TS1-TS2	suicide vector with up-/down-stream region of *fabF* for deletion in *P. putida* KT2440; oriT, traJ, ori(R6K), $P_{14g(BCD2)}$→msfGFP; KmR	Pathway engineering for prodiginine production	this thesis
pSNW2-pvdQ	suicide vector with up-/down-stream region of *pvdQ* for deletion in *P. putida* KT2440; oriT, traJ, ori(R6K), $P_{14g(BCD2)}$→msfGFP; KmR	OMV formation in double mutants; Cycloprodigiosin production and OMV formation	[445]
pQure6-high	oriV(RK2), XylS/P_m→*trfA*, XylS/P_m→I-SceI, $P_{14g(BCD2)}$→mRFP, GmR	knockout strains	[296]
pVLT33-pigCB-prub680 (c.a.)	*lacIq*, P_{tac}→*pigCB*, *prub680 (c.a.)*, KmR, RSF1010 ori, *mob*, repABC	Cycloprodigiosin production and OMV formation	Publication VI
pYTNB04K_1G7	KmR, oriT-mob, Tn7-L, *nagR*-P_{nagAa}→*rebODCP*, eYFP, GmR, Tn7 tnsA-D, Tn7-R	OMV formation in double mutants	[419]
strains			
name	**features**	**application**	**reference**
P. putida pig21	*P. putida* KT2440::yTREX-*pig*, TcR	Pathway engineering for prodiginine production	[99]
P. putida pig21 Δ*fabF*	*P. putida* KT2440::yTREX-*pig*, TcR, seamless deletion of *fabF*		this thesis
P. putida KT2440	wild type, derivative of mt-2	OMV formation in double mutants	[255]
P. putida Δ*mlaE*	wild type, seamless deletion of *mlaE*		[419]
P. putida Δ*mlaEpvdQ*	wild type, seamless deletion of *mlaE* and *pvdQ*		this thesis

P. putida KT2440 *ΔmlaE/Tn7-*P_{nagAa}*-rebODCP*	*P. putida* KT2440 with seamless deletion of *mlaE* *nagR*-P_{nagAa}→*rebODCP*, eYFP, GmR, tnsA-D		[419]
P. putida KT2440 *ΔmlaEpvdQ/Tn7-*P_{nagAa}*-rebODCP*	*P. putida* KT2440 with seamless deletion of *mlaE* and *pvdQ* *nagR*-P_{nagAa}→*rebODCP*, eYFP, GmR, tnsA-D		this thesis
P. putida MBC18	*P. putida* KT2440::yTREX-*pigA,F-N*, TcR	Cycloprodigiosin production and OMV formation	[429]
P. putida MBC18 Δ*pvdQ*	*P. putida* KT2440::yTREX-*pigA,F-N*, TcR, seamless deletion of *pvdQ*		this thesis

Pathway engineering for prodiginine production:

The knockout mutant of *P. putida* pig21 was generated based on the previously established I-SceI-based engineering system[296]. The suicide vector pSNW2 was linearized by EcoRI and XbaI and the PCR amplified up-stream (880 bp, primer **1** and **2**) and down-stream regions (880 bp, primer **3** and **4**) of the *fabF* gene were assembled into the vector by InFusion® cloning (InFusion® Snap Assembly, Takara Bio Europe, St Germain en Laye, France). The procedure for construction of the knockout strain *P. putida* pig21 Δ*fabF* was performed as previously described[445].

For prodigiosin production, 10 mL LB medium, supplemented with 50 µg mL^{-1} tetracycline, were inoculated to an optical density of $OD_{700\ nm}$ of 0.05 and incubated at 30 °C, 120 rpm for 24 h. For a comparative study, both strains, *P. putida* pig21 and *P. putida* pig21 Δ*fabF*, were used. Prodigiosin was extracted from the cell pellet using 1 mL of acidified ethanol (4% 1 M HCl) and the amount was quantified by measuring the absorption as described before[445].

OMV formation in double mutants:

To evaluate the influence of a combinatorial deletion, the gene *pvdQ* was deleted in the hypervesiculation mutant *P. putida* Δ*mlaE*. For generation, the above-described engineering system was applied, and the strains were analyzed regarding OMV formation using the Bradford and NileRed assay as previously described (**Figure V-1**)[445].

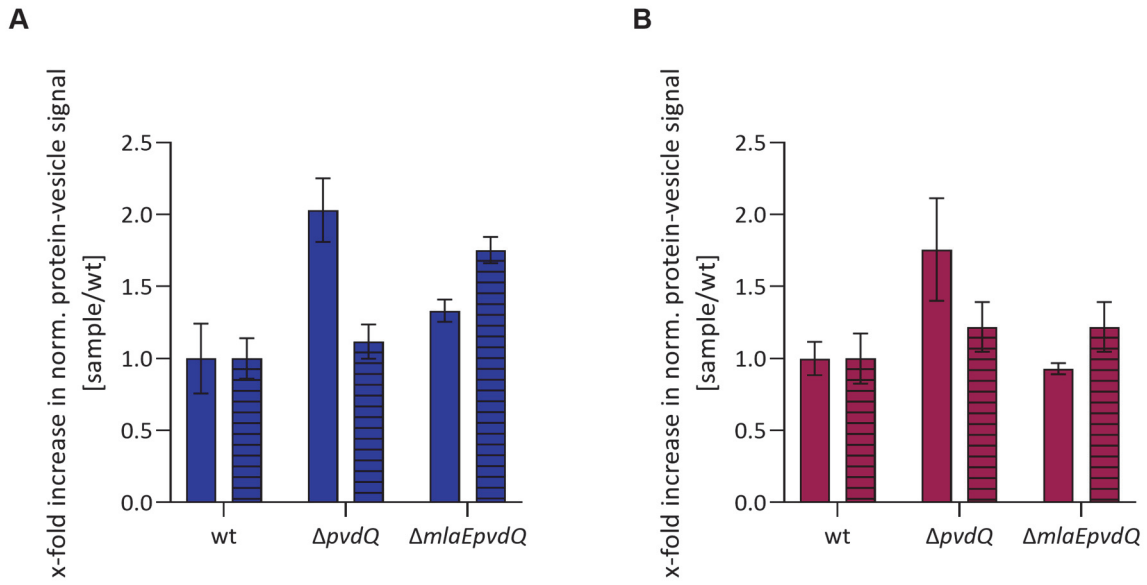

Figure V-1: Investigation of the effect of combinatorial deletions on the OMV formation in *P. putida*.
The effect of combinatorial deletions of the genes *pvdQ* and *mlaE* on the OMV formation was determined by analyzing the protein content (Bradford assay, **A**) and the lipid content (Nile red assay, **B**) of the isolated vesicle fraction. The *P. putida* KT2440 wild type strain (wt) was used for comparison and the data are shown as x-fold increase compared to this strain. Blank bars show the signal for OMV isolation after 7 h of cultivation, horizontally striped bars show the signal after 24 h. The data are mean values of biological triplicates with their corresponding standard deviation.

To further investigate the influence of combinatorial deletion on the recombinant production, the genes *rebODCP* are introduced at the *att*Tn7 site of the *P. putida* mutants under control of the inducible salicylic acid promoter P_{nagAa} using the pYT vector pYTNB04K_1G7[136]. Arcyriaflavin A production with PU foam cubes (50 mL culture volume), isolation, analyzation and quantification were performed as described before[419].

Cycloprodigiosin production and OMV formation:

Engineered vesiculation in a cycloprodigiosin producer was explored with *P. putida* MBC18 Δ*pvdQ*, which was generated as described above. *P. putida* MBC18 and the newly constructed mutant were freshly transformed with the plasmid pVLT33-pigCB-prub680 (h) (**Publication VI**).

Cycloprodigiosin production was performed in 1 mL LB medium (supplemented with 50 µg mL^{-1} tetracycline, 25 µg mL^{-1} kanamycin) in a FlowerPlate® (Beckman Coulter GmbH (formerly m2p-labs GmbH), Baesweiler, Germany). The culture was inoculated to an optical density of $OD_{600\ nm}$ of 0.05 and incubated at 30 °C and 1200 rpm for 4 h. Then, 0.5 mM IPTG and 1 mM chemically synthesized MAP were added, and the incubation was continued for 20 h at 20 °C. Cycloprodigiosin was extracted from the cell pellet with 250 µL acidified ethanol (**Publication VI**). In addition, the supernatant was extracted with 2x500 µL ethyl acetate. The solvent was removed under reduced pressure and the cycloprodigiosin was resuspended in 250 µL acidified ethanol. The analyzation and quantification were performed by HPLC as described in Publication VI.

Alternative sequences of cyclizing enzymes:

In a previous study, the established mutasynthesis platform for cycloprodigiosin production was already expanded by selection of four further candidate enzymes, whose production led to the formation of cycloprodigiosin and derivatives in *P putida* (**Publication VI**). A screening of other putative cyclases has been supposed to be promising in the future. Besides the already examined candidates, 25 putative enzyme homologs, identified via BLASTp analysis, are listed in **Table V-3**.

Table V-3: Summary of potential cyclases identified via BLASTp analysis.
Cells filled in gray represent enzymes that have already been investigated.

NCBI accession	organism	gene fragment name	pers. identity
WP_010386914.1	*P. rubra*		(reference sequence)
WP_049864432.1	*P. rubra*	2_Prubra_harm	99.29%
WP_239445344.1	*Pseudoalteromonas* sp. McH1-42	4_Prubra_harm	99.05%
WP_125562796.1	*P. rubra*	5_Prubra_harm	98.82%
WP_054015532.1	*Pseudoalteromonas* sp. R3	6_PR3_harm	93.84%
WP_125722037.1	*P. rubra*	7_Prubra_harm	93.84%
WP_253048581.1	*Pseudoalteromonas* sp. XMcav2-N	8_Prubra_harm	93.36%
WP_052713016.1	*P. rubra*	9_Prubra_harm	93.84%
WP_130245642.1	*P. rubra*	10_Prubra_harm	93.36%
WP_138544838.1	*P. rubra*	11_Prubra_harm	93.60%
WP_209052464.1	*P. viridis*	12_Pviridis_harm	93.60%
WP_125779618.1	*P. rubra*	13_Prubra_harm	93.36%
WP_235412117.1	*Pseudoalteromonas* sp. DL2-H2.2	14_PDL2_harm	93.60%
WP_138553295.1	*P. rubra*	15_Prubra_harm	92.89%
WP_095368148.1	*Pseudoalteromonas* sp. NBT06-2	16_PNBT06_harm	72.04%
WP_091980140.1	*P. denitrificans*		72.04%
WP_087478959.1	*V. mangrovi*	18_Vmangrov_harm	70.10%
WP_182287486.1	*V. spartinae*	19_Vspartinae_harm	68.38%
WP_072958698.1	*V. gazogenes*		68.38%
WP_208843821.1	*P. xiamenensis*	22_Pxiam_harm	61.56%
WP_215820965.1	*Zooshikella* sp. WH53	23_ZWH53_harm	54.37%
WP_094788782.1	*Z. ganghwensis*	24_Zgang_harm	54.53%
WP_212720964.1	*Z. ganghwensis*		54.59%
WP_163833151.1	*S. ruber*		48.07%
WP_120606176.1	*C. carmarthensis*	28_Ccarmar_harm	39.67%
WP_223762583.1	*Corallococcus* sp. AS-1-6	29_CAS1-6_harm	38.34%
MBL0692321.1	*Comamonas* sp. JC664	30_CJC664_harm	40.53%
WP_002635586.1	*M. hansupus*	31_Mhansupus_harm	38.60%
WP_223742966.1	*Corallococcus* sp. AS-1-12	32_CAS1-12_harm	38.34%
WP_201423855.1	*M. xanthus*	35_Mxanthus_harm	40.20%

VI. CONFERENCE CONTRIBUTIONS

B.1. Poster presentations

Kruse L*, **Bitzenhofer NL**, Schmidgall T, Eberlein C, Loeschcke A, Heipieper H, Jaeger K-E, Thies S (2022) From unexplored strains to robust *chassis* platforms – evolving the novel stress tolerant *Pseudomonas* species. Annual Conference 2022 of the Association for General and Applied Microbiology (VAAM), Düsseldorf/Germany (virtual)

Bitzenhofer NL*, Kruse L, Reiter A, Schatton M, Oldiges M, Wiechert W, Pietruszka J, Thies S, Loeschcke A, Jaeger K-E (2022) ARcyria: Biologically active indolocarbazoles – Advanced Recombinant production of Arcyriaflavins. BioSC Symposium 2022, Düsseldorf/Germany (with poster pitch)

Kruse L, **Bitzenhofer NL**, Kubicki S, Weihmann R, Jaeger K-E, Loeschcke A, Thies S* (2022) *Pseudomonas* whole-cell biocatalysts for complex biotransformation cascades. 10th International Congress on Biocatalysis, Hamburg/Germany.

B.2. Oral presentations

Bitzenhofer NL*, Höfel C, Kruse L, Thies S, Pietruszka J, Jaeger K-E, Loeschcke A (2022) Evolving *Pseudomonas putida* as robust production platform for the synthesis of bioactive natural products. Annual Conference 2022 of the Association for General and Applied Microbiology (VAAM), Düsseldorf/Germany (virtual)

Bitzenhofer NL*, Höfel C, Thies S, Eberlein C, Heipieper H, Jaeger K-E, Loeschcke A (2022) Tuning outer membrane vesicle formation to increase production of natural compounds in *Pseudomonas putida* KT2440. International Biennial Conference: *Pseudomonas* 2022, Atlanta/USA.

*presenting author

VII. PUBLICATIONS

Bitzenhofer NL*, Kruse L*, Thies S, Wynands B, Lechtenberg T, Rönitz J, Kozaeva E, Wirth NT, Eberlein C, Jaeger K-E, Nikel PI, Heipieper HJ, Wierckx N, and Loeschcke A (2021). Towards robust *Pseudomonas* cell factories to harbour novel biosynthetic pathways. *Essays in Biochemistry*. 65(2):319-336. doi: 10.1042/EBC20200173

Weihmann R*, Kubicki S*, **Bitzenhofer NL**, Domröse A, Bator I, Kirschen L-M, Kofler F, Funk A, Tiso T, Blank LM, Jaeger K-E, Drepper T, Thies S, and Loeschcke A (**2023**) The modular pYT vector series employed for chromosomal gene integration and expression to produce carbazoles and glycolipids in *P. putida*. *FEMS Microbes*. 4:1-17. doi: 10.1093/femsmc/xtac030

Kossmann DF*, Huang M*, Weihmann R*, Xiao X, Gätgens F, Weber TM, Brass HUC, **Bitzenhofer NL**, Ibrahim S, Bangert K, Rehling L, Müller C, Tiso T, Blank LM, Drepper T, Jaeger K-E, Grundler FMW, Pietruszka J, Schleker S, and Loeschcke A (**2023**) Production of tailored hydroxylated prodiginine showing combinatorial activity with rhamnolipids against plant-parasitic nematodes. *Frontiers in Microbiology*. 14:1151882. doi: 10.3389/fmicb.2023.1151882

Bitzenhofer NL, Höfel C, Thies S, Weiler AJ, Eberlein C, Heipieper HJ, Batra-Safferling R, Sundermeyer P, Heidler T, Sachse C, Busche T, Kalinowski J, Belthle T, Drepper T, Jaeger K-E, and Loeschcke A (**2023**) Exploring engineered vesiculation by *Pseudomonas putida* KT2440 for natural product biosynthesis. *Microbial Biotechnology*. 00:1-18. doi: 10.1111/1751-7915.14312

Bitzenhofer NL, Classen T, Jaeger K-E, and Loeschcke A (**2023**) Biotransformation of L-Tryptophan to produce Arcyriaflavin A with *Pseudomonas putida* KT2440. *ChemBioChem*. 00:e202300576. doi: 10.1002/cbic.202300576

Bitzenhofer NL*, Bleser M*, Sieberichs A, Kossmann DF, Weber TM, Warth V, Germes D, Weihmann R, Jaeger K-E, Pietruszka J, and Loeschcke A. Substrate tolerance of Prub680 and homologous enzymes allows the mutasynthesis of cycloprodiginines in *Pseudomonas putida* KT2440. *in preparation*

*these authors contributed equally

VIII. ACKNOWLEDGEMENTS AND AFFIDAVIT

Ich möchte hiermit noch die Gelegenheit nutzen und allen Personen danken, die mich während der letzten Jahre begleitet und unterstützt haben.
Zuallererst möchte ich Ihnen, Herr Prof. Karl-Erich Jaeger, für die Möglichkeit danken, dass ich meine Promotion am Institut für Molekulare Enzymtechnologie durchführen durfte. Ebenfalls danke ich Ihnen für die Konzeption meines Promotionsthemas sowie die fachliche Unterstützung in all den Jahren meiner Ausbildung am IMET.

Frau Prof. Martina Pohl möchte ich für die Zeit als Mentorin und Ihre damit verbundenen Mühen sowie für die Übernahme des Zweigutachtens herzlich danken.

Mein besonderer Dank geht an Dr. Anita Loeschcke und Dr. Stephan Thies. Vielen Dank Euch beiden für die engagierte Betreuung, Eure Unterstützung und Euer ständiges Interesse an meiner Arbeit. Ich habe unsere kleinen ‚Projekt-Kaffeekränzchen' immer sehr zu schätzen gewusst. Liebe Anita, dir möchte ich zudem von Herzen für dein stets offenes Ohr, dein Engagement, deine Geduld und deine lieben, aufbauenden und motivierenden Worte, vor allem in den letzten Monaten, danken – du warst eine tolle Betreuerin und ich wünsche Dir für die Zukunft alles Gute!

Vielen Dank auch an Apl. Prof. Thomas Drepper und Dr. Achim Heck. Ihr Beide standet mir ebenfalls bei jeglichen fachlichen oder organisatorischen Fragen in den ganzen Jahren im Institut zur Seite und habt mit Eurem Humor selbst angespannte und anstrengende Tage erträglich gemacht. Und auch den weiteren IMET-Kollegen, insbesondere Vera Svensson, Marzena Malek, Esther Knieps-Grünhagen und allen Dreppern/Loeschcke/Thies-Mitgliedern, möchte ich für Eure Unterstützung, die großartige Arbeitsatmosphäre sowie die lustigen Stunden danken. Ich werde sie vermissen!

Ein besonderer Dank gilt auch „meinen Studenten" Jana, Lars, Carolin, Max und Anka, die ich auf Ihrem Weg begleiten durfte. Ich danke Euch für die tolle Arbeit und Eure Hilfe bei der Bearbeitung meiner vielen Projekte und hoffe, dass ich Euch gerecht werden konnte. Viel Erfolg für die Zukunft!

Für die großartige Zusammenarbeit in meinen verschiedenen Projekten möchte ich allen Kooperationspartnern danken. Ich danke Dr. Christian Eberlein und Dr. Hermann Heipieper sowie allen NoStress-Mitgliedern für die tolle Zusammenarbeit und die großartigen Projekt-Treffen. Es war jedes Mal sehr produktiv, fachlich aufschlussreich und gesellig mit Euch!

Vielen Dank auch an die Kollegen aus dem Institut für Bioorganische Chemie, insbesondere an Matthias Bleser, Dorothea Kossmann, Dr. Thomas Classen und Prof. Jörg Pietruszka für die großartige Zusammenarbeit und die tatkräftige Unterstützung bei chemischen Fragestellungen. Jörg, dir möchte ich nicht nur für deine fachliche Unterstützung danken, sondern auch für deine stets offene Tür sowie die netten Gespräche, die Du mit mir als „Fremde“ im Institut geführt hast.

Liebe Mitglieder der „Fahrgemeinschaft“, falls ihr Euch bisher gewundert habt, dass ich Euch nicht namentlich bei den Kollegen erwähnt habe, liegt es daran, dass aus Euch enge Freunde geworden sind. Fabienne, Andreas, Luzie, Oliver, Andrea, Robin, und Patrick vielen Dank für die letzten Jahre. Wir haben nicht nur zahlreiche Arbeitstage und Kaffeepausen miteinander verbracht, sondern privat auch viele lustige Unternehmungen, Treffen und besondere Momente geteilt. Und ich freue mich auf viele weitere schöne Momente mit Euch! Danke für die großartige gemeinsame Zeit im IMET!

Ich möchte zudem auch Lea, Anne, Florestan, Vivian, Leonie, Manuel, Maurice, und Niklas für die moralische und seelische Unterstützung der letzten Jahre danken. Insbesondere die Gelegenheiten abzuschalten, wie ich es gerade wieder mit Euch erleben durfte, waren sehr kostbar und bleiben mir lange in Erinnerung. Ich möchte unser jährliches Holland-Wochenende nicht mehr missen und ich bin gespannt, was uns die nächsten 10 Jahre bringen werden.
Oli, Fabi, Luzie, Lea, Anne und Vivian, ich möchte Euch noch einmal für Eure Unterstützung, Euer offenes Ohr und die gemeinsamen Gespräche vor allem in der letzten Zeit meiner bzw. unserer Promotion danken.

Meiner gesamten Familie danke ich dafür, dass Ihr immer für mich da seid und mich unterstützt. Liebe „Rheidter“, dank Euch habe ich im Rheinland ein zweites Zuhause gefunden und hatte immer einen Ort und Personen, zu denen ich gehen konnte und denen ich mich in allen Belangen anvertrauen konnte. Vielen Dank dafür, dass es Euch gibt.
Corni, du hast mir immer gut zugesprochen, auch wenn es hätte andersherum sein müssen. Danke dafür, dass du mich immer wieder aufbaust, mir neue Perspektiven auf verschiedene Dinge gibst und mich manchmal auf den Boden der Tatsachen zurückholst. Ich hoffe, wir können uns ab jetzt wieder gegenseitig mehr Zeit widmen.
Mama, Papa, wenn es zwei Menschen gibt, denen ich auf jeden Fall danken müsste, dann seid Ihr das. Uns haben die vergangenen Jahre mehrere hundert Kilometer getrennt, aber Ihr habt mir nie das Gefühl gegeben, weit weg zu sein. Ihr hattet immer ein offenes Ohr, wart neugierig wie es läuft und habt mich bei so vielen kleinen wie großen Dingen unterstützt. Danke, dass Ihr

so großartige Eltern seid und zumindest versucht, zu verstehen, was ich da eigentlich die ganzen Jahre gemacht habe.

Es gibt eine weitere Person, die für mich in den letzten Jahren von unschätzbarem Wert war und ohne die diese Arbeit nicht in der Form existieren würde. Alex, du hast mich nicht nur durch die gesamte Promotion begleitet und unterstützt, sondern hast mir insbesondere in den letzten Monaten unermüdliche Unterstützung, viel Verständnis und eine bewundernswerte Geduld entgegengebracht. Ohne Dich hätte ich diese Herausforderung nicht gemeistert. Von Herzen vielen Dank dafür! Immer wieder hast du während des Schreibens betont, dass es nach der Abgabe ein Leben jenseits von Formatvorlagen und Zitationsprogrammen gibt. Jetzt freue ich mich darauf, diesen neuen Abschnitt mit dir zu erkunden.

Eidesstattliche Versicherung

Ich, Nora Lisa Bitzenhofer, versichere an Eides statt, dass die vorliegende Dissertation von mir selbstständig und ohne unzulässige fremde Hilfe unter Beachtung der „Grundsätze zur Sicherung guter wissenschaftlicher Praxis an der Heinrich-Heine-Universität Düsseldorf“ erstellt worden ist.

Die Dissertation wurde in der vorgelegten oder in ähnlicher Form noch bei keiner anderen Institution eingereicht. Ich habe bisher keine erfolglosen Promotionsversuche unternommen.

Düsseldorf, den _____ _____

Nora Lisa Bitzenhofer